



Universitetet  
i Stavanger

**FACULTY OF SCIENCE AND TECHNOLOGY**

## **MASTER'S THESIS**

Study programme/specialisation: Offshore Technology – Marine and Subsea	Spring semester 2017  Open
Author: Karina Hellevik	..... (signature of author)
Faculty supervisor: Ove Tobias Gudmestad	
Title of master's thesis: Effects of nonlinearities in the Equation of motion for one degree of freedom systems	
Credits: 30	
Keywords: - Phase plane method - Limit cycles - Nonlinear damping - Negative damping - Drag force - Nonlinear forcing term - Resonance - Critical nonlinear damping value	Number of pages: 140  + supplemental material/other: 156  Stavanger, ..... date/year

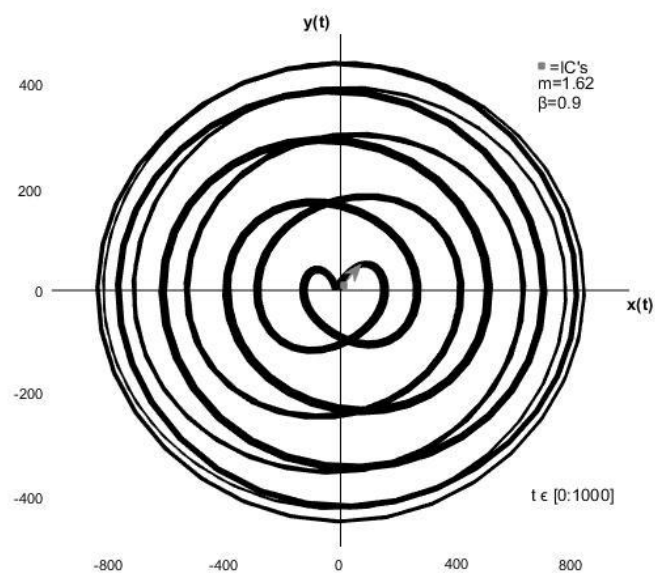
# Effects of nonlinearities in the Equation of motion for one degree of freedom systems.

Master thesis

Spring 2017

Karina Hellevik

12.06.2017



# Abstract

Most natural phenomena in the world have a nonlinear behaviour. If systems are to be described by linear equations they must follow the superposition principle. The superposition principle, consisting of additivity and homogeneity, states that the response caused by several inputs are equal to the sum of each input separately. Even though a minimal amount of systems in the world follow this principle, linearization of systems is widely used. The classical thoughts that the world could be described linearly were not disputed until the late 19<sup>th</sup> century.

Dynamical systems describe how all points of the system evolve with time. Most nonlinear systems cannot be explicitly solved, so phase diagrams are widely used. Phase diagrams map the velocity and position as time increases, making it possible to investigate how the system travels after some time. Trajectories with different initial values also tells us how sensitive the system is to its starting values.

This thesis has been divided into two parts. Part I consists of chapters 1-4, while part II consists of chapter 5-9.

Chapter 1 gives an introduction briefly describing important terms and the history of nonlinearity in engineering. Chapter 2 gives a description of an unforced, linear dynamical system with different values of damping, using the *method of the phase plane*. In chapter 3, a linear forcing term is added to the system, and *limit cycles* are explained.

The Pendulum equation, van der Pol equation and the Morison equation, which all describe known nonlinear systems are presented in chapter 4.

Part II of this thesis consists of a parameter study of an equation of motion with nonlinearity in either the forcing or the damping term.

Chapter 5 gives the presentation of what is termed the “base-case system”, which is an undamped system subjected to a *nonlinear forcing term* representing the *drag force* from the Morison equation. The parameters are varied separately to look at their effect on the system.

In chapter 6, linear, constant damping is added to the base-case system and some selected systems with varied parameters from chapter 5. The results are as expected, with decaying amplitudes due to the damping. The systems mass parameter is also varied to get systems close to and at *resonance*. These systems have a behaviour similar to the results obtained from the van der Pol equation in chapter 4.

Chapter 7 and 8 look at systems with a **nonlinear damping term**. In chapter 7, the homogenous base-case system is investigated, as well as systems with some degree of resonance. **Critical values of the nonlinear damping parameter** are found, where **negative damping** overtakes the systems. These critical values are different for each system. In chapter 8, a linear forcing term is added. The results from this chapter show that the critical values of the nonlinear damping parameter are the same with force added.

In chapter 9, **limit cycles** are found for the base-case system with linear, constant damping and **nonlinear forcing**. The limit cycles are found for systems with the mass parameter varied to make the systems have some degree of **resonance**. As the damping is linear and constant, and some trajectories with initial conditions inside the limit cycle increase their amplitudes, it is concluded that the **drag force** from the Morison equation will to some degree work as **negative damping**.

The thesis ends with a summary of conclusions and suggestions for further work within this subject.

This thesis consists of a great deal of figures, plotted in Matlab. To make the figures easily readable the size of each diagram is rather large. This causes the thesis to be of significant length. To make it lighter, the presentation of the separate diagrams in chapter 7 and 8 is put into Appendix C and D respectively.

Keywords:

- **Phase plane method**
- **Limit cycles**
- **Nonlinear damping**
- **Negative damping**
- **Drag force**
- **Nonlinear forcing term**
- **Resonance**
- **Critical nonlinear damping value**

# Acknowledgements

To my mother Siv Bente Hellevik, thank you for making everything achievable for me. Thank you for believing in me, and for showing me possibilities when something goes wrong.

To my brother Henning Hellevik, thank you for always being there for me, more than what is expected from a brother. You have always been my role model and you were the biggest influence in making me pursue the academic world.

To my boyfriend Thomas Nøstbakken, thank you for believing in me more than I do myself. Thank you for always encouraging me, and for making me laugh every single day.

To Professor Ove Tobias Gudmestad, thank you for being such a great teacher during the entire master studies. Thank you for letting me pursue such a mathematical thesis, and for being so available when I have needed guidance. I feel very fortunate having had the opportunity to learn from you. You have my deepest respect and admiration.

# Content

<b>ABSTRACT</b>	<b>I</b>
<b>ACKNOWLEDGEMENTS</b>	<b>III</b>
<b>LIST OF FIGURES</b>	<b>X</b>
<b>LIST OF TABLES</b>	<b>XXIII</b>
<b>PART I</b>	<b>1</b>
<b>CHAPTER 1 – INTRODUCTION</b>	<b>2</b>
<b>1.1 DIFFERENTIAL EQUATIONS IN ENGINEERING</b>	<b>2</b>
<b>1.2 ORDINARY DIFFERENTIAL EQUATIONS</b>	<b>2</b>
1.2.1 LINEAR AND NONLINEAR SYSTEMS	3
1.2.2 NONLINEAR DYNAMICAL SYSTEMS	4
<b>1.3 FROM LINEARITY TO NONLINEARITY</b>	<b>4</b>
<b>1.4 NONLINEARITY IN ENGINEERING</b>	<b>5</b>
<b>CHAPTER 2- LINEAR SECOND ORDER ORDINARY DIFFERENTIAL EQUATION</b>	<b>6</b>
<b>2.1 CASE 1- SYSTEM WITHOUT DAMPING</b>	<b>7</b>
2.1.1 FREE RESPONSE	7
2.1.2 PHASE PLANE DIAGRAM	8
<b>2.2 CASE 2- UNDERDAMPED SYSTEM</b>	<b>9</b>
2.2.1 FREE RESPONSE	10
2.2.2 PHASE PLANE DIAGRAM	10
<b>2.3 CASE 3- OVERDAMPED SYSTEM</b>	<b>12</b>
2.3.1 FREE RESPONSE	12
2.3.2 PHASE PLANE DIAGRAM	13
<b>2.4 CASE 4- CRITICALLY DAMPED SYSTEM</b>	<b>16</b>
2.4.1 FREE RESPONSE	17
2.4.2 PHASE PLANE DIAGRAM	17
<b>2.5 CASE 5- NEGATIVE STIFFNESS</b>	<b>19</b>
<b>CHAPTER 3 – FORCED OSCILLATIONS AND LIMIT CYCLES</b>	<b>21</b>
<b>3.1 FORCED OSCILLATIONS</b>	<b>21</b>
3.1.1 FORCED RESPONSE	21
3.1.2 RESONANCE AND PHASE CURVES	23
3.1.3 PHASE PLANE DIAGRAMS	24

3.1.3.1 No damping	24
3.1.3.2 Underdamped system	25
3.1.3.3 Overdamped system	26
3.1.3.4 Critically damped system	26
<b>3.2 LIMIT CYCLES</b>	<b>27</b>

---

**CHAPTER 4- ONE DEGREE OF FREEDOM EQUATIONS FOR KNOWN NONLINEAR SYSTEMS 28**

<b>4.1 THE VAN DER POL EQUATION</b>	<b>28</b>
4.1.1 FREE RESPONSE	29
4.1.2 PHASE PLANE DIAGRAM	30
4.1.3 APPLICATIONS OF THE VAN DER POL EQUATION	31
<b>4.2 THE PENDULUM EQUATION</b>	<b>32</b>
4.2.1 FREE RESPONSE	32
4.2.2 PHASE PLANE DIAGRAM	33
<b>4.5 THE MORISON EQUATION</b>	<b>35</b>

---

**PART II 37**

---

**CHAPTER 5- NONLINEAR FORCING TERM IN THE EQUATION OF MOTION WITHOUT DAMPING. 38**

<b>5.1 NONLINEAR FORCING TERM</b>	<b>38</b>
<b>5.2 BASE-CASE SYSTEM</b>	<b>39</b>
5.2.1 DEVELOPMENT FOR THE BASE-CASE SYSTEM	41
<b>5.3 VARYING THE STIFFNESS COEFFICIENT</b>	<b>42</b>
5.3.1 $k=0,1$	42
5.3.2 $k=0,2$	43
5.3.3 $k=0,3$	44
5.3.4 $k=0,4$	45
5.3.5 $k=0,6$	46
5.3.6 $k=0,7$	47
5.3.7 $k=0,8$	48
5.3.8 $k=0,9$	49
5.3.9 $k=1,0$	50
5.4.12 CONCLUSION	51
<b>5.4 VARYING THE AMPLITUDE PARAMETER, <math>F_0</math>.</b>	<b>52</b>
5.4.1 $F_0=10$	52
5.4.2 $F_0=20$	53
5.4.3 $F_0=30$	54
5.4.4 $F_0=40$	55
5.4.5 $F_0=60$	56
5.4.6 $F_0=70$	57
5.4.7 $F_0=80$	58
5.4.8 $F_0=90$	59
5.4.9 $F_0=100$	60
5.4.10 CONCLUSION	61

<b>5.5 VARYING THE LOADING FREQUENCY, <math>\omega</math></b>	<b>62</b>
5.5.1 $\omega = 0,1$	62
5.5.2 $\omega = 0,2$	62
5.5.3 $\omega = 0,3$	63
5.5.4 $\omega = 0,4$	64
5.5.5 $\omega = 0,6$	65
5.5.6 $\omega = 0,7$	66
5.5.7 $\omega = 0,8$	67
5.5.8 $\omega = 0,9$	68
5.5.9 $\omega = 1,0$	69
5.5.10 CONCLUSION	70
<b>5.6 VARYING THE MASS PARAMETER, <math>m</math>.</b>	<b>71</b>
5.6.1 $m = 50$	71
5.6.2 $m = 60$	72
5.6.3 $m = 70$	73
5.6.4 $m = 80$	74
5.6.5 $m = 90$	75
5.6.6 $m = 110$	76
5.6.7 $m = 120$	77
5.6.8 $m = 130$	78
5.6.9 $m = 140$	79
5.6.5 CONCLUSION	80
<b>5.7 THE BASE-CASE SYSTEM NEAR RESONANCE</b>	<b>81</b>
5.7.1 VARYING THE MASS NEAR RESONANCE	81
5.7.1.1 $\beta = 0,8$	81
5.7.1.2 $\beta = 0,9$	81
5.7.1.3 $\beta = 1,0$	82
5.7.1.4 $\beta = 1,1$	82
5.7.1.5 $\beta = 1,2$	83
5.7.2 VARYING THE LOADING FREQUENCY, $\omega$ , NEAR RESONANCE	84
5.7.2.1 $\beta = 0,8$	84
5.7.2.2 $\beta = 0,9$	84
5.7.2.3 $\beta = 1,0$	85
5.7.2.4 $\beta = 1,1$	85
5.7.2.5 $\beta = 1,2$	86
5.7.3 CONCLUSION	86
<b>5.8 CONCLUSION</b>	<b>88</b>

---

**CHAPTER 6- NONLINEAR FORCING TERM IN THE EQUATION OF MOTION WITH LINEAR, CONSTANT DAMPING.** **89**

<b>6.1 BASE-CASE SYSTEM</b>	<b>89</b>
<b>6.2 BASE-CASE SYSTEM WITH CHANGED STIFFNESS PARAMETER, <math>k</math>.</b>	<b>90</b>
<b>6.3 BASE-CASE SYSTEM WITH CHANGED AMPLITUDE PARAMETER, <math>F_0</math>.</b>	<b>93</b>
<b>6.4 BASE-CASE SYSTEM WITH CHANGED FREQUENCY PARAMETER, <math>\omega</math>.</b>	<b>96</b>
<b>6.5 BASE-CASE SYSTEM WITH VARIED MASS PARAMETER, <math>m</math>.</b>	<b>99</b>
<b>6.6 BASE-CASE SYSTEM AT AND NEAR RESONANCE.</b>	<b>102</b>



<b>6.7 CONCLUSION</b>	<b>107</b>
<hr/>	
<b>CHAPTER 7- NONLINEAR DAMPING TERM IN THE HOMOGENOUS EQUATION OF MOTION FOR ONE DEGREE OF FREEDOM SYSTEMS</b>	<b>108</b>
<hr/>	
<b>CHAPTER 8 – NONLINEAR DAMPING TERM IN THE EQUATION OF MOTION WITH LINEAR FORCING TERM FOR ONE DEGREE OF FREEDOM SYSTEMS</b>	<b>116</b>
<hr/>	
<b>CHAPTER 9 - LIMIT CYCLES FOR A SYSTEM WITH DRAG LOADING SUBJECTED TO LINEAR, CONSTANT DAMPING.</b>	<b>123</b>
<hr/>	
<b>9.1 EXPLORATION OF LIMIT CYCLES FOR BASE-CASE SYSTEM WITH <math>\beta=0,8</math></b>	<b>123</b>
<b>9.2 EXPLORATION OF LIMIT CYCLES FOR BASE-CASE SYSTEMS WITH <math>\beta = 1/3, \beta = 1/2, \beta = 1,0, \beta = 3/2</math> and <math>\beta = 2,0</math></b>	<b>125</b>
9.2.1 $\beta = 1/3$	126
9.2.2 $\beta = 1/2$	128
9.2.3 $\beta = 1,0$	130
9.2.4 $\beta = 3/2$	132
9.2.5 $\beta = 2,0$	134
<b>9.3 CONCLUSION</b>	<b>137</b>
<b>9.4 CONSEQUENCES FOR OFFSHORE STRUCTURES</b>	<b>137</b>
<hr/>	
<b>CHAPTER 10 - CONCLUSIONS AND FURTHER WORK</b>	<b>138</b>
<hr/>	
<b>10.1 PART I</b>	<b>138</b>
<b>10.2 PART II</b>	<b>138</b>
<b>10.3 FURTHER WORK</b>	<b>140</b>
<hr/>	
<b>REFERENCES</b>	<b>141</b>
<hr/>	
<b>APPENDIX A– MATLAB CODES</b>	<b>143</b>
<hr/>	
<b>APPENDIX B – CALCULATIONS FOR EQUATIONS (3.4)-(3.12)</b>	<b>156</b>
<hr/>	
<b>APPENDIX C – DIAGRAMS FOR CHAPTER 7</b>	<b>158</b>
<hr/>	
<b>C.1 BASE-CASE SYSTEM</b>	<b>158</b>
C.1.1 $a = 0$	158
C.1.1.1 $c_0=0,0015$	158
C.1.1.2 $c_0=0,005$	159
C.1.2 $a=0,5$	160
C.1.2.1 $c_0=0,0015$	160
C.1.2.2 $c_0=0,005$	161
C.1.3 $a=1,0$	162
C.1.3.1 $c_0=0,0015$	162

C.1.3.2 $c_0=0,005$	163
C.1.4 $a=1,19$	164
C.1.4.1 $c_0=0,0015$	164
C.1.4.2 $c_0=0,005$	165
C.1.5 $a=1,2$	166
C.1.5.1 $c_0=0,0015$	166
C.1.4.2 $c_0=0,005$	167
<b>C.2 <math>\beta = 1/3</math></b>	<b>168</b>
C.2.1 $a=0$	168
C.2.2 $a=1,0$	170
C.2.3 $a=2,0$	172
C.2.4 $a=3,45$	174
C.2.5 $a=3,46$	176
<b>C.3 <math>\beta = 1/2</math></b>	<b>178</b>
C.3.1 $a=0$	178
C.3.2 $a=0,5$	180
C.3.3 $a=1,0$	182
C.3.4 $a=1,60$	184
C.3.5 $a=1,61$	186
<b>C.4 <math>\beta = 1,0</math></b>	<b>188</b>
C.4.1 $a=0$	188
C.4.2 $a=0,5$	190
C.4.3 $a=1,0$	192
C.4.4 $a=1,03$	194
C.4.5 $a=1,04$	196
<b>C.5 <math>\beta = 3/2</math></b>	<b>198</b>
C.5.1 $a=0$	198
C.5.2 $a=0,1$	200
C.5.3 $a=0,2$	202
C.5.4 $a=0,36$	204
C.5.5 $a=0,37$	206
<b>C.6 <math>\beta = 2,0</math></b>	<b>208</b>
C.6.1 $a=0$	208
C.6.2 $a=0,01$	210
C.6.3 $a=0,02$	212

---

**APPENDIX D – DIAGRAMS FOR CHAPTER 8** **214**

<b>D.1 BASE-CASE SYSTEM</b>	<b>214</b>
D.1.1 $a=0$	214
D.1.1.1 $c_0=0,0015$	214
D.1.1.2 $c_0=0,005$	215
D.1.2 $a=0,5$	216
D.1.2.1 $c_0=0,0015$	216
D.1.2.2 $c_0=0,005$	217
D.1.3 $a=1,0$	218
D.1.3.1 $c_0=0,0015$	218

D.1.3.2 $c_0=0,005$	219
D.1.4 $a=1,19$	220
D.1.4.1 $c_0=0,0015$	220
D.1.4.2 $c_0=0,005$	221
D.1.5 $a=1,2$	222
D.1.5.1 $c_0=0,0015$	222
D.1.4.2 $c_0=0,005$	223
<b>D.2 <math>\beta = 1/3</math></b>	<b>224</b>
D.2.1 $a=0$	224
D.2.2 $a=1,0$	226
D.2.3 $a=2,0$	228
D.2.4 $a=3,45$	230
D.2.5 $a=3,46$	232
<b>D.3 <math>\beta = 1/2</math></b>	<b>234</b>
D.3.1 $a=0$	234
D.3.2 $a=0,5$	236
D.3.3 $a=1,0$	238
D.3.4 $a=1,60$	240
D.3.5 $a=1,61$	242
<b>D.4 <math>\beta = 1, 0</math></b>	<b>244</b>
D.4.1 $a=0$	244
D.4.2 $a=0,5$	246
D.4.3 $a=1,0$	248
D.4.4 $a=1,03$	250
D.4.5 $a=1,04$	252
<b>D.5 <math>\beta = 3/2</math></b>	<b>254</b>
D.5.1 $a=0$	254
D.5.2 $a=0,1$	256
D.5.3 $a=0,2$	258
D.5.4 $a=0,36$	260
D.5.5 $a=0,37$	262
<b>D.6 <math>\beta = 2, 0</math></b>	<b>264</b>
D.6.1 $a=0$	264
D.6.2 $a=0,01$	266
D.6.3 $a=0,01$	268

---

<b>APPENDIX E</b>	<b>270</b>
-------------------	------------

<b>E.1 CONTEXT</b>	<b>270</b>
<b>E.2 INTERVIEW</b>	<b>270</b>
<b>E.3 COMPLEMENTARY COMMENTS</b>	<b>271</b>
<b>E.4 CONCLUSION</b>	<b>271</b>

# List of figures

Figure 2.1: Free response without damping.	8
Figure 2.2: Trajectory in the phase plane of an unforced system without damping.	9
Figure 2.3: Free response of an underdamped system.	10
Figure 2.4: Trajectories in the uv-plane of an underdamped, unforced system.	11
Figure 2.5: Trajectories in the phase plane of an underdamped, unforced system.	12
Figure 2.6: Free response of an overdamped system.	13
Figure 2.7: Trajectories in the uv-plane of an overdamped, unforced system.	15
Figure 2.8: Trajectories in the phase plane of an overdamped, unforced system.	16
Figure 2.9: Free response of a critically damped system	17
Figure 2.10: Trajectories in the uv-plane of a critically damped, unforced system.	18
Figure 2.11: Trajectories in the phase plane of a critically damped, unforced system.	19
Figure 2.12: Trajectories in the uv-plane for an overdamped, unforced system with negative stiffness.	20
Figure 2.13: Trajectories in the phase plane for an overdamped, unforced system with negative stiffness.	20
Figure 3.1: Response of a forced damped system, note the initial transient motion caused by the initial conditions for displacement and velocity.	22
Figure 3.2: Resonance curves for different values of damping.	23
Figure 3.3: Phase curves for different values of damping.	24
Figure 3.4: Phase diagram for an undamped forced system.	25
Figure 3.5: Phase diagram for an underdamped forced system.	25
Figure 3.6: Trajectories in the phase plane for an overdamped forced system.	26
Figure 3.7: Trajectories in the phase plane for a critically damped forced system.	26
Figure 3.8: Stable, half-stable and unstable limit cycles.	27
Figure 4.1: Free response of the unforced van der Pol Equation with $\mu=0.5$ .	28
Figure 4.2: Free response of the unforced van der Pol Equation with $\mu=5$ .	29
Figure 4.3: Free response of the unforced van der Pol Equation with $\mu=10$ .	29
Figure 4.4: Phase plane diagram for the unforced van der Pol equation with $\mu=1$ .	30
Figure 4.5: Limit cycles for the van der Pol equation with different values of $\mu$ .	31
Figure 4.6: Angular response as a function of time for an undamped, unforced pendulum for both linear and non-linear systems.	33
Figure 4.7: Phase plane diagram for the undamped, unforced pendulum equation.	33
Figure 4.8: Phase plane diagram for the damped, unforced pendulum equation.	34
Figure 5.1: Typical phase plane diagrams for undamped systems with nonlinear force with different initial conditions(IC's) from $t=0$ to $t=500s$ (left) and $t=1000s$ (right).	39
Figure 5.2: Position curves for systems with nonlinear force for different IC's, separated by different colours.	39
Figure 5.3: Velocity curves for systems with nonlinear force for different IC's, separated by different colours.	40
Figure 5.4: Development in the phase plane for the base-case system from $t=0$ to $t=267s$ (left) and to $t=500s$ (right).	41
Figure 5.5: Position curve for the base-case system.	41
Figure 5.6: Development in the phase plane for the base-case system with $k=0,1$ from $t=0$ to $t=199s$ (left) and to $t=1000s$ (right).	42
Figure 5.7: Position curve for the base-case system with $k=0,1$ .	42
Figure 5.8: Development in the phase plane for the base-case system with $k=0,2$ from $t=0$ to $t=141s$ (left) and to $t=1000s$ (right).	43
Figure 5.9: Position curve for the base-case system with $k=0,2$ .	43
Figure 5.10: Development in the phase plane for the base-case system with $k=0,3$ from $t=0$ to $t=115s$ (left) and to $t=1000s$ (right).	44
Figure 5.11: Position curve for the base-case system with $k=0,3$ .	44

Figure 5.12: Development in the phase plane for the base-case system with $k=0,4$ from $t=0$ to $t=100$ (left) and to $t=1000$ s(right).	45
Figure 5.13: Position curve for the base-case system with $k=0,4$ .	45
Figure 5.14: Development in the phase plane for the base-case system with $k=0,6$ from $t=0$ to $t=81$ (left) and to $t=1000$ s(right).	46
Figure 5.15: Position curve for the base-case system with $k=0,6$ .	46
Figure 5.16: Development in the phase plane for the base-case system with $k=0,7$ from $t=0$ to $t=75$ (left) and to $t=1000$ s(right).	47
Figure 5.17: Position curve for the base-case system with $k=0,7$ .	47
Figure 5.18: Development in the phase plane for the base-case system with $k=0,8$ from $t=0$ to $t=70$ (left) and to $t=1000$ s(right).	48
Figure 5.19: Position curve for the base-case system with $k=0,8$ .	48
Figure 5.20: Development in the phase plane for the base-case system with $k=0,9$ from $t=0$ to $t=67$ s(left) and to $t=1000$ s(right).	49
Figure 5.21: Position curve for the base-case system with $k=0,9$ .	49
Figure 5.22: Development in the phase plane for the base-case system with $k=1,0$ from $t=0$ to $t=63$ (left) and to $t=1000$ s(right).	50
Figure 5.23: Position curve for the base-case system with $k=1,0$ .	50
Figure 5.24: Development in the phase plane for the base-case system with $F_0=10$ from $t=0$ to $t=89$ s(left) and to $t=1000$ s(right).	52
Figure 5.25: Position curve for the base-case system with $F_0=10$ .	52
Figure 5.26: Development in the phase plane for the base-case system with $F_0=20$ from $t=0$ to $t=89$ s(left) and to $t=1000$ s(right).	53
Figure 5.27: Position curve for the base-case system with $F_0=20$ .	53
Figure 5.28: Development in the phase plane for the base-case system with $F_0=30$ from $t=0$ to $t=89$ s(left) and to $t=1000$ s(right).	54
Figure 5.29: Position curve for the base-case system with $F_0=30$ .	54
Figure 5.30: Development in the phase plane for the base-case system with $F_0=40$ from $t=0$ to $t=89$ s(left) and to $t=1000$ s(right).	55
Figure 5.31: Position curve for the base-case system with $F_0=40$ .	55
Figure 5.32: Development in the phase plane for the base-case system with $F_0=60$ from $t=0$ to $t=89$ s(left) and to $t=1000$ s(right).	56
Figure 5.33: Position curve for the base-case system with $F_0=60$ .	56
Figure 5.34: Development in the phase plane for the base-case system with $F_0=70$ from $t=0$ to $t=89$ s(left) and to $t=1000$ s(right).	57
Figure 5.35: Position curve for the base-case system with $F_0=70$ .	57
Figure 5.36: Development in the phase plane for the base-case system with $F_0=80$ from $t=0$ to $t=89$ s(left) and to $t=1000$ s(right).	58
Figure 5.37: Position curve for the base-case system with $F_0=80$ .	58
Figure 5.38: Development in the phase plane for the base-case system with $F_0=90$ from $t=0$ to $t=89$ s(left) and to $t=1000$ s(right).	59
Figure 5.39: Position curve for the base-case system with $F_0=90$ .	59
Figure 5.40: Development in the phase plane for the base-case system with $F_0=100$ from $t=0$ to $t=89$ s(left) and to $t=1000$ s(right).	60
Figure 5.41: Position curve for the base-case system with $F_0=100$ .	60
Figure 5.42: Development in the phase plane(left) and position curve(right) for the base-case system with $\omega=0,1$ from $t=0$ to $t=1000$ s.	62
Figure 5.43: Development in the phase plane(left) and position curve(right) for the base-case system with $\omega=0,2$ from $t=0$ to $t=1000$ s.	62
Figure 5.44: Development in the phase plane for the base-case system with $\omega=0,3$ from $t=0$ to $t=89$ s(left) and to $t=1000$ s(right).	63
Figure 5.45: Position curve for the base-case system with $\omega=0,3$ .	63

Figure 5.46: Development in the phase plane for the base-case system with $\omega=0,4$ from $t=0$ to $t=89s$ (left) and to $t=1000s$ (right).	64
Figure 5.47: Position curve for the base-case system with $\omega=0,4$ .	64
Figure 5.48: Development in the phase plane for the base-case system with $\omega=0,6$ from $t=0$ to $t=89s$ (left) and to $t=1000s$ (right).	65
Figure 5.49: Position curve for the base-case system with $\omega=0,6$ .	65
Figure 5.50: Development in the phase plane for the base-case system with $\omega=0,7$ from $t=0$ to $t=89s$ (left) and to $t=1000s$ (right).	66
Figure 5.51: Position curve for the base-case system with $\omega=0,7$ .	66
Figure 5.52: Development in the phase plane for the base-case system with $\omega=0,8$ from $t=0$ to $t=89s$ (left) and to $t=1000s$ (right).	67
Figure 5.53: Position curve for the base-case system with $\omega=0,8$ .	67
Figure 5.54: Development in the phase plane for the base-case system with $\omega=0,9$ from $t=0$ to $t=89s$ (left) and to $t=1000s$ (right).	68
Figure 5.55: Position curve for the base-case system with $\omega=0,9$ .	68
Figure 5.56: Development in the phase plane for the base-case system with $\omega=1,0$ from $t=0$ to $t=89s$ (left) and to $t=1000s$ (right).	69
Figure 5.57: Position curve for the base-case system with $\omega=1,0$ .	69
Figure 5.58: Development in the phase plane for the base-case system with $m=50$ from $t=0$ to $t=63s$ (left) and to $t=1000s$ (right).	71
Figure 5.59: Position curve for the base-case system with $m=50$ .	71
Figure 5.60: Development in the phase plane for the base-case system with $m=60$ from $t=0$ to $t=69s$ (left) and to $t=1000s$ (right).	72
Figure 5.61: Position curve for the base-case system with $m=60$ .	72
Figure 5.62: Development in the phase plane for the base-case system with $m=60$ from $t=0$ to $t=74s$ (left) and to $t=1000s$ (right).	73
Figure 5.63: Position curve for the base-case system with $m=70$ .	73
Figure 5.64: Development in the phase plane for the base-case system with $m=80$ from $t=0$ to $t=80s$ (left) and to $t=1000s$ (right).	74
Figure 5.65: Position curve for the base-case system with $m=80$ .	74
Figure 5.66: Development in the phase plane for the base-case system with $m=90$ from $t=0$ to $t=84s$ (left) and to $t=1000s$ (right).	75
Figure 5.67: Position curve for the base-case system with $m=90$ .	75
Figure 5.68: Development in the phase plane for the base-case system with $m=110$ from $t=0$ to $t=94s$ (left) and to $t=1000s$ (right).	76
Figure 5.69: Position curve for the base-case system with $m=110$ .	76
Figure 5.70: Development in the phase plane for the base-case system with $m=120$ from $t=0$ to $t=97s$ (left) and to $t=1000s$ (right).	77
Figure 5.71: Position curve for the base-case system with $m=120$ .	77
Figure 5.72: Development in the phase plane for the base-case system with $m=130$ from $t=0$ to $t=102s$ (left) and to $t=1000s$ (right).	78
Figure 5.73: Position curve for the base-case system with $m=130$ .	78
Figure 5.74: Development in the phase plane for the base-case system with $m=140$ from $t=0$ to $t=105s$ (left) and to $t=1000s$ (right).	79
Figure 5.75: Position curve for the base-case system with $m=140$ .	79
Figure 5.76: Phase plane diagram(left) and position curve(right) for the base-case system with $m=1,28$ , making $\beta =0,8$ , from $t=0$ to $t=1000s$ .	81
Figure 5.77: Phase plane diagram(left) and position curve(right) for the base-case system with $m=1,62$ , making $\beta =0,9$ , from $t=0$ to $t=1000s$ .	81
Figure 5.78: Development in the phase plane(left) and position curve(right) for the base-case with $m=2$ from $t=0$ to $t=200s$ .	82
Figure 5.79: Phase plane diagram for the base-case system with $m=2,42$ , making $\beta =1,1$ , from $t=0$ to $t=1000s$ .	82

Figure 5.80: Phase plane diagram for the base-case system with $m=2,88$ , making $\beta =1,2$ , from $t=0$ to $t=1000s$ .	83
Figure 5.81: Phase plane diagram(left) and position curve(right) for the base-case system with $\omega=0,057$ , making $\beta =0,8$ , from $t=0$ to $t=1000s$ .	84
Figure 5.82: Phase plane diagram(left) and position curve(right) for the base-case system with $\omega=0,064$ , making $\beta =0,9$ , from $t=0$ to $t=1000s$ .	84
Figure 5.83: Phase plane diagram(left) and position curve(right) for the base-case with $\omega=0,071$ , making the system at resonance, from $t=0$ to $t=1000s$ .	85
Figure 5.84: Phase plane diagram(left) and position curve(right) for the base-case system with $\omega=0,078$ , making $\beta =1,1$ , from $t=0$ to $t=1000s$ .	85
Figure 5.85: Phase plane diagram(left) and position curve(right) for the base-case system with $\omega=0,081$ , making $\beta =1,2$ , from $t=0$ to $t=1000s$ .	86
Figure 6.1: Phase plane diagrams for the base-case system with $c=0,15$ (left) and $c=0,5$ (right).	89
Figure 6.2: Position curves for the base-case system with $c=0,15$ (left) and $c=0,5$ (right).	90
Figure 6.3: Phase plane diagrams for the base-case system with $k=0,1$ , and $c=0,15$ (left) and $c=0,5$ (right).	90
Figure 6.4: Position curves for the base-case system with $k=0,1$ , and $c=0,15$ (left) and $c=0,5$ (right).	91
Figure 6.5: Phase plane diagrams for the base-case system with $k=1,0$ , and $c=0,15$ (left) and $c=0,5$ (right).	91
Figure 6.6: Position curves for the base-case system with $k=1,0$ , and $c=0,15$ (left) and $c=0,5$ (right).	91
Figure 6.7: Phase plane diagrams for the base-case system with $F_0=10$ , and $c=0,15$ (left) and $c=0,5$ (right).	93
Figure 6.8: Position curves for the base-case system with $F_0=10$ , and $c=0,15$ (left) and $c=0,5$ (right).	93
Figure 6.9: Phase plane diagrams for the base-case system with $F_0=100$ , and $c=0,15$ (left) and $c=0,5$ (right).	94
Figure 6.10: Position curves for the base-case system with $F_0=100$ , and $c=0,15$ (left) and $c=0,5$ (right).	94
Figure 6.11: Phase plane diagrams for the base-case system with $\omega=0,2$ , and $c=0,15$ (left) and $c=0,5$ (right).	96
Figure 6.12: Position curves for the base-case system with $\omega=0,2$ , and $c=0,15$ (left) and $c=0,5$ (right).	96
Figure 6.13: Phase plane diagrams for the base-case system with $\omega=1,0$ , and $c=0,15$ (left) and $c=0,5$ (right).	97
Figure 6.14: Position curves for the base-case system with $\omega=1,0$ , and $c=0,15$ (left) and $c=0,5$ (right).	97
Figure 6.15: Phase plane diagrams for the base-case system with $m=50$ , and $c=0,15$ (left) and $c=0,5$ (right).	99
Figure 6.16: Position curves for the base-case system with $m=50$ , and $c=0,15$ (left) and $c=0,5$ (right).	99
Figure 6.17: Phase plane diagrams for the base-case system with $m=140$ , and $c=0,15$ (left) and $c=0,5$ (right).	100
Figure 6.18: Position curves for the base-case system with $m=140$ , and $c=0,15$ (left) and $c=0,5$ (right).	100
Figure 6.19: Phase plane diagrams for the base-case system with $m=1,28$ , making $\beta=0,8$ , with $c=0,15$ (left) and $c=0,5$ (right).	102
Figure 6.20: Position curves for the base-case system with $m=1,28$ , making $\beta=0,8$ , with $c=0,15$ (left) and $c=0,5$ (right).	102
Figure 6.21: Phase plane diagrams for the base-case system with $m=1,62$ , making $\beta=0,9$ , with $c=0,15$ (left) and $c=0,5$ (right).	103
Figure 6.22: Position curves for the base-case system with $m=1,62$ , making $\beta=0,9$ , with $c=0,15$ (left) and $c=0,5$ (right).	103
Figure 6.23: Phase plane diagrams for the base-case system with $m=2,0$ , making $\beta=1,0$ , with $c=0,15$ (left) and $c=0,5$ (right).	103
Figure 6.24: Position curves for the base-case system with $m=2,0$ , making $\beta=1,0$ , with $c=0,15$ (left) and $c=0,5$ (right).	104
Figure 6.25: Phase plane diagrams for the base-case system with $m=2,42$ , making $\beta=1,1$ , with $c=0,15$ (left) and $c=0,5$ (right).	104
Figure 6.26: Position curves for the base-case system with $m=2,42$ , making $\beta=1,1$ , with $c=0,15$ (left) and $c=0,5$ (right).	104
Figure 6.27: Phase plane diagrams for the base-case system with $m=2,88$ , making $\beta=1,2$ , with $c=0,15$ (left) and $c=0,5$ (right).	105
Figure 6.28: Position curves for the base-case system with $m=2,88$ , making $\beta=1,2$ , with $c=0,15$ (left) and $c=0,5$ (right).	105
Figure 9.1: Base-case system with $m=1,28$ , making $\beta=0,8$ with $c=0,15$ for four different initial conditions.	123
Figure 9.2: Base-case system with $m=1,28$ , making $\beta=0,8$ with $c=0,5$ (left) and $c=1,0$ (right) for four different initial conditions.	124

Figure 9.3: Limit cycles in the base-case system with $\beta$ between 0,8 and 1,0(left) and between 1,0 and 1,2(right), with $c=0,15$ .	124
Figure 9.4: Limit cycles in the base-case system with $\beta$ between 0,8 and 1,0(left) and between 1,0 and 1,2(right), with $c=0,5$ .	125
Figure 9.5: Limit cycles in the base-case system with $\beta$ between 0,8 and 1,0(left) and between 1,0 and 1,2(right), with $c=1,0$ .	125
Figure 9.6: Base-case system with $m=0,222$ , making $\beta=1/3$ with $c=0,15$ (left) and $c=0,5$ (right) for four different set of initial conditions.	126
Figure 9.7: Position curves for the system with $\beta=1/3$ , $c=0,15$ (left) and $c=0,5$ (right) for four different set of initial conditions represented by separate colours.	127
Figure 9.8: Velocity curves for the system with $\beta=1/3$ , $c=0,15$ (left) and $c=0,5$ (right) for four different set of initial conditions represented by separate colours.	127
Figure 9.9: The first 35s of the position curves for the system with $\beta=1/3$ , $c=0,15$ (left) and $c=0,5$ (right) for four different set of initial conditions represented by separate colours.	127
Figure 9.10: Base-case system with $m=0,5$ , making $\beta=1/2$ with $c=0,15$ (left) and $c=0,5$ (right) for four different set of initial conditions represented with separate colours.	128
Figure 9.11: Position curves for the system with $\beta=1/2$ , $c=0,15$ (left) and $c=0,5$ (right) for four different set of initial conditions represented by separate colours.	128
Figure 9.12: Velocity curves for the system with $\beta=1/2$ , $c=0,15$ (left) and $c=0,5$ (right) for four different set of initial conditions represented by separate colours.	129
Figure 9.13: The first 35s of the position curves for the system with $\beta=1/2$ , $c=0,15$ (left) and $c=0,5$ (right) for four different set of initial conditions represented by separate colours.	129
Figure 9.14: Base-case system with $m=2,0$ , making $\beta=1/2$ with $c=0,15$ (left) and $c=0,5$ (right) for four different set of initial conditions represented with separate colours.	130
Figure 9.15: Position curves for the system with $\beta=1,0$ , $c=0,15$ (left) and $c=0,5$ (right) for four different set of initial conditions represented by separate colours.	130
Figure 9.16: Velocity curves for the system with $\beta=1,0$ , $c=0,15$ (left) and $c=0,5$ (right) for four different set of initial conditions represented by separate colours.	131
Figure 9.17: The first 100s of the position curves for the system with $\beta=1,0$ , $c=0,15$ (left) and $c=0,5$ (right) for four different set of initial conditions represented by separate colours.	131
Figure 9.18: Base-case system with $m=4,5$ , making $\beta=3/2$ with $c=0,15$ (left) and $c=0,5$ (right) for four different set of initial conditions represented with separate colours.	132
Figure 9.19: Position curves for the system with $\beta=3/2$ , $c=0,15$ (left) and $c=0,5$ (right) for four different set of initial conditions represented by separate colours.	132
Figure 9.20: Velocity curves for the system with $\beta=3/2$ , $c=0,15$ (left) and $c=0,5$ (right) for four different set of initial conditions represented by separate colours.	133
Figure 9.21: The first 100s of the position curves for the system with $\beta=3/2$ , $c=0,15$ (left) and $c=0,5$ (right) for four different set of initial conditions represented by separate colours.	133
Figure 9.22: Base-case system with $m=8,0$ , making $\beta=2,0$ with $c=0,15$ (left) and $c=0,5$ (right) for four different set of initial conditions represented with separate colours.	134
Figure 9.23: Position curves for the system with $\beta=2,0$ , $c=0,15$ (left) and $c=0,5$ (right) for four different set of initial conditions represented by separate colours.	134
Figure 9.24: Velocity curves for the system with $\beta=2,0$ , $c=0,15$ (left) and $c=0,5$ (right) for four different set of initial conditions represented by separate colours.	135
Figure 9.25: The first 100s of the position curves for the system with $\beta=2,0$ , $c=0,15$ (left) and $c=0,5$ (right) for four different set of initial conditions represented by separate colours.	135
Figure C.1: Position curve(left) and velocity curve(right) for the base-case system with $a=0$ and $c_0=0,0015$ .	158
Figure C.2: Phase plane diagram for the base-case system with $a=0$ and $c_0=0,0015$ .	158
Figure C.3: Position curve(left) and velocity curve(right) for the base-case system with $a=0$ and $c_0=0,005$ .	159
Figure C.4: Phase plane diagram for the base-case system with $a=0$ and $c_0=0,005$ .	159
Figure C.5: Position curve(left) and velocity curve(right) for the base-case system with $a=0,5$ and $c_0=0,0015$ .	160
Figure C.6: Phase plane diagram for the base-case system with $a=0,5$ and $c_0=0,0015$ .	160
Figure C.7: Position curve(left) and velocity curve(right) for the base-case system with $a=0,5$ and $c_0=0,005$ .	161



Figure C.8: Phase plane diagram for the base-case system with $a=0,5$ and $c_0=0,005$ .	161
Figure C.9: Position curve(left) and velocity curve(right) for the base-case system with $a=1,0$ and $c_0=0,0015$ .	162
Figure C.10: Phase plane diagram for the base-case system with $a=1,0$ and $c_0=0,0015$ .	162
Figure C.11: Position curve(left) and velocity curve(right) for the base-case system with $a=1,0$ and $c_0=0,005$ .	163
Figure C.12: Phase plane diagram for the base-case system with $a=1,0$ and $c_0=0,005$ .	163
Figure C.13: Position curve(left) and velocity curve(right) for the base-case system with $a=1,19$ and $c_0=0,0015$ .	164
Figure C.14: Phase plane diagram for the base-case system with $a=1,19$ and $c_0=0,0015$ .	164
Figure C.15: Position curve(left) and velocity curve(right) for the base-case system with $a=1,19$ and $c_0=0,005$ .	165
Figure C.16: Phase plane diagram for the base-case system with $a=1,19$ and $c_0=0,005$ .	165
Figure C.17: Position curve(left) and velocity curve(right) for the base-case system with $a=1,2$ and $c_0=0,0015$ .	166
Figure C.18: Phase plane diagram for the base-case system with $a=1,2$ and $c_0=0,0015$ .	166
Figure C.19: Position curve(left) and velocity curve(right) for the base-case system with $a=1,2$ and $c_0=0,005$ .	167
Figure C.20: Phase plane diagram for the base-case system with $a=1,2$ and $c_0=0,005$ .	167
Figure C.21: Position curve(left) and velocity curve(right) for the base-case system with $m=0,222$ , making $\beta=1/3$ , with $c_0=0,0015$ and $a=0$ .	168
Figure C.22: Phase plane diagram for the base-case system with $m=0,222$ , making $\beta=1/3$ , with $c_0=0,0015$ and $a=0$ .	168
Figure C.23: Position curve(left) and velocity curve(right) for the base-case system with $m=0,222$ , making $\beta=1/3$ , with $c_0=0,005$ and $a=0$ .	169
Figure C.24: Phase plane diagram for the base-case system with $m=0,222$ , making $\beta=1/3$ , with $c_0=0,005$ and $a=0$ .	169
Figure C.25: Position curve(left) and velocity curve(right) for the base-case system with $m=0,222$ , making $\beta=1/3$ , with $c_0=0,0015$ and $a=1,0$ .	170
Figure C.26: Phase plane diagram for the base-case system with $m=0,222$ , making $\beta=1/3$ , with $c_0=0,0015$ and $a=1,0$ .	170
Figure C.27: Position curve(left) and velocity curve(right) for the base-case system with $m=0,222$ , making $\beta=1/3$ , with $c_0=0,005$ and $a=1,0$ .	171
Figure C.28: Phase plane diagram for the base-case system with $m=0,222$ , making $\beta=1/3$ , with $c_0=0,005$ and $a=1,0$ .	171
Figure C.29: Position curve(left) and velocity curve(right) for the base-case system with $m=0,222$ , making $\beta=1/3$ , with $c_0=0,0015$ and $a=2$ .	172
Figure C.30: Phase plane diagram for the base-case system with $m=0,222$ , making $\beta=1/3$ , with $c_0=0,0015$ and $a=2,0$ .	172
Figure C.31: Position curve(left) and velocity curve(right) for the base-case system with $m=0,222$ , making $\beta=1/3$ , with $c_0=0,005$ and $a=2,0$ .	173
Figure C.32: Phase plane diagram for the base-case system with $m=0,222$ , making $\beta=1/3$ , with $c_0=0,005$ and $a=2,0$ .	173
Figure C.33: Position curve(left) and velocity curve(right) for the base-case system with $m=0,222$ , making $\beta=1/3$ , with $c_0=0,0015$ and $a=3,45$ .	174
Figure C.34: Phase plane diagram for the base-case system with $m=0,222$ , making $\beta=1/3$ , with $c_0=0,0015$ and $a=3,45$ .	174
Figure C.35: Position curve(left) and velocity curve(right) for the base-case system with $m=0,222$ , making $\beta=1/3$ , with $c_0=0,005$ and $a=3,45$ .	175
Figure C.36: Phase plane diagram for the base-case system with $m=0,222$ , making $\beta=1/3$ , with $c_0=0,005$ and $a=3,45$ .	175
Figure C.37: Position curve(left) and velocity curve(right) for the base-case system with $m=0,222$ , making $\beta=1/3$ , with $c_0=0,0015$ and $a=3,46$ .	176
Figure C.38: Phase plane diagram for the base-case system with $m=0,222$ , making $\beta=1/3$ , with $c_0=0,0015$ and $a=3,46$ .	176

Figure C.39: Position curve(left) and velocity curve(right) for the base-case system with $m=0,222$ , making $\beta=1/3$ , with $c_0=0,005$ and $a=3,46$ .	177
Figure C.40: Phase plane diagram for the base-case system with $m=0,222$ , making $\beta=1/3$ , with $c_0=0,005$ and $a=3,46$ .	177
Figure C.41: Position curve(left) and velocity curve(right) for the base-case system with $m=0,5$ , making $\beta=1/2$ , with $c_0=0,0015$ and $a=0$ .	178
Figure C.42: Phase plane diagram for the base-case system with $m=0,5$ , making $\beta=1/2$ , with $c_0=0,0015$ and $a=0$ .	178
Figure C.43: Position curve(left) and velocity curve(right) for the base-case system with $m=0,5$ , making $\beta=1/2$ , with $c_0=0,005$ and $a=0$ .	179
Figure C.44: Phase plane diagram for the base-case system with $m=0,5$ , making $\beta=1/2$ , with $c_0=0,005$ and $a=0$ .	179
Figure C.45: Position curve(left) and velocity curve(right) for the base-case system with $m=0,5$ , making $\beta=1/2$ , with $c_0=0,0015$ and $a=0,5$ .	180
Figure C.46: Phase plane diagram for the base-case system with $m=0,5$ , making $\beta=1/2$ , with $c_0=0,0015$ and $a=0,5$ .	180
Figure C.47: Position curve(left) and velocity curve(right) for the base-case system with $m=0,5$ , making $\beta=1/2$ , with $c_0=0,005$ and $a=0,5$ .	181
Figure C.48: Phase plane diagram for the base-case system with $m=0,5$ , making $\beta=1/2$ , with $c_0=0,005$ and $a=0,5$ .	181
Figure C.49: Position curve(left) and velocity curve(right) for the base-case system with $m=0,5$ , making $\beta=1/2$ , with $c_0=0,0015$ and $a=1,0$ .	182
Figure C.50: Phase plane diagram for the base-case system with $m=0,5$ , making $\beta=1/2$ , with $c_0=0,0015$ and $a=1,0$ .	182
Figure C.51: Position curve(left) and velocity curve(right) for the base-case system with $m=0,5$ , making $\beta=1/2$ , with $c_0=0,005$ and $a=1,0$ .	183
Figure C.52: Phase plane diagram for the base-case system with $m=0,5$ , making $\beta=1/2$ , with $c_0=0,005$ and $a=1,0$ .	183
Figure C.53: Position curve(left) and velocity curve(right) for the base-case system with $m=0,5$ , making $\beta=1/2$ , with $c_0=0,0015$ and $a=1,60$ .	184
Figure C.54: Phase plane diagram for the base-case system with $m=0,5$ , making $\beta=1/2$ , with $c_0=0,0015$ and $a=1,60$ .	184
Figure C.55: Position curve(left) and velocity curve(right) for the base-case system with $m=0,5$ , making $\beta=1/2$ , with $c_0=0,005$ and $a=1,60$ .	185
Figure C.56: Phase plane diagram for the base-case system with $m=0,5$ , making $\beta=1/2$ , with $c_0=0,005$ and $a=1,60$ .	185
Figure C.57: Position curve(left) and velocity curve(right) for the base-case system with $m=0,5$ , making $\beta=1/2$ , with $c_0=0,0015$ and $a=1,61$ .	186
Figure C.58: Phase plane diagram for the base-case system with $m=0,5$ , making $\beta=1/2$ , with $c_0=0,0015$ and $a=1,61$ .	186
Figure C.59: Position curve(left) and velocity curve(right) for the base-case system with $m=0,5$ , making $\beta=1/2$ , with $c_0=0,005$ and $a=1,61$ .	187
Figure C.60: Phase plane diagram for the base-case system with $m=0,5$ , making $\beta=1/2$ , with $c_0=0,005$ and $a=1,61$ .	187
Figure C.61: Position curve(left) and velocity curve(right) for the base-case system with $m=2,0$ , making $\beta=1,0$ , with $c_0=0,0015$ and $a=0$ .	188
Figure C.62: Phase plane diagram for the base-case system with $m=2,0$ , making $\beta=1,0$ , with $c_0=0,0015$ and $a=0$ .	188
Figure C.63: Position curve(left) and velocity curve(right) for the base-case system with $m=2,0$ , making $\beta=1,0$ , with $c_0=0,005$ and $a=0$ .	189
Figure C.64: Phase plane diagram for the base-case system with $m=2,0$ , making $\beta=1,0$ , with $c_0=0,005$ and $a=0$ .	189

Figure C.65: Position curve(left) and velocity curve(right) for the base-case system with $m=2,0$ , making $\beta=1,0$ , with $c_0=0,0015$ and $a=0,5$ .	190
Figure C.66: Phase plane diagram for the base-case system with $m=2,0$ , making $\beta=1,0$ , with $c_0=0,0015$ and $a=0,5$ .	190
Figure C.67: Position curve(left) and velocity curve(right) for the base-case system with $m=2,0$ , making $\beta=1,0$ , with $c_0=0,005$ and $a=0,5$ .	191
Figure C.68: Phase plane diagram for the base-case system with $m=2,0$ , making $\beta=1,0$ , with $c_0=0,005$ and $a=0,5$ .	191
Figure C.69: Position curve(left) and velocity curve(right) for the base-case system with $m=2,0$ , making $\beta=1,0$ , with $c_0=0,0015$ and $a=1,0$ .	192
Figure C.70: Phase plane diagram for the base-case system with $m=2,0$ , making $\beta=1,0$ , with $c_0=0,0015$ and $a=1,0$ .	192
Figure C.71: Position curve(left) and velocity curve(right) for the base-case system with $m=2,0$ , making $\beta=1,0$ , with $c_0=0,005$ and $a=1,0$ .	193
Figure C.72: Phase plane diagram for the base-case system with $m=2,0$ , making $\beta=1,0$ , with $c_0=0,005$ and $a=1,0$ .	193
Figure C.73: Position curve(left) and velocity curve(right) for the base-case system with $m=2,0$ , making $\beta=1,0$ , with $c_0=0,0015$ and $a=1,03$ .	194
Figure C.74: Phase plane diagram for the base-case system with $m=2,0$ , making $\beta=1,0$ , with $c_0=0,0015$ and $a=1,03$ .	194
Figure C.75: Position curve(left) and velocity curve(right) for the base-case system with $m=2,0$ , making $\beta=1,0$ , with $c_0=0,005$ and $a=1,03$ .	195
Figure C.76: Phase plane diagram for the base-case system with $m=2,0$ , making $\beta=1,0$ , with $c_0=0,005$ and $a=1,03$ .	195
Figure C.77: Position curve(left) and velocity curve(right) for the base-case system with $m=2,0$ , making $\beta=1,0$ , with $c_0=0,0015$ and $a=1,04$ .	196
Figure C.78: Phase plane diagram for the base-case system with $m=2,0$ , making $\beta=1,0$ , with $c_0=0,0015$ and $a=1,04$ .	196
Figure C.79: Position curve(left) and velocity curve(right) for the base-case system with $m=2,0$ , making $\beta=1,0$ , with $c_0=0,005$ and $a=1,04$ .	197
Figure C.80: Phase plane diagram for the base-case system with $m=2,0$ , making $\beta=1,0$ , with $c_0=0,005$ and $a=1,04$ .	197
Figure C.81: Position curve(left) and velocity curve(right) for the base-case system with $m=4,5$ , making $\beta=3/2$ , with $c_0=0,0015$ and $a=0$ .	198
Figure C.82: Phase plane diagram for the base-case system with $m=4,5$ , making $\beta=3/2$ , with $c_0=0,0015$ and $a=0$ .	198
Figure C.83: Position curve(left) and velocity curve(right) for the base-case system with $m=4,5$ , making $\beta=3/2$ , with $c_0=0,005$ and $a=0$ .	199
Figure C.84: Phase plane diagram for the base-case system with $m=4,5$ , making $\beta=3/2$ , with $c_0=0,005$ and $a=0$ .	199
Figure C.85: Position curve(left) and velocity curve(right) for the base-case system with $m=4,5$ , making $\beta=3/2$ , with $c_0=0,0015$ and $a=0,1$ .	200
Figure C.86: Phase plane diagram for the base-case system with $m=4,5$ , making $\beta=3/2$ , with $c_0=0,0015$ and $a=0,1$ .	200
Figure C.87: Position curve(left) and velocity curve(right) for the base-case system with $m=4,5$ , making $\beta=3/2$ , with $c_0=0,005$ and $a=0,1$ .	201
Figure C.88: Phase plane diagram for the base-case system with $m=4,5$ , making $\beta=3/2$ , with $c_0=0,005$ and $a=0,1$ .	201
Figure C.89: Position curve(left) and velocity curve(right) for the base-case system with $m=4,5$ , making $\beta=3/2$ , with $c_0=0,0015$ and $a=0,2$ .	202
Figure C.90: Phase plane diagram for the base-case system with $m=4,5$ , making $\beta=3/2$ , with $c_0=0,0015$ and $a=0,2$ .	202

Figure C.91: Position curve(left) and velocity curve(right) for the base-case system with $m=4,5$ , making $\beta=3/2$ , with $c_0=0,005$ and $a=0,2$ .	203
Figure C.92: Phase plane diagram for the base-case system with $m=4,5$ , making $\beta=3/2$ , with $c_0=0,005$ and $a=0,2$ .	203
Figure C.93: Position curve(left) and velocity curve(right) for the base-case system with $m=4,5$ , making $\beta=3/2$ , with $c_0=0,0015$ and $a=0,36$ .	204
Figure C.94: Phase plane diagram for the base-case system with $m=4,5$ , making $\beta=3/2$ , with $c_0=0,0015$ and $a=0,36$ .	204
Figure C.95: Position curve(left) and velocity curve(right) for the base-case system with $m=4,5$ , making $\beta=3/2$ , with $c_0=0,005$ and $a=0,36$ .	205
Figure C.96: Phase plane diagram for the base-case system with $m=4,5$ , making $\beta=3/2$ , with $c_0=0,005$ and $a=0,36$ .	205
Figure C.97: Position curve(left) and velocity curve(right) for the base-case system with $m=4,5$ , making $\beta=3/2$ , with $c_0=0,0015$ and $a=0,37$ .	206
Figure C.98: Phase plane diagram for the base-case system with $m=4,5$ , making $\beta=3/2$ , with $c_0=0,0015$ and $a=0,37$ .	206
Figure C.99: Position curve(left) and velocity curve(right) for the base-case system with $m=4,5$ , making $\beta=3/2$ , with $c_0=0,005$ and $a=0,37$ .	207
Figure C.100: Phase plane diagram for the base-case system with $m=4,5$ , making $\beta=3/2$ , with $c_0=0,005$ and $a=0,37$ .	207
Figure C.101: Position curve(left) and velocity curve(right) for the base-case system with $m=8,0$ , making $\beta=2,0$ , with $c_0=0,0015$ and $a=0$ .	208
Figure C.102: Phase plane diagram for the base-case system with $m=8,0$ , making $\beta=2,0$ , with $c_0=0,0015$ and $a=0$ .	208
Figure C.103: Position curve(left) and velocity curve(right) for the base-case system with $m=8,0$ , making $\beta=2,0$ , with $c_0=0,005$ and $a=0$ .	209
Figure C.104: Phase plane diagram for the base-case system with $m=8,0$ , making $\beta=2,0$ , with $c_0=0,005$ and $a=0$ .	209
Figure C.105: Position curve(left) and velocity curve(right) for the base-case system with $m=8,0$ , making $\beta=2,0$ , with $c_0=0,0015$ and $a=0,01$ .	210
Figure C.106: Phase plane diagram for the base-case system with $m=8,0$ , making $\beta=2,0$ , with $c_0=0,0015$ and $a=0,01$ .	210
Figure C.107: Position curve(left) and velocity curve(right) for the base-case system with $m=8,0$ , making $\beta=2,0$ , with $c_0=0,005$ and $a=0,01$ .	211
Figure C.108: Phase plane diagram for the base-case system with $m=8,0$ , making $\beta=2,0$ , with $c_0=0,005$ and $a=0,01$ .	211
Figure C.109: Position curve(left) and velocity curve(right) for the base-case system with $m=8,0$ , making $\beta=2,0$ , with $c_0=0,0015$ and $a=0,02$ .	212
Figure C.110: Phase plane diagram for the base-case system with $m=8,0$ , making $\beta=2,0$ , with $c_0=0,0015$ and $a=0,02$ .	212
Figure C.111: Position curve(left) and velocity curve(right) for the base-case system with $m=8,0$ , making $\beta=2,0$ , with $c_0=0,005$ and $a=0,02$ .	213
Figure C.112: Phase plane diagram for the base-case system with $m=8,0$ , making $\beta=2,0$ , with $c_0=0,005$ and $a=0,02$ .	213
Figure D.1: Position curve(left) and velocity curve(right) for the base-case system with $a=0$ and $c_0=0,0015$ .	214
Figure D.2: Phase plane diagram for the base-case system with $a=0$ and $c_0=0,0015$ .	214
Figure D.3: Position curve(left) and velocity curve(right) for the base-case system with $a=0$ and $c_0=0,005$ .	215
Figure D.4: Phase plane diagram for the base-case system with $a=0$ and $c_0=0,005$ .	215
Figure D.5: Position curve(left) and velocity curve(right) for the base-case system with $a=0,5$ and $c_0=0,0015$ .	216
Figure D.6: Phase plane diagram for the base-case system with $a=0,5$ and $c_0=0,0015$ .	216
Figure D.7: Position curve(left) and velocity curve(right) for the base-case system with $a=0,5$ and $c_0=0,005$ .	217
Figure D.8: Phase plane diagram for the base-case system with $a=0,5$ and $c_0=0,005$ .	217
Figure D.9: Position curve(left) and velocity curve(right) for the base-case system with $a=1,0$ and $c_0=0,0015$ .	218

Figure D.10: Phase plane diagram for the base-case system with $a=1,0$ and $c_0=0,0015$ .	218
Figure D.11: Position curve(left) and velocity curve(right) for the base-case system with $a=1,0$ and $c_0=0,005$ .	219
Figure D.12: Phase plane diagram for the base-case system with $a=1,0$ and $c_0=0,005$ .	219
Figure D.13: Position curve(left) and velocity curve(right) for the base-case system with $a=1,19$ and $c_0=0,0015$ .	220
Figure D.14: Phase plane diagram for the base-case system with $a=1,19$ and $c_0=0,0015$ .	220
Figure D.15: Position curve(left) and velocity curve(right) for the base-case system with $a=1,19$ and $c_0=0,005$ .	221
Figure D.16: Phase plane diagram for the base-case system with $a=1,19$ and $c_0=0,005$ .	221
Figure D.17: Position curve(left) and velocity curve(right) for the base-case system with $a=1,2$ and $c_0=0,0015$ .	222
Figure D.18: Phase plane diagram for the base-case system with $a=1,2$ and $c_0=0,0015$ .	222
Figure D.19: Position curve(left) and velocity curve(right) for the base-case system with $a=1,2$ and $c_0=0,005$ .	223
Figure D.20: Phase plane diagram for the base-case system with $a=1,2$ and $c_0=0,005$ .	223
Figure D.21: Position curve(left) and velocity curve(right) for the base-case system with $m=0,222$ , making $\beta=1/3$ , with $c_0=0,0015$ and $a=0$ .	224
Figure D.22: Phase plane diagram for the base-case system with $m=0,222$ , making $\beta=1/3$ , with $c_0=0,0015$ and $a=0$ .	224
Figure D.23: Position curve(left) and velocity curve(right) for the base-case system with $m=0,222$ , making $\beta=1/3$ , with $c_0=0,005$ and $a=0$ .	225
Figure D.24: Phase plane diagram for the base-case system with $m=0,222$ , making $\beta=1/3$ , with $c_0=0,005$ and $a=0$ .	225
Figure D.25: Position curve(left) and velocity curve(right) for the base-case system with $m=0,222$ , making $\beta=1/3$ , with $c_0=0,0015$ and $a=1,0$ .	226
Figure D.26: Phase plane diagram for the base-case system with $m=0,222$ , making $\beta=1/3$ , with $c_0=0,0015$ and $a=1,0$ .	226
Figure D.27: Position curve(left) and velocity curve(right) for the base-case system with $m=0,222$ , making $\beta=1/3$ , with $c_0=0,005$ and $a=1,0$ .	227
Figure D.28: Phase plane diagram for the base-case system with $m=0,222$ , making $\beta=1/3$ , with $c_0=0,005$ and $a=1,0$ .	227
Figure D.29: Position curve(left) and velocity curve(right) for the base-case system with $m=0,222$ , making $\beta=1/3$ , with $c_0=0,0015$ and $a=2$ .	228
Figure D.30: Phase plane diagram for the base-case system with $m=0,222$ , making $\beta=1/3$ , with $c_0=0,0015$ and $a=2,0$ .	228
Figure D.31: Position curve(left) and velocity curve(right) for the base-case system with $m=0,222$ , making $\beta=1/3$ , with $c_0=0,005$ and $a=2,0$ .	229
Figure D.32: Phase plane diagram for the base-case system with $m=0,222$ , making $\beta=1/3$ , with $c_0=0,005$ and $a=2,0$ .	229
Figure D.33: Position curve(left) and velocity curve(right) for the base-case system with $m=0,222$ , making $\beta=1/3$ , with $c_0=0,0015$ and $a=3,45$ .	230
Figure D.34: Phase plane diagram for the base-case system with $m=0,222$ , making $\beta=1/3$ , with $c_0=0,0015$ and $a=3,45$ .	230
Figure D.35: Position curve(left) and velocity curve(right) for the base-case system with $m=0,222$ , making $\beta=1/3$ , with $c_0=0,005$ and $a=3,45$ .	231
Figure D.36: Phase plane diagram for the base-case system with $m=0,222$ , making $\beta=1/3$ , with $c_0=0,005$ and $a=3,45$ .	231
Figure D.37: Position curve(left) and velocity curve(right) for the base-case system with $m=0,222$ , making $\beta=1/3$ , with $c_0=0,0015$ and $a=3,46$ .	232
Figure D.38: Phase plane diagram for the base-case system with $m=0,222$ , making $\beta=1/3$ , with $c_0=0,0015$ and $a=3,46$ .	232
Figure D.39: Position curve(left) and velocity curve(right) for the base-case system with $m=0,222$ , making $\beta=1/3$ , with $c_0=0,005$ and $a=3,46$ .	233

Figure D.40: Phase plane diagram for the base-case system with $m=0,222$ , making $\beta=1/3$ , with $c_0=0,005$ and $a=3,46$ .	233
Figure D.41: Position curve(left) and velocity curve(right) for the base-case system with $m=0,5$ , making $\beta=1/2$ , with $c_0=0,0015$ and $a=0$ .	234
Figure D.42: Phase plane diagram for the base-case system with $m=0,5$ , making $\beta=1/2$ , with $c_0=0,0015$ and $a=0$ .	234
Figure D.43: Position curve(left) and velocity curve(right) for the base-case system with $m=0,5$ , making $\beta=1/2$ , with $c_0=0,005$ and $a=0$ .	235
Figure D.44: Phase plane diagram for the base-case system with $m=0,5$ , making $\beta=1/2$ , with $c_0=0,005$ and $a=0$ .	235
Figure D.45: Position curve(left) and velocity curve(right) for the base-case system with $m=0,5$ , making $\beta=1/2$ , with $c_0=0,0015$ and $a=0,5$ .	236
Figure D.46: Phase plane diagram for the base-case system with $m=0,5$ , making $\beta=1/2$ , with $c_0=0,0015$ and $a=0,5$ .	236
Figure D.47: Position curve(left) and velocity curve(right) for the base-case system with $m=0,5$ , making $\beta=1/2$ , with $c_0=0,005$ and $a=0,5$ .	237
Figure D.48: Phase plane diagram for the base-case system with $m=0,5$ , making $\beta=1/2$ , with $c_0=0,005$ and $a=0,5$ .	237
Figure D.49: Position curve(left) and velocity curve(right) for the base-case system with $m=0,5$ , making $\beta=1/2$ , with $c_0=0,0015$ and $a=1,0$ .	238
Figure D.50: Phase plane diagram for the base-case system with $m=0,5$ , making $\beta=1/2$ , with $c_0=0,0015$ and $a=1,0$ .	238
Figure D.51: Position curve(left) and velocity curve(right) for the base-case system with $m=0,5$ , making $\beta=1/2$ , with $c_0=0,005$ and $a=1,0$ .	239
Figure D.52: Phase plane diagram for the base-case system with $m=0,5$ , making $\beta=1/2$ , with $c_0=0,005$ and $a=1,0$ .	239
Figure D.53: Position curve(left) and velocity curve(right) for the base-case system with $m=0,5$ , making $\beta=1/2$ , with $c_0=0,0015$ and $a=1,60$ .	240
Figure D.54: Phase plane diagram for the base-case system with $m=0,5$ , making $\beta=1/2$ , with $c_0=0,0015$ and $a=1,60$ .	240
Figure D.55: Position curve(left) and velocity curve(right) for the base-case system with $m=0,5$ , making $\beta=1/2$ , with $c_0=0,005$ and $a=1,60$ .	241
Figure D.56: Phase plane diagram for the base-case system with $m=0,5$ , making $\beta=1/2$ , with $c_0=0,005$ and $a=1,60$ .	241
Figure D.57: Position curve(left) and velocity curve(right) for the base-case system with $m=0,5$ , making $\beta=1/2$ , with $c_0=0,0015$ and $a=1,61$ .	242
Figure D.58: Phase plane diagram for the base-case system with $m=0,5$ , making $\beta=1/2$ , with $c_0=0,0015$ and $a=1,61$ .	242
Figure D.59: Position curve(left) and velocity curve(right) for the base-case system with $m=0,5$ , making $\beta=1/2$ , with $c_0=0,005$ and $a=1,61$ .	243
Figure D.60: Phase plane diagram for the base-case system with $m=0,5$ , making $\beta=1/2$ , with $c_0=0,005$ and $a=1,61$ .	243
Figure D.61: Position curve(left) and velocity curve(right) for the base-case system with $m=2,0$ , making $\beta=1,0$ , with $c_0=0,0015$ and $a=0$ .	244
Figure D.62: Phase plane diagram for the base-case system with $m=2,0$ , making $\beta=1,0$ , with $c_0=0,0015$ and $a=0$ .	244
Figure D.63: Position curve(left) and velocity curve(right) for the base-case system with $m=2,0$ , making $\beta=1,0$ , with $c_0=0,005$ and $a=0$ .	245
Figure D.64: Phase plane diagram for the base-case system with $m=2,0$ , making $\beta=1,0$ , with $c_0=0,005$ and $a=0$ .	245
Figure D.65: Position curve(left) and velocity curve(right) for the base-case system with $m=2,0$ , making $\beta=1,0$ , with $c_0=0,0015$ and $a=0,5$ .	246

Figure D.66: Phase plane diagram for the base-case system with $m=2,0$ , making $\beta=1,0$ , with $c_0=0,0015$ and $a=0,5$ .	246
Figure D.67: Position curve(left) and velocity curve(right) for the base-case system with $m=2,0$ , making $\beta=1,0$ , with $c_0=0,005$ and $a=0,5$ .	247
Figure D.68: Phase plane diagram for the base-case system with $m=2,0$ , making $\beta=1,0$ , with $c_0=0,005$ and $a=0,5$ .	247
Figure D.69: Position curve(left) and velocity curve(right) for the base-case system with $m=2,0$ , making $\beta=1,0$ , with $c_0=0,0015$ and $a=1,0$ .	248
Figure D.70: Phase plane diagram for the base-case system with $m=2,0$ , making $\beta=1,0$ , with $c_0=0,0015$ and $a=1,0$ .	248
Figure D.71: Position curve(left) and velocity curve(right) for the base-case system with $m=2,0$ , making $\beta=1,0$ , with $c_0=0,005$ and $a=1,0$ .	249
Figure D.72: Phase plane diagram for the base-case system with $m=2,0$ , making $\beta=1,0$ , with $c_0=0,005$ and $a=1,0$ .	249
Figure D.73: Position curve(left) and velocity curve(right) for the base-case system with $m=2,0$ , making $\beta=1,0$ , with $c_0=0,0015$ and $a=1,03$ .	250
Figure D.74: Phase plane diagram for the base-case system with $m=2,0$ , making $\beta=1,0$ , with $c_0=0,0015$ and $a=1,03$ .	250
Figure D.75: Position curve(left) and velocity curve(right) for the base-case system with $m=2,0$ , making $\beta=1,0$ , with $c_0=0,005$ and $a=1,03$ .	251
Figure D.76: Phase plane diagram for the base-case system with $m=2,0$ , making $\beta=1,0$ , with $c_0=0,005$ and $a=1,03$ .	251
Figure D.77: Position curve(left) and velocity curve(right) for the base-case system with $m=2,0$ , making $\beta=1,0$ , with $c_0=0,0015$ and $a=1,04$ .	252
Figure D.78: Phase plane diagram for the base-case system with $m=2,0$ , making $\beta=1,0$ , with $c_0=0,0015$ and $a=1,04$ .	252
Figure D.79: Position curve(left) and velocity curve(right) for the base-case system with $m=2,0$ , making $\beta=1,0$ , with $c_0=0,005$ and $a=1,04$ .	253
Figure D.80: Phase plane diagram for the base-case system with $m=2,0$ , making $\beta=1,0$ , with $c_0=0,005$ and $a=1,04$ .	253
Figure D.81: Position curve(left) and velocity curve(right) for the base-case system with $m=4,5$ , making $\beta=3/2$ , with $c_0=0,0015$ and $a=0$ .	254
Figure D.82: Phase plane diagram for the base-case system with $m=4,5$ , making $\beta=3/2$ , with $c_0=0,0015$ and $a=0$ .	254
Figure D.83: Position curve(left) and velocity curve(right) for the base-case system with $m=4,5$ , making $\beta=3/2$ , with $c_0=0,005$ and $a=0$ .	255
Figure D.84: Phase plane diagram for the base-case system with $m=4,5$ , making $\beta=3/2$ , with $c_0=0,005$ and $a=0$ .	255
Figure D.85: Position curve(left) and velocity curve(right) for the base-case system with $m=4,5$ , making $\beta=3/2$ , with $c_0=0,0015$ and $a=0,1$ .	256
Figure D.86: Phase plane diagram for the base-case system with $m=4,5$ , making $\beta=3/2$ , with $c_0=0,0015$ and $a=0,1$ .	256
Figure D.87: Position curve(left) and velocity curve(right) for the base-case system with $m=4,5$ , making $\beta=3/2$ , with $c_0=0,005$ and $a=0,1$ .	257
Figure D.88: Phase plane diagram for the base-case system with $m=4,5$ , making $\beta=3/2$ , with $c_0=0,005$ and $a=0,1$ .	257
Figure D.89: Position curve(left) and velocity curve(right) for the base-case system with $m=4,5$ , making $\beta=3/2$ , with $c_0=0,0015$ and $a=0,2$ .	258
Figure D.90: Phase plane diagram for the base-case system with $m=4,5$ , making $\beta=3/2$ , with $c_0=0,0015$ and $a=0,2$ .	258
Figure D.91: Position curve(left) and velocity curve(right) for the base-case system with $m=4,5$ , making $\beta=3/2$ , with $c_0=0,005$ and $a=0,2$ .	259

Figure D.92: Phase plane diagram for the base-case system with $m=4,5$ , making $\beta=3/2$ , with $c_0=0,005$ and $a=0,2$ .	259
Figure D.93: Position curve(left) and velocity curve(right) for the base-case system with $m=4,5$ , making $\beta=3/2$ , with $c_0=0,0015$ and $a=0,36$ .	260
Figure D.94: Phase plane diagram for the base-case system with $m=4,5$ , making $\beta=3/2$ , with $c_0=0,0015$ and $a=0,36$ .	260
Figure D.95: Position curve(left) and velocity curve(right) for the base-case system with $m=4,5$ , making $\beta=3/2$ , with $c_0=0,005$ and $a=0,36$ .	261
Figure D.96: Phase plane diagram for the base-case system with $m=4,5$ , making $\beta=3/2$ , with $c_0=0,005$ and $a=0,36$ .	261
Figure D.97: Position curve(left) and velocity curve(right) for the base-case system with $m=4,5$ , making $\beta=3/2$ , with $c_0=0,0015$ and $a=0,37$ .	262
Figure D.98: Phase plane diagram for the base-case system with $m=4,5$ , making $\beta=3/2$ , with $c_0=0,0015$ and $a=0,37$ .	262
Figure D.99: Position curve(left) and velocity curve(right) for the base-case system with $m=4,5$ , making $\beta=3/2$ , with $c_0=0,005$ and $a=0,37$ .	263
Figure D.100: Phase plane diagram for the base-case system with $m=4,5$ , making $\beta=3/2$ , with $c_0=0,005$ and $a=0,37$ .	263
Figure D.101: Position curve(left) and velocity curve(right) for the base-case system with $m=8,0$ , making $\beta=2,0$ , with $c_0=0,0015$ and $a=0$ .	264
Figure D.102: Phase plane diagram for the base-case system with $m=8,0$ , making $\beta=2,0$ , with $c_0=0,0015$ and $a=0$ .	264
Figure D.103: Position curve(left) and velocity curve(right) for the base-case system with $m=8,0$ , making $\beta=2,0$ , with $c_0=0,005$ and $a=0$ .	265
Figure D.104: Phase plane diagram for the base-case system with $m=8,0$ , making $\beta=2,0$ , with $c_0=0,005$ and $a=0$ .	265
Figure D.105: Position curve(left) and velocity curve(right) for the base-case system with $m=8,0$ , making $\beta=2,0$ , with $c_0=0,0015$ and $a=0,01$ .	266
Figure D.106: Phase plane diagram for the base-case system with $m=8,0$ , making $\beta=2,0$ , with $c_0=0,0015$ and $a=0,01$ .	266
Figure D.107: Position curve(left) and velocity curve(right) for the base-case system with $m=8,0$ , making $\beta=2,0$ , with $c_0=0,005$ and $a=0,01$ .	267
Figure D.108: Phase plane diagram for the base-case system with $m=8,0$ , making $\beta=2,0$ , with $c_0=0,005$ and $a=0,01$ .	267
Figure D.109: Position curve(left) and velocity curve(right) for the base-case system with $m=8,0$ , making $\beta=2,0$ , with $c_0=0,0015$ and $a=0,02$ .	268
Figure D.110: Phase plane diagram for the base-case system with $m=8,0$ , making $\beta=2,0$ , with $c_0=0,0015$ and $a=0,02$ .	268
Figure D.111: Position curve(left) and velocity curve(right) for the base-case system with $m=8,0$ , making $\beta=2,0$ , with $c_0=0,005$ and $a=0,02$ .	269
Figure D.112: Phase plane diagram for the base-case system with $m=8,0$ , making $\beta=2,0$ , with $c_0=0,005$ and $a=0,02$ .	269



# List of tables

Table 5.1: Review of phase plane diagrams and position curves for the base-case system with different values of $k$ .	51
Table 5.2: Review of phase plane diagrams and position curves for the base-case system with different values of $F_0$ .	61
Table 5.3: Review of phase plane diagrams and position curves for the base-case system with different values of $\omega$ .	70
Table 5.4: Review of phase plane diagrams and position curves for the base-case system with different values of $m$ .	80
Table 5.5: Review of phase plane diagrams and position curves for the base-case system with different values of $m$ , making the system near resonance.	87
Table 5.6: Review of phase plane diagrams and position curves for the base-case system with different values of $\omega$ , making the system near resonance.	87
Table 6.1: Review of phase plane diagrams and position curves for the base-case system with different values of the stiffness parameter, $k$ , with different values of linear damping, $c$ .	92
Table 6.2: Review of phase plane diagrams and position curves for the base-case system with different values of the amplitude parameter, $F_0$ , with different values of linear damping, $c$ .	95
Table 6.3: Review of phase plane diagrams and position curves for the base-case system with different values of the frequency parameter, $\omega$ , with different values of linear damping, $c$ .	98
Table 6.4: Review of phase plane diagrams and position curves for the base-case system with different values of the mass parameter, $m$ , with different values of linear damping, $c$ .	101
Table 6.5: Review of phase plane diagrams and position curves for the base-case system with different values of $m$ , making the system at and near resonance, with different values of linear damping, $c$ .	106
Table 7.1: Review of position curves, velocity curves and phase plane diagrams for the base-case system with varying nonlinear damping, for two values of linear, constant damping, $c_0=0,0015$ and $c_0=0,005$ .	110
Table 7.2: Review of position curves, velocity curves and phase plane diagrams for the system with $\beta=1/3$ , with $c_0=0,0015$ and $c_0=0,005$ , for increasing values of $a$ .	111
Table 7.3: Review of position curves, velocity curves and phase plane diagrams for the base-case system with $\beta=1/2$ , with varying nonlinear damping, for two values of linear, constant damping, $c_0=0,0015$ and $c_0=0,005$ .	112
Table 7.4: Review of position curves, velocity curves and phase plane diagrams for the system with $\beta=1,0$ , with $c_0=0,0015$ and $c_0=0,005$ , for increasing values of $a$ .	113
Table 7.5: Review of position curves, velocity curves and phase plane diagrams for the system with $\beta=3/2$ , with $c_0=0,0015$ and $c_0=0,005$ , for increasing values of $a$ .	114
Table 7.6: Review of position curves, velocity curves and phase plane diagrams for the system with $\beta=2,0$ , with $c_0=0,0015$ and $c_0=0,005$ , for increasing values of $a$ .	115
Table 8.1: Review of position curves, velocity curves and phase plane diagrams for the base-case system, for $c_0=0,0015$ and $c_0=0,005$ , and increasing values of $a$ .	117
Table 8.2: Review of position curves, velocity curves and phase plane diagrams for the system with $\beta=1/3$ , for $c_0=0,0015$ and $c_0=0,005$ , and increasing values of $a$ .	118
Table 8.3: Review of position curves, velocity curves and phase plane diagrams for the system with $\beta=1/2$ , for $c_0=0,0015$ and $c_0=0,005$ , and increasing values of $a$ .	119
Table 8.4: Review of position curves, velocity curves and phase plane diagrams for the system with $\beta=1,0$ , for $c_0=0,0015$ and $c_0=0,005$ , and increasing values of $a$ .	120
Table 8.5: Review of position curves, velocity curves and phase plane diagrams for the system with $\beta=3/2$ , for $c_0=0,0015$ and $c_0=0,005$ , and increasing values of $a$ .	121
Table 8.6: Review of position curves, velocity curves and phase plane diagrams for the system with $\beta=2,0$ , for $c_0=0,0015$ and $c_0=0,005$ , and increasing values of $a$ .	122
Table 9.1: Review of position curves, velocity curves and phase plane diagrams for the base-case system with the mass varied close to resonance, for two types of linear damping, $c=0,15$ and $c=0,5$ , for four different set of initial conditions.	136

# PART I

Part I of this thesis presents the preliminary considerations which were necessary to achieve part II.

Chapter 1 introduces differential equations and nonlinearity.

Second order linear differential equations are presented and investigated using the **phase plane method** in chapter 2. The book "*Nonlinear Differential Equations*" by Struble R.A and Martin W.T was a great reference for the preparation of this chapter.

Chapter 3 presents the forced oscillations in the phase plane and explain the concept of **limit cycles**.

In chapter 4, known nonlinear equations are presented. The Van der Pol's equation and the Pendulum equation are worked through, presenting the typical phase plane diagrams showing the behaviour they exhibit. Lastly in chapter 4, the Morison equation is presented, from where the **drag force** is used in the parameter studies in part II.

# Chapter 1 – Introduction

## 1.1 Differential equations in engineering

Differential equations are equations that involve the derivatives of some function. These equations describe the change in the system, and its solutions are functions themselves. The origin of differential equation is traced back to Isaac Newton's work written in 1671, and published in 1736 on what he called "fluxional equations." Newton classified three kinds of equations:

$$\frac{dy}{dx} = f(x) \quad (1.1)$$

$$\frac{dy}{dx} = f(x, y) \quad (1.2)$$

$$x_1 \frac{\partial y}{\partial x_1} + x_2 \frac{\partial y}{\partial x_2} = y \quad (1.3)$$

The first two equations, (1.1) and (1.2), are classified as ordinary differential equations, while the last equation, (1.3) is a partial differential equation. Newton used a different notation, using dots for the derivative. These equations are written in the modern notation, by Leibniz, which also introduced the term "differential equations" in 1680. The Bernoulli brothers and others further studied the work of Leibniz. The application of the theory has stretched from first being mostly towards geometry and mechanics, to involving all fields of science and engineering, such as astronomy, electricity, magnetism, quantum mathematics, dynamical systems, and relativity theory. [1]

## 1.2 Ordinary differential equations

Differential equations can be divided into ordinary and partial differential equations. Ordinary Differential Equations, (ODEs) contain only one independent variable. Partial differential equations contain two or more independent variables. Example of an ODE is the following which has x as its independent variable:

$$\frac{dy}{dx} = f(x) \quad (1.4)$$

specifying the slope of a graph,  $y(x)$ . Another example is the equation with variable t, describing a function that varies with time (t):

$$m \frac{d^2y}{dt^2} = f(t) \quad (1.5)$$

(1.5) is Newton's second law of motion  $F=ma$ . The heat equation, describing the variation of heatflux is an example of a partial differential equations, where  $h(x,t)$  are the independent variables; position( $x$ ) and time( $t$ ):

$$\frac{\partial h}{\partial t} = k \frac{\partial^2 h}{\partial x^2} \quad (1.6)$$

In this thesis, only ODEs will be considered.

The order of the differential equation is determined by the highest order derivative that occurs in the equation. The equation specifying the slope of a graph is of first order, while Newton's second law of motion is a second order ODE. An equation that occurs in the theory of fluid boundary layers is:

$$\frac{d^3 \phi}{dx^3} + \frac{1}{2} \phi \frac{d\phi}{dx} = 0 \quad (1.7)$$

Which is a third order ODE as it contains the third derivative for  $\phi(x)$ . [2]. Furthermore, it is a nonlinear equation as it contains the nonlinear term  $\phi \frac{d\phi}{dx}$ .

### 1.2.1 Linear and nonlinear systems

A nonlinear system is a system that is not linear. It is a set of equations that do not follow the superposition principle. The superposition principle consists of the additivity and homogeneity properties:

$$F(x_1 + x_2) = F(x_1) + F(x_2) \quad \textit{Additivity} \quad (1.8)$$

$$F(ax) = aF(x) \quad \textit{Homogeneity} \quad (1.9)$$

The superposition principle states that the response caused by several inputs is the same as the sum of the response from each input separately.

Linear systems are possible to solve to find an explicit solution. Nonlinear systems cannot be solved explicitly except from some special cases. An ODE for  $y(t)$  of the  $n^{\text{th}}$  order is said to be linear if it can be written as:

$$a_n(t) \frac{d^n y}{dt^n} + a_{n-1}(t) \frac{d^{n-1} y}{dt^{n-1}} + \dots + a_1(t) \frac{dy}{dt} + a_0(t)y = f(t) \quad (1.10)$$

where only  $y$  and derivatives of  $y$  occur. If  $f(t)=0$  the equation is said to be homogenous. If  $f(t) \neq 0$  the equation is inhomogenous. [2]

## 1.2.2 Nonlinear dynamical systems

A dynamical system is a system that can be described by how all points of the system evolve with time. What happens to the system over time is described by a mathematical rule, typically a differential equation for continuous time. The solution space can be presented as points of the position and the velocities of the system. The initial position tells us where the system is placed and using the mathematical rule we can identify the location of the system at all other times.

The nonlinear ODEs can rarely be solved analytically. Nonlinear systems may have no solutions to an initial value problem, or they may have an infinite number of solutions. Studying these systems evolve around finding certain properties of the solutions. Plotting the positions and velocities of the solutions over time gives us a trajectory, telling us how the system travels as time passes. These trajectories can be very useful in analysing how, or if the system will settle after some time. [3]

Examples of a nonlinear dynamical system are the Pendulum equation:

$$\frac{d^2\theta}{dt^2} + \frac{g}{l}\sin\theta = 0 \quad (1.11)$$

the van der Pol equation:

$$\frac{d^2x}{dt^2} - \mu(1 - x^2)\frac{dx}{dt} + x = 0 \quad (1.12)$$

and the Morison equation:

$$m\frac{d^2x}{dt^2} + c\frac{dx}{dt} + kx(t) = \rho C_m V \frac{du}{dt} + \frac{1}{2}\rho C_D A u |u| \quad (1.13)$$

All of which will be studied in chapter 4.

## 1.3 From linearity to nonlinearity

Classical science evolved around the concept of a linear world. Isaac Newton's laws of physics presented the universe as constant and static with time and space with linear variables having no beginning nor end. The realization that the world is very much nonlinear has by some been considered a new paradigm, while others have seen it as a natural evolution of the sciences. The classical thoughts grounded in Newtonian mechanics and Euclidian geometry began to be disputed in the late 19<sup>th</sup> century. Einstein and his theory of relativity in 1915 revealed that time and space are related and relative to the observer and that space-time is a dynamic non-Euclidean geometry. Heisenberg encountered obstacles to measurement which revealed the complex and dynamical patterns of the nature. Roger Penrose and Stephen Hawking's work implied that the universe had a specific beginning in space-time, overthrowing Newton's assumption. [4]

The invention of radio, laser, radar and computers in the 20<sup>th</sup> century made it crucial to look at the nonlinearity that occurred. Henri Poincaré pointed at problems regarding the linear description of the world in 1903. Edward Lorenz brought attention to dynamical systems in meteorology and published the first nonlinear phenomena mathematical model in 1963. [4]

## 1.4 Nonlinearity in engineering

The world consists of nonlinearity in most physical systems, across the different sciences. Linearization is a much used tool to be able to solve the system equation and predict what will occur at any time. Linearization is possible if the amplitude is small enough, so that higher order terms can almost be negligible. The following are some examples of nonlinearity in engineering, and illustrates the importance of studying nonlinearity.

The simplest example is to look at the bending of a branch. When the applied load is sufficiently small, the bending of the branch is approximately proportional to the applied force. But when increasing the load, the branch will at some point break. [5]

The most important nonlinearities in engineering are geometrical, physical and structural. The pendulum is an example of a geometrical nonlinearity. The linearization of the pendulum equation is based on the Taylor series:

$$\sin(\theta) = \theta - \frac{\theta^3}{3!} + \frac{\theta^5}{5!} - \dots \quad (1.14)$$

At small angles the pendulum equation can be linearized ( $\sin(\theta) \sim \theta$ ), as the  $\theta$  part is clearly dominating in the series. For larger oscillations or rotational motion the pendulum must be studied as a nonlinear equation as  $\theta$  is not the only part contributing in the series given by (1.14).

The stress-strain diagrams for steel and rubber are examples of physical or material nonlinearities. The stiffness of a system of springs illustrates structural nonlinearity as the stiffness will increase or decrease after a certain value of load or deflection is reached. Another source of nonlinearity is damping, which is very complex. Damping slows the system, normally through friction. [5]

# Chapter 2- Linear second order ordinary differential equation

Linear ordinary differential equations are possible to solve to find an explicit solution based only on the initial condition. The free response equation of motion will be studied in this chapter. The equation will involve only linear terms and the results for different damping cases will be presented. The trajectories in the phase plane will show what happens to the position and velocity of the system as time increases. **The method using the phase plane** was adapted from “*Nonlinear Differential Equations*” by Struble R.A and Martin W.T. [7]

The equation:

$$m \frac{d^2x}{dt^2} + c \frac{dx}{dt} + kx(t) = 0 \quad (2.1)$$

is a second order ordinary differential equation that describes a free response of a single degree of freedom system. The  $m$  represents the mass,  $c$  is the damping coefficient and  $k$  represents the stiffness of the system. It is known as an equation of motion as  $x(t)$  describes position, its first derivative describes velocity, and the second derivative gives the acceleration.

Introducing new variables for simpler equations:

$$\omega_0 = \sqrt{\frac{k}{m}} \quad (2.2)$$

$$\sigma = \frac{c}{m} \quad (2.3)$$

Substituting  $x(t)=Xe^{\lambda t}$  in (2.1) results in:

$$\lambda^2 X e^{\lambda t} + \sigma \lambda X e^{\lambda t} + \omega_0^2 X e^{\lambda t} = 0 \quad (2.4)$$

$$(\lambda^2 + \sigma \lambda + \omega_0^2) X e^{\lambda t} = 0 \quad (2.5)$$

Initial conditions are represented by:

$$x(0) = d_0 \quad (2.6)$$

$$\frac{dx}{dt}(0) = v_0 \quad (2.7)$$

which describe the initial displacement  $d_0$  and the initial velocity  $v_0$  at time  $t=0$ .

(2.5) is satisfied trivially when  $X=0$  and the non-trivial solution is the quadric equation

$$\lambda^2 + \sigma\lambda + \omega_0^2 = 0 \quad (2.8)$$

with roots

$$\lambda_{1,2} = -\frac{\sigma}{2} \pm \sqrt{\left(\frac{\sigma}{2}\right)^2 - \omega_0^2} \quad (2.9)$$

The quadratic roots (2.9) are affected by the amount of damping,  $c$ . In this chapter four cases of damping will be presented: no damping, underdamping, overdamping and critical damping. Lastly, phase diagram for a system with negative stiffness will be presented.

We are also introducing a new variable for the description of the velocity:

$$y(t) = \frac{dx}{dt} \quad (2.10)$$

## 2.1 Case 1- System without damping

$$\left(\frac{\sigma}{2}\right)^2 = 0 \quad (2.11)$$

When  $\left(\frac{\sigma}{2}\right)^2 = 0$  the system has no damping, and the system will oscillate freely.

The roots (2.9) become imaginary:

$$\lambda_{1,2} = \pm \sqrt{-\omega_0^2} = \pm i\omega_0 \quad (2.12)$$

where  $\omega_n$  is called the natural frequency of the system and the system will oscillate freely around this frequency as shown in figure 2.1.

### 2.1.1 Free response

The solution of (2.1) becomes:

$$x(t) = a\cos(\omega_0 t) + b\sin(\omega_0 t) \quad (2.13)$$

where  $a$  and  $b$  depend on the initial conditions (2.6) and (2.7). Applying initial conditions gives the solution:

$$x(t) = d_0 \cos(\omega_0 t) + \frac{v_0}{\omega_0} \sin(\omega_0 t) \quad (2.14)$$



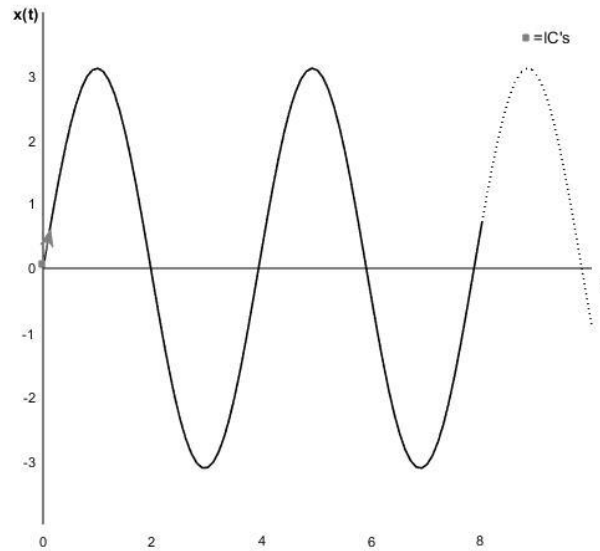


Figure 2.1: Free response without damping.

Figure 2.1 shows that the free response without damping of the system will be a sinusoidal response. The initial position,  $d_0$ , is set to 0, and the starting point when  $t=0$  is indicated by the arrow.

### 2.1.2 Phase plane diagram

The velocity (2.10) of an undamped system is:

$$y(t) = \frac{dx}{dt} = -a\omega_0 \sin(\omega_0 t) + b\omega_0 \cos(\omega_0 t) \quad (2.15)$$

with initial values (2.6) and (2.7):

$$y(t) = -d_0\omega_0 \sin(\omega_0 t) + v_0 \cos(\omega_0 t)$$

Plotting the position  $x$  and the velocity  $y$  gives us the trajectory in the phase plane. Figure 2.2 shows that the trajectory is an ellipse with centre in the origin,  $x=0$  and  $y=0$ .

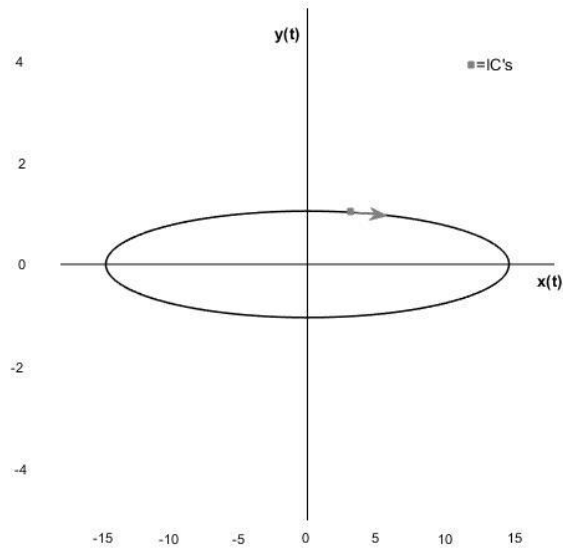


Figure 2.2: Trajectory in the phase plane of an unforced system without damping.

The origin is here called a center, as the trajectories neither move away or converge towards it. [6]

## 2.2 Case 2- Underdamped system

$$\left(\frac{\sigma}{2}\right)^2 < \omega_0^2 \quad (2.16)$$

When the damping rate is below the critical damping rate, the system is regarded as “underdamped”. The critical damping rate is given as:

$$c_c = 2m\omega_0 \quad (2.17)$$

Underdamped systems will oscillate freely from the initial displacement and velocity. The roots become imaginary. Introducing a new variable for the rooted part of (2.9):

$$\omega_d = \pm \sqrt{\left(\frac{\sigma}{2}\right)^2 - \omega_0^2} = \pm i\omega_0 \sqrt{1 - \frac{c}{c_c}} \quad (2.18)$$

### 2.2.1 Free response

(2.1) gives the solution of:

$$x(t) = e^{-\frac{\sigma}{2}t} (a \sin(\omega_d t) + b \cos(\omega_d t)) \quad (2.19)$$

Using initial conditions (2.6) and (2.7), the solution becomes:

$$x(t) = e^{-\frac{\sigma}{2}t} \left( \left( \frac{v_0}{\omega_d} + \frac{\sigma}{2\omega_d} d_0 \right) \sin(\omega_d t) + d_0 \cos(\omega_d t) \right) \quad (2.20)$$

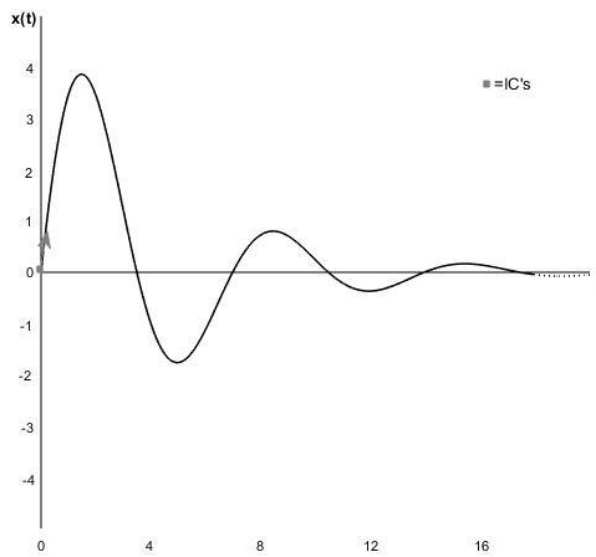


Figure 2.3: Free response of an underdamped system.

Figure 2.3 shows the free response of an underdamped system and is of the same form as figure 2.2, but with decreasing oscillations due to the damping. At  $t=0$ , we set  $d_0=0$ .

### 2.2.2 Phase plane diagram

Recognizing that:

$$x(t) = e^{-\frac{\sigma}{2}t} (a \sin(\omega_d t) + b \cos(\omega_d t)) = A e^{-\frac{\sigma}{2}t} \sin(\omega_d t + \phi) \quad (2.21)$$

for arbitrary  $A$  and  $\phi$ , we get a velocity function (2.10):

$$y(t) = \frac{dx}{dt} = -\frac{\sigma}{2} A e^{-\frac{\sigma}{2}t} \sin(\omega_d t + \phi) + A \omega_d e^{-\frac{\sigma}{2}t} \cos(\omega_d t + \phi) \quad (2.22)$$

Introducing new dependent variables:

$$u(t) = \omega_d x(t) = A\omega_d e^{-\frac{\sigma}{2}t} \sin(\omega_d t + \varphi) \quad (2.23)$$

$$v(t) = y(t) + \frac{\sigma}{2}x(t) = A\omega_d e^{-\frac{\sigma}{2}t} \cos(\omega_d t + \varphi) \quad (2.24)$$

Where equations (2.23) and (2.24) represent a spiral as shown in Figure 2.4. [7]

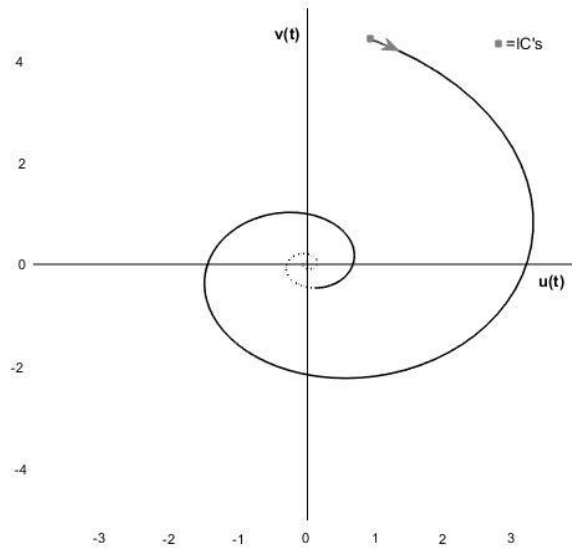


Figure 2.4: Trajectories in the  $uv$ -plane of an underdamped, unforced system.

Going back to the  $xy$ -plane by using (2.23) and (2.24):

$$x(t) = \frac{u(t)}{\omega_d} \quad (2.25)$$

$$y(t) = v(t) - \frac{u(t)\sigma}{2\omega_d} \quad (2.26)$$

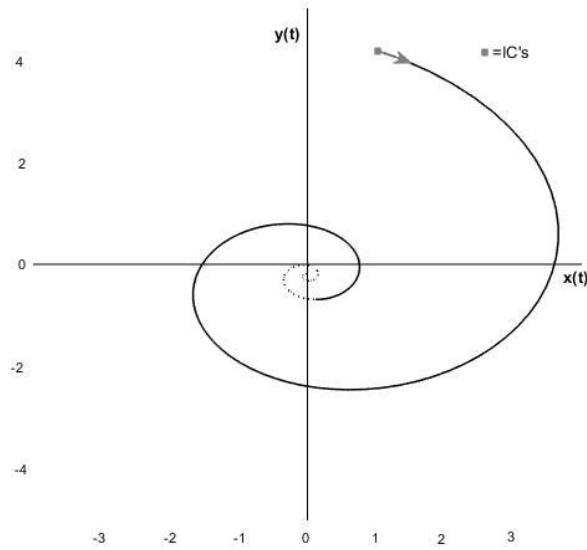


Figure 2.5: Trajectories in the phase plane of an underdamped, unforced system.

The origin is called a spiral point. When the damping coefficient  $c$  is positive, the spiral goes toward this point as time increases, as shown in figure 2.4. If  $c < 0$ , the spiral will spiral away from the point [6]. The spiral in figure 2.5 shows a distorted spiral in the phase plane. The dotted line shows how the figures will continue to spiral if time is increased.

### 2.3 Case 3- Overdamped system

$$\left(\frac{\sigma}{2}\right)^2 > \omega_0^2 \quad (2.27)$$

When  $c > c_c$ , where  $c_c$  is defined in equation (2.17), the system is “overdamped”.

#### 2.3.1 Free response

The overdamped system will not oscillate freely and the solution of equation (2.1) becomes:

$$x(t) = ae^{\lambda_1 t} + be^{\lambda_2 t} \quad (2.28)$$

where  $a$  and  $b$  again are determined from the initial conditions from equations (2.6) and (2.7), and the solution becomes:

$$x(t) = \left( \frac{d_0 \lambda_2 - v_0}{\lambda_2 - \lambda_1} \right) e^{\lambda_1 t} + \left( \frac{v_0 - d_0 \lambda_1}{\lambda_2 - \lambda_1} \right) e^{\lambda_2 t} \quad (2.29)$$

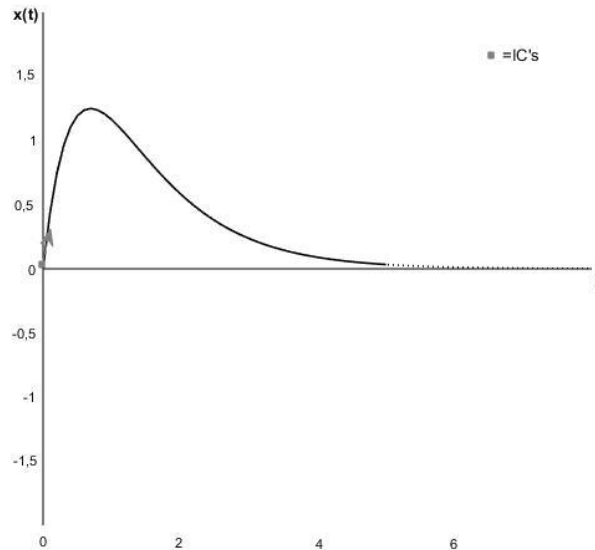


Figure 2.6: Free response of an overdamped system.

Figure 2.6 shows the free response of the overdamped system. The initial position  $d_0=0$  is chosen, and the starting point is indicated by the arrow. The figure shows that the system goes to zero position without oscillation.

### 2.3.2 Phase plane diagram

Rewriting the equation (2.1) by using the expression for velocity (2.10) we get:

$$\frac{d^2 x}{dt^2} = \frac{dy}{dt} = -\frac{k}{m} x(t) - \frac{c}{m} y(t) = -\omega_0^2 x(t) - \sigma y(t) \quad (2.30)$$

Seeking a system of the form:

$$\frac{du}{dt} = \alpha_1 u(t) \quad (2.31)$$

$$\frac{dv}{dt} = \alpha_2 v(t) \quad (2.32)$$

By applying linear transformation of the form:

$$u(t) = b_{11} x(t) + b_{12} y(t) \quad (2.33)$$

$$v(t) = b_{21}x(t) + b_{22}y(t) \quad (2.34)$$

where  $x(t)$  can be expressed as (2.10) and  $y(t)$  as (2.30).

The following is obtained:

$$b_{11}y(t) + b_{12}(-\omega_0^2x(t) - \sigma y(t)) = \alpha_1(b_{11}x(t) + b_{12}y(t)) \quad (2.35)$$

$$b_{21}y(t) + b_{22}(-\omega_0^2x(t) - \sigma y(t)) = \alpha_2(b_{21}x(t) + b_{22}y(t)) \quad (2.36)$$

For these equations to hold identically in  $x$  and  $y$ , each of the total coefficients of  $x(t)$  and  $y(t)$  must disappear.[7]

Considering the sets of equations:

$$-\omega_0^2b_{12} = \alpha_1b_{11} \quad (2.37)$$

$$b_{11} - \sigma b_{12} = \alpha_1b_{12} \quad (2.38)$$

Will give:

$$\frac{b_{12}}{b_{11}} = -\frac{\alpha_1}{\omega_0^2} \quad (2.39)$$

$$1 + \frac{\alpha_1\sigma}{\omega_0^2} = -\frac{\alpha_1^2}{\omega_0^2} \quad (2.40)$$

and

$$-\omega_0^2b_{22} = \alpha_2b_{21} \quad (2.41)$$

$$b_{21} - \sigma b_{22} = \alpha_2b_{22} \quad (2.42)$$

giving:

$$\frac{b_{22}}{b_{21}} = -\frac{\alpha_2}{\omega_0^2} \quad (2.43)$$

$$1 + \frac{\alpha_2\sigma}{\omega_0^2} = -\frac{\alpha_2^2}{\omega_0^2} \quad (2.44)$$

Recognizing that equations (2.40) and (2.44) yield the characteristic equation,  $\alpha_1$  and  $\alpha_2$  become roots,  $\lambda_1$  and  $\lambda_2$ . Setting  $b_{11}=b_{21}=\omega_0^2$  gives the desired transformation (2.33) and (2.34):

$$u(t) = \omega_0^2x(t) - \lambda_1y(t) \quad (2.45)$$

$$v(t) = \omega_0^2x(t) - \lambda_2y(t) \quad (2.46)$$

Noting that the determinant:

$$\begin{vmatrix} \omega_0^2 & -\lambda_1 \\ \omega_0^2 & -\lambda_2 \end{vmatrix} = \omega_0^2(\lambda_1 - \lambda_2) \quad (2.47)$$

is different from zero, since  $\lambda_1 \neq \lambda_2$ . This makes (2.45) and (2.46) nonsingular. [7]

The solutions become:

$$u(t) = u_0 e^{\lambda_1 t} \quad (2.48)$$

$$v(t) = v_0 e^{\lambda_2 t} \quad (2.49)$$

where the pair  $u_0$  and  $v_0$  represents the initial condition (IC). Figure 2.7 shows the trajectories for different IC's, marked by starting points. The arrows show that all trajectories tend towards the origin as time increases.

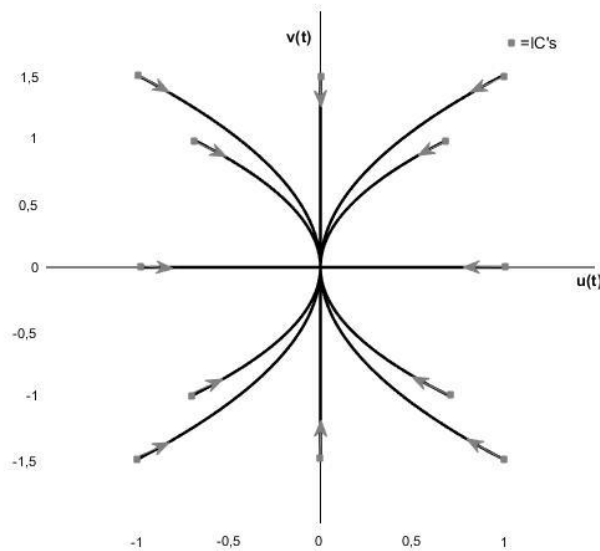


Figure 2.7: Trajectories in the  $uv$ -plane of an overdamped, unforced system.

Going back to  $x$  and  $y$  by using (2.45) and (2.46):

$$x(t) = \frac{u(t)}{\omega_0^2} + \frac{\lambda_1(v(t) - u(t))}{\lambda_1 - \lambda_2} \quad (2.50)$$

$$y(t) = \frac{v(t) - u(t)}{\lambda_1 - \lambda_2} \quad (2.51)$$



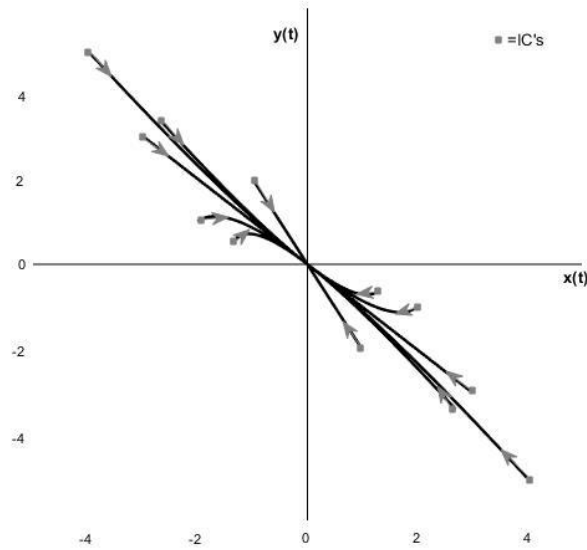


Figure 2.8: Trajectories in the phase plane of an overdamped, unforced system.

The trajectories in the phase-plane are given in figure 2.8. They are similar to those in the  $uv$ -plane, but appear rotated and stretched. The arrows in figures 2.7 and 2.8 indicate the starting position when  $t=0$ . The origin is called a node, and the trajectories converge to the point when the roots are negative as shown in figures 2.7 and 2.8. If the roots were both positive, the trajectories would move away from the origin. [6]

## 2.4 Case 4- Critically damped system

$$\left(\frac{\sigma}{2}\right)^2 = \omega_0^2 \quad (2.52)$$

When  $c=c_c$  the system is described as “critically damped” and will not oscillate freely.

The quadratic equation (2.8) gets the roots:

$$\lambda_{1,2} = -\frac{\sigma}{2} \pm \sqrt{\left(\frac{\sigma}{2}\right)^2 - \omega_0^2} = -\omega_0 = -\frac{\sigma}{2} \quad (2.53)$$

### 2.4.1 Free response

The roots are equal and the solution of equation (2.1) becomes:

$$x(t) = ae^{-\omega_0 t} + bte^{-\omega_0 t} \quad (2.54)$$

where the constants  $a$  and  $b$  are determined from the initial conditions (2.6) and (2.7). Applying initial conditions gives solution:

$$x(t) = d_0 e^{-\omega_0 t} + (v_0 + \omega_0 d_0) t e^{-\omega_0 t} \quad (2.55)$$

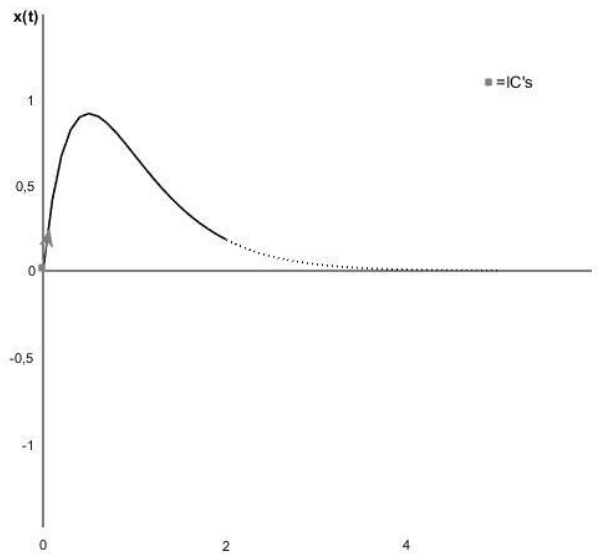


Figure 2.9: Free response of a critically damped system

The response of a critically damped system shown in figure 2.9 is as figure 2.6 of the overdamped system. The only difference is that it reaches zero earlier. The initial condition  $d_0$  is set to 0 when  $t=0$ .

### 2.4.2 Phase plane diagram

In case of critical damping, the characteristic roots (2.53) are equal and the equations cannot be completely uncoupled. There is a need to find a linear transformation (2.33) and (2.34) to make one of the equations independent of the other. Using equation (2.45), and a second arbitrary equation independent of the first [7]:

$$u(t) = \omega_0^2 x(t) - \lambda_1 y(t) = \left(\frac{\sigma}{2}\right)^2 x(t) + \frac{\sigma}{2} y(t) \quad (2.56)$$

$$v(t) = \frac{\sigma}{2} x(t) \quad (2.57)$$

By using equations (2.56) and (2.57), the derivatives become:

$$\begin{aligned}\frac{du}{dt} &= \left(\frac{\sigma}{2}\right)^2 \frac{dx}{dt} + \frac{\sigma}{2} \frac{dy}{dt} = \left(\frac{\sigma}{2}\right)^2 y(t) + \frac{\sigma}{2} (-\omega_0^2 x(t) - \sigma y(t)) \\ &= -\frac{\sigma}{2} \left( \left(\frac{\sigma}{2}\right)^2 x(t) + \frac{\sigma}{2} y(t) \right) = -\frac{\sigma}{2} u(t)\end{aligned}\quad (2.58)$$

$$\frac{dv}{dt} = \frac{\sigma}{2} \frac{dx}{dt} = \frac{\sigma}{2} y(t) = u(t) - \left(\frac{\sigma}{2}\right)^2 x(t) = u(t) - \frac{\sigma}{2} v(t)\quad (2.59)$$

Making:

$$u(t) = u_0 e^{-\frac{\sigma}{2}t}\quad (2.60)$$

where  $u_0$  depends on initial conditions.

(2.60) in (2.59) gives:

$$\frac{dv}{dt} = u_0 e^{-\frac{\sigma}{2}t} - \frac{\sigma}{2} v(t)\quad (2.61)$$

Giving the solution of  $v$ :

$$v(t) = u_0 t e^{-\frac{\sigma}{2}t} + v_0 e^{-\frac{\sigma}{2}t}\quad (2.62)$$

where also  $v_0$  depends on initial conditions.

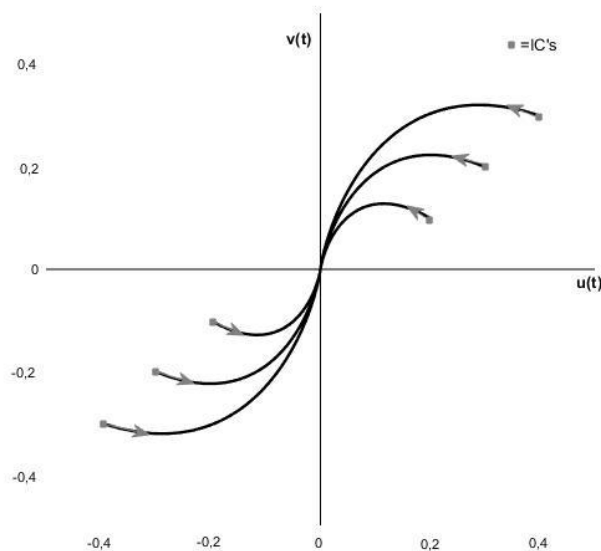


Figure 2.10: Trajectories in the  $uv$ -plane of a critically damped, unforced system.

By using equations (2.56) and (2.57) we obtain expressions for  $x(t)$  and  $y(t)$ :

$$x(t) = \frac{2}{\sigma} v(t) \quad (2.63)$$

$$y(t) = \frac{2}{\sigma} u(t) - v(t) \quad (2.64)$$

Plotting these expressions gives the trajectories in the phase-plane shown in figure 2.11. The linear transformations appears to involve rotation, stretching and reflection. [7]

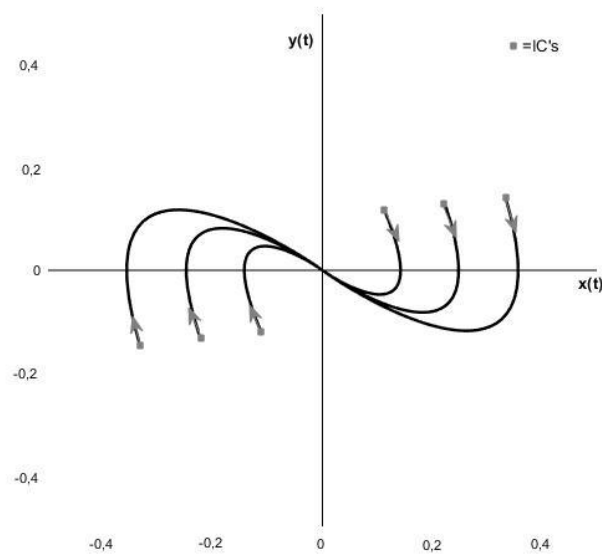


Figure 2.11: Trajectories in the phase plane of a critically damped, unforced system.

The origin is here called an improper node. All trajectories converge to this point when the root is negative, as shown in figure 2.10 and 2.11. If the root was positive, the trajectories would move away from the point. [6]

## 2.5 Case 5- Negative stiffness

$$k < 0$$

When  $k < 0$ ,  $\omega_0^2 < 0$ , leading to an overdamped case. The solution is (2.48) and (2.49), with one root negative and the other positive. Figure 2.12 shows the trajectories in the  $uv$ -plane. Figure 2.13 shows the trajectories in the phase plane, obtained by using (2.50) and (2.51). [7]

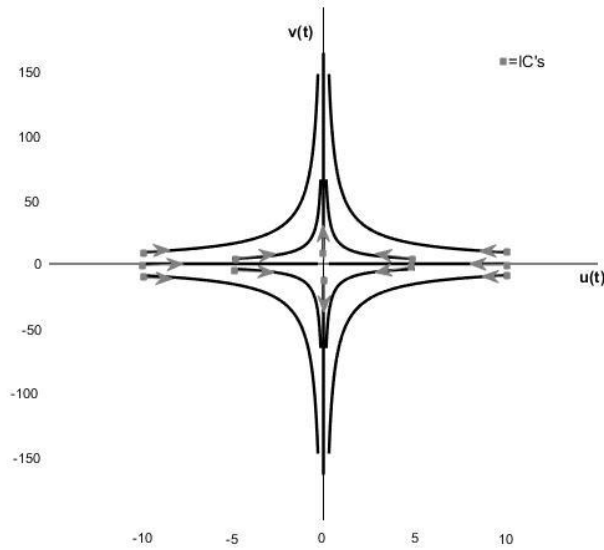


Figure 2.12: Trajectories in the  $uv$ -plane for an overdamped, unforced system with negative stiffness.

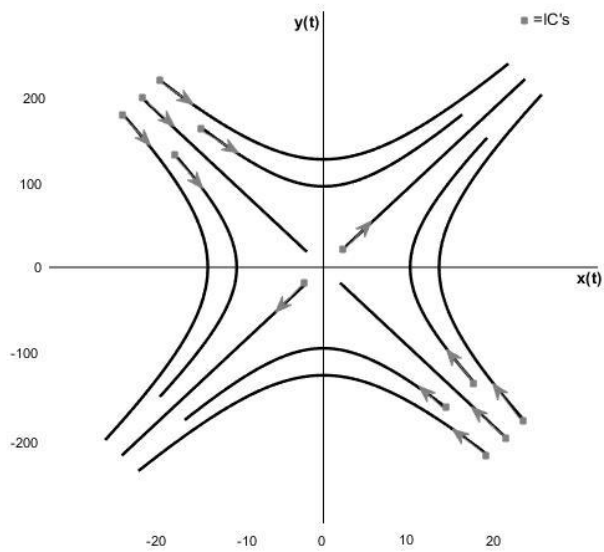


Figure 2.13: Trajectories in the phase plane for an overdamped, unforced system with negative stiffness.

Figures 2.12 and 2.13 both have the origin as a saddle point. A saddle point is a critical point where the trajectories of the negative eigenvalue goes towards the critical point, while the trajectories of the positive eigenvalue moves away from the point. All other trajectories starting away from the point, go towards, but never reach the point, before moving away from the point. [6]

Usually, for elastic systems, the stiffness is positive. When a system has positive stiffness, it experiences force in the same direction as the deformation of the system. Systems with negative stiffness contain stored energy leading to larger damping. Examples of systems with negative stiffness are pre-strained objects including post-buckled elements. [8]

# Chapter 3 – Forced oscillations and limit cycles

## 3.1 Forced oscillations

When the equation of motion (2.1) has a forcing term added, it is called an equation for forced oscillations:

$$m \frac{d^2 x}{dt^2} + c \frac{dx}{dt} + kx(t) = F(t) \quad (3.1)$$

The loading may be harmonic or some arbitrary type of loading. As the harmonic loading case is relevant for waves, this type will be presented here. The loading is given as:

$$F(t) = F_0 \sin(\omega t) \quad (3.2)$$

It should be noted that all load functions can be given as sums of harmonic loading through Fourier expansion of the loads time history.

### 3.1.1 Forced response

The solution of (3.1) consists of two parts, called the “homogenous solution”,  $x_h$ , and the “particular solution”,  $x_p$ . The homogenous solution is (2.20), that of the unforced one. It is also called the “transient solution”, and will as time increases be damped out.

$$x_h(t) = e^{-\frac{\sigma}{2}t} \left( \left( \frac{v_0}{\omega_d} + \frac{\sigma}{2\omega_d} d_0 \right) \sin(\omega_d t) + d_0 \cos(\omega_d t) \right) \quad (3.3)$$

The particular solution will be of the form:

$$x_p(t) = a \sin(\omega t - \theta) \quad (3.4)$$

where  $a$  is the amplitude of the system,  $\omega$  is the loading frequency of the system and  $\theta$  represents the phase difference between the resultant motion and the driving force. Introducing a new variable:

$$A = \frac{F_0}{m} \quad (3.5)$$

Derivation of (3.4) in (3.2), and expansion of the sine and cosines terms gives:

$$\begin{aligned} & \sin(\omega t)(A + a((\omega^2 - \omega_0^2) \cos(\theta) - \sigma\omega \sin(\theta))) \\ & + \cos(\omega t)(a((\omega_0^2 - \omega^2) \sin(\theta) - \sigma\omega \cos(\theta))) = 0 \end{aligned} \quad (3.6)$$

Sine and cosine of the same angle are linearly independent; making (3.6) only satisfied in general if the coefficients of those terms vanish.

From the  $\cos(\omega t)$  coefficient we get:

$$\tan(\theta) = \frac{\sigma\omega}{\omega_0^2 - \omega^2} \quad (3.7)$$

Which further leads to the expressions:

$$\sin(\theta) = \frac{\omega_0^2 - \omega^2}{\sqrt{\sigma^2\omega^2 + (\omega_0^2 - \omega^2)^2}} \quad (3.8)$$

$$\cos(\theta) = \frac{\sigma\omega}{\sqrt{\sigma^2\omega^2 + (\omega_0^2 - \omega^2)^2}} \quad (3.9)$$

From the  $\sin(\omega t)$  coefficient we get:

$$a = \frac{A}{\sqrt{(\omega_0^2 - \omega^2)^2 + \sigma^2\omega^2}} \quad (3.10)$$

Using (3.10) in (3.4) gives an expression for the particular solution:

$$x_p(t) = \frac{A}{\sqrt{(\omega_0^2 - \omega^2)^2 + \sigma^2\omega^2}} \sin(\omega t - \theta) \quad (3.11)$$

where from (3.7) we have that:

$$\theta = \tan^{-1} \frac{\sigma\omega}{\omega_0^2 - \omega^2} \quad (3.12)$$

The full calculation of the resulting equations (3.4)-(3.12) is given in Appendix B.

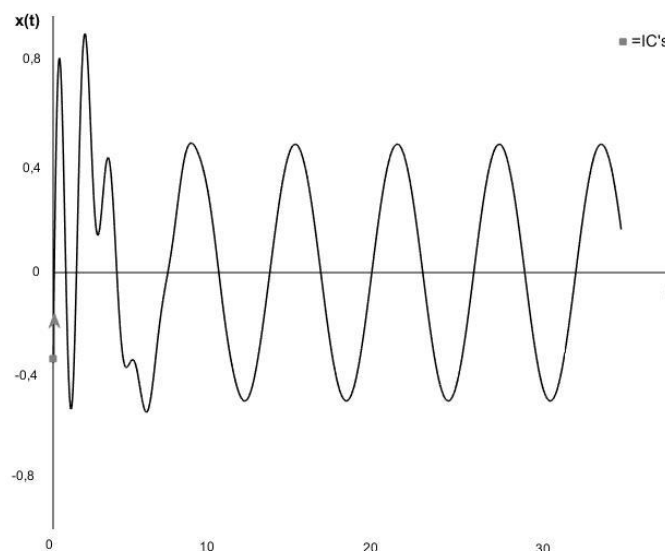


Figure 3.1: Response of a forced damped system, note the initial transient motion caused by the initial conditions for displacement and velocity.

Figure 3.1 shows the full response of the forced equation of motion as a sum of the homogenous solution (3.3) and the particular solution (3.4). The homogenous solution will be damped out as time

increases, leaving only the particular solution which is a sinusoidal wave. From this, we see that the particular solution gives the steady state solution, the response the system will have after some time. This response does not depend on the initial condition. [9]

### 3.1.2 Resonance and phase curves

Figure 3.2 shows the resonance curves for different values of damping. When the damping rate is increased, the resonance frequency,  $\omega_d$ , is lowered. Resonance occurs when the loading frequency,  $\omega$ , is equal to the Eigen frequency,  $\omega_0$ , of the system. [10]

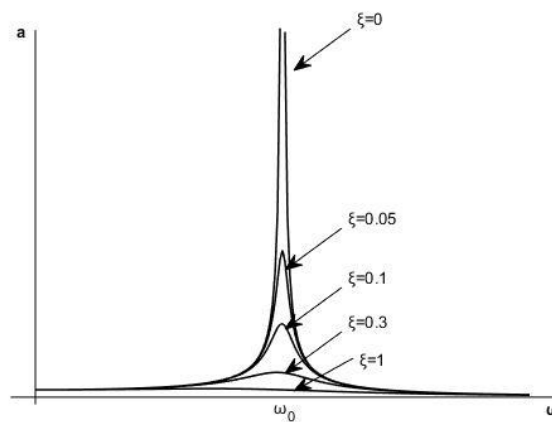


Figure 3.2: Resonance curves for different values of damping.

The quantity (3.12) represents the phase difference between the force and the motion as a result of the force. Keeping  $\omega_0$  fixed, figure 3.3 shows how the phase difference increases for different values of damping. For all values of damping the phase is 0 at  $\omega=0$ , increases to  $\frac{\pi}{2}$  at  $\omega= \omega_0$  and ends towards  $\pi$  when  $\omega$  increases. [9]



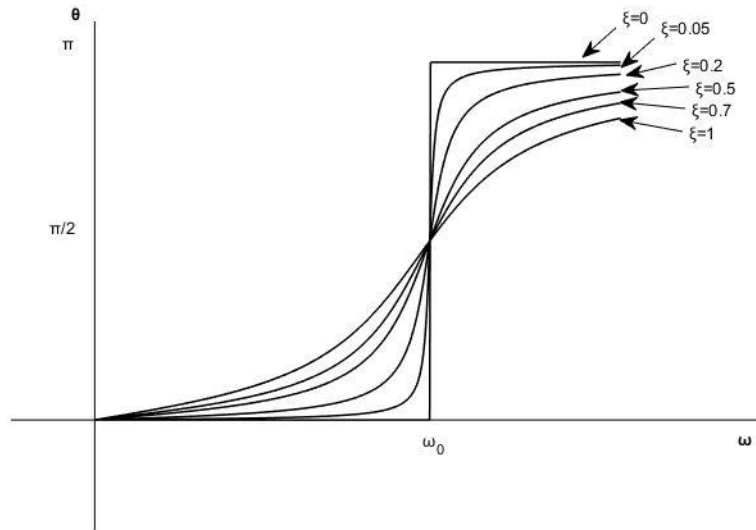


Figure 3.3: Phase curves for different values of damping.

From figures 3.2 and 3.3 we see that when the loading frequency is a lot less than the Eigen frequency of the system the motion is controlled by the stiffness of the system and is in phase with the loading. When the loading frequency is about the same as the system's Eigen frequency, the motion is controlled by damping and is out of phase with the loading. Loading frequencies larger than the systems' Eigen frequency leads to a mass controlled motion, in phase opposite to the loading. At this frequency, the mass or inertia force acts against the loading and thus reduces the response. [9]

### 3.1.3 Phase plane diagrams

In this part, we look at what happens in the phase plane when the equations from chapter 2 are subjected to a sinusoidal loading.

#### 3.1.3.1 No damping

A forced system with no damping can be described by the equation:

$$m \frac{d^2x}{dt^2} + kx(t) = F_0 \sin(\omega t) \quad (3.13)$$

When there is no damping, the phase plane of an unforced system is an ellipse as shown in figure 2.2. Figure 3.4 shows the phase plane for equation (3.13). The form of the trajectory is still an ellipse, but is now a wavy line due to the forcing term. The initial conditions are marked on the figure as well as the starting point. Different initial values will give the same ellipse but with different starting values. The mass and the stiffness coefficient will decide the shape of the ellipse. The force coefficient decides the amplitude and the frequency  $\omega$  decides the wavelength of the wavy line.

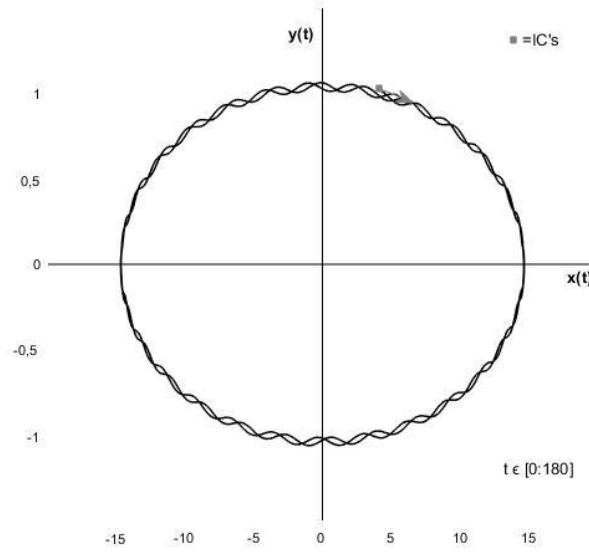


Figure 3.4: Phase diagram for an undamped forced system.

### 3.1.3.2 Underdamped system

In the case of the underdamped system, the trajectory in the phase plane is as a spiral going towards or away from the origin. Figure 2.5 shows the case of a positive damping coefficient, resulting in a trajectory spiralling towards the origin.

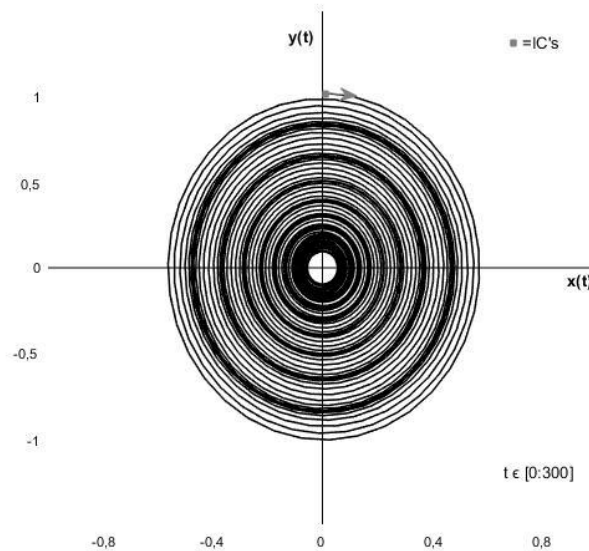


Figure 3.5: Phase diagram for an underdamped forced system.

The trajectory in the phase plane for an underdamped forced system will still spiral toward the origin, as shown in figure 3.5. Now, however, the trajectory seems to be spiralling into a circle in

which it continues a couple of revolutions before continuing to spiral towards the origin. New circles appear more and more closely as time increases.

### 3.1.3.3 Overdamped system

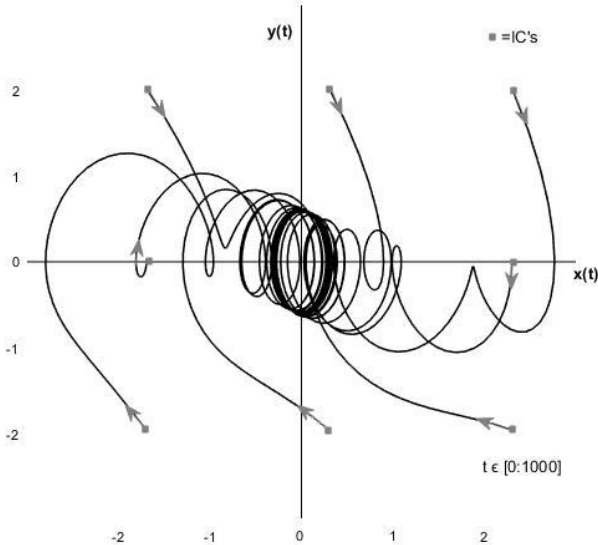


Figure 3.6: Trajectories in the phase plane for an overdamped forced system.

The trajectories in the phase plane for an overdamped forced system will spiral towards the origin making loops on their way. The trajectories do not reach the origin but end in one steady loop where they stay as time is increased. These loops are different for different initial conditions but lay close together as shown in figure 3.6. This means that different trajectories for different initial conditions will after some time end up similar.

### 3.1.3.4 Critically damped system

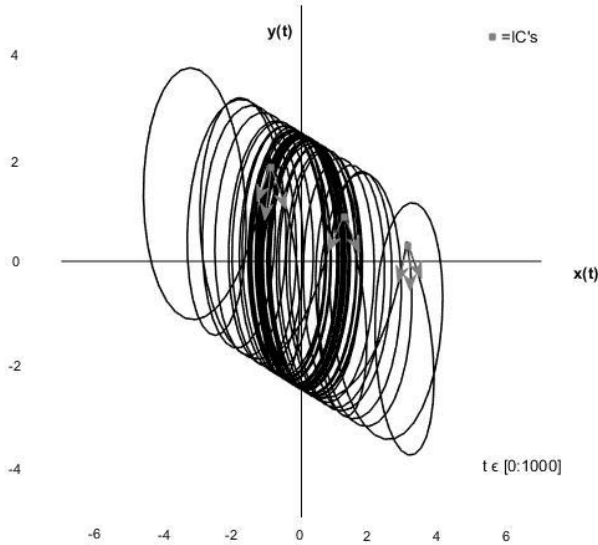


Figure 3.7: Trajectories in the phase plane for a critically damped forced system.

The trajectories in the phase plane for a critically damped forced system appears as a zoomed version of the underdamped one. The IC's and the time span are the same for figures 3.6 and 3.7. The trajectories go directly into loops for the critically damped system and loops continuously until reaching a steady loop around the origin. The amplitudes are as for the overdamped system.

### 3.2 Limit cycles

An isolated trajectory is called a limit cycle. Trajectories around a limit cycle spiral towards or away from the limit cycle, and are not closed. Limit cycles occur only in nonlinear systems. A linear system may have closed trajectories, as seen for the undamped case in figure 2.2, but the trajectories will be surrounded by other closed orbits. Limit cycles can be stable, half-stable or unstable as shown in figure 3.4. Stable limit cycles attract all near trajectories towards it. Unstable limit cycle will have near trajectories spiralling away from them. Half-stable limit cycles, where one trajectory spirals towards the limit cycle while another spirals away, are more uncommon. Stable limit cycles are important as they model systems with self-sustained oscillations. Examples of this phenomena are the beating of a heart or the self-excited vibrations in bridges and airplane wings. [11]

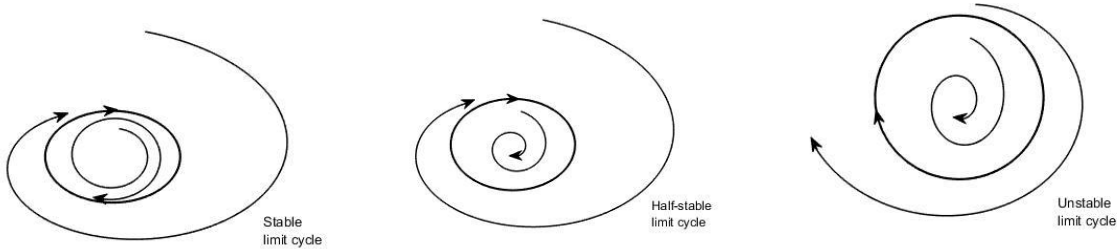


Figure 3.8: Stable, half-stable and unstable limit cycles.

# Chapter 4- One degree of freedom equations for known nonlinear systems

## 4.1 The van der Pol Equation

The unforced van der Pol equation is of the form:

$$\frac{d^2x}{dt^2} - \mu(1 - x^2) \frac{dx}{dt} + x = 0 \quad (4.1)$$

Balthazar van der Pol proposed the nonlinear equation (4.1) to describe the behaviour found in experiments with oscillations in a vacuum tube triode circuit. These vacuum tubes were used during the first half of the twentieth century to control the flow of electricity in the circuitry of transmitters and receivers. Van der Pol's work, alongside Lorentz, Thompson, and Appleton has had a significant impact in the fields of radio and telecommunications. [13]

Equation (4.1) is nonlinear as it contains the nonlinear multiplier  $(1-x^2)$  in the damping term. When  $\mu=0$ , the equation represents a simple harmonic oscillator. From the nonlinear term, we can observe that for  $|x| > 1$ , the system has ordinary damping, i.e. decaying oscillations. For  $|x| < 1$ , the system experiences **negative damping** which pumps energy into the system. This indicates that the system may settle into some oscillations of a given amplitude, a **limit cycle** where there is a balance between the generation and dissipation of energy. [12]. The value of  $\mu$  indicates the strength of nonlinearity in the system. For more about this see "Asymptotic methods in the theory of non-linear oscillations" by Bogoliubov N.N. and Mitropolsky Y.A. [21] from page 186.

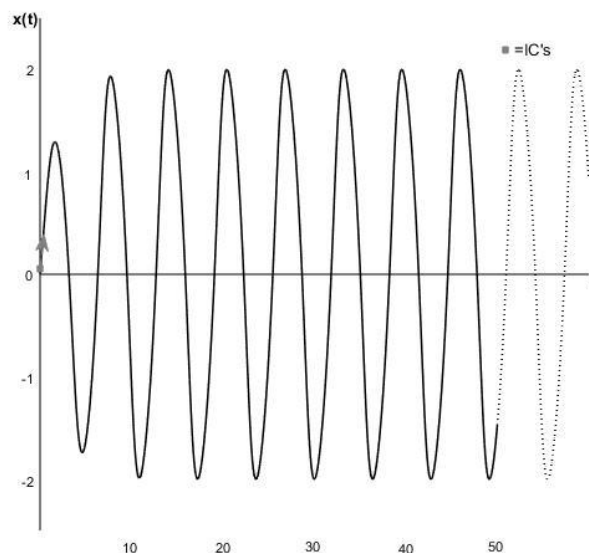


Figure 4.1: Free response of the unforced van der Pol Equation with  $\mu=0.5$ .

### 4.1.1 Free response

Figures 4.1-4.3, made from using a build in function for the van der Pol equation in Matlab shows the response of the equation (4.1) as a function of time for different values of  $\mu$ . Small values of  $\mu$  leads to a weakly nonlinear system and the response is close to that of a simple harmonic oscillator. Figure 4.1 shows the response for  $\mu=0.5$  with IC's of  $x=0$  and  $\frac{dx}{dt} = 1$  at  $t=0$ . The response is shown from  $t=0$  to  $t=60$ .

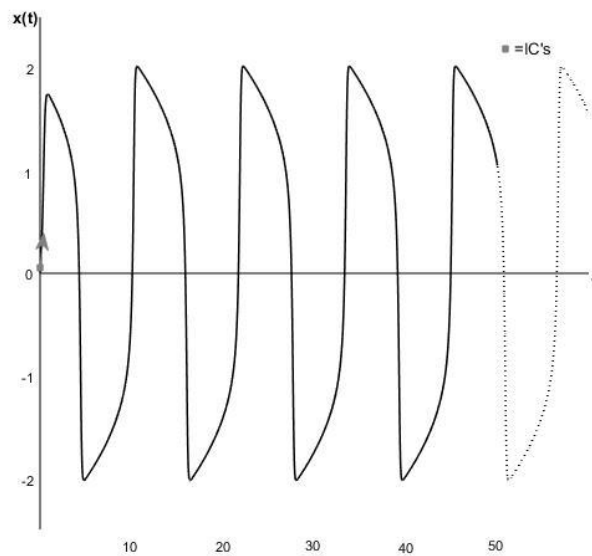


Figure 4.2: Free response of the unforced van der Pol Equation with  $\mu=5$ .

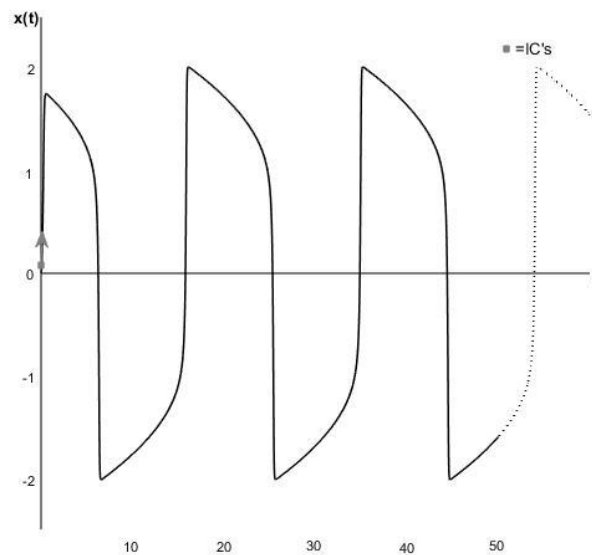


Figure 4.3: Free response of the unforced van der Pol Equation with  $\mu=10$ .

The response for a system with  $\mu=5$  is shown in figure 4.2. The system has a stronger nonlinearity than the one in figure 4.1 and we can see a shift in response for  $|x| = 1$ . The response decays slowly for  $x>1$  and reaches a faster shift at  $x=1$  to  $x=-2$ . From  $x=-2$  the system's amplitude slowly grows before another fast shift occurs at  $x=-1$  to  $x=2$ . The system continues this response with a steady amplitude of 2 as time increases. The IC's and duration of the system in figure 4.2 is the same as for the system in Figure 4.1

Figure 4.3 shows the response with  $\mu=10$  and the same IC's and duration as figures 4.1 and 4.2. This system is strongly nonlinear and the shift at  $|x| = 1$  is seen clearly. From figures 4.1-4.3 we see that larger values of  $\mu$  gives a stronger nonlinearity in a system and longer periods.

### 4.1.2 Phase plane diagram

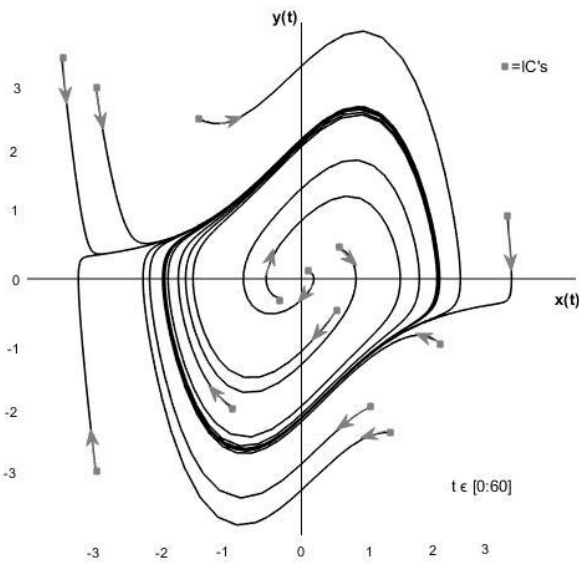


Figure 4.4: Phase plane diagram for the unforced van der Pol equation with  $\mu=1$ .

The phase plane diagram for the unforced van der Pol equation with  $\mu=1$  exhibits a clear limit cycle shown in figure 4.2. It is seen that all the trajectories, despite of their initial conditions, which are marked with squares on the figure, reach the limit cycle after some time. The limit cycle is stable as all near trajectories spiral towards it.

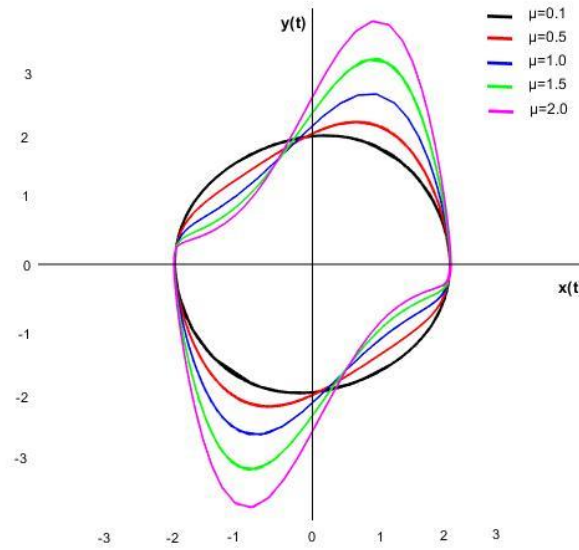


Figure 4.5: Limit cycles for the van der Pol equation with different values of  $\mu$ .

The system in equation (4.1) have different limit cycles for different values of  $\mu$ . The limit cycles start as a circle for  $\mu=0$  and become more sharp as  $\mu$  increases. Limit cycles for increasing values of  $\mu$  are shown in Figure 4.5. Limit cycles for  $\mu \gg 1$  are often called “relaxation oscillations” as they alternate between long relaxation periods and short fast shifts.

#### 4.1.3 Applications of the van der Pol equation

The limit cycles that appear in the phase plane for the van der Pol equation have been used in many difference sciences to describe systems with nonlinear behaviour.

Parkinson’s disease is a neurodegenerative disorder often characterized by tremors. The van der Pol equation have been proposed to model these tremors, since the limit cycles are not sinusoidal, but have flattened segments. [15]

The cell model used to model the gastric mill central pattern generator of the lobster uses a generalization and extension of the van der Pol equation. [16]

In the field of excitable media, the model of van der Pol, Fitz Hugh and Nagumo is used to describe the frictional sliding dynamics of a number of materials. [17]. Note that the term excitability originally referred to the property of living organisms (or of their constituent cells) to respond strongly to the action of a relatively weak external stimulus. [18]

It has been proposed further study on the forced Van der Pol’s equation:

$$\frac{d^2x}{dt^2} - \mu(1 - x^2) \frac{dx}{dt} + x = A \sin(\omega t) \quad (4.2)$$

by Cao W. in “Van der Pol Oscillator” [22].

This has been attempted by Wallace T.L. and Homer T.H in “Mathematical Model of Forced Van Der Pol’s Equation” [23].



## 4.2 The pendulum equation

The equation of motion for the pendulum is derived from Newton's Second Law of motion:

$$ma = F \quad (4.3)$$

Here  $m$  represents the mass of the system,  $a$  is the acceleration and  $F$  is the sum of forces working on the system. For the pendulum,  $m$  is the mass of the ball as the pendulum rod (with length  $l$ ) is seen as massless. As the rod is stiff, no motion is possible in the radial direction. The position of the pendulum from the resting position is dependent only on the angular displacement  $\theta$  and is  $l\theta$ . The acceleration is therefore described as:

$$a = l \frac{d^2\theta}{dt^2} \quad (4.4)$$

For an unforced, undamped pendulum the sum of forces is:

$$F = -mgsin\theta \quad (4.5)$$

Equations (4.3) and (4.4) with (4.5) gives:

$$ml \frac{d^2\theta}{dt^2} = -mgsin\theta \quad (4.6)$$

Which leads to the equation of motion for an undamped, unforced pendulum of:

$$\frac{d^2\theta}{dt^2} + \frac{g}{l} sin\theta = 0 \quad (4.7)$$

Where  $g$  represents the gravitational constant, which is acceleration due to gravity,  $l$  is the length of the pendulum and  $\theta$  represents the angular displacement from the stable equilibrium. Note the nonlinear term  $sin\theta$ .

### 4.2.1 Free response

The pendulum equation is often linearized using small angle approximation. For small angles, the dominating term in the Taylor series (1.14) is  $\theta$ , which can replace  $sin\theta$  in (4.9). Figure 4.6 shows the linear response in black line and the response for a nonlinear system in red. The top graphs represent a system with IC  $\theta(0) = \frac{\pi}{2}$ , while the lower graphs have IC of  $\theta(0) = \frac{\pi}{6}$ . All graphs have IC  $\frac{d\theta}{dt} = 0$  at  $t=0$  (no initial velocity). For the graph with a lower starting angle, the linear and nonlinear solutions match exactly from the start and become somewhat different as time increases. For even lower angles, the graphs will match even more. For the graphs starting at the larger angle the mismatch is clear from the start. The graph difference increases as time increases.

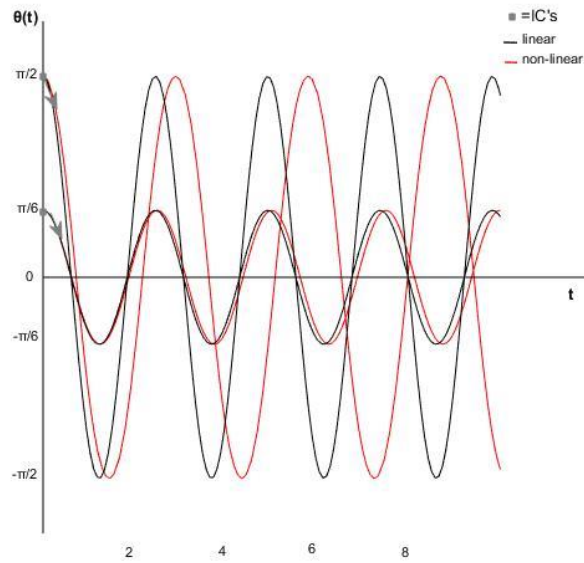


Figure 4.6: Angular response as a function of time for an undamped, unforced pendulum for both linear and non-linear systems.

#### 4.2.2 Phase plane diagram

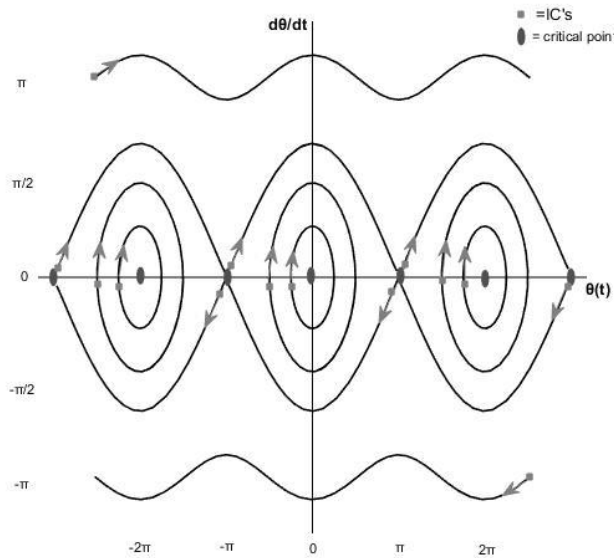


Figure 4.7: Phase plane diagram for the undamped, unforced pendulum equation.

The phase plane diagram for the undamped, unforced pendulum gives a picture of what happens with a pendulum and is shown in figure 4.7. Critical points, marked in the figure with a grey circle, are the vertical position  $\theta=0$  and the inverted vertical position  $\theta=\pi$ . The positions  $|\theta| = 2\pi$  is of course the same position as  $\theta=0$ . The pendulum motion cannot start at the critical point as with no velocity the pendulum would rest in either its vertical or inverted vertical position. The arrows in the figure represent the initial condition of the trajectory and indicate the direction in which the mass travels. When the pendulum has IC where  $\theta$  is close to the vertical position, it will swing around this position.

Releasing the pendulum from rest, near the inverted vertical position will increase its velocity until it reaches the vertical position. It will continue until it reaches the inverted vertical position, but the velocity will now decrease. Since the initial velocity is zero, the pendulum will only make one turn, reaching rest in the inverted vertical position. [14]

When the initial velocity of the pendulum is large, it will, without damping, continue to spin around indefinitely. The velocity will decrease from the vertical position but then increase on the way down from the inverted vertical position. This is shown by the wavy graphs on the top and bottom of figure 4.7. The top shows the pendulum going in the counter clockwise direction, and the bottom shows the clockwise direction. [14]

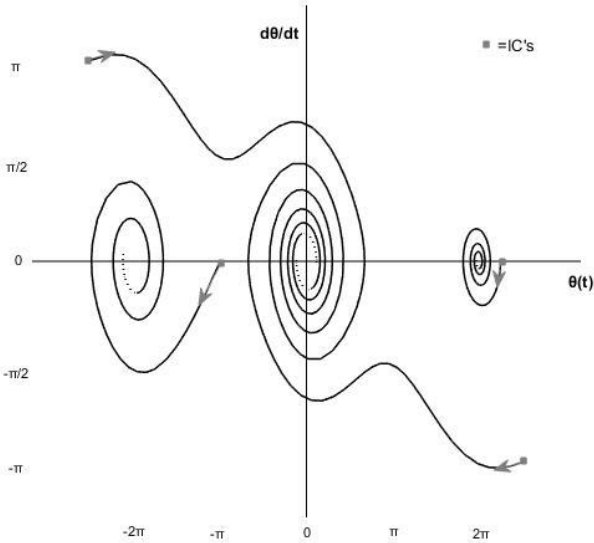


Figure 4.8: Phase plane diagram for the damped, unforced pendulum equation.

Normally there is always friction in a system, which makes the swinging of the pendulum decay and reach the resting position after some time. Figure 4.8 shows the phase plane for the same system as before, but with a damping coefficient added (linear damping). When the pendulum is released, now the velocity will decay no matter the initial velocity or displacement. The pendulum will not rest in the inverted vertical position. In the figure, each trajectory's end is marked with a dotted line indicating that it will continue to spiral towards the resting position and no velocity if time were increased.

## 4.5 The Morison Equation

The Morison Equation, which is used to describe the force on a cylinder in oscillatory flow is given by:

$$m \frac{d^2x}{dt^2} + c \frac{dx}{dt} + kx(t) = F(t) \quad (4.8)$$

The total force acting on the entire cylinder is given as:

$$F(t) = \int_{-d}^{surface} f(z, t) dz = \int_{-d}^{\alpha} f_M(z, t) dz + \int_{-d}^{\alpha} f_D(z, t) dz \quad (4.9)$$

Together the mass force and the **drag force** are assumed to be sufficient for the calculation of forces on a cylinder in waves, which gives the Morison formula describing a total force acting on a submerged cylinder per unit length:

$$f(z, t) = f_M + f_D = \rho \frac{\pi D^2}{4} \frac{du}{dt} C_M + \frac{1}{2} \rho C_D D u |u| \quad (4.10)$$

From experiments, see for example [10], it has been shown that an approximation for the drag force per unit length of a cylinder exposed to a uniform current is:

$$f_D = \frac{1}{2} \rho C_D D u |u| \quad (4.11)$$

where  $\rho$  is the density of the water,  $C_D$  is the drag coefficient,  $D$  is the diameter of the cylinder, and  $u$  is the horizontal water particle velocity. The force has the same sign as the flow direction, due to the absolute value of one of the velocity components. The drag force in the Morison equation is nonlinear, due to the square velocity force. The drag coefficient is determined from experiments and is a function of parameters such as the Reynolds number and the roughness of the cylinder's surface. The horizontal velocity varies normally with water depth, making the total drag force acting on the submerged cylinder to be:

$$F_D(t) = \int_{-d}^{surface} f_D(z, t) dz \quad (4.12)$$

The mass force acting on a submerged cylinder in constant accelerated flow per unit length is given as:

$$f_M = \rho \frac{\pi D^2}{4} \frac{du}{dt} C_M \quad (4.13)$$

where  $\rho$  is the fluid density,  $\frac{\rho \pi D^2}{4}$  is the mass of a unit length of the cylinder,  $\frac{du}{dt}$  is wave acceleration and  $C_M$  is the mass coefficient which is determined using wave tank experiments or computer software. The acceleration is as the velocity dependent on water depth, so the total mass force on the cylinder is:

$$F_M(t) = \int_{-d}^{surface} f_M(z, t) dz \quad (4.14)$$

The mass and drag coefficients  $C_M$  and  $C_D$  are derived from experiments, making the Morison equation empirical. The development of equation (4.9) is taken from “Marine Technology and Operation” written by O.T Gudmestad [10].

Equation (4.8) is also applicable for other types of geometries than a cylinder. The term  $\frac{\pi D^2}{4}$  is the cross-sectional area of the structure and  $D$  is the projected area of the structure and may be replaced with other formulas for the appropriate geometry. The Morison equation is used for regular waves that do not break. A regular wave in deep water does not break if the wave height divided on the wave length is smaller than 0.14. In addition, the diameter of the cylinder divided on the wave length needs to be smaller than 0.2 to ensure that the acceleration do not change too much over the diameter. The last requirement for the Morison equation is that the amplitude divided on the cylinder diameter should be smaller than 0.2 to ensure that the motion of the cylinder is not too big. [10]

The drag term will dominate for:

$$\frac{D}{H} < 0.1 \quad (4.15)$$

The mass term will dominate for:

$$0.5 < \frac{D}{H} < 1.0 \quad (4.16)$$

For values in between, both the mass and drag term will need to be calculated and the sum represents the total wave force.

# PART II

Part II of this thesis consist of a parameter study of an equation of motion with nonlinearity in either the forcing or the damping term.

Chapter 5 gives the presentation of what is termed the “base-case system”, which is an undamped system subjected to a **nonlinear forcing term** representing the **drag force** from the Morison equation. The parameters are varied separately to look at their effect on the system.

In chapter 6, linear, constant damping is added to the base-case system and some selected systems with varied parameters from chapter 5. The results are as expected, with decaying amplitudes due to the damping. The systems mass parameter is also varied to get system close to and at **resonance**. These systems have a behaviour similar to the results obtained from the van der Pol equation in chapter 4.

Chapter 7 and 8 looks at systems **nonlinear damping term**. In chapter 7, the homogenous base-case system is looked at, as well as systems with some degree of resonance. **Critical values of the nonlinear damping parameter** are found, where **negative damping** overtakes the systems. These critical values are different for different systems. In chapter 8, a linear forcing term is added. The results from this chapter show that the critical values of the nonlinear damping parameter are the same with force added. For chapter 7 and 8, only the tables are presented, while the presentation of each diagram is added as Appendix C and Appendix D respectively.

In chapter 9, **limit cycles** are found for the base-case system with linear, constant damping and **nonlinear forcing**. The limit cycles are found for systems with the mass parameter varied to make the systems have some degree of **resonance**. As the damping is linear and constant, and some trajectories with initial conditions inside the limit cycle increase their amplitudes, it is concluded that the **drag force** from the Morison equation will to some degree work as **negative damping**.

# Chapter 5- Nonlinear forcing term in the equation of motion without damping.

## 5.1 Nonlinear forcing term

The response and phase plane diagram of a forced second order linear equation of motion was showed in chapter 3. The forced equation of motion is expressed as:

$$m \frac{d^2x}{dt^2} + c \frac{dx}{dt} + kx(t) = F(t) \quad (5.1)$$

where  $F(t)$  in chapter 3 was equal to  $F_0 \sin(\omega t)$ . In this chapter, equation (5.1) will be studied with  $F(t)$  being a **nonlinear forcing term**. The equation studied here is given as:

$$m \frac{d^2x}{dt^2} + c \frac{dx}{dt} + kx(t) = F_0 \sin(\omega t) |\sin(\omega t)| \quad (5.2)$$

This forcing term represent the **drag force** in the Morison equation, described by equation (4.8). This is used for calculating wave and current loading on fixed offshore structures. Notice that the forcing term is representing a term proportional to the velocity squared, representing turbulent flow past a cylinder (an obstacle in the flow path).

A system of random variables is looked at, from where a base-case system is chosen. The values of the variables were chosen more or less at random as the aim with this chapter is to look at this system and evaluate the effect of each parameter. The parameters will, one by one, be varied to look at the response in the base-case system. It should be noted that physical systems always have some degree of damping, but for the sake of this analysis the systems will in this chapter be evaluated without damping, i.e.  $c=0$ . Other values of the variables could be chosen; however we would not expect large changes from the parameter studies conducted in this thesis.

## 5.2 Base-case system

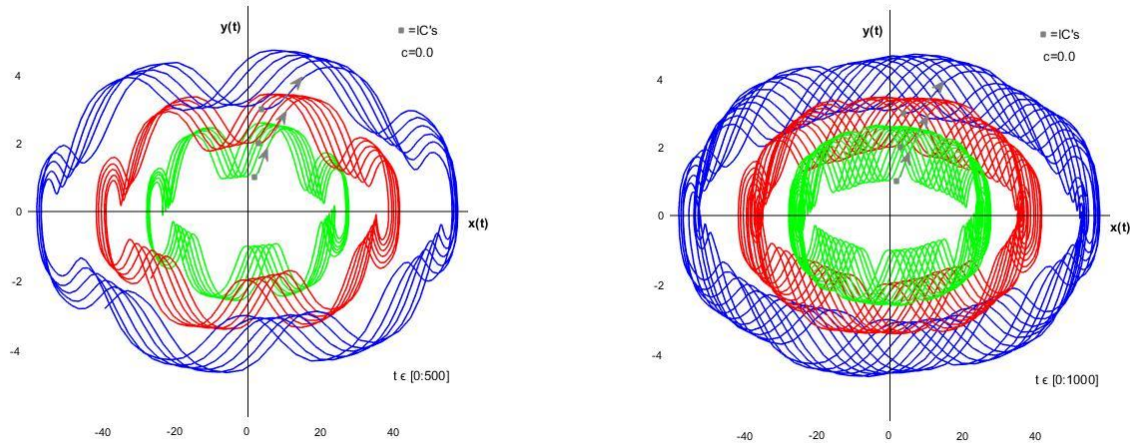


Figure 5.1: Typical phase plane diagrams for undamped systems with nonlinear force with different initial conditions (IC's) from  $t=0$  to  $t=500s$  (left) and  $t=1000s$  (right).

The trajectories in the phase plane shown in figure 5.1 have similar behaviour. The colour of the graph indicates the trajectory of one given set of initial conditions, IC's. IC's represent a measure of the starting conditions; IC=1 means that at  $t=0$  both the velocity and displacement are equal to 1.  $x(t)$  is the displacement while  $y(t)$  represents the velocity. The green trajectory has IC's of 1 for both position and velocity. The blue trajectory has IC's of 3 for position and velocity, while the red trajectory has IC's of 2 for position and velocity.

Figures 5.2 and 5.3 shows the position and velocity curves for the system respectively, with different initial conditions. The systems have equal periods of approximately 89s, and amplitudes of approximately 27, 41 and 55.

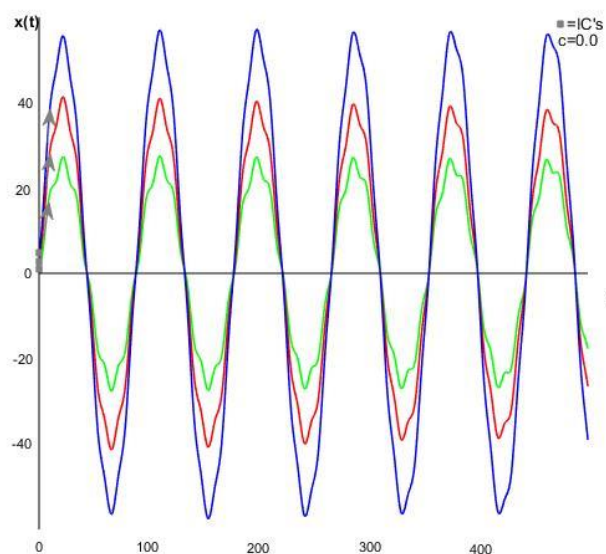


Figure 5.2: Position curves for systems with nonlinear force for different IC's, separated by different colours.



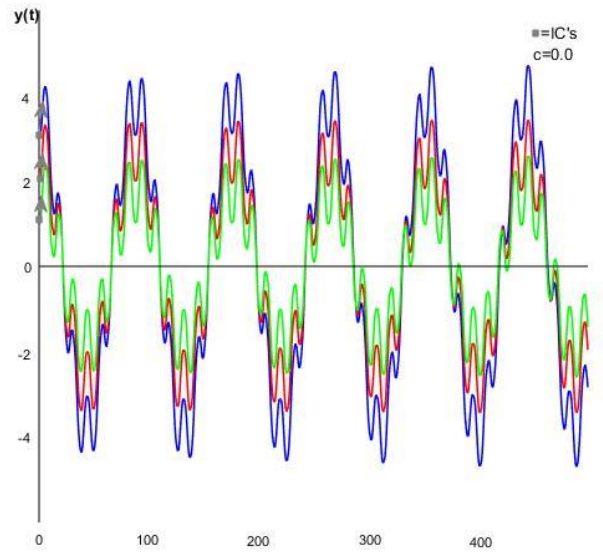


Figure 5.3: Velocity curves for systems with nonlinear force for different IC's, separated by different colours.

The system represented by the red trajectory from figure 5.2 will from this point be referred to as the “base-case system”. In the following in this chapter, we will investigate what happens to this system when the parameters are varied.

The base-case system has the following values of the parameters:

- Linear, constant damping coefficient,  $c=0$
- Stiffness parameter,  $k=0,5$
- Mass parameter,  $m=100$
- Amplitude parameter,  $F_0=50$
- Loading frequency,  $\omega=0,5$
- Initial displacement,  $x_{(0)}=2$
- Initial velocity,  $y_{(0)}=2$

Introducing a new variable:

$$\beta = \frac{\omega}{\omega_0} \quad (5.3)$$

If  $\beta=1,0$ , i.e.  $\omega=\omega_0$ , the system is at resonance. For the base-case system is  $\beta=7,07$ .

5.2.1 Development for the base-case system

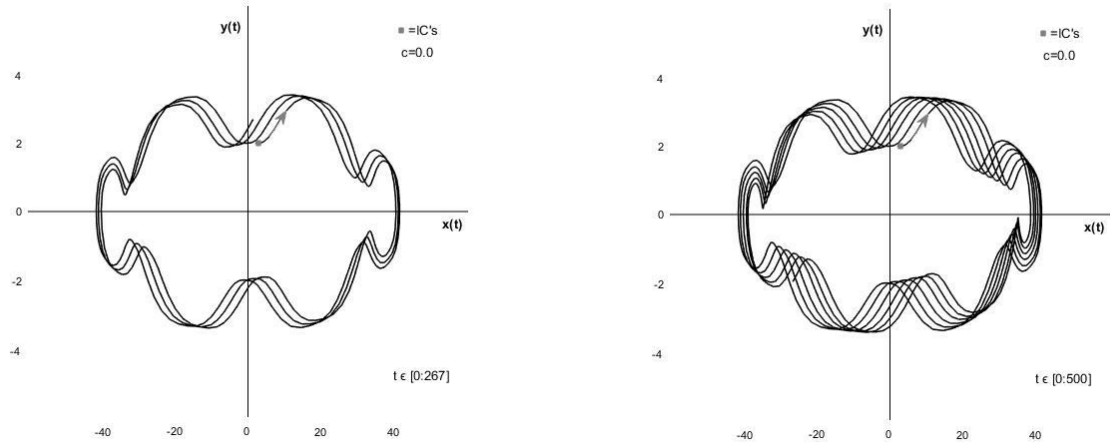


Figure 5.4: Development in the phase plane for the base-case system from  $t=0$  to  $t=267s$ (left) and to  $t=500s$ (right).

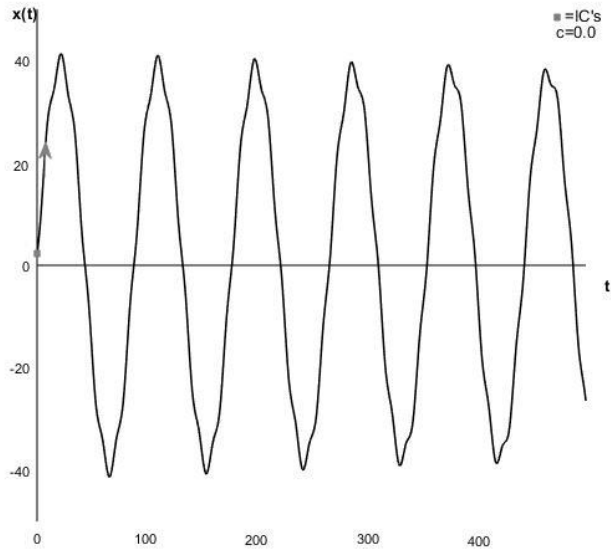


Figure 5.5: Position curve for the base-case system.

Figures 5.4 and 5.5 show the behaviour for the base-case system. Figure 5.4 shows the system in the phase plane, while figure 5.5 shows the position curve. The system has periods of approximately 89s.

### 5.3 Varying the stiffness coefficient

The stiffness coefficient,  $k$ , will here be varied from 0,1 to 2,0, while all other variables will be as for the base-case system. The original value of  $k$  in the base-case system is  $k=0,5$ .

#### 5.3.1 $k=0,1$

The base-case system with a stiffness of  $k=0,1$  has a natural period of approximately 199s. Figure 5.6 shows the development in the phase plane. On the left in the figure, the first revolution is shown, while the system is shown for 1000s on the right. Figure 5.7 shows the position curve for the system.

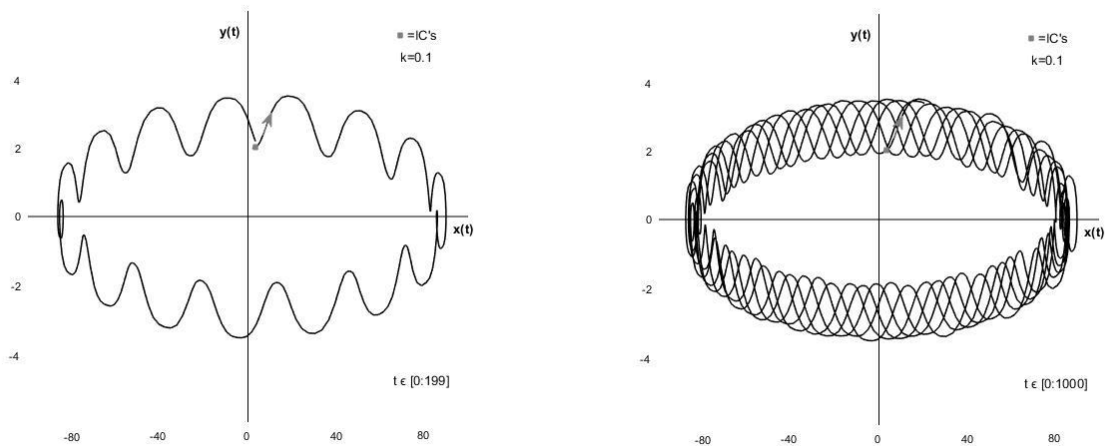


Figure 5.6: Development in the phase plane for the base-case system with  $k=0,1$  from  $t=0$  to  $t=199$ s(left) and to  $t=1000$ s(right).

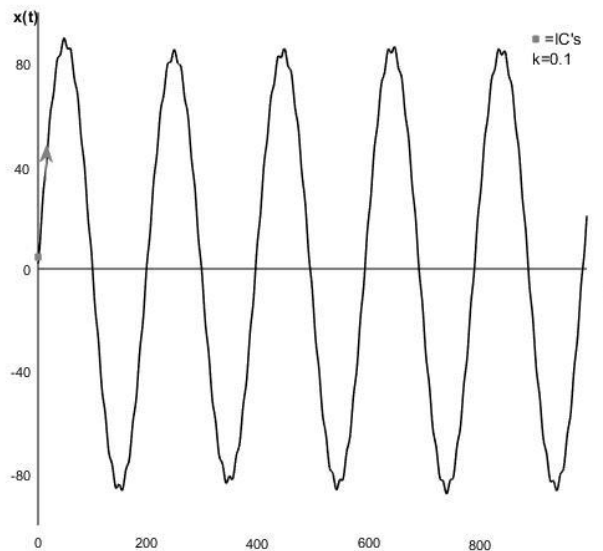


Figure 5.7: Position curve for the base-case system with  $k=0,1$ .

### 5.3.2 $k=0,2$

Figures 5.8 and 5.9 show the development of the base-case system with  $k=0,2$  for the first 1000s. Figure 5.8 shows the system in the phase plane. The first revolution is shown to the left in the figure, while to the right the system is shown until  $t=1000s$ . Figure 5.9 shows the system's position curve. The system has periods of approximately 140s.

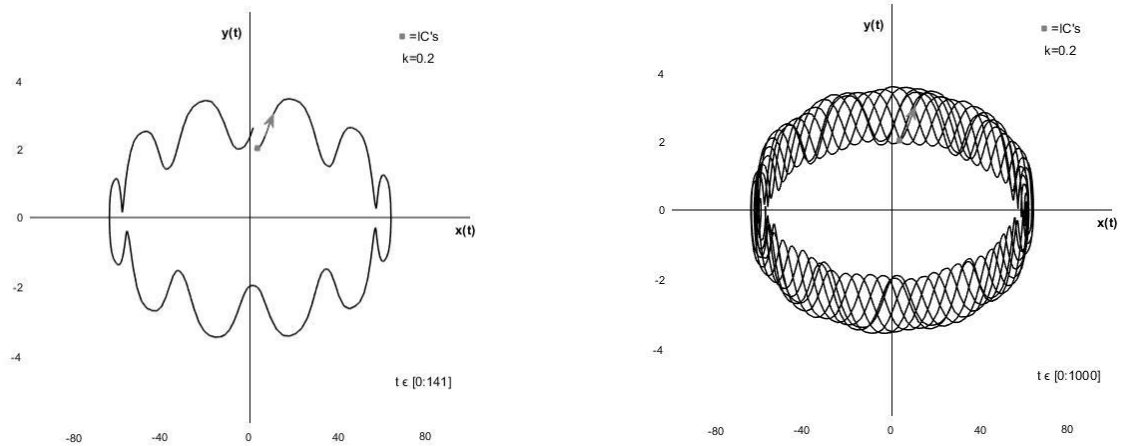


Figure 5.8: Development in the phase plane for the base-case system with  $k=0,2$  from  $t=0$  to  $t=141s$ (left) and to  $t=1000s$ (right).

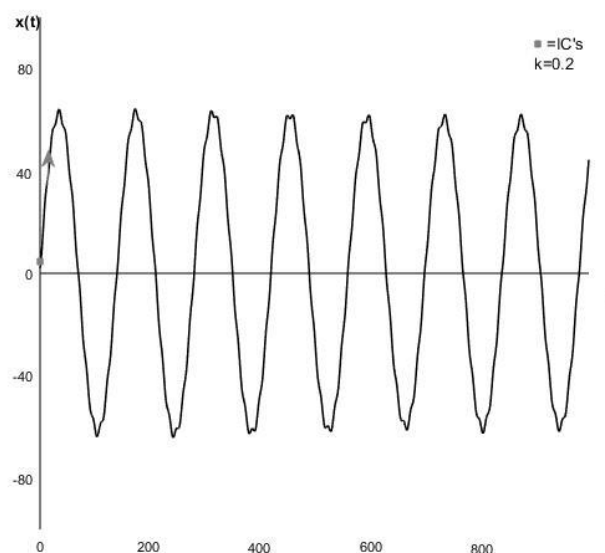


Figure 5.9: Position curve for the base-case system with  $k=0,2$ .

### 5.3.3 $k=0,3$

Figures 5.10 and 5.11 show the development of the base-case system with  $k=0,3$  for the first 1000s. Figure 5.10 shows the system in the phase plane. The first revolution is shown to the left in the figure, while to the right the system is shown until  $t=1000$ s. Figure 5.11 shows the system's position curve. The system has periods of approximately 115s.

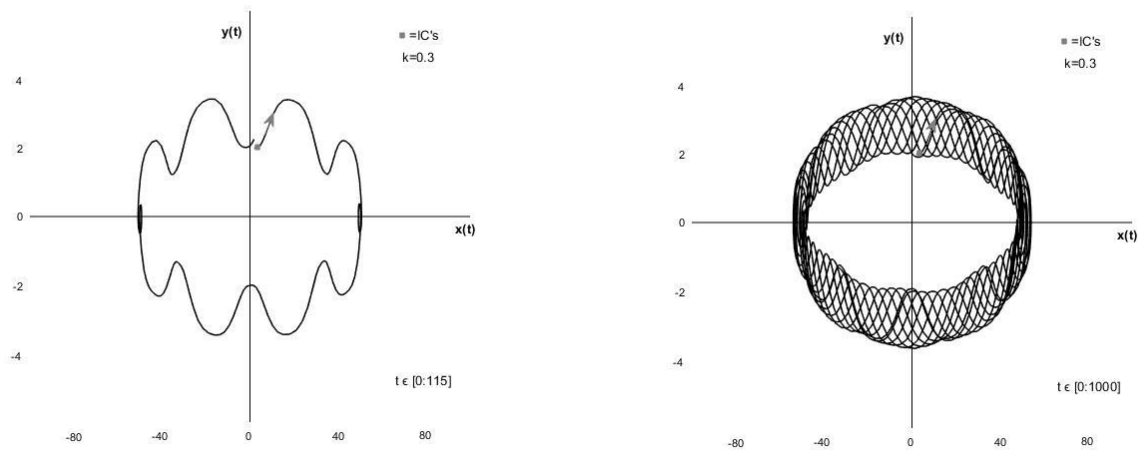


Figure 5.10: Development in the phase plane for the base-case system with  $k=0,3$  from  $t=0$  to  $t=115$ (left) and to  $t=1000$ s(right).

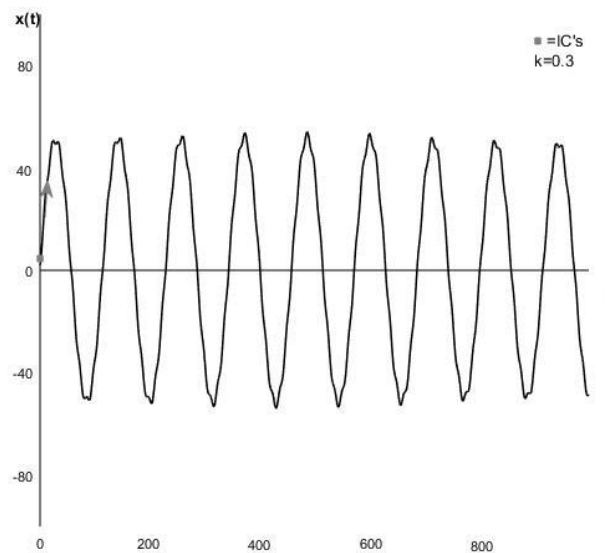


Figure 5.11: Position curve for the base-case system with  $k=0,3$ .

### 5.3.4 $k=0,4$

Figures 5.12 and 5.13 show the development of the base-case system with  $k=0,4$  for the first 1000s. Figure 5.12 shows the system in the phase plane. The first revolution is shown to the left in the figure, while to the right the system is shown until  $t=1000$ s. Figure 5.13 shows the system's position curve. The system has periods of approximately 100s.

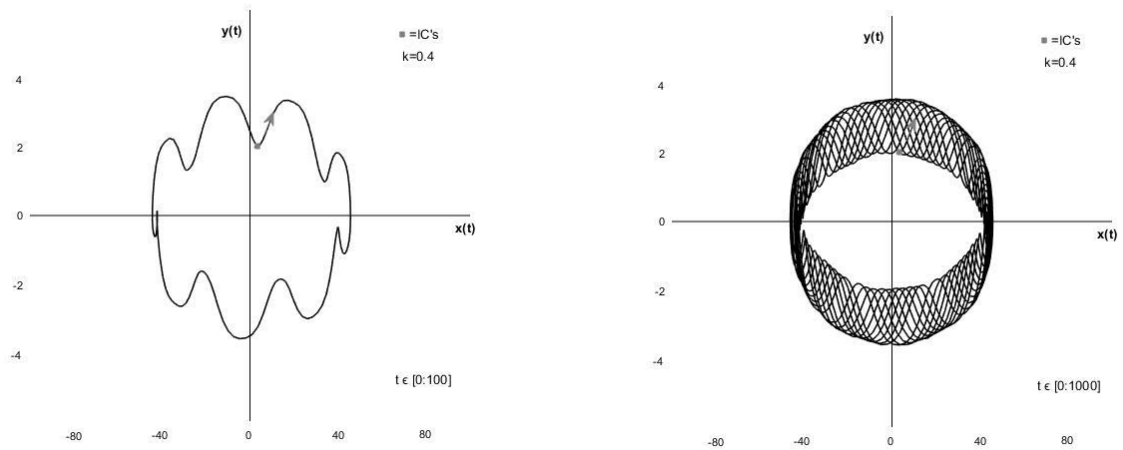


Figure 5.12: Development in the phase plane for the base-case system with  $k=0,4$  from  $t=0$  to  $t=100$ (left) and to  $t=1000$ s(right).

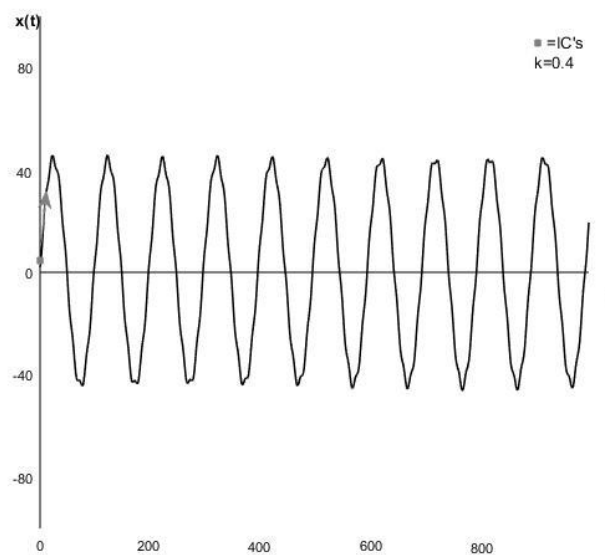


Figure 5.13: Position curve for the base-case system with  $k=0,4$ .

### 5.3.5 $k=0,6$

Figures 5.14 and 5.15 show the development of the base-case system with  $k=0,6$  for the first 1000s. Figure 5.14 shows the system in the phase plane. The first revolution is shown to the left in the figure, while to the right the system is shown until  $t=1000$ s. Figure 5.15 shows the system's position curve. The system has periods of approximately 81s.

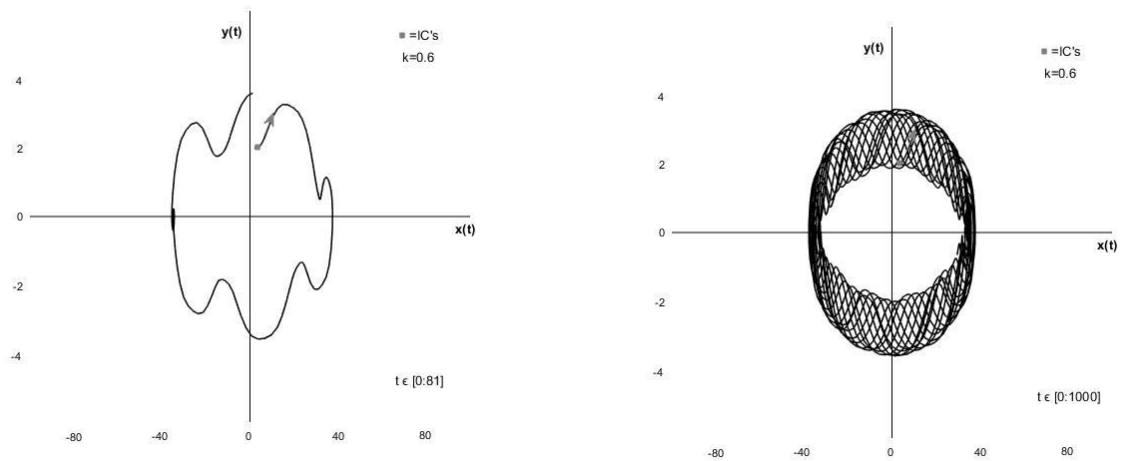


Figure 5.14: Development in the phase plane for the base-case system with  $k=0,6$  from  $t=0$  to  $t=81$ (left) and to  $t=1000$ s(right).

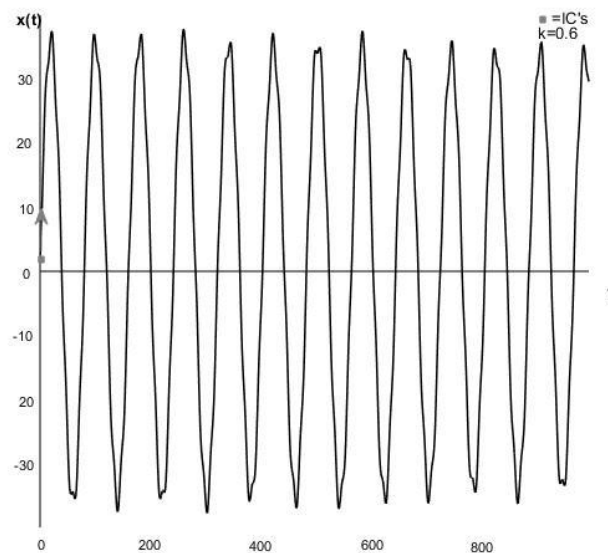


Figure 5.15: Position curve for the base-case system with  $k=0,6$ .

### 5.3.6 $k=0,7$

Figures 5.16 and 5.17 show the development of the base-case system with  $k=0,7$  for the first 1000s. Figure 5.16 shows the system in the phase plane. The first revolution is shown to the left in the figure, while to the right the system is shown until  $t=1000$ s. Figure 5.17 shows the system's position curve. The system has periods of approximately 75s.

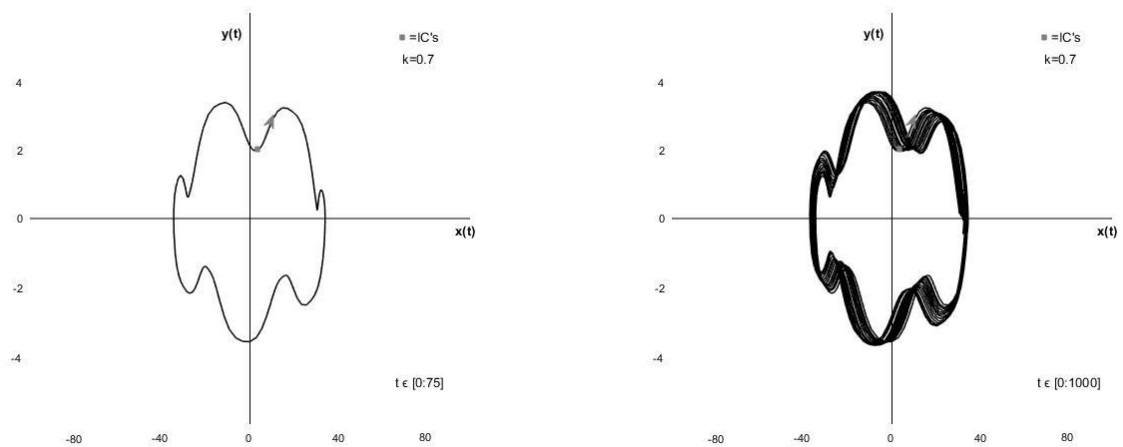


Figure 5.16: Development in the phase plane for the base-case system with  $k=0,7$  from  $t=0$  to  $t=75$ (left) and to  $t=1000$ s(right).

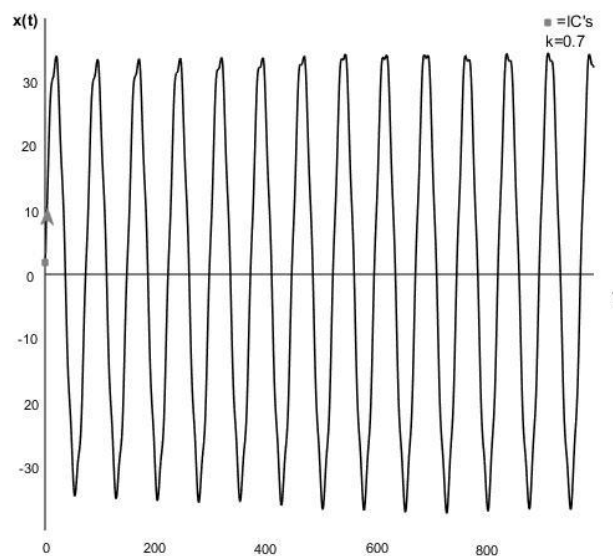


Figure 5.17: Position curve for the base-case system with  $k=0,7$ .



### 5.3.7 $k=0,8$

Figures 5.18 and 5.19 show the development of the base-case system with  $k=0,8$  for the first 1000s. Figure 5.18 shows the system in the phase plane. The first revolution is shown to the left in the figure, while to the right the system is shown until  $t=1000$ s. Figure 5.19 shows the system's position curve. The system has periods of approximately 70s.

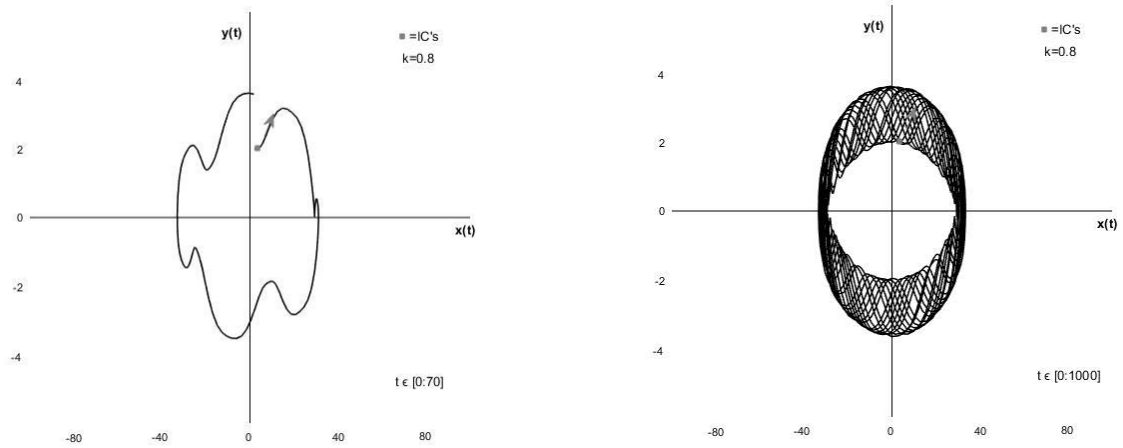


Figure 5.18: Development in the phase plane for the base-case system with  $k=0,8$  from  $t=0$  to  $t=70$ (left) and to  $t=1000$ s(right).

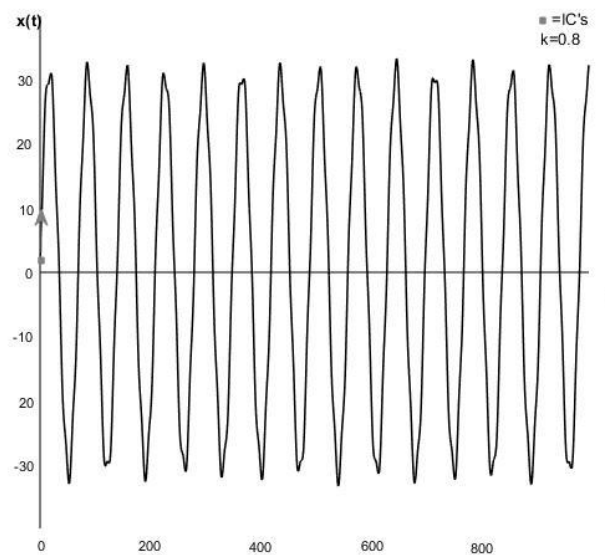


Figure 5.19: Position curve for the base-case system with  $k=0,8$ .

### 5.3.8 $k=0,9$

Figures 5.20 and 5.21 show the development of the base-case system with  $k=0,9$  for the first 1000s. Figure 5.20 shows the system in the phase plane. The first revolution is shown to the left in the figure, while to the right the system is shown until  $t=1000$ s. Figure 5.21 shows the system's position curve. The system has periods of approximately 67s.

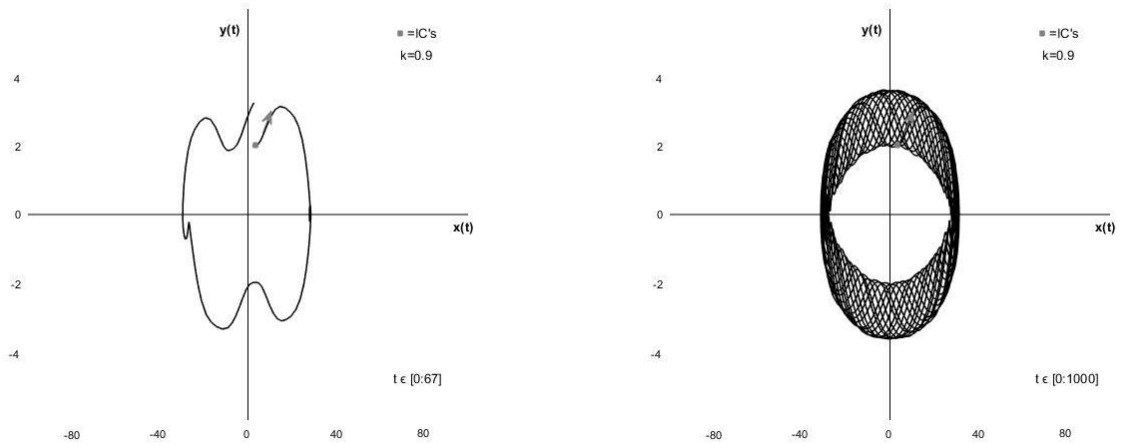


Figure 5.20: Development in the phase plane for the base-case system with  $k=0,9$  from  $t=0$  to  $t=67$ s(left) and to  $t=1000$ s(right).

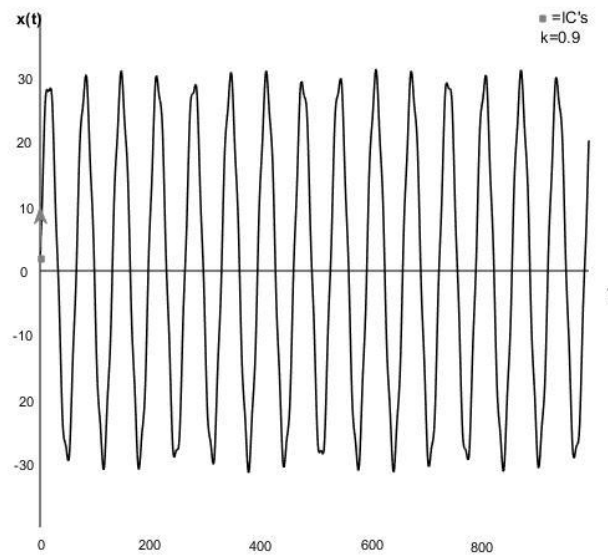


Figure 5.21: Position curve for the base-case system with  $k=0,9$ .

### 5.3.9 $k=1,0$

Figures 5.22 and 5.23 show the development of the base-case system with  $k=1,0$  for the first 1000s. Figure 5.22 shows the system in the phase plane. The first revolution is shown to the left in the figure, while to the right the system is shown until  $t=1000$ s. Figure 5.23 shows the system's position curve. The system has periods of approximately 63s.

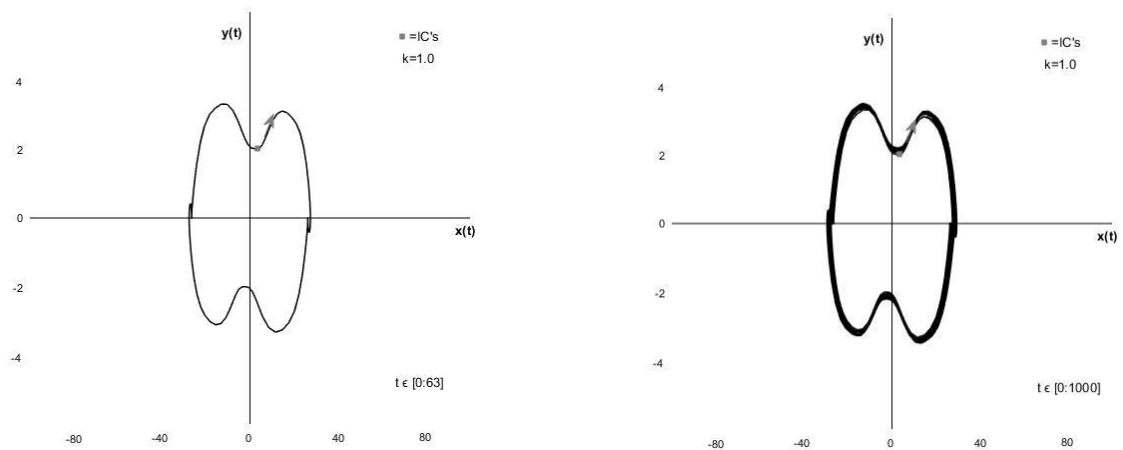


Figure 5.22: Development in the phase plane for the base-case system with  $k=1,0$  from  $t=0$  to  $t=63$ (left) and to  $t=1000$ s(right).

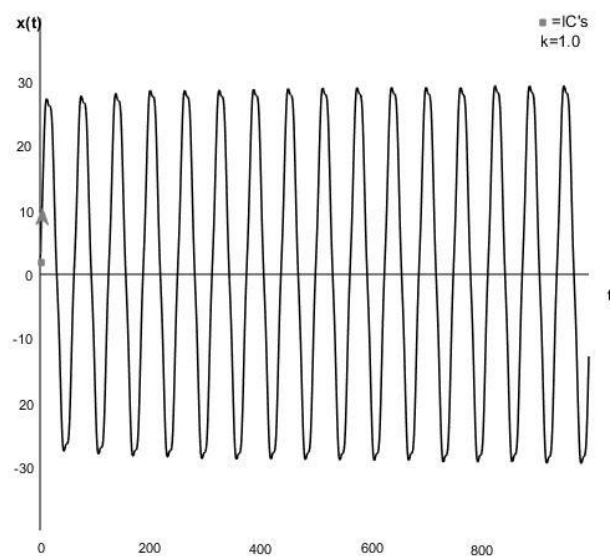


Figure 5.23: Position curve for the base-case system with  $k=1,0$ .

### 5.4.12 Conclusion

k	0,1	0,2	0,3	0,4	0,5 (base-case system)	0,6	0,7	0,8	0,9	1,0
Periods	199	141	115	100	89	81	75	70	67	63
$\beta$	15,81	11,18	9,13	7,91	7,07	6,45	5,98	5,59	5,27	5,0
Phase plane diagrams										
Position curves										

*Table 5.1: Review of phase plane diagrams and position curves for the base-case system with different values of k.*

Table 5.1 shows the phase plane diagrams and position curves for the base-case system with varying values of the stiffness parameter, k. The periods and the values of  $\beta$ , in the systems are also shown. The table shows that increasing the stiffness will lead to a reduced period, as well as lower amplitudes in the position curves. The velocity in the system does not seem to be affected by the variation of the stiffness parameter. The position curves get more smooth as the stiffness is increased, i.e. the nonlinearity in the forcing term gets less prominent.

## 5.4 Varying the amplitude parameter, $F_0$ .

The amplitude parameter,  $F_0$ , will here be varied from 10 to 100. The value of  $F_0$  in the base-case system is  $F_0=50$ .

### 5.4.1 $F_0=10$

Figures 5.24 and 5.25 show the development of the base-case system with  $F_0=10$  for the first 1000s. Figure 5.24 shows the system in the phase plane. The first revolution is shown to the left in the figure, while to the right the system is shown until  $t=1000$ s. Figure 5.25 shows the system's position curve. The system has periods of approximately 89s.

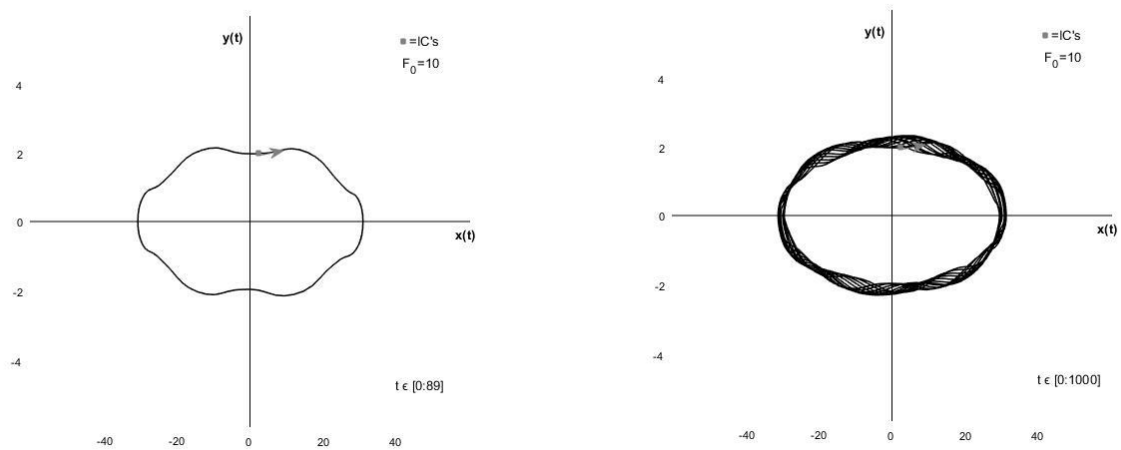


Figure 5.24: Development in the phase plane for the base-case system with  $F_0=10$  from  $t=0$  to  $t=89$ s(left) and to  $t=1000$ s(right).

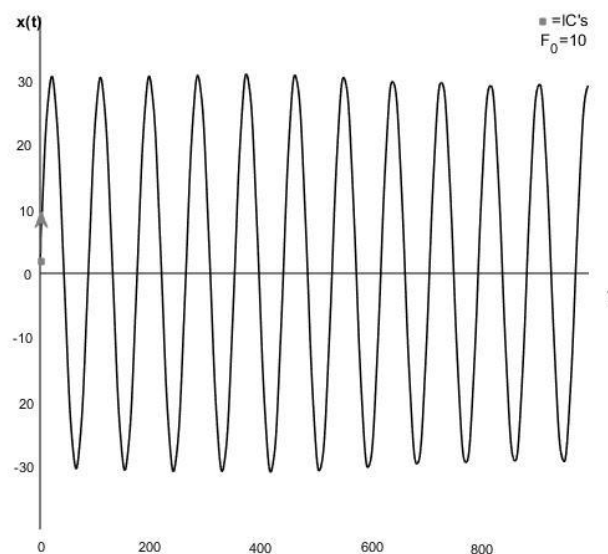


Figure 5.25: Position curve for the base-case system with  $F_0=10$ .

## 5.4.2 $F_0=20$

Figures 5.26 and 5.27 show the development of the base-case system with  $F_0=20$  for the first 1000s. Figure 5.26 shows the system in the phase plane. The first revolution is shown to the left in the figure, while to the right the system is shown until  $t=1000$ s. Figure 5.27 shows the system's position curve. The system has periods of approximately 89s.

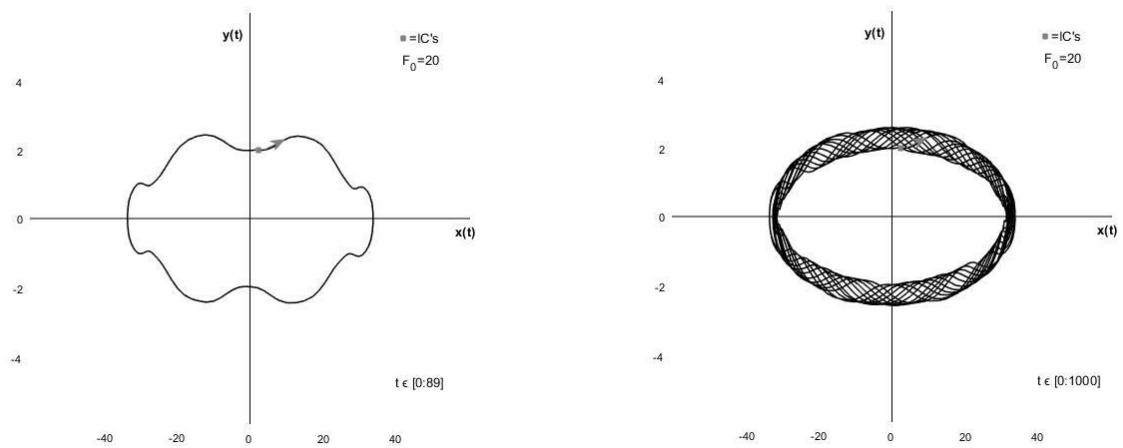


Figure 5.26: Development in the phase plane for the base-case system with  $F_0=20$  from  $t=0$  to  $t=89$ s(left) and to  $t=1000$ s(right).

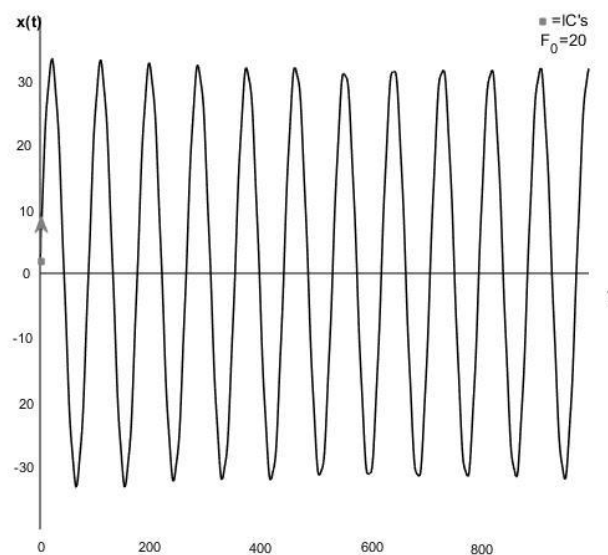


Figure 5.27: Position curve for the base-case system with  $F_0=20$ .

5.4.3  $F_0=30$

Figures 5.28 and 5.29 show the development of the base-case system with  $F_0=30$  for the first 1000s. Figure 5.28 shows the system in the phase plane. The first revolution is shown to the left in the figure, while to the right the system is shown until  $t=1000s$ . Figure 5.29 shows the system's position curve. The system has periods of approximately 89s.

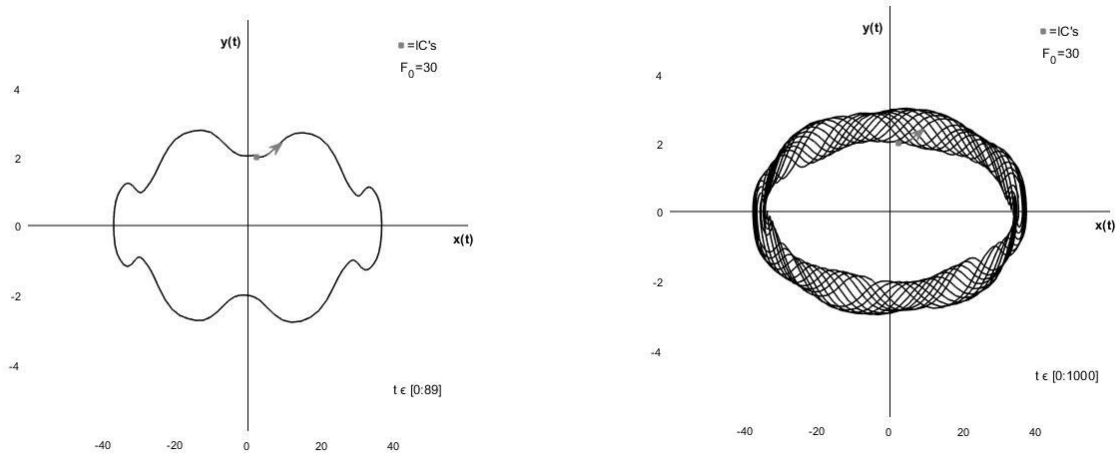


Figure 5.28: Development in the phase plane for the base-case system with  $F_0=30$  from  $t=0$  to  $t=89s$ (left) and to  $t=1000s$ (right).

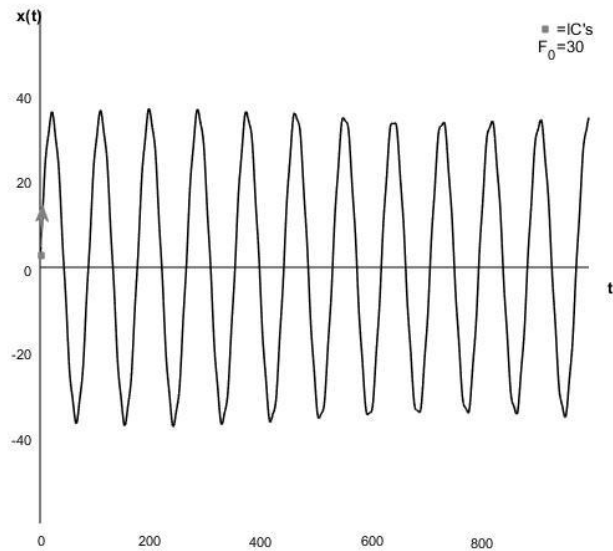


Figure 5.29: Position curve for the base-case system with  $F_0=30$ .

#### 5.4.4 $F_0=40$

Figures 5.30 and 5.31 show the development of the base-case system with  $F_0=40$  for the first 1000s. Figure 5.30 shows the system in the phase plane. The first revolution is shown to the left in the figure, while to the right the system is shown until  $t=1000$ s. Figure 5.31 shows the system's position curve. The system has periods of approximately 89s.

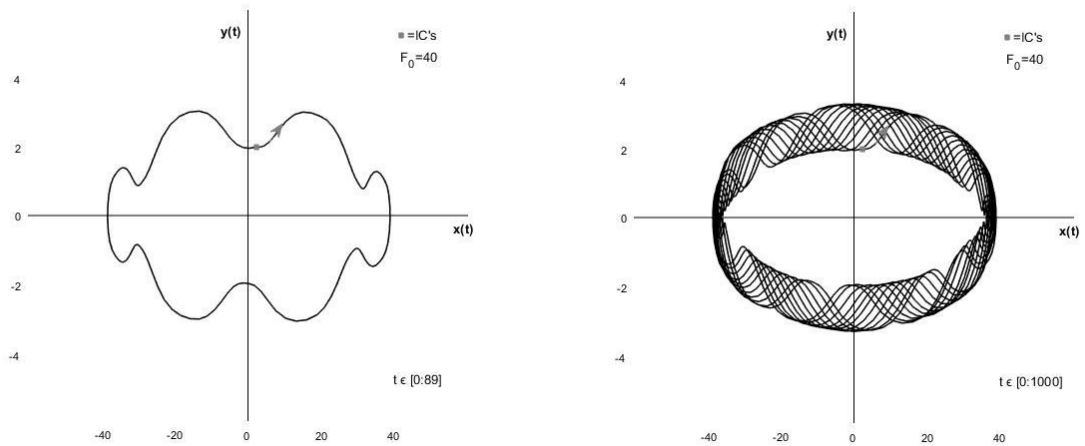


Figure 5.30: Development in the phase plane for the base-case system with  $F_0=40$  from  $t=0$  to  $t=89$ s(left) and to  $t=1000$ s(right).

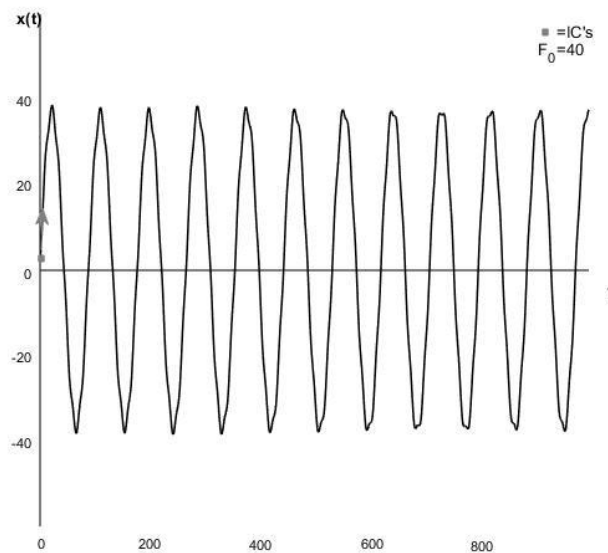


Figure 5.31: Position curve for the base-case system with  $F_0=40$ .



### 5.4.5 $F_0=60$

Figures 5.32 and 5.33 show the development of the base-case system with  $F_0=60$  for the first 1000s. Figure 5.32 shows the system in the phase plane. The first revolution is shown to the left in the figure, while to the right the system is shown until  $t=1000$ s. Figure 5.33 shows the system's position curve. The system has periods of approximately 89s.

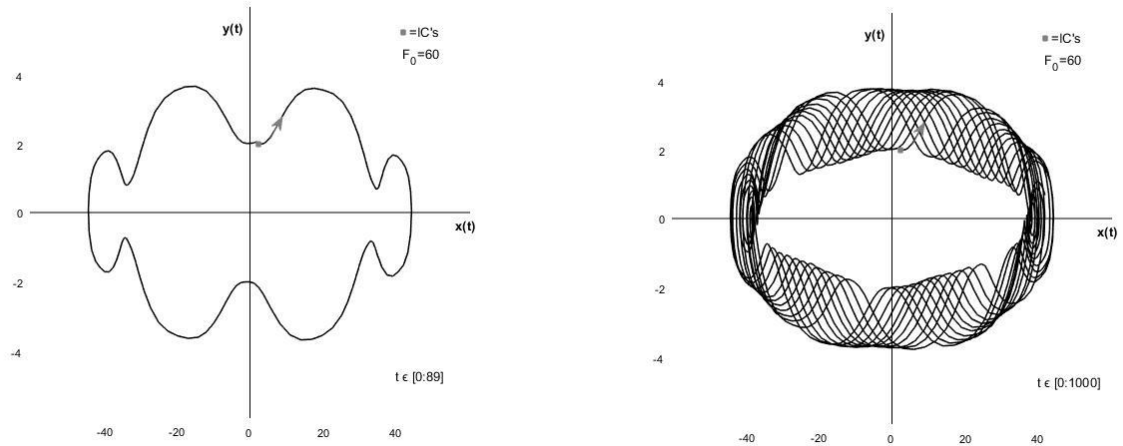


Figure 5.32: Development in the phase plane for the base-case system with  $F_0=60$  from  $t=0$  to  $t=89$ s(left) and to  $t=1000$ s(right).

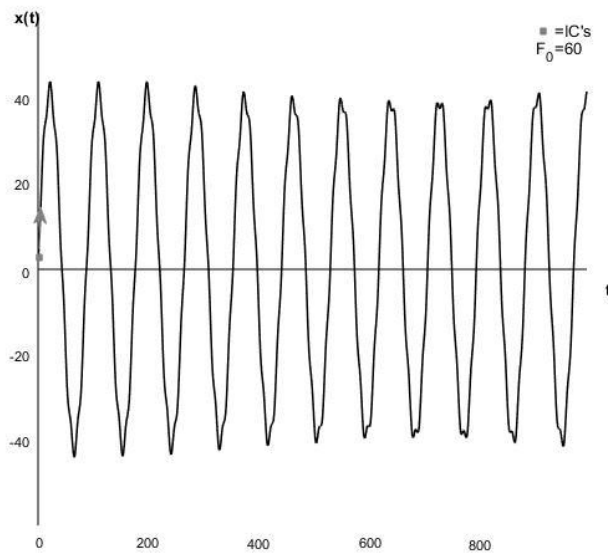


Figure 5.33: Position curve for the base-case system with  $F_0=60$ .

5.4.6  $F_0=70$

Figures 5.34 and 5.35 show the development of the base-case system with  $F_0=70$  for the first 1000s. Figure 5.34 shows the system in the phase plane. The first revolution is shown to the left in the figure, while to the right the system is shown until  $t=1000$ s. Figure 5.35 shows the system's position curve. The system has periods of approximately 89s.

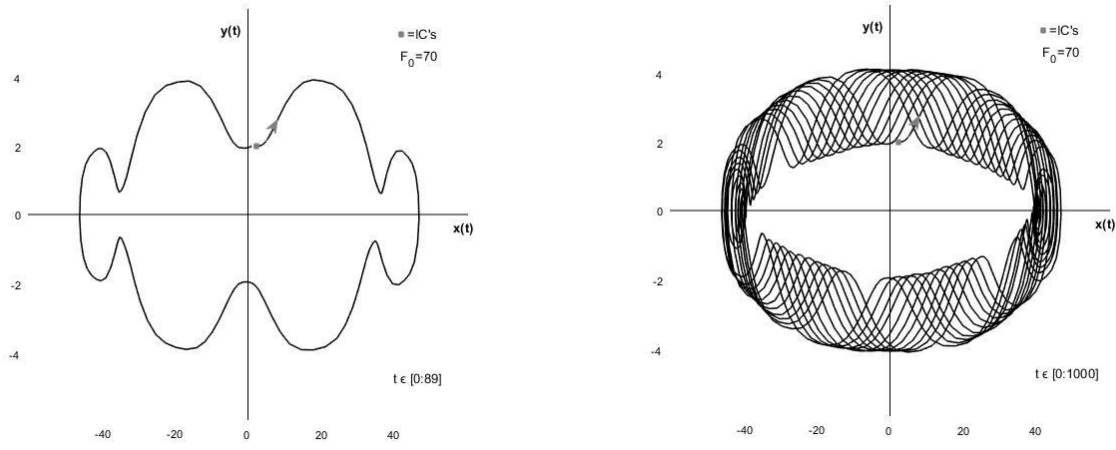


Figure 5.34: Development in the phase plane for the base-case system with  $F_0=70$  from  $t=0$  to  $t=89$ s(left) and to  $t=1000$ s(right).

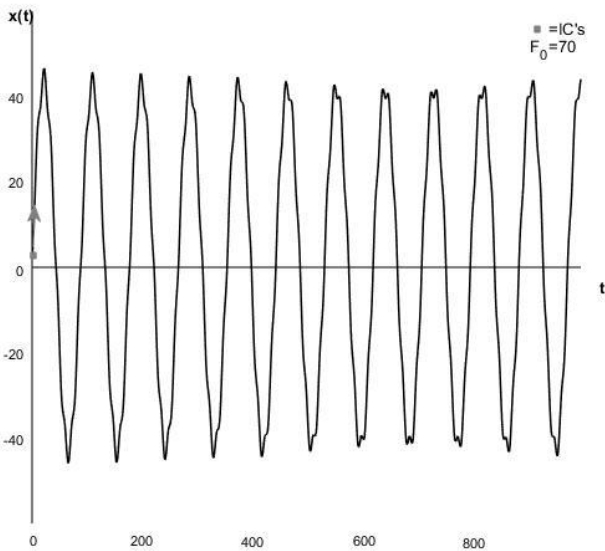


Figure 5.35: Position curve for the base-case system with  $F_0=70$ .

### 5.4.7 $F_0=80$

Figures 5.36 and 5.37 show the development of the base-case system with  $F_0=80$  for the first 1000s. Figure 5.36 shows the system in the phase plane. The first revolution is shown to the left in the figure, while to the right the system is shown until  $t=1000$ s. Figure 5.37 shows the system's position curve. The system has periods of approximately 89s.

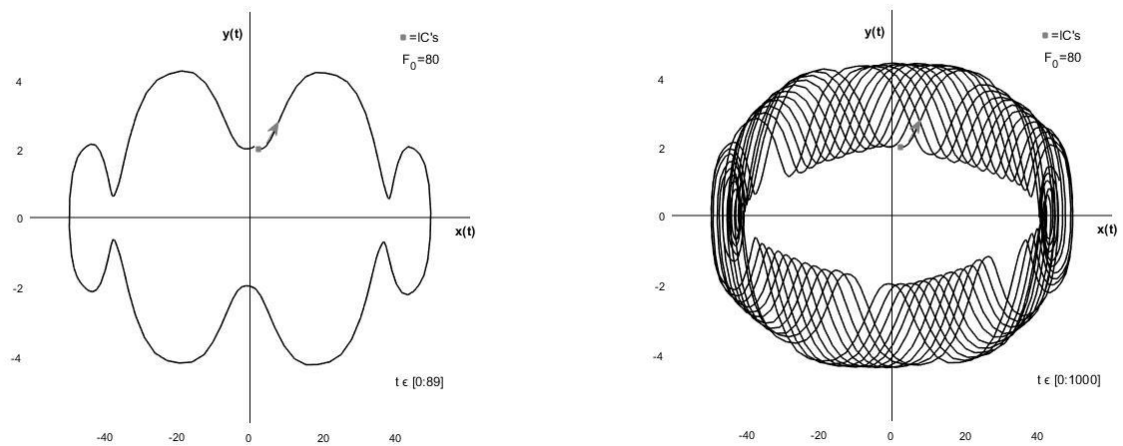


Figure 5.36: Development in the phase plane for the base-case system with  $F_0=80$  from  $t=0$  to  $t=89$ s(left) and to  $t=1000$ s(right).

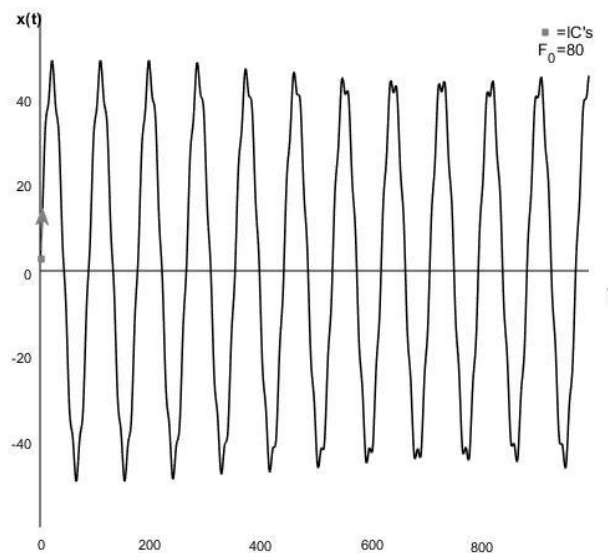


Figure 5.37: Position curve for the base-case system with  $F_0=80$ .

### 5.4.8 $F_0=90$

Figures 5.38 and 5.39 show the development of the base-case system with  $F_0=90$  for the first 1000s. Figure 5.38 shows the system in the phase plane. The first revolution is shown to the left in the figure, while to the right the system is shown until  $t=1000$ s. Figure 5.39 shows the system's position curve. The system has periods of approximately 89s.

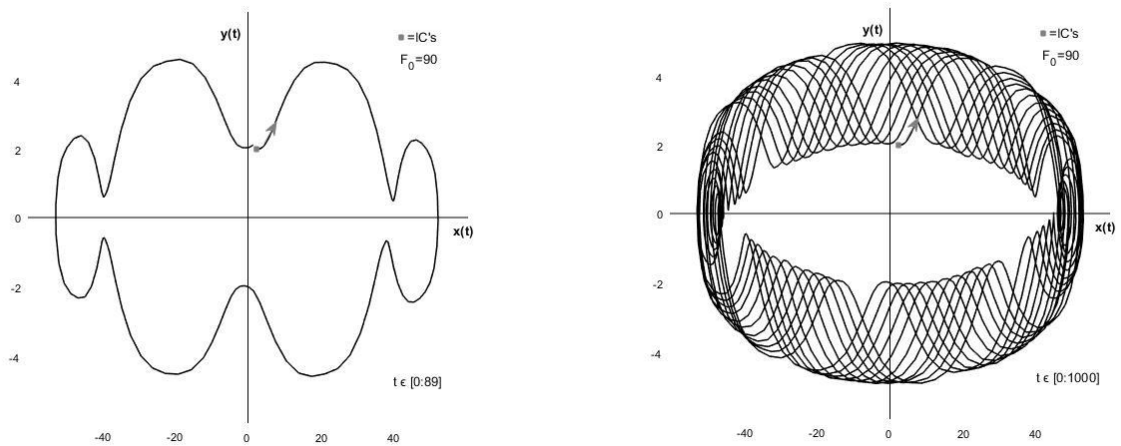


Figure 5.38: Development in the phase plane for the base-case system with  $F_0=90$  from  $t=0$  to  $t=89$ s(left) and to  $t=1000$ s(right).

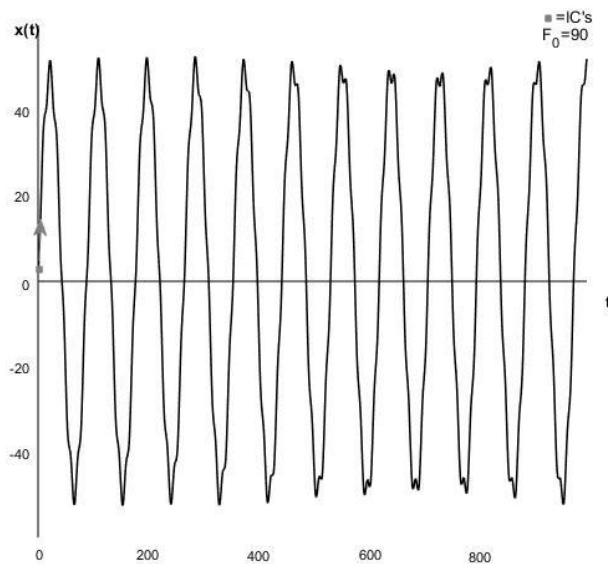


Figure 5.39: Position curve for the base-case system with  $F_0=90$ .

### 5.4.9 $F_0=100$

Figures 5.40 and 5.41 show the development of the base-case system with  $F_0=100$  for the first 1000s. Figure 5.40 shows the system in the phase plane. The first revolution is shown to the left in the figure, while to the right the system is shown until  $t=1000$ s. Figure 5.41 shows the system's position curve. The system has periods of approximately 89s.

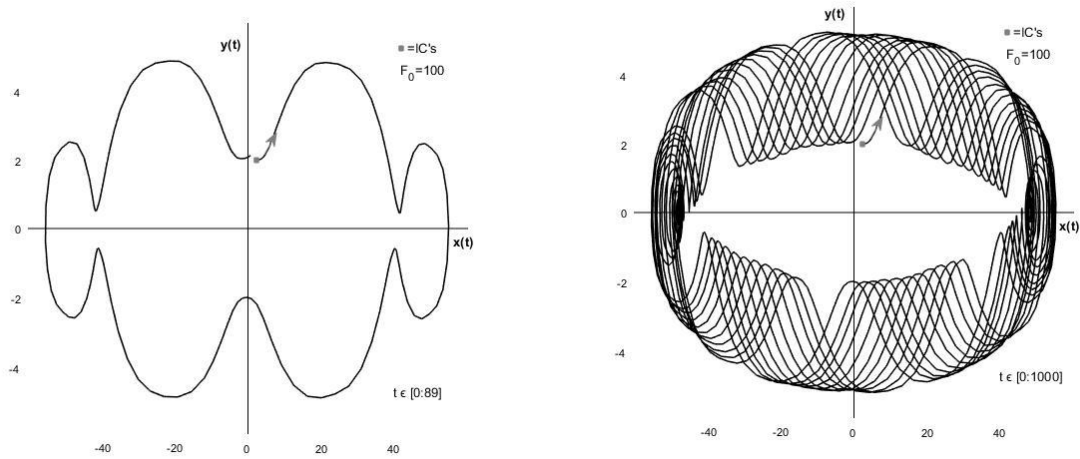


Figure 5.40: Development in the phase plane for the base-case system with  $F_0=100$  from  $t=0$  to  $t=89$ s(left) and to  $t=1000$ s(right).

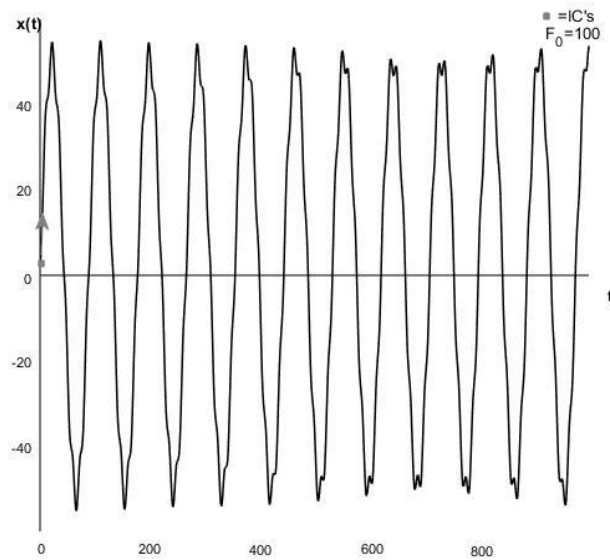


Figure 5.41: Position curve for the base-case system with  $F_0=100$ .

5.4.10 Conclusion

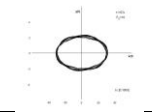
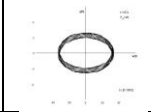
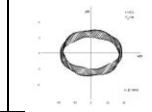
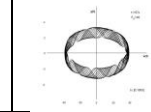

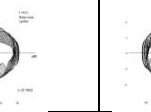
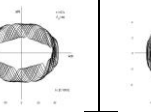
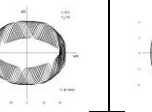
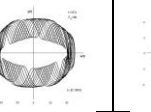
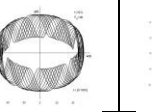
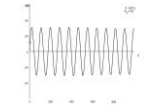
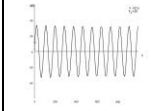
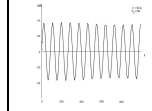
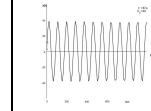
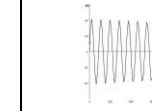
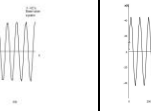
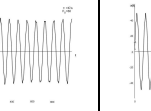
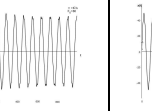
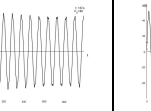
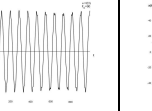
$F_0$	10	20	30	40	50 (base-case system)	60	70	80	90	100
Periods	89	89	89	89	89	89	89	89	89	89
$\beta$	7,07	7,07	7,07	7,07	7,07	7,07	7,07	7,07	7,07	7,07
Phase plane diagrams										
Position curves										

Table 5.2: Review of phase plane diagrams and position curves for the base-case system with different values of  $F_0$ .

Table 5.2 shows the phase plane diagrams and position curves for the base-case system with varying values of the amplitude parameter,  $F_0$ . The period and value of  $\beta$  is constant when varying  $F_0$ . The position curves show an increase in position amplitude as  $F_0$  gets larger. The velocity also increases as  $F_0$  increases, this is shown in the phase plane diagrams in the table. When  $F_0$  is increased, the effect of the nonlinear forcing term increases.

## 5.5 Varying the loading frequency, $\omega$

In this part the loading frequency,  $\omega$ , will be varied from 0,1 to 1,0. In the base-case system the value of  $\omega$  is 0,5.

### 5.5.1 $\omega=0,1$

Figures 5.42 shows the development of the base-case system with  $\omega=0,1$  for the first 1000s. The phase plane diagram is showed to the left and the position curve to the right in the figure.

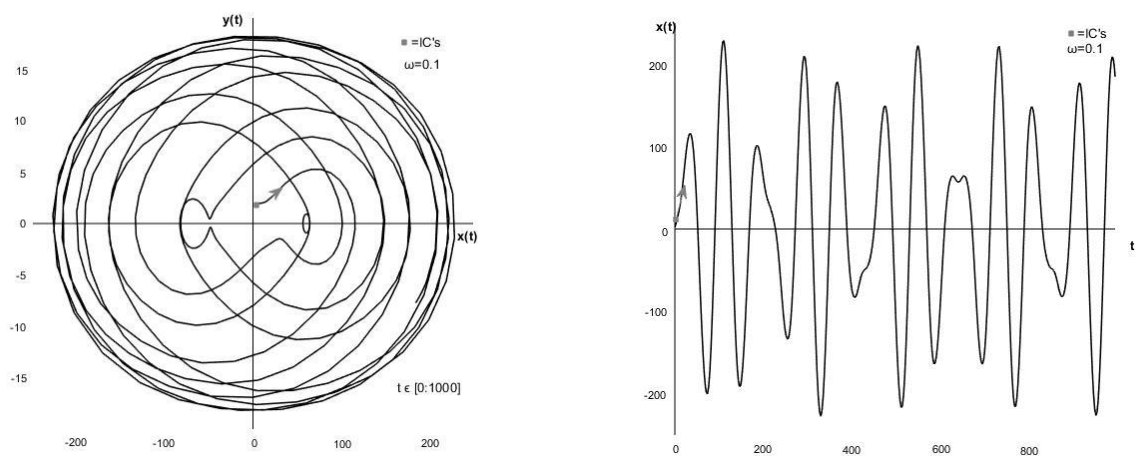


Figure 5.42: Development in the phase plane(left) and position curve(right) for the base-case system with  $\omega=0,1$  from  $t=0$  to  $t=1000s$ .

### 5.5.2 $\omega=0,2$

Figures 5.43 shows the development of the base-case system with  $\omega=0,2$  for the first 1000s. The system is shown in the phase plane to the left, and the position curve is showed to the right in the figure.

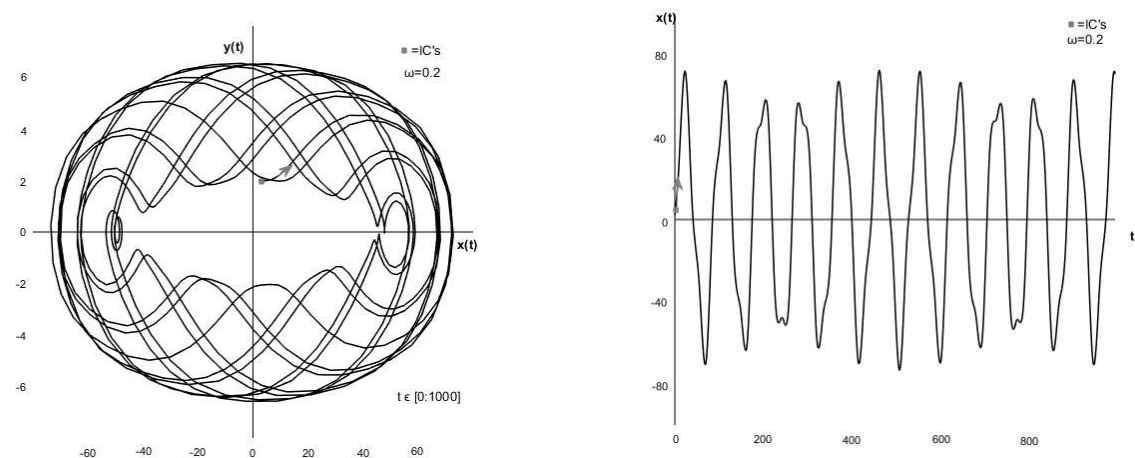


Figure 5.43: Development in the phase plane(left) and position curve(right) for the base-case system with  $\omega=0,2$  from  $t=0$  to  $t=1000s$ .

### 5.5.3 $\omega = 0,3$

Figures 5.44 and 5.45 show the development of the base-case system with  $\omega=0,3$  for the first 1000s. Figure 5.44 shows the system in the phase plane. The first revolution is shown to the left in the figure, while to the right the system is shown until  $t=1000s$ . Figure 5.45 shows the system's position curve. The system has periods of approximately 89s.

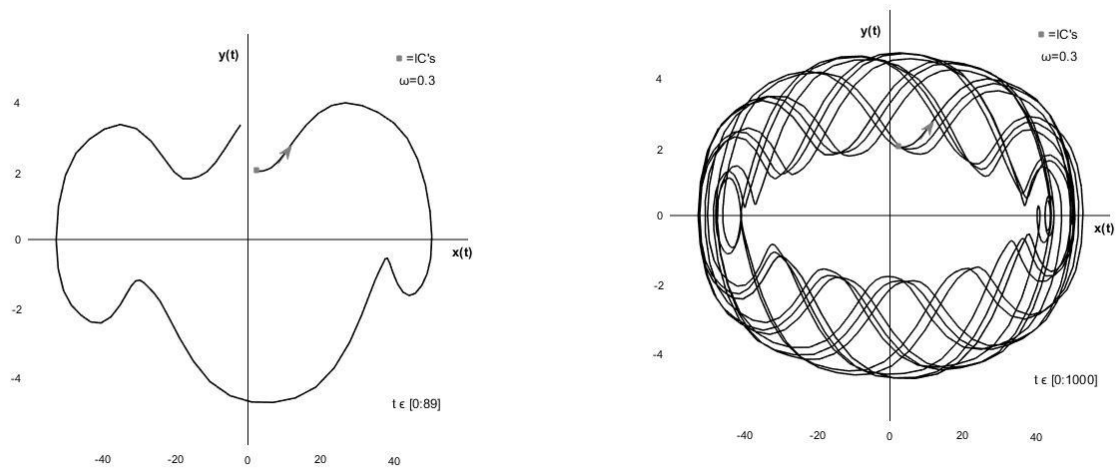


Figure 5.44: Development in the phase plane for the base-case system with  $\omega=0,3$  from  $t=0$  to  $t=89s$ (left) and to  $t=1000s$ (right).

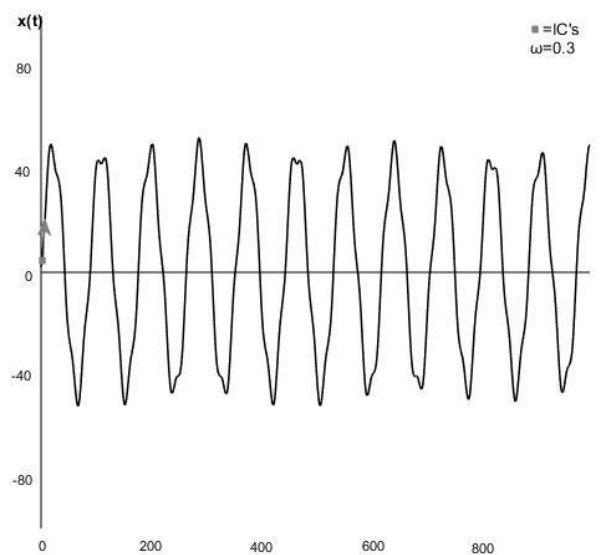


Figure 5.45: Position curve for the base-case system with  $\omega=0,3$ .



### 5.5.4 $\omega = 0,4$

Figures 5.46 and 5.47 show the development of the base-case system with  $\omega=0,4$  for the first 1000s. Figure 5.46 shows the system in the phase plane. The first revolution is shown to the left in the figure, while to the right the system is shown until  $t=1000$ s. Figure 5.47 shows the system's position curve. The system has periods of approximately 89s.

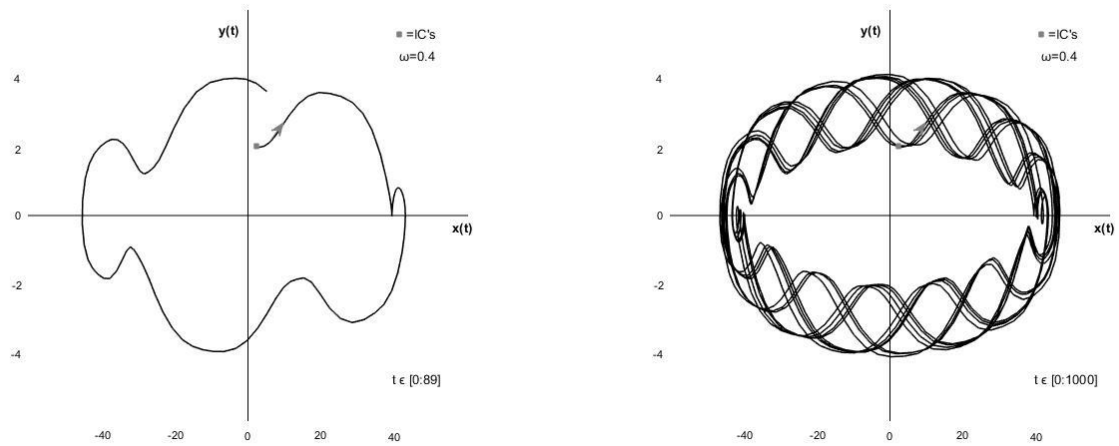


Figure 5.46: Development in the phase plane for the base-case system with  $\omega=0,4$  from  $t=0$  to  $t=89$ s(left) and to  $t=1000$ s(right).

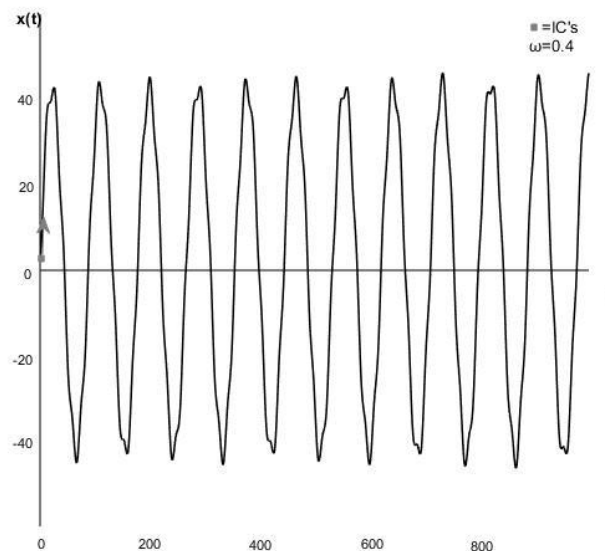


Figure 5.47: Position curve for the base-case system with  $\omega=0,4$ .

### 5.5.5 $\omega = 0,6$

Figures 5.48 and 5.49 show the development of the base-case system with  $\omega=0,6$  for the first 1000s. Figure 5.48 shows the system in the phase plane. The first revolution is shown to the left in the figure, while to the right the system is shown until  $t=1000$ s. Figure 5.49 shows the system's position curve. The system has periods of approximately 89s.

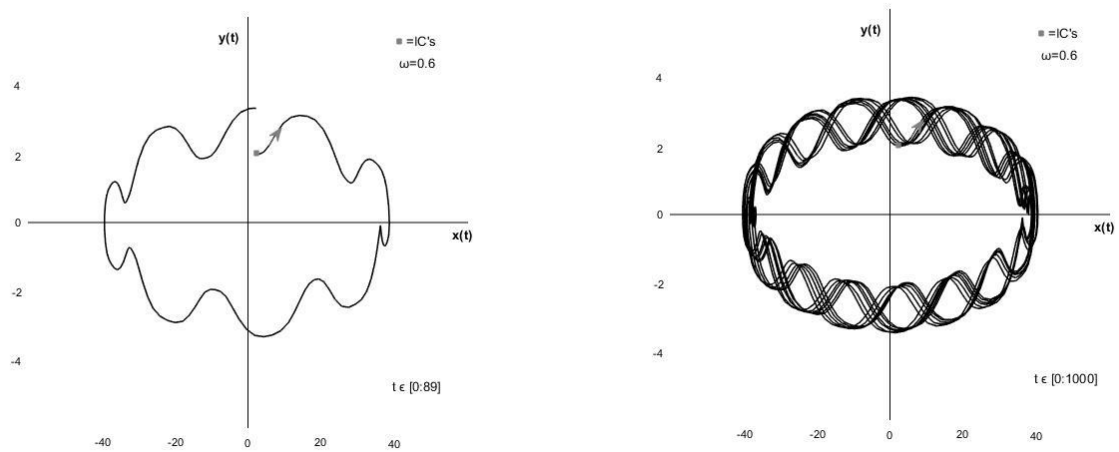


Figure 5.48: Development in the phase plane for the base-case system with  $\omega=0,6$  from  $t=0$  to  $t=89$ s (left) and to  $t=1000$ s (right).

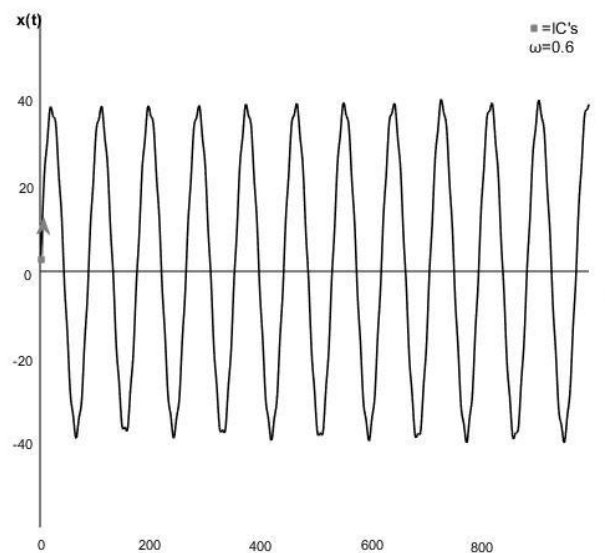


Figure 5.49: Position curve for the base-case system with  $\omega=0,6$ .

### 5.5.6 $\omega = 0,7$

Figures 5.50 and 5.51 show the development of the base-case system with  $\omega=0,7$  for the first 1000s. Figure 5.50 shows the system in the phase plane. The first revolution is shown to the left in the figure, while to the right the system is shown until  $t=1000$ s. Figure 5.51 shows the system's position curve. The system has periods of approximately 89s.

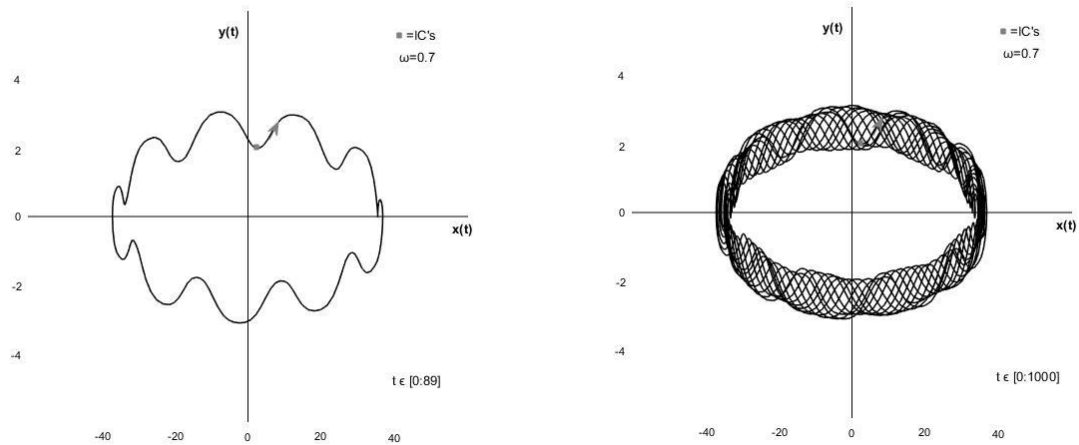


Figure 5.50: Development in the phase plane for the base-case system with  $\omega=0,7$  from  $t=0$  to  $t=89$ s(left) and to  $t=1000$ s(right).

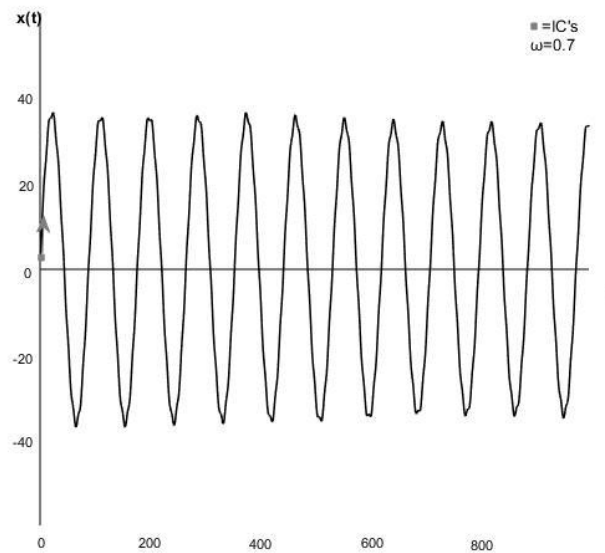


Figure 5.51: Position curve for the base-case system with  $\omega=0,7$ .

### 5.5.7 $\omega = 0,8$

Figures 5.52 and 5.53 show the development of the base-case system with  $\omega=0,8$  for the first 1000s. Figure 5.52 shows the system in the phase plane. The first revolution is shown to the left in the figure, while to the right the system is shown until  $t=1000s$ . Figure 5.53 shows the system's position curve. The system has periods of approximately 89s.

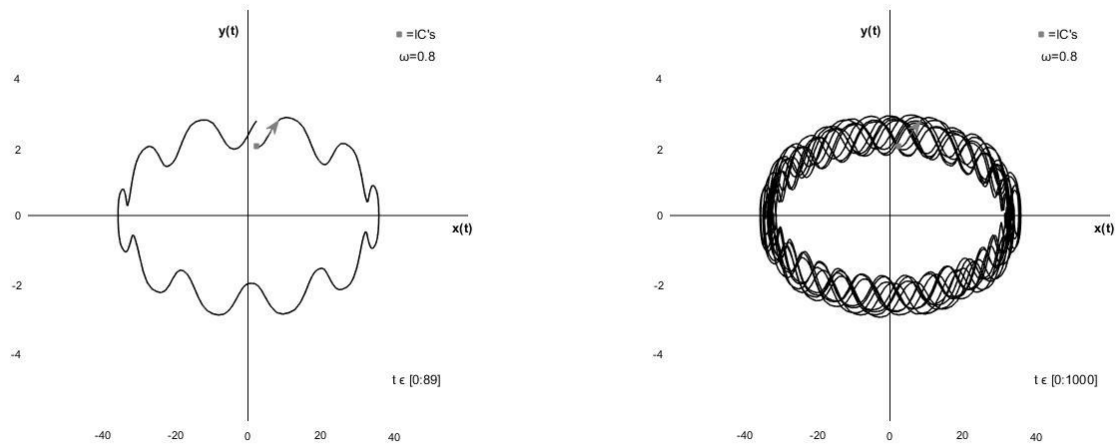


Figure 5.52: Development in the phase plane for the base-case system with  $\omega=0,8$  from  $t=0$  to  $t=89s$ (left) and to  $t=1000s$ (right).

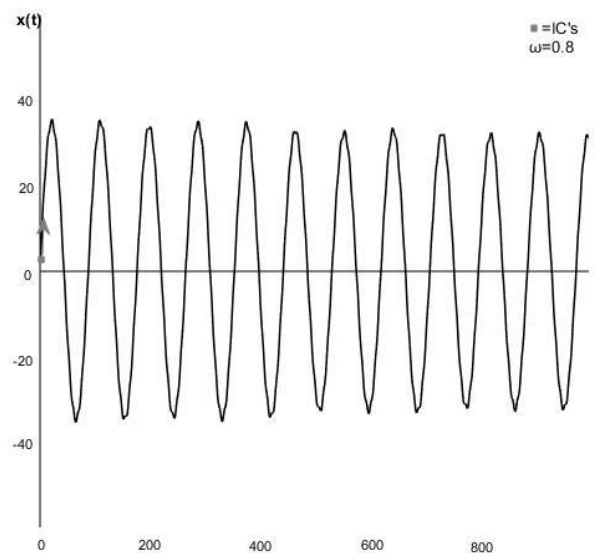


Figure 5.53: Position curve for the base-case system with  $\omega=0,8$ .

### 5.5.8 $\omega = 0,9$

Figures 5.54 and 5.55 show the development of the base-case system with  $\omega=0,9$  for the first 1000s. Figure 5.54 shows the system in the phase plane. The first revolution is shown to the left in the figure, while to the right the system is shown until  $t=1000$ s. Figure 5.55 shows the system's position curve. The system has periods of approximately 89s.

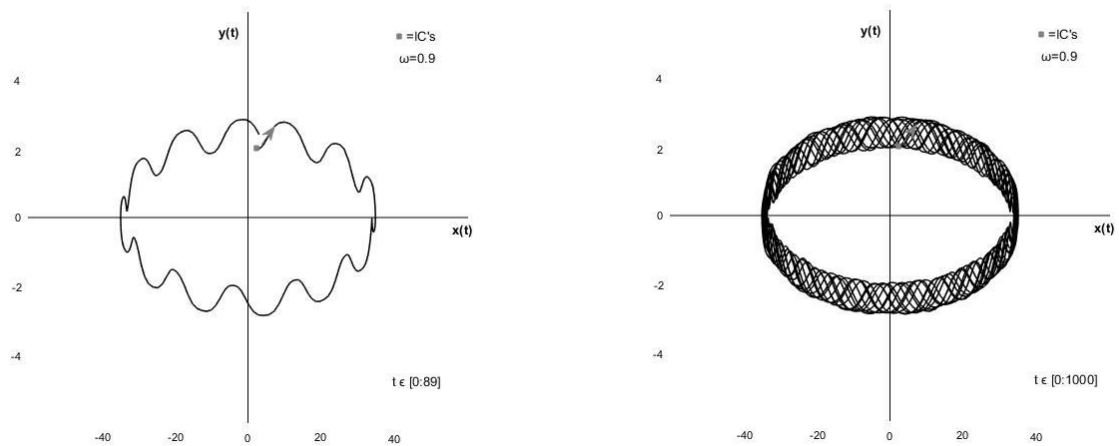


Figure 5.54: Development in the phase plane for the base-case system with  $\omega=0,9$  from  $t=0$  to  $t=89$ s(left) and to  $t=1000$ s(right).

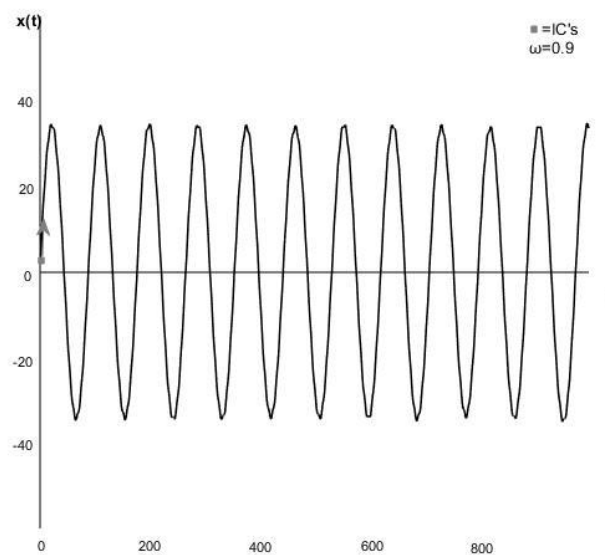


Figure 5.55: Position curve for the base-case system with  $\omega=0,9$ .

### 5.5.9 $\omega = 1,0$

Figures 5.56 and 5.57 show the development of the base-case system with  $\omega=1,0$  for the first 1000s. Figure 5.56 shows the system in the phase plane. The first revolution is shown to the left in the figure, while to the right the system is shown until  $t=1000$ s. Figure 5.57 shows the system's position curve. The system has periods of approximately 89s.

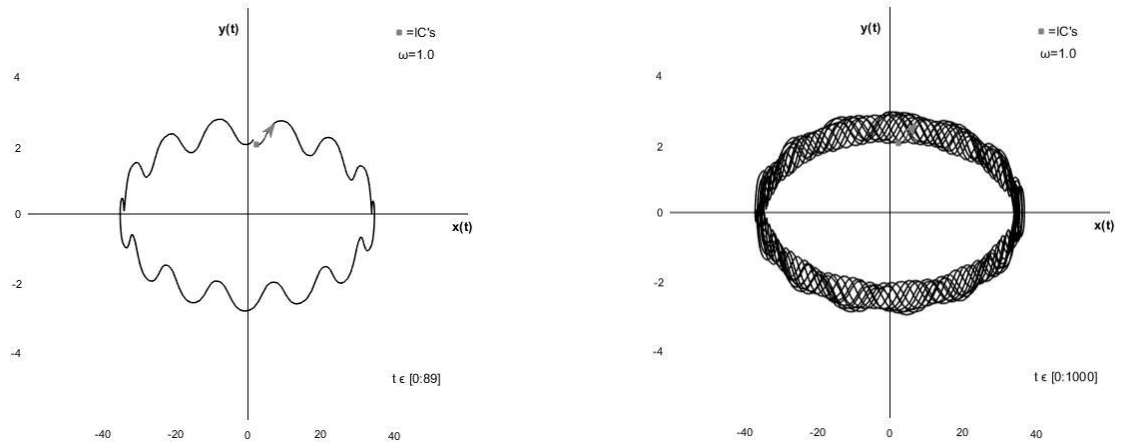


Figure 5.56: Development in the phase plane for the base-case system with  $\omega=1,0$  from  $t=0$  to  $t=89$ s(left) and to  $t=1000$ s(right).

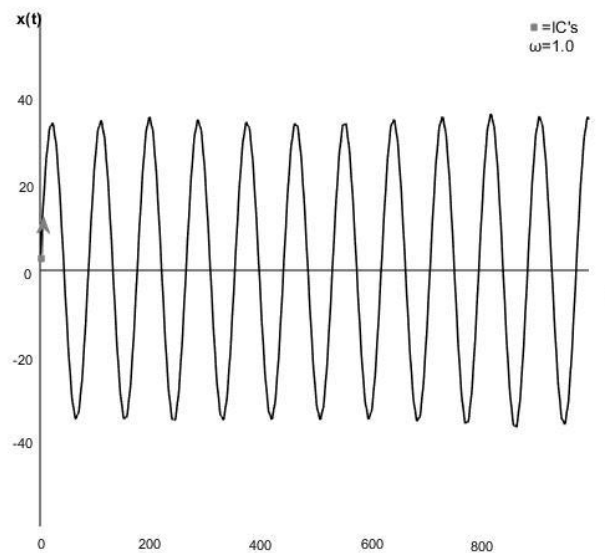


Figure 5.57: Position curve for the base-case system with  $\omega=1,0$ .

### 5.5.10 Conclusion

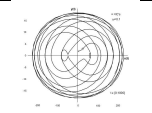
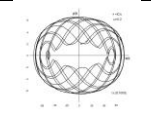
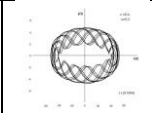
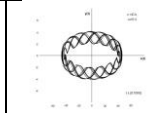


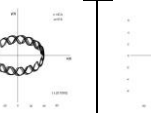
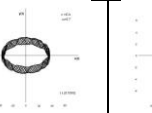
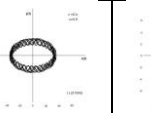
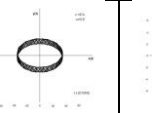

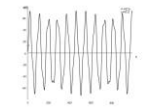
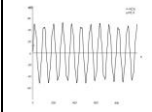
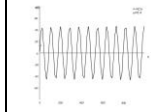
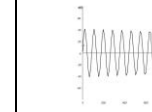
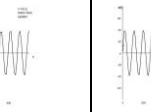
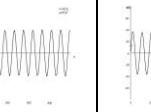
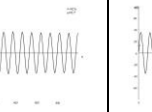

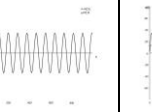
$\omega$	0,1	0,2	0,3	0,4	0,5 (base-case system)	0,6	0,7	0,8	0,9	1,0
Periods	89	89	89	89	89	89	89	89	89	89
$\beta$	1,41	2,83	4,24	5,66	7,07	8,49	9,10	11,31	12,73	14,14
Phase plane diagrams										
Position curves										

Table 5.3: Review of phase plane diagrams and position curves for the base-case system with different values of  $\omega$ .

Table 5.3 shows the phase plane diagrams and position curves for the base-case system with varying values of  $\omega$ . The loading frequency does not affect the period of the system, which remains at 89s. The value of  $\beta$  is shown in the table, and it increases with the increase of the parameter. When  $\omega=0,1$ ,  $\beta=1,41$ , which means the system is close to resonance, i.e. when  $\omega=\omega_0$ . Because of this, the diagrams for this value have larger axes than the rest, and should not be compared directly with the other diagrams in the table. The axes are also different for the system with  $\omega=0,2$ . The diagrams for the other values of  $\omega$  show that the amplitudes decrease as the parameter is increased. From the phase plane diagrams, it is seen that also the velocities decrease as the loading frequency is increased. The decrease in amplitudes is most visible for the lower values of  $\omega$ , which are closer to resonance. When  $\omega$  is increased, the effect of the nonlinear forcing term decreases.

## 5.6 Varying the mass parameter, $m$ .

The last parameter to be varied is that of the mass,  $m$ , which will be varied from 50 to 150. The mass coefficient will also, in the end of this chapter, be set to very small values, to look at what happens with the base-case system at resonance. The original value of  $m$  in the base-case system is 100.

### 5.6.1 $m=50$

Figures 5.58 and 5.59 show the development of the base-case system with  $m=50$  for the first 1000s. Figure 5.58 shows the system in the phase plane. The first revolution is shown to the left in the figure, while to the right the system is shown until  $t=1000$ s. Figure 5.59 shows the system's position curve. The system has periods of approximately 63s.

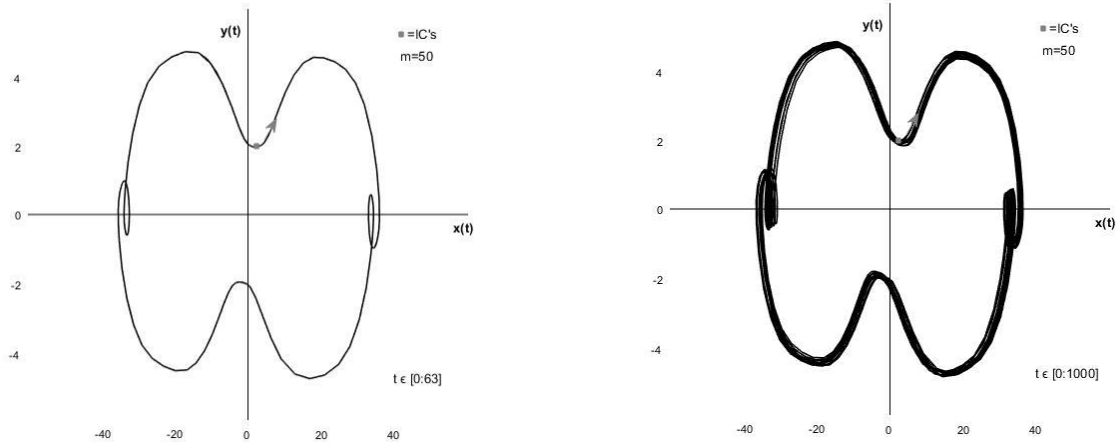


Figure 5.58: Development in the phase plane for the base-case system with  $m=50$  from  $t=0$  to  $t=63$ s(left) and to  $t=1000$ s(right).

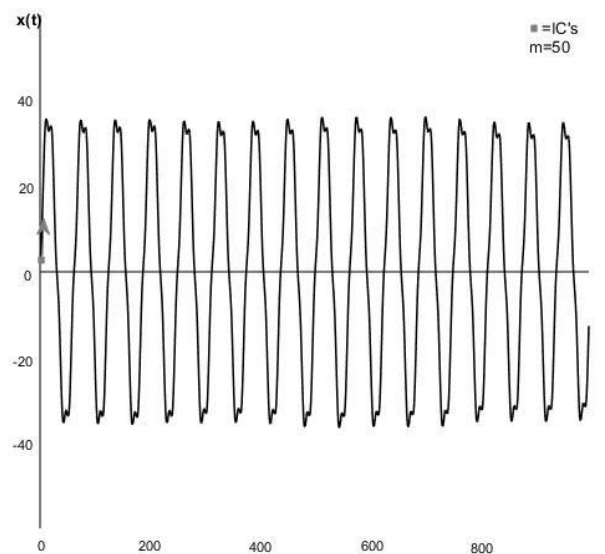


Figure 5.59: Position curve for the base-case system with  $m=50$ .



## 5.6.2 $m=60$

Figures 5.60 and 5.61 show the development of the base-case system with  $m=60$  for the first 1000s. Figure 5.60 shows the system in the phase plane. The first revolution is shown to the left in the figure, while to the right the system is shown until  $t=1000$ s. Figure 5.61 shows the system's position curve. The system has periods of approximately 69s.

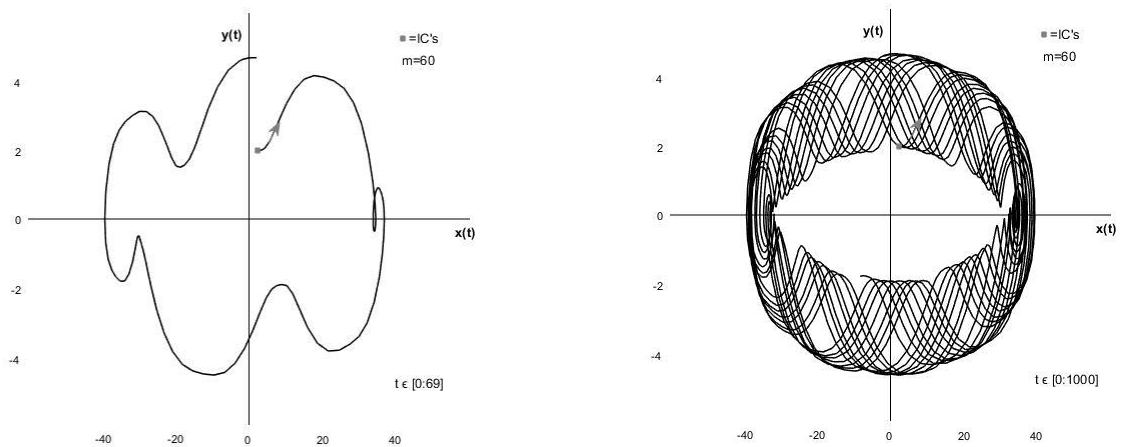


Figure 5.60: Development in the phase plane for the base-case system with  $m=60$  from  $t=0$  to  $t=69$ s(left) and to  $t=1000$ s(right).

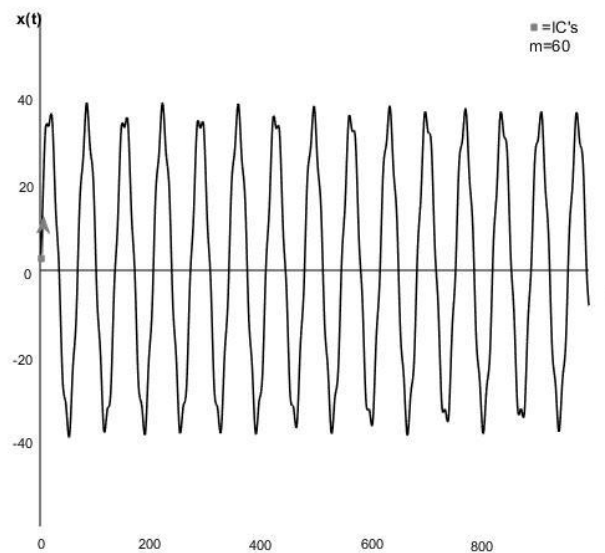


Figure 5.61: Position curve for the base-case system with  $m=60$ .

### 5.6.3 $m=70$

Figures 5.62 and 5.63 show the development of the base-case system with  $m=70$  for the first 1000s. Figure 5.62 shows the system in the phase plane. The first revolution is shown to the left in the figure, while to the right the system is shown until  $t=1000$ s. Figure 5.63 shows the system's position curve. The system has periods of approximately 74s.

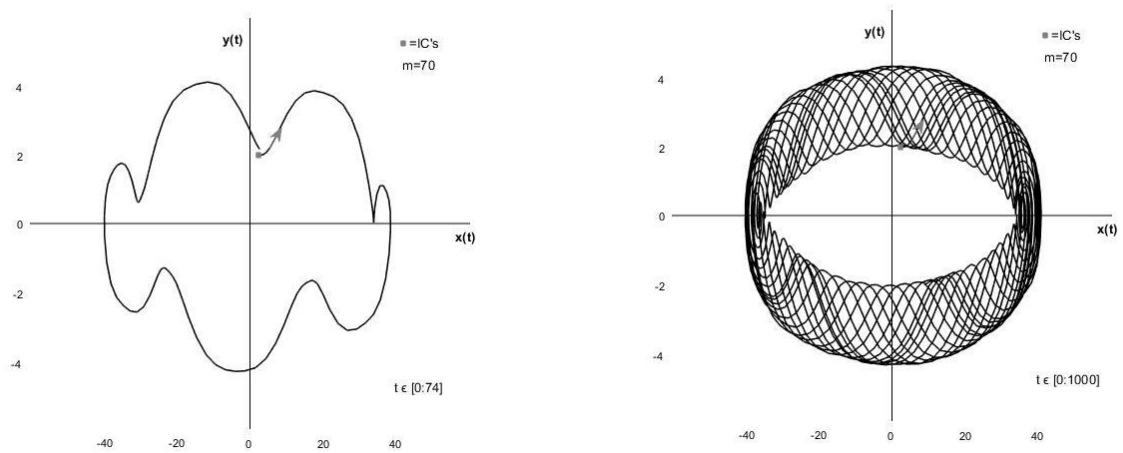


Figure 5.62: Development in the phase plane for the base-case system with  $m=60$  from  $t=0$  to  $t=74$ s(left) and to  $t=1000$ s(right).

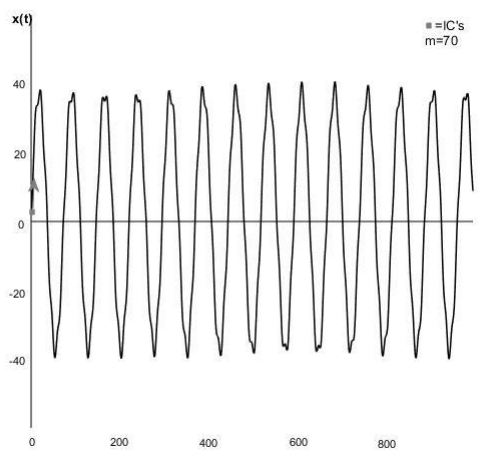


Figure 5.63: Position curve for the base-case system with  $m=70$ .

### 5.6.4 $m=80$

Figures 5.64 and 5.65 show the development of the base-case system with  $m=80$  for the first 1000s. Figure 5.64 shows the system in the phase plane. The first revolution is shown to the left in the figure, while to the right the system is shown until  $t=1000$ s. Figure 5.65 shows the system's position curve. The system has periods of approximately 80s.

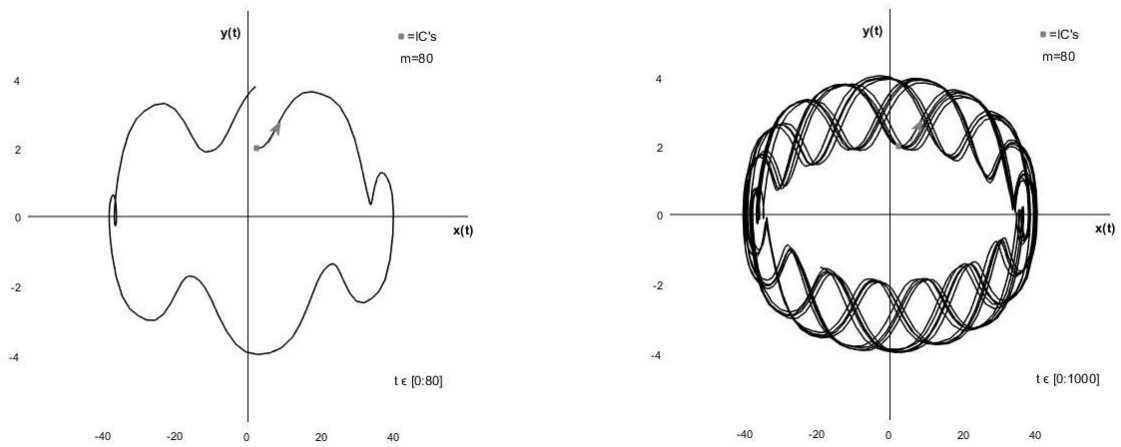


Figure 5.64: Development in the phase plane for the base-case system with  $m=80$  from  $t=0$  to  $t=80$ s(left) and to  $t=1000$ s(right).

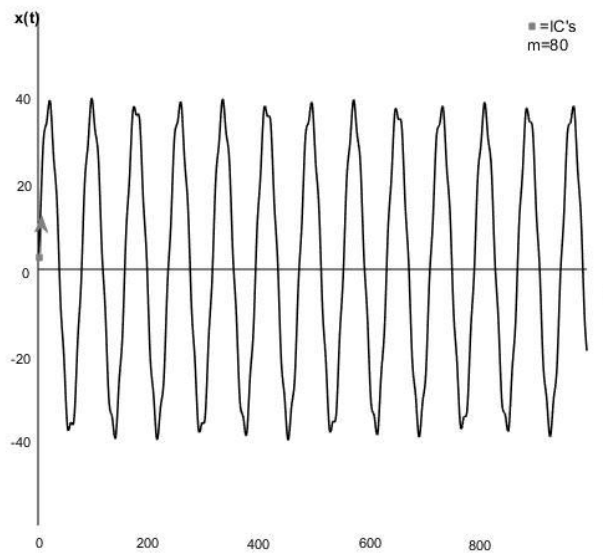


Figure 5.65: Position curve for the base-case system with  $m=80$ .

### 5.6.5 $m=90$

Figures 5.66 and 5.67 show the development of the base-case system with  $m=90$  for the first 1000s. Figure 5.66 shows the system in the phase plane. The first revolution is shown to the left in the figure, while to the right the system is shown until  $t=1000$ s. Figure 5.67 shows the system's position curve. The system has periods of approximately 84s.

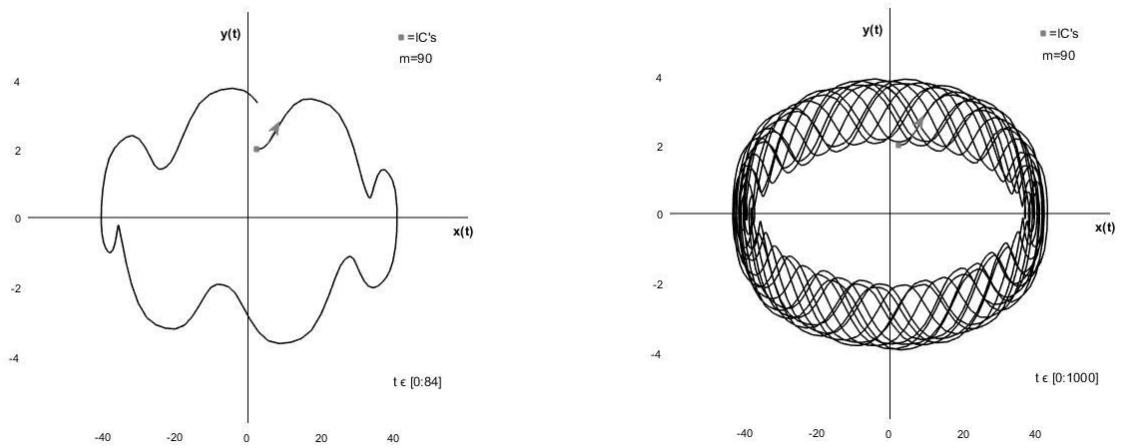


Figure 5.66: Development in the phase plane for the base-case system with  $m=90$  from  $t=0$  to  $t=84$ s(left) and to  $t=1000$ s(right).

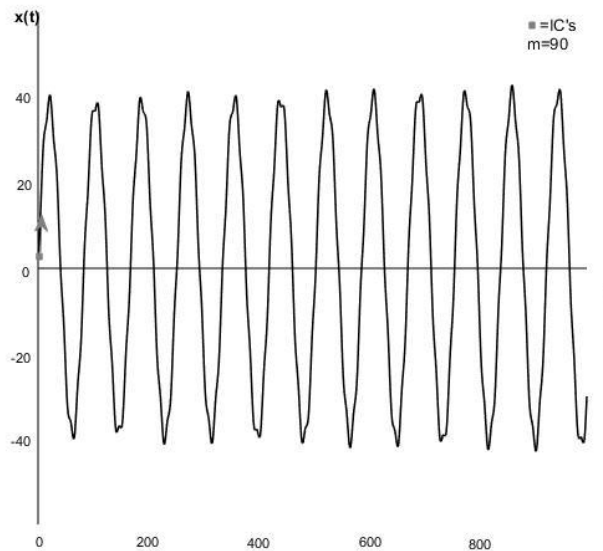


Figure 5.67: Position curve for the base-case system with  $m=90$ .

### 5.6.6 $m=110$

Figures 5.68 and 5.69 show the development of the base-case system with  $m=110$  for the first 1000s. Figure 5.68 shows the system in the phase plane. The first revolution is shown to the left in the figure, while to the right the system is shown until  $t=1000$ s. Figure 5.69 shows the system's position curve. The system has periods of approximately 94s.

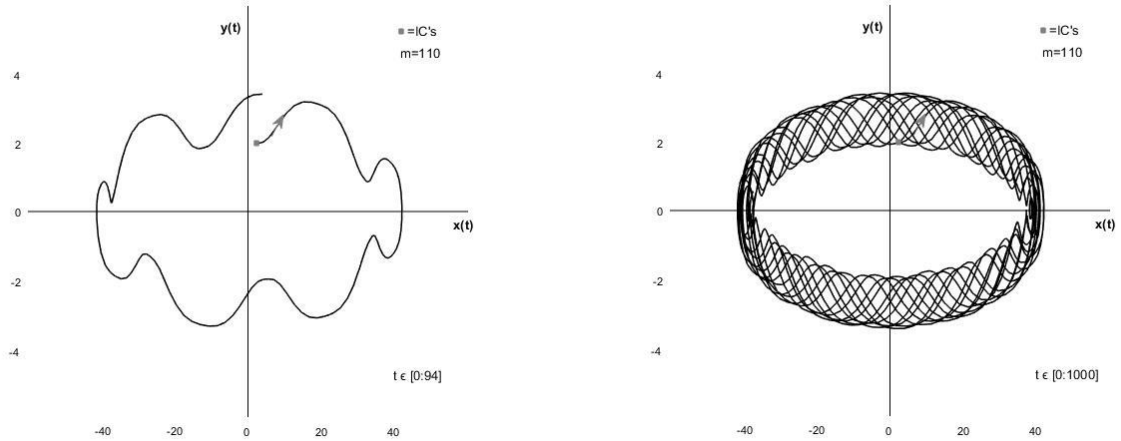


Figure 5.68: Development in the phase plane for the base-case system with  $m=110$  from  $t=0$  to  $t=94$ s(left) and to  $t=1000$ s(right).

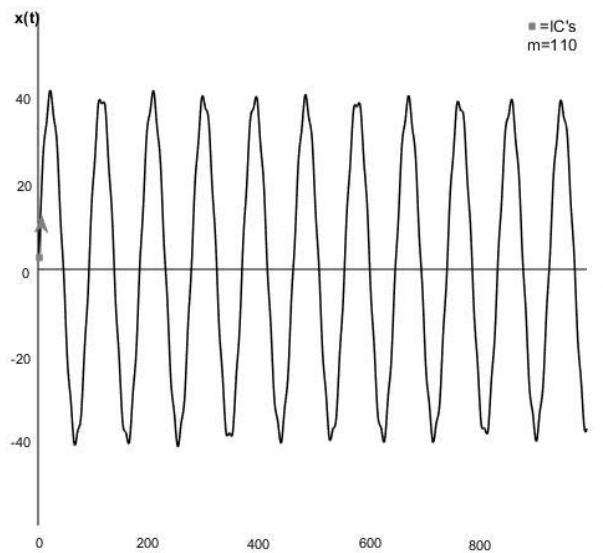


Figure 5.69: Position curve for the base-case system with  $m=110$ .

### 5.6.7 $m=120$

Figures 5.70 and 5.71 show the development of the base-case system with  $m=120$  for the first 1000s. Figure 5.70 shows the system in the phase plane. The first revolution is shown to the left in the figure, while to the right the system is shown until  $t=1000$ s. Figure 5.71 shows the system's position curve. The system has periods of approximately 97s.

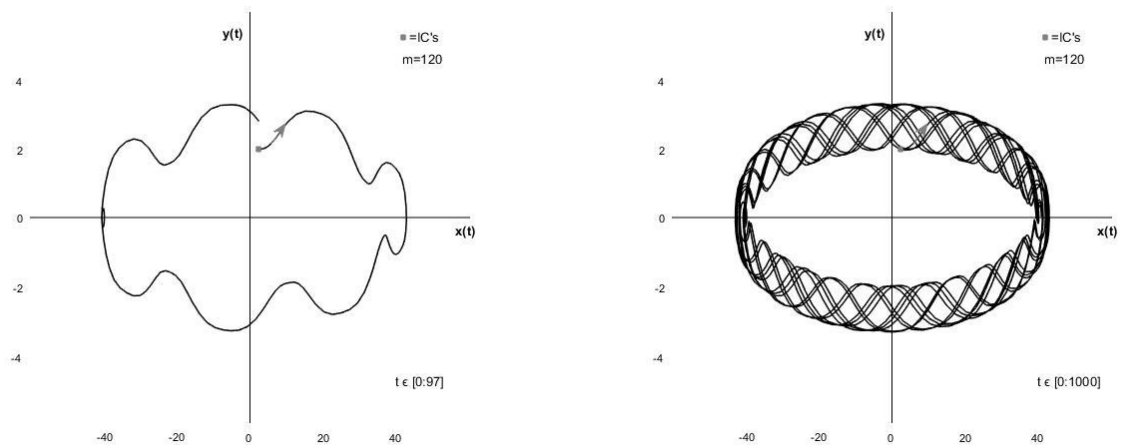


Figure 5.70: Development in the phase plane for the base-case system with  $m=120$  from  $t=0$  to  $t=97$ s(left) and to  $t=1000$ s(right).

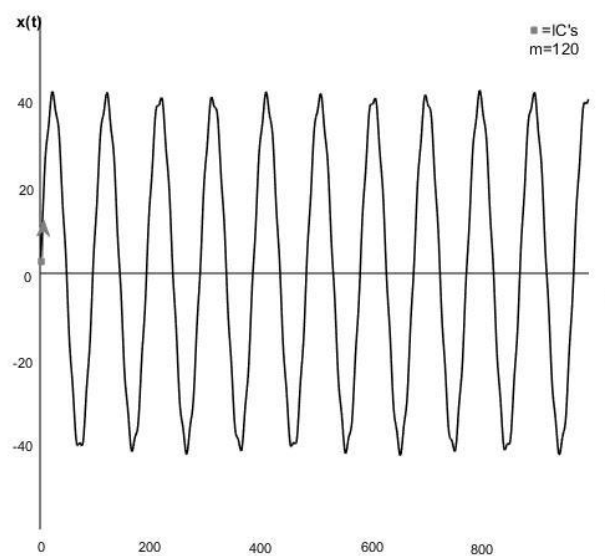


Figure 5.71: Position curve for the base-case system with  $m=120$ .

### 5.6.8 $m=130$

Figures 5.72 and 5.73 show the development of the base-case system with  $m=130$  for the first 1000s. Figure 5.72 shows the system in the phase plane. The first revolution is shown to the left in the figure, while to the right the system is shown until  $t=1000$ s. Figure 5.73 shows the system's position curve. The system has periods of approximately 102s.

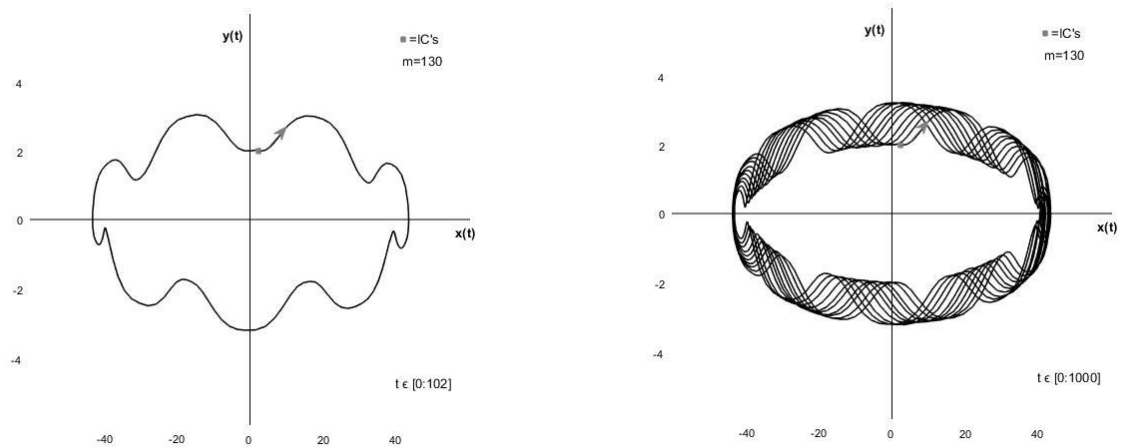


Figure 5.72: Development in the phase plane for the base-case system with  $m=130$  from  $t=0$  to  $t=102$ s(left) and to  $t=1000$ s(right).

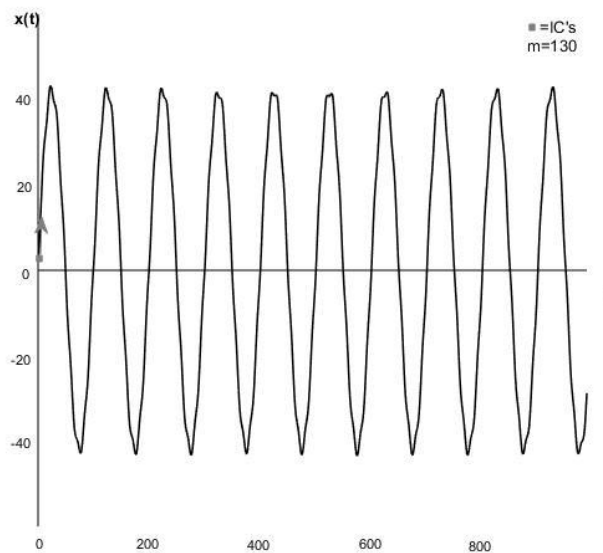


Figure 5.73: Position curve for the base-case system with  $m=130$ .

### 5.6.9 $m=140$

Figures 5.74 and 5.75 show the development of the base-case system with  $m=140$  for the first 1000s. Figure 5.74 shows the system in the phase plane. The first revolution is shown to the left in the figure, while to the right the system is shown until  $t=1000$ s. Figure 5.75 shows the system's position curve. The system has periods of approximately 105.

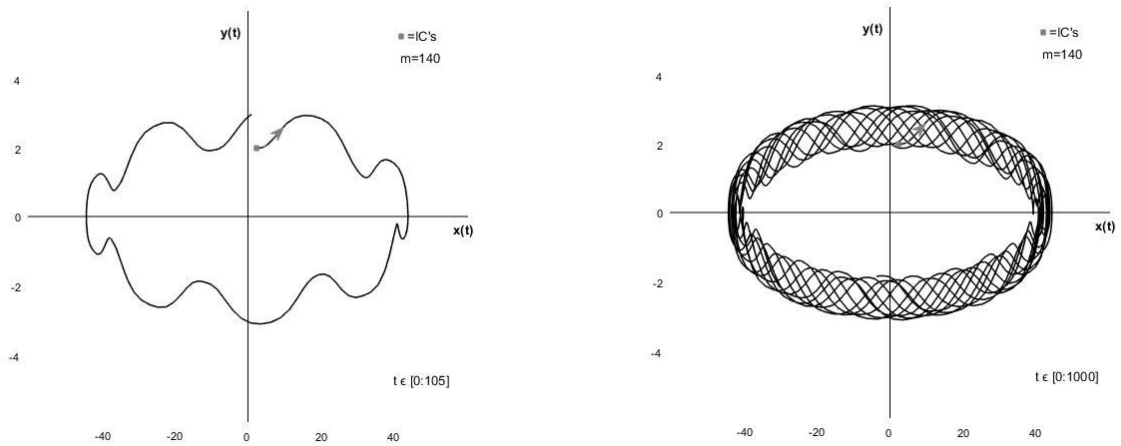


Figure 5.74: Development in the phase plane for the base-case system with  $m=140$  from  $t=0$  to  $t=105$ s(left) and to  $t=1000$ s(right).

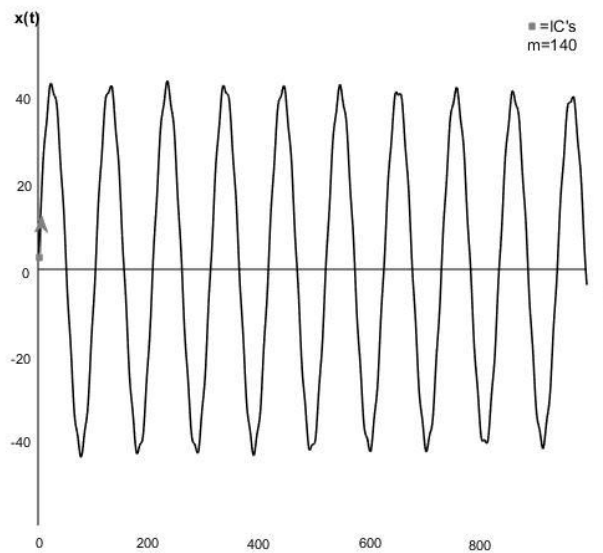
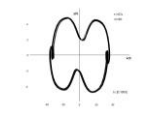
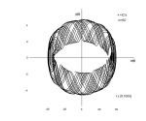
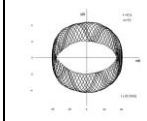
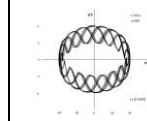
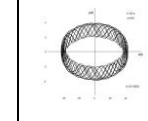
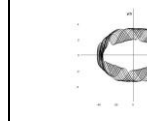

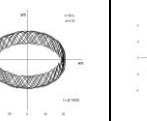
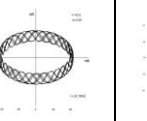
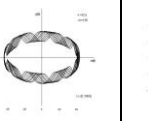
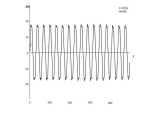
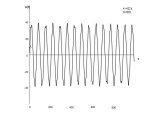
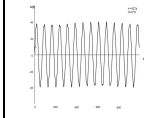
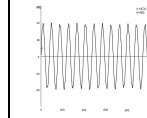
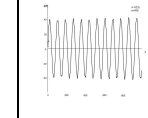
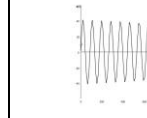
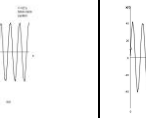
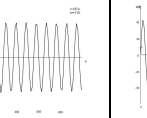
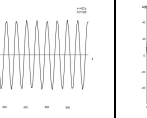
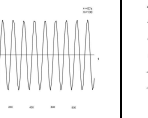


Figure 5.75: Position curve for the base-case system with  $m=140$ .



### 5.6.5 Conclusion

<b>m</b>	<b>50</b>	<b>60</b>	<b>70</b>	<b>80</b>	<b>90</b>	<b>100</b> (base-case system)	<b>110</b>	<b>120</b>	<b>130</b>	<b>140</b>
<b>Periods</b>	62	69	74	80	84	89	94	96	102	105
<b><math>\beta</math></b>	5,0	5,48	5,92	6,32	6,71	7,07	7,41	7,75	8,06	8,37
<b>Phase plane diagrams</b>										
<b>Position curves</b>										

*Table 5.4: Review of phase plane diagrams and position curves for the base-case system with different values of  $m$ .*

Table 5.4 shows the phase plane diagrams and position curves for the base-case system with varying values of the mass parameter,  $m$ . Increasing the mass leads to increased periods, and increased value of  $\beta$  for the system. The increase of the mass parameter decreases the amplitude for velocity, but does not seem to affect the position amplitude. When  $m$  is increased, the effect of the nonlinear forcing term is not noticeably different.

## 5.7 The base-case system near resonance

In this part, the parameters will be varied to achieve systems at and near resonance.

### 5.7.1 Varying the mass near resonance

#### 5.7.1.1 $\beta=0,8$

When  $m=1,28$ ,  $\beta=0,8$ . The phase plane diagram is shown to the left in figure 5.76, and the position curve is shown to the right.

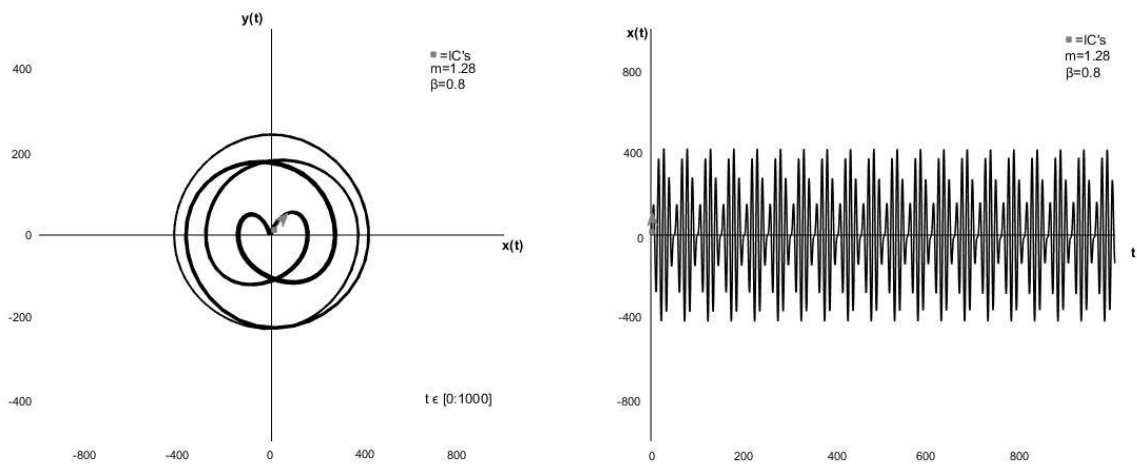


Figure 5.76: Phase plane diagram(left) and position curve(right) for the base-case system with  $m=1,28$ , making  $\beta=0,8$ , from  $t=0$  to  $t=1000s$ .

#### 5.7.1.2 $\beta=0,9$

When  $m=1,62$ ,  $\beta=0,9$ . The phase plane diagram is shown to the left in figure 5.77, and the position curve is shown to the right.

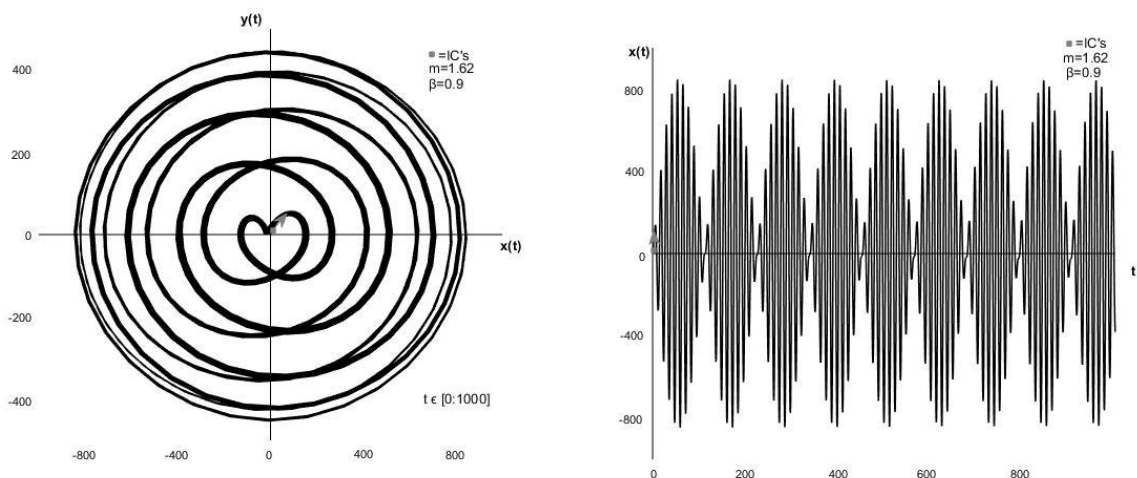


Figure 5.77: Phase plane diagram(left) and position curve(right) for the base-case system with  $m=1,62$ , making  $\beta=0,9$ , from  $t=0$  to  $t=1000s$ .

### 5.7.1.3 $\beta=1,0$

When  $m=2$ ,  $\beta=1$ , which means that the system is at resonance. The system is shown in the phase plane to the left in figure 5.78, while the position curve is shown to the right.

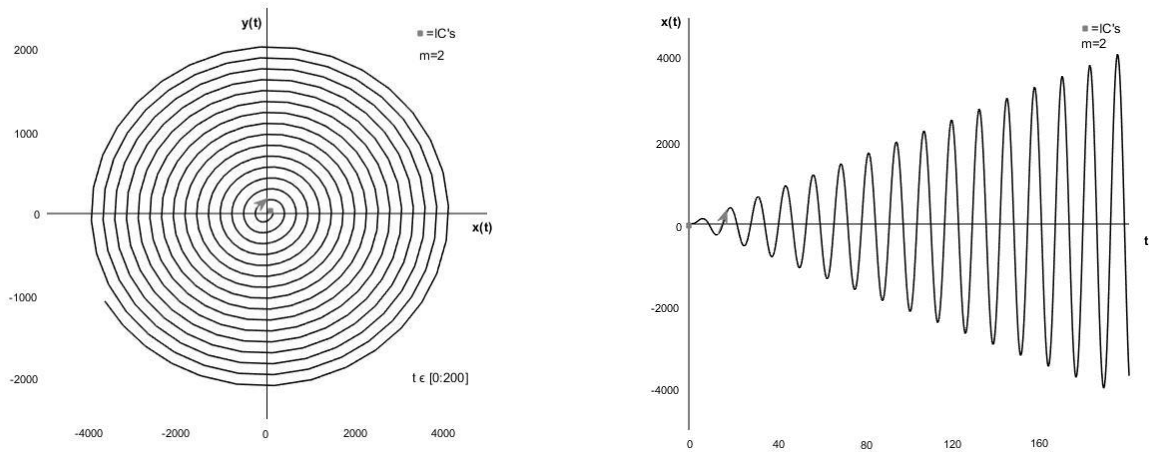


Figure 5.78: Development in the phase plane(left) and position curve(right) for the base-case with  $m=2$  from  $t=0$  to  $t=200s$ .

### 5.7.1.4 $\beta=1,1$

When  $m=2,42$ ,  $\beta=1,1$ . The phase plane diagram is shown to the left in figure 5.79, and the position curve is shown to the right.

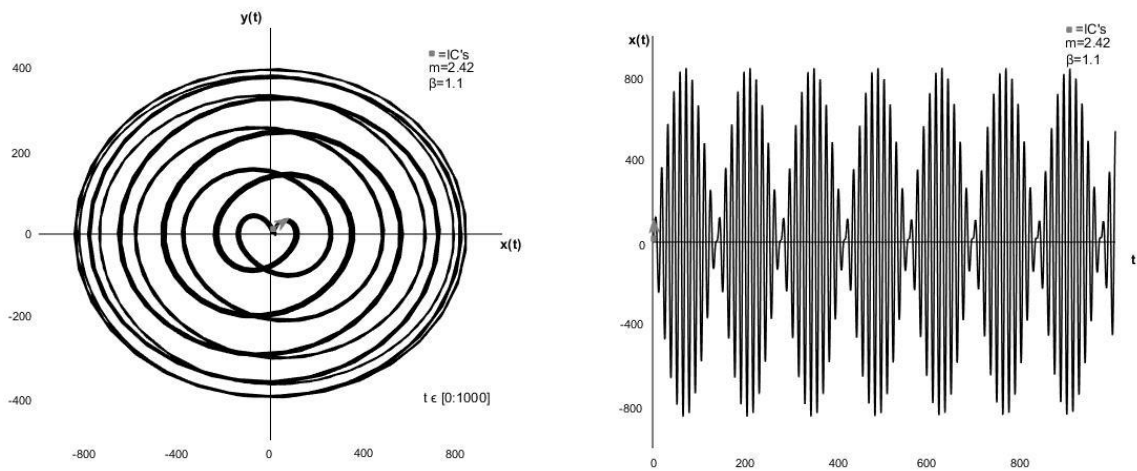


Figure 5.79: Phase plane diagram for the base-case system with  $m=2,42$ , making  $\beta=1,1$ , from  $t=0$  to  $t=1000s$ .

### 5.7.1.5 $\beta=1,2$

When  $m=2,88$ ,  $\beta=1,2$ . The phase plane diagram is shown to the left in figure 5.80, and the position curve is shown to the right.

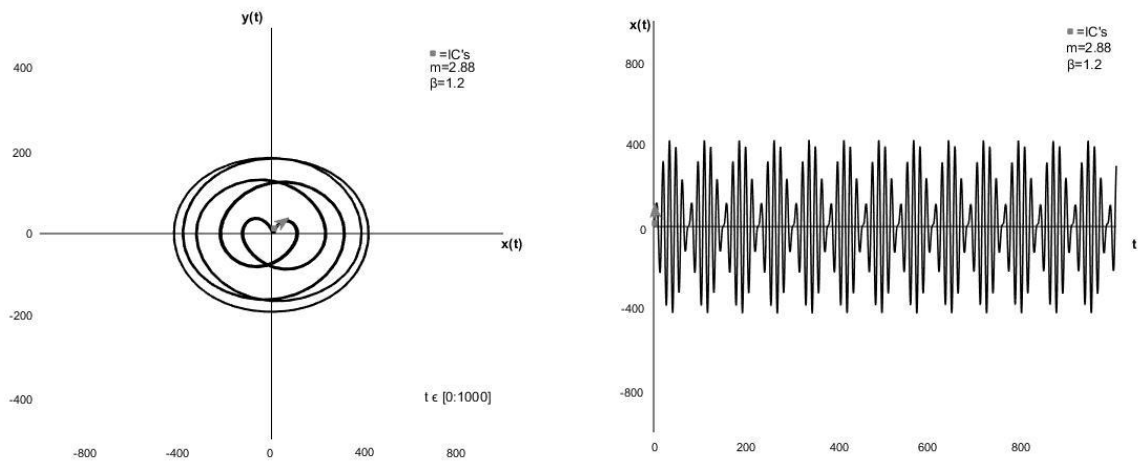


Figure 5.80: Phase plane diagram for the base-case system with  $m=2,88$ , making  $\beta=1,2$ , from  $t=0$  to  $t=1000$ s.

## 5.7.2 Varying the loading frequency, $\omega$ , near resonance

### 5.7.2.1 $\beta=0,8$

When  $\omega=0,057$ ,  $\beta=0,8$ . The phase plane diagram is shown to the left in figure 5.81, and the position curve is shown to the right.

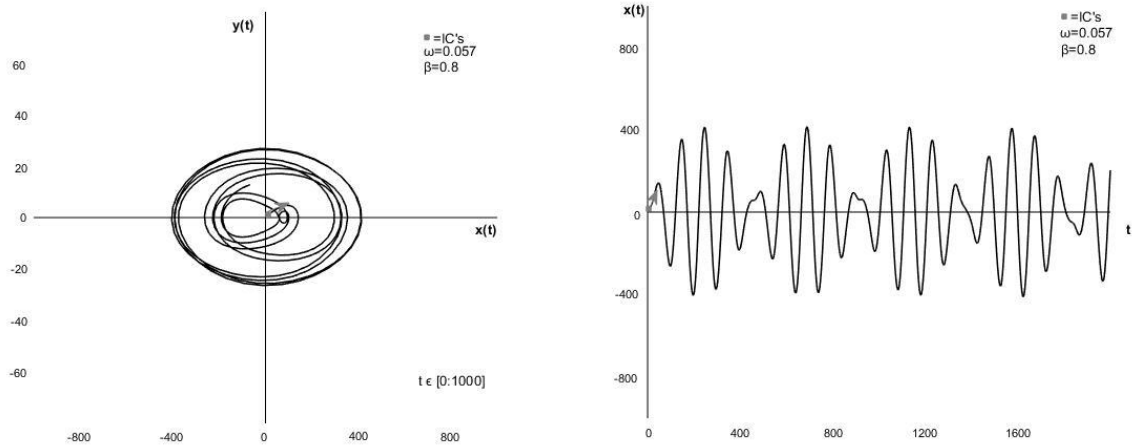


Figure 5.81: Phase plane diagram(left) and position curve(right) for the base-case system with  $\omega=0,057$ , making  $\beta=0,8$ , from  $t=0$  to  $t=1000s$ .

### 5.7.2.2 $\beta=0,9$

When  $\omega=0,064$ ,  $\beta=0,9$ . The phase plane diagram is shown to the left in figure 5.82, and the position curve is shown to the right.

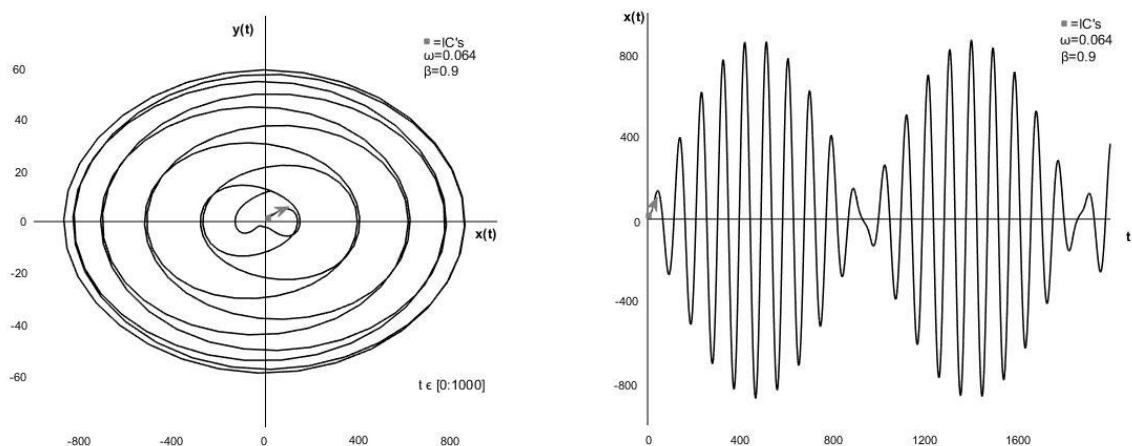


Figure 5.82: Phase plane diagram(left) and position curve(right) for the base-case system with  $\omega=0,064$ , making  $\beta=0,9$ , from  $t=0$  to  $t=1000s$ .

### 5.7.2.3 $\beta=1,0$

When  $\omega=0,071$ ,  $\beta=1$ , which means that the system is at resonance. The system is shown in the phase plane on the left in figure 5.83, while the position curve is showed to the right.

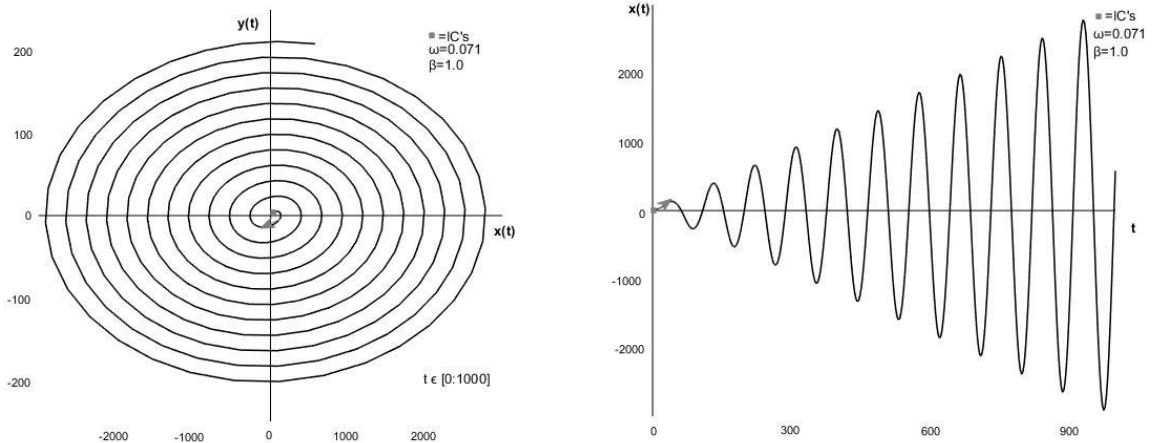


Figure 5.83: Phase plane diagram(left) and position curve(right) for the base-case with  $\omega=0,071$ , making the system at resonance, from  $t=0$  to  $t=1000s$ .

### 5.7.2.4 $\beta=1,1$

When  $\omega=0,078$ ,  $\beta=1,1$ . The phase plane diagram is shown to the left in figure 5.84, and the position curve is shown to the right.

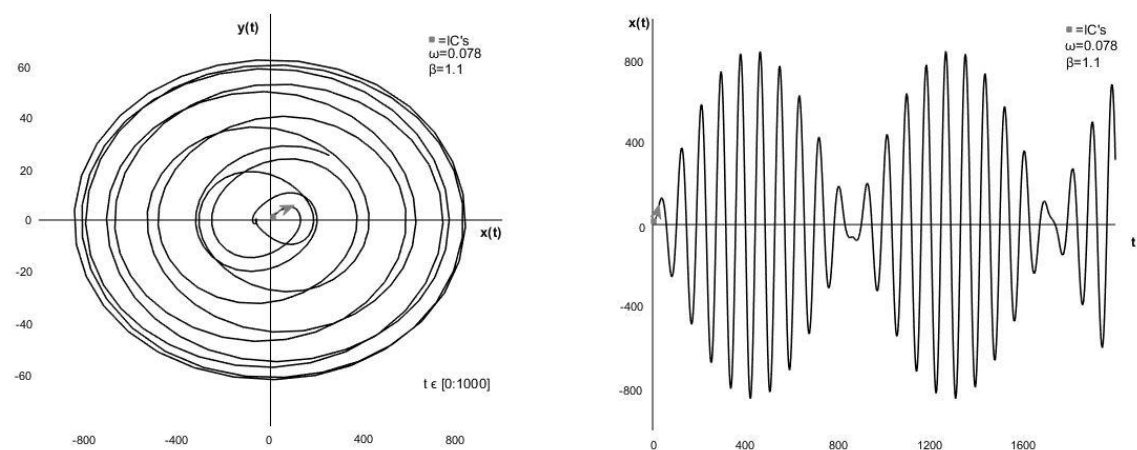


Figure 5.84: Phase plane diagram(left) and position curve(right) for the base-case system with  $\omega=0,078$ , making  $\beta=1,1$ , from  $t=0$  to  $t=1000s$ .

### 5.7.2.5 $\beta=1,2$

When  $\omega=0,085$ ,  $\beta=1,2$ . The phase plane diagram is shown to the left in figure 5.85, and the position curve is shown to the right.

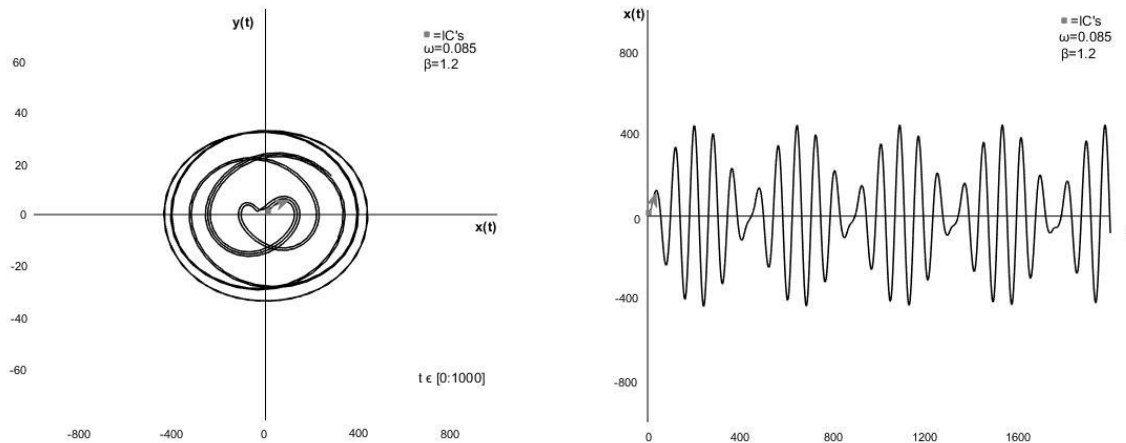


Figure 5.85: Phase plane diagram(left) and position curve(right) for the base-case system with  $\omega=0,081$ , making  $\beta=1,2$ , from  $t=0$  to  $t=1000s$ .

### 5.7.3 Conclusion

Tables 5.5 and 5.6 show the phase plane diagrams and position curves for the base-case system at and near resonance. Table 5.5 shows the system with different values of the mass parameter,  $m$ , and table 5.6 shows the system with different values of the frequency parameter,  $\omega$ . It should be noted that the axes are not the same in the two tables. The axes are also different for the diagrams at resonance, i.e.  $\beta=1,0$ , compared to those near resonance in each table. This is due to the rapid growth when the system reaches resonance, making the axes too large. Higher order resonances;  $\beta=1/3$  and  $\beta=1/2$  will be discussed in chapter 9.

The tables show that the systems go in a steady path of increase and decrease in both position and velocity as the parameters are set to values near resonance. The position and velocity amplitudes increase as  $\beta$  gets larger, up until  $\beta=1,0$ . At resonance, i.e.  $\beta=1,0$ , both systems experience an unlimited growth in both velocity and position. When the parameters,  $m$  and  $\omega$ , are increased making systems with  $\beta>1,0$ , the systems go back to the steady path of increase and decrease in amplitudes. The increase of  $\beta$  after  $\beta=1,0$ , decreases the position and velocity amplitudes. The phase plane diagrams show that the values over and under resonance values are very similar to each other.

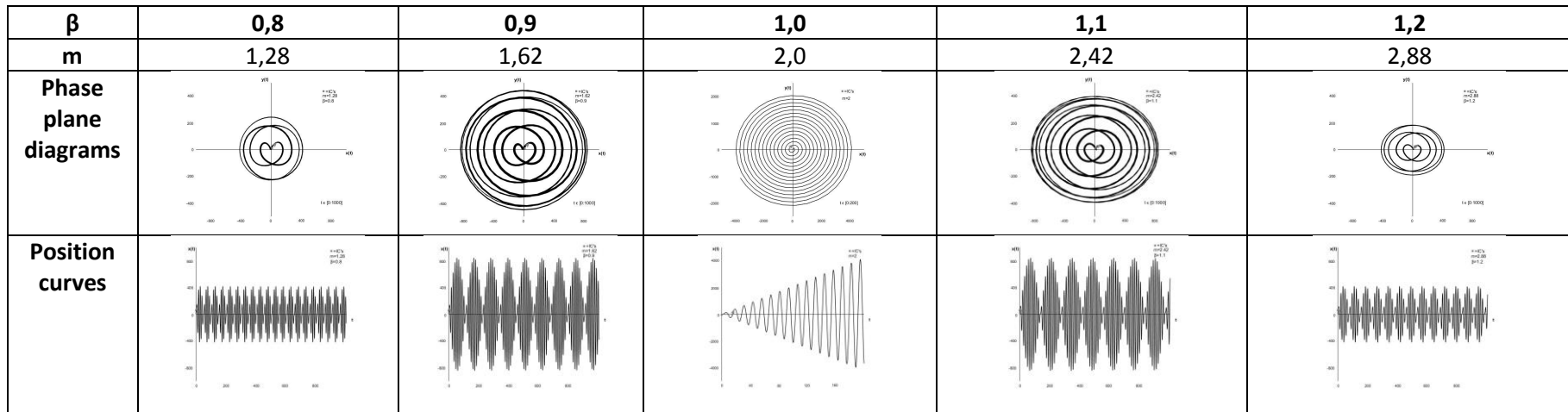


Table 5.5: Review of phase plane diagrams and position curves for the base-case system with different values of  $m$ , making the system near resonance.

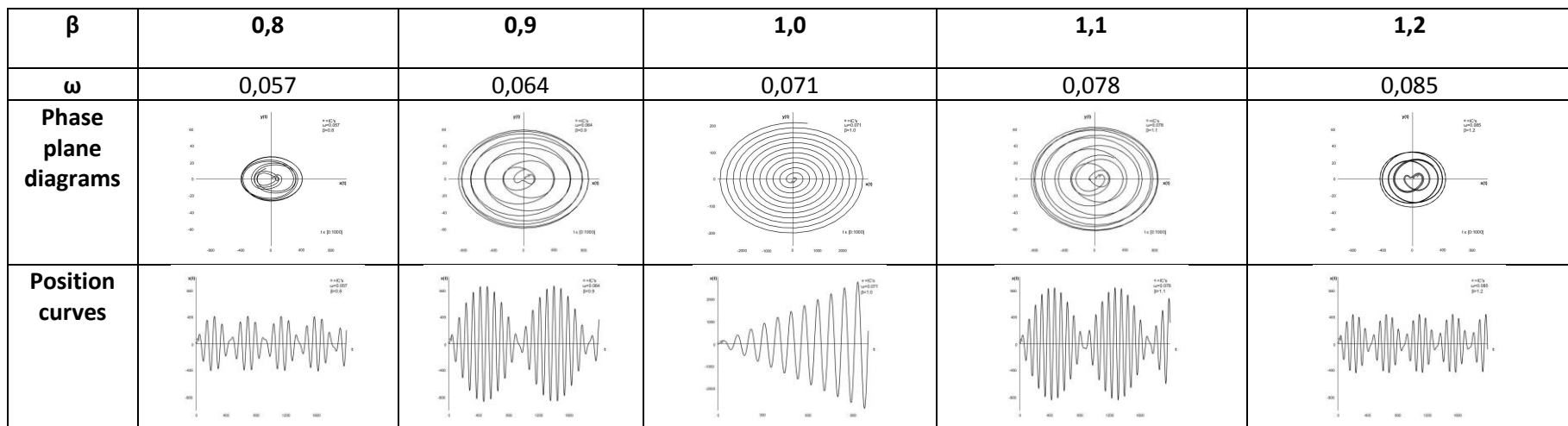


Table 5.6: Review of phase plane diagrams and position curves for the base-case system with different values of  $\omega$ , making the system near resonance.



## 5.8 Conclusion

This chapter started with an introduction of a system we termed “the base-case system”. This system was selected more or less randomly, however, it should be representative for the nonlinear effects we are considering within this thesis. A parameter study was conducted, where each parameter was varied separately, while all other parameters were held equal to the values in the base-case system. In addition, the mass and the loading frequency were set to values making systems close to and at resonance, i.e.  $\beta=1,0$ . The following are the results of the analysis:

- When the stiffness parameter,  $k$ , is increased, the periods decrease, the position amplitude decrease (which is expected also for a static system<sup>9</sup>, while the velocity amplitudes are not affected. The effect of the nonlinearity in the forcing term is decreased as  $k$  is increased.
- The increase of the amplitude parameter,  $F_0$ , does not affect the period, while both the position and velocity amplitude is increased. The effect of the nonlinearity increases as  $F_0$  is increased.
- The loading frequency,  $\omega$ , does not affect the period (notice that this system is undamped, making the systems natural frequency important). Some decrease in the position and velocity amplitude were noticed when  $\omega$  was increased. This was most visible in the lower values of  $\omega$ , where the systems were closer to resonance. The increase of  $\omega$  shows that the effect of the nonlinearity in the forcing term decreases.
- When the mass parameter,  $m$ , was increased, the periods increased as the natural frequency  $\omega_0$  of the system varies. The position amplitudes do not seem to be affected, while a little decrease in velocity amplitude was observed. The variation of the mass parameter does not seem to affect the nonlinearity caused by the forcing term.
- When the system’s mass or loading frequency is increased to values making systems close to resonance, i.e.  $\omega=\omega_0$ , the systems’ position and velocity amplitudes increase as  $\beta$  gets larger, up until  $\beta=1,0$ . At resonance, i.e.  $\beta=1,0$ , both systems experience an unlimited growth in both velocity and position (note that there is no linear damping in the system). When the parameters are increased over the resonance values the systems go back to the steady path of increase and decrease in amplitudes. The increase of  $\beta$  after  $\beta=1,0$ , decreases the position and velocity amplitudes.

In this chapter, to achieve systems close to and at resonance, both the mass parameter and the loading frequency were varied. Due to the similar effects of these parameter, it has been decided that when looking at the systems at and near resonance in the following of the thesis, only the mass parameter will be varied.

# Chapter 6- Nonlinear forcing term in the equation of motion with linear, constant damping.

As mentioned in the previous chapter, all physical systems have some degree of damping inherent. In this chapter, the base-case system will be presented with damping, as well as some selected systems from the cases where the parameters are changed. The systems at and near resonance will also be presented with damping.

The equation of motion which is considered in this chapter is:

$$m \frac{d^2x}{dt^2} + c \frac{dx}{dt} + kx(t) = F_0 \sin(\omega t) |\sin(\omega t)| \quad (6.1)$$

which is equal to equation (5.1), but with  $c \neq 0$ .

The systems will be presented with two types of constant, linear damping,  $c=0,15$  and  $c=0,5$ . The systems selected is the base-case system, and the lowest and highest cases of each parameter as presented in chapter 5.

Introducing new variable:

$$\xi = \frac{c}{c_c} \quad (6.1)$$

where  $\xi$  is the damping ratio in the system. For the base-case system  $c_c=14,14$ .

## 6.1 Base-case system

The base-case system is shown in the phase plane in figure 6.1 with two values of linear damping,  $c=0,15$  ( $\xi=0,012$ ) on the left and  $c=0,5$  ( $\xi=0,035$ ) on the right. The position curves are shown in figure 6.2.

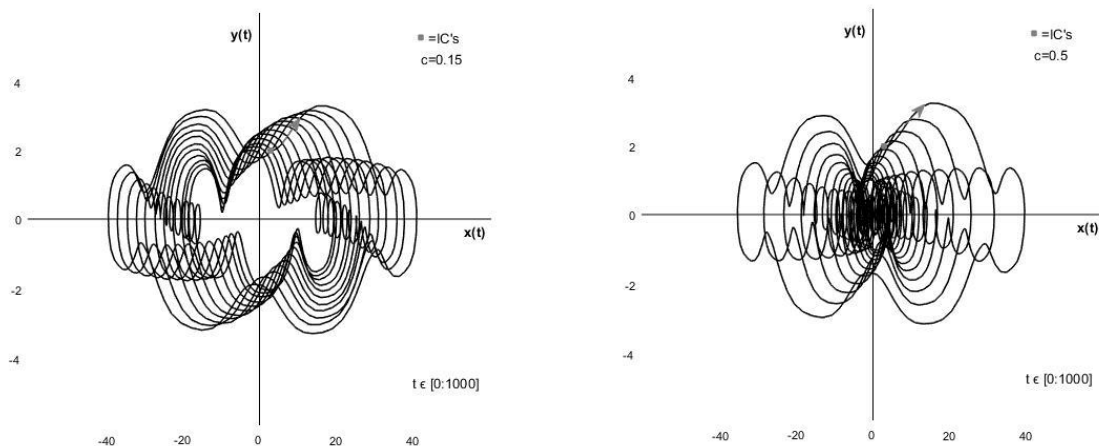


Figure 6.1: Phase plane diagrams for the base-case system with  $c=0,15$ (left) and  $c=0,5$ (right).

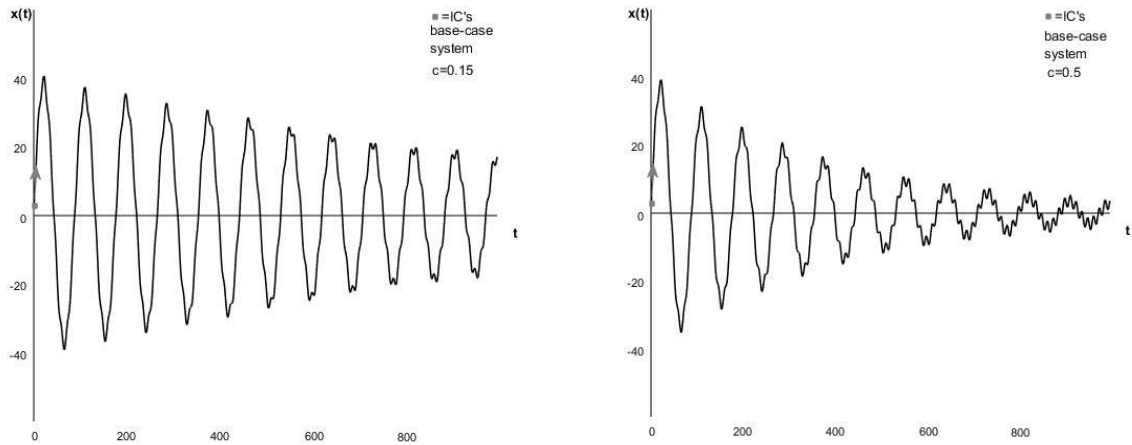


Figure 6.2: Position curves for the base-case system with  $c=0,15$ (left) and  $c=0,5$ (right).

## 6.2 Base-case system with changed stiffness parameter, $k$ .

The base-case system with  $k=0,1$  and  $k=1,0$  is shown in the phase plane in figures 6.3 and 6.5 respectively, with two values of linear damping,  $c=0,15$  on the left and  $c=0,5$  on the right. The position curves are shown in figure 6.4 for the system with  $k=0,1$ . The system is showed with  $c=0,15$  ( $\xi=2,37$ ) to the left, and with  $c=0,5$  ( $\xi=7,91$ ) to the right. The system with  $k=1,0$  is showed in figure 6.6, where  $c=0,15$  ( $\xi=0,75$ ) is showed on the left and  $c=0,5$  ( $\xi=2,5$ ) is showed on the right.

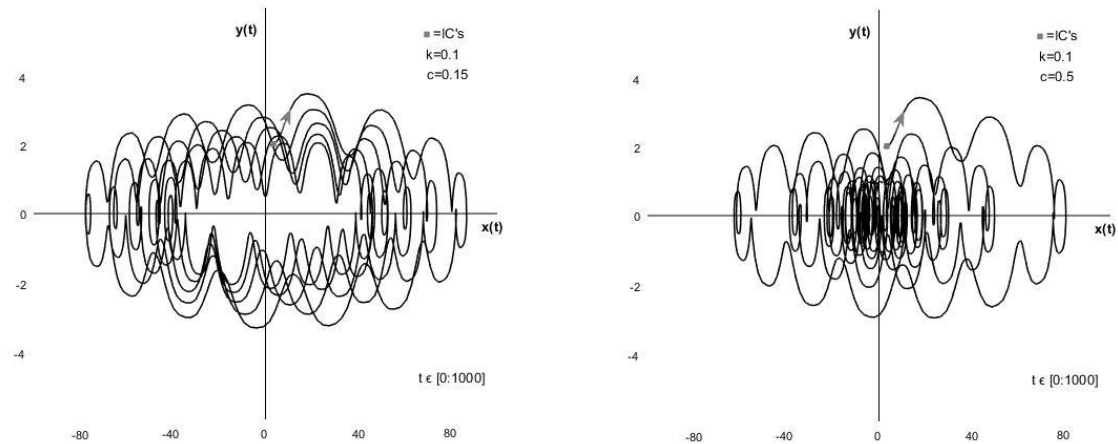


Figure 6.3: Phase plane diagrams for the base-case system with  $k=0,1$ , and  $c=0,15$ (left) and  $c=0,5$ (right).

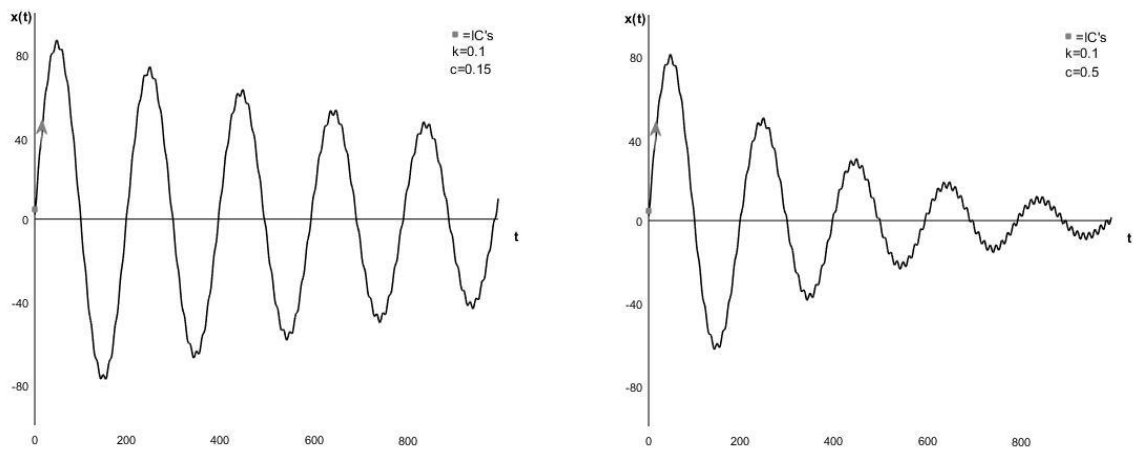


Figure 6.4: Position curves for the base-case system with  $k=0,1$ , and  $c=0,15$ (left) and  $c=0,5$ (right).

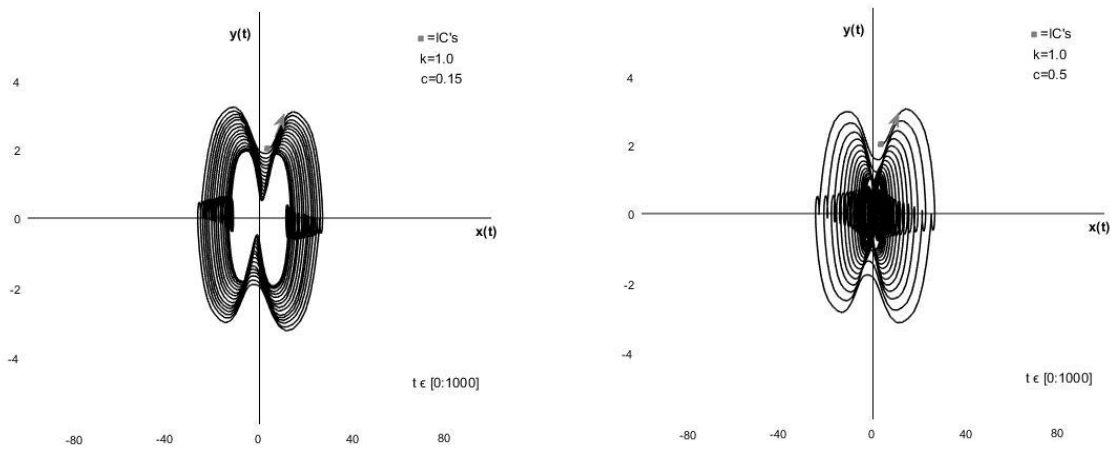


Figure 6.5: Phase plane diagrams for the base-case system with  $k=1,0$ , and  $c=0,15$ (left) and  $c=0,5$ (right).

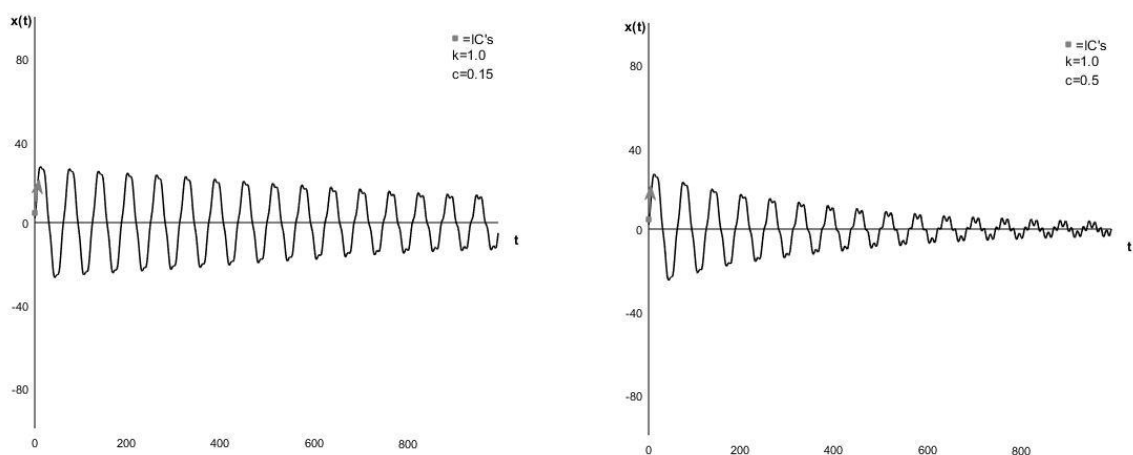


Figure 6.6: Position curves for the base-case system with  $k=1,0$ , and  $c=0,15$ (left) and  $c=0,5$ (right).

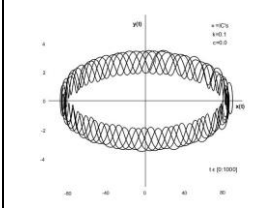
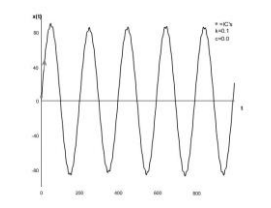
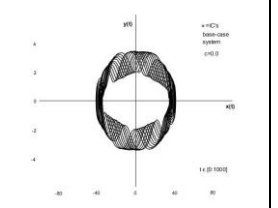
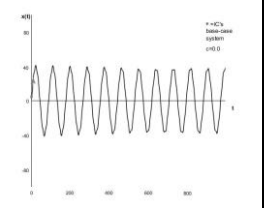
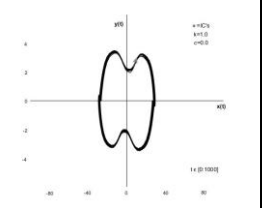
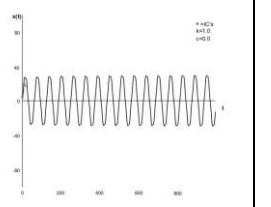
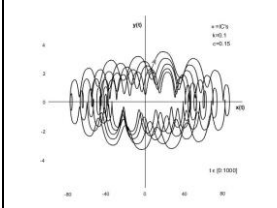
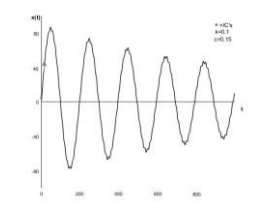
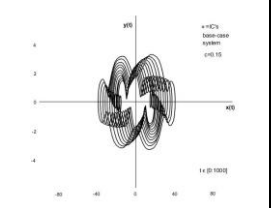
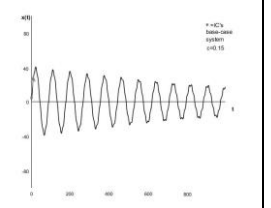
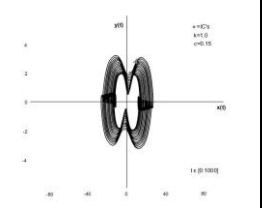
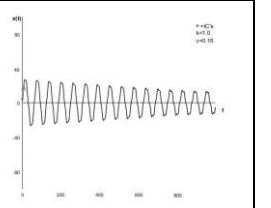
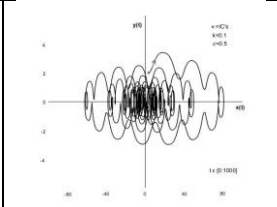
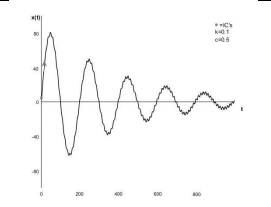
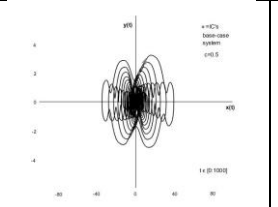
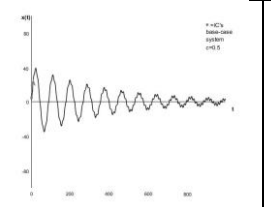
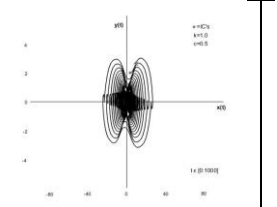
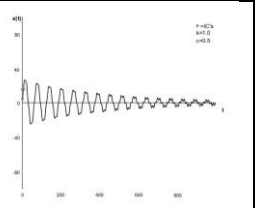
		<b>k</b>					
<b>c</b>	<b>0,1</b> $\beta=15,81$		<b>0,5</b> (base-case system) $\beta=7,07$		<b>1,0</b> $\beta=5,0$		
	Phase plane diagrams	Position curves	Phase plane diagrams	Position curves	Phase plane diagrams	Position curves	
<b>0</b>							
<b>0,15</b>							
<b>0,5</b>							

Table 6.1: Review of phase plane diagrams and position curves for the base-case system with different values of the stiffness parameter,  $k$ , with different values of linear damping,  $c$ .

### 6.3 Base-case system with changed amplitude parameter, $F_0$ .

The base-case system with  $F_0=10$  and  $F_0=100$  is shown in the phase plane in figures 6.7 and 6.9 respectively, with two values of linear damping,  $c=0,15$  on the left and  $c=0,5$  on the right. The position curves are shown in figure 6.8 for the system with  $F_0=10$  and in figure 6.10 for the system with  $F_0=100$ , also with  $c=0,15$  on the left and  $c=0,5$  on the right. The amplitude parameter does not affect the critical damping, making the damping ratio equal to that of the base-case system, namely  $\xi=0,012$  for  $c=0,15$  and  $\xi=0,035$  for  $c=0,5$ .

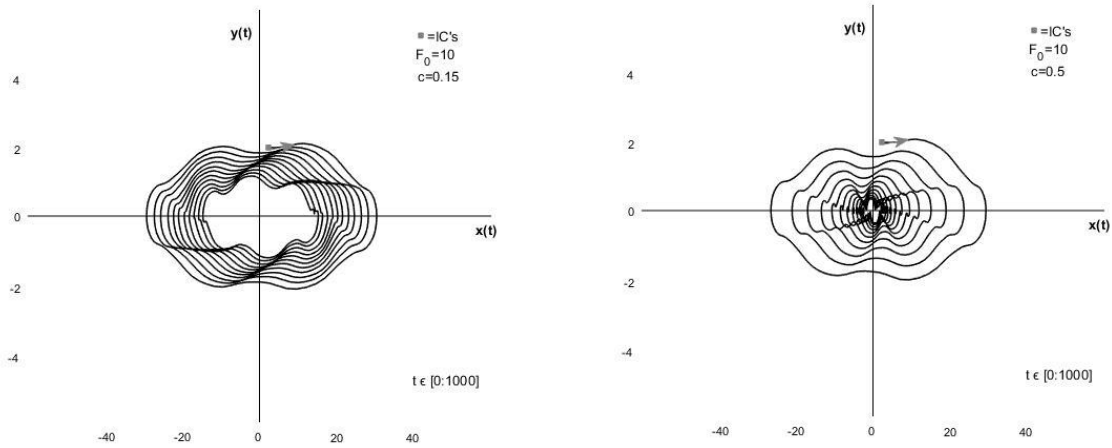


Figure 6.7: Phase plane diagrams for the base-case system with  $F_0=10$ , and  $c=0,15$ (left) and  $c=0,5$ (right).

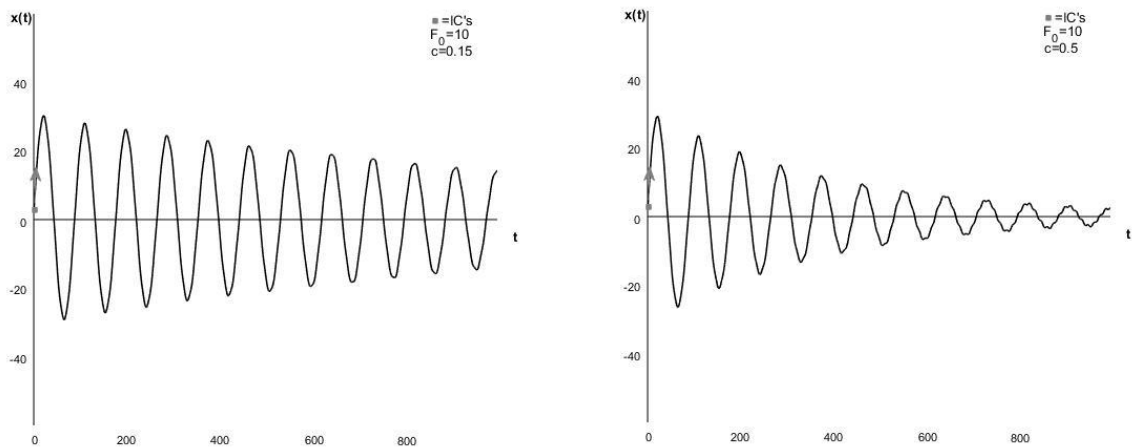


Figure 6.8: Position curves for the base-case system with  $F_0=10$ , and  $c=0,15$ (left) and  $c=0,5$ (right).

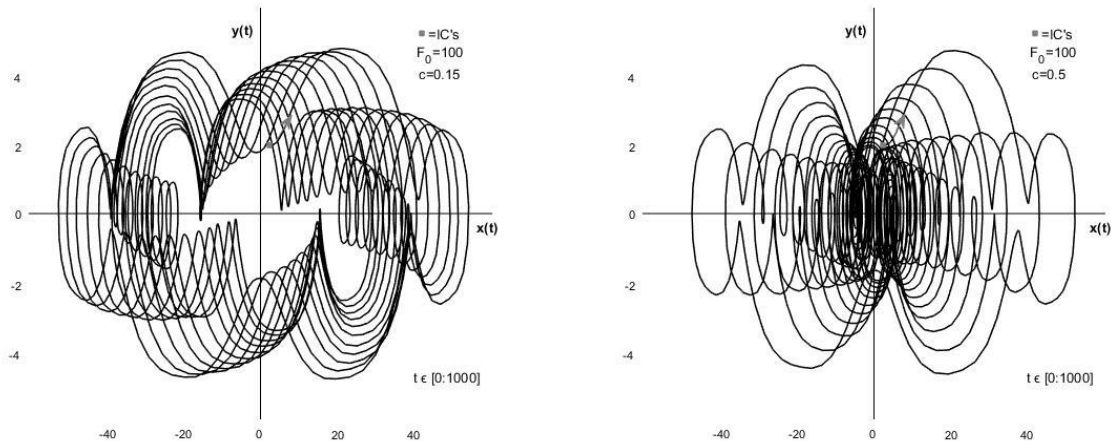


Figure 6.9: Phase plane diagrams for the base-case system with  $F_0=100$ , and  $c=0,15$ (left) and  $c=0,5$ (right).

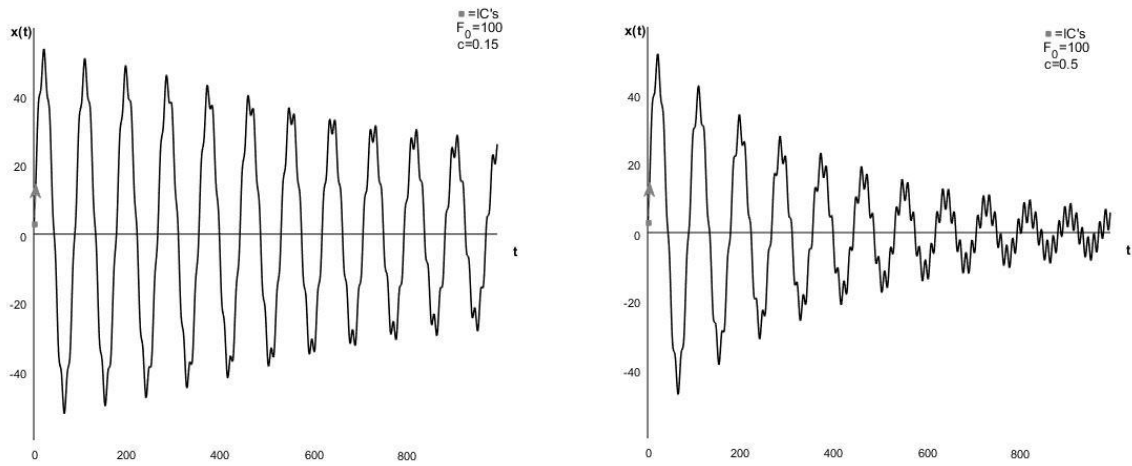


Figure 6.10: Position curves for the base-case system with  $F_0=100$ , and  $c=0,15$ (left) and  $c=0,5$ (right).

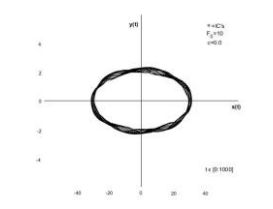
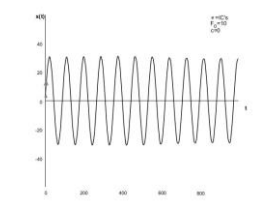
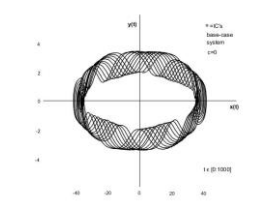
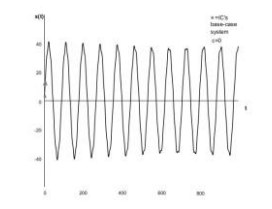
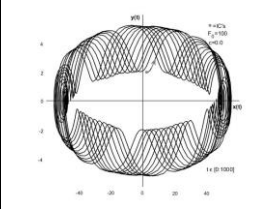
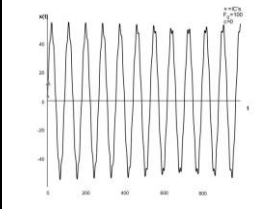
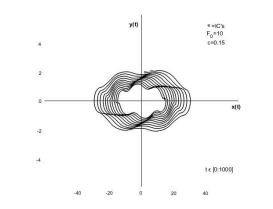
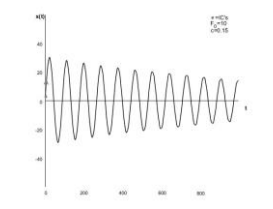
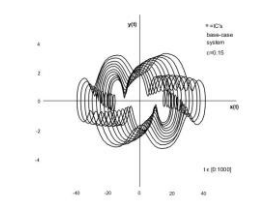
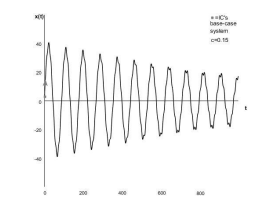
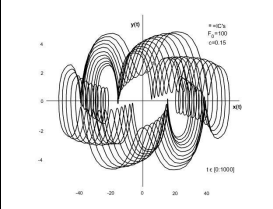
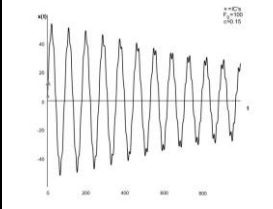
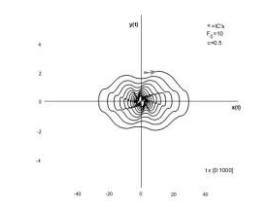
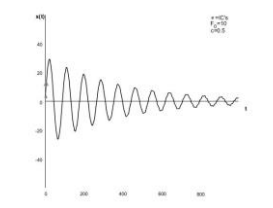
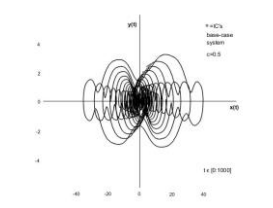
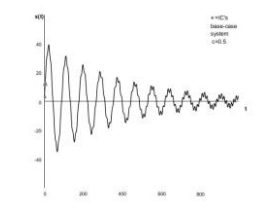
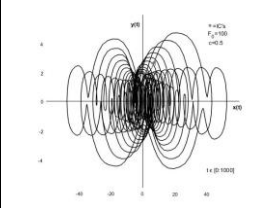
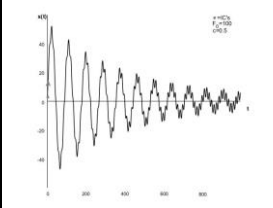
		$F_0$					
<b>c</b>	<b>10</b>		<b>50</b> (base-case system)		<b>100</b>		
	Phase plane diagrams	Position curves	Phase plane diagrams	Position curves	Phase plane diagrams	Position curves	
<b>0</b>							
<b>0,15</b>							
<b>0,5</b>							

Table 6.2: Review of phase plane diagrams and position curves for the base-case system with different values of the amplitude parameter,  $F_0$ , with different values of linear damping,  $c$ .



## 6.4 Base-case system with changed frequency parameter, $\omega$ .

The base-case system with  $\omega=0,2$  and  $\omega=1,0$  is shown in the phase plane in figures 6.11 and 6.13 respectively, with two values of linear damping,  $c=0,15$  on the left and  $c=0,5$  on the right. The system with  $\omega=0,1$  is not shown as it is a system close to resonance, which will be presented in 6.1.6. The position curves are shown in figure 6.12 for the system with  $\omega=0,2$  and in figure 6.14 for the system with  $\omega=1,0$ , also with  $c=0,15$  on the left and  $c=0,5$  on the right. The frequency parameter does not affect the critical damping, making the damping ratio equal to that of the base-case system, namely  $\xi=0,012$  for  $c=0,15$  and  $\xi=0,035$  for  $c=0,5$ .

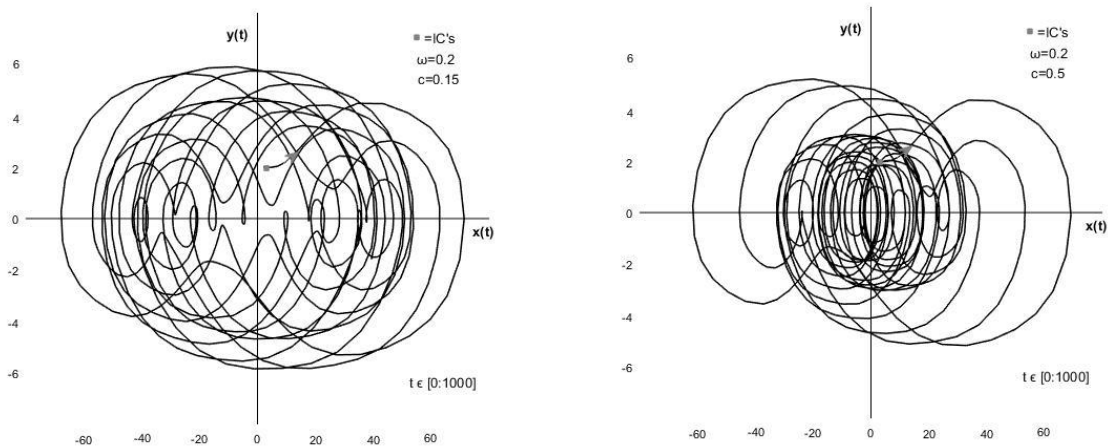


Figure 6.11: Phase plane diagrams for the base-case system with  $\omega=0,2$ , and  $c=0,15$ (left) and  $c=0,5$ (right).

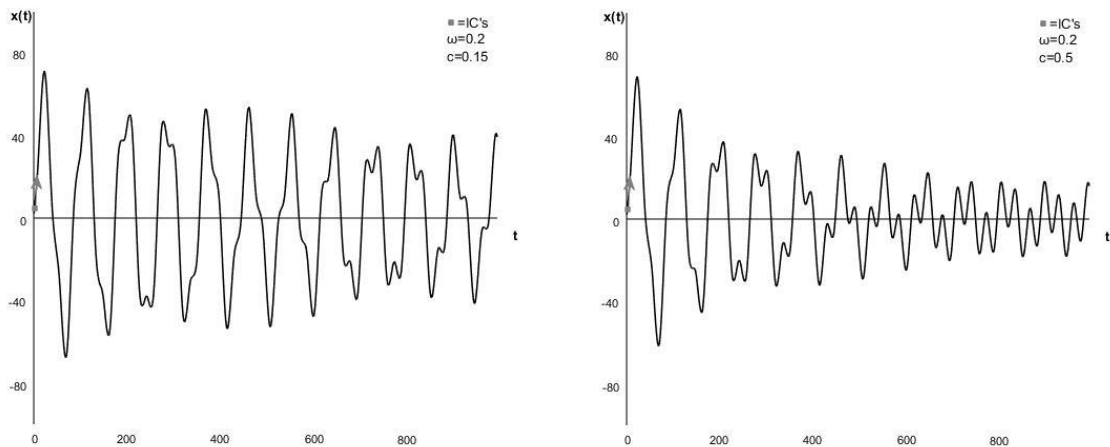


Figure 6.12: Position curves for the base-case system with  $\omega=0,2$ , and  $c=0,15$ (left) and  $c=0,5$ (right).

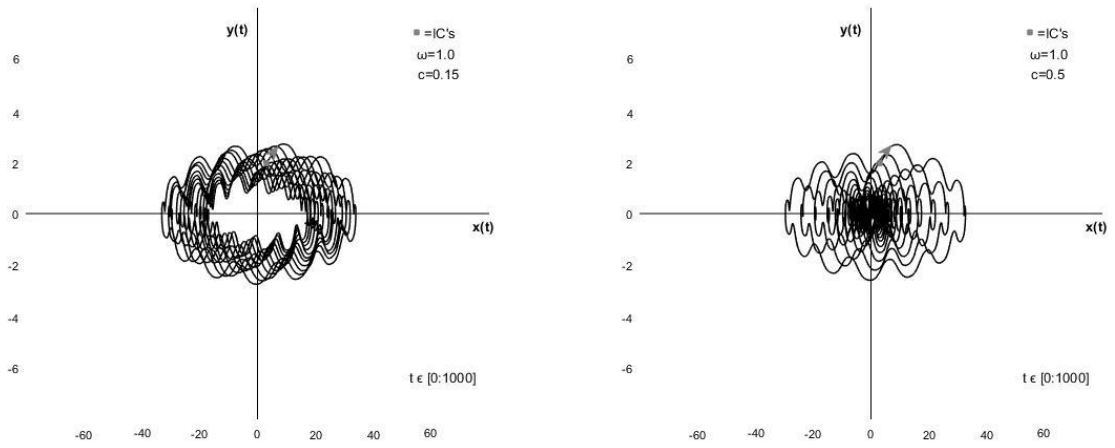


Figure 6.13: Phase plane diagrams for the base-case system with  $\omega=1,0$ , and  $c=0,15$ (left) and  $c=0,5$ (right).

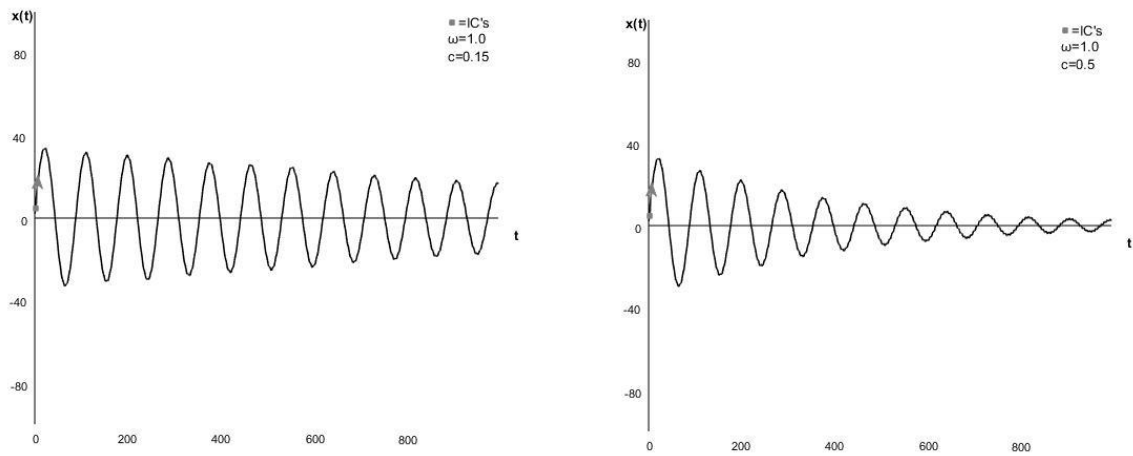


Figure 6.14: Position curves for the base-case system with  $\omega=1,0$ , and  $c=0,15$ (left) and  $c=0,5$ (right).

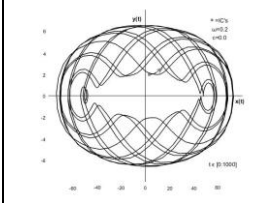
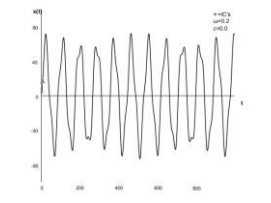
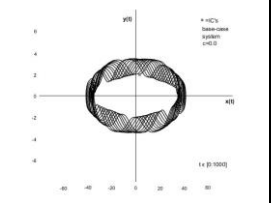
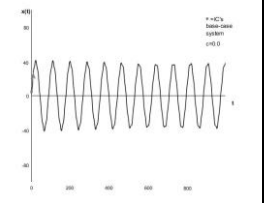
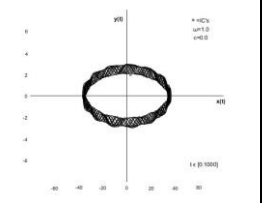
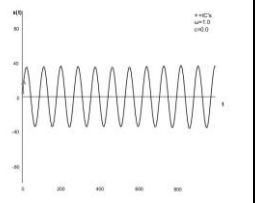
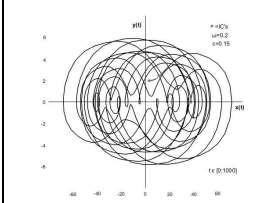
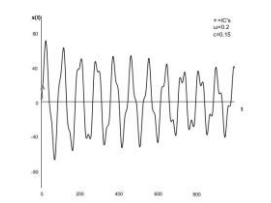
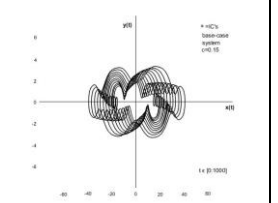
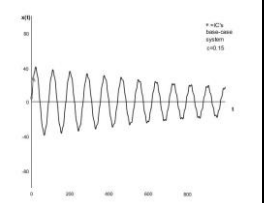
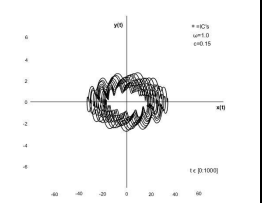
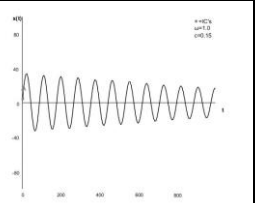
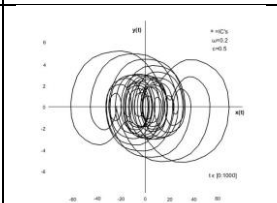
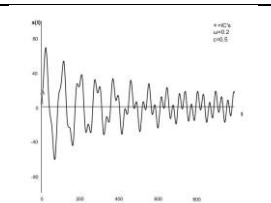
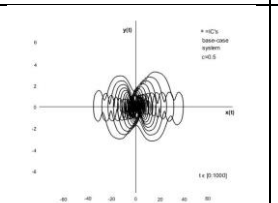
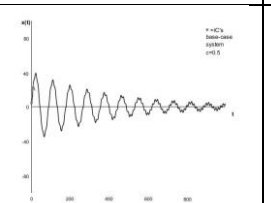
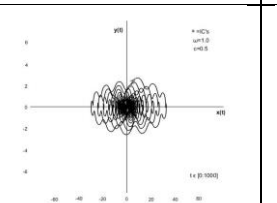
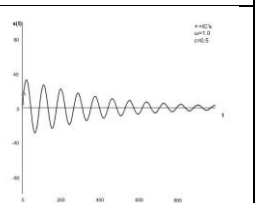
		$\omega$					
$c$	0,2 $\beta=2,83$		0,5 (base-case system) $\beta=7,07$		1,0 $\beta=14,14$		
	Phase plane diagrams	Position curves	Phase plane diagrams	Position curves	Phase plane diagrams	Position curves	
0							
0,15							
0,5							

Table 6.3: Review of phase plane diagrams and position curves for the base-case system with different values of the frequency parameter,  $\omega$ , with different values of linear damping,  $c$ .

## 6.5 Base-case system with varied mass parameter, $m$ .

The base-case system with  $m=50$  and  $m=140$  is shown in the phase plane in figures 6.15 and 6.17 respectively, with two values of linear damping,  $c=0,15$  on the left and  $c=0,5$  on the right. The position curves are shown in figure 6.16 for the system with  $m=50$  and in figure 6.18 for the system with  $m=140$ , also with  $c=0,15$  on the left and  $c=0,5$  on the right. The system with  $m=50$  has  $\xi=0,75$  for  $c=0,15$  and  $\xi=2,50$  for  $c=0,5$ . When  $m=140$ ,  $\xi=1,25$  for  $c=0,15$  and  $\xi=4,18$  for  $c=0,5$ .

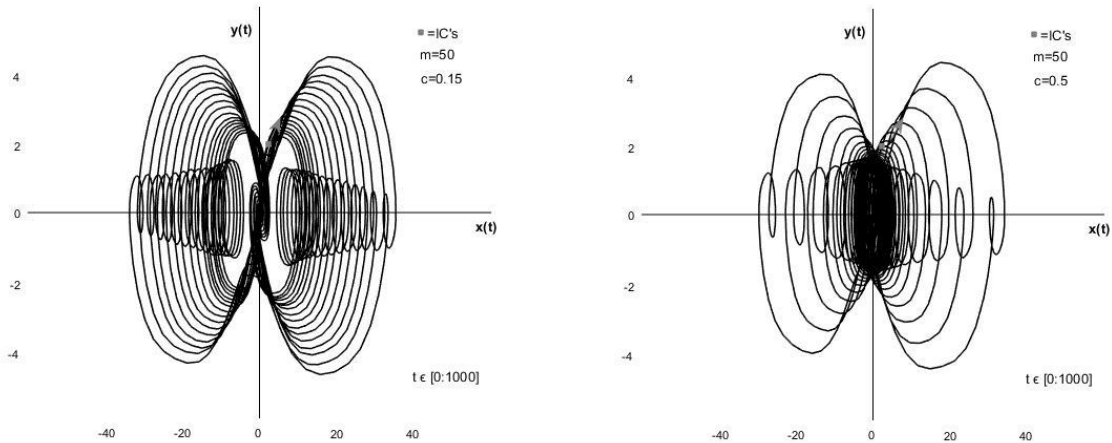


Figure 6.15: Phase plane diagrams for the base-case system with  $m=50$ , and  $c=0,15$ (left) and  $c=0,5$ (right).

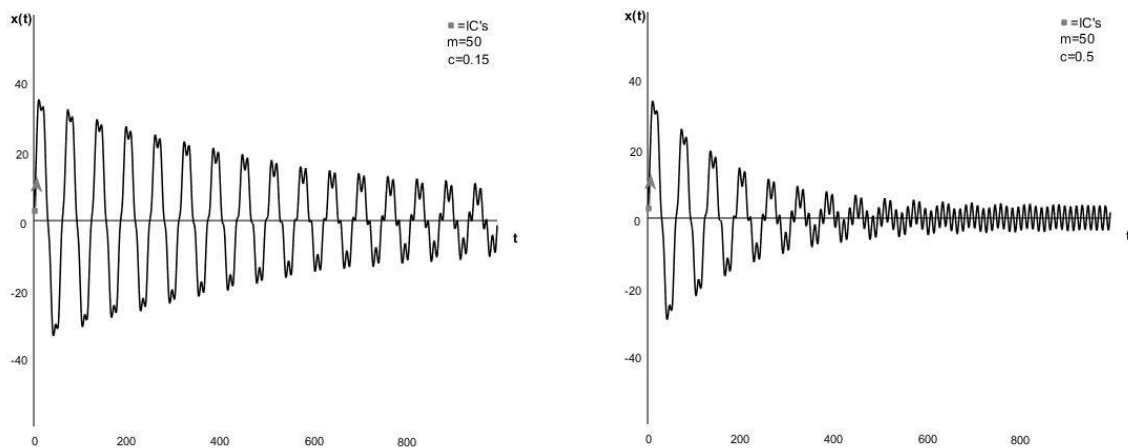


Figure 6.16: Position curves for the base-case system with  $m=50$ , and  $c=0,15$ (left) and  $c=0,5$ (right).

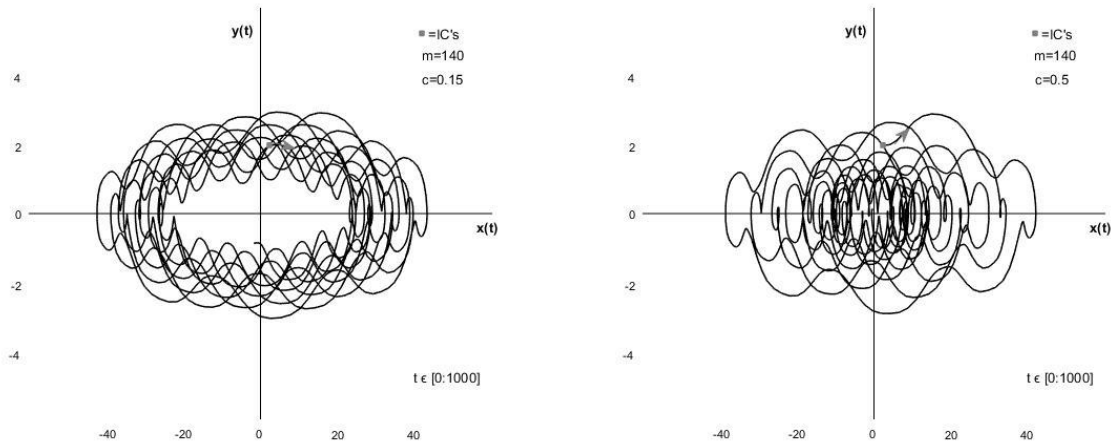


Figure 6.17: Phase plane diagrams for the base-case system with  $m=140$ , and  $c=0,15$ (left) and  $c=0,5$ (right).

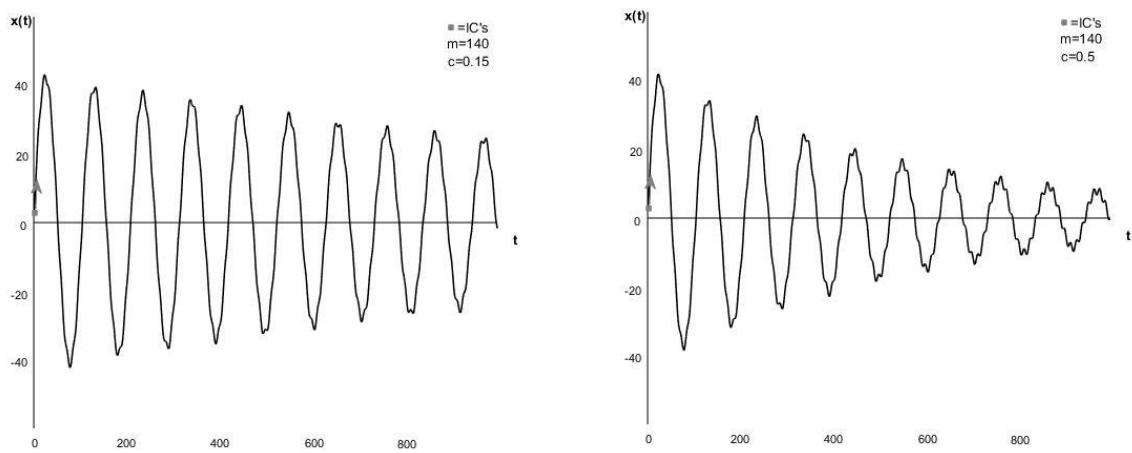


Figure 6.18: Position curves for the base-case system with  $m=140$ , and  $c=0,15$ (left) and  $c=0,5$ (right).

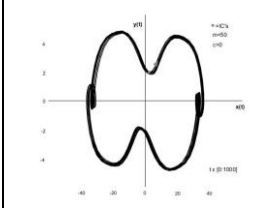
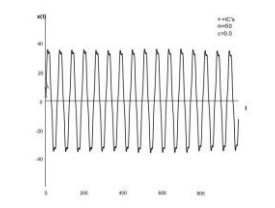
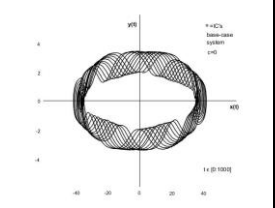
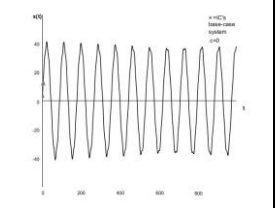
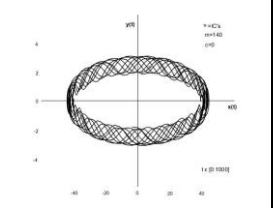
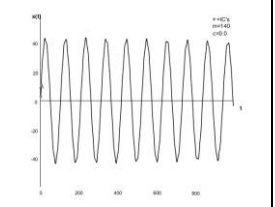
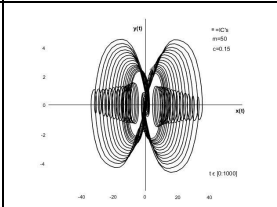
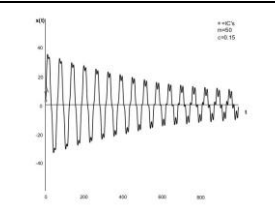
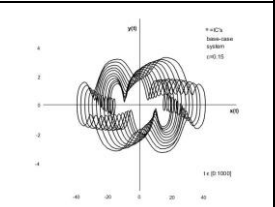
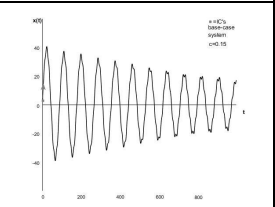
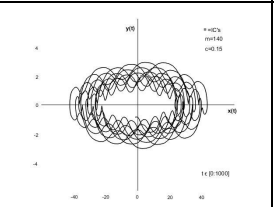
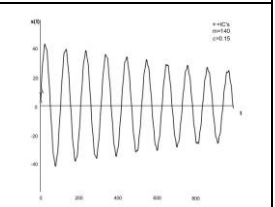
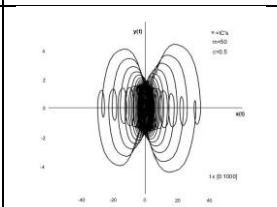
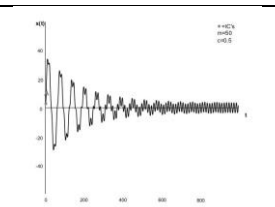
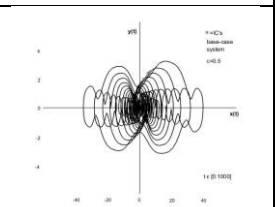
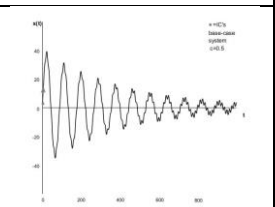
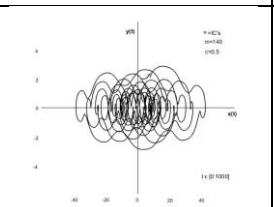
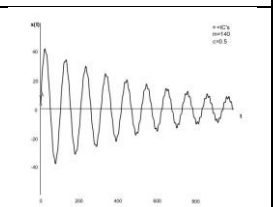
		<b>m</b>					
<b>c</b>	<b>50</b> $\beta=5,0$		<b>100</b> (base-case system) $\beta=7,07$		<b>140</b> $\beta=8,37$		
	Phase plane diagrams	Position curves	Phase plane diagrams	Position curves	Phase plane diagrams	Position curves	
<b>0</b>							
<b>0,15</b>							
<b>0,5</b>							

Table 6.4: Review of phase plane diagrams and position curves for the base-case system with different values of the mass parameter,  $m$ , with different values of linear damping,  $c$ .

## 6.6 Base-case system at and near resonance.

The base-case system with the mass varied so that the system is at and near resonance, i.e.  $\beta=0,8-1,2$  is shown with two values of linear damping,  $c=0,15$  on the left and  $c=0,5$  on the right in the figures. The phase plane diagrams for  $\beta=0,8-1,2$  is shown in figures 6.19, 6.21, 6.23, 6.25 and 6.27 respectively. The position curves are shown in figures 6.20, 6.22, 6.24, 6.26 and 6.28, also with  $c=0,15$  on the left and  $c=0,5$  on the right. The damping ratio vary from  $\xi=0,12$  to  $\xi=0,18$  for  $c=0,15$  and from  $\xi=0,40$  to  $\xi=0,60$  for  $c=0,5$ .

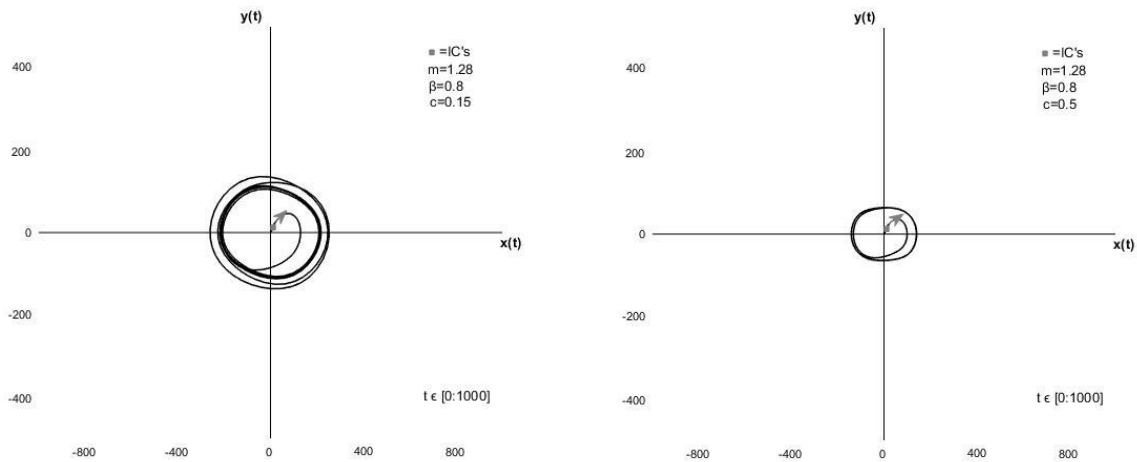


Figure 6.19: Phase plane diagrams for the base-case system with  $m=1,28$ , making  $\beta=0,8$ , with  $c=0,15$ (left) and  $c=0,5$ (right).

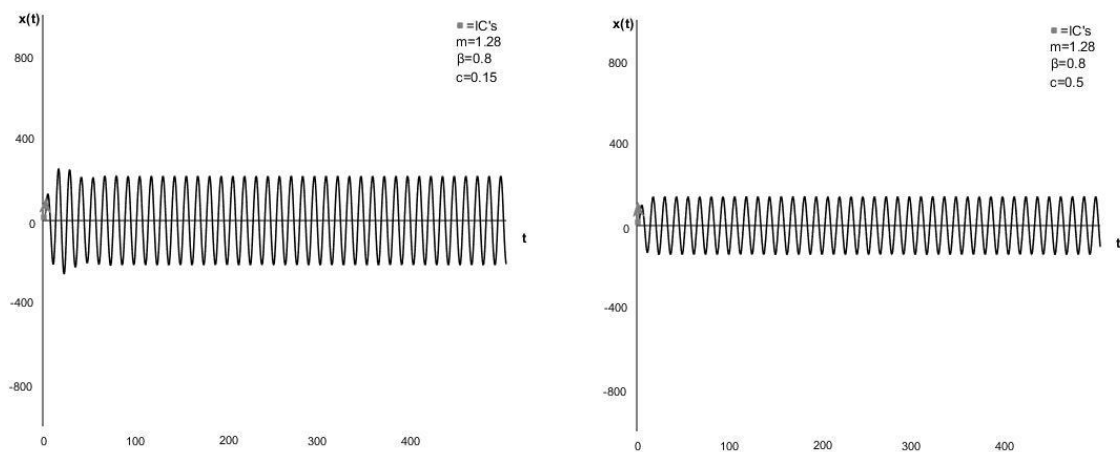


Figure 6.20: Position curves for the base-case system with  $m=1,28$ , making  $\beta=0,8$ , with  $c=0,15$ (left) and  $c=0,5$ (right).

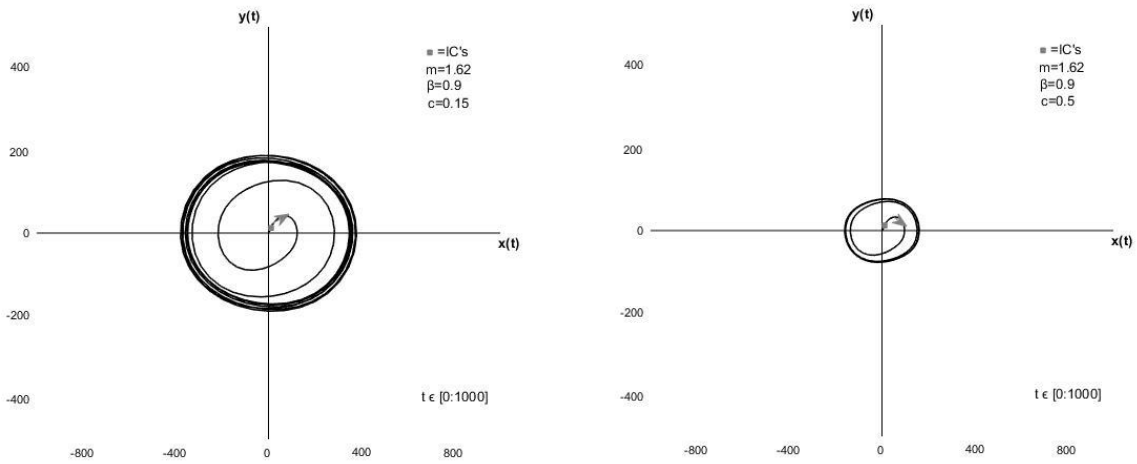


Figure 6.21: Phase plane diagrams for the base-case system with  $m=1,62$ , making  $\beta=0,9$ , with  $c=0,15$ (left) and  $c=0,5$ (right).

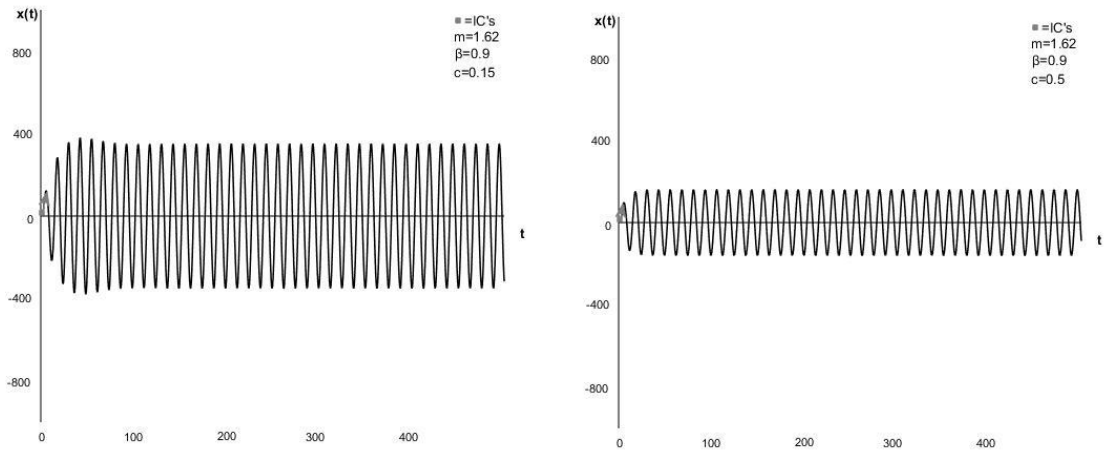


Figure 6.22: Position curves for the base-case system with  $m=1,62$ , making  $\beta=0,9$ , with  $c=0,15$ (left) and  $c=0,5$ (right).

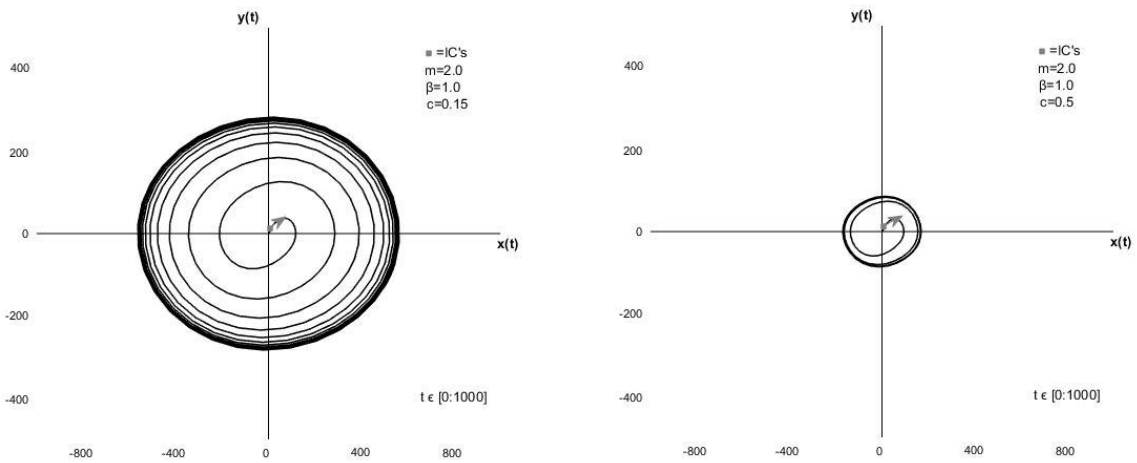


Figure 6.23: Phase plane diagrams for the base-case system with  $m=2,0$ , making  $\beta=1,0$ , with  $c=0,15$ (left) and  $c=0,5$ (right).



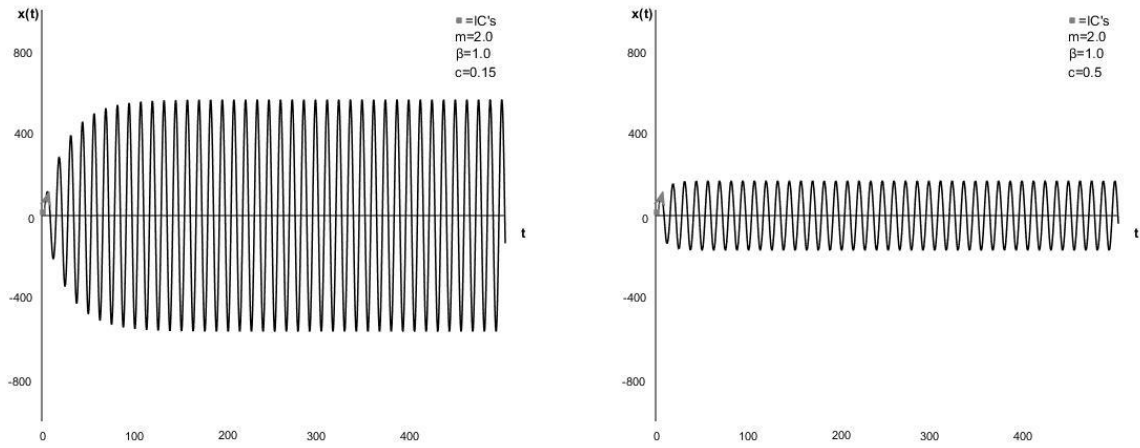


Figure 6.24: Position curves for the base-case system with  $m=2,0$ , making  $\beta=1,0$ , with  $c=0,15$ (left) and  $c=0,5$ (right).

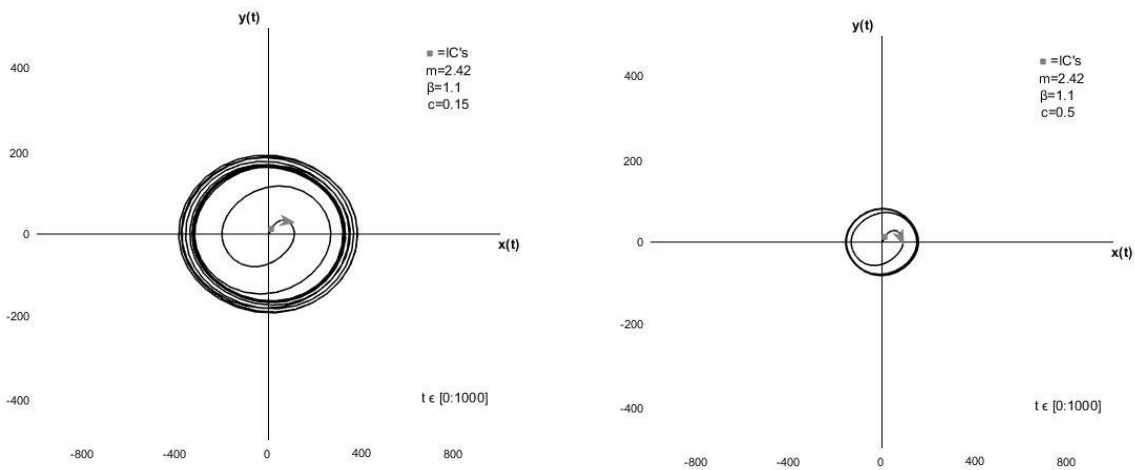


Figure 6.25: Phase plane diagrams for the base-case system with  $m=2,42$ , making  $\beta=1,1$ , with  $c=0,15$ (left) and  $c=0,5$ (right).

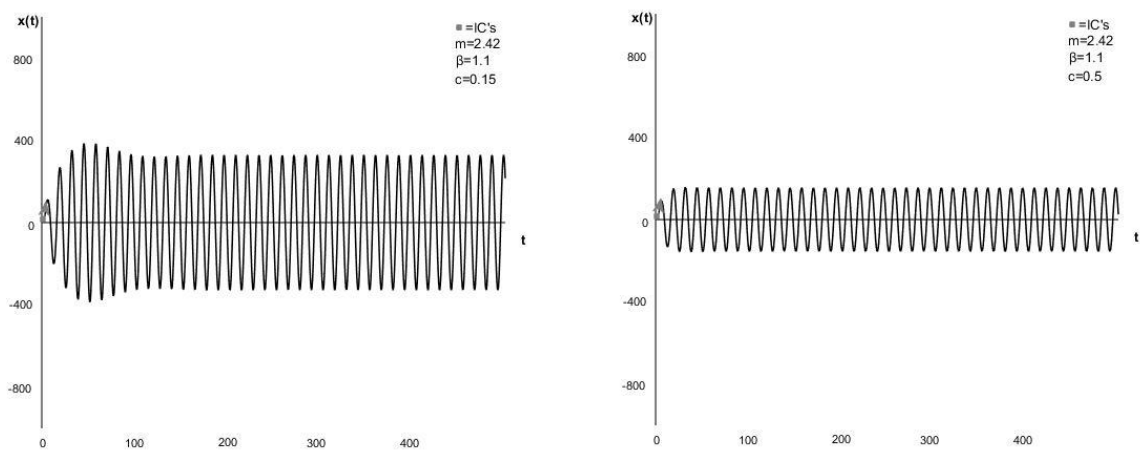


Figure 6.26: Position curves for the base-case system with  $m=2,42$ , making  $\beta=1,1$ , with  $c=0,15$ (left) and  $c=0,5$ (right).

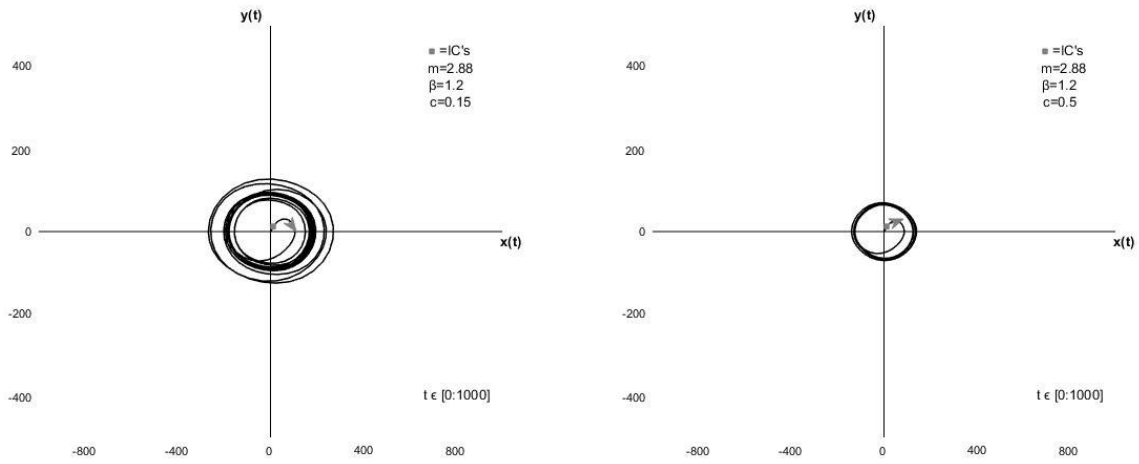


Figure 6.27: Phase plane diagrams for the base-case system with  $m=2,88$ , making  $\beta=1,2$ , with  $c=0,15$ (left) and  $c=0,5$ (right).

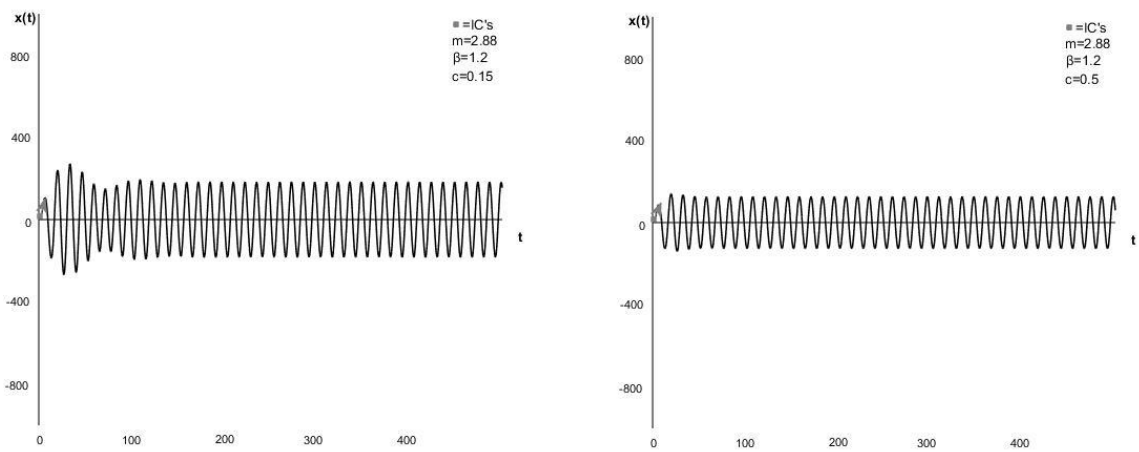


Figure 6.28: Position curves for the base-case system with  $m=2,88$ , making  $\beta=1,2$ , with  $c=0,15$ (left) and  $c=0,5$ (right).

Table 6.5 shows the phase plane diagrams and position curves for the base-case system when the mass is varied so that the system is near and at resonance. When a system is at resonance, the input frequency,  $\omega$ , is equal to the natural frequency of the system,  $\omega_0$ .

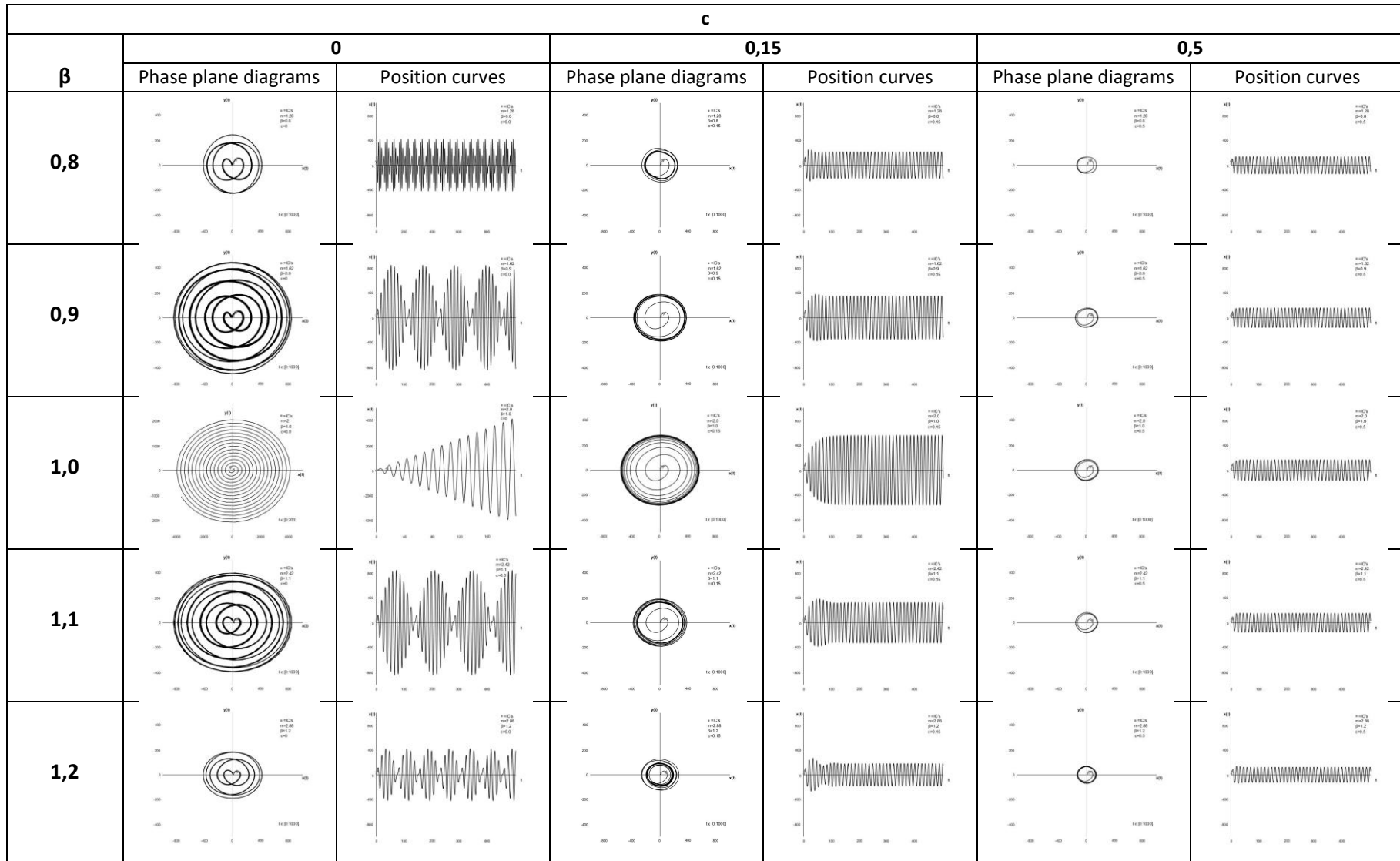


Table 6.5: Review of phase plane diagrams and position curves for the base-case system with different values of  $m$ , making the system at and near resonance, with different values of linear damping,  $c$ .

## 6.7 Conclusion

In this chapter, the base-case system, as well as some chosen systems from chapter 5 have been investigated when linear, constant damping is added. For the systems with parameters varied around the value in the base-case system, the results are as expected, the systems start to spiral towards the origin in the phase plane diagrams, i.e. the amplitudes decrease with time.

The base-case system with the mass parameter set to values making the system near and at resonance experiences an increase in position and velocity. When there is no damping inherent, the system at resonance,  $\beta=1,0$ , will continue to grow, and the systems near resonance will have a repeated cycle of increasing and decreasing amplitudes in both position and velocity. When damping is added, both the systems near and at resonance will increase until some point, where they have a steady trajectory in the phase plane. This trajectory has similarities to that of the van der Pol equation, leading to an exploration if they may in fact be limit cycles. This is investigated in chapter 9.

# Chapter 7- Nonlinear damping term in the homogenous equation of motion for one degree of freedom systems

In this chapter equation (5.1) is investigated with a nonlinear damping term. The equation is homogenous, i.e. the external force  $F(t)=0$ .

In the Marintek report “*Comparing simple models for prediction of ringing loads and responses*” [24] from 2009, the following equation is **proposed to simulate structural motions of an offshore fixed platform**:

$$a(t) + (\beta(t)f_e(t) + b_0)v(t) + \omega_0^2x(t) = f_e(t) \quad (7.1)$$

where  $\beta$  represents the possible nonlinear damping term, while  $b_0$  represents constant linear damping. See also [21]. Using this in equation (5.1) and making the equation homogenous (no external forces), we get:

$$\frac{d^2x}{dt^2} + (a \sin(\omega t) |\sin(\omega t)| + c_0) \frac{dx}{dt} + \frac{k}{m}x(t) = 0 \quad (7.2)$$

Equation (7.2) is investigated with values from the base-case system presented in chapter 5. The parameters are varied to look at their effect on the system. The variations of the parameters are the same as in chapter 6, i.e. only the lowest and highest values from chapter 5 are investigated.

It should be noted that as for the nonlinear damping term for the van der Pol equation, described in chapter 4, the damping could become **negative**. When  $a > c_0$ , the damping term will for some values of  $t$ , become negative. As the nonlinear damping term is multiplied with the velocity of the system, both position and velocity curves are included in this chapter, as well as the phase plane diagrams.

The nonlinear damping will be varied by varying  $a$ . This is done for two values of the constant damping coefficient,  $c_0=0,005$  and  $c_0=0,0015$ .

The diagrams are only shown in summary tables in this chapter. Presentation of all the diagrams for the different values of  $c_0$  and  $a$ , has been put into Appendix C.

The tables in this chapter show the position curves, velocity curves and phase plane diagrams for the systems with two values of linear, constant damping,  $c_0$ , and with varying values of nonlinear damping. Table 7.1 show the base-case system. Tables 7.2-7.6 show the systems with  $\beta=1/3, 1/2, 1, 3/2, \text{ and } 2,0$  respectively.

The tables show that the increase of the nonlinear coefficient,  $a$ , increases the nonlinearity in the systems. When the nonlinear coefficient,  $a$ , reaches a certain value, which is different for every system, the negative damping is almost balancing the positive damping in the system. When  $a$  is increased just slightly more, the negative damping takes control, making the amplitudes grow continuously. The increase of the linear, constant coefficient,  $c_0$ , slows the increase down.

The following are the **critical values** of  $a$ , where the systems have a continued incline in their amplitudes:

- $a=1,20$  for the base-case system, where  $\beta=7,07$ .
- $a=3,46$  for the system with  $\beta=1/3$  for both values of  $c_0$
- $a=1,61$  for the system with  $\beta=1/2$  for both values of  $c_0$
- $a=1,04$  for the system with  $\beta=1,0$  for both values of  $c_0$
- $a=0,37$  for the system with  $\beta=3/2$  for both values of  $c_0$
- $a=0,01$  for the system with  $\beta=2,0$  and  $c_0=0,0015$
- $a=0,02$  for the system with  $\beta=2,0$  and  $c_0=0,005$

This shows that as the value of  $\beta$  is increased, the systems need less value of the nonlinear coefficient,  $a$ , to reach a continued grow in amplitudes. The system with  $\beta=2,0$ , only need  $a=0,01$  when  $c_0=0,0015$ .

No further discussion of these results are included as we will propose that more research be done to investigate the appropriateness of the model equation (7.1) for structural systems.

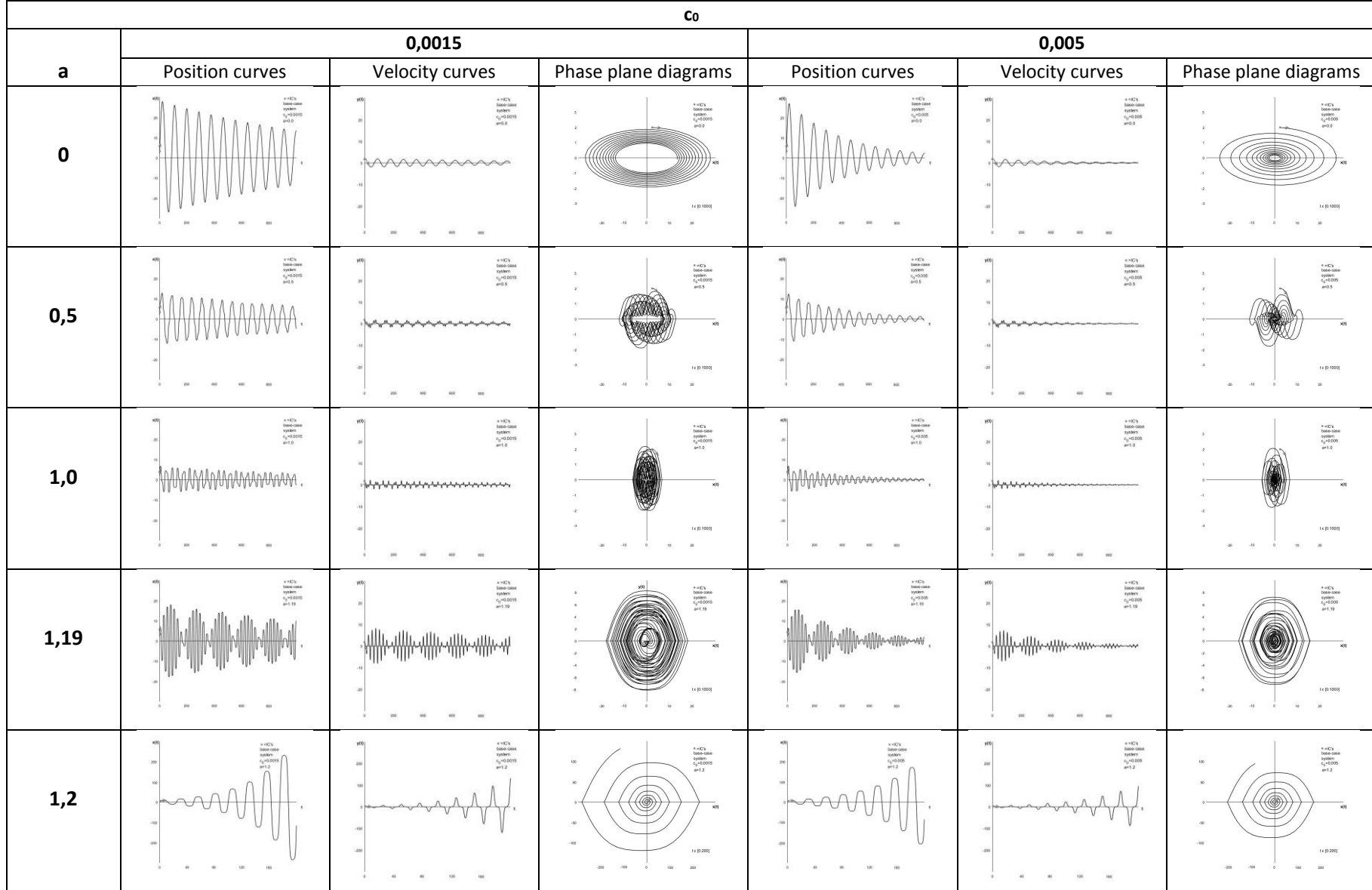


Table 7.1: Review of position curves, velocity curves and phase plane diagrams for the base-case system with varying nonlinear damping, for two values of linear, constant damping,  $c_0=0,0015$  and  $c_0=0,005$ .

It should be noted that the axis for the value  $a=1,2$  is different from the axis in the other diagrams.

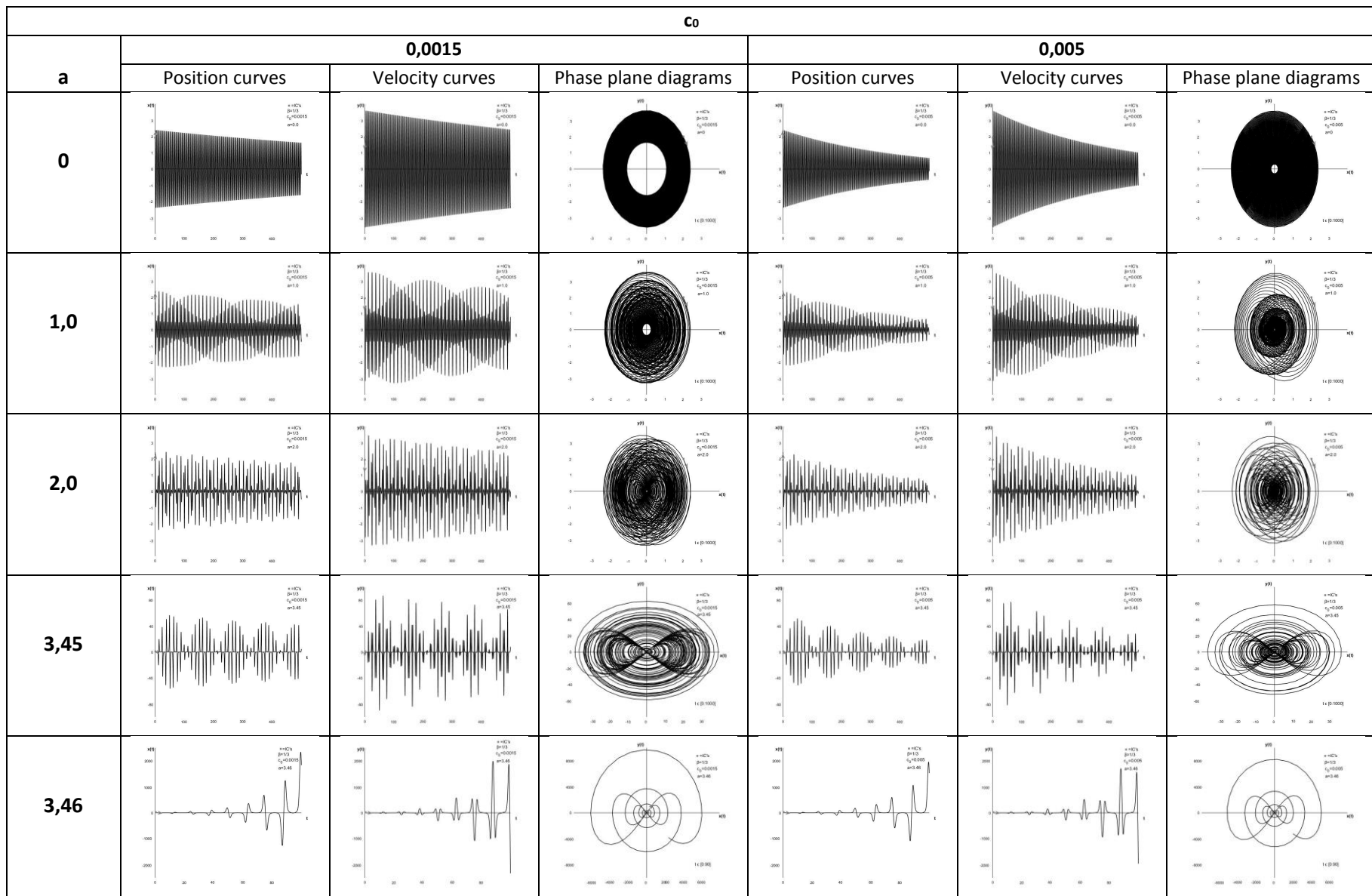


Table 7.2: Review of position curves, velocity curves and phase plane diagrams for the system with  $\beta=1/3$ , with  $c_0=0,0015$  and  $c_0=0,005$ , for increasing values of  $a$ .

It should be noted that for the values  $a=3,45$  and  $3,46$  the axis are different from the rest.



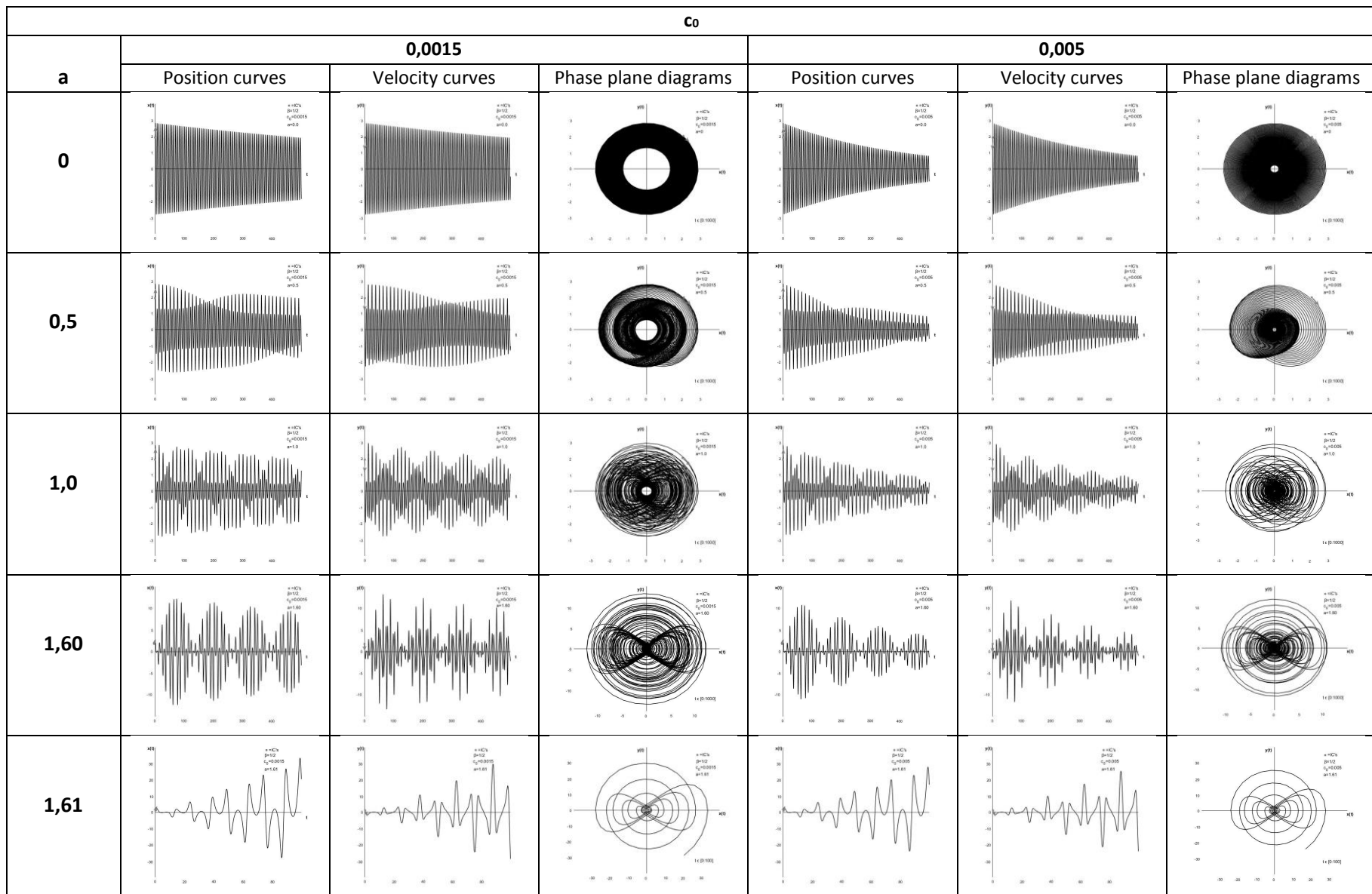


Table 7.3: Review of position curves, velocity curves and phase plane diagrams for the base-case system with  $\beta=1/2$ , with varying nonlinear damping, for two values of linear, constant damping,  $c_0=0,0015$  and  $c_0=0,005$ .

It should be noted that for the values  $a=1,60$  and  $1,61$  the axis are different from the rest.

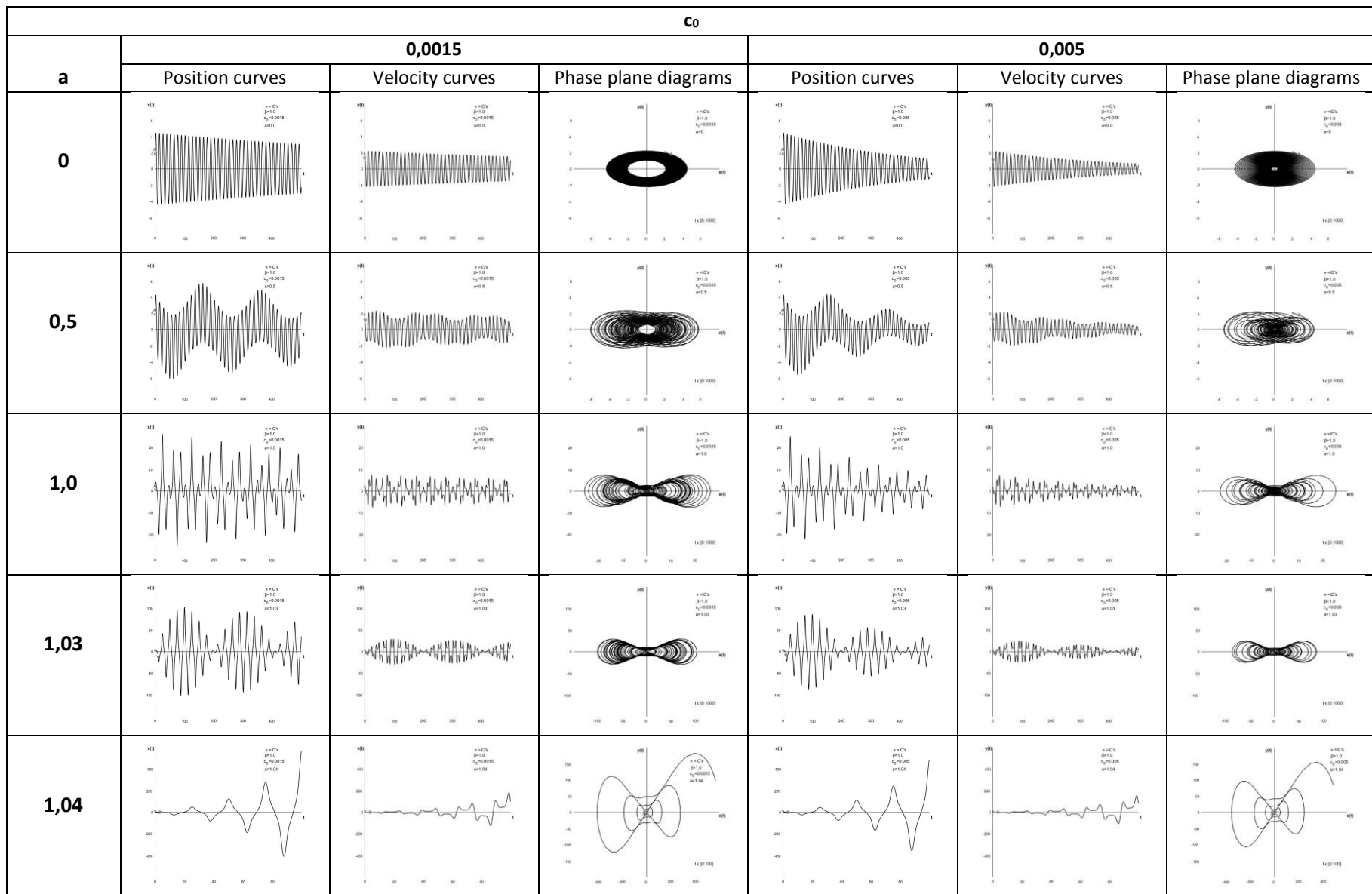


Table 7.4: Review of position curves, velocity curves and phase plane diagrams for the system with  $\beta=1,0$ , with  $c_0=0,0015$  and  $c_0=0,005$ , for increasing values of  $a$ .

It should be noted that for the values  $a=1,0$ ,  $a=1,03$  and  $a=1,04$ , the axis are changed compared to the other diagrams.

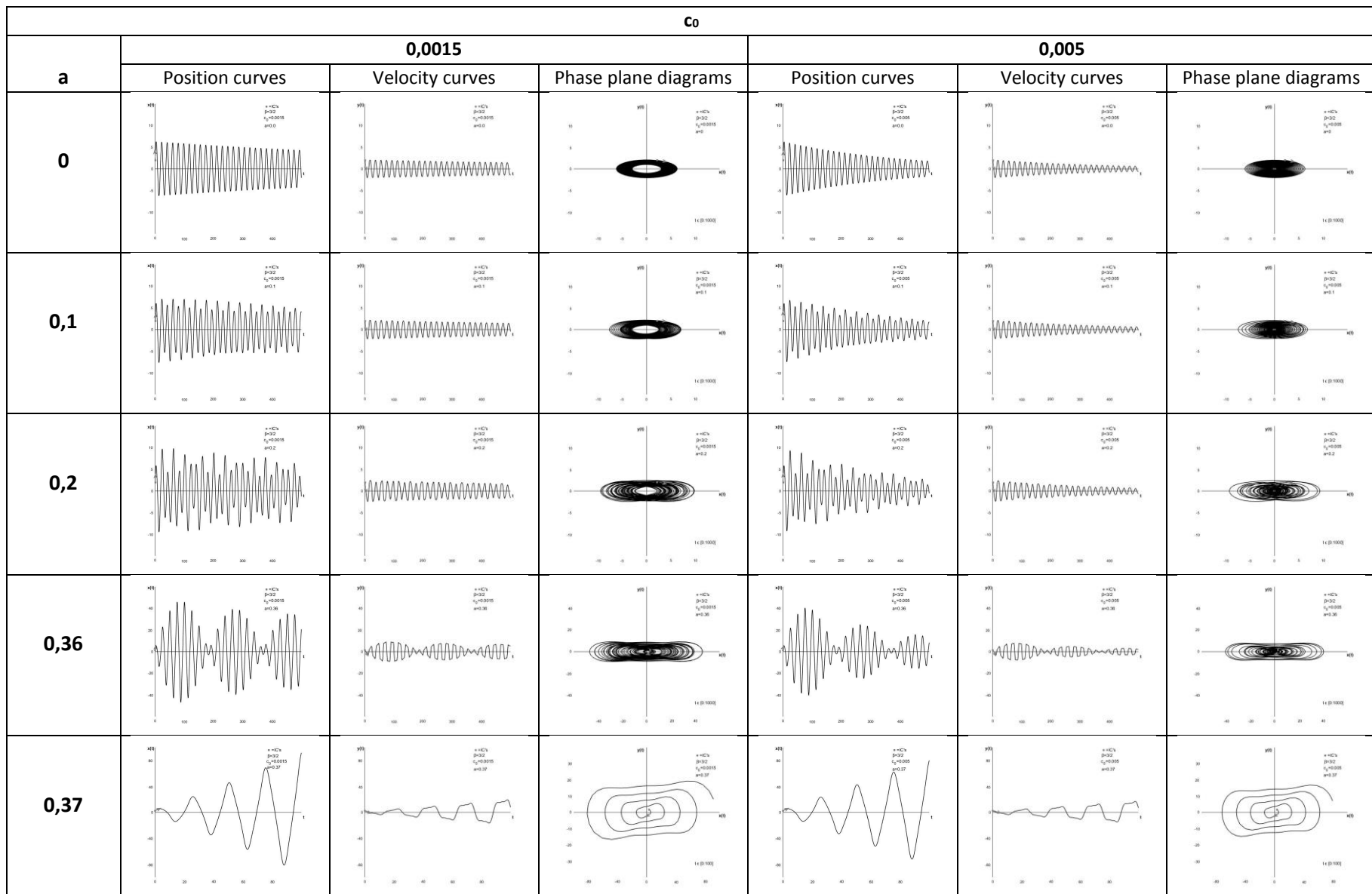


Table 7.5: Review of position curves, velocity curves and phase plane diagrams for the system with  $\beta=3/2$ , with  $c_0=0,0015$  and  $c_0=0,005$ , for increasing values of  $a$ .

It should be noted that for the values  $a=0,36$  and  $a=0,37$ , the axis differ from the other diagrams.

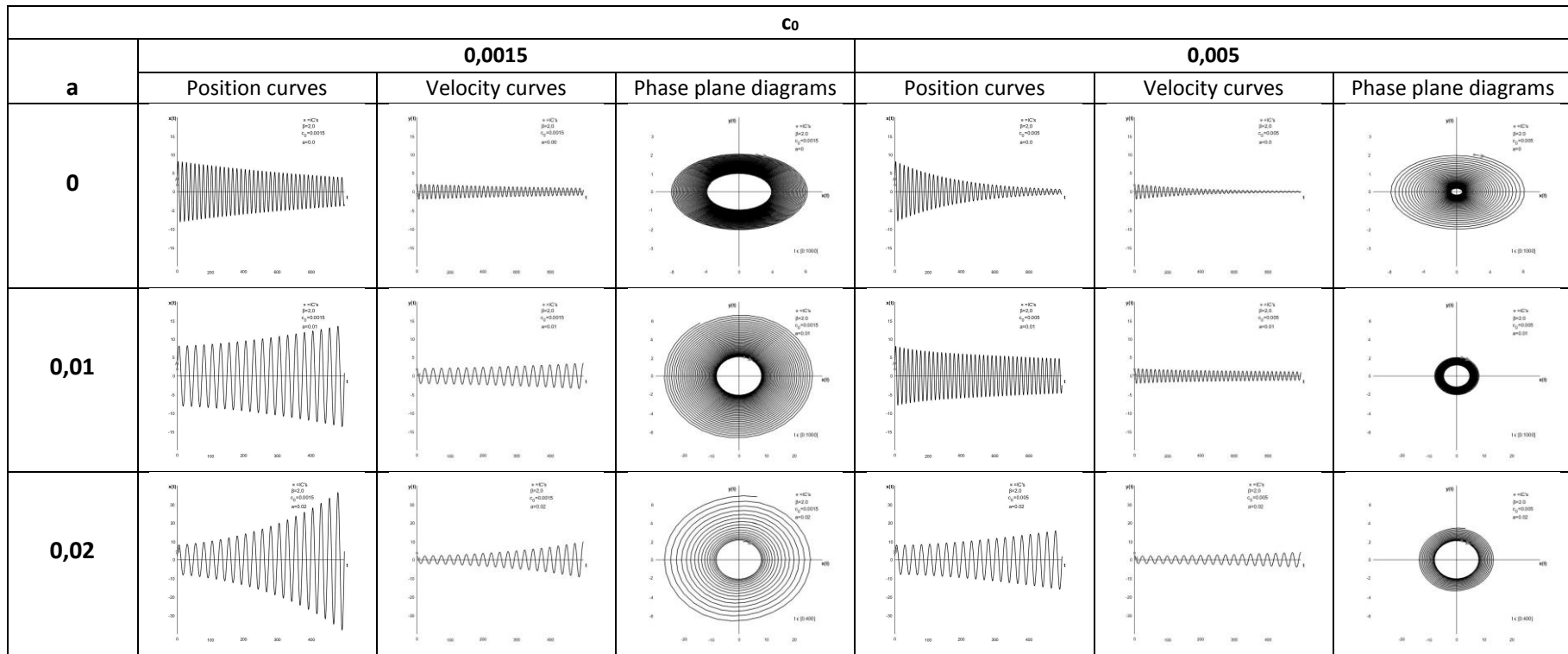


Table 7.6: Review of position curves, velocity curves and phase plane diagrams for the system with  $\beta=2,0$ , with  $c_0=0,0015$  and  $c_0=0,005$ , for increasing values of  $a$ .

It should be noted that for the value  $a=0,02$ , the axis and timespans differ from the other diagrams.

# Chapter 8 – Nonlinear damping term in the equation of motion with linear forcing term for one degree of freedom systems

In this chapter equation (5.1) is investigated with nonlinear damping term equal to that in chapter 7, and with a linear forcing term  $F(t)$ , see [24]. The equation becomes:

$$\frac{d^2x}{dt^2} + (a \sin(\omega t) |\sin(\omega t)| + c_0) \frac{dx}{dt} + \frac{k}{m} x(t) = \frac{F_0}{m} \sin(\omega t) \quad (8.1)$$

The base-case system is presented with two values of the linear damping coefficient,  $c_0=0,005$  and  $c_0=0,0015$ , for increasing values of the nonlinear damping coefficient,  $a$ . The system is also investigated for the same values of the mass parameter, making the system close to and at resonance, as in chapter 7.

Only the tables are presented in this chapter, the presentation of each diagram separately is in Appendix D.

Table 8.1 shows the position curves, velocity curves and phase plane diagrams for the base-case system with two values of linear, constant damping,  $c_0$ , and with varying values of nonlinear damping. Tables 8.2-8.6 show the same for the systems with  $\beta=1/3$ ,  $\beta=1/2$ ,  $\beta=1,0$ ,  $\beta=3/2$  and  $\beta=2,0$ , respectively.

The systems will have a value of the nonlinear damping coefficient,  $a$ , where it has continuous increase in its amplitudes. This value is different for all the systems, but is the same as was found in chapter 7, when the system was not subjected to any loading. The behaviour of the systems up until this value of  $a$ , are similar to those in chapter 7, but because of the linear forcing term, the amplitudes are significantly higher and the system uses longer time to obtain a decrease of the amplitudes.

The system at resonance, i.e.  $\beta=1,0$ , subjected to only linear, constant damping,  $c_0$ , experience continuous growth in amplitudes. When nonlinear damping is added, the system does not experience this growth until  $a$  reaches its **critical value**,  $a=1,2$ .

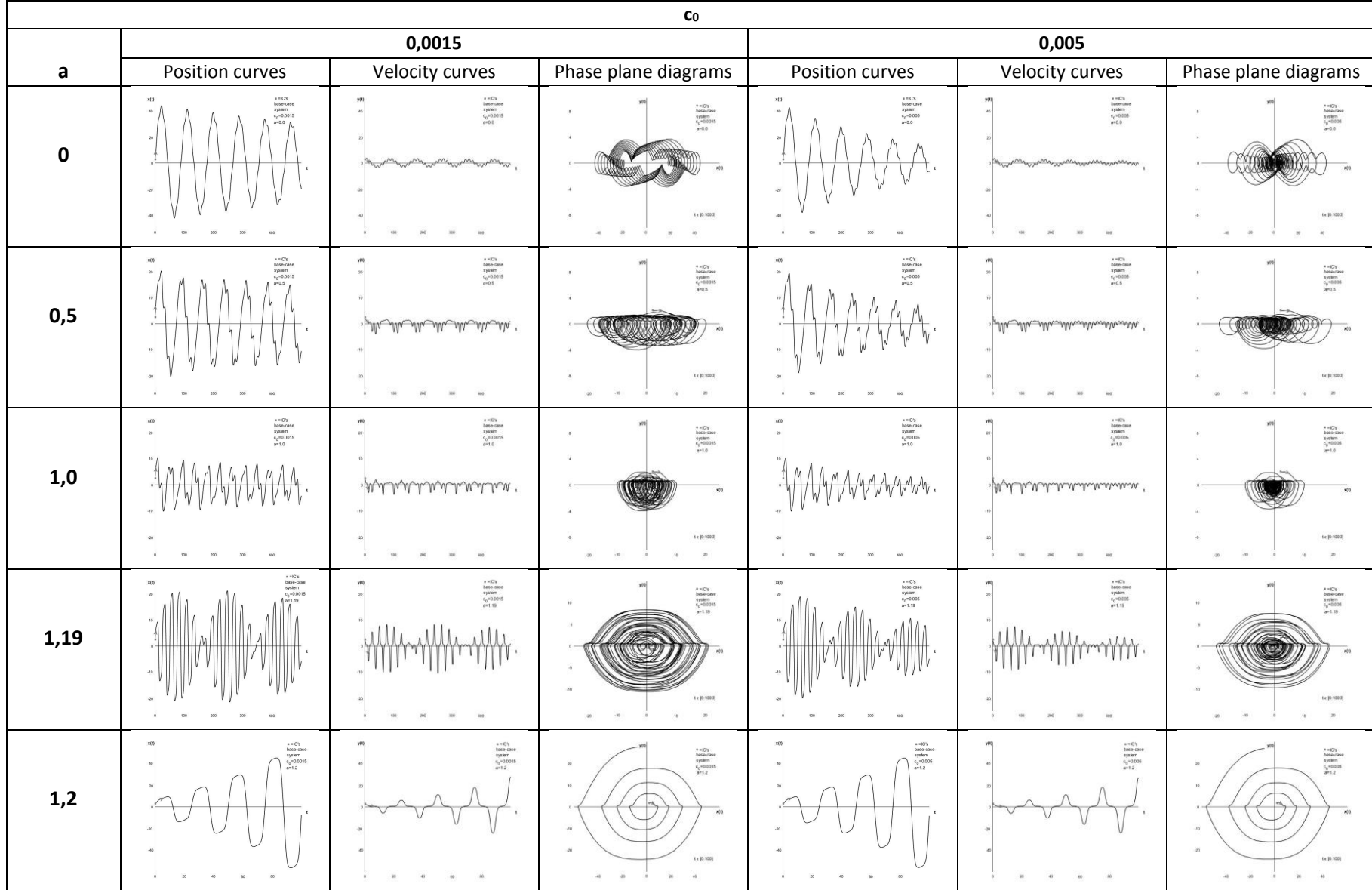


Table 8.1: Review of position curves, velocity curves and phase plane diagrams for the base-case system, for  $c_0=0,0015$  and  $c_0=0,005$ , and increasing values of  $a$ .

Note that the axis for the values  $a=0$  and  $a=1,2$  are different from the other diagrams.

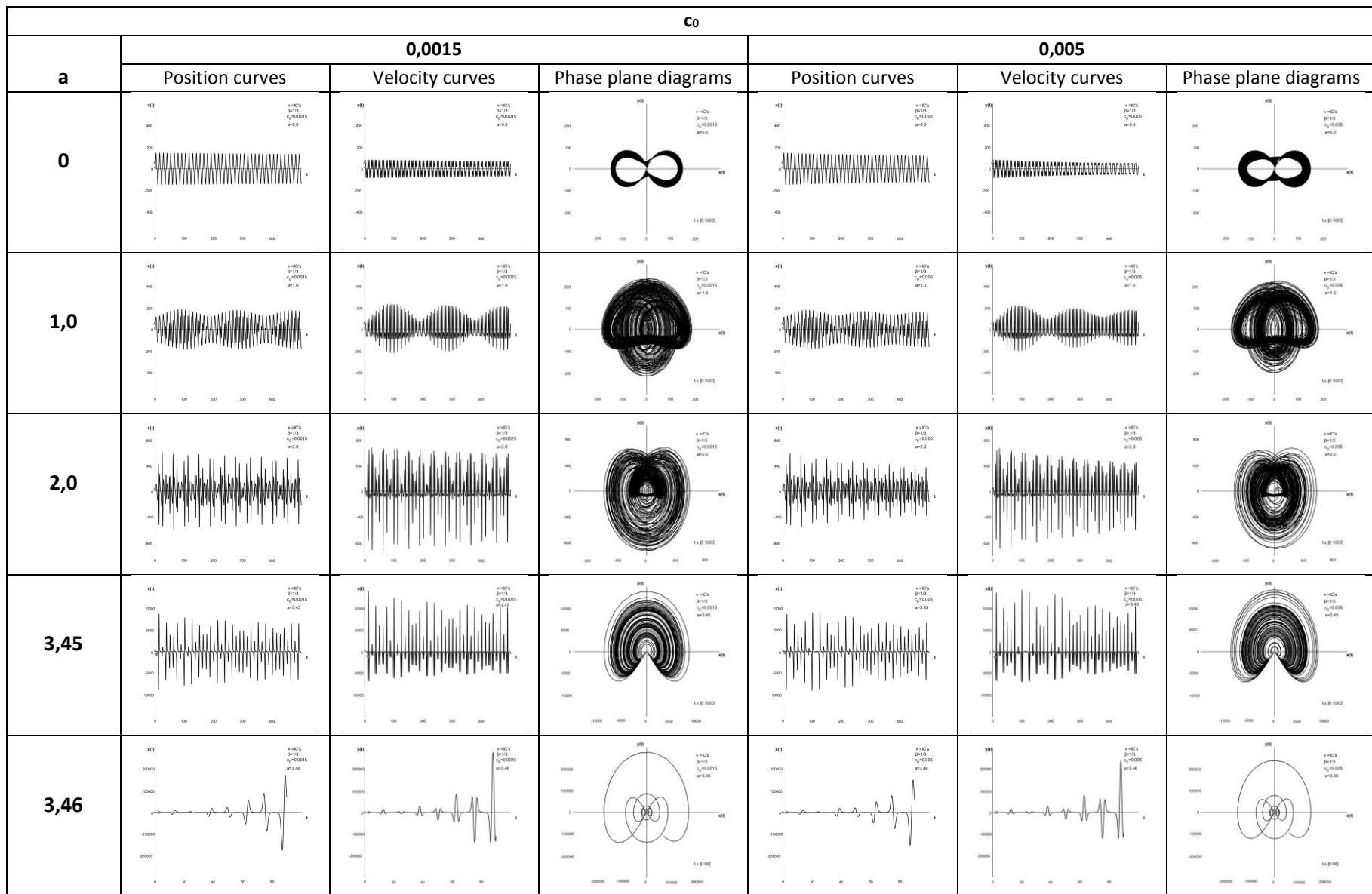


Table 8.2: Review of position curves, velocity curves and phase plane diagrams for the system with  $\beta=1/3$ , for  $c_0=0,0015$  and  $c_0=0,005$ , and increasing values of  $a$ .

Note that the axis in the diagrams for the system with values  $a=2,0$ ,  $a=3,45$  and  $a=3,46$  are different from the other systems diagram axis.

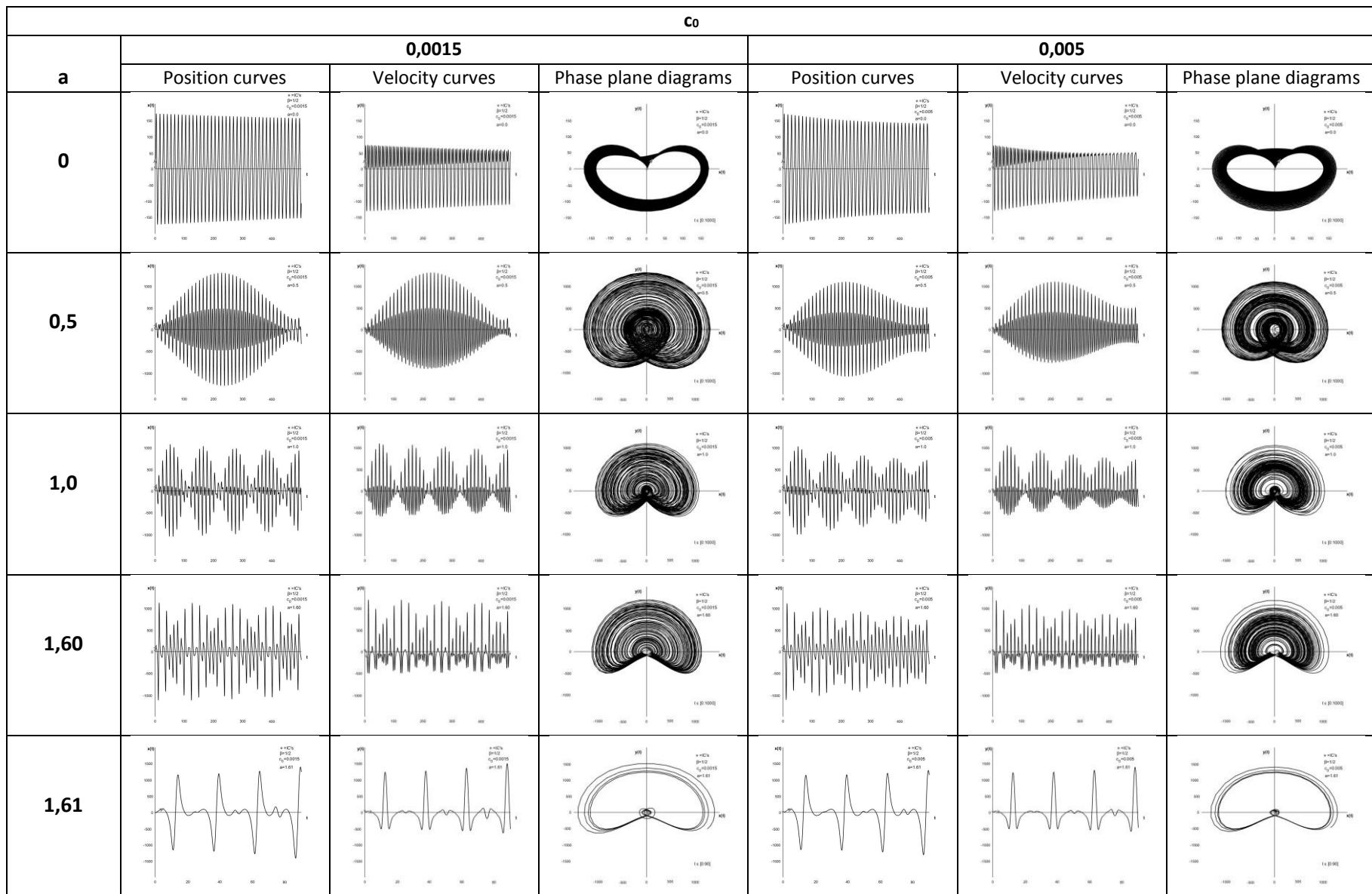


Table 8.3: Review of position curves, velocity curves and phase plane diagrams for the system with  $\beta=1/2$ , for  $c_0=0,0015$  and  $c_0=0,005$ , and increasing values of  $a$ .

Note that the axis in the diagrams for the system with values  $a=0$  and  $a=1,61$  are different from the other systems diagram axis.



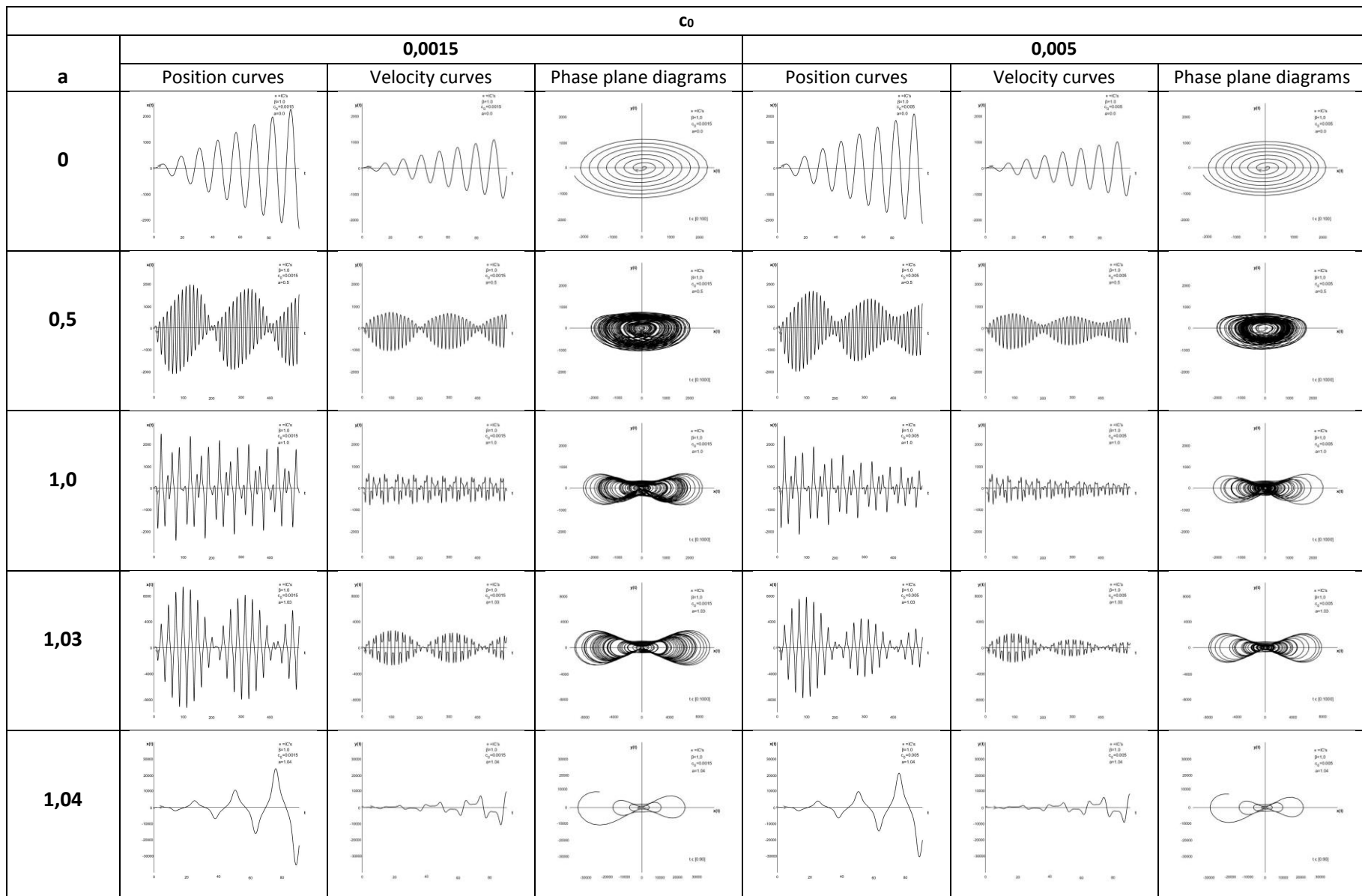


Table 8.4: Review of position curves, velocity curves and phase plane diagrams for the system with  $\beta=1,0$ , for  $c_0=0,0015$  and  $c_0=0,005$ , and increasing values of  $a$ .

Note that the axis in the diagrams for the system with values  $a=0$ ,  $a=1,03$  and  $a=1,04$  are different from the other systems diagram axis.

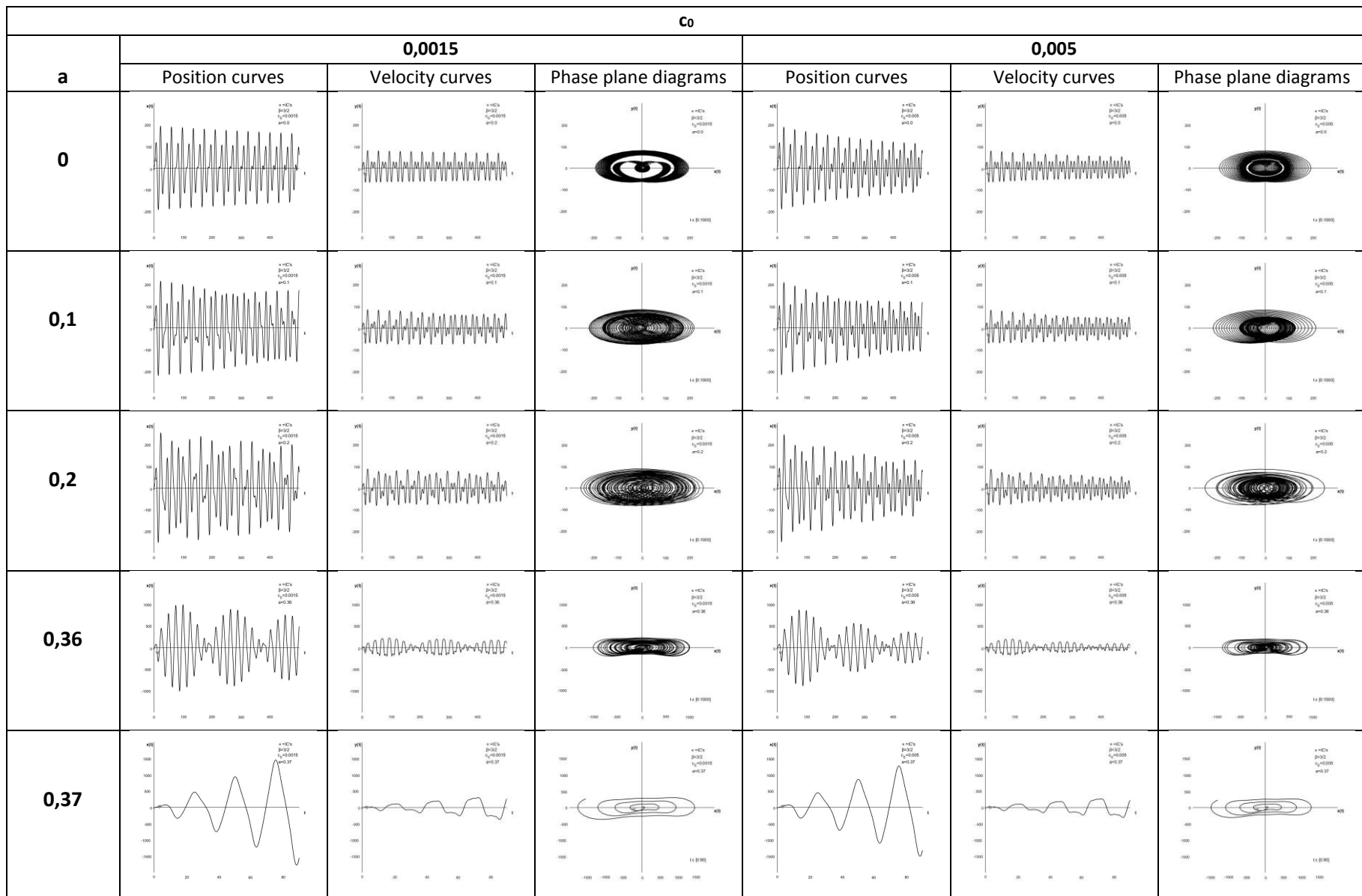


Table 8.5: Review of position curves, velocity curves and phase plane diagrams for the system with  $\beta=3/2$ , for  $c_0=0,0015$  and  $c_0=0,005$ , and increasing values of  $a$ .

Note that the axis in the diagrams for the system with values  $a=0,36$  and  $a=0,37$  are different from the other systems diagram axis.

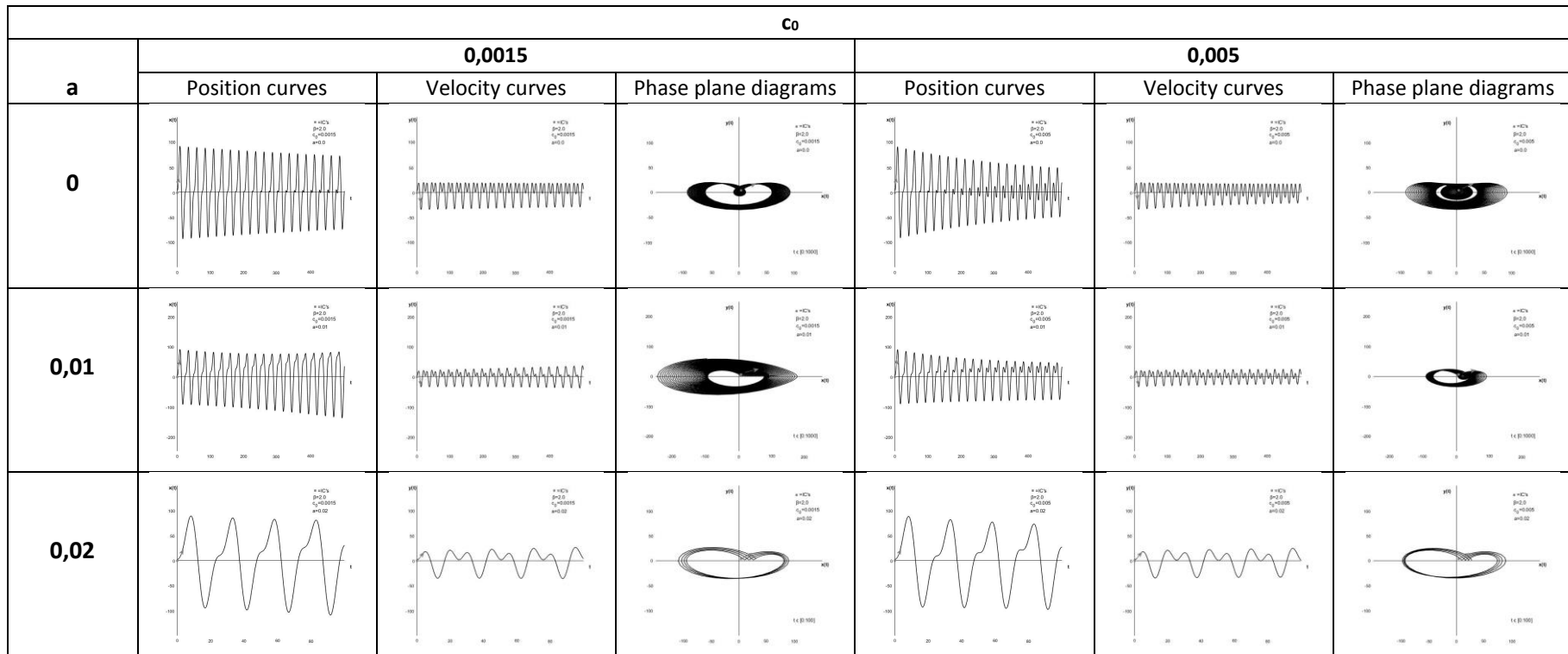


Table 8.6: Review of position curves, velocity curves and phase plane diagrams for the system with  $\beta=2,0$ , for  $c_0=0,0015$  and  $c_0=0,005$ , and increasing values of  $a$ .

Note that the axis in the diagrams differs for every value of  $a$ .

# Chapter 9 - Limit cycles for a system with drag loading subjected to linear, constant damping.

Limit cycles were discussed in chapter 3 and shown for the van der Pol equation in chapter 4. The van der Pol equation contains nonlinearity in the damping term, which can be both positive and negative. This leads to the system experiencing both generation and dissipation of energy from the damping term. The limit cycles are shown in figure 4.5 for different degrees of damping.

In chapter 6, the phase plane diagrams for the systems with the mass parameter set to values making the system at and near resonance showed some similarities to those found for the van der Pol equation. In this chapter, those systems are further analysed, and limit cycles are found.

## 9.1 Exploration of limit cycles for base-case system with $\beta=0,8$

The base-case system with  $m=1,28$ , making  $\beta=0,8$ , is shown for different initial conditions in figure 9.1, with damping,  $c=0,15$ . The different coloured trajectories represents different initial conditions, which are marked in the figure. All the trajectories spiral towards the limit cycle, making it a stable limit cycle. Figure 9.2 shows the system with more damping,  $c=0,5$  to the left and  $c=1,0$  to the right. These systems also have clear limit cycles, with amplitudes which are lower in both position and velocity. The more damping in the system, the more the transient response is limited, making the steady state solution occurring earlier.

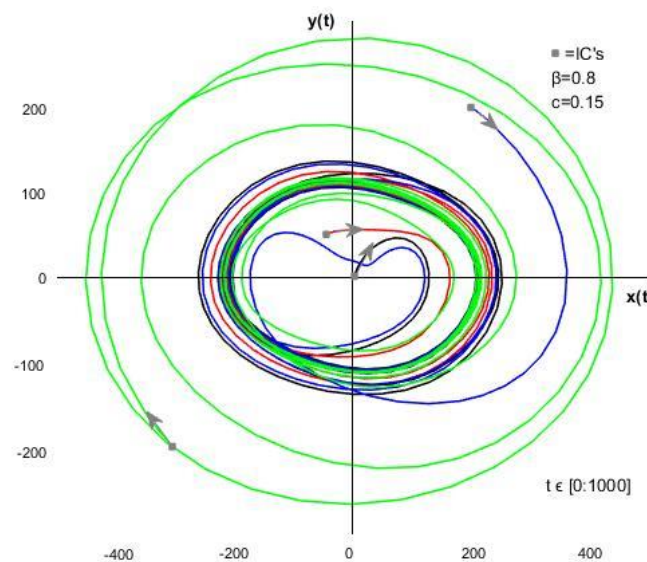


Figure 9.1: Base-case system with  $m=1,28$ , making  $\beta=0,8$  with  $c=0,15$  for four different initial conditions.

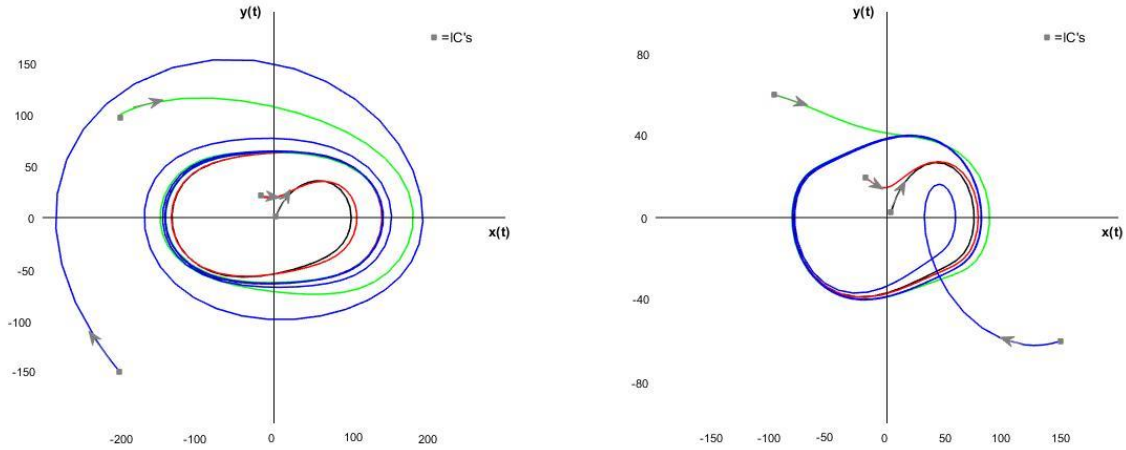


Figure 9.2: Base-case system with  $m=1,28$ , making  $\beta=0,8$  with  $c=0,5$ (left) and  $c=1,0$ (right) for four different initial conditions.

Further investigation shows that all the systems presented in table 6.4 exhibits limit cycles in the phase plane when subjected to linear, constant damping. Figure 9.3 shows the limit cycles in the base-case system with varying mass, making  $\beta$  between 0,8 and 1,2, with  $c=0,15$ . The increase of  $\beta$  increases the amplitudes of the limit cycles until the system is at resonance. When further increasing  $\beta$ , the limit cycles occur lower in position and velocity. For a static system, the amplitude of the displacement is  $x(t) = \frac{F_0}{k}$ , and for a dynamic system the amplitude at resonance is  $x(t) = \frac{F_0}{2kc_c}$  [19].

Figures 9.4 and 9.5 shows the limit cycles for varying  $\beta$  for larger damping,  $c=0,5$  and  $c=1,0$ . The limit cycles occur earlier, as was found for the system with  $\beta=0,8$ . The cycles also seem to be closer arranged when the damping is increased.

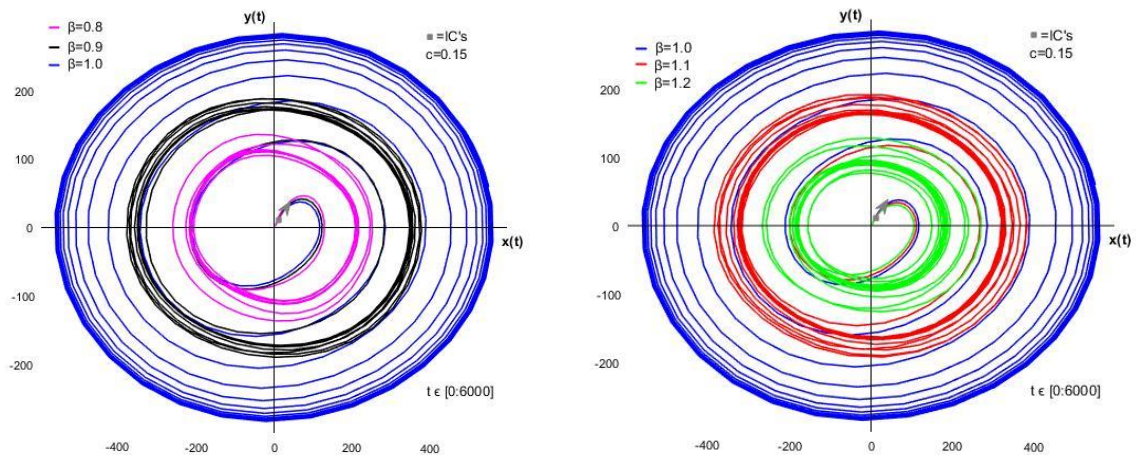


Figure 9.3: Limit cycles in the base-case system with  $\beta$  between 0,8 and 1,0(left) and between 1,0 and 1,2(right), with  $c=0,15$ .

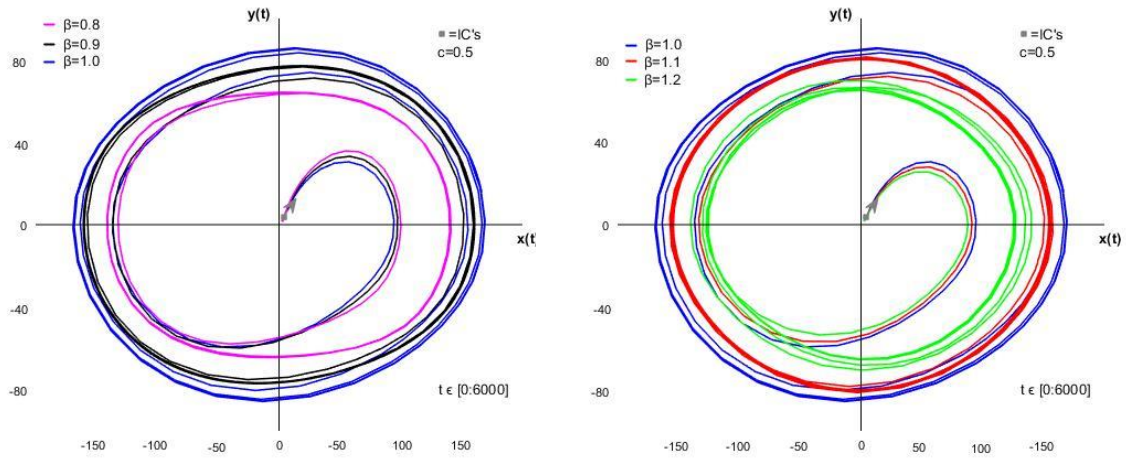


Figure 9.4: Limit cycles in the base-case system with  $\beta$  between 0,8 and 1,0(left) and between 1,0 and 1,2(right), with  $c=0,5$ .

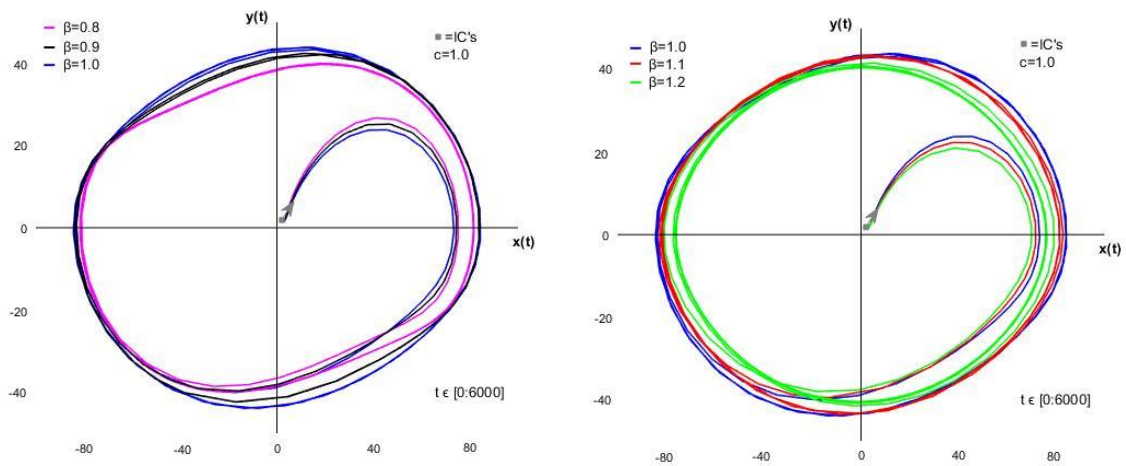


Figure 9.5: Limit cycles in the base-case system with  $\beta$  between 0,8 and 1,0(left) and between 1,0 and 1,2(right), with  $c=1,0$ .

## 9.2 Exploration of limit cycles for base-case systems

with  $\beta = \frac{1}{3}, \beta = \frac{1}{2}, \beta = 1,0, \beta = \frac{3}{2}$  and  $\beta = 2,0$

When  $\beta=1,0$ , the loading frequency,  $\omega$ , is equal to the natural frequency of the system,  $\omega_0$ . The periods of the system are given by:

$$T_0 = \frac{2\pi}{\omega_0} \quad (9.1)$$

$$T = \frac{2\pi}{\omega} \quad (9.2)$$

$T_0$  is the natural period of the system, and  $T$  is the loading period. This makes it possible to express  $\beta$  as:

$$\beta = \frac{\omega}{\omega_0} = \frac{T_0}{T} \quad (9.3)$$

This means that when  $\beta=1,0$ , the period of the loading is equal to the natural period of the system. Resonance is thereby the phenomena that occurs when for example a wave has the same period as the structure it encounters.

In the following part, the following systems will be investigated for limit cycles in the phase plane for **higher order resonances** [26]:

- $\beta=1/3$ , i.e. the period of the wave is three times bigger than the period of the structure.
- $\beta=1/2$ , i.e. the period of the wave is double the period of the structure.
- $\beta=3/2$ , i.e. the period of the wave is 2/3 of the period of the structure.
- $\beta=2,0$ , i.e. the period of the wave is half of the period of the structure.

### 9.2.1 $\beta = \frac{1}{3}$

When adjusting the mass coefficient in the base-case system to  $m=0,222$ , we get a system with  $\beta = \frac{1}{3}$ . Figure 9.6 shows the phase plane diagrams for the systems with  $c=0,15$  to the left and with  $c=0,5$  to the right. The systems have clear limit cycles, and the increase of a linear damping coefficient,  $c$ , seems to decrease to limit cycle amplitude, as well as making it appear earlier. Figure 9.7 show the position curves for the systems, also here with  $c=0,15$  on the left and  $c=0,5$  on the right. The different colours in the plot represents the four different initial conditions, which are the same as in the phase plane diagrams. Figure 9.8 show the velocity curves for the same systems. When  $\beta=1/3$ , i.e. the period of the wave is three times the period of the structure, the limit cycles occur rather quickly. Figure 9.9 show the position curve for the systems for the first 35s.

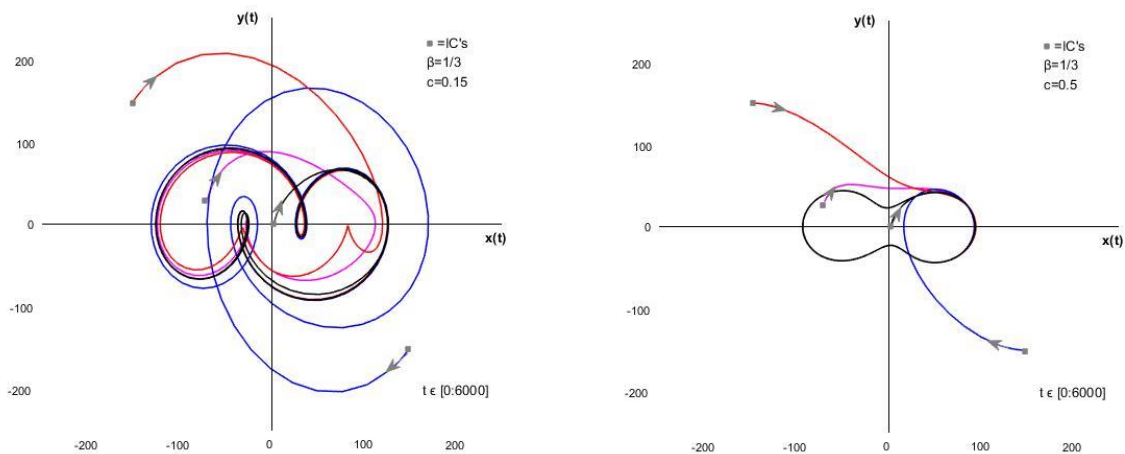


Figure 9.6: Base-case system with  $m=0,222$ , making  $\beta=1/3$  with  $c=0,15$ (left) and  $c=0,5$ (right) for four different set of initial conditions.

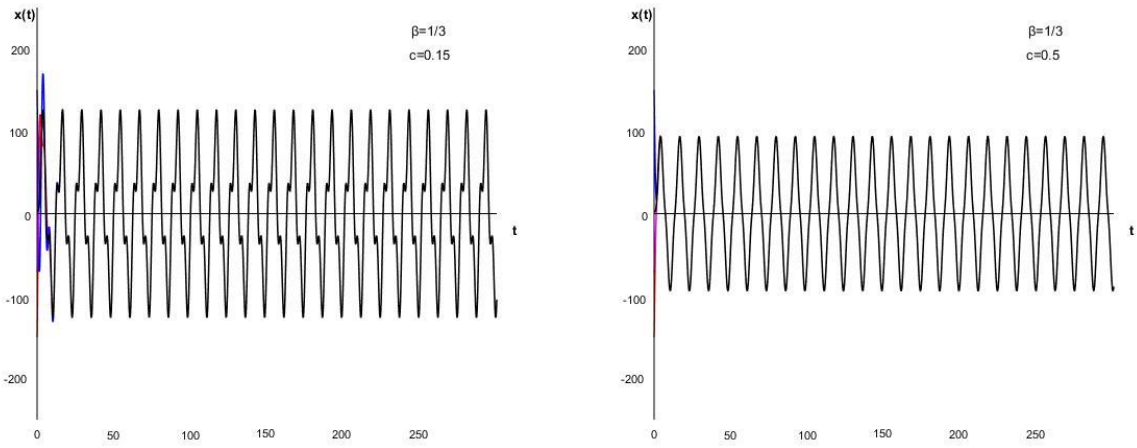


Figure 9.7: Position curves for the system with  $\beta=1/3$ ,  $c=0,15$ (left) and  $c=0,5$ (right) for four different set of initial conditions represented by separate colours.

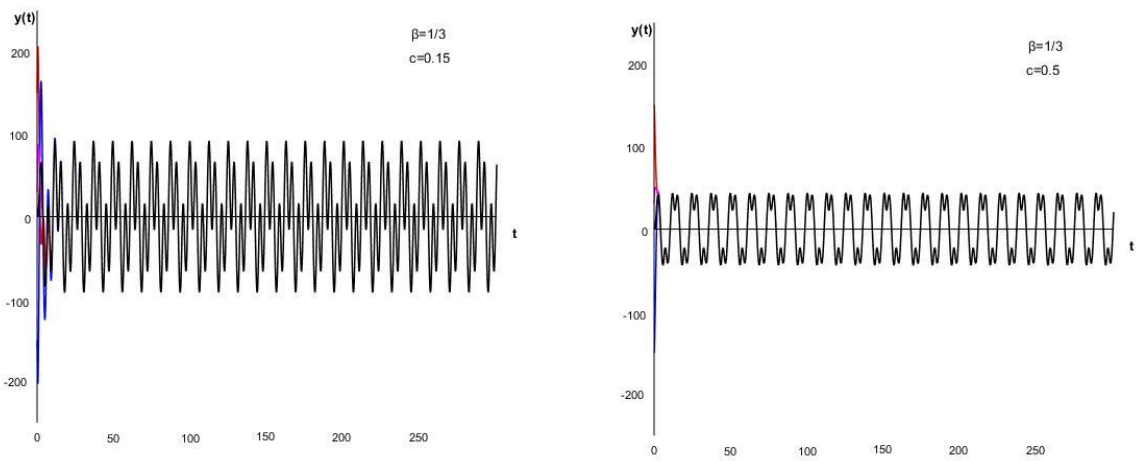


Figure 9.8: Velocity curves for the system with  $\beta=1/3$ ,  $c=0,15$ (left) and  $c=0,5$ (right) for four different set of initial conditions represented by separate colours.

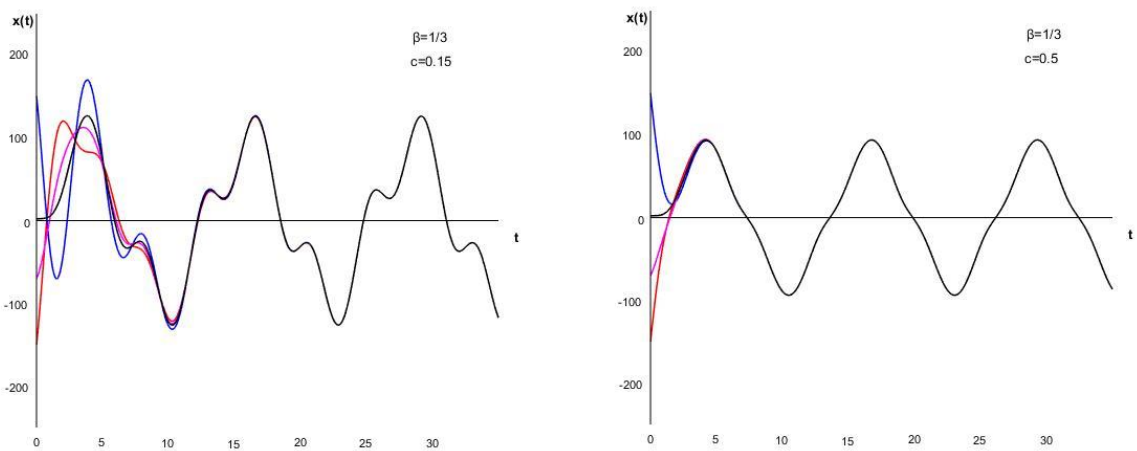


Figure 9.9: The first 35s of the position curves for the system with  $\beta=1/3$ ,  $c=0,15$ (left) and  $c=0,5$ (right) for four different set of initial conditions represented by separate colours.



### 9.2.2 $\beta = \frac{1}{2}$

When adjusting the mass coefficient in the base-case system to  $m=0,5$ , we get a system with  $\beta = \frac{1}{2}$ . Figure 9.10 show the phase plane diagrams for the systems with  $c=0,15$  to the left and with  $c=0,5$  to the right. The systems have clear limit cycles. Figures 9.11 and 9.12 show the position and velocity curves respectively. Also for these systems, the limit cycles occur rather fast. Figure 9.13 show the position curves for the systems for the first 35s.

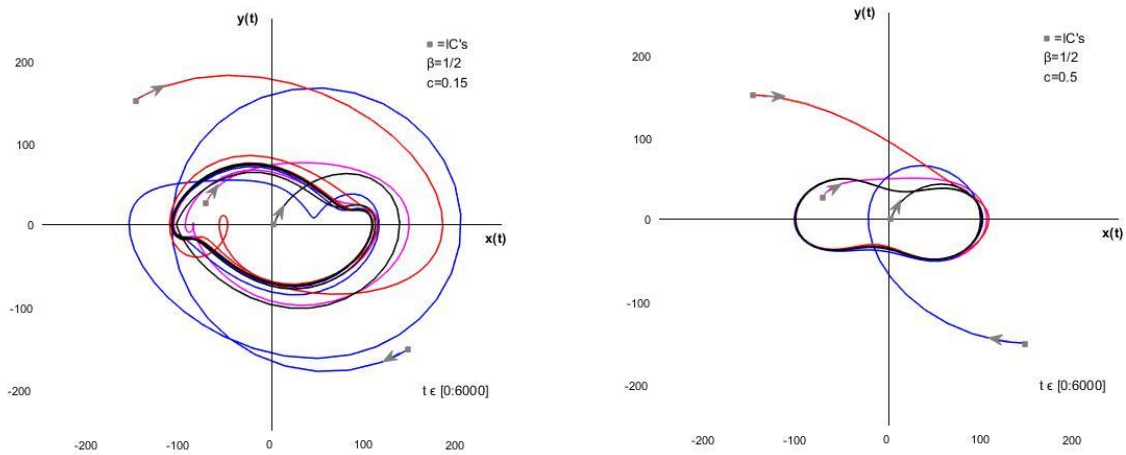


Figure 9.10: Base-case system with  $m=0,5$ , making  $\beta=1/2$  with  $c=0,15$ (left) and  $c=0,5$ (right) for four different set of initial conditions represented with separate colours.

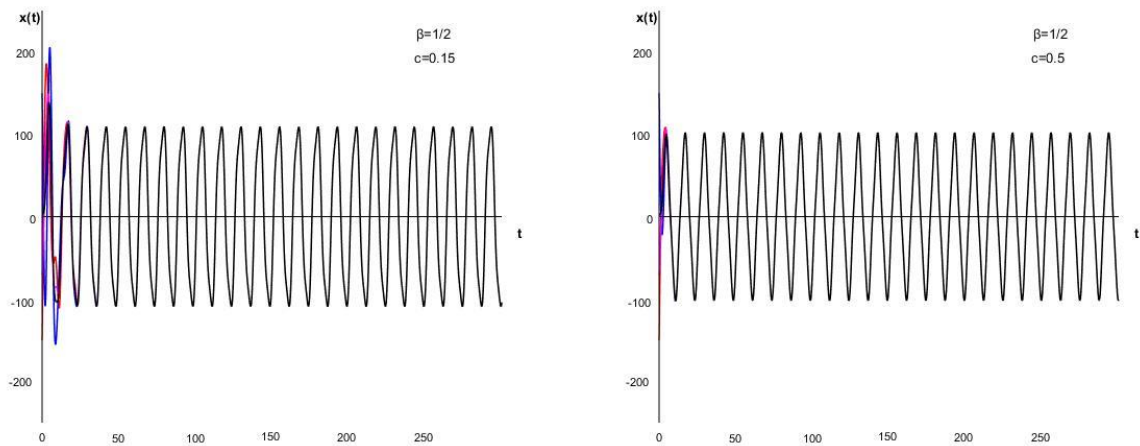


Figure 9.11: Position curves for the system with  $\beta=1/2$ ,  $c=0,15$ (left) and  $c=0,5$ (right) for four different set of initial conditions represented by separate colours.

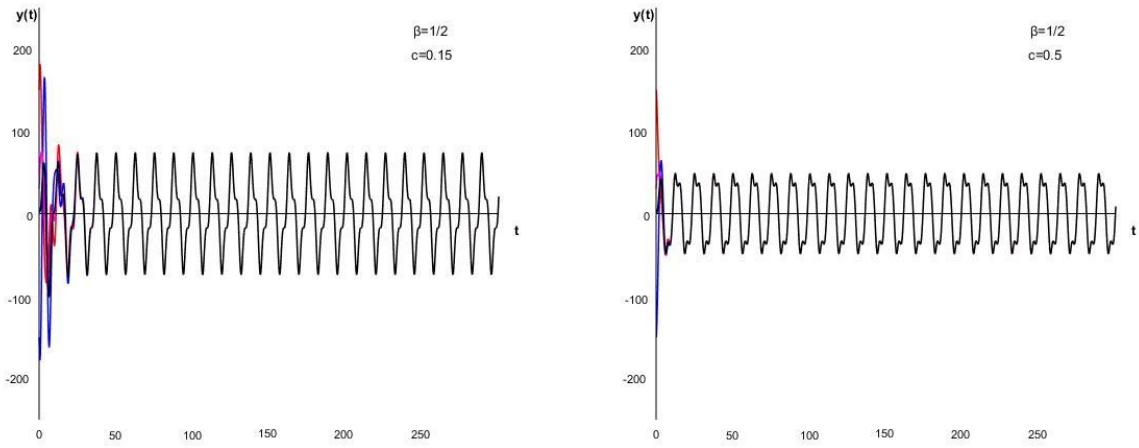


Figure 9.12: Velocity curves for the system with  $\beta=1/2$ ,  $c=0,15$ (left) and  $c=0,5$ (right) for four different set of initial conditions represented by separate colours.

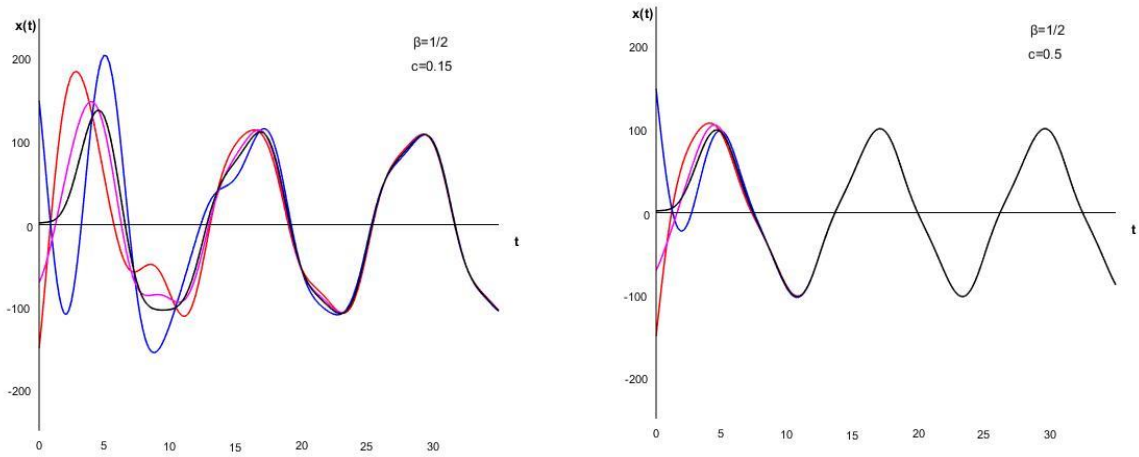


Figure 9.13: The first 35s of the position curves for the system with  $\beta=1/2$ ,  $c=0,15$ (left) and  $c=0,5$ (right) for four different set of initial conditions represented by separate colours.

### 9.2.3 $\beta = 1,0$

When the mass parameter in the base-case system is set to  $m=2,0$ , we get a system at resonance,  $\beta=1,0$ , which means that the period of the wave is equal to the natural period of the structure. Figure 9.14 show the system with two values of linear damping,  $c=0,15$  to the left and  $c=0,5$  to the right. Figures 9.15 and 9.16 show the systems position and velocity curves respectively. Figure 9.17 shows the position curve for the system in the first 100s. It should be noted that the sets of initial conditions are different for these systems than the others. The systems at resonance have limit cycles in the phase plane diagrams, and the trajectories spiral quickly towards them. The increase of the damping coefficient,  $c$ , rapidly increases the amplitude where the limit cycle occurs.

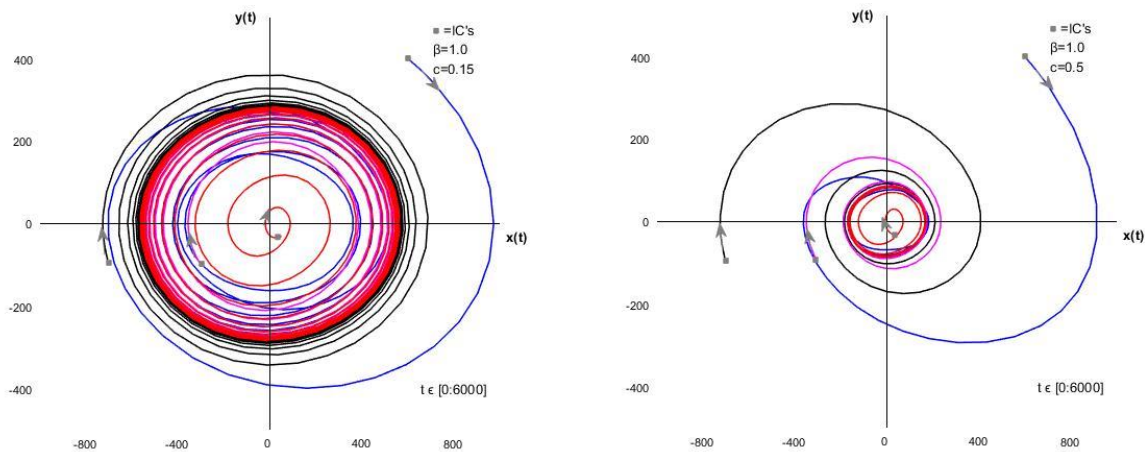


Figure 9.14: Base-case system with  $m=2,0$ , making  $\beta=1/2$  with  $c=0,15$ (left) and  $c=0,5$ (right) for four different set of initial conditions represented with separate colours.

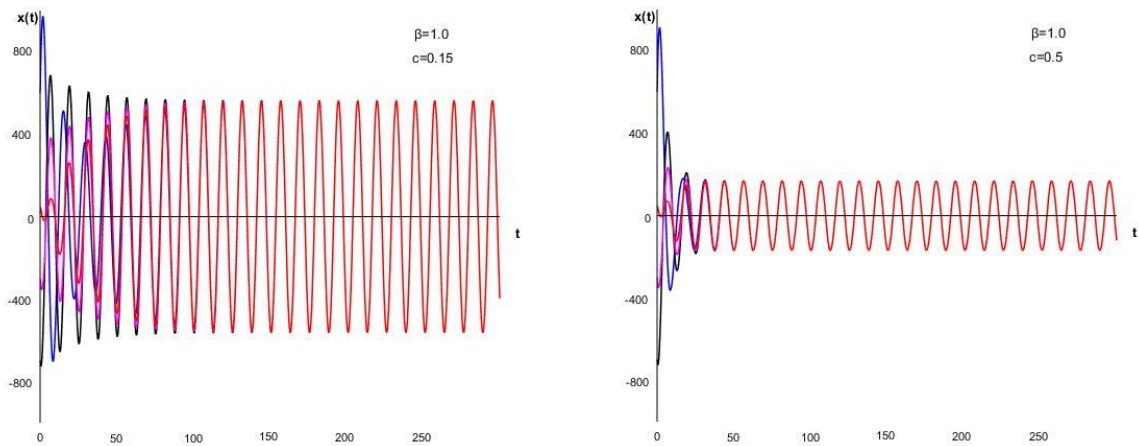


Figure 9.15: Position curves for the system with  $\beta=1,0$ ,  $c=0,15$ (left) and  $c=0,5$ (right) for four different set of initial conditions represented by separate colours.

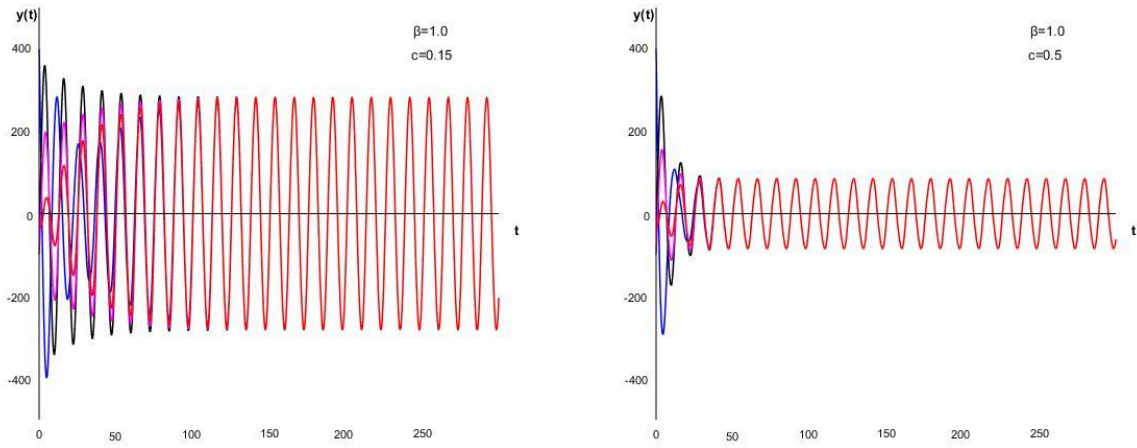


Figure 9.16: Velocity curves for the system with  $\beta=1,0$ ,  $c=0,15$ (left) and  $c=0,5$ (right) for four different set of initial conditions represented by separate colours.

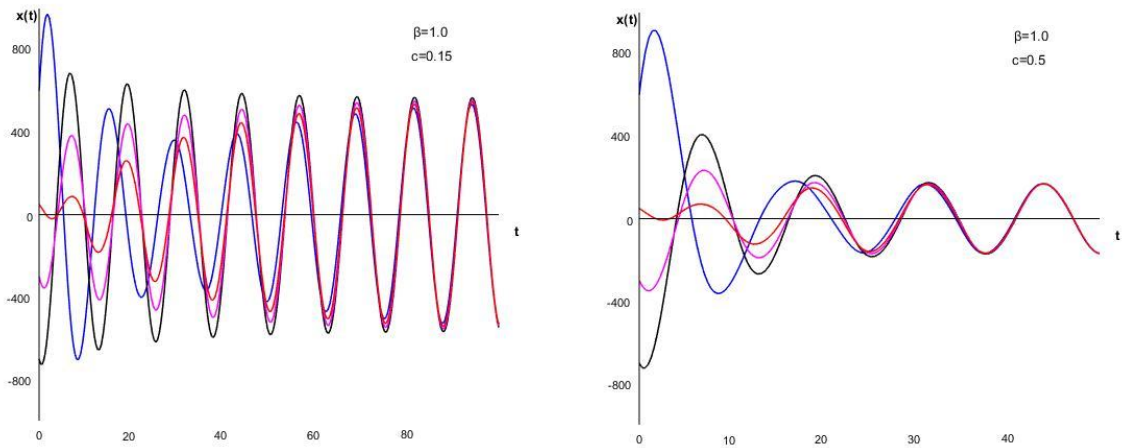


Figure 9.17: The first 100s of the position curves for the system with  $\beta=1,0$ ,  $c=0,15$ (left) and  $c=0,5$ (right) for four different set of initial conditions represented by separate colours.

### 9.2.4 $\beta = \frac{3}{2}$

When the mass parameter in the base-case system is set to  $m=4,5$ , we get  $\beta=3/2$ , which means that the period of the wave is  $2/3$  of the period of the structure. Figure 9.18 show the system with two values of linear damping,  $c=0,15$  to the left and  $c=0,5$  to the right. Figures 9.19 and 9.20 show the systems position and velocity curves respectively. Figure 9.21 show the position curves for the first 100s. The systems exhibit limit cycles in the phase plane, but the trajectories use longer time to get there, i.e. the transient solution is more visible. The effect of increasing the linear damping coefficient,  $c$ , is also more visible.

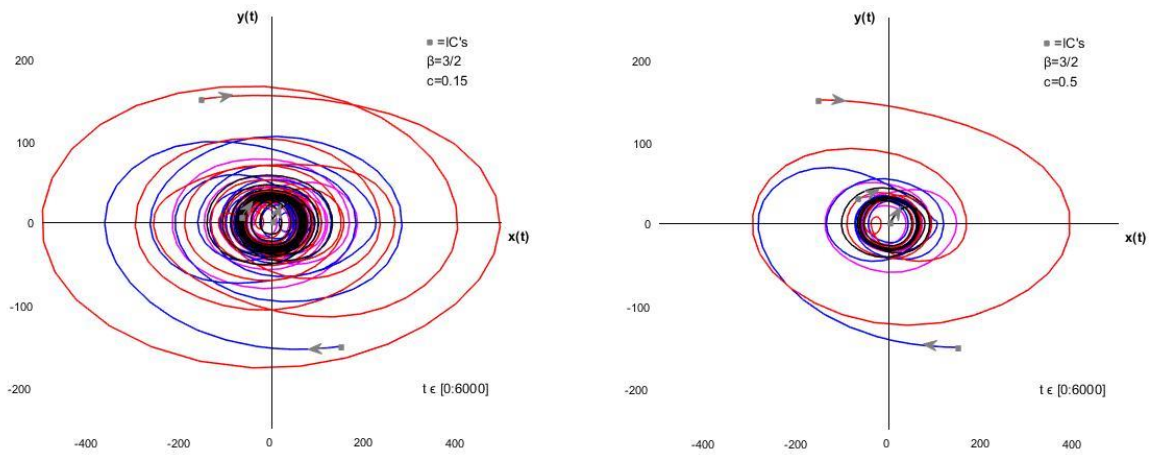


Figure 9.18: Base-case system with  $m=4,5$ , making  $\beta=3/2$  with  $c=0,15$ (left) and  $c=0,5$ (right) for four different set of initial conditions represented with separate colours.

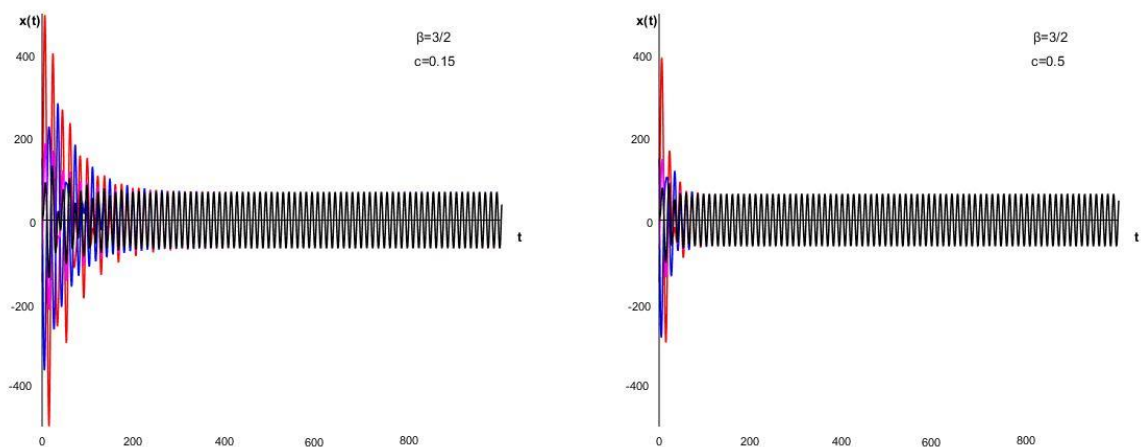


Figure 9.19: Position curves for the system with  $\beta=3/2$ ,  $c=0,15$ (left) and  $c=0,5$ (right) for four different set of initial conditions represented by separate colours.

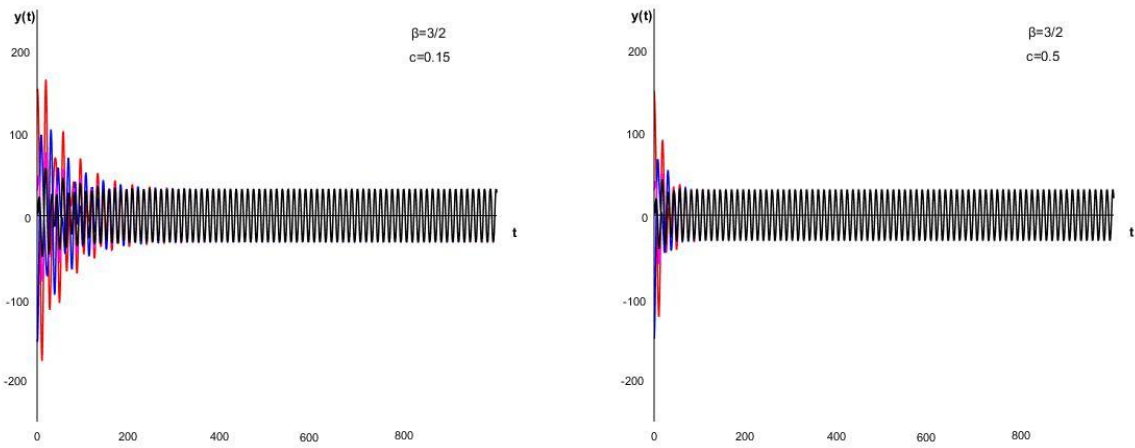


Figure 9.20: Velocity curves for the system with  $\beta=3/2$ ,  $c=0,15$ (left) and  $c=0,5$ (right) for four different set of initial conditions represented by separate colours.

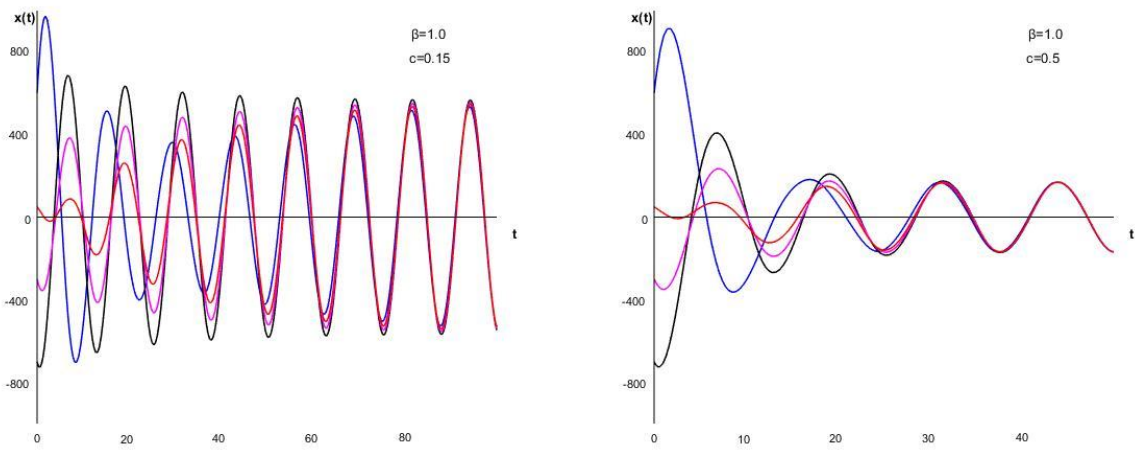


Figure 9.21: The first 100s of the position curves for the system with  $\beta=3/2$ ,  $c=0,15$ (left) and  $c=0,5$ (right) for four different set of initial conditions represented by separate colours.

### 9.2.5 $\beta = 2,0$

When adjusting the mass coefficient in the base-case system to  $m=8,0$ , we get a system with  $\beta = 2$ . This means that the period of the wave is half of the period of the structure. Figure 9.22 show the phase plane diagrams for the systems with  $c=0,15$  to the left and with  $c=0,5$  to the right. Figures 9.23 and 9.24 show the position and velocity curves for the systems respectively. Figure 9.24 show the position curves for the first 100s. It should be noted that the systems with  $\beta=2,0$  have different initial conditions than the systems for the other values.

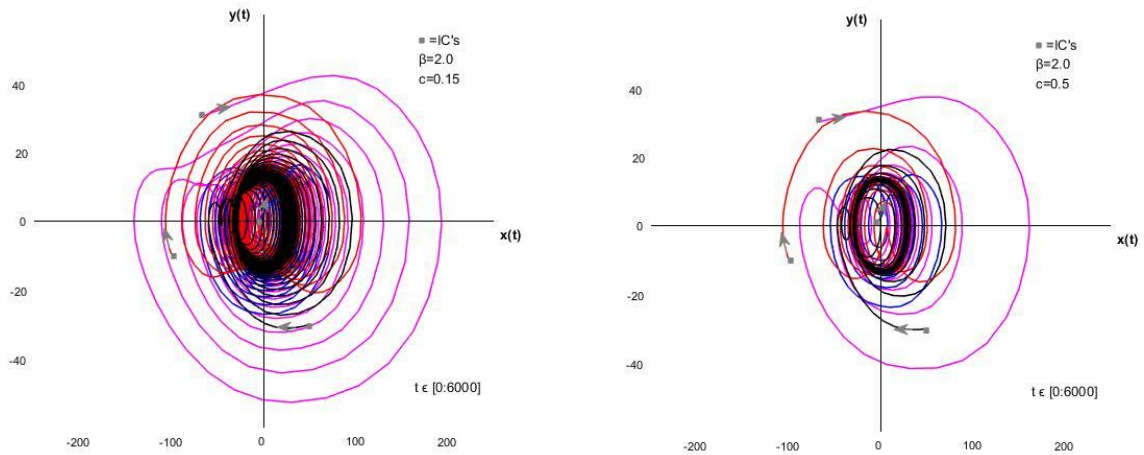


Figure 9.22: Base-case system with  $m=8,0$ , making  $\beta=2,0$  with  $c=0,15$ (left) and  $c=0,5$ (right) for four different set of initial conditions represented with separate colours.

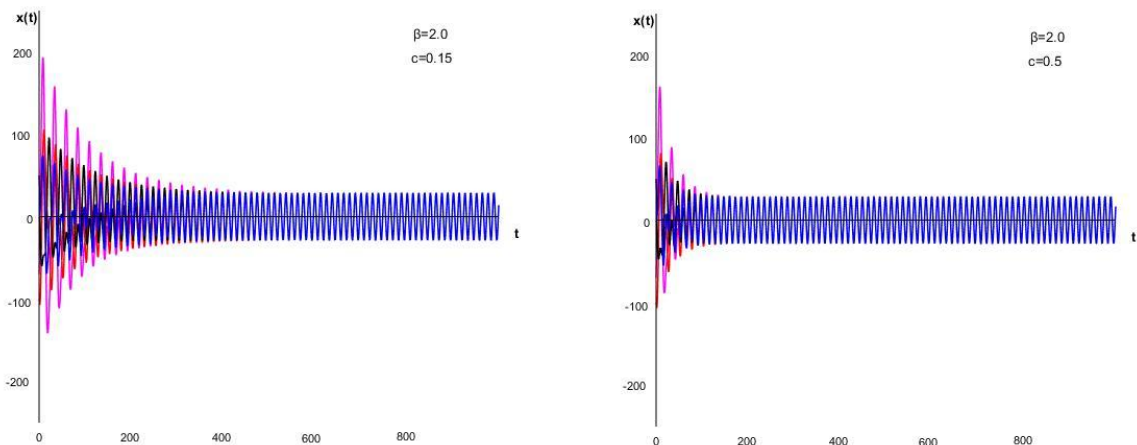


Figure 9.23: Position curves for the system with  $\beta=2,0$ ,  $c=0,15$ (left) and  $c=0,5$ (right) for four different set of initial conditions represented by separate colours.

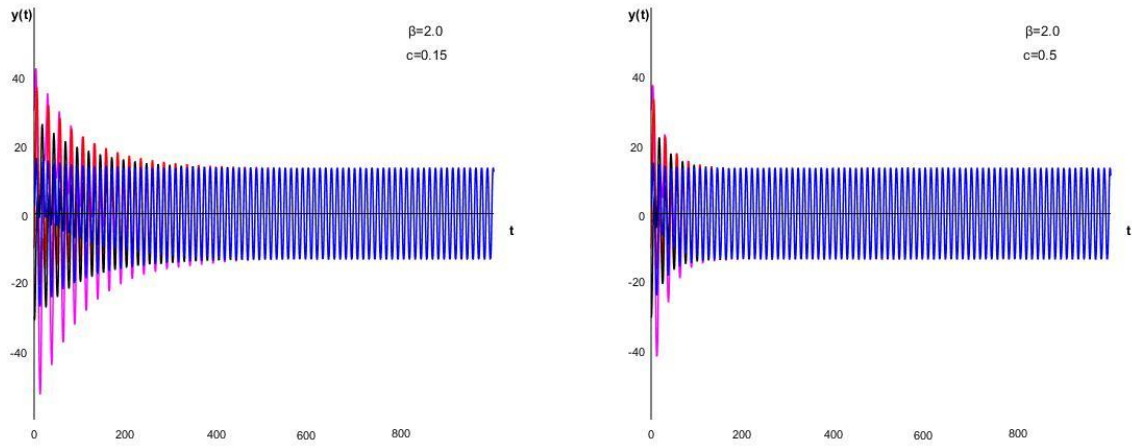


Figure 9.24: Velocity curves for the system with  $\beta=2,0$ ,  $c=0,15$ (left) and  $c=0,5$ (right) for four different set of initial conditions represented by separate colours.

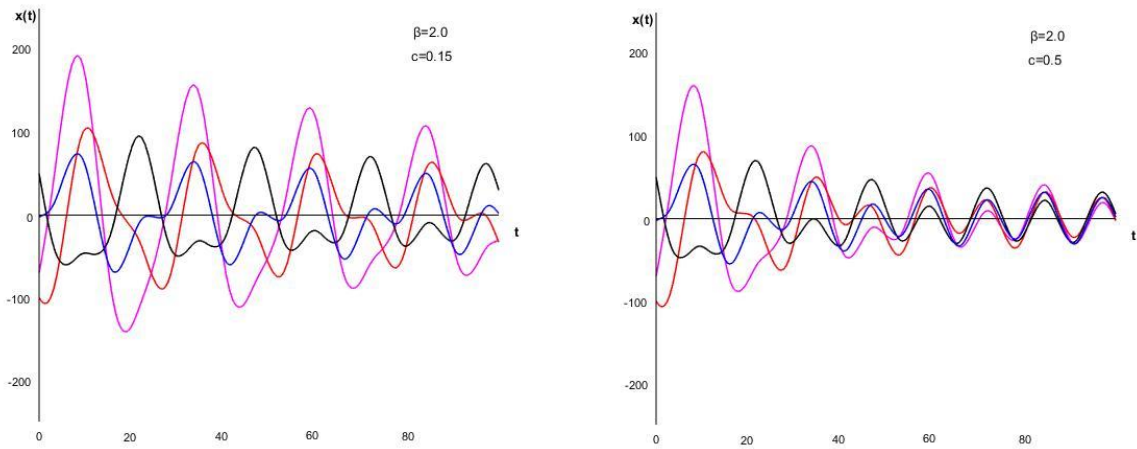


Figure 9.25: The first 100s of the position curves for the system with  $\beta=2,0$ ,  $c=0,15$ (left) and  $c=0,5$ (right) for four different set of initial conditions represented by separate colours.



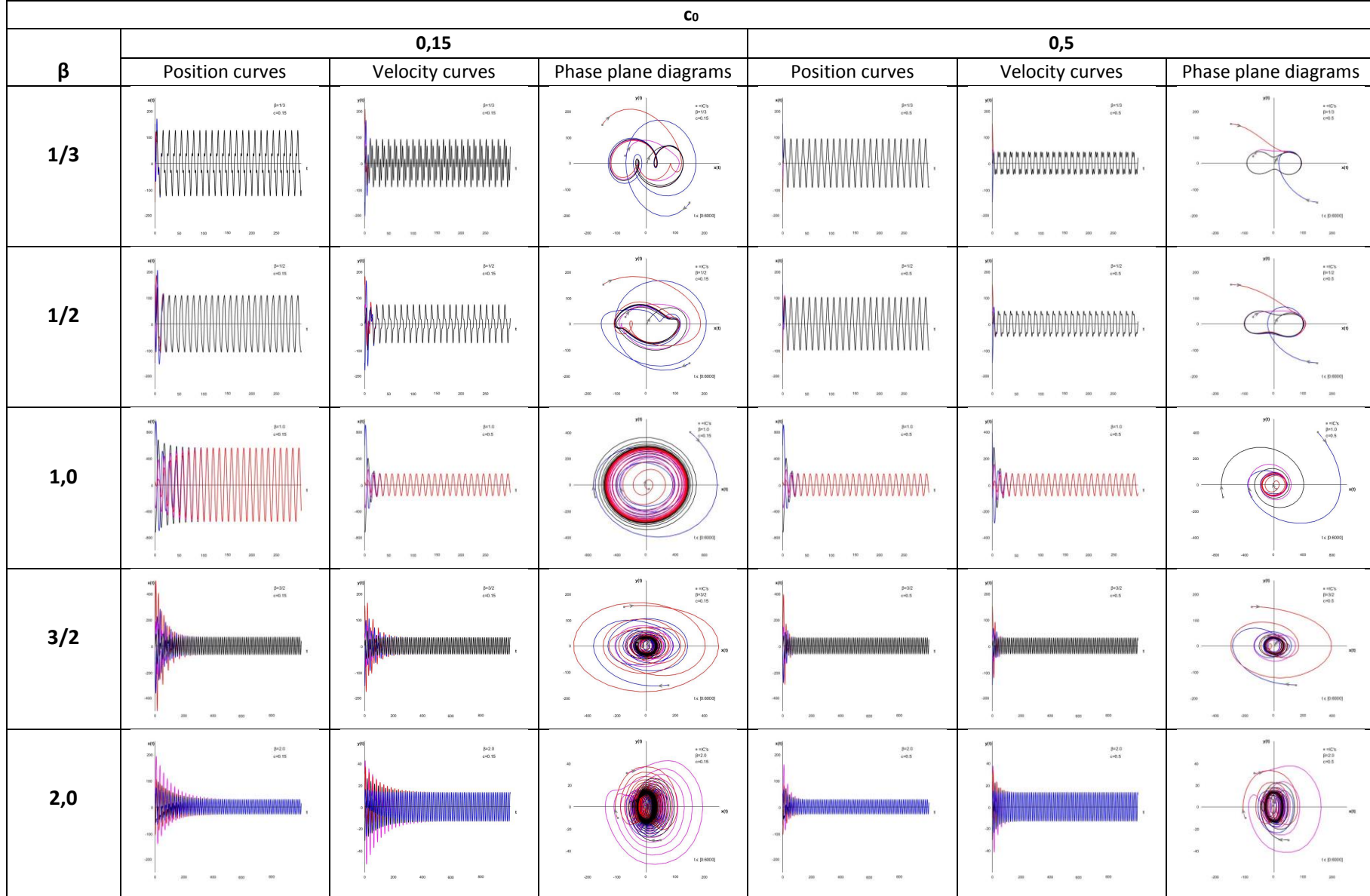


Table 9.1: Review of position curves, velocity curves and phase plane diagrams for the base-case system with the mass varied close to resonance, for two types of linear damping,  $c=0,15$  and  $c=0,5$ , for four different set of initial conditions.

It should be noted that the axis and timespans for  $\beta=1,0$ ,  $\beta=3/2$  and  $\beta=2,0$  differ from the axis in the diagrams for the other vales of  $\beta$ .

### 9.3 Conclusion

A one degree of freedom system subjected to drag loading and linear, constant damping will have limit cycles near and at resonance. As the damping is constant and linear, the drag loading will to some degree work as **negative damping**, making the generation and dissipation of energy in the system balanced. The trajectories having initial conditions outside the limit cycle decrease their amplitudes, while the trajectories starting inside the limit cycle increase their amplitudes into the limit cycles.

### 9.4 Consequences for offshore structures

For waves that have periods in resonance with the construction ( $\omega=\omega_0$ ,  $\beta=1$ ), we get a limit cycle behaviour of the response (at least for small values of damping), giving systems starting at some initial conditions an increase in amplitude. This behaviour is discussed in the report "*Transient motions of an oscillating system caused by forcing terms proportional to the velocity of the structural motion*" by Gudmestad O.T [20]. The forcing term does thus include a negative damping component, which can be seen when linearizing the forcing term [20].

For higher order resonances,  $\beta=1/2$  and  $\beta=1/3$  as well as for  $\beta=3/2$  and  $\beta=2,0$ , similar behaviour is observed, thereby energy from waves with higher periods, for example 15 seconds and 10 seconds, respectively, is fed into a system with natural period of 5 seconds. In storm situations, the energy spectrum has high values for higher periodic waves and considerable displacements and velocities can be expected, see also Appendix E.

# Chapter 10 - Conclusions and further work

## 10.1 Part I

This thesis has been divided into two parts. Part I starts with preliminary considerations, a short historic overview of the nonlinearity in engineering as well as the introduction of the **phase plane method**. The method is in part I used to describe linear systems with different degrees of damping inherent. In chapter 2, the system is homogenous, i.e.  $F(t)=0$ , while in chapter 3, a linear forcing term is added to the systems.

Chapter 4 gives a presentation of one degree of freedom equations for known nonlinear systems. The van der Pol equation is well known for describing systems with a **nonlinear damping term**. Systems described using the van der Pol equation exhibits **limit cycles**. Limit cycles are closed orbits in the phase plane, in which all near trajectories with different initial conditions will either spiral towards or away from. A limit cycle is said to be stable when all trajectories spiral towards it.

The pendulum equation is a known equation for describing the pendulum which has a **nonlinear stiffness**. The pendulum equation is often linearized by using small angle approximation. The angular response as a function of time is presented in chapter 4 for both the linearized and the non-linearized pendulum equation. It clearly shows the problem with linearization when the angles are increased. The phase plane diagram for the unforced pendulum equation is also presented, both without and with damping inherent.

The Morison equation is a well-known equation within the marine engineering community. It is used to describe the inline force on a body in oscillatory flow. The Morison equation consists of the drag force and the mass force.

## 10.2 Part II

In part I, the systems and diagrams plotted are well known. In part II, a system with random values of the parameters is chosen. This system is named the base-case system. The aim of part II is to analyse what happens in this system when varying the values of the parameters. The base-case system is in chapter 5 subjected to a nonlinear force, representing the drag force from the Morison equation. The system's parameters for stiffness, amplitude, loading frequency and mass are varied to look at their impact on the system, and the system is in chapter 5 looked at without damping. The results obtained from chapter 5 are:

- When the stiffness parameter,  $k$ , is increased, the periods decrease, the position amplitude decrease, while the velocity amplitudes are not affected. The effect of the nonlinearity in the forcing term is decreased as  $k$  is increased.
- The increase of the amplitude parameter,  $F_0$ , does not affect the period, while both the position and velocity amplitude is increased. The effect of the nonlinearity increases as  $F_0$  is increased.
- The loading frequency,  $\omega$ , does not affect the period. Some decrease in the position and velocity amplitude were noticed when  $\omega$  was increased. This was most visible in the lower values of  $\omega$ , where

the systems were closer to resonance. The increase of  $\omega$ , makes the effect of the nonlinearity in the forcing term decrease.

- When the mass parameter,  $m$ , was increased, the periods increased. The position amplitudes do not seem to be affected, while a little decrease in velocity amplitude was seen. The variation of the mass parameter does not seem to affect the nonlinearity from the forcing term.

- When the systems mass or loading frequency are increased to values close to resonance, i.e.  $\omega=\omega_0$ , the systems positions and velocities amplitudes increase as  $\beta$  gets larger, up until  $\beta=1,0$ . At resonance, i.e.  $\beta=1,0$ , both systems experience an unlimited growth in both velocity and position. When the parameters are increased over the resonance values the systems go back to the steady path of increase and decrease in amplitudes. The increase of  $\beta$  after  $\beta=1,0$ , decreases the position and velocity amplitudes.

In chapter 6, linear, constant damping is added to the base-case system, as well as for some selected systems from chapter 5. When varying the parameters around the values from the base-case system, we get results as expected. The linear, constant damping will decay the oscillations, making the systems spiral towards the origin in the phase plane diagrams. When the mass parameter is set to values making the base-case system close to and at resonance, the results are a bit different. The addition of damping makes the systems' amplitudes increase up until the point where they have a steady trajectory in the phase plane. These trajectories are similar to those showed for the van der Pol equation in chapter 4.

In chapter 7 nonlinear damping was added to the base-case system, and the system was made homogenous, i.e.  $F(t)=0$ . The base-case system was investigated as well as the systems with the mass varied to make systems with  $\beta=1/3-2,0$ . It was found that all the systems had their own **critical value** of the nonlinear damping coefficient  $a$ . At this value, the systems were overtaken by the negative damping leading to a continuous growth in amplitudes. The following values of  $a$  was found:

- $a=1,20$  for the base-case system, where  $\beta=7,07$ .
- $a=3,46$  for the system with  $\beta=1/3$  for both values of  $c_0$
- $a=1,61$  for the system with  $\beta=1/2$  for both values of  $c_0$
- $a=1,04$  for the system with  $\beta=1,0$  for both values of  $c_0$
- $a=0,37$  for the system with  $\beta=3/2$  for both values of  $c_0$
- $a=0,01$  for the system with  $\beta=2,0$  and  $c_0=0,0015$
- $a=0,02$  for the system with  $\beta=2,0$  and  $c_0=0,005$

In chapter 8, a linear forcing term was added to the systems from chapter 7, and the same investigations were conducted. It was found that the systems were still overtaken by the negative damping at the same **critical values** of  $a$ , as was found in chapter 7. In the Marintek report "Comparing simple models for prediction of ringing loads and responses", 3.2.2 [24], it is mentioned that their nonlinear damping parameter,  $\beta$ , which the nonlinear damping parameter in this thesis,  $a$ , is based on, will be different for different systems.

An exploration around limit cycles was conducted in chapter 9. The base-case system with nonlinear forcing term and linear, constant damping was investigated for values of the mass parameter making

$\beta=1/3-2,0$ . It was in this chapter concluded that a one degree of freedom system subjected to drag loading and linear, constant damping will have limit cycles near and at resonance. As the damping is constant and linear, the drag loading will to some degree work as **negative damping**, making the generation and dissipation of energy in the system balanced.

For higher order resonances,  $\beta=1/2$  and  $\beta=1/3$  as well as for  $\beta=3/2$  and  $\beta=2,0$ , similar behaviour is observed, thereby energy from waves with higher periods, for example 15 seconds and 10 seconds, respectively, is fed into a system with natural period of 5 seconds. In storm situations, the energy spectrum has high values for higher periodic waves and considerable displacements and velocities can be expected, see also Appendix E.

### 10.3 Further work

The following is suggested:

- As suggested in the Marintek report [24], further work to establish a **“normalized” parameter** for the nonlinear damping that does not depend on the actual system would be favourable. Also the load model suggested in [24] needs more investigation.
- The “base-case system” chosen to investigate in this thesis has been chosen more or less at random. **Further work would include to use values to describe an actual physical system.** A natural place to start with this is the values from the Draugen monotower model from the Marintek report [24], as the nonlinear damping term in this thesis is based on that report.
- Appendix E in this thesis is directly copied from the master thesis *“Apparent Negative Damping an Original Approach to the Oscillations of Offshore Structures”* by Rayne Babbiste from 2016. [25] It consists of an interview with the platform manager, Nils Gunnar Gundersen, of the Shell Draugen platform, about an incident occurring in 1995. The platform was hit by a great wave, but fortunately the platform was designed in such a way that no significant harm occurred. Rayne concludes that this wave may have been the result of crossflow oscillations. From the work conducted in this thesis, the large response **may have been the result of negative damping from the drag force in the Morison equation, causing a wave with a large period and a large amplitude, hitting a structure, resulting in some degree of resonance.** This should be further investigated.
- The drag load from the Morison equation is used to describe oscillatory flow past an obstacle. It is suggested that there might be some interest in the medical science to use this equation to describe the flow in blood veins past obstacles as for example blood clots. Note that the loading is oscillatory (the heart pumps the blood at a certain frequency). The research question is therefore if **certain frequencies of the heartbeat would cause resonance in the system and possible movements of the clots**, a situation most undesirable for the patient.

# References

- [1] Archibald T, Fraser C, Grattan-Guinness I. *The History of Differential Equations, 1670-1950*. Mathematisches Forschungsinstitut Oberwolfach; Report No. 51/2004 Available from: <https://www.scribd.com/doc/31730457/The-History-of-Differential-Equations-1670-1950>
- [2] Robinson J.C. *An Introduction to Ordinary Differential Equations*. Cambridge University Press; 2004 Available from: [http://faculty.mu.edu.sa/public/uploads/1358974368.6105An\\_Introduction\\_to\\_Ordinary\\_Differential\\_Equations.pdf](http://faculty.mu.edu.sa/public/uploads/1358974368.6105An_Introduction_to_Ordinary_Differential_Equations.pdf)
- [3] Hirsch M.W, Smale S, Devaney R.L. *Differential Equations, Dynamical Systems & An Introduction to Chaos*. Second Edition. Elsevier Academic Press; 2004 Available from: <https://www.math.upatras.gr/~bountis/files/def-eq.pdf>
- [4] Burke K.M. *Nonlinearity: The history and philosophy of the science*[paper]. University of Missouri-St.Louis; 2009 Available from: <http://files.eric.ed.gov/fulltext/ED504453.pdf>
- [5] Fidlin A. *Nonlinear Oscillations in Mechanical Engineering*. N.D. Springer-Verlag Berlin Heidelberg; 2006
- [6] *The phase plane*. [lecture notes]. Pennsylvania State University; 2008 Available from: <http://www.math.psu.edu/tseng/class/Math251/Notes-PhasePlane.pdf>
- [7] Struble R.A, Martin W.T. *Nonlinear Differential Equations*. McGraw-Hill Book Company, INC; 1962
- [8] Wagg D, Bond I, Weaver P, Friswell M. *Adaptive Structures: Engineering Applications*. John Wiley & Sons, Ltd; 2007
- [9] Marion J.B, Thornton S.T. *Classical Dynamics of Particles & Systems*. Third Edition. Harcourt Brace Jovanovich, Inc; 1988
- [10] Gudmestad O.T. *Marine Technology and Operations. Theory and Practice*. WIT Press; 2015
- [11] Strogatz S.H. *Nonlinear Dynamics and Chaos. With Applications to Physics, Biology, Chemistry, and Engineering*. Perseus Books Publishing, LLC; 1994
- [12] Guckenheimer J, Holmes P. *Nonlinear Oscillations, Dynamical Systems, and Bifurcations of Vector Fields*. Springer-Verlag Berlin Heidelberg; 2002
- [13] Guckenheimer J, Hoffman K, Weckesser W. *The Forced van der Pol Equation I: The Slow Flow and Its Bifurcations*. Society for Industrial and Applied Mathematics; 2003
- [14] Brown University. *Chapter Seven: The Pendulum and phase-plane plots*. Lecture notes; 2006 Available from: <http://www.dam.brown.edu/people/mumford/beyond/coursenotes/2006PartIIb.pdf>
- [15] Beuter A, Glass L, Mackey M.C, Titcombe M.S. *Nonlinear Dynamics in Physiology and Medicine*. Springer-Verlag New York, Inc; 2003
- [16] Rowat F.P, Selverston I. A. *Modeling the Gastric Mill Central Pattern Generator of the Lobster With a Relaxation-Oscillator Network*. Journal of Neurophysiology; Vol. 70. No. 3, September 1993 Available from: <http://citeseerx.ist.psu.edu/viewdoc/download?doi=10.1.1.423.5860&rep=rep1&type=pdf>

[17] Cartwright J.H.E., Eguiluz V.M., Hernandez-Garcia E, Piro O. *Dynamics of elastic excitable media*. International Journal of Bifurcation and Chaos; Vol. 9, No 11 1999

Available from:

<https://pdfs.semanticscholar.org/3f5b/e3261cb7bc4df50c08d9c138e2b924c0fa1a.pdf>

[18] Zykov V.S. *Excitable media*. Scholarpedia; 2008 Available from:

[http://www.scholarpedia.org/article/Excitable\\_media](http://www.scholarpedia.org/article/Excitable_media)

[19] Brownjohn J.M.W. *Single degree of freedom(SDOF) systems*. University of Plymouth; 2005

Available from: [http://www.tech.plym.ac.uk/soe/james/my\\_papers/STRC201\\_SDOF\\_JMWB.pdf](http://www.tech.plym.ac.uk/soe/james/my_papers/STRC201_SDOF_JMWB.pdf)

[20] Gudmestad O.T. *Transient motions of an oscillating system caused by forcing terms proportional to the velocity of the structural motion*. Philosophical Transactions of The Royal Society; 2011, 369

[21] Bogoliubov N.N. and Mitropolsky Y.A. *Asymptotic methods in the theory of non-linear oscillations*. Hindustan Publishing Corpn(India); 1961

[22] Cao W. *Van der Pol Oscillator*. Celestial Mechanics: N.D

Available from: [http://www.math.cornell.edu/~templier/junior/final\\_paper/Wesley\\_Cao-vanderpol.pdf](http://www.math.cornell.edu/~templier/junior/final_paper/Wesley_Cao-vanderpol.pdf)

[23] Wallace T.T.L. and Homer L.T.H. *Mathematical Model of Forced Van Der Pol's Equation*; 2015

Available from: <https://www.overleaf.com/articles/forced-van-der-pols-equation/yjyxdhvbrcgq/viewer.pdf>

[24] Stansberg C.T. *Comparing simple models for prediction of ringing roads and responses*. Marintek report;2009

[25] Rayne B. *Apparent Negative Damping an Original Approach to the Oscillations of Offshore Structures*. Master thesis; 2016

[26] Gudmestad O.T. and Poubouras G.A. *Time and frequency domain wave forced on offshore structures*. Applied Ocean Research, Vol. 10, No. 1, 1988.

# Appendix A– Matlab codes

```

%%%%%%%%%%%%%%%%%%%%%%%%%%%%%%%%%%%%%%%%%%%%%%%%%%%%%%%%%%%%%%%%%%%%%%%%
%%Free response without damping%%
%%%%%%%%%%%%%%%%%%%%%%%%%%%%%%%%%%%%%%%%%%%%%%%%%%%%%%%%%%%%%%%%%%%%%%%%
d0=0; v0=5; w0=1.6;          %%Variables
t1=0:0.1:8; t2=0:0.1:10;    %%Timespans

x1=d0.*cos(w0.*t1)+(v0/w0).*sin(w0.*t1);
x2=d0.*cos(w0.*t2)+(v0/w0).*sin(w0.*t2);

plot(t1,x1,'k','LineWidth',1.2)    %%Plot whole line
hold on
plot(t2,x2,':k','LineWidth',1.2)   %%Plot dotted line

plot([0 10],[0 0],'k'); plot([0 0], [-4 4],'k'); %%Making new axis

axis off

%%%%%%%%%%%%%%%%%%%%%%%%%%%%%%%%%%%%%%%%%%%%%%%%%%%%%%%%%%%%%%%%%%%%%%%%
%%Unforced system in the phase plane without damping%%
%%%%%%%%%%%%%%%%%%%%%%%%%%%%%%%%%%%%%%%%%%%%%%%%%%%%%%%%%%%%%%%%%%%%%%%%

d0=4; v0=1; k=0.5; m=100; w0=sqrt(k/m);    %%Variables
t=0:0.1:180;                               %%Timespan

x=(d0.*cos(w0.*t))+((v0/w0).*sin(w0.*t));
y=(-d0.*w0.*sin(w0.*t))+v0.*cos(w0.*t);

plot(x,y,'k','Linewidth',1.2)
hold on

plot([-18 18],[0 0],'k');plot([0 0], [-5 5],'k'); %%Making new axis

axis off

%%%%%%%%%%%%%%%%%%%%%%%%%%%%%%%%%%%%%%%%%%%%%%%%%%%%%%%%%%%%%%%%%%%%%%%%
%%Response of unforced, underdamped system%%
%%%%%%%%%%%%%%%%%%%%%%%%%%%%%%%%%%%%%%%%%%%%%%%%%%%%%%%%%%%%%%%%%%%%%%%%

wd=0.9; c=0.9; m=2; d0=0; v0=5;          %%Variables
t1=0:0.1:18; t2=0:0.1:20;               %%Timespans

x1=exp((-c./(2.*m)).*t1).*(((v0/wd)+(c/(2*m*wd)*d0)).*sin((wd.*t1)+(d0.*cos(wd.*t1)))));
x2=exp((-c./(2.*m)).*t2).*(((v0/wd)+(c/(2*m*wd)*d0)).*sin((wd.*t2)+(d0.*cos(wd.*t2)))));

plot(t1,x1,'k','LineWidth',1.2)    %%Plot whole line
hold on
plot(t2,x2,':k','LineWidth',1.2)   %%Plot dotted line

plot([0 20],[0 0],'k'); plot([0 0], [-5 5],'k'); %%Making new axis

```



axis off

```
%%%%%%%%%%%%%%%%%%%%%%%%%%%%%%%%%%%%%%%%%%%%%%%%%%%%%%%%%%%%%%%%%%%%%%%%%  
%%unforced, underdamped system in u-v plane%%  
%%%%%%%%%%%%%%%%%%%%%%%%%%%%%%%%%%%%%%%%%%%%%%%%%%%%%%%%%%%%%%%%%%%%%%%%%  
A=5; wd=0.9; c=0.9; m=2; phi=0.2;          %%Variables  
t1=0:0.1:10; t2=0:0.1:22;                 %%Timespans
```

```
u1=A.*wd.*exp((-c./(2.*m)).*t1).*sin((wd.*t1)+phi);  
u2=A.*wd.*exp((-c./(2.*m)).*t2).*sin((wd.*t2)+phi);  
v1=A.*wd.*exp((-c./(2.*m)).*t1).*cos((wd.*t1)+phi);  
v2=A.*wd.*exp((-c./(2.*m)).*t2).*cos((wd.*t2)+phi);
```

```
plot(u1,v1,'k','LineWidth',1.2)           %%Plot whole line  
hold on  
plot(u2,v2,':k','LineWidth',1.2)         %%Plot dotted line
```

```
plot([-4 4],[0 0], 'k'); plot([0 0], [-5 5], 'k'); %%Making new axis
```

axis off

```
%%%%%%%%%%%%%%%%%%%%%%%%%%%%%%%%%%%%%%%%%%%%%%%%%%%%%%%%%%%%%%%%%%%%%%%%%  
%%unforced, underdamped system in phase plane%%  
%%%%%%%%%%%%%%%%%%%%%%%%%%%%%%%%%%%%%%%%%%%%%%%%%%%%%%%%%%%%%%%%%%%%%%%%%  
A=5; wd=0.9; c=0.9; m=2; phi=0.2;          %%Variables  
t1=0:0.1:10; t2=0:0.1:22;                 %%Timespans
```

```
u1=A.*wd.*exp((-c./(2.*m)).*t1).*sin((wd.*t1)+phi);  
u2=A.*wd.*exp((-c./(2.*m)).*t2).*sin((wd.*t2)+phi);  
v1=A.*wd.*exp((-c./(2.*m)).*t1).*cos((wd.*t1)+phi);  
v2=A.*wd.*exp((-c./(2.*m)).*t2).*cos((wd.*t2)+phi);  
x1=u1./wd;  
x2=u2./wd;  
y1=v1-c./(2.*m);  
y2=v2-c./(2.*m);
```

```
plot(x1,y1,'k','LineWidth',1.2)           %%Plot whole line  
hold on  
plot(x2,y2,':k','LineWidth',1.2)         %%Plot dotted line
```

```
plot([-4 4],[0 0], 'k'); plot([0 0], [-5 5], 'k'); %%Making new axis
```

axis off

```
%%%%%%%%%%%%%%%%%%%%%%%%%%%%%%%%%%%%%%%%%%%%%%%%%%%%%%%%%%%%%%%%%%%%%%%%%  
%%Free response overdamped system%%  
%%%%%%%%%%%%%%%%%%%%%%%%%%%%%%%%%%%%%%%%%%%%%%%%%%%%%%%%%%%%%%%%%%%%%%%%%
```

```
d0=0; v0=5; s1=-1; s2=-2;                %%Variables  
t1=0:0.1:5; t2=0:0.1:8;                 %%Timespans
```

```
x1=(((d0*s2)-v0)/(s2-s1)).*exp(s1.*t1)+((v0-(d0*s1))/(s2-s1)).*exp(s2.*t1);
```

```
x2=((d0*s2-v0)/(s2-s1)).*exp(s1.*t2)+((v0-(d0*s1))/(s2-s1)).*exp(s2.*t2);
```

```
plot(t1,x1,'k','LineWidth',1.2) %%Plot whole line
```

```
hold on
```

```
plot(t2,x2,'k','LineWidth',1.2) %%Plot dotted line
```

```
plot([0 8],[0 0],'k'); plot([0 0], [-2 2],'k'); %%Making new axis
```

```
axis off
```

```
%%%%%%%%%%%%%%%%%%%%%%%%%%%%%%%%%%%%%%%%%%%%%%%%%%%%%%%%%%%%%%%%%%%%%%%%  
%%unforced, overdamped system in u-v plane%%  
%%%%%%%%%%%%%%%%%%%%%%%%%%%%%%%%%%%%%%%%%%%%%%%%%%%%%%%%%%%%%%%%%%%%%%%%
```

```
a0=1; b0=1.5; a1=0; b1=1.5; a2=1; b2=0; a3=0; b3=-1.5; a4=-1; b4=0;
```

```
a5=0.7; b5=1; a6=-1; b6=-1.5; a7=-0.7; b7=-1; a8=-1; b8=1.5; a9=1;
```

```
b9=-1.5; a10=-0.7; b10=1; a11=0.7; b11=-1; s1=-1; s2=-0.5; %%Variables
```

```
t=0:0.1:10; %%Timespan
```

```
u0=a0.*exp(s1.*t);v0=b0.*exp(s2.*t);u1=a1.*exp(s1.*t);v1=b1.*exp(s2.*t);
```

```
u2=a2.*exp(s1.*t);v2=b2.*exp(s2.*t);u3=a3.*exp(s1.*t);v3=b3.*exp(s2.*t);
```

```
u4=a4.*exp(s1.*t);v4=b4.*exp(s2.*t);u5=a5.*exp(s1.*t);v5=b5.*exp(s2.*t);
```

```
u6=a6.*exp(s1.*t);v6=b6.*exp(s2.*t);u7=a7.*exp(s1.*t);v7=b7.*exp(s2.*t);
```

```
u8=a8.*exp(s1.*t);v8=b8.*exp(s2.*t);u9=a9.*exp(s1.*t);v9=b9.*exp(s2.*t);
```

```
u10=a10.*exp(s1.*t);v10=b10.*exp(s2.*t);u11=a11.*exp(s1.*t);
```

```
v11=b11.*exp(s2.*t);
```

```
plot(u0,v0,'k',u1,v1,'k',u2,v2,'k',u3,v3,'k',u4,v4,'k',u5,v5,'k',u6,v6,'k',u7,v7,'k',u8,v8,'k',u9,v9,'k',u10,v10,'k',u11,v11,'k','LineWidth',1.8)
```

```
hold on
```

```
plot([-1.5 1.5],[0 0],'k');plot([0 0], [-2 2],'k'); %%Making new axis
```

```
axis off
```

```
%%%%%%%%%%%%%%%%%%%%%%%%%%%%%%%%%%%%%%%%%%%%%%%%%%%%%%%%%%%%%%%%%%%%%%%%  
%%unforced, overdamped system in phase plane%%  
%%%%%%%%%%%%%%%%%%%%%%%%%%%%%%%%%%%%%%%%%%%%%%%%%%%%%%%%%%%%%%%%%%%%%%%%
```

```
a0=1; b0=1.5; a1=0; b1=1.5; a2=1; b2=0; a3=0; b3=-1.5; a4=-1; b4=0;
```

```
a5=0.7; b5=1; a6=-1; b6=-1.5; a7=-0.7; b7=-1; a8=-1; b8=1.5; a9=1;
```

```
b9=-1.5; a10=-0.7; b10=1; a11=0.7; b11=-1; s1=-1; s2=-0.5; %%Variables
```

```
t=0:0.1:10; %%Timespans
```

```
u0=a0.*exp(s1.*t);v0=b0.*exp(s2.*t);u1=a1.*exp(s1.*t);v1=b1.*exp(s2.*t);
```

```
u2=a2.*exp(s1.*t);v2=b2.*exp(s2.*t);u3=a3.*exp(s1.*t);v3=b3.*exp(s2.*t);
```

```
u4=a4.*exp(s1.*t);v4=b4.*exp(s2.*t);u5=a5.*exp(s1.*t);v5=b5.*exp(s2.*t);
```

```
u6=a6.*exp(s1.*t);v6=b6.*exp(s2.*t);u7=a7.*exp(s1.*t);v7=b7.*exp(s2.*t);
```

```
u8=a8.*exp(s1.*t);v8=b8.*exp(s2.*t);u9=a9.*exp(s1.*t);v9=b9.*exp(s2.*t);
```

```
u10=a10.*exp(s1.*t);v10=b10.*exp(s2.*t);u11=a11.*exp(s1.*t);
```

```
v11=b11.*exp(s2.*t);
```

```
hold on
```

```
x0=(u0./w0)+((s1*(v0-u0))./(s1-s2));y0=(v0-u0)./(s1-s2);
```

```
x1=(u1./w0)+((s1*(v1-u1))./(s1-s2));y1=(v1-u1)./(s1-s2);
```

```
x2=(u2./w0)+((s1*(v2-u2))./(s1-s2));y2=(v2-u2)./(s1-s2);
```

```
x3=(u3./w0)+((s1*(v3-u3))./(s1-s2));y3=(v3-u3)./(s1-s2);
```

```
x4=(u4./w0)+((s1*(v4-u4))./(s1-s2));y4=(v4-u4)./(s1-s2);
```

```

x5=(u5./w0)+((s1*(v5-u5))./(s1-s2));y5=(v5-u5)./(s1-s2);
x6=(u6./w0)+((s1*(v6-u6))./(s1-s2));y6=(v6-u6)./(s1-s2);
x7=(u7./w0)+((s1*(v7-u7))./(s1-s2));y7=(v7-u7)./(s1-s2);
x8=(u8./w0)+((s1*(v8-u8))./(s1-s2));y8=(v8-u8)./(s1-s2);
x9=(u9./w0)+((s1*(v9-u9))./(s1-s2));y9=(v9-u9)./(s1-s2);
x10=(u10./w0)+((s1*(v10-u10))./(s1-s2));y10=(v10-u10)./(s1-s2);
x11=(u11./w0)+((s1*(v11-u11))./(s1-s2));y11=(v11-u11)./(s1-s2);
plot(x0,y0,'k',x1,y1,'k',x2,y2,'k',x3,y3,'k',x4,y4,'k',x5,y5,'k',x6,y6,'k',x7,y7,'k',x8,y8,'k',x9,y9,'k',x10,y10,'k',x11,y11,
'k','LineWidth',1.8)
plot([-5 5],[0 0],'k');plot([0 0], [-6 6], 'k');    %%Making new axis

```

axis off

%%Response of unforced, critically damped system%%  
%%

```

d0=0; v0=5; w0=2;                %%Variables
t1=0:0.1:2; t2=0:0.1:5;         %%Timespans

```

```

x1=d0.*exp(-w0.*t1)+(v0+(w0.*d0)).*t1.*exp(-w0.*t1);
x2=d0.*exp(-w0.*t2)+(v0+(w0.*d0)).*t2.*exp(-w0.*t2);
plot(t1,x1,'k','LineWidth',1.2)    %%Plot whole line
hold on
plot(t2,x2,':k','LineWidth',1.2)    %%Plot dotted line

```

```

plot([0 6],[0 0], 'k'); plot([0 0], [-1.5 1.5], 'k');%%Making new axis

```

axis off

%%  
%%unforced, overdamped system in u-v plane%%  
%%

```

a0=0.4;b0=0.3;a1=0.3;b1=0.2;a2=0.2;b2=0.1;a3=-0.4;
b3=-0.3;a4=-0.3;b4=-0.2;a5=-0.2;b5=-0.1;    %%Variables
t=0:0.1:10;                                  %%Timespan
u0=a0*exp(-c.*t);v0=(exp(-c.*t)).*((a0.*t)+b0);
u1=a1*exp(-c.*t);v1=(exp(-c.*t)).*((a1.*t)+b1);
u2=a2*exp(-c.*t);v2=(exp(-c.*t)).*((a2.*t)+b2);
u3=a3*exp(-c.*t);v3=(exp(-c.*t)).*((a3.*t)+b3);
u4=a4*exp(-c.*t);v4=(exp(-c.*t)).*((a4.*t)+b4);
u5=a5*exp(-c.*t);v5=(exp(-c.*t)).*((a5.*t)+b5);
plot(u0,v0,'k',u1,v1,'k',u2,v2,'k',u3,v3,'k',u4,v4,'k',u5,v5,'k','LineWidth',1.8)
hold on
plot([-0.5 0.5],[0 0], 'k');plot([0 0], [-0.5 0.5], 'k'); %%Making new axis

```

axis off

%%  
%%unforced, overdamped system in phase plane%%  
%%

```

a0=0.4;b0=0.3;a1=0.3;b1=0.2;a2=0.2;b2=0.1;a3=-0.4;

```

```

b3=-0.3;a4=-0.3;b4=-0.2;a5=-0.2;b5=-0.1;    %%Variables
t=0:0.1:10;                                %%Timespan
u0=a0*exp(-c.*t);v0=(exp(-c.*t)).*((a0.*t)+b0);
u1=a1*exp(-c.*t);v1=(exp(-c.*t)).*((a1.*t)+b1);
u2=a2*exp(-c.*t);v2=(exp(-c.*t)).*((a2.*t)+b2);
u3=a3*exp(-c.*t);v3=(exp(-c.*t)).*((a3.*t)+b3);
u4=a4*exp(-c.*t);v4=(exp(-c.*t)).*((a4.*t)+b4);
u5=a5*exp(-c.*t);v5=(exp(-c.*t)).*((a5.*t)+b5);
x0=v0./c;y0=(u0./c)-v0;x1=v1./c;y1=(u1./c)-v1;
x2=v2./c;y2=(u2./c)-v2;x3=v3./c;y3=(u3./c)-v3;
x4=v4./c;y4=(u4./c)-v4;x5=v5./c;y5=(u5./c)-v5;
plot(x0,y0,'k',x1,y1,'k',x2,y2,'k',x3,y3,'k',x4,y4,'k',x5,y5,'k','LineWidth',1.8)
hold on

```

```

plot([-0.5 0.5],[0 0],'k');plot([0 0], [-0.5 0.5],'k'); %%Making new axis

```

```

axis off

```

```

%%%%%%%%%%%%%%%%%%%%%%%%%%%%%%%%%%%%%%%%%%%%%%%%%%%%%%%%%%%%%%%%%%%%%%%%
%%unforced system with negative stiffness in u-v plane%%
%%%%%%%%%%%%%%%%%%%%%%%%%%%%%%%%%%%%%%%%%%%%%%%%%%%%%%%%%%%%%%%%%%%%%%%%

```

```

a0=10;b0=0;a1=0;b1=10;a2=0;b2=-10;a3=10;b3=9;a4=5;b4=4;a5=10;b5=-9;a6=5;b6=-4;a7=-10;b7=-9;a8=-
5;b8=-4;a9=-10;b9=9;a10=-5;b10=4;a11=-10;b11=0;s1=-0.5;s2=0.4; %%Variables
t=0:0.1:7;    %%Timespan
u0=a0.*exp(s1.*t);v0=b0.*exp(s2.*t);
u1=a1.*exp(s1.*t);v1=b1.*exp(s2.*t);u2=a2.*exp(s1.*t);v2=b2.*exp(s2.*t);
u3=a3.*exp(s1.*t);v3=b3.*exp(s2.*t);u4=a4.*exp(s1.*t);v4=b4.*exp(s2.*t);
u5=a5.*exp(s1.*t);v5=b5.*exp(s2.*t);u6=a6.*exp(s1.*t);v6=b6.*exp(s2.*t);
u7=a7.*exp(s1.*t);v7=b7.*exp(s2.*t);u8=a8.*exp(s1.*t);v8=b8.*exp(s2.*t);
u9=a9.*exp(s1.*t);v9=b9.*exp(s2.*t);u10=a10.*exp(s1.*t);v10=b10.*exp(s2.*t);
u11=a11.*exp(s1.*t);v11=b11.*exp(s2.*t);

```

```

plot(u0,v0,'k',u1,v1,'k',u2,v2,'k',u3,v3,'k',u4,v4,'k',u5,v5,'k',u6,v6,'k',u7,v7,'k',u8,v8,'k',u9,v9,'k',u10,v10,'k',u11,v
11,'k','LineWidth',1.8)
hold on
plot([-15 15],[0 0],'k');plot([0 0], [-200 200],'k'); %%Making new axis

```

```

axis off

```

```

%%%%%%%%%%%%%%%%%%%%%%%%%%%%%%%%%%%%%%%%%%%%%%%%%%%%%%%%%%%%%%%%%%%%%%%%
%%Resonance curves%%
%%%%%%%%%%%%%%%%%%%%%%%%%%%%%%%%%%%%%%%%%%%%%%%%%%%%%%%%%%%%%%%%%%%%%%%%

```

```

A=1;w0=1;c1=0;c2=0.05;c4=0.1;c5=0.3;c6=1;w=0:0.01:2;    %%Variables

```

```

a1=A./(sqrt(((w0.^2-w.^2).^2)+(c1.^2.*w.^2)));
a2=A./(sqrt(((w0.^2-w.^2).^2)+(c2.^2.*w.^2)));
a4=A./(sqrt(((w0.^2-w.^2).^2)+(c4.^2.*w.^2)));
a5=A./(sqrt(((w0.^2-w.^2).^2)+(c5.^2.*w.^2)));
a6=A./(sqrt(((w0.^2-w.^2).^2)+(c6.^2.*w.^2)));

plot(w,a1,'k',w,a2,'k',w,a4,'k',w,a6,'k',w,a5,'k','LineWidth',1.2)
hold on

```

```

plot([-0.1 2.1],[0 0], 'k');plot([0 0], [-1 50], 'k'); %%Making new axis
axis off

%%%%%%%%%%%%%%%%%%%%%%%%%%%%%%%%%%%%%%%%%%%%%%%%%%%%%%%%%%%%%%%%%%%%%%%%
%%Phasecurves%%
%%%%%%%%%%%%%%%%%%%%%%%%%%%%%%%%%%%%%%%%%%%%%%%%%%%%%%%%%%%%%%%%%%%%%%%%

w0=4;c1=0;c2=0.05;c3=0.2;c4=0.5;c5=0.7;c6=1;w=0:0.01:2*pi; %%Variables

te1=atan2((c1.*w),(w0.^2-w.^2));
te2=atan2((c2.*w),(w0.^2-w.^2));
te3=atan2((c3.*w),(w0.^2-w.^2));
te4=atan2((c4.*w),(w0.^2-w.^2));
te5=atan2((c5.*w),(w0.^2-w.^2));
te6=atan2((c6.*w),(w0.^2-w.^2));

plot(w,te1,'k',w,te2,'k',w,te3,'k',w,te4,'k',w,te5,'k',w,te6,'k','LineWidth',1.2)
hold on
plot([-1 8],[0 0], 'k');plot([0 0], [-1 3.5], 'k'); %%Making new axis

Axis off

%%%%%%%%%%%%%%%%%%%%%%%%%%%%%%%%%%%%%%%%%%%%%%%%%%%%%%%%%%%%%%%%%%%%%%%%
%%forced system without damping in the phase plane%%
%%%%%%%%%%%%%%%%%%%%%%%%%%%%%%%%%%%%%%%%%%%%%%%%%%%%%%%%%%%%%%%%%%%%%%%%

m=100; F0=5; k=0.5; c=0; sig=c/m; A=F0/m; w=2; wd=sqrt((sig/2)^2-w0^2);
d0=4; v0=1; w0=sqrt(k/m);thet=atan((sig*m)/(w0^2-w^2)); %%Variables
t=0:0.1:180; %%Timespan
xp=(A/sqrt((w0^2-w^2)^2+(sig^2*w^2)))*sin((w.*t)-thet);
yh=(d0.*cos(w0.*t))+((v0/w0). *sin(w0*t));
yp=((A*w)/sqrt((w0^2-w^2)^2+(sig^2*w^2)))*cos((w.*t)-thet);
yh=(-d0.*w0.*sin(w0.*t))+v0.*cos(w0.*t);
x=xh+xp;
y=yh+yp;

plot(x,y,'k','Linewidth',1.2)
hold on
plot([-20 20],[0 0], 'k'); plot([0 0], [-1.5 1.5], 'k'); %%Making new axis

axis off

%%%%%%%%%%%%%%%%%%%%%%%%%%%%%%%%%%%%%%%%%%%%%%%%%%%%%%%%%%%%%%%%%%%%%%%%
%%forced, underdamped system the phase plane%%
%%%%%%%%%%%%%%%%%%%%%%%%%%%%%%%%%%%%%%%%%%%%%%%%%%%%%%%%%%%%%%%%%%%%%%%%

m=100; F0=5; c=1.5; k=1.69; sig=c/m; w02=k/m; A=F0/m; w=2; wd=sqrt(w^2-(k/2)^2);
v0=1; d0=0;thet=atan((sig*m)/(w02-w^2)); %%Variables
t=0:0.1:300; %%Timespan
xp=(A/sqrt((w02-w^2)^2+(sig^2*w^2)))*sin((w.*t)-thet);
yh=exp((-sig/2). *t). *(((v0/wd)+(sig/2*wd)). *sin(wd.*t)+(d0.*cos(wd.*t)));
yp=((A*w)/sqrt((w02-w^2)^2+(sig^2*w^2)))*cos((w.*t)-thet);
yh=exp((-sig/2). *t). *((( -sig*v0)/(2*wd))-((sig^2*d0)/(4*wd))-(d0*wd)). *sin(wd.*t)+(v0.*cos(wd.*t)));

```

```

x=xh+xp;
y=yh+yp;

plot(x,y,'k','Linewidth',1.2)
hold on
plot([0 0], [-1.5 1.5],'k'); plot([-1 1], [0 0], 'k') %%Making new axis

axis off

%%%%%%%%%%%%%%%%%%%%%%%%%%%%%%%%%%%%%%%%%%%%%%%%%%%%%%%%%%%%%%%%%%%%%%%%
%%forced, overdamped system the phase plane%%
%%%%%%%%%%%%%%%%%%%%%%%%%%%%%%%%%%%%%%%%%%%%%%%%%%%%%%%%%%%%%%%%%%%%%%%%

m=10; F0=50; c=80; k=1.69; sig=c/m; w02=k/m; A=F0/m; w=2; wd=sqrt(w^2-(k/2)^2);
b=(v0-(s1*d0))/(s2-s1); a=d0-b; s1=-1; s2=-0.5;thet=atan((sig*m)/(w02-w^2)); %%Variables

hold on
for d0=[-2 0 2] %%Initial displacement
    for v0=[-2 0 2] %%Initial velocity
        t=0:0.1:1000; %%Timespan
        b=(v0-(s1*d0))/(s2-s1); a=d0-b;
        xp=(A/sqrt((w02-w^2)^2+(sig^2*w^2)))*sin((w.*t)-thet);
        xh=a.*exp(s1.*t)+b.*exp(s2.*t);
        yp=((A*w)/sqrt((w02-w^2)^2+(sig^2*w^2)))*cos((w.*t)-thet);
        yh=(s1.*a.*exp(s1.*t))+s2.*b.*exp(s2.*t);
        x=xh+xp;
        y=yh+yp;
        plot(x,y,'k','Linewidth',1.2)
    end
end

plot([0 0], [-3 3],'k'); plot([-3 3], [0 0], 'k') %%Making new axis

axis off

%%%%%%%%%%%%%%%%%%%%%%%%%%%%%%%%%%%%%%%%%%%%%%%%%%%%%%%%%%%%%%%%%%%%%%%%
%%forced, critically damped system the phase plane%%
%%%%%%%%%%%%%%%%%%%%%%%%%%%%%%%%%%%%%%%%%%%%%%%%%%%%%%%%%%%%%%%%%%%%%%%%

m=10; F0=50; k=1.69; c=4*k; sig=c/m; w02=k/m; w0=sqrt(k/m); A=F0/m; w=2; wd=sqrt(w^2-(k/2)^2);
s1=-w0; s2=-w0; thet=atan((sig*m)/(w02-w^2)); %%Variables

hold on
for d0=[-2 0 2] %%Initial displacement
    for v0=[-2 0 2] %%Initial velocity
        t=0:0.1:1000; %%Timespan
        a=d0; b=v0+(w0*d0);
        xp=(A/sqrt((w02-w^2)^2+(sig^2*w^2)))*sin((w.*t)-thet);
        xh=(a.*exp(s1.*t)+(b.*t.*exp(s2.*t)));
        yp=((A*w)/sqrt((w02-w^2)^2+(sig^2*w^2)))*cos((w.*t)-thet);
        yh=(-w0.*a.*exp(s1.*t)-(w0.*b.*t.*exp(s2.*t)));
        x=xh+xp;

```

```

y=yh+yp;
plot(x,y,'k','LineWidth',1.2)
    end
end

```

```

plot([0 0], [-5 5],'k');plot([-7 7], [0 0], 'k') %%Making new axis

```

```

axis off

```

```

%%%%%%%%%%%%%%%%%%%%%%%%%%%%%%%%%%%%%%%%%%%%%%%%%%%%%%%%%%%%%%%%%%%%%%%%
%%Position curve Van der Pol with mu=0,5%%
%%%%%%%%%%%%%%%%%%%%%%%%%%%%%%%%%%%%%%%%%%%%%%%%%%%%%%%%%%%%%%%%%%%%%%%%

```

```

type vanderpoldemo
tspan=[0, 60];                %%Timespan
y0=[0;1];Mu1=0.5;            %%Variables
ode1=@(t,y) vanderpoldemo(t,y,Mu1);
[t,y1]=ode15s(ode1,tspan,y0);

```

```

plot(t,y1(:,1),'k','LineWidth',1.2)
hold on

```

```

plot([0 60],[0 0],'k');plot([0 0], [-2.5 2.5],'k'); %%Making new axis

```

```

axis off

```

```

%%%%%%%%%%%%%%%%%%%%%%%%%%%%%%%%%%%%%%%%%%%%%%%%%%%%%%%%%%%%%%%%%%%%%%%%
%%Position curve Van der Pol with mu=5%%
%%%%%%%%%%%%%%%%%%%%%%%%%%%%%%%%%%%%%%%%%%%%%%%%%%%%%%%%%%%%%%%%%%%%%%%%

```

```

type vanderpoldemo
tspan=[0, 50];                %%Timespan
y0=[0;1];Mu1=5;                %%Variables
ode1=@(t,y) vanderpoldemo(t,y,Mu1);
[t,y1]=ode15s(ode1,tspan,y0);

```

```

plot(t,y1(:,1),'k','LineWidth',1.2)
hold on

```

```

plot([0 60],[0 0],'k');plot([0 0], [-2.5 2.5],'k'); %%Making new axis

```

```

axis off

```

```

%%%%%%%%%%%%%%%%%%%%%%%%%%%%%%%%%%%%%%%%%%%%%%%%%%%%%%%%%%%%%%%%%%%%%%%%
%%Position curve Van der Pol with mu=10 %%
%%%%%%%%%%%%%%%%%%%%%%%%%%%%%%%%%%%%%%%%%%%%%%%%%%%%%%%%%%%%%%%%%%%%%%%%

```

```

type vanderpoldemo
tspan=[0, 60];                %%Timespan
y0=[0;1];Mu1=10;            %%Variables
ode1=@(t,y) vanderpoldemo(t,y,Mu1);

```

```

[t,y1]=ode15s(ode1,tspan,y0);

plot(t,y1(:,1),'k','LineWidth',1.2)
hold on

plot([0 60],[0 0],'k');plot([0 0], [-2.5 2.5],'k'); %%Making new axis

axis off

%%%%%%%%%%%%%%%%%%%%%%%%%%%%%%%%%%%%%%%%%%%%%%%%%%%%%%%%%%%%%%%%%%%%%%%%
%%phaseplane vanderpol mu=1%%
%%%%%%%%%%%%%%%%%%%%%%%%%%%%%%%%%%%%%%%%%%%%%%%%%%%%%%%%%%%%%%%%%%%%%%%%

type vanderpoldemo
tspan=[0, 60]; %%Timespan
y0=[2;0];y02=[3;1];y03=[-1;-2];y04=[-3;3];y05=[2;-1];y06=[1;-2];y07=[0.1;0.1];y08=[-0.3;-0.3];y09=[-
3.5;3.5];y010=[0.5;-0.5];y011=[1.3;-2.4];y012=[0.5;0.5];y013=[-1.5;2.5];y014=[-3;-3]; %%Variables
Mu=1;
ode=@(t,y) vanderpoldemo(t,y,Mu);
[t,y1]=ode15s(ode,tspan,y0);
plot(y1(:,1),y1(:,2),'k','LineWidth',1.2)
hold on
[t,y2]=ode15s(ode,tspan,y02);
plot(y2(:,1),y2(:,2),'k','LineWidth',1.2)
[t,y3]=ode15s(ode,tspan,y03);
plot(y3(:,1),y3(:,2),'k','LineWidth',1.2)
[t,y4]=ode15s(ode,tspan,y04);
plot(y4(:,1),y4(:,2),'k','LineWidth',1.2)
[t,y5]=ode15s(ode,tspan,y05);
plot(y5(:,1),y5(:,2),'k','LineWidth',1.2)
[t,y6]=ode15s(ode,tspan,y06);
plot(y6(:,1),y6(:,2),'k','LineWidth',1.2)
[t,y7]=ode15s(ode,tspan,y07);
plot(y7(:,1),y7(:,2),'k','LineWidth',1.2)
[t,y8]=ode15s(ode,tspan,y08);
plot(y8(:,1),y8(:,2),'k','LineWidth',1.2)
[t,y9]=ode15s(ode,tspan,y09);
plot(y9(:,1),y9(:,2),'k','LineWidth',1.2)
[t,y10]=ode15s(ode,tspan,y010);
plot(y10(:,1),y10(:,2),'k','LineWidth',1.2)
[t,y11]=ode15s(ode,tspan,y011);
plot(y11(:,1),y11(:,2),'k','LineWidth',1.2)
[t,y12]=ode15s(ode,tspan,y012);
plot(y12(:,1),y12(:,2),'k','LineWidth',1.2)
[t,y13]=ode15s(ode,tspan,y013);
plot(y13(:,1),y13(:,2),'k','LineWidth',1.2)
[t,y14]=ode15s(ode,tspan,y014);
plot(y14(:,1),y14(:,2),'k','LineWidth',1.2)
axis off

plot([0 0], [-4 4],'k');plot([-4 4], [0 0],'k'); %%Making new axis

```



```

%%%%%%%%%%%%%%
%% Van der Pol limit cycles%%
%%%%%%%%%%%%%%
type vanderpoldemo
tspan=[0, 150];
y0=[2;0];y01=[1;0];y02=[3;1];y03=[-1;-2];y04=[-3;3];y05=[2;-1];y06=[1;-2];y07=[0.1;0.1];y08=[-0.3;-0.3];y09=[-
3.5;3.5];y010=[0.5;-0.5];y011=[1.3;-2.4];y012=[0.5;0.5];y013=[-1.5;2.5];y014=[-3;-3]; %%Variables
Mu1=0.1;
ode1=@(t,y) vanderpoldemo(t,y,Mu1);
[t,y1]=ode15s(ode1,tspan,y0);
plot(y1(:,1),y1(:,2),'k','LineWidth',1.2)
hold on
Mu3=0.5;
ode3=@(t,y) vanderpoldemo(t,y,Mu3);
[t,y3]=ode15s(ode3,tspan,y0);
plot(y3(:,1),y3(:,2),'r','LineWidth',1.2)
Mu4=1;
ode4=@(t,y) vanderpoldemo(t,y,Mu4);
[t,y4]=ode15s(ode4,tspan,y0);
plot(y4(:,1),y4(:,2),'b','LineWidth',1.2)
Mu5=1.5;
ode5=@(t,y) vanderpoldemo(t,y,Mu5);
[t,y5]=ode15s(ode5,tspan,y0);
plot(y5(:,1),y5(:,2),'g','LineWidth',1.2)
Mu6=2;
ode6=@(t,y) vanderpoldemo(t,y,Mu6);
[t,y6]=ode15s(ode6,tspan,y0);
plot(y6(:,1),y6(:,2),'m','LineWidth',1.2)
plot([-4 4], [0 0],'k');plot([0 0], [-4 4],'k'); %%Making new axis

```

```

%%%%%%%%%%%%%%
%%Response of the Pendulum equation%%
%%%%%%%%%%%%%%

```

```
L=1.5; g=9.81; m=0.3; b=0.05;k=0;r=g/L; %%Variables
```

```

f=@(t,x) [x(2);-k*x(2)-r*x(1)];
init=[pi/6;0]
[t,x]=ode45(f,[0 10], init);
plot(t,x(:,1),'k');
hold on

```

```
plot([0 10],[0 0],'k');plot([0 0], [-2 2],'k'); %%Making new axis
```

```
axis off
```

```

%%%%%%%%%%%%%%
%%Pendulum phaseplane%%
%%%%%%%%%%%%%%

```

```
L=9; g=9.81; m=0.3; b=0.05;
k=0.2;
r=g/L;
```

```
f=@(t,x) [x(2);-k*x(2)-r*sin(x(1))];
```

```

init1=[-3.15;0];
[t,x1]=ode45(f,[0 22], init1);
plot(x1(:,1),x1(:,2),'k','LineWidth',1.2);
hold on
axis off
plot([-10 10],[0 0],'k');
plot([0 0], [-4 4],'k');

%%%%%%%%%%%%%%%%%%%%%%%%%%%%%%%%%%%%%%%%%%%%%%%%%%%%%%%%%%%%%%%%%%%%%%%%
%% Phase plane plots for nonlinear force %%
%%%%%%%%%%%%%%%%%%%%%%%%%%%%%%%%%%%%%%%%%%%%%%%%%%%%%%%%%%%%%%%%%%%%%%%%

m=8; F0=50; c=0; k=0.5; w=0.5; %% Setting the variables to appropriate values.

f=@(t,x) [x(2);((F0/m)*sin(w.*t)*abs(sin(w.*t)))-((c/m)*x(2))-((k/m)*x(1))];
init1=[2;2]; %% Initial conditions
[t,x1]=ode45(f,[0 3600], init1)
plot(x1(:,1),x1(:,2),'k','LineWidth',1.2);
hold on

axis off
plot([-40 40],[0 0],'k');
plot([0 0], [-10 10],'k'); %% Making axis through the origin.

%%%%%%%%%%%%%%%%%%%%%%%%%%%%%%%%%%%%%%%%%%%%%%%%%%%%%%%%%%%%%%%%%%%%%%%%
%%Position/velocity curves for nonlinear force%%
%%%%%%%%%%%%%%%%%%%%%%%%%%%%%%%%%%%%%%%%%%%%%%%%%%%%%%%%%%%%%%%%%%%%%%%%

m=8; F0=50; c=0.0; k=0.5; w=0.5; %% Setting the variables to appropriate values.

f=@(t,x) [x(2);((F0/m)*sin(w.*t)*abs(sin(w.*t)))-((c/m)*x(2))-((k/m)*x(1))];
init1=[2;2]; %% Initial conditions
[t,x1]=ode45(f,[0 3600], init1)
plot(t,x1(:,1),'k','LineWidth',1.2);
hold on

axis off
plot([0 3800],[0 0],'k');
plot([0 0], [-40 40],'k'); %% Making axis through the origin.

%%%%%%%%%%%%%%%%%%%%%%%%%%%%%%%%%%%%%%%%%%%%%%%%%%%%%%%%%%%%%%%%%%%%%%%%
%% Phase plane plots for homogenous equation with nonlinear damping%%
%%%%%%%%%%%%%%%%%%%%%%%%%%%%%%%%%%%%%%%%%%%%%%%%%%%%%%%%%%%%%%%%%%%%%%%%

m=100; F0=50; c0=0; a=0; k=0.5; w=0.5; %% Setting the variables to
appropriate values.

f=@(t,x) [x(2);-(((a.*sin(w.*t)).*abs(sin(w.*t))+c0)/m).*x(2))-
((k/m).*x(1))];
init1=[2;2]; %% Initial conditions
[t,x1]=ode45(f,[0 3600], init1)
plot(x1(:,1),x1(:,2),'k','LineWidth',1.2);
hold on

```

```

axis off
plot([-40 40],[0 0], 'k');
plot([0 0], [-10 10], 'k');           %% Making axis through the
origin.

%%%%%%%%%%%%%%%%%%%%%%%%%%%%%%%%%%%%%%%%%%%%%%%%%%%%%%%%%%%%%%%%%%%%%%%%
%%Position/velocity for homogenous equation with nonlinear damping%%
%%%%%%%%%%%%%%%%%%%%%%%%%%%%%%%%%%%%%%%%%%%%%%%%%%%%%%%%%%%%%%%%%%%%%%%%

m=100; F0=50; c0=0.005; a=0.5; k=0.5; w=0.5;           %% Setting the variables
to appropriate values.

f=@(t,x) [x(2);-(((a.*sin(w.*t)).*abs(sin(w.*t)))+c0)).*x(2))-
((k/m).*x(1))];
init1=[2;2];                                           %% Initial conditions
[t,x1]=ode45(f,[0 3600], init1)
plot(t,x1(:,1), 'k', 'LineWidth',1.2);
hold on

axis off
plot([0 3800],[0 0], 'k');
plot([0 0], [-40 40], 'k');           %% Making axis through the
origin.

%%%%%%%%%%%%%%%%%%%%%%%%%%%%%%%%%%%%%%%%%%%%%%%%%%%%%%%%%%%%%%%%%%%%%%%%
%% Phase plane plots for linear forced equation with nonlinear damping%%
%%%%%%%%%%%%%%%%%%%%%%%%%%%%%%%%%%%%%%%%%%%%%%%%%%%%%%%%%%%%%%%%%%%%%%%%

m=100; F0=50; c0=0.0015; a=0.5; k=0.5; w=0.5;       %% Setting the variables
to appropriate values.

f=@(t,x) [x(2);((F0/m).*sin(w.*t))-
(((a.*sin(w.*t)).*abs(sin(w.*t)))+c0)).*x(2))-((k/m).*x(1))];
init1=[2;2];                                           %% Initial conditions
[t,x1]=ode45(f,[0 2000], init1)
plot(x1(:,1),x1(:,2), 'k', 'LineWidth',1.2);
hold on

plot([-30 30],[0 0], 'k');
plot([0 0], [-8 8], 'k');           %% Making axis through the origin.

axis off

%%%%%%%%%%%%%%%%%%%%%%%%%%%%%%%%%%%%%%%%%%%%%%%%%%%%%%%%%%%%%%%%%%%%%%%%
%%
%%Position/velocity plots for linear forced equation with nonlinear
damping%%
%%%%%%%%%%%%%%%%%%%%%%%%%%%%%%%%%%%%%%%%%%%%%%%%%%%%%%%%%%%%%%%%%%%%%%%%
%%

m=8; F0=50; c0=0.005; a=0.02; k=0.5; w=0.5;         %% Setting the variables to
appropriate values.

f=@(t,x) [x(2);((F0/m).*sin(w.*t))-
(((a.*sin(w.*t)).*abs(sin(w.*t)))+c0)).*x(2))-((k/m).*x(1))];
init1=[2;2];                                           %% Initial conditions
[t,x1]=ode45(f,[0 500], init1)
plot(t,x1(:,1), 'k', 'LineWidth',1.2);

```

```
hold on

plot([0 500],[0 0],'k');
plot([0 0], [-40 40],'k');      %% Making axis through the
origin.

axis off
```

## Appendix B – Calculations for equations (3.4)-(3.12)

$$x_p(t) = a \sin(\omega t - \theta) = a(\sin(\omega t) \cos(\theta) - \cos(\omega t) \sin(\theta))$$

$$\frac{dx}{dt} = a\omega \cos(\omega t - \theta) = a\omega(\cos(\omega t) \cos(\theta) + \sin(\omega t) \sin(\theta))$$

$$\frac{d^2x}{dt^2} = -a\omega^2 \sin(\omega t - \theta) = -a\omega^2(\sin(\omega t) \cos(\theta) - \cos(\omega t) \sin(\theta))$$

$$A \sin(\omega t) + a\omega^2(\sin(\omega t) \cos(\theta) - \cos(\omega t) \sin(\theta)) - \sigma a\omega(\cos(\omega t) \cos(\theta) + \sin(\omega t) \sin(\theta)) - \omega_0^2 a(\sin(\omega t) \cos(\theta) - \cos(\omega t) \sin(\theta)) = 0$$

$$A \sin(\omega t) + a\omega^2 \sin(\omega t) \cos(\theta) - a\omega^2 \cos(\omega t) \sin(\theta) - \sigma a\omega \cos(\omega t) \cos(\theta) - \sigma a\omega \sin(\omega t) \sin(\theta) - \omega_0^2 a \sin(\omega t) \cos(\theta) + \omega_0^2 a \cos(\omega t) \sin(\theta) = 0$$

$$\sin(\omega t)(A + a\omega^2 \cos(\theta) - \sigma a\omega \sin(\theta) - \omega_0^2 a \cos(\theta)) + \cos(\omega t)(-a\omega^2 \sin(\theta) - \sigma a\omega \cos(\theta) + \omega_0^2 a \sin(\theta)) = 0$$

$$\sin(\omega t)(A + a(\omega^2 \cos(\theta) - \sigma\omega \sin(\theta) - \omega_0^2 \cos(\theta))) + \cos(\omega t)(a(-\omega^2 \sin(\theta) - \sigma\omega \cos(\theta) + \omega_0^2 \sin(\theta))) = 0$$

$$\sin(\omega t) \left( A - a((\omega_0^2 - \omega^2) \cos(\theta) + \sigma\omega \sin(\theta)) \right) + \cos(\omega t) \left( a((\omega_0^2 - \omega^2) \sin(\theta) - \sigma\omega \cos(\theta)) \right) = 0$$

$$a((\omega_0^2 - \omega^2) \sin(\theta) - \sigma\omega \cos(\theta)) = 0$$

$$(\omega_0^2 - \omega^2) \sin(\theta) = \sigma\omega \cos(\theta)$$

$$\frac{\sin(\theta)}{\cos(\theta)} = \frac{\sigma\omega}{\omega_0^2 - \omega^2}$$

$$\tan(\theta) = \frac{\sigma\omega}{\omega_0^2 - \omega^2}$$

$$\sin(\theta) = \frac{(\omega_0^2 - \omega^2) \cos(\theta)}{\sigma\omega}$$

$$\sin^2(\theta) = \frac{(\omega_0^2 - \omega^2)^2 \cos^2(\theta)}{\sigma^2 \omega^2}$$

$$\sin^2(\theta) + \cos^2(\theta) = 1$$

$$\cos^2(\theta) = 1 - \sin^2(\theta)$$

$$\sin^2(\theta) = \frac{(\omega_0^2 - \omega^2)^2 (1 - \sin^2(\theta))}{\sigma^2 \omega^2}$$

$$\sin^2(\theta) = \frac{(\omega_0^2 - \omega^2)^2 - (\omega_0^2 - \omega^2)^2 \sin^2(\theta)}{\sigma^2 \omega^2}$$

$$\sin^2(\theta) \sigma^2 \omega^2 = (\omega_0^2 - \omega^2)^2 - (\omega_0^2 - \omega^2)^2 \sin^2(\theta)$$

$$\sin^2(\theta) \sigma^2 \omega^2 + (\omega_0^2 - \omega^2)^2 \sin^2(\theta) = (\omega_0^2 - \omega^2)^2$$

$$\sin^2(\theta) (\sigma^2 \omega^2 + (\omega_0^2 - \omega^2)^2) = (\omega_0^2 - \omega^2)^2$$

$$\sin^2(\theta) = \frac{(\omega_0^2 - \omega^2)^2}{\sigma^2 \omega^2 + (\omega_0^2 - \omega^2)^2}$$

$$\sin(\theta) = \frac{\omega_0^2 - \omega^2}{\sqrt{\sigma^2 \omega^2 + (\omega_0^2 - \omega^2)^2}}$$

$$\cos(\theta) = \frac{\sigma\omega \sin(\theta)}{\omega_0^2 - \omega^2}$$

$$\cos(\theta) = \frac{\sigma\omega(\omega_0^2 - \omega^2)}{(\omega_0^2 - \omega^2)\sqrt{\sigma^2\omega^2 + (\omega_0^2 - \omega^2)^2}}$$

$$\cos(\theta) = \frac{\sigma\omega}{\sqrt{\sigma^2\omega^2 + (\omega_0^2 - \omega^2)^2}}$$

$$A - a((\omega_0^2 - \omega^2) \cos(\theta) + \sigma\omega \sin(\theta))$$

$$a = \frac{A}{(\omega_0^2 - \omega^2) \cos(\theta) + \sigma\omega \sin(\theta)}$$

$$a = \frac{A}{\sqrt{(\omega_0^2 - \omega^2)^2 + \sigma^2\omega^2}}$$

# Appendix C – Diagrams for chapter 7

## C.1 Base-case system

### C.1.1 $a=0$

When  $a=0$ , the system only has linear, constant damping from the coefficient  $c_0$ .

#### C.1.1.1 $c_0=0,0015$

Figures C.1 and C.2 show the base-case system with the linear damping coefficient,  $c_0=0,0015$ . Figure C.1 shows the position curve to the left and the velocity curve to the right, while figure C.2 shows the phase plane diagram. The system has a steady decline in both position and velocity creating a spiral towards the origin in the phase plane.

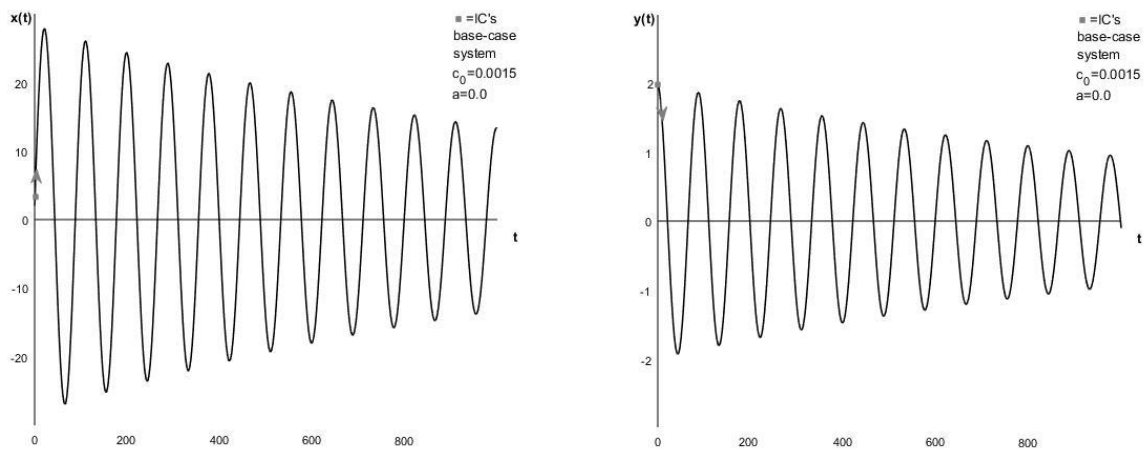


Figure C.1: Position curve(left) and velocity curve(right) for the base-case system with  $a=0$  and  $c_0=0,0015$ .

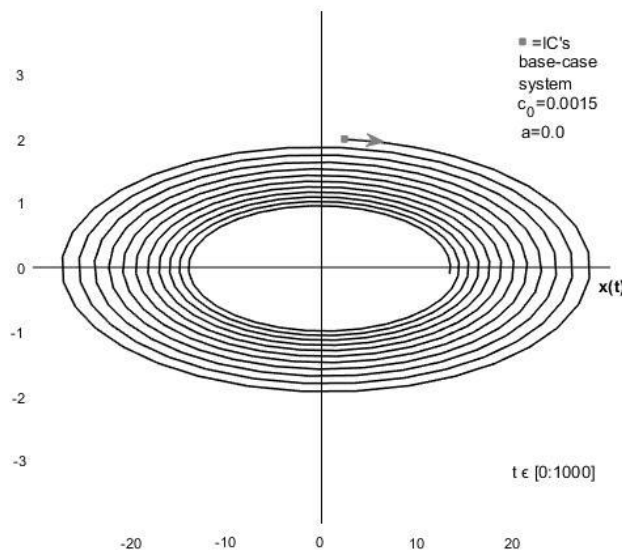


Figure C.2: Phase plane diagram for the base-case system with  $a=0$  and  $c_0=0,0015$ .

C.1.1.2  $c_0=0,005$

Figures C.3 and C.4 show the base-case system with the linear damping coefficient,  $c_0=0,005$ . Figure C.3 shows the position curve to the left and the velocity curve to the right, while figure C.4 shows the phase plane diagram. The system has a more rapid decline in both position and velocity due to the increase in damping compared to the system with  $c_0=0,0015$ .

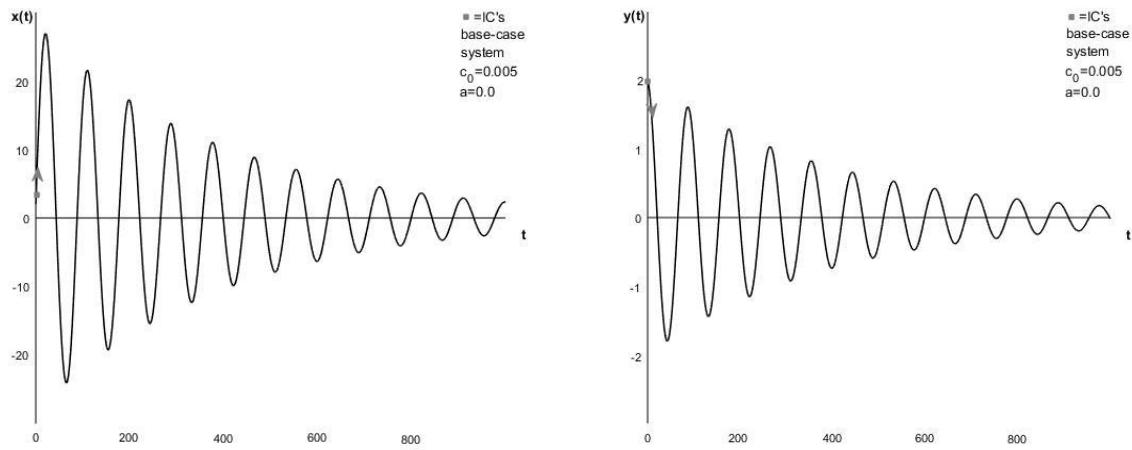


Figure C.3: Position curve(left) and velocity curve(right) for the base-case system with  $a=0$  and  $c_0=0,005$ .

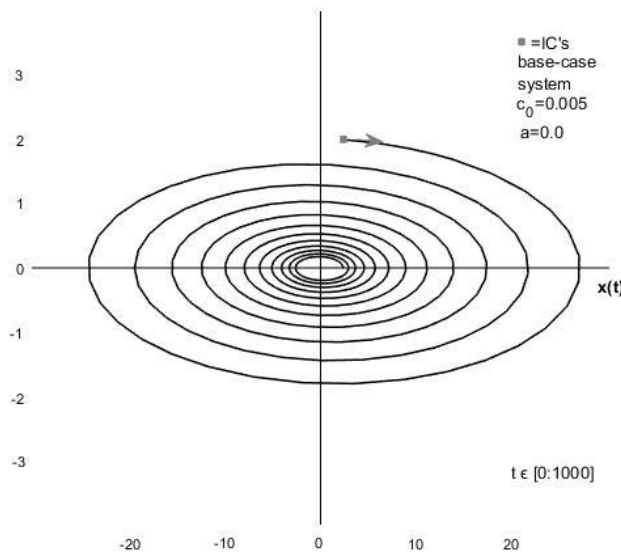


Figure C.4: Phase plane diagram for the base-case system with  $a=0$  and  $c_0=0,005$ .



### C.1.2 $a=0,5$

In this part, the system will be subjected to both a linear damping coefficient,  $c_0$ , as well as the nonlinear damping coefficient,  $a=0,5$ .

#### C.1.2.1 $c_0=0,0015$

Figures C.5 and C.6 show the base-case system with the linear damping coefficient,  $c_0=0,0015$ , and the nonlinear damping coefficient,  $a=0,5$ . Figure C.5 shows the position curve to the left and the velocity curve to the right, while figure C.6 shows the phase plane diagram. The nonlinearity is visible in the position curve, but is much more prominent in the velocity curve. The phase plane diagram is distorted as it moves very slowly towards the origin.

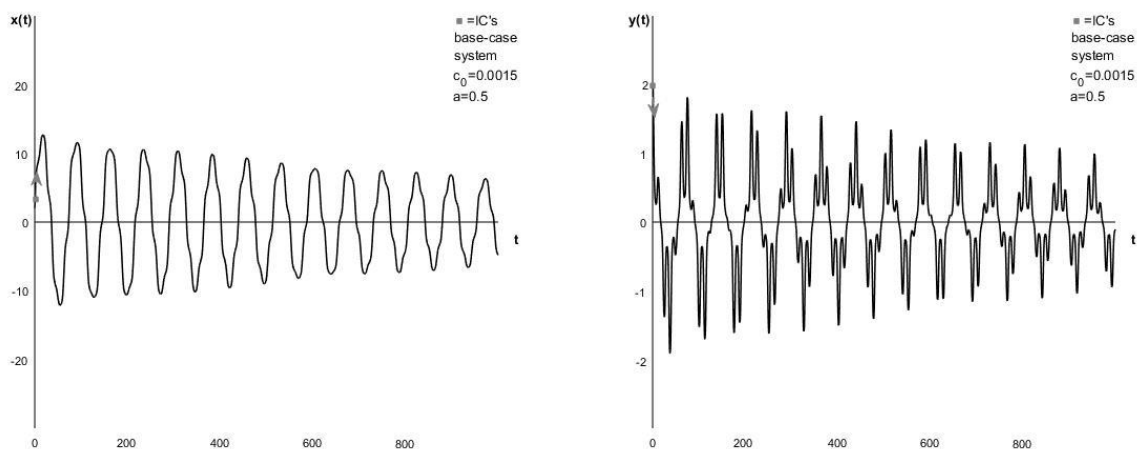


Figure C.5: Position curve(left) and velocity curve(right) for the base-case system with  $a=0,5$  and  $c_0=0,0015$ .

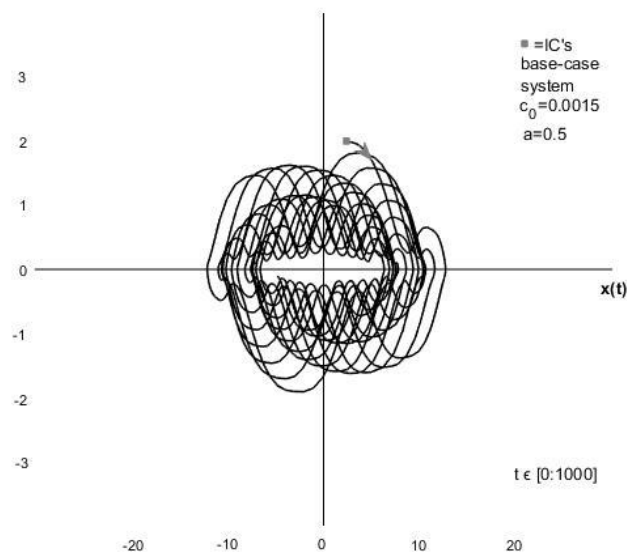


Figure C.6: Phase plane diagram for the base-case system with  $a=0,5$  and  $c_0=0,0015$ .

### C.1.2.2 $c_0=0,005$

Figures C.7 and C.8 show the base-case system with the linear damping coefficient,  $c_0=0,005$ , and the nonlinear damping coefficient,  $a=0,5$ . Figure C.7 shows the position curve to the left and the velocity curve to the right, while figure C.8 shows the phase plane diagram. Since the linear damping coefficient is increased, all the graphs move faster towards zero.

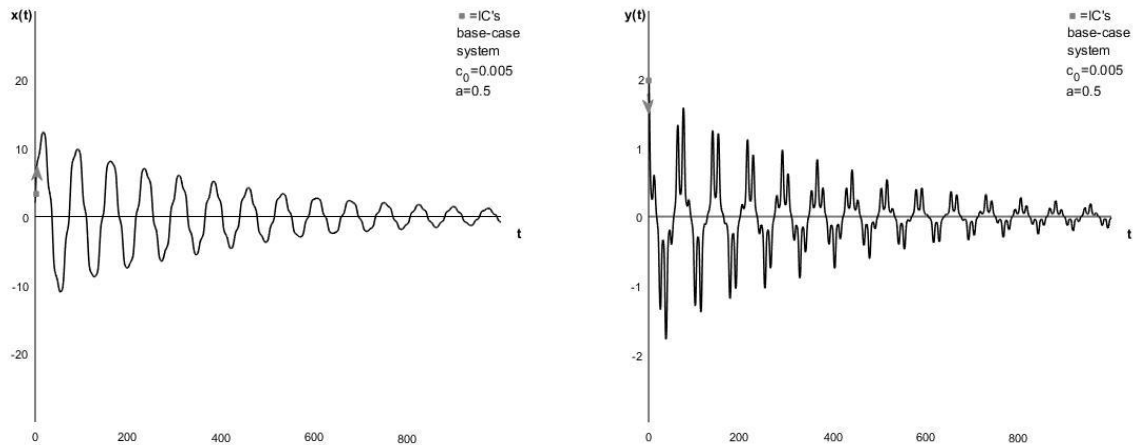


Figure C.7: Position curve(left) and velocity curve(right) for the base-case system with  $a=0,5$  and  $c_0=0,005$ .

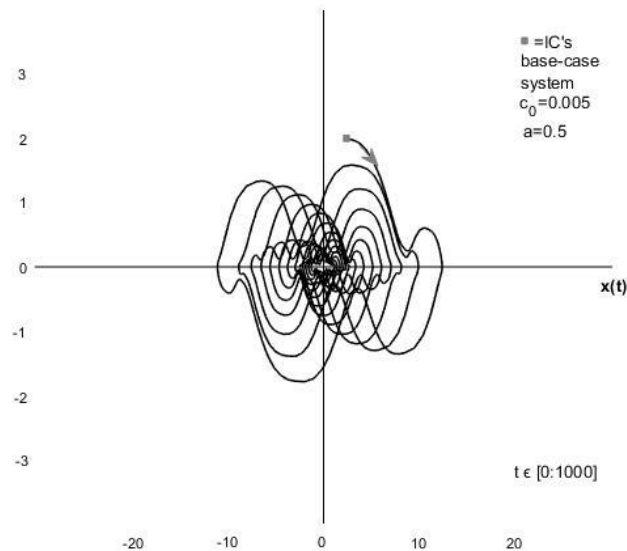


Figure C.8: Phase plane diagram for the base-case system with  $a=0,5$  and  $c_0=0,005$ .

### C.1.3 $a=1,0$

In this part, the nonlinear damping coefficient is increased to  $a=1,0$ .

#### C.1.3.1 $c_0=0,0015$

Figures C.9 and C.19 show the base-case system with the linear damping coefficient,  $c_0=0,0015$ , and the nonlinear damping coefficient,  $a=1,0$ . Figure C.9 shows the position curve to the left and the velocity curve to the right, while figure C.10 shows the phase plane diagram. In all the diagrams, it is clear that the nonlinearity is being more dominant. It is also visible that the damping at some times becomes negative, giving an incline in amplitude for the position and velocity.

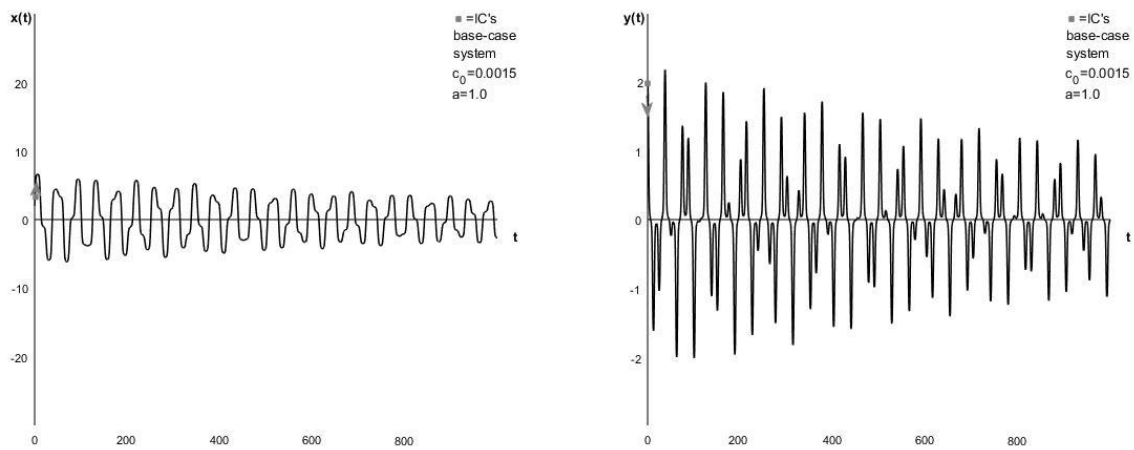


Figure C.9: Position curve(left) and velocity curve(right) for the base-case system with  $a=1,0$  and  $c_0=0,0015$ .

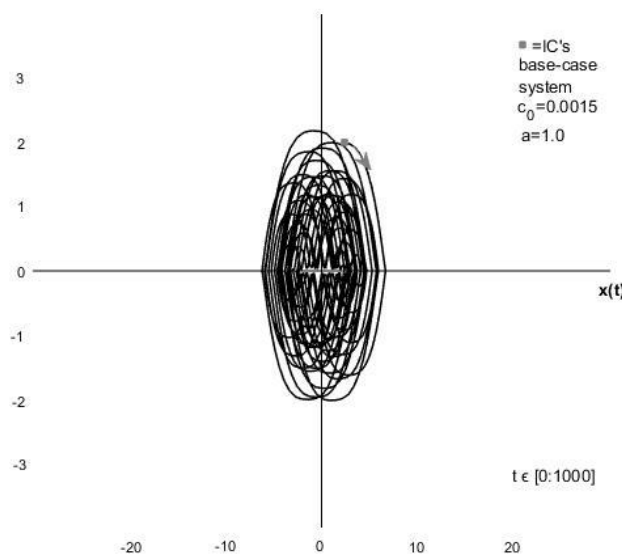


Figure C.10: Phase plane diagram for the base-case system with  $a=1,0$  and  $c_0=0,0015$ .

C.1.3.2  $c_0=0,005$

Figures C.11 and C.12 show the base-case system with the linear damping coefficient,  $c_0=0,005$ , and the nonlinear damping coefficient,  $a=1,0$ . Figure C.11 shows the position curve to the left and the velocity curve to the right, while figure C.12 shows the phase plane diagram.

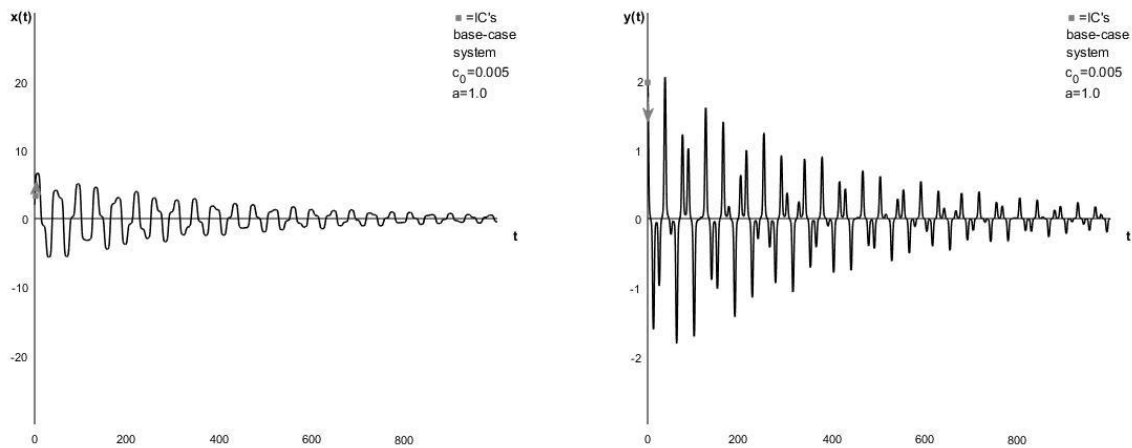


Figure C.11: Position curve(left) and velocity curve(right) for the base-case system with  $a=1,0$  and  $c_0=0,005$ .

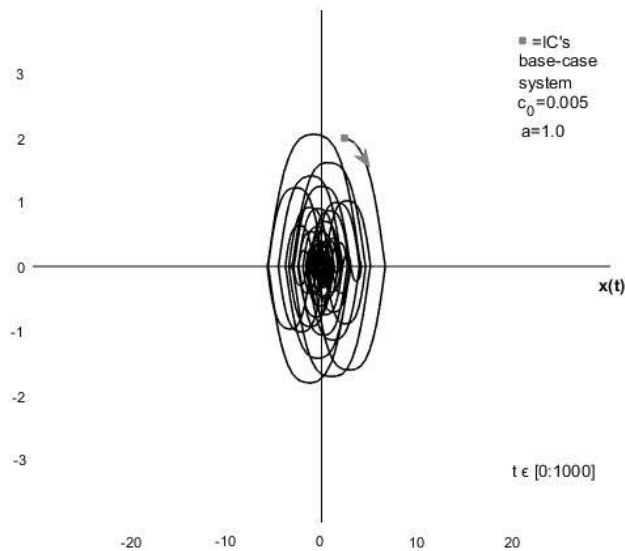


Figure C.12: Phase plane diagram for the base-case system with  $a=1,0$  and  $c_0=0,005$ .

### C.1.4 $a=1,19$

#### C.1.4.1 $c_0=0,0015$

Figures C.13 and C.14 show the base-case system with the linear damping coefficient,  $c_0=0,0015$ , and the nonlinear damping coefficient,  $a=1,19$ . Figure C.13 shows the position curve to the left and the velocity curve to the right, while figure C.14 shows the phase plane diagram. The diagrams show that the negative damping from the nonlinearity in the damping term is almost balancing the linear damping coefficient.

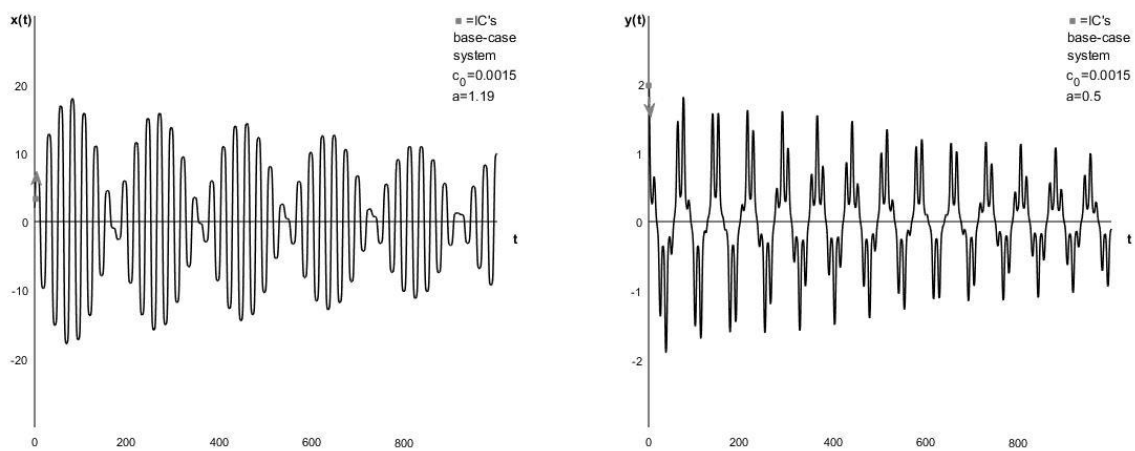


Figure C.13: Position curve(left) and velocity curve(right) for the base-case system with  $a=1,19$  and  $c_0=0,0015$ .

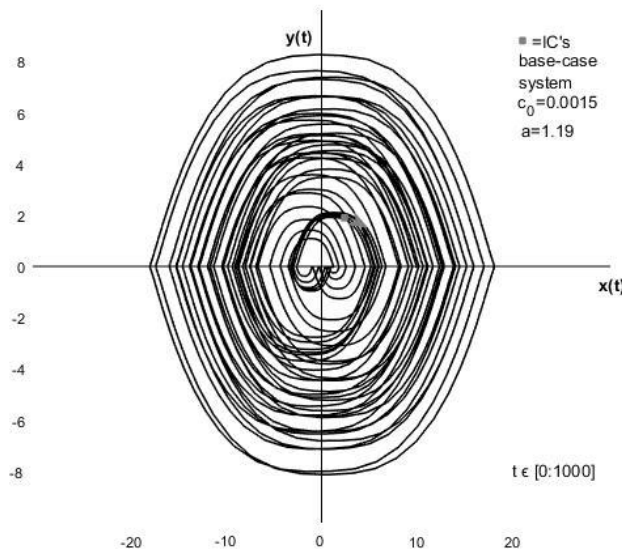


Figure C.14: Phase plane diagram for the base-case system with  $a=1,19$  and  $c_0=0,0015$ .

### C.1.4.2 $c_0=0,005$

Figures C.15 and C.16 show the base-case system with the linear damping coefficient,  $c_0=0,005$ , and the nonlinear damping coefficient,  $a=1,19$ . Figure C.15 shows the position curve to the left and the velocity curve to the right, while figure C.16 shows the phase plane diagram. Even with greater linear damping coefficient, the nonlinearity is very visible. With  $a=1,19$ , the nonlinearity becomes more prominent in the position curve as well.

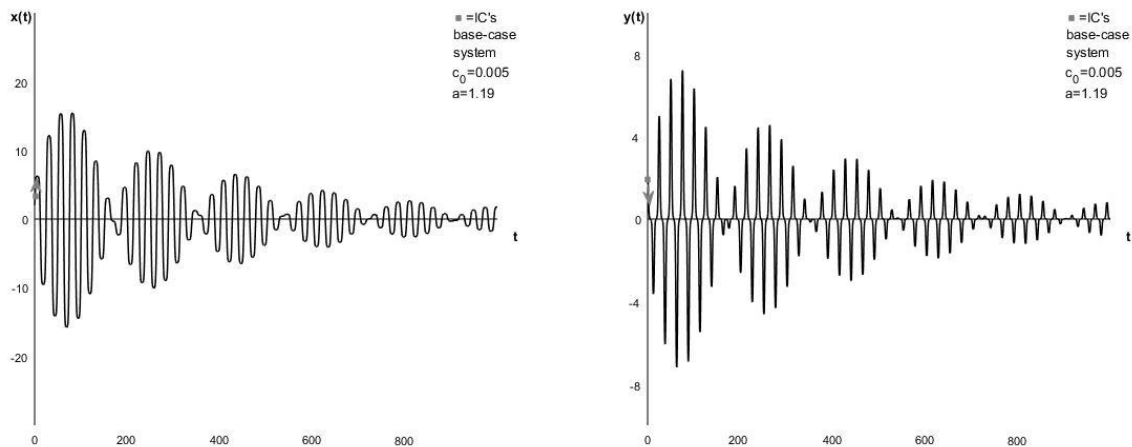


Figure C.15: Position curve(left) and velocity curve(right) for the base-case system with  $a=1,19$  and  $c_0=0,005$ .

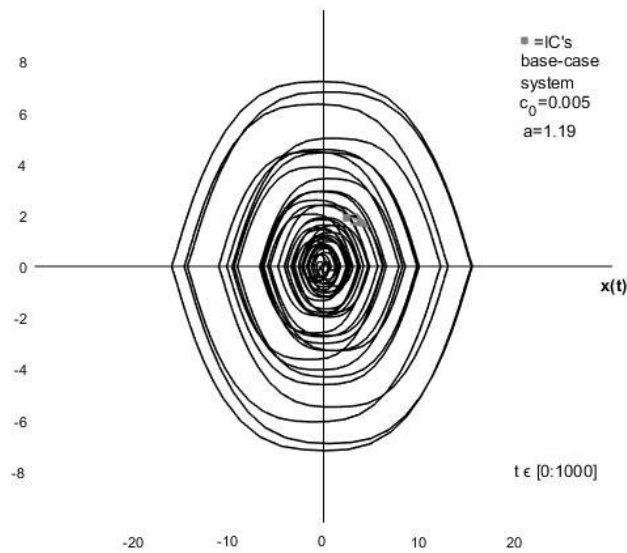


Figure C.16: Phase plane diagram for the base-case system with  $a=1,19$  and  $c_0=0,005$ .

### C.1.5 $a=1,2$

#### C.1.5.1 $c_0=0,0015$

Figures C.17 and C.18 show the base-case system with the linear damping coefficient,  $c_0=0,0015$ , and the nonlinear damping coefficient,  $a=1,2$ . Figure C.17 shows the position curve to the left and the velocity curve to the right, while figure C.18 shows the phase plane diagram. When  $a=1,2$ , the negative damping has overtaken the system, making it have a constant incline in both position and velocity.

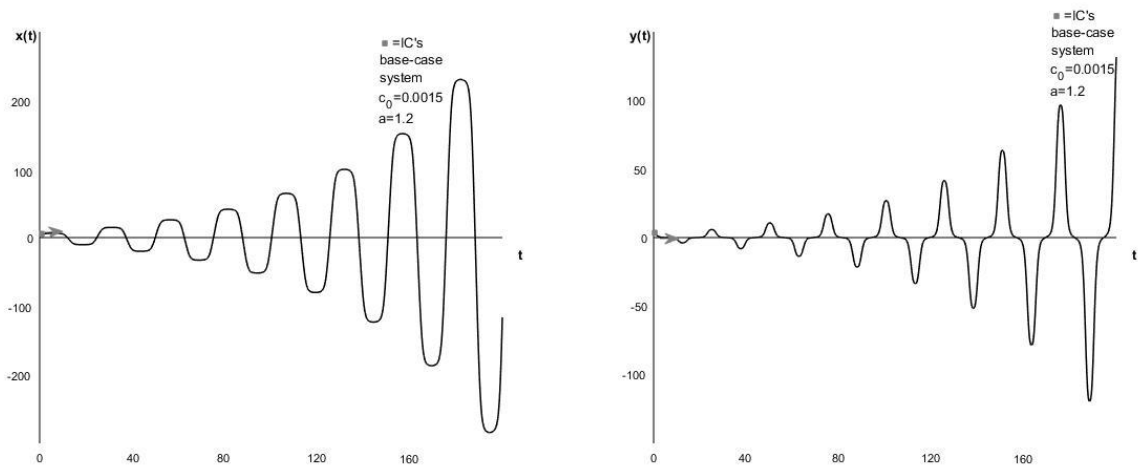


Figure C.17: Position curve(left) and velocity curve(right) for the base-case system with  $a=1,2$  and  $c_0=0,0015$ .

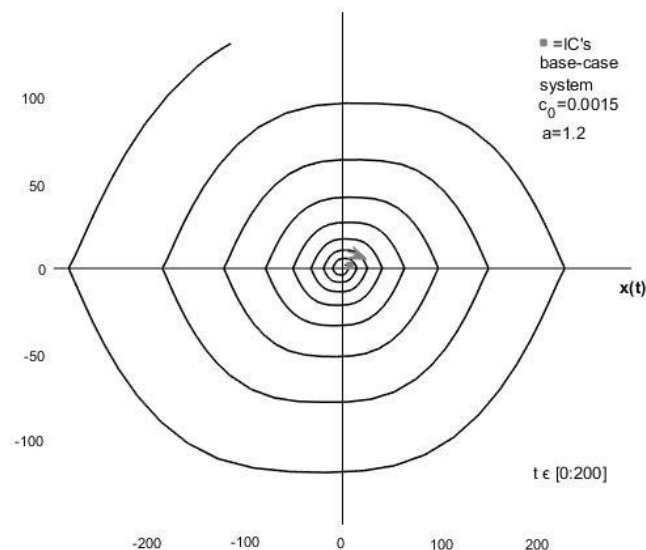


Figure C.18: Phase plane diagram for the base-case system with  $a=1,2$  and  $c_0=0,0015$ .

C.1.4.2  $c_0=0,005$

Figures C.19 and C.20 show the base-case system with the linear damping coefficient,  $c_0=0,005$ , and the nonlinear damping coefficient,  $a=1,2$ . Figure C.19 shows the position curve to the left and the velocity curve to the right, while figure C.20 shows the phase plane diagram. The negative damping is still making the system constantly increasing the position and velocity, but the linear damping coefficient slows the system more down when increased.

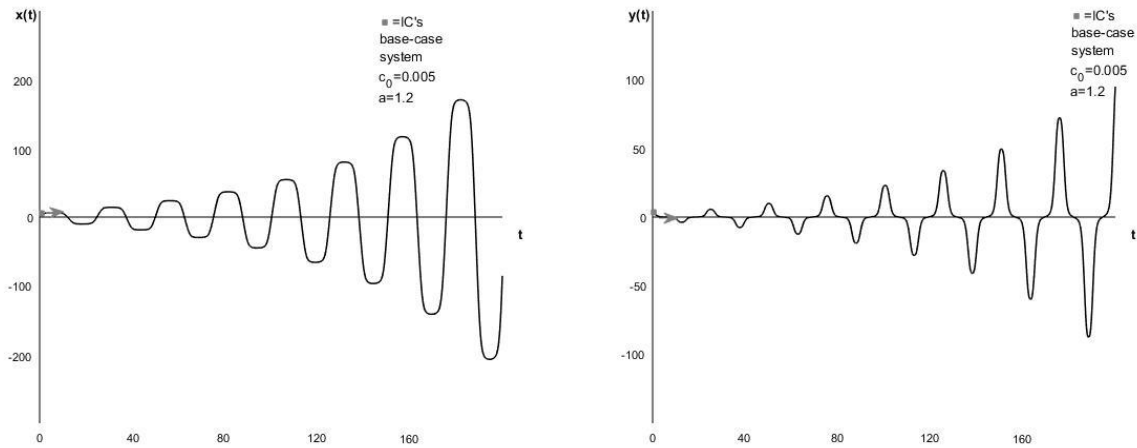


Figure C.19: Position curve(left) and velocity curve(right) for the base-case system with  $a=1,2$  and  $c_0=0,005$ .

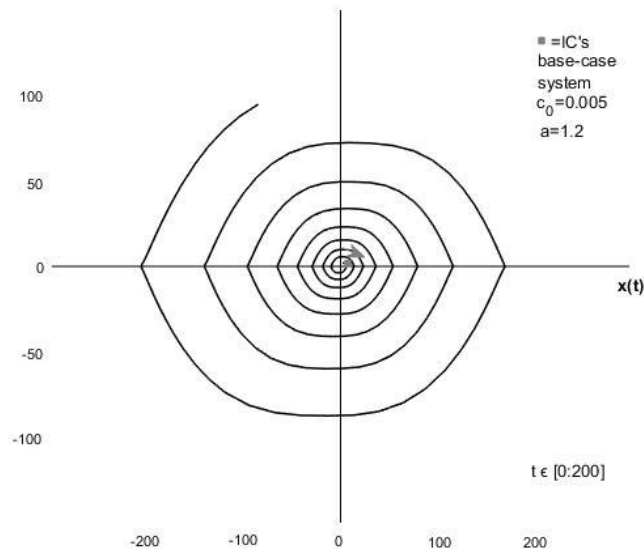


Figure C.20: Phase plane diagram for the base-case system with  $a=1,2$  and  $c_0=0,005$ .



## C.2 $\beta = \frac{1}{3}$

When the mass parameter,  $m=0,222$ , the system has a loading frequency,  $\omega$ , one third of the natural frequency,  $\omega_0$ , i.e.  $\beta = \frac{1}{3}$ .

### C.2.1 $a=0$

When  $a=0$ , the system is only subjected to linear, constant damping,  $c_0$ . Figure C.21 shows the position and velocity curve for the system with  $c_0=0,0015$ . Figure C.22 shows the system with  $c_0=0,0015$  in the phase plane. Figures C.23 and C.24 show the position and velocity curve and phase plane diagram respectively for the system with  $c_0=0,005$ . The systems spirals towards the origin in the phase plane, as expected, faster for the system with higher damping coefficient.

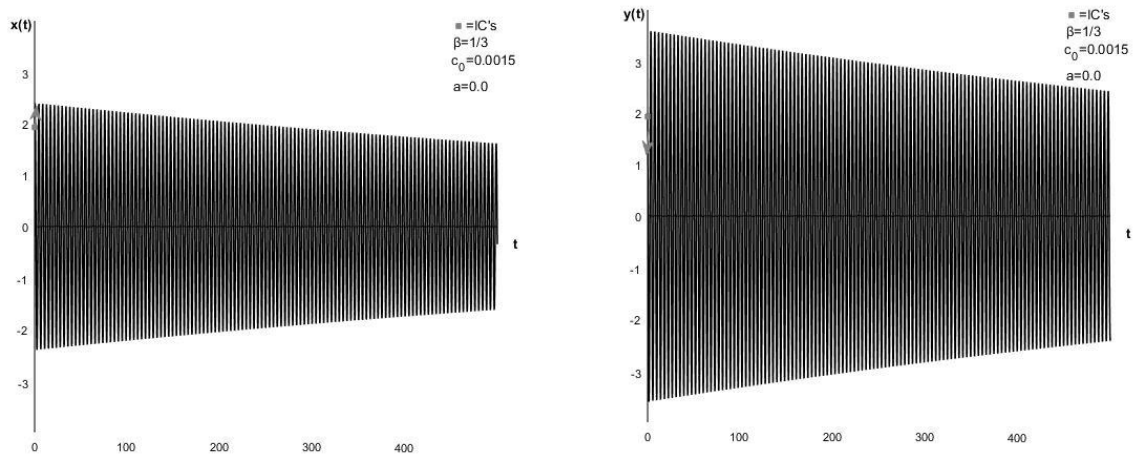


Figure C.21: Position curve(left) and velocity curve(right) for the base-case system with  $m=0,222$ , making  $\beta=1/3$ , with  $c_0=0,0015$  and  $a=0$ .

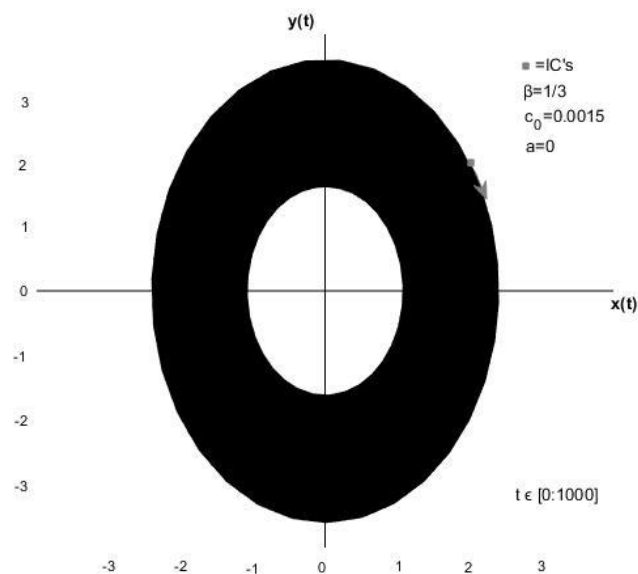


Figure C.22: Phase plane diagram for the base-case system with  $m=0,222$ , making  $\beta=1/3$ , with  $c_0=0,0015$  and  $a=0$ .

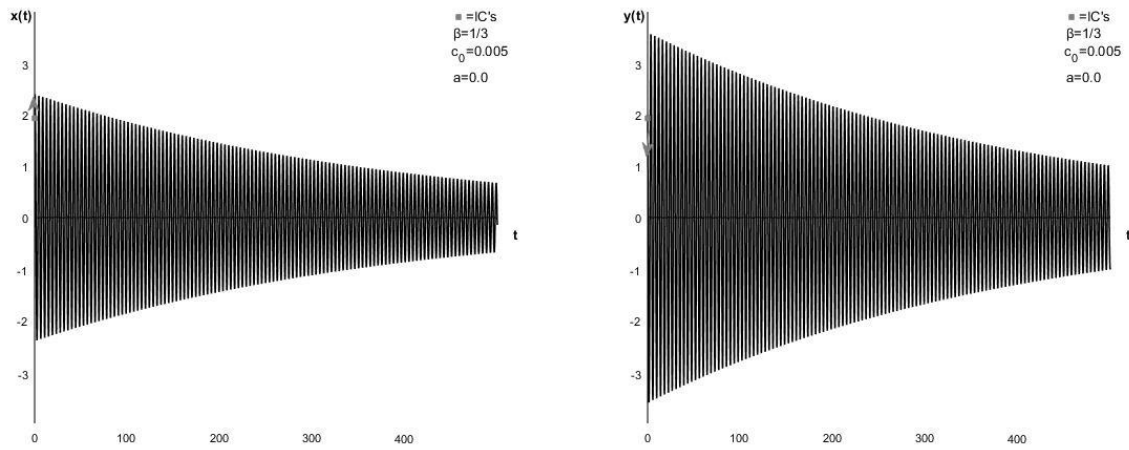


Figure C.23: Position curve(left) and velocity curve(right) for the base-case system with  $m=0,222$ , making  $\beta=1/3$ , with  $c_0=0,005$  and  $a=0$ .

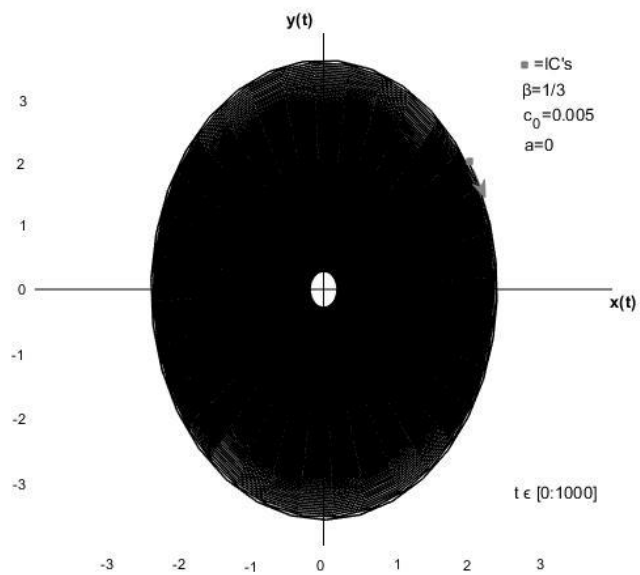


Figure C.24: Phase plane diagram for the base-case system with  $m=0,222$ , making  $\beta=1/3$ , with  $c_0=0,005$  and  $a=0$ .

### C.2.2 $a=1,0$

Figures C.25 and C.26 show the position curve, velocity curve and phase plane diagram respectively for the system with  $a=1,0$  and  $c_0=0,0015$ . Figures C.27 and C.28 show the same for the system with  $a=1,0$  and  $c_0=0,0015$ . It is clear that the damping term at some times becomes negative, leading to an increase in the amplitude.

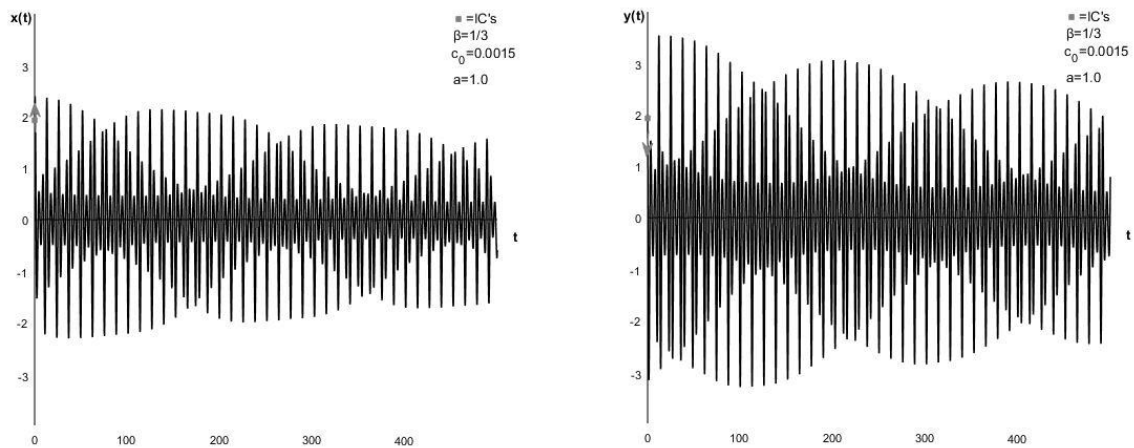


Figure C.25: Position curve(left) and velocity curve(right) for the base-case system with  $m=0,222$ , making  $\beta=1/3$ , with  $c_0=0,0015$  and  $a=1,0$

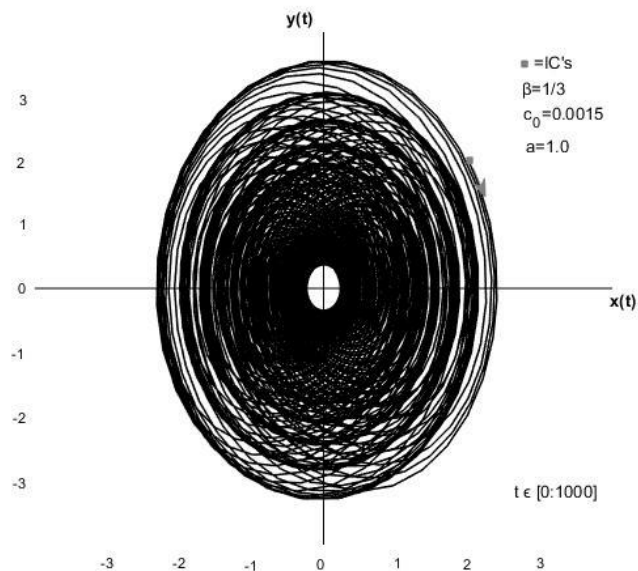


Figure C.26: Phase plane diagram for the base-case system with  $m=0,222$ , making  $\beta=1/3$ , with  $c_0=0,0015$  and  $a=1,0$ .

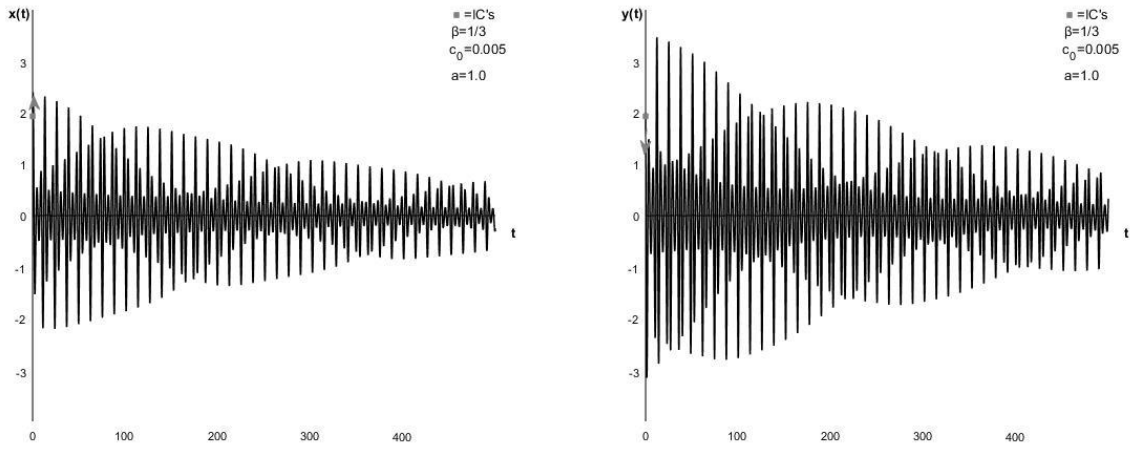


Figure C.27: Position curve(left) and velocity curve(right) for the base-case system with  $m=0,222$ , making  $\beta=1/3$ , with  $c_0=0,005$  and  $a=1,0$ .

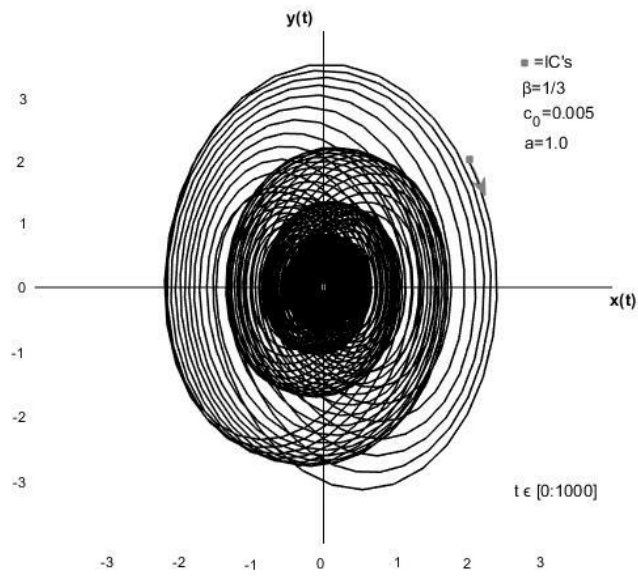


Figure C.28: Phase plane diagram for the base-case system with  $m=0,222$ , making  $\beta=1/3$ , with  $c_0=0,005$  and  $a=1,0$ .

### C.2.3 $a=2,0$

Figures C.29 and C.30 show the position curve, velocity curve and phase plane diagram respectively for the system with  $a=2,0$  and  $c_0=0,005$ . Figures C.31 and C.32 show the same for the system with  $a=2,0$  and  $c_0=0,005$ . The negativity in the damping term is almost balancing the positive damping, especially for the system with the lowest linear, constant damping coefficient,  $c_0=0,0015$ .

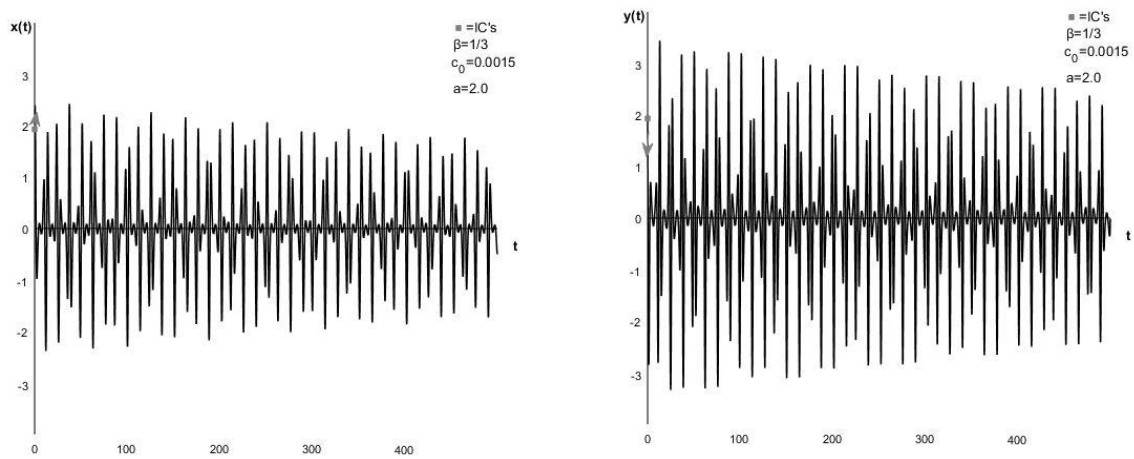


Figure C.29: Position curve(left) and velocity curve(right) for the base-case system with  $m=0,222$ , making  $\beta=1/3$ , with  $c_0=0,0015$  and  $a=2,0$ ,

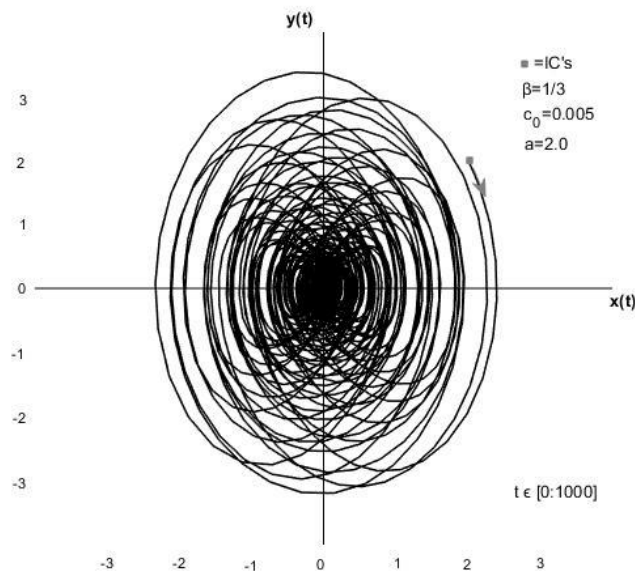


Figure C.30: Phase plane diagram for the base-case system with  $m=0,222$ , making  $\beta=1/3$ , with  $c_0=0,0015$  and  $a=2,0$ .

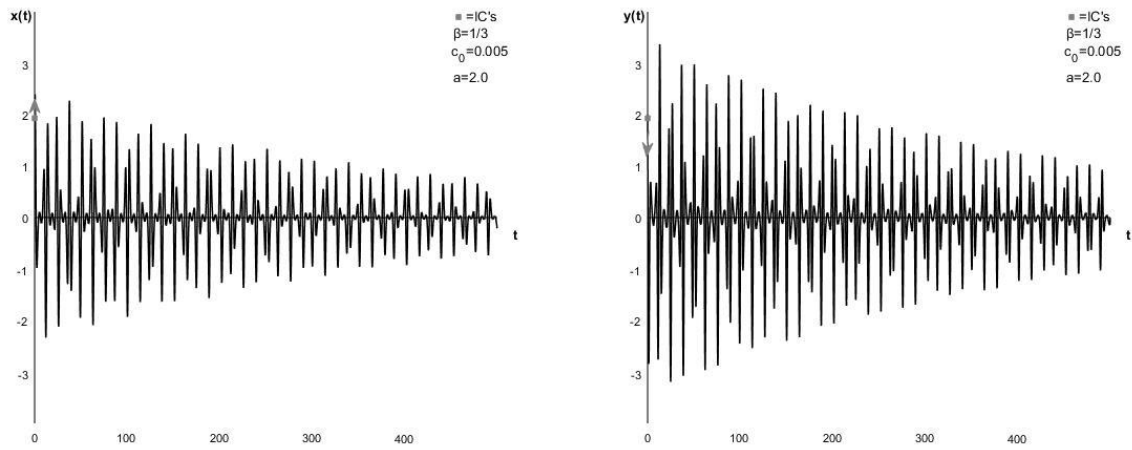


Figure C.31: Position curve(left) and velocity curve(right) for the base-case system with  $m=0,222$ , making  $\beta=1/3$ , with  $c_0=0,005$  and  $a=2,0$ .

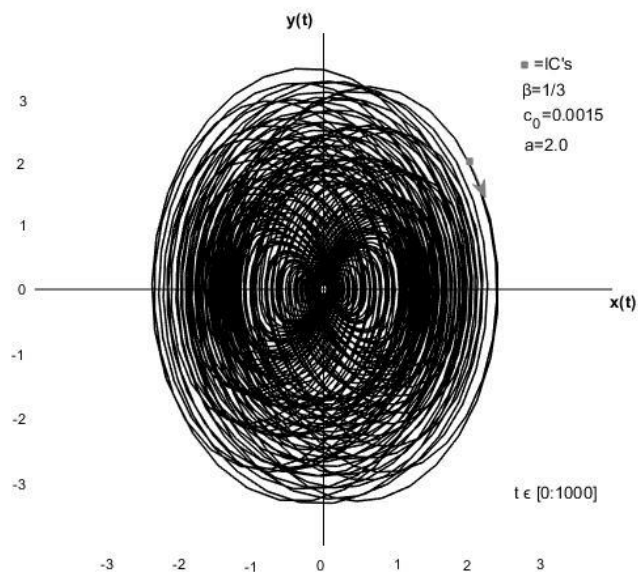


Figure C.32: Phase plane diagram for the base-case system with  $m=0,222$ , making  $\beta=1/3$ , with  $c_0=0,005$  and  $a=2,0$ .

### C.2.4 $a=3,45$

Figures C.33 and C.34 show the position curve, velocity curve and phase plane diagram respectively for the system with  $a=3,45$  and  $c_0=0,005$ . Figures C.35 and C.36 show the same for the system with  $a=3,45$  and  $c_0=0,005$ . The negativity in the damping term is almost taking over for the positive damping.

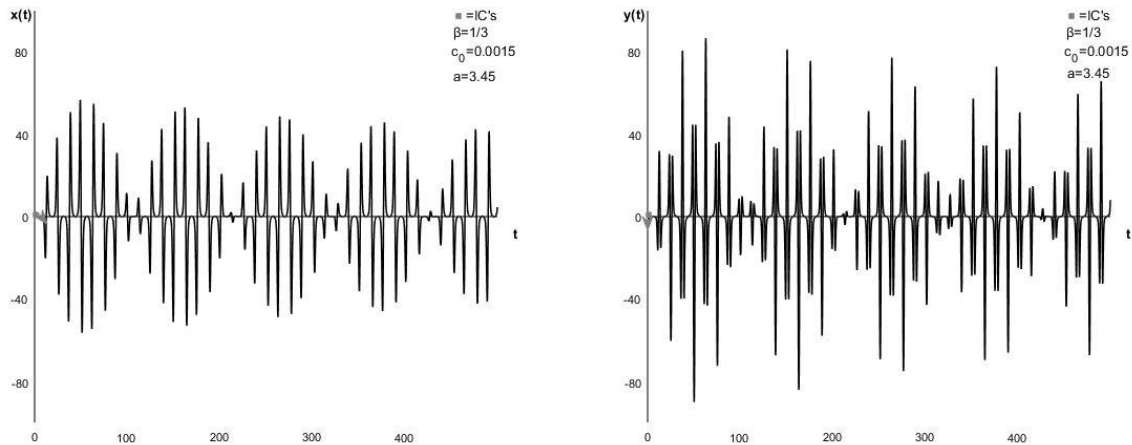


Figure C.33: Position curve(left) and velocity curve(right) for the base-case system with  $m=0,222$ , making  $\beta=1/3$ , with  $c_0=0,0015$  and  $a=3,45$ .

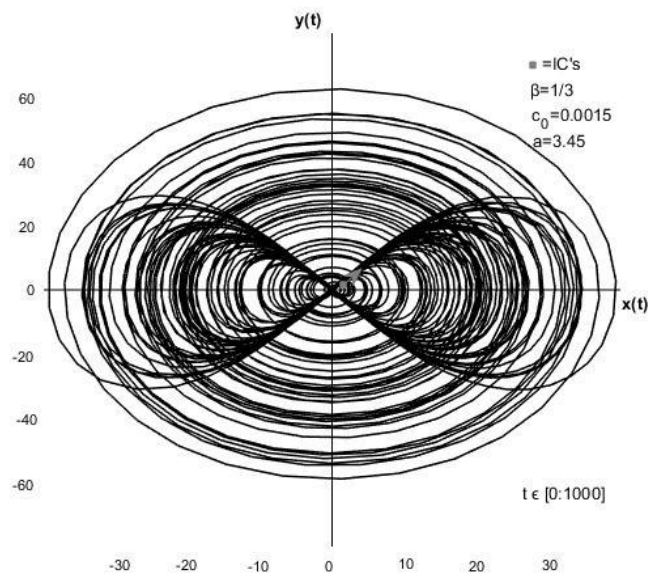


Figure C.34: Phase plane diagram for the base-case system with  $m=0,222$ , making  $\beta=1/3$ , with  $c_0=0,0015$  and  $a=3,45$ .

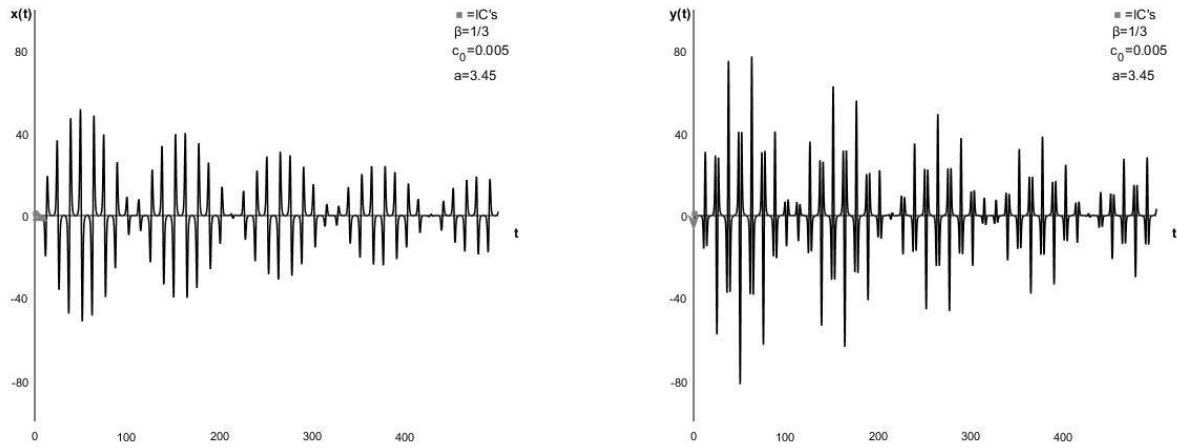


Figure C.35: Position curve(left) and velocity curve(right) for the base-case system with  $m=0,222$ , making  $\beta=1/3$ , with  $c_0=0,005$  and  $a=3,45$ .

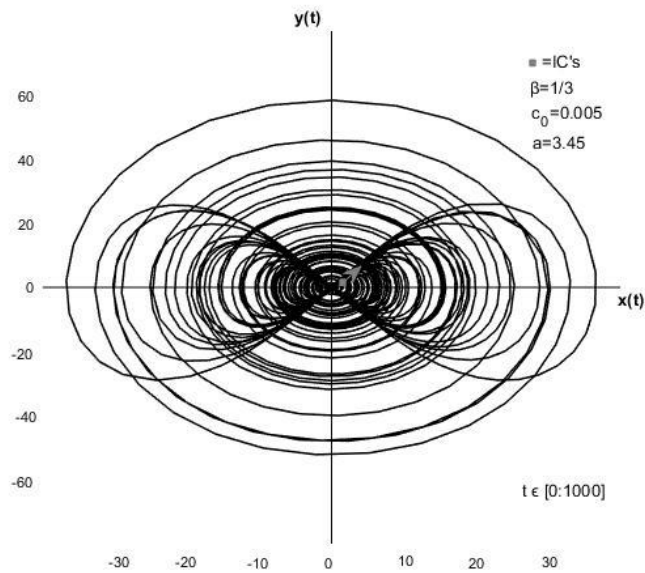


Figure C.36: Phase plane diagram for the base-case system with  $m=0,222$ , making  $\beta=1/3$ , with  $c_0=0,005$  and  $a=3,45$ .



### C.2.5 $a=3,46$

Figures C.37 and C.38 show the position curve, velocity curve and phase plane diagram respectively for the system with  $a=3,46$  and  $c_0=0,005$ . Figures C.39 and C.40 show the same for the system with  $a=3,46$  and  $c_0=0,005$ . The negativity in the damping term has taken completely control of the system, leading to a continued incline in amplitude. Note that the timespan for the phase plane diagrams is set to only 90s, as the growth is rapid.

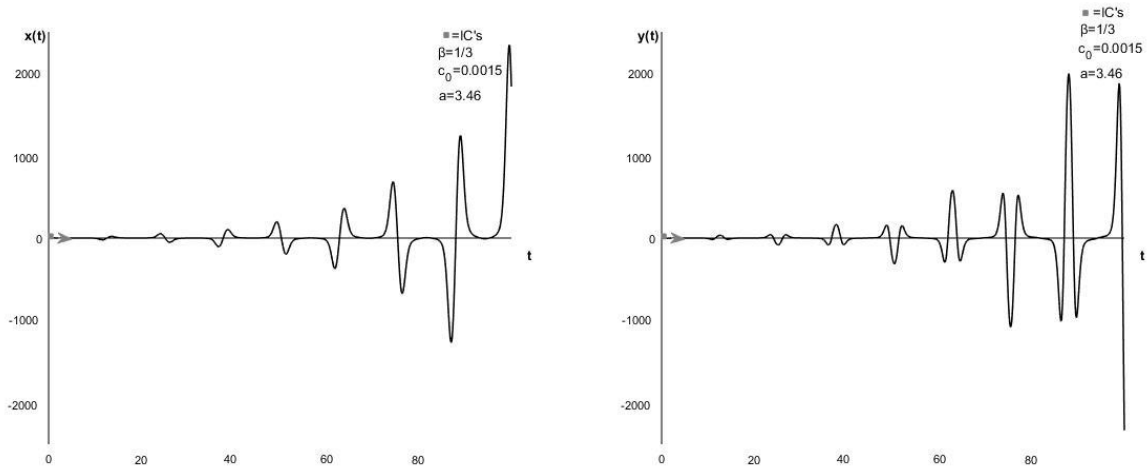


Figure C.37: Position curve(left) and velocity curve(right) for the base-case system with  $m=0,222$ , making  $\beta=1/3$ , with  $c_0=0,0015$  and  $a=3,46$ .

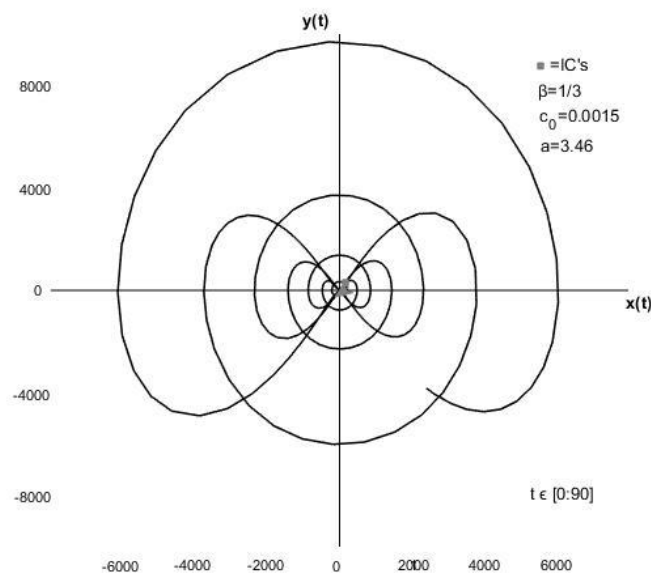


Figure C.38: Phase plane diagram for the base-case system with  $m=0,222$ , making  $\beta=1/3$ , with  $c_0=0,0015$  and  $a=3,46$ .

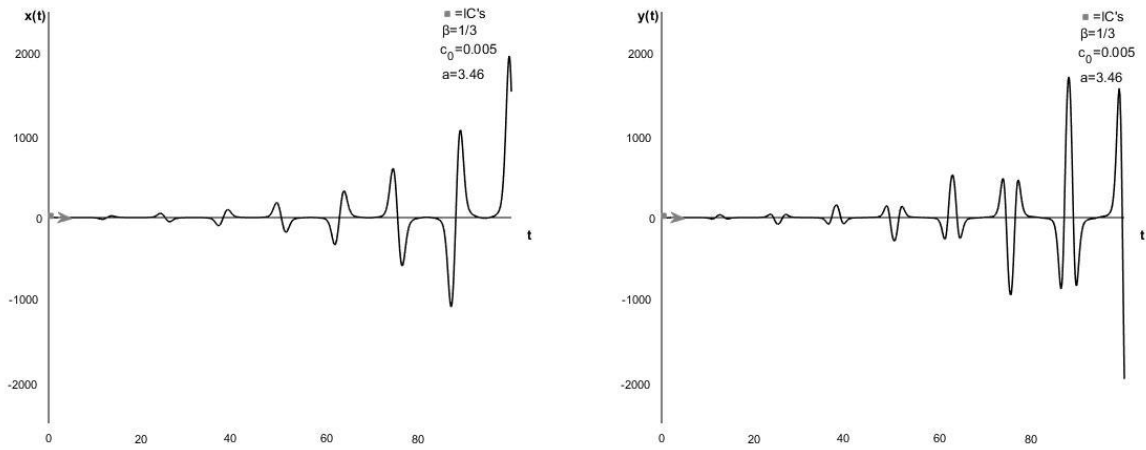


Figure C.39: Position curve(left) and velocity curve(right) for the base-case system with  $m=0,222$ , making  $\beta=1/3$ , with  $c_0=0,005$  and  $a=3,46$ .

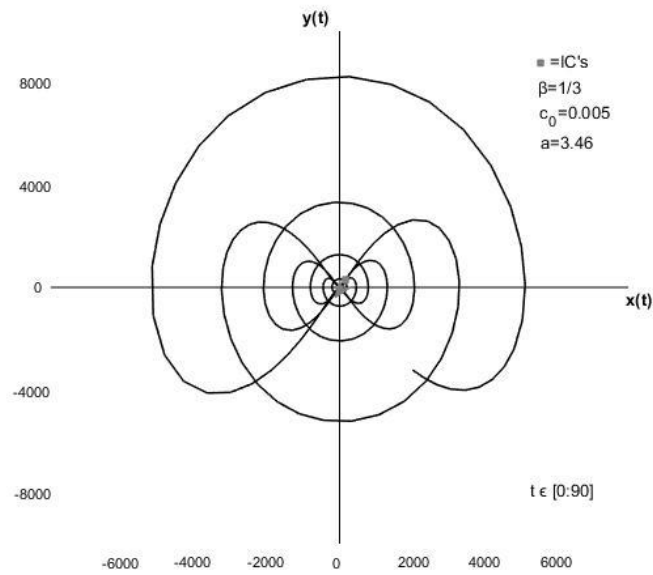


Figure C.40: Phase plane diagram for the base-case system with  $m=0,222$ , making  $\beta=1/3$ , with  $c_0=0,005$  and  $a=3,46$ .

### C.3 $\beta = \frac{1}{2}$

When the mass parameter,  $m=0,5$ , the system has a frequency,  $\omega$ , half of the natural frequency,  $\omega_0$ , i.e.  $\beta = \frac{1}{2}$ .

#### C.3.1 $a=0$

When  $a=0$ , the system is only subjected to linear, constant damping,  $c_0$ . Figure C.41 shows the position and velocity curve for the system with  $c_0=0,0015$ . Figure C.42 shows the system with  $c_0=0,0015$  in the phase plane. Figures C.43 and C.44 show the position and velocity curve and phase plane diagram respectively for the system with  $c_0=0,005$ . The systems have similar behaviour as for  $\beta=1/3$ .

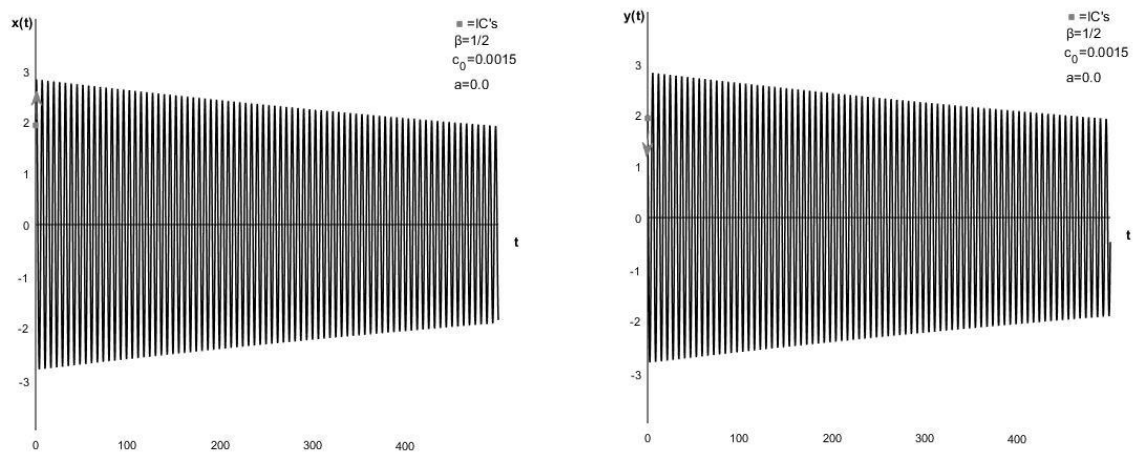


Figure C.41: Position curve(left) and velocity curve(right) for the base-case system with  $m=0,5$ , making  $\beta=1/2$ , with  $c_0=0,0015$  and  $a=0$ .

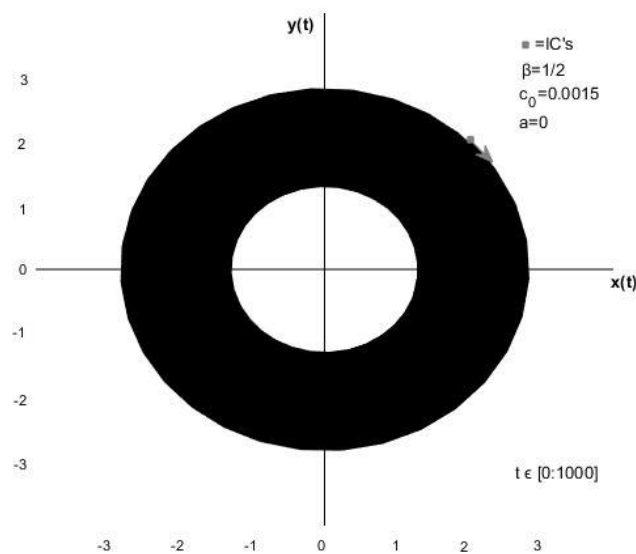


Figure C.42: Phase plane diagram for the base-case system with  $m=0,5$ , making  $\beta=1/2$ , with  $c_0=0,0015$  and  $a=0$ .

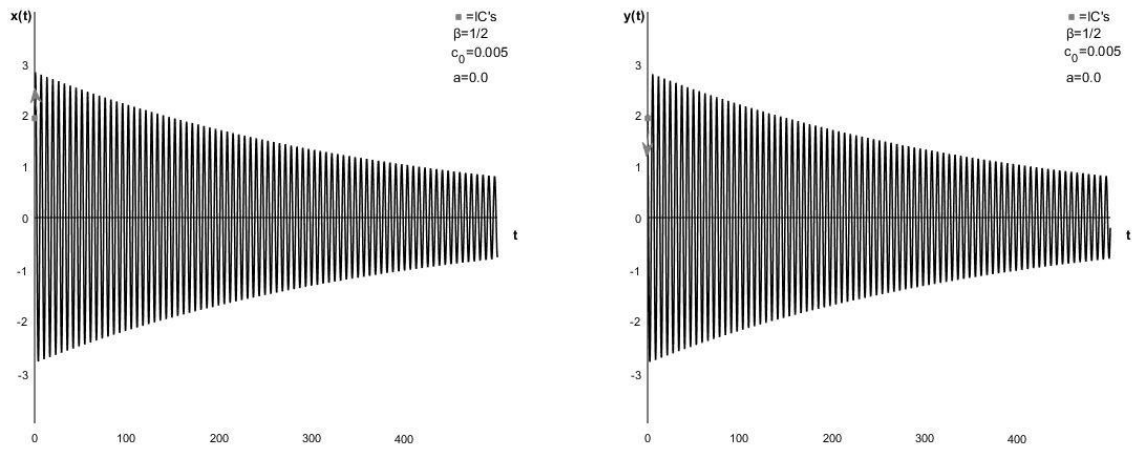


Figure C.43: Position curve(left) and velocity curve(right) for the base-case system with  $m=0,5$ , making  $\beta=1/2$ , with  $c_0=0,005$  and  $a=0$ .

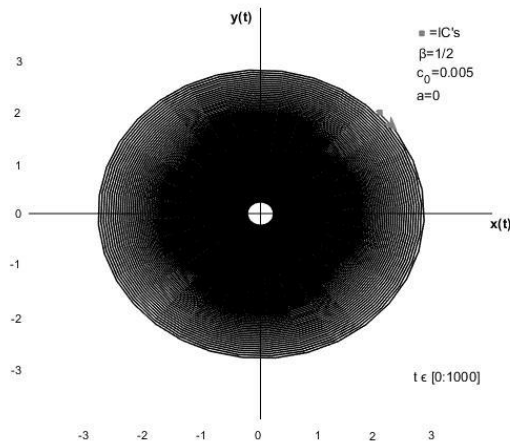


Figure C.44: Phase plane diagram for the base-case system with  $m=0,5$ , making  $\beta=1/2$ , with  $c_0=0,005$  and  $a=0$ .

### C.3.2 $a=0,5$

Figures C.45 and C.46 show the position curve, velocity curve and phase plane diagram respectively for the system with  $a=0,5$  and  $c_0=0,0015$ . Figures C.47 and C.48 show the same for the system with  $a=0,5$  and  $c_0=0,0015$ .

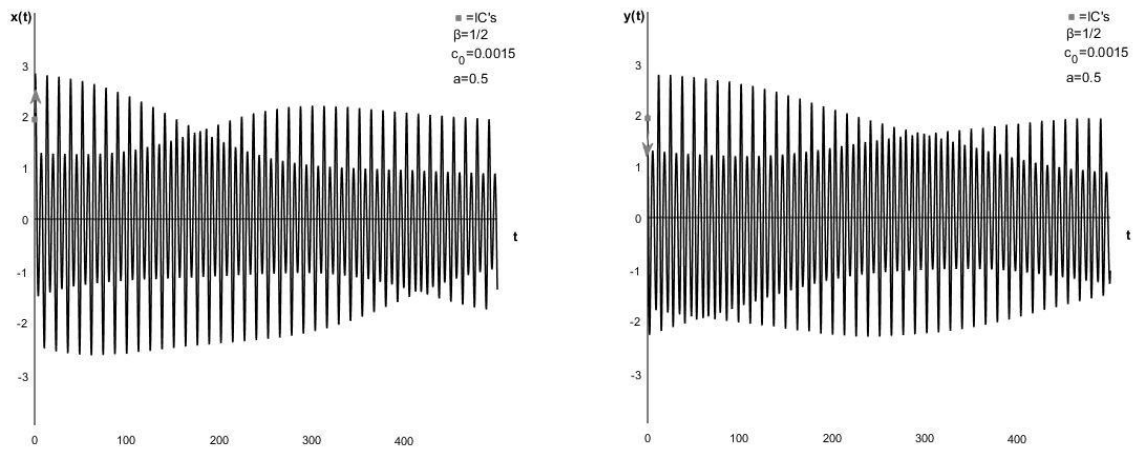


Figure C.45: Position curve(left) and velocity curve(right) for the base-case system with  $m=0,5$ , making  $\beta=1/2$ , with  $c_0=0,0015$  and  $a=0,5$ .

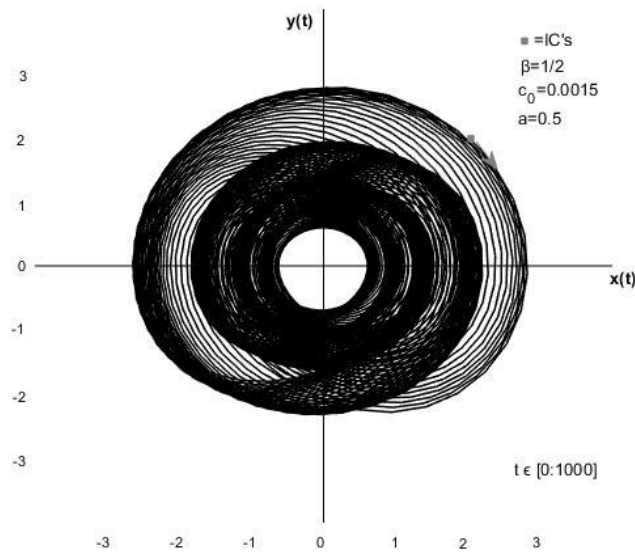


Figure C.46: Phase plane diagram for the base-case system with  $m=0,5$ , making  $\beta=1/2$ , with  $c_0=0,0015$  and  $a=0,5$ .

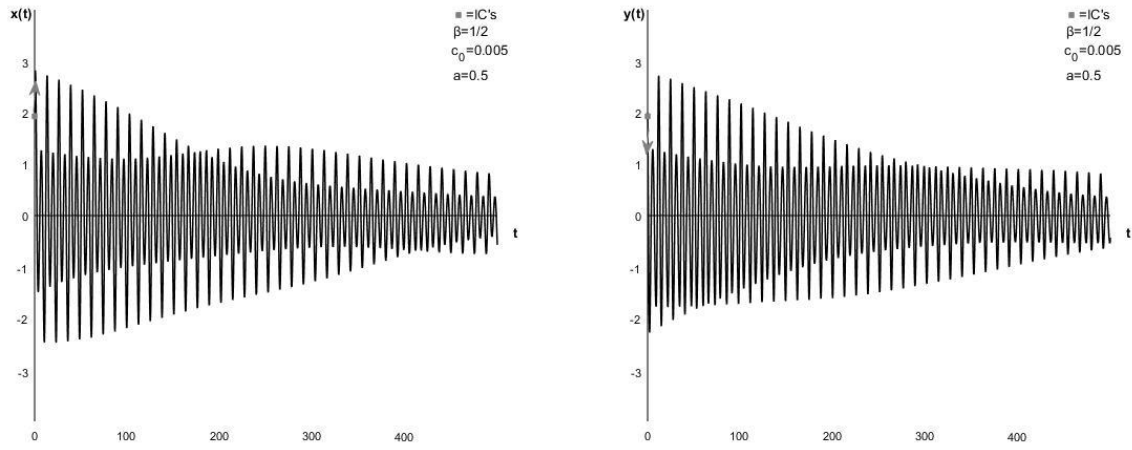


Figure C.47: Position curve(left) and velocity curve(right) for the base-case system with  $m=0,5$ , making  $\beta=1/2$ , with  $c_0=0,005$  and  $a=0,5$ .

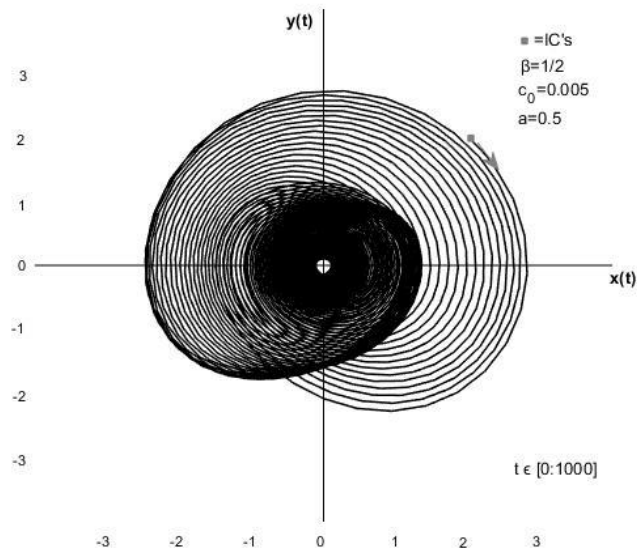


Figure C.48: Phase plane diagram for the base-case system with  $m=0,5$ , making  $\beta=1/2$ , with  $c_0=0,005$  and  $a=0,5$ .

### C.3.3 $a=1,0$

Figures C.49 and C.50 show the position curve, velocity curve and phase plane diagram respectively for the system with  $a=1,0$  and  $c_0=0,005$ . Figures C.51 and C.52 show the same for the system with  $a=1,0$  and  $c_0=0,005$ .

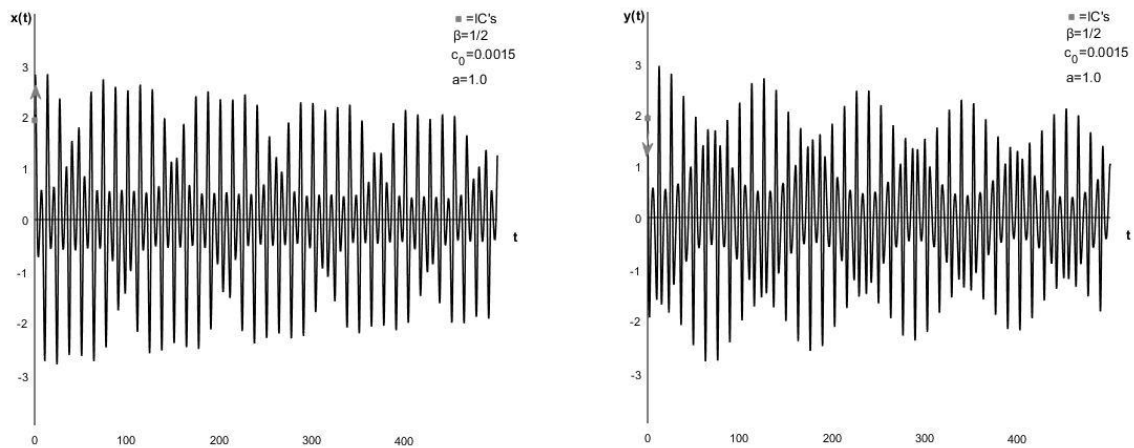


Figure C.49: Position curve(left) and velocity curve(right) for the base-case system with  $m=0,5$ , making  $\beta=1/2$ , with  $c_0=0,0015$  and  $a=1,0$ .

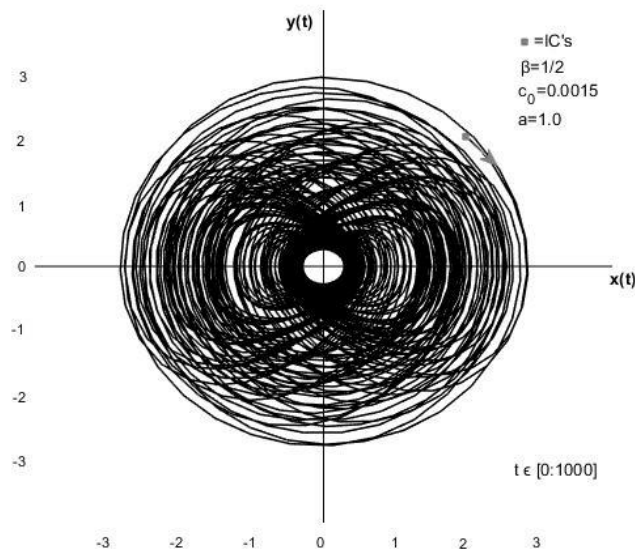


Figure C.50: Phase plane diagram for the base-case system with  $m=0,5$ , making  $\beta=1/2$ , with  $c_0=0,0015$  and  $a=1,0$ .

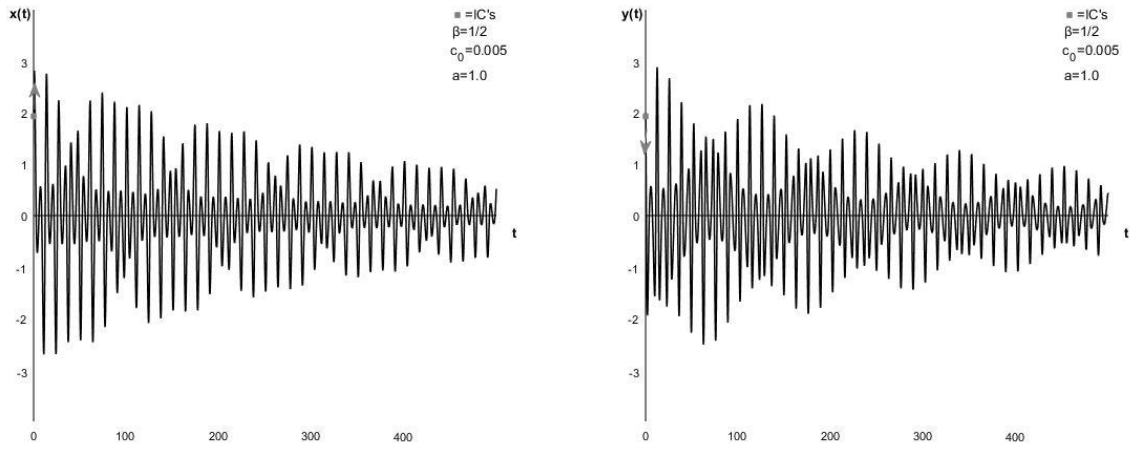


Figure C.51: Position curve(left) and velocity curve(right) for the base-case system with  $m=0,5$ , making  $\beta=1/2$ , with  $c_0=0,005$  and  $a=1,0$ .

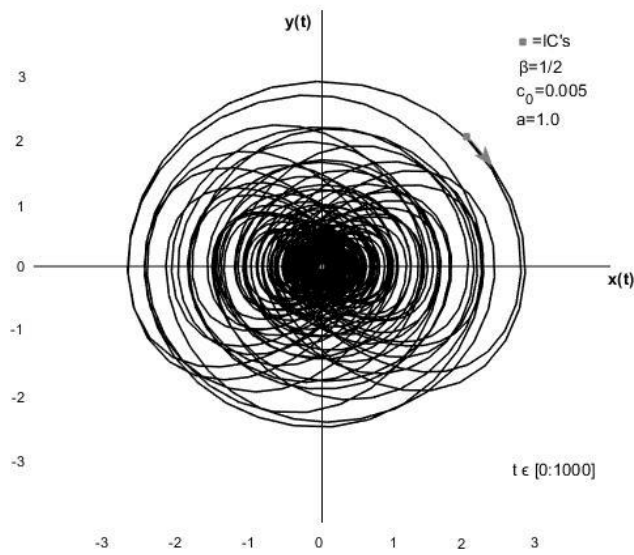


Figure C.52: Phase plane diagram for the base-case system with  $m=0,5$ , making  $\beta=1/2$ , with  $c_0=0,005$  and  $a=1,0$ .



### C.3.4 $a=1,60$

Figures C.53 and C.54 show the position curve, velocity curve and phase plane diagram respectively for the system with  $a=1,60$  and  $c_0=0,005$ . Figures C.55 and C.56 show the same for the system with  $a=1,60$  and  $c_0=0,005$ .

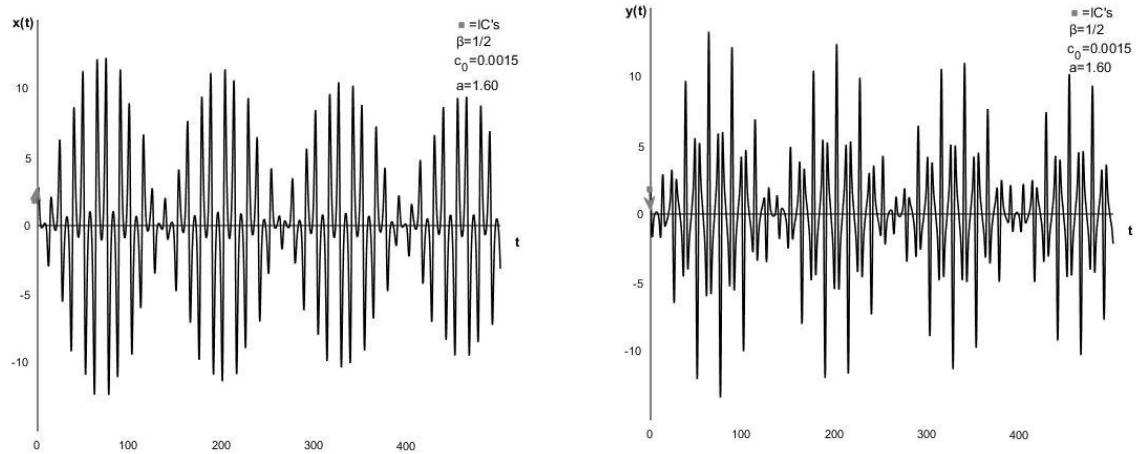


Figure C.53: Position curve(left) and velocity curve(right) for the base-case system with  $m=0,5$ , making  $\beta=1/2$ , with  $c_0=0,0015$  and  $a=1,60$ .

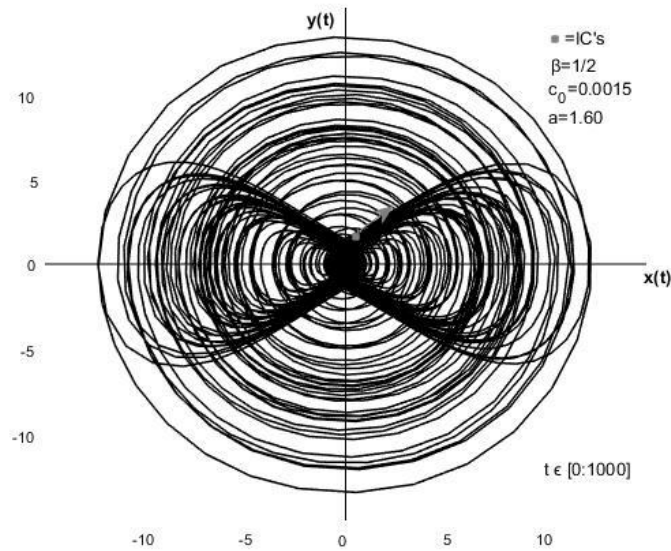


Figure C.54: Phase plane diagram for the base-case system with  $m=0,5$ , making  $\beta=1/2$ , with  $c_0=0,0015$  and  $a=1,60$ .

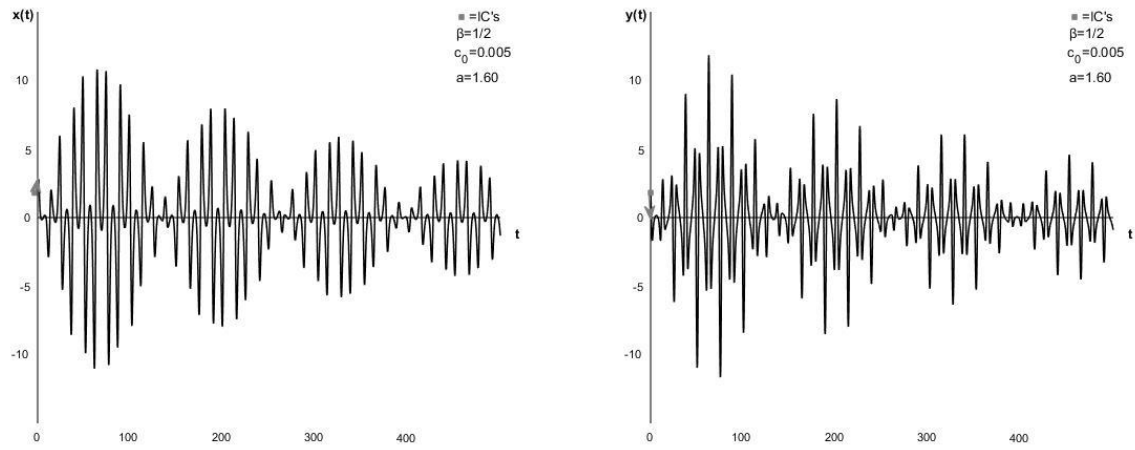


Figure C.55: Position curve(left) and velocity curve(right) for the base-case system with  $m=0,5$ , making  $\beta=1/2$ , with  $c_0=0,005$  and  $a=1,60$ .

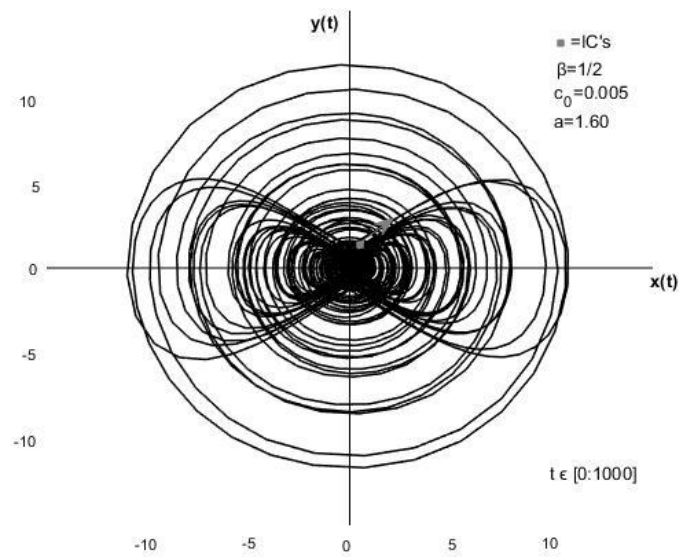


Figure C.56: Phase plane diagram for the base-case system with  $m=0,5$ , making  $\beta=1/2$ , with  $c_0=0,005$  and  $a=1,60$ .

### C.3.5 $a=1,61$

Figures C.57 and C.58 show the position curve, velocity curve and phase plane diagram respectively for the system with  $a=1,61$  and  $c_0=0,005$ . Figures C.59 and C.60 show the same for the system with  $a=1,61$  and  $c_0=0,005$ .

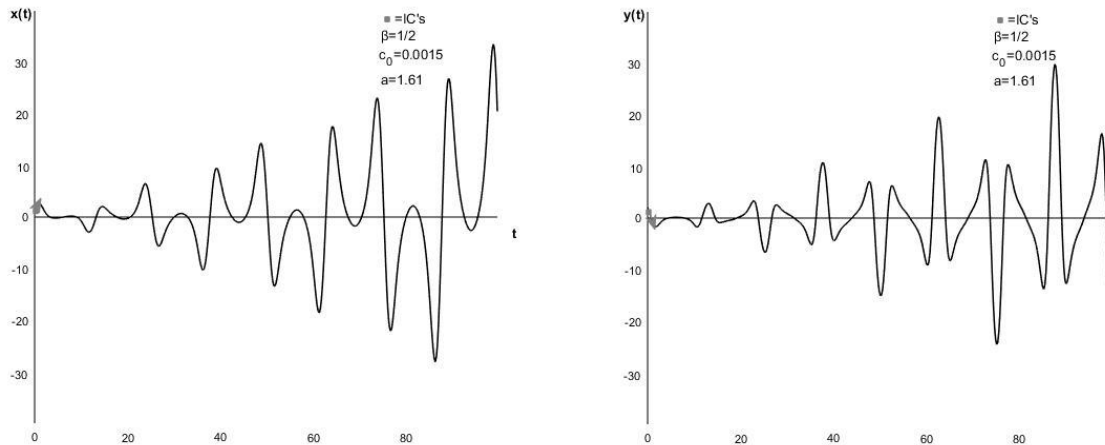


Figure C.57: Position curve(left) and velocity curve(right) for the base-case system with  $m=0,5$ , making  $\beta=1/2$ , with  $c_0=0,0015$  and  $a=1,61$ .

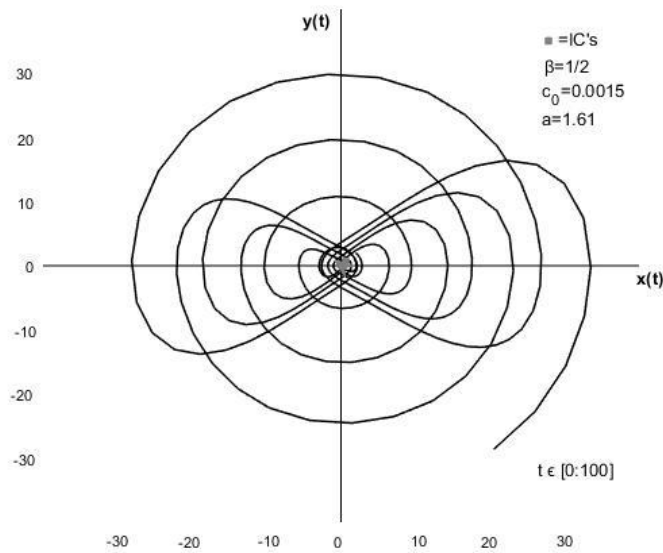


Figure C.58: Phase plane diagram for the base-case system with  $m=0,5$ , making  $\beta=1/2$ , with  $c_0=0,0015$  and  $a=1,61$ .

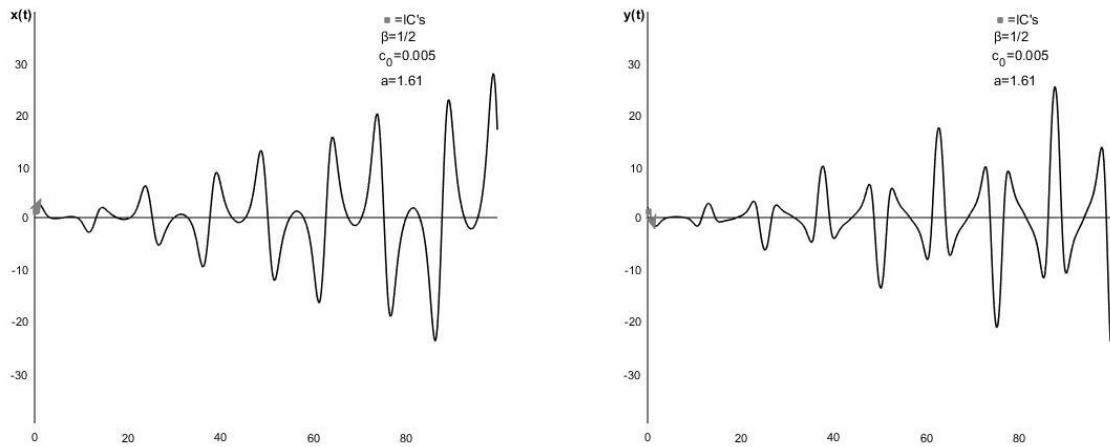


Figure C.59: Position curve(left) and velocity curve(right) for the base-case system with  $m=0,5$ , making  $\beta=1/2$ , with  $c_0=0,005$  and  $a=1,61$ .

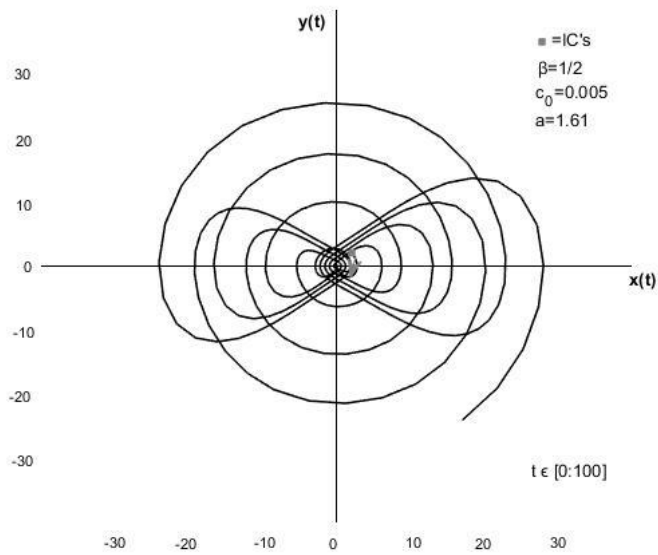


Figure C.60: Phase plane diagram for the base-case system with  $m=0,5$ , making  $\beta=1/2$ , with  $c_0=0,005$  and  $a=1,61$ .

## C.4 $\beta = 1,0$

When the mass parameter,  $m=2,0$ , the system has a frequency,  $\omega$ , equal to the natural frequency,  $\omega_0$ , i.e.  $\beta = 1,0$ .

### C.4.1 $a=0$

When  $a=0$ , the system is only subjected to linear, constant damping,  $c_0$ . Figure C.61 shows the position and velocity curve for the system with  $c_0=0,0015$ . Figure C.62 shows the system with  $c_0=0,0015$  in the phase plane. Figures C.63 and C.64 show the position and velocity curve and phase plane diagram respectively for the system with  $c_0=0,005$ .

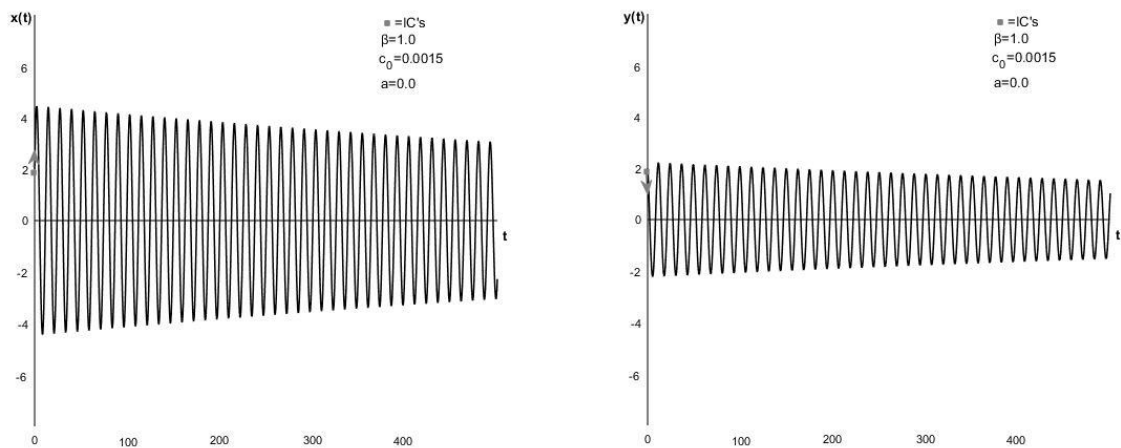


Figure C.61: Position curve(left) and velocity curve(right) for the base-case system with  $m=2,0$ , making  $\beta=1,0$ , with  $c_0=0,0015$  and  $a=0$ .

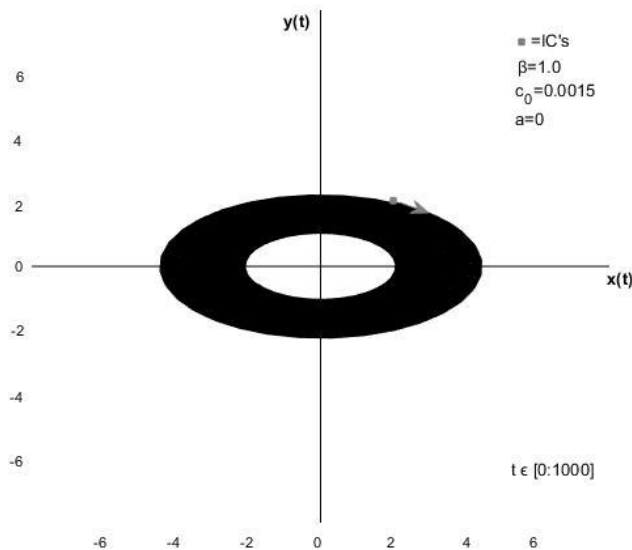


Figure C.62: Phase plane diagram for the base-case system with  $m=2,0$ , making  $\beta=1,0$ , with  $c_0=0,0015$  and  $a=0$ .

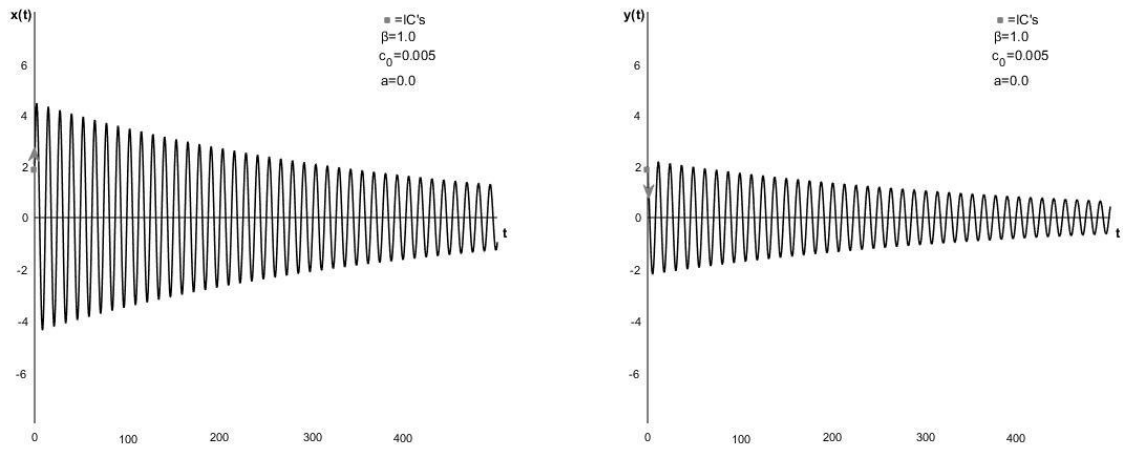


Figure C.63: Position curve(left) and velocity curve(right) for the base-case system with  $m=2,0$ , making  $\beta=1,0$ , with  $c_0=0,005$  and  $a=0$ .

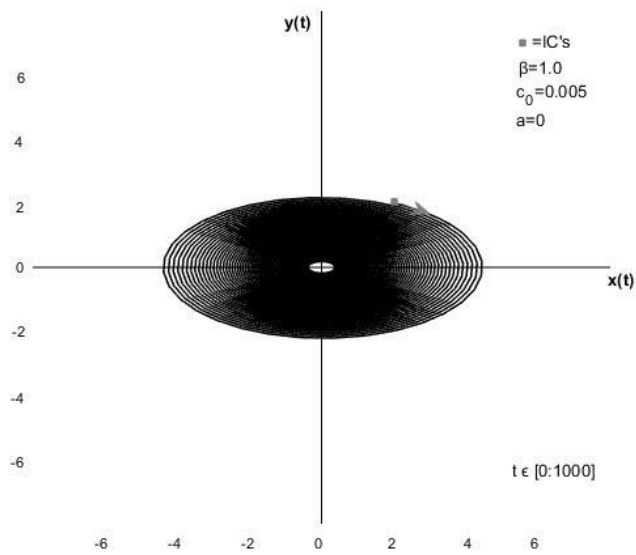


Figure C.64: Phase plane diagram for the base-case system with  $m=2,0$ , making  $\beta=1,0$ , with  $c_0=0,005$  and  $a=0$ .

### C.4.2 $a=0,5$

Figures C.65 and C.66 show the position curve, velocity curve and phase plane diagram respectively for the system with  $a=0,5$  and  $c_0=0,0015$ . Figures C.67 and C.68 show the same for the system with  $a=0,5$  and  $c_0=0,0015$ .

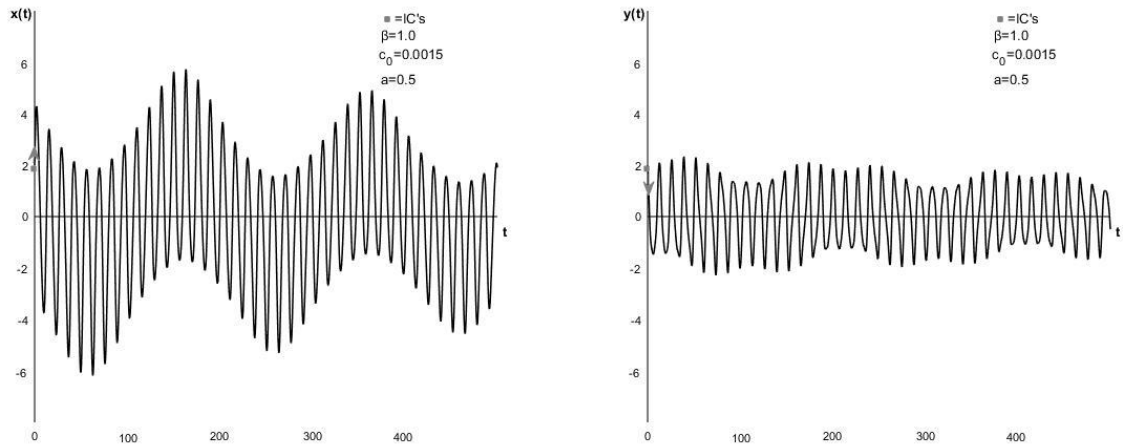


Figure C.65: Position curve(left) and velocity curve(right) for the base-case system with  $m=2,0$ , making  $\beta=1,0$ , with  $c_0=0,0015$  and  $a=0,5$ .

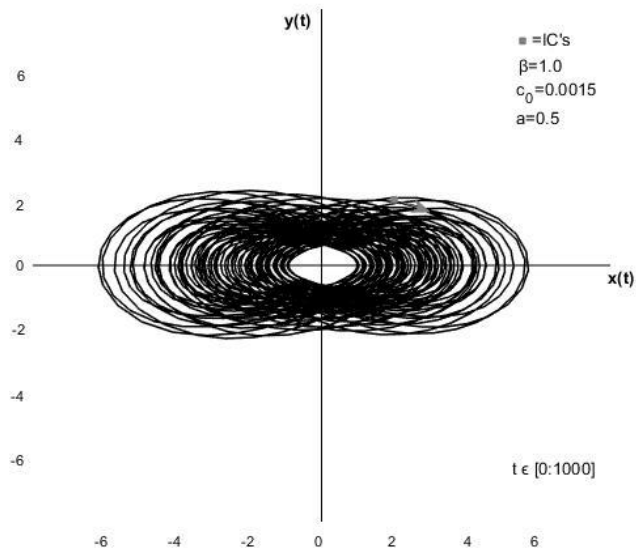


Figure C.66: Phase plane diagram for the base-case system with  $m=2,0$ , making  $\beta=1,0$ , with  $c_0=0,0015$  and  $a=0,5$ .

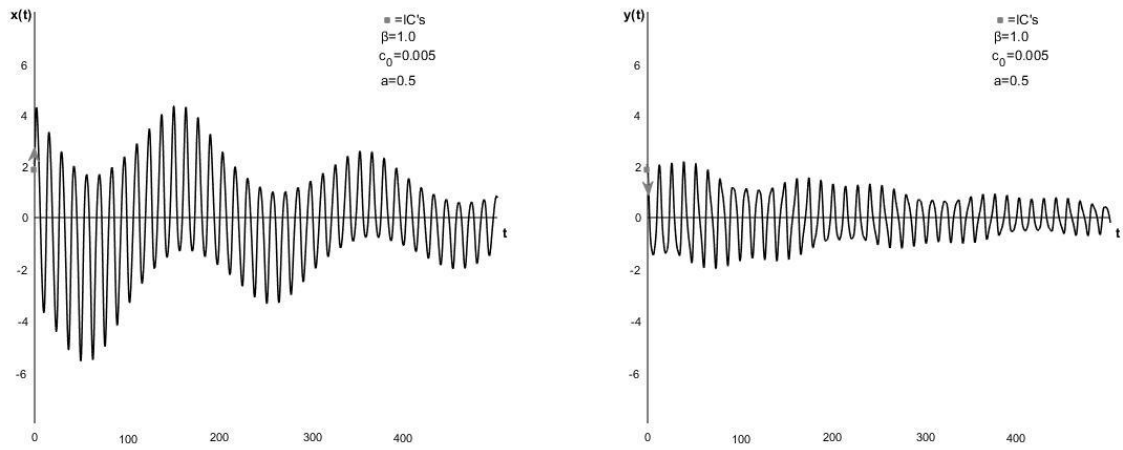


Figure C.67: Position curve(left) and velocity curve(right) for the base-case system with  $m=2,0$ , making  $\beta=1,0$ , with  $c_0=0,005$  and  $a=0,5$ .

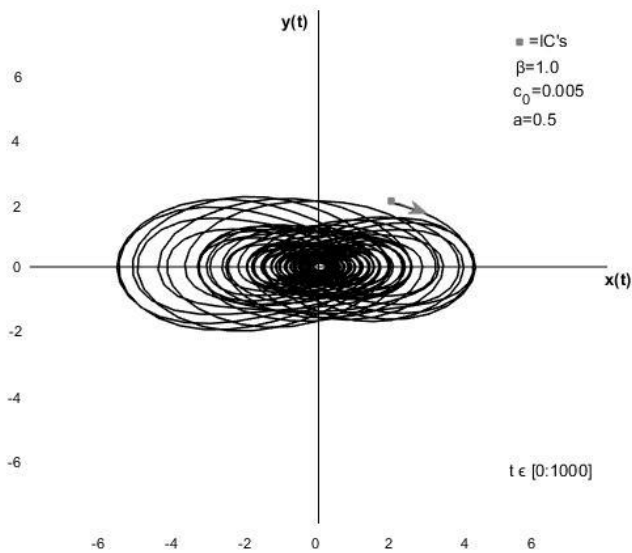


Figure C.68: Phase plane diagram for the base-case system with  $m=2,0$ , making  $\beta=1,0$ , with  $c_0=0,005$  and  $a=0,5$ .



### C.4.3 $a=1,0$

Figures C.69 and C.70 show the position curve, velocity curve and phase plane diagram respectively for the system with  $a=1,0$  and  $c_0=0,005$ . Figures C.71 and C.72 show the same for the system with  $a=1,0$  and  $c_0=0,005$ .

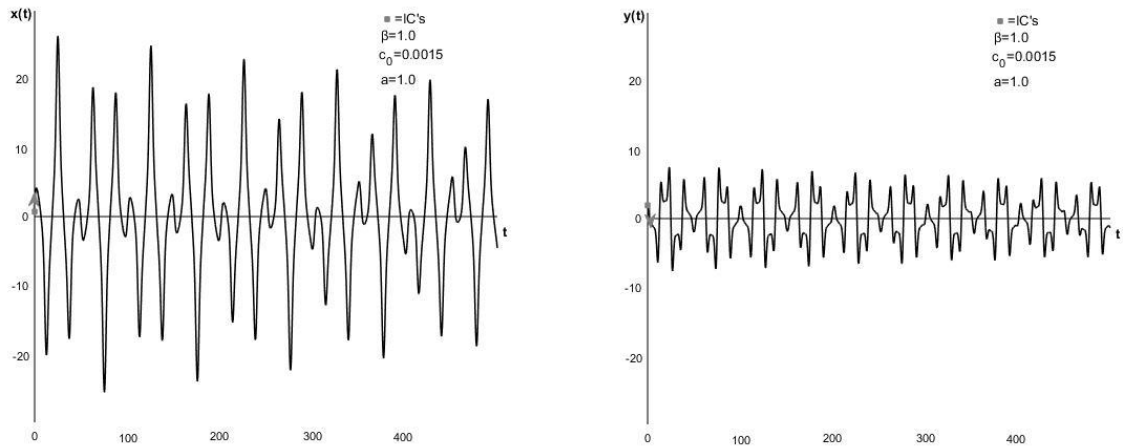


Figure C.69: Position curve(left) and velocity curve(right) for the base-case system with  $m=2,0$ , making  $\beta=1,0$ , with  $c_0=0,0015$  and  $a=1,0$ .

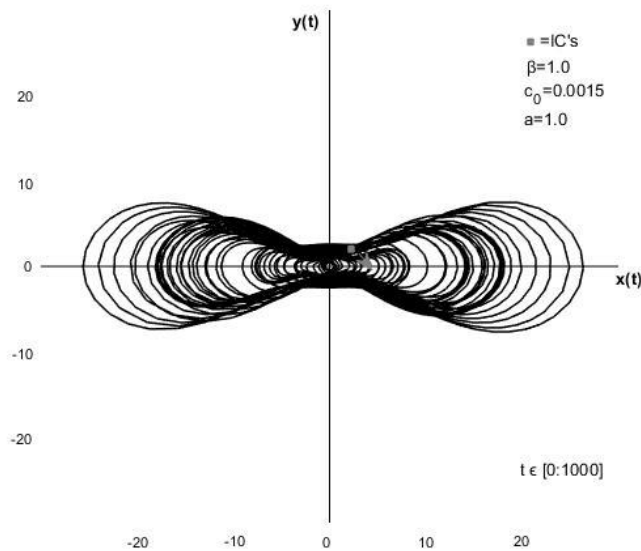


Figure C.70: Phase plane diagram for the base-case system with  $m=2,0$ , making  $\beta=1,0$ , with  $c_0=0,0015$  and  $a=1,0$ .

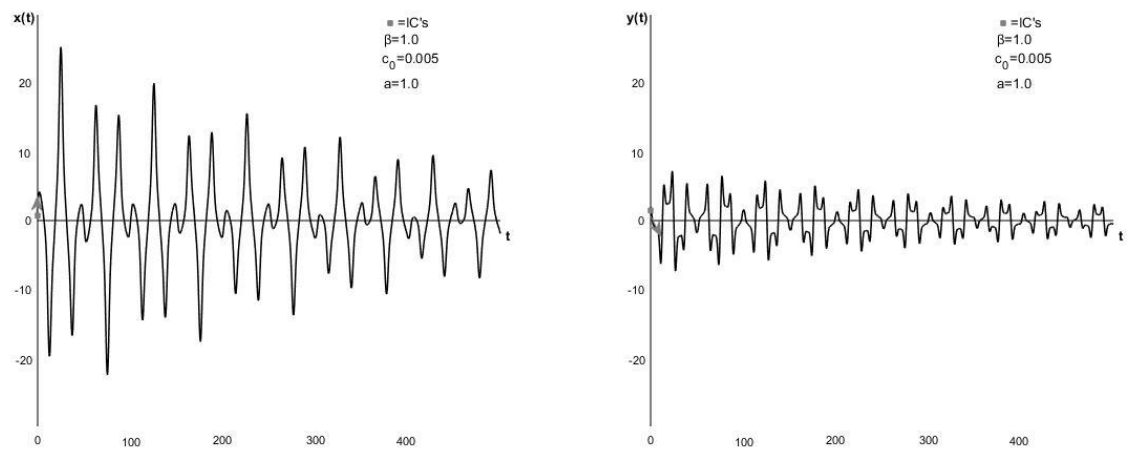


Figure C.71: Position curve(left) and velocity curve(right) for the base-case system with  $m=2,0$ , making  $\beta=1,0$ , with  $c_0=0,005$  and  $a=1,0$ .

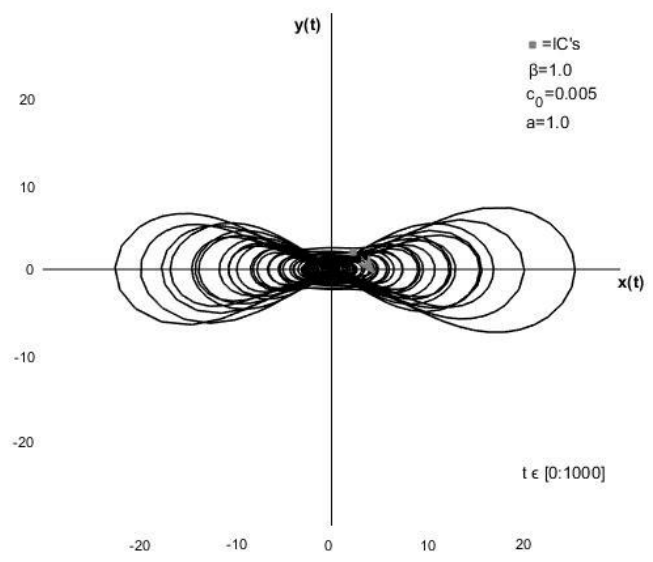


Figure C.72: Phase plane diagram for the base-case system with  $m=2,0$ , making  $\beta=1,0$ , with  $c_0=0,005$  and  $a=1,0$ .

#### C.4.4 $a=1,03$

Figures C.73 and C.74 show the position curve, velocity curve and phase plane diagram respectively for the system with  $a=1,03$  and  $c_0=0,005$ . Figures C.75 and C.76 show the same for the system with  $a=1,03$  and  $c_0=0,005$ .

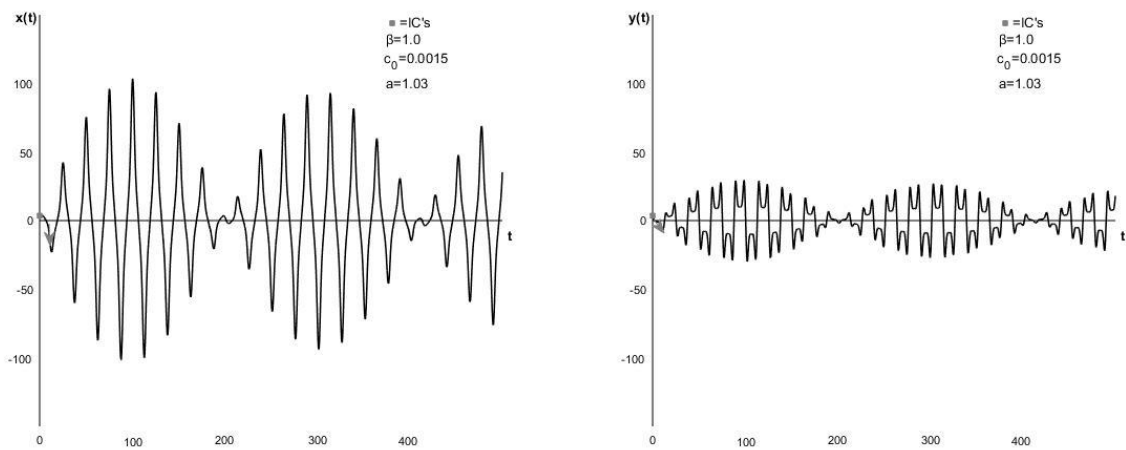


Figure C.73: Position curve(left) and velocity curve(right) for the base-case system with  $m=2,0$ , making  $\beta=1,0$ , with  $c_0=0,0015$  and  $a=1,03$ .

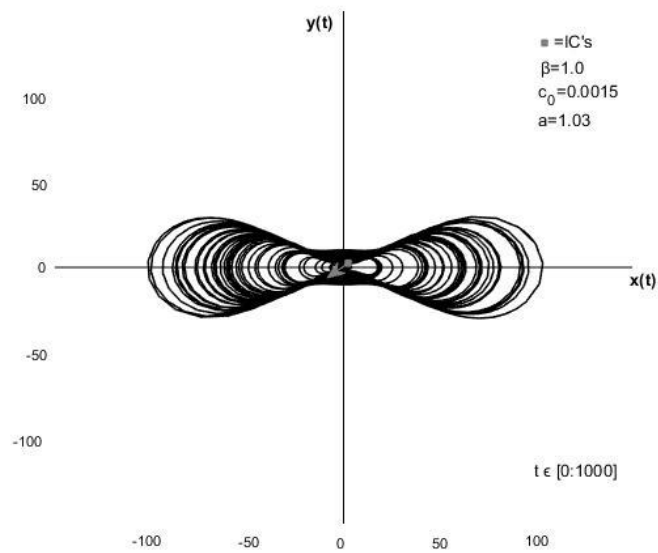


Figure C.74: Phase plane diagram for the base-case system with  $m=2,0$ , making  $\beta=1,0$ , with  $c_0=0,0015$  and  $a=1,03$ .

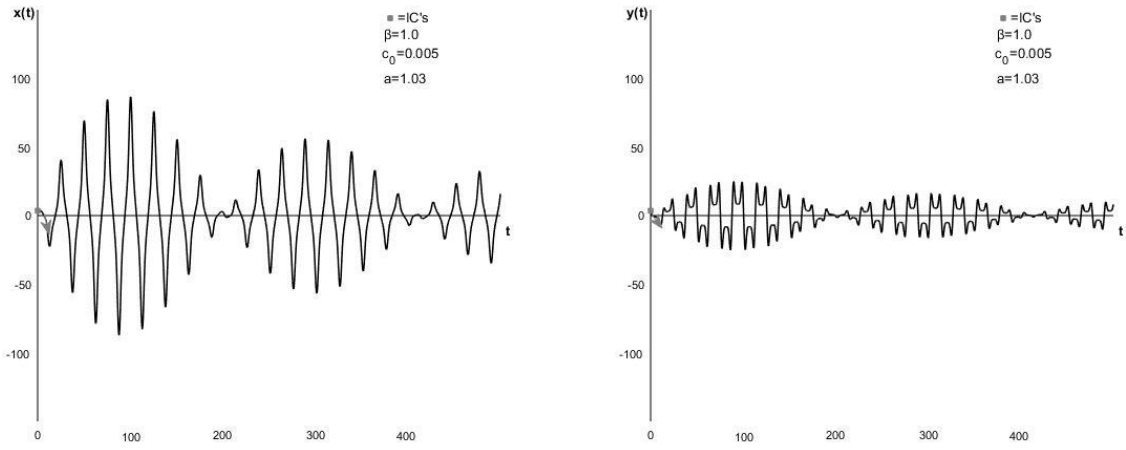


Figure C.75: Position curve(left) and velocity curve(right) for the base-case system with  $m=2,0$ , making  $\beta=1,0$ , with  $c_0=0,005$  and  $a=1,03$ .

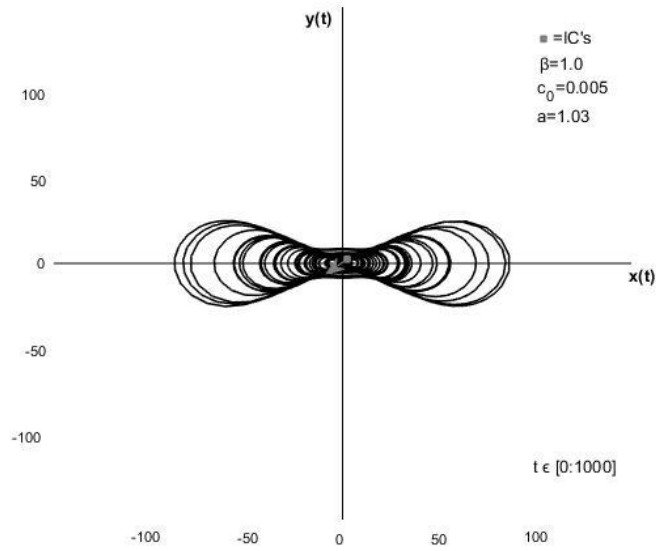


Figure C.76: Phase plane diagram for the base-case system with  $m=2,0$ , making  $\beta=1,0$ , with  $c_0=0,005$  and  $a=1,03$ .

C.4.5  $a=1,04$

Figures C.77 and C.78 show the position curve, velocity curve and phase plane diagram respectively for the system with  $a=1,04$  and  $c_0=0,005$ . Figures C.79 and C.80 show the same for the system with  $a=1,04$  and  $c_0=0,005$ .

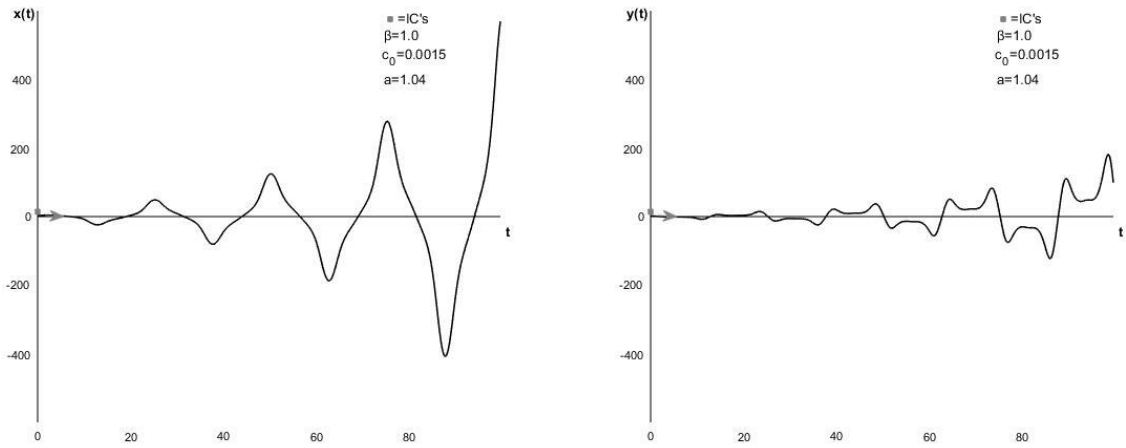


Figure C.77: Position curve(left) and velocity curve(right) for the base-case system with  $m=2,0$ , making  $\beta=1,0$ , with  $c_0=0,0015$  and  $a=1,04$ .

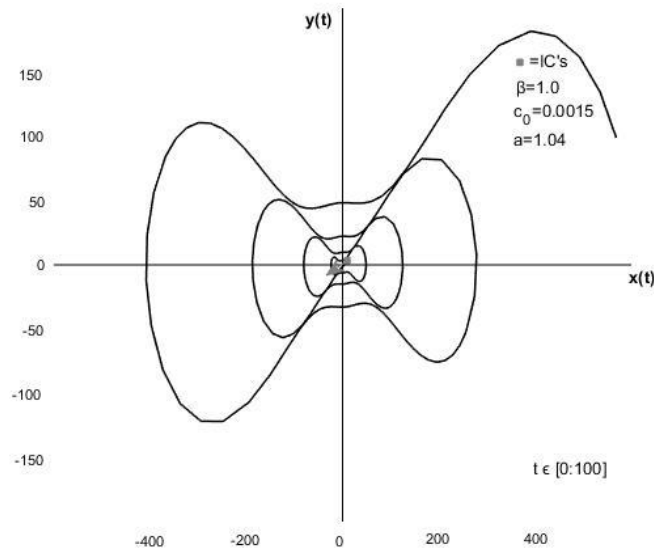


Figure C.78: Phase plane diagram for the base-case system with  $m=2,0$ , making  $\beta=1,0$ , with  $c_0=0,0015$  and  $a=1,04$ .

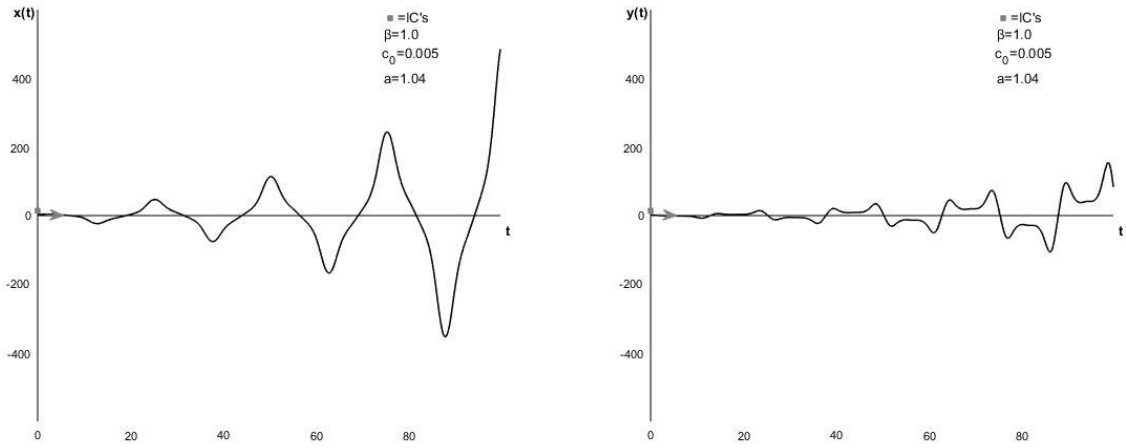


Figure C.79: Position curve(left) and velocity curve(right) for the base-case system with  $m=2,0$ , making  $\beta=1,0$ , with  $c_0=0,005$  and  $a=1,04$ .

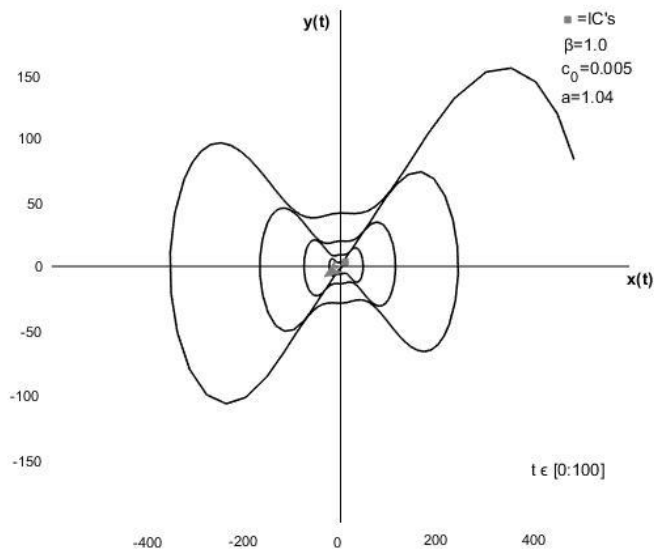


Figure C.80: Phase plane diagram for the base-case system with  $m=2,0$ , making  $\beta=1,0$ , with  $c_0=0,005$  and  $a=1,04$ .

C.5  $\beta = \frac{3}{2}$

When the mass parameter,  $m=4,5$ , the system has a frequency,  $\omega$ , is 50% bigger than the natural frequency,  $\omega_0$ , i.e.  $\beta = \frac{3}{2}$ .

C.5.1  $a=0$

When  $a=0$ , the system is only subjected to linear, constant damping,  $c_0$ . Figure C.81 shows the position and velocity curve for the system with  $c_0=0,0015$ . Figure C.82 shows the system with  $c_0=0,0015$  in the phase plane. Figures C.83 and C.84 show the position and velocity curve and phase plane diagram respectively for the system with  $c_0=0,005$ .

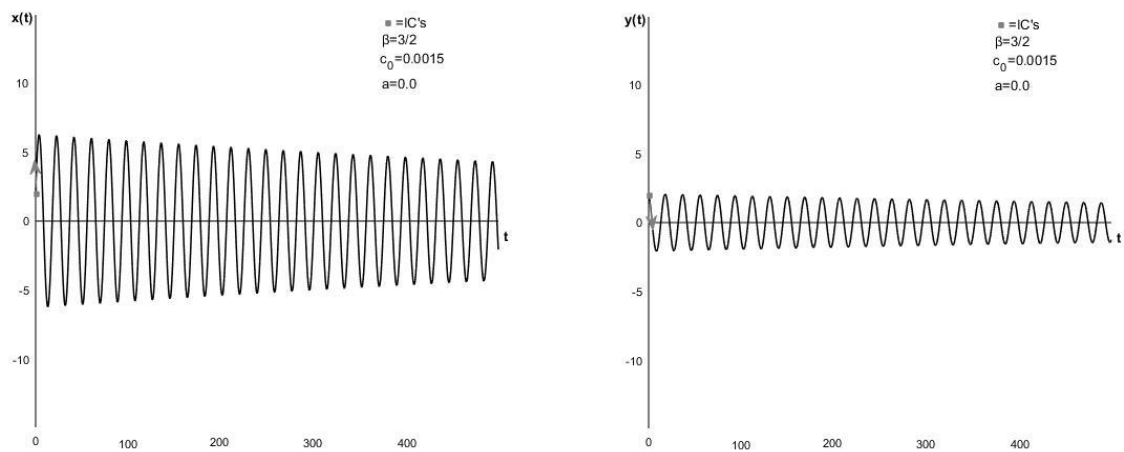


Figure C.81: Position curve(left) and velocity curve(right) for the base-case system with  $m=4,5$ , making  $\beta=3/2$ , with  $c_0=0,0015$  and  $a=0$ .

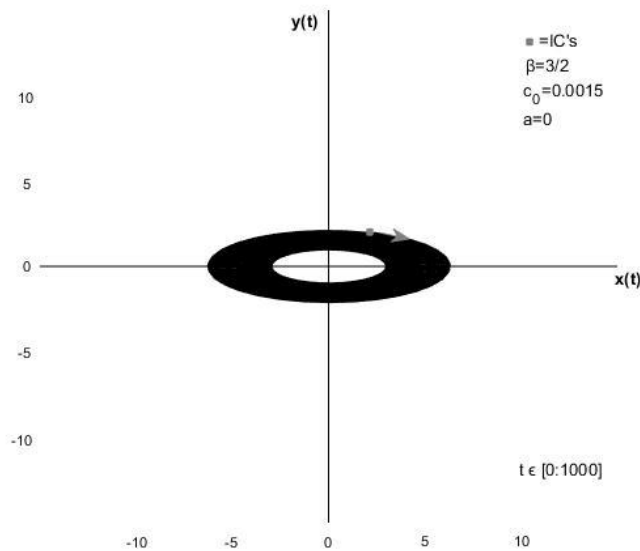


Figure C.82: Phase plane diagram for the base-case system with  $m=4,5$ , making  $\beta=3/2$ , with  $c_0=0,0015$  and  $a=0$ .

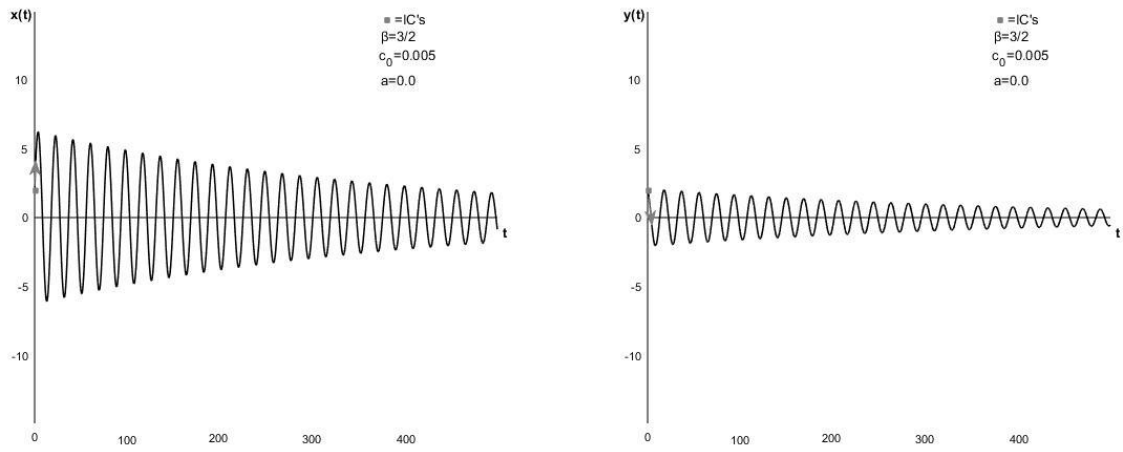


Figure C.83: Position curve(left) and velocity curve(right) for the base-case system with  $m=4,5$ , making  $\beta=3/2$ , with  $c_0=0,005$  and  $a=0$ .

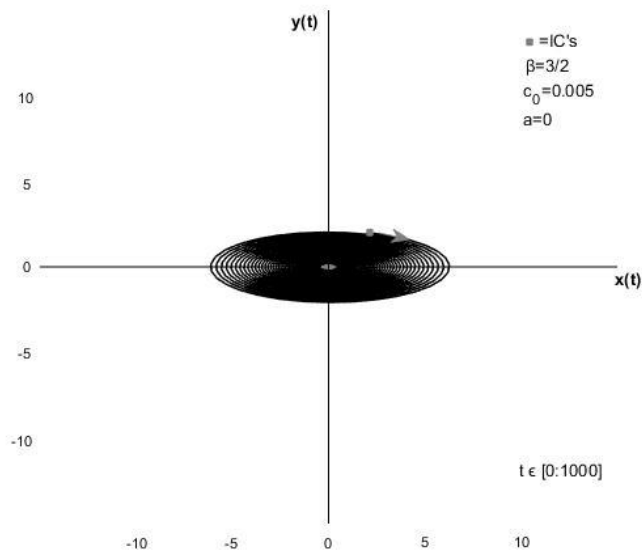


Figure C.84: Phase plane diagram for the base-case system with  $m=4,5$ , making  $\beta=3/2$ , with  $c_0=0,005$  and  $a=0$ .



### C.5.2 $a=0,1$

Figures C.85 and C.86 show the position curve, velocity curve and phase plane diagram respectively for the system with  $a=0,1$  and  $c_0=0,0015$ . Figures C.87 and C.88 show the same for the system with  $a=0,1$  and  $c_0=0,0015$ .

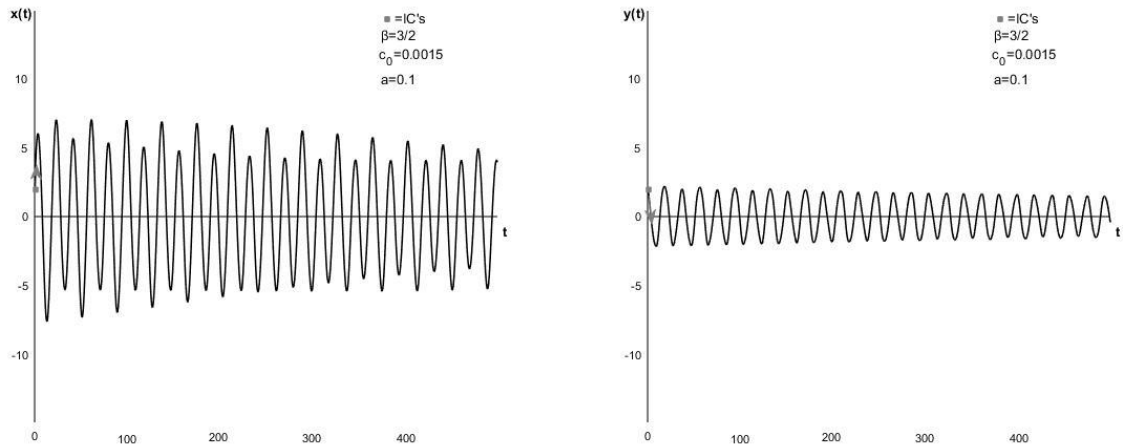


Figure C.85: Position curve(left) and velocity curve(right) for the base-case system with  $m=4,5$ , making  $\beta=3/2$ , with  $c_0=0,0015$  and  $a=0,1$ .

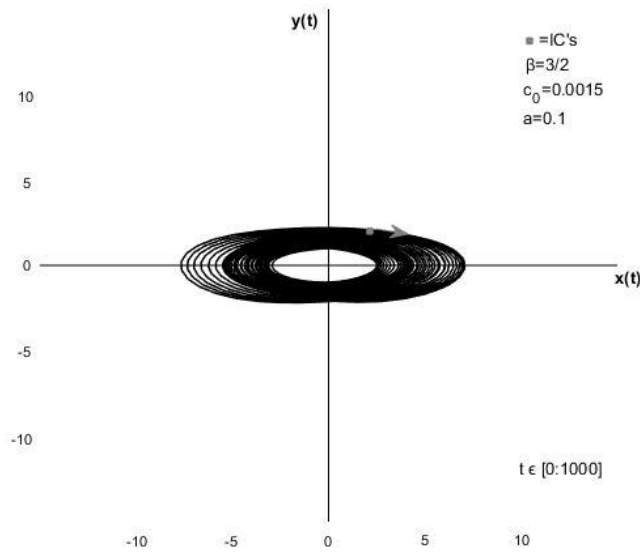


Figure C.86: Phase plane diagram for the base-case system with  $m=4,5$ , making  $\beta=3/2$ , with  $c_0=0,0015$  and  $a=0,1$ .

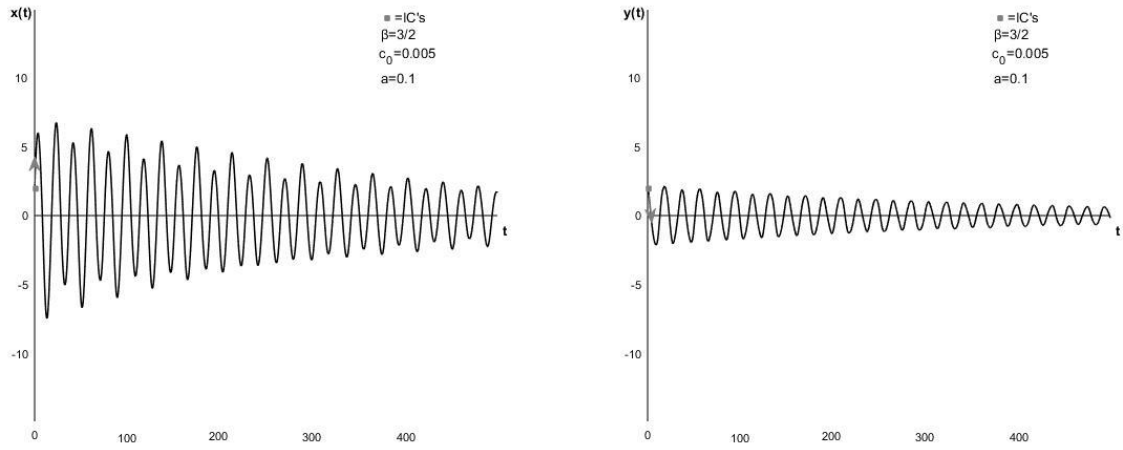


Figure C.87: Position curve(left) and velocity curve(right) for the base-case system with  $m=4,5$ , making  $\beta=3/2$ , with  $c_0=0,005$  and  $a=0,1$ .

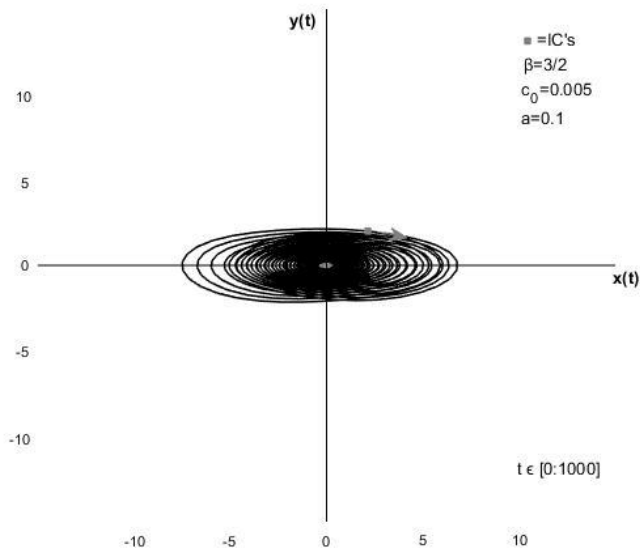


Figure C.88: Phase plane diagram for the base-case system with  $m=4,5$ , making  $\beta=3/2$ , with  $c_0=0,005$  and  $a=0,1$ .

### C.5.3 $a=0,2$

Figures C.89 and C.90 show the position curve, velocity curve and phase plane diagram respectively for the system with  $a=0,2$  and  $c_0=0,005$ . Figures C.91 and C.92 show the same for the system with  $a=0,2$  and  $c_0=0,005$ .

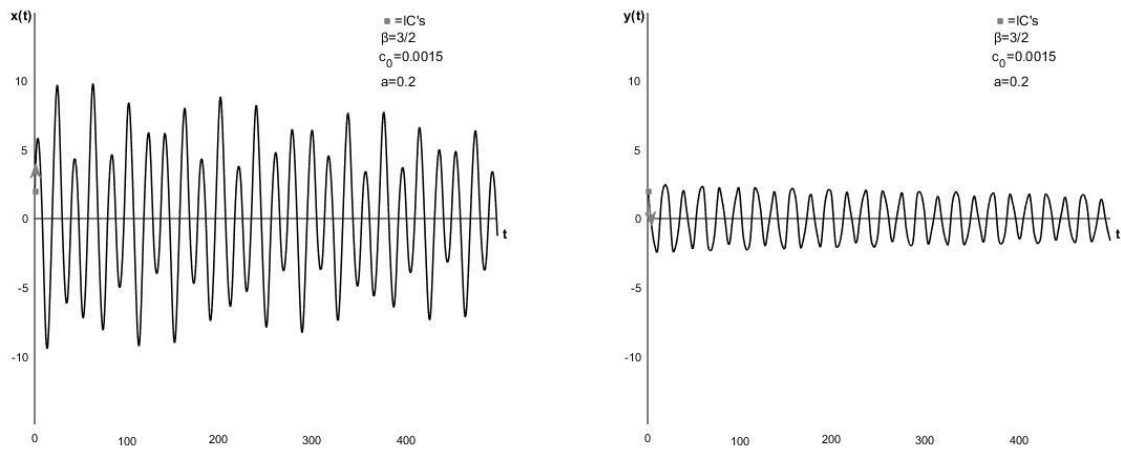


Figure C.89: Position curve(left) and velocity curve(right) for the base-case system with  $m=4,5$ , making  $\beta=3/2$ , with  $c_0=0,0015$  and  $a=0,2$ .

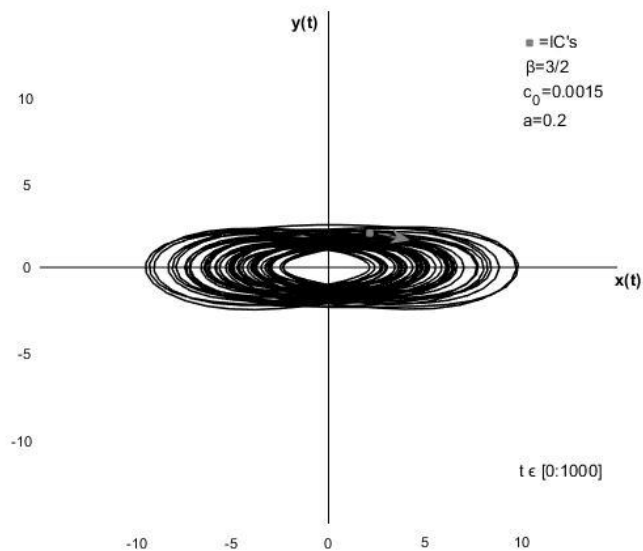


Figure C.90: Phase plane diagram for the base-case system with  $m=4,5$ , making  $\beta=3/2$ , with  $c_0=0,0015$  and  $a=0,2$ .

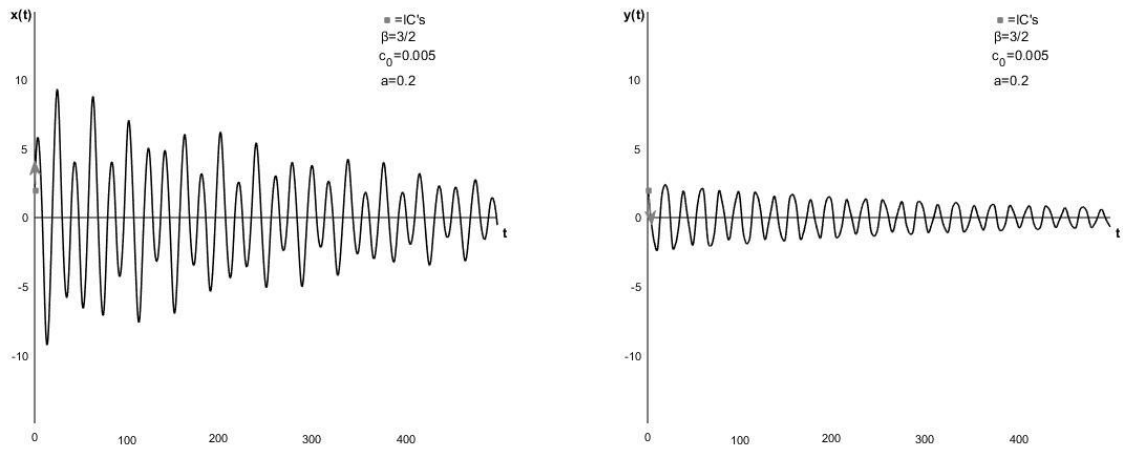


Figure C.91: Position curve(left) and velocity curve(right) for the base-case system with  $m=4,5$ , making  $\beta=3/2$ , with  $c_0=0,005$  and  $a=0,2$ .

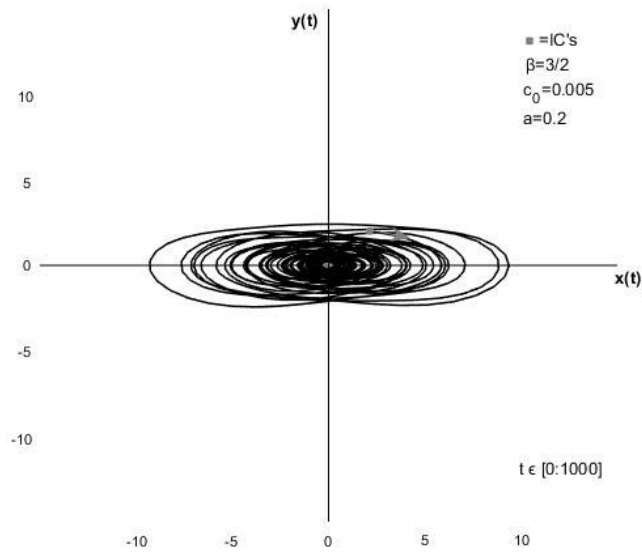


Figure C.92: Phase plane diagram for the base-case system with  $m=4,5$ , making  $\beta=3/2$ , with  $c_0=0,005$  and  $a=0,2$ .

### C.5.4 $a=0,36$

Figures C.93 and C.94 show the position curve, velocity curve and phase plane diagram respectively for the system with  $a=0,36$  and  $c_0=0,005$ . Figures C.95 and C.96 show the same for the system with  $a=0,36$  and  $c_0=0,005$ .

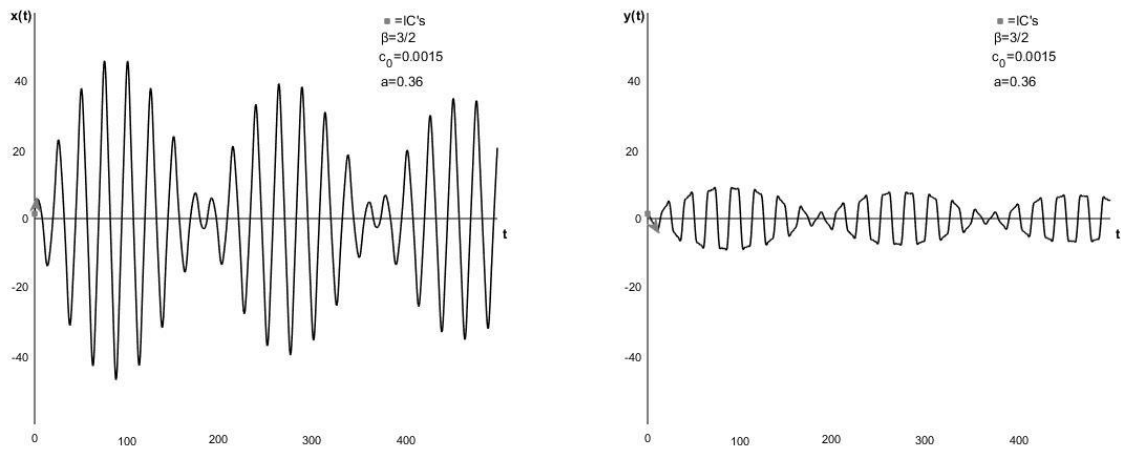


Figure C.93: Position curve(left) and velocity curve(right) for the base-case system with  $m=4,5$ , making  $\beta=3/2$ , with  $c_0=0,0015$  and  $a=0,36$ .

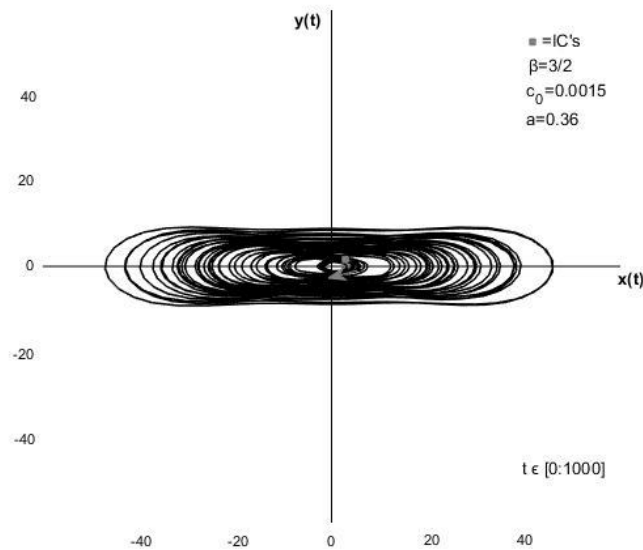


Figure C.94: Phase plane diagram for the base-case system with  $m=4,5$ , making  $\beta=3/2$ , with  $c_0=0,0015$  and  $a=0,36$ .

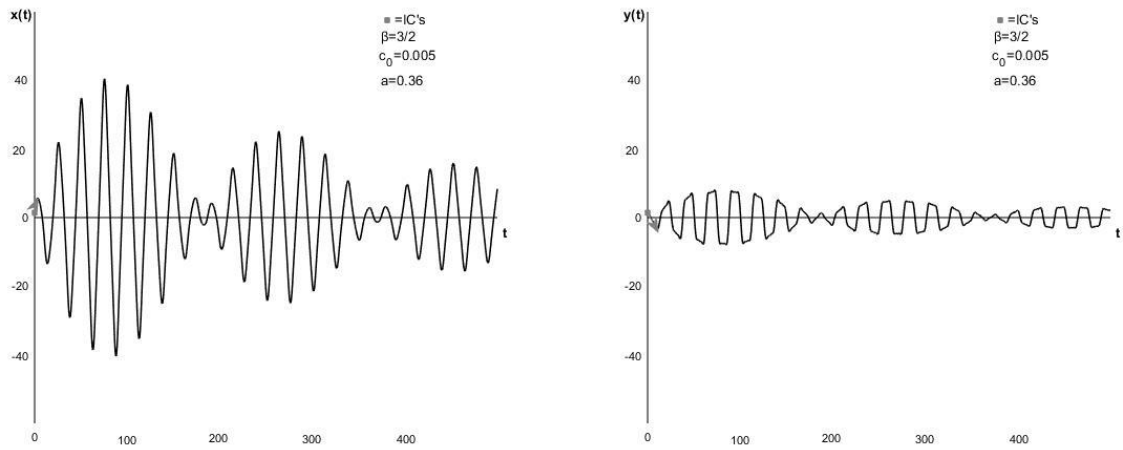


Figure C.95: Position curve(left) and velocity curve(right) for the base-case system with  $m=4,5$ , making  $\beta=3/2$ , with  $c_0=0,005$  and  $a=0,36$ .

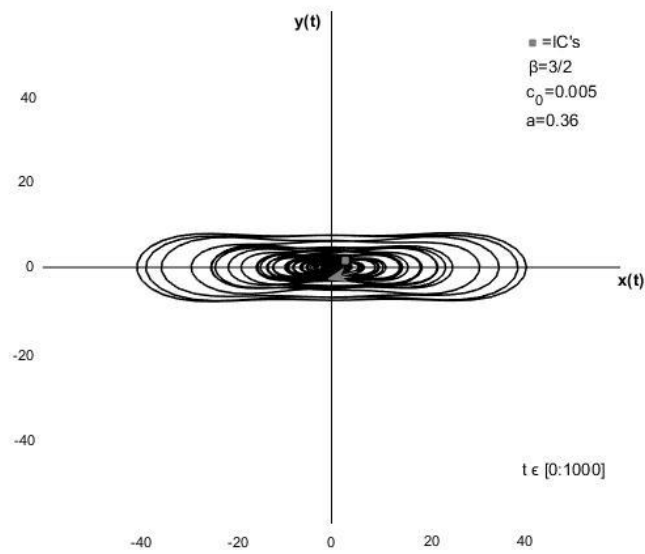


Figure C.96: Phase plane diagram for the base-case system with  $m=4,5$ , making  $\beta=3/2$ , with  $c_0=0,005$  and  $a=0,36$ .

C.5.5  $a=0,37$

Figures C.97 and C.98 show the position curve, velocity curve and phase plane diagram respectively for the system with  $a=0,37$  and  $c_0=0,005$ . Figures C.99 and C.100 show the same for the system with  $a=0,37$  and  $c_0=0,005$ .

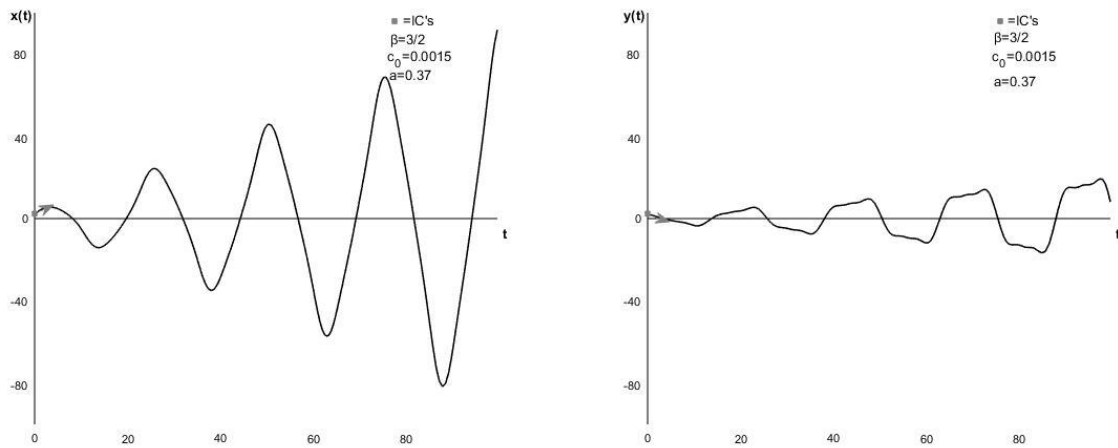


Figure C.97: Position curve(left) and velocity curve(right) for the base-case system with  $m=4,5$ , making  $\beta=3/2$ , with  $c_0=0,0015$  and  $a=0,37$ .

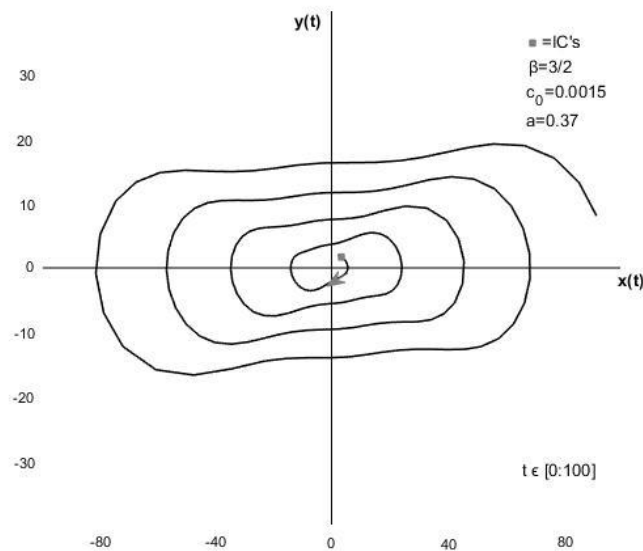


Figure C.98: Phase plane diagram for the base-case system with  $m=4,5$ , making  $\beta=3/2$ , with  $c_0=0,0015$  and  $a=0,37$ .

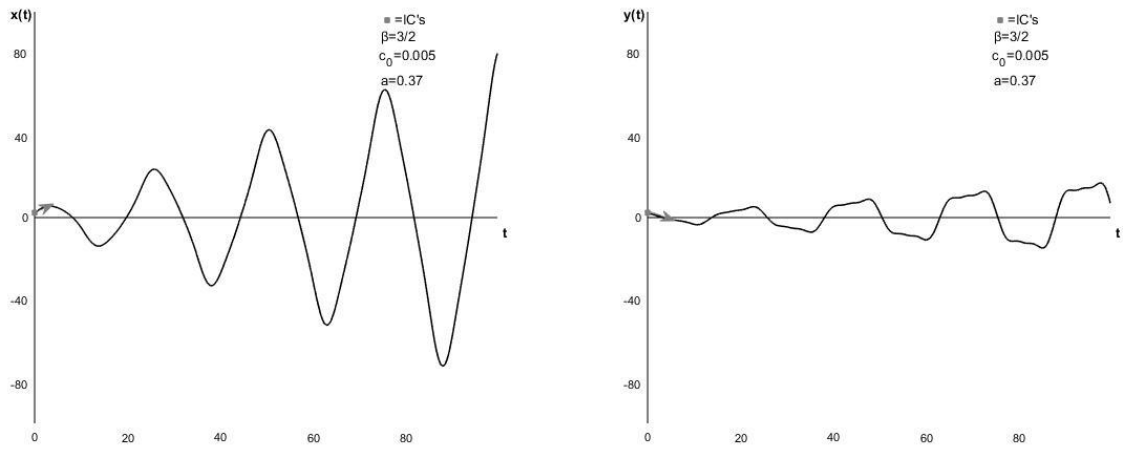


Figure C.99: Position curve(left) and velocity curve(right) for the base-case system with  $m=4,5$ , making  $\beta=3/2$ , with  $c_0=0,005$  and  $a=0,37$ .

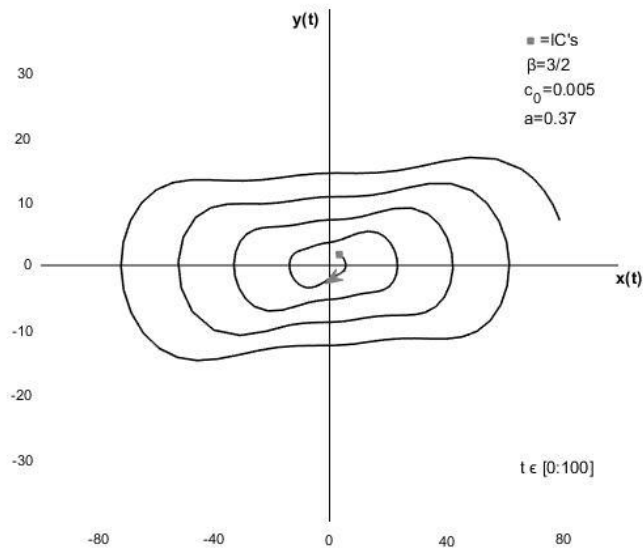


Figure C.100: Phase plane diagram for the base-case system with  $m=4,5$ , making  $\beta=3/2$ , with  $c_0=0,005$  and  $a=0,37$ .



## C.6 $\beta = 2,0$

When the mass parameter,  $m=8,0$ , the system has a frequency,  $\omega$ , is twice the natural frequency,  $\omega_0$ , i.e.  $\beta = 2,0$ . The system is presented for two values of linear, constant damping,  $c_0=0,0015$  and  $c_0=0,005$ , with an increasing nonlinear coefficient,  $a$ .

### C.6.1 $a=0$

When  $a=0$ , the system is only subjected to linear, constant damping,  $c_0$ . Figure C.101 shows the position and velocity curve for the system with  $c_0=0,0015$ . Figure C.102 shows the system with  $c_0=0,0015$  in the phase plane. Figures C.103 and C.104 show the position and velocity curve and phase plane diagram respectively for the system with  $c_0=0,005$ .

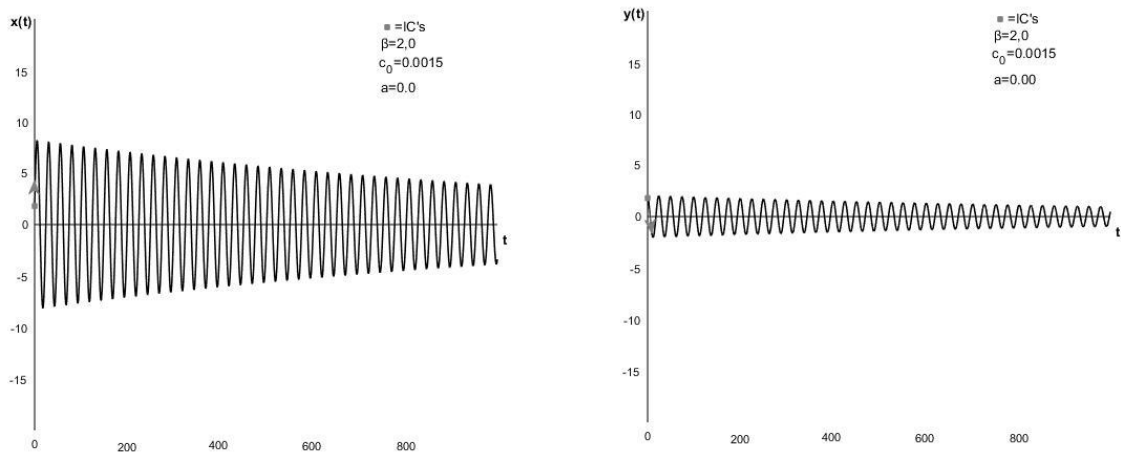


Figure C.101: Position curve(left) and velocity curve(right) for the base-case system with  $m=8,0$ , making  $\beta=2,0$ , with  $c_0=0,0015$  and  $a=0$ .

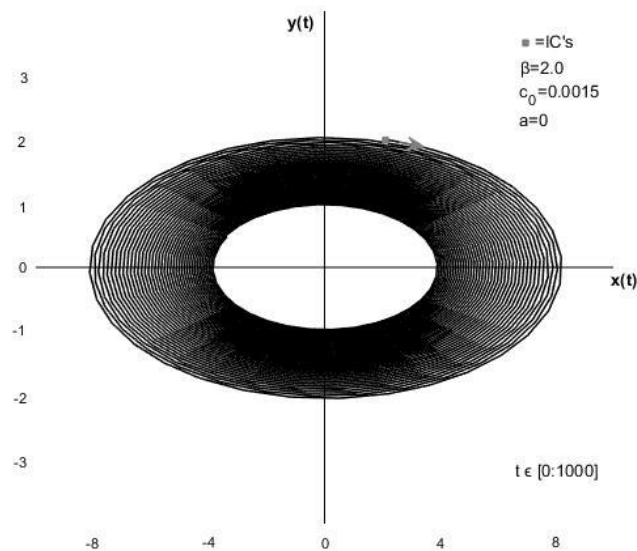


Figure C.102: Phase plane diagram for the base-case system with  $m=8,0$ , making  $\beta=2,0$ , with  $c_0=0,0015$  and  $a=0$ .

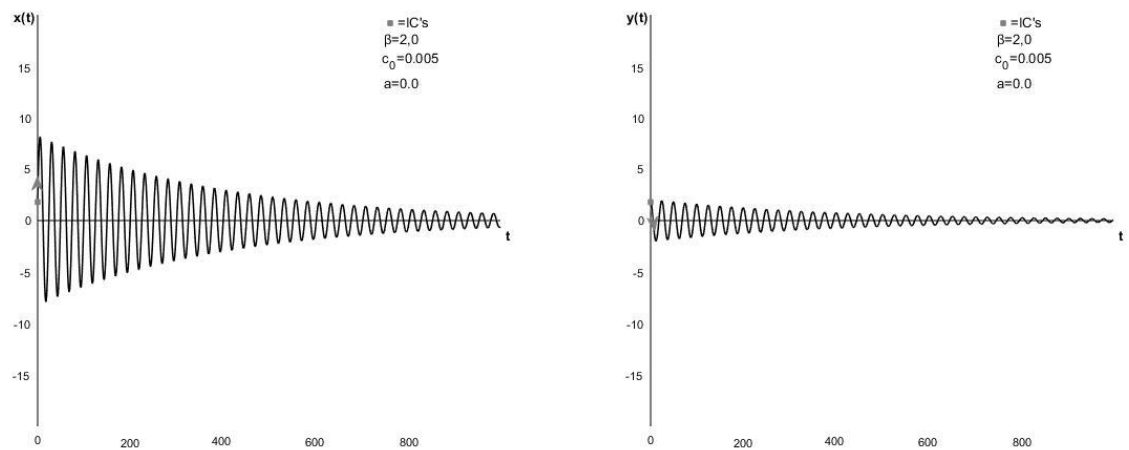


Figure C.103: Position curve(left) and velocity curve(right) for the base-case system with  $m=8,0$ , making  $\beta=2,0$ , with  $c_0=0,005$  and  $a=0$ .

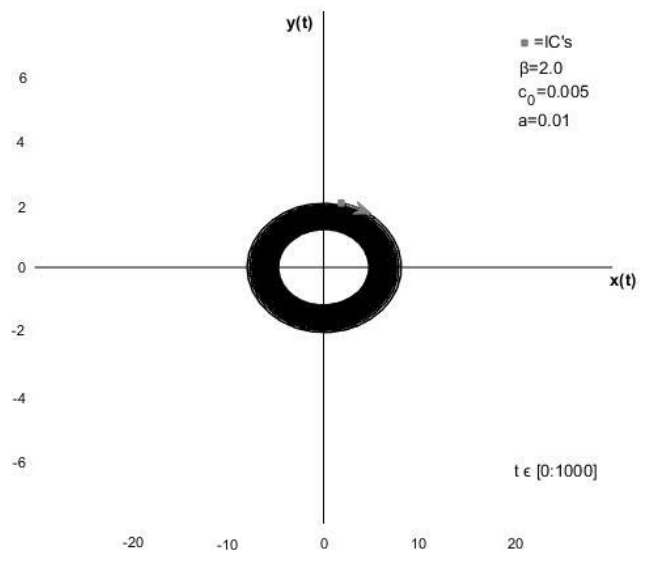


Figure C.104: Phase plane diagram for the base-case system with  $m=8,0$ , making  $\beta=2,0$ , with  $c_0=0,005$  and  $a=0$ .

### C.6.2 $a=0,01$

Figures C.105 and C.106 show the position curve, velocity curve and phase plane diagram respectively for the system with  $a=0,01$  and  $c_0=0,0015$ . Figures C.107 and C.108 show the same for the system with  $a=0,01$  and  $c_0=0,0015$ . When the base-case system is at double resonance, the system is very sensitive to the nonlinear damping. At  $a=0,01$ , the system with  $c_0=0,0015$  is overtaken by the negative damping, while the system with  $c_0=0,005$  still decreases its amplitudes.

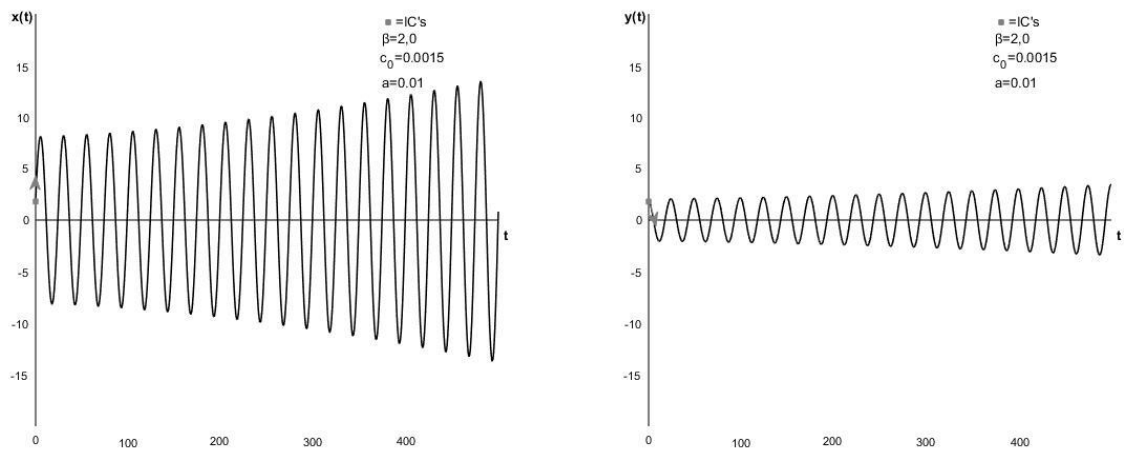


Figure C.105: Position curve(left) and velocity curve(right) for the base-case system with  $m=8,0$ , making  $\beta=2,0$ , with  $c_0=0,0015$  and  $a=0,01$ .

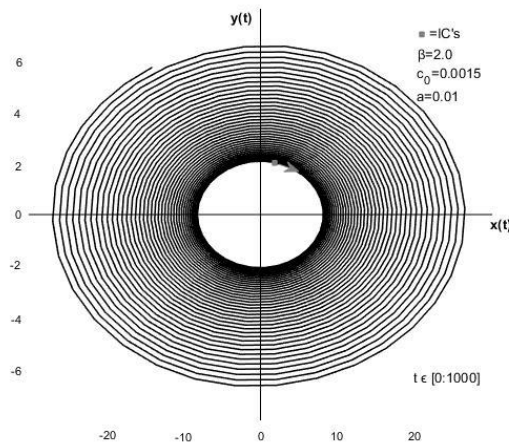


Figure C.106: Phase plane diagram for the base-case system with  $m=8,0$ , making  $\beta=2,0$ , with  $c_0=0,0015$  and  $a=0,01$ .

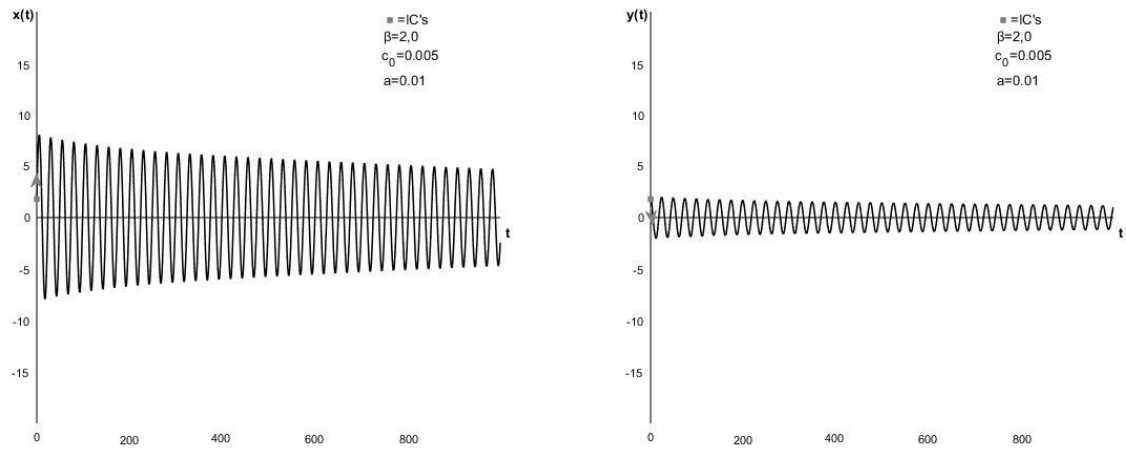


Figure C.107: Position curve(left) and velocity curve(right) for the base-case system with  $m=8,0$ , making  $\beta=2,0$ , with  $c_0=0,005$  and  $a=0,01$ .

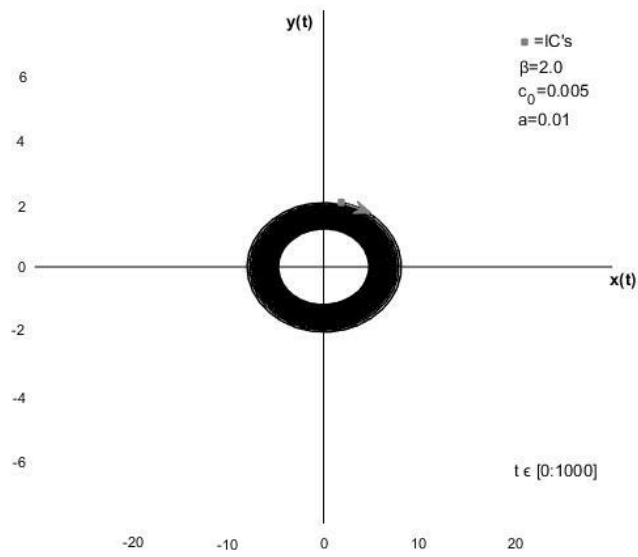


Figure C.108: Phase plane diagram for the base-case system with  $m=8,0$ , making  $\beta=2,0$ , with  $c_0=0,005$  and  $a=0,01$ .

### C.6.3 $a=0,02$

Figures C.109 and C.110 show the position curve, velocity curve and phase plane diagram respectively for the system with  $a=0,02$  and  $c_0=0,005$ . Figures C.111 and C.112 show the same for the system with  $a=0,02$  and  $c_0=0,005$ . At  $a=0,02$ , both systems experience a continued increase in amplitudes.

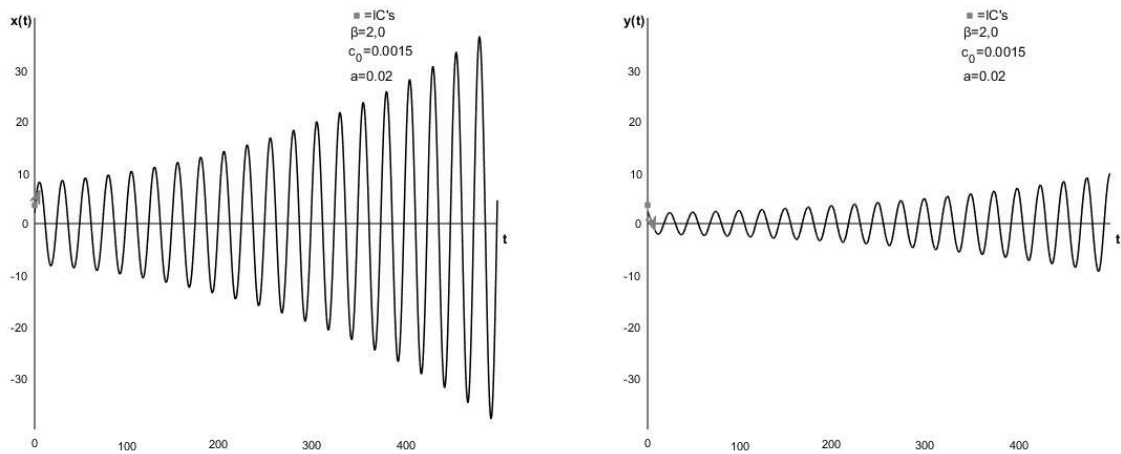


Figure C.109: Position curve(left) and velocity curve(right) for the base-case system with  $m=8,0$ , making  $\beta=2,0$ , with  $c_0=0,0015$  and  $a=0,02$ .

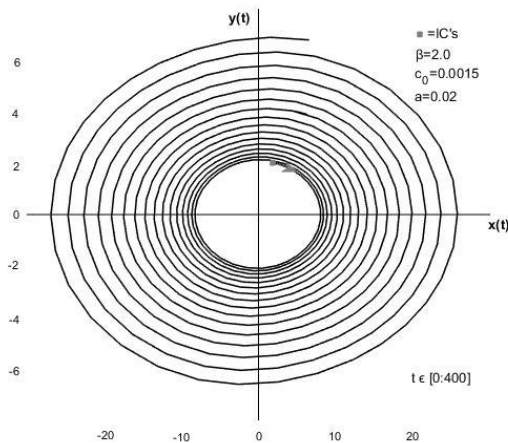


Figure C.110: Phase plane diagram for the base-case system with  $m=8,0$ , making  $\beta=2,0$ , with  $c_0=0,0015$  and  $a=0,02$ .

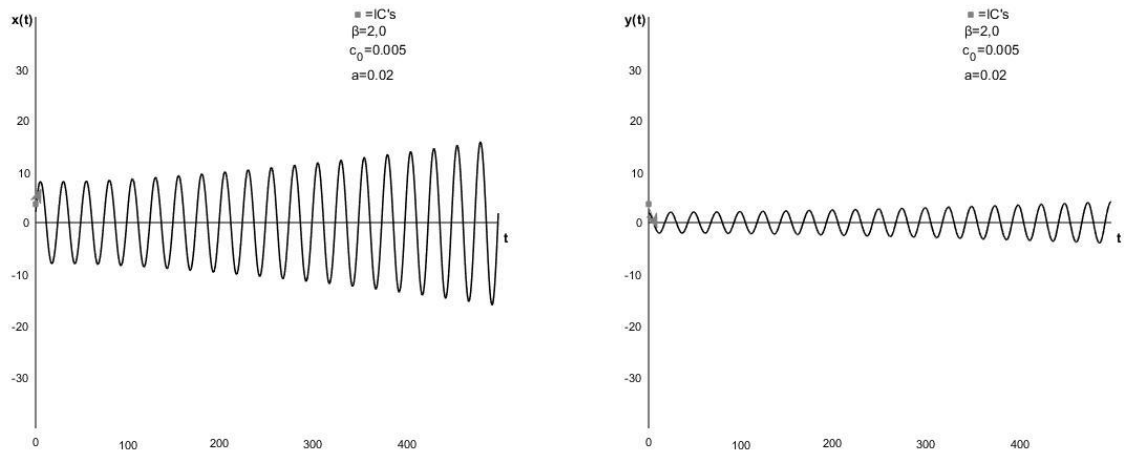


Figure C.111: Position curve(left) and velocity curve(right) for the base-case system with  $m=8,0$ , making  $\beta=2,0$ , with  $c_0=0,005$  and  $a=0,02$ .

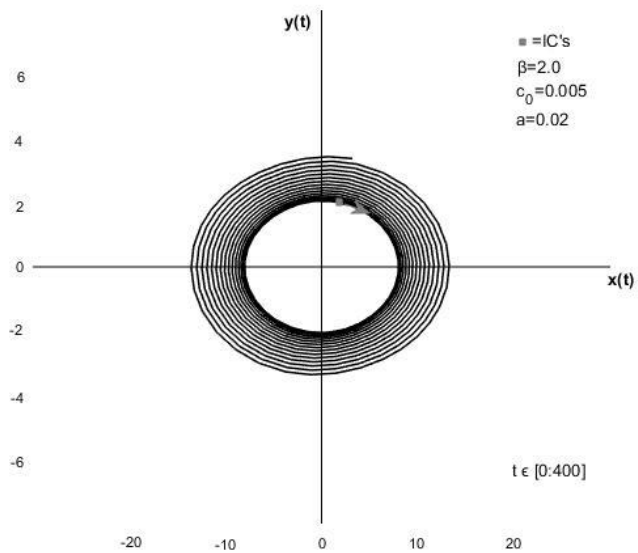


Figure C.112: Phase plane diagram for the base-case system with  $m=8,0$ , making  $\beta=2,0$ , with  $c_0=0,005$  and  $a=0,02$ .

# Appendix D – Diagrams for chapter 8

## D.1 Base-case system

### D.1.1 $a=0$

When  $a=0$ , the system only has linear, constant damping from the coefficient  $c_0$ .

#### D.1.1.1 $c_0=0,0015$

Figures D.1 and D.2 show the base-case system with the linear damping coefficient,  $c_0=0,0015$ . Figure D.1 shows the position curve to the left and the velocity curve to the right, while figure D.2 shows the phase plane diagram.

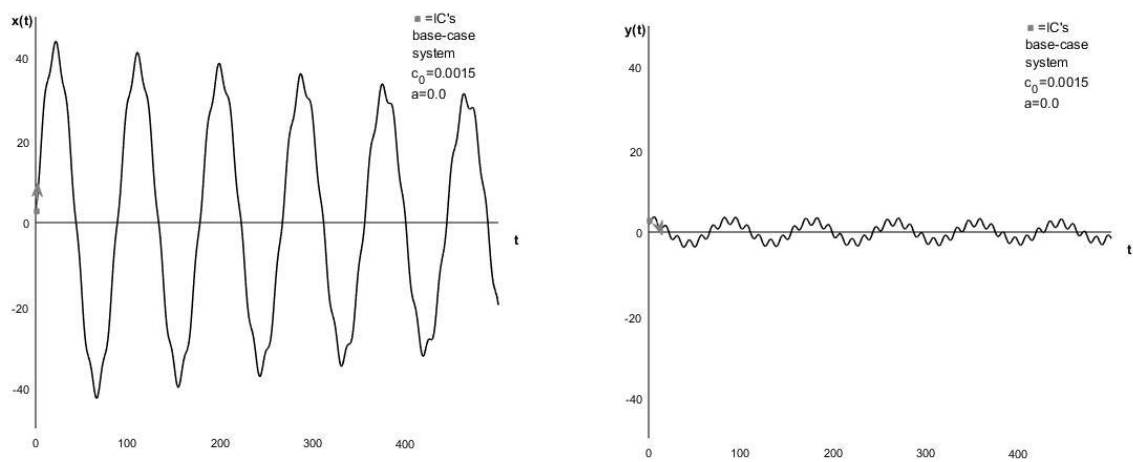


Figure D.1: Position curve(left) and velocity curve(right) for the base-case system with  $a=0$  and  $c_0=0,0015$ .

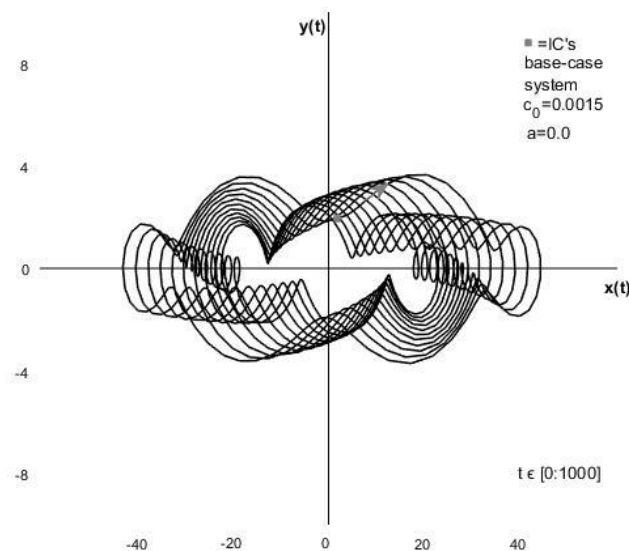


Figure D.2: Phase plane diagram for the base-case system with  $a=0$  and  $c_0=0,0015$ .

D.1.1.2  $c_0=0,005$

Figures D.3 and D.4 show the base-case system with the linear damping coefficient,  $c_0=0,005$ . Figure D.3 shows the position curve to the left and the velocity curve to the right, while figure D.4 shows the phase plane diagram.

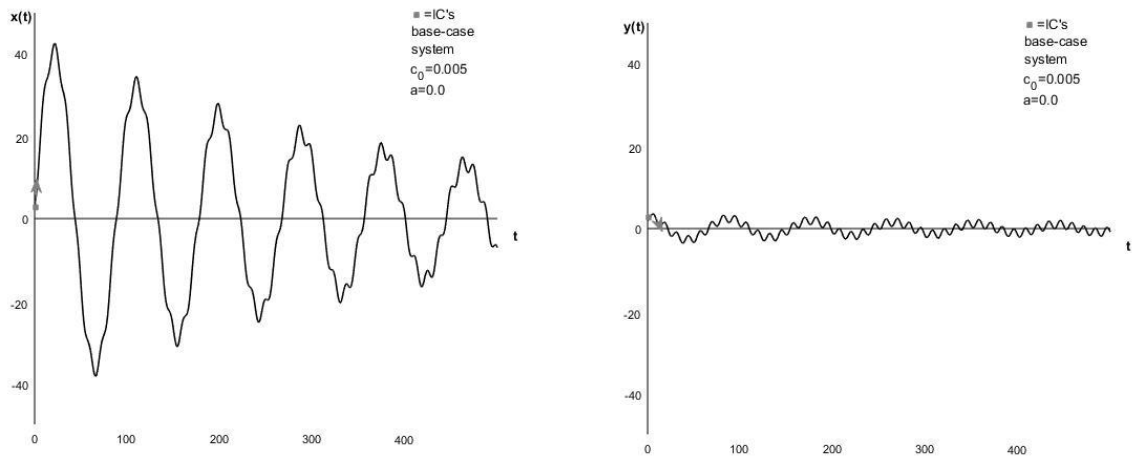


Figure D.3: Position curve(left) and velocity curve(right) for the base-case system with  $a=0$  and  $c_0=0,005$ .

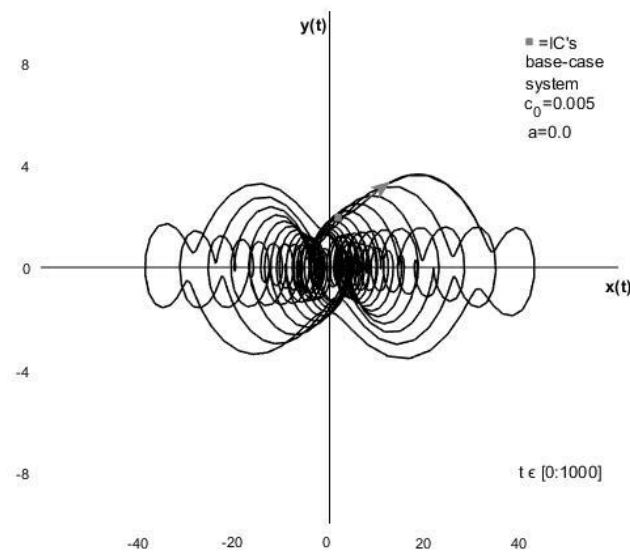


Figure D.4: Phase plane diagram for the base-case system with  $a=0$  and  $c_0=0,005$ .



### D.1.2 $a=0,5$

In this part, the system will be subjected to both a linear damping coefficient,  $c_0$ , as well as the nonlinear damping coefficient,  $a=0,5$ .

#### D.1.2.1 $c_0=0,0015$

Figures D.5 and D.6 show the base-case system with the linear damping coefficient,  $c_0=0,0015$ , and the nonlinear damping coefficient,  $a=0,5$ . Figure D.5 shows the position curve to the left and the velocity curve to the right, while figure D.6 shows the phase plane diagram.

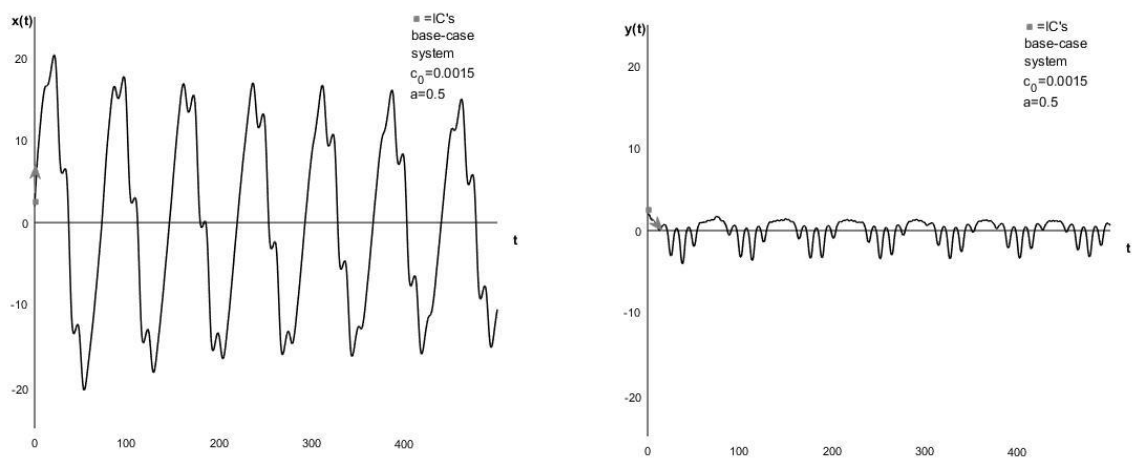


Figure D.5: Position curve(left) and velocity curve(right) for the base-case system with  $a=0,5$  and  $c_0=0,0015$ .

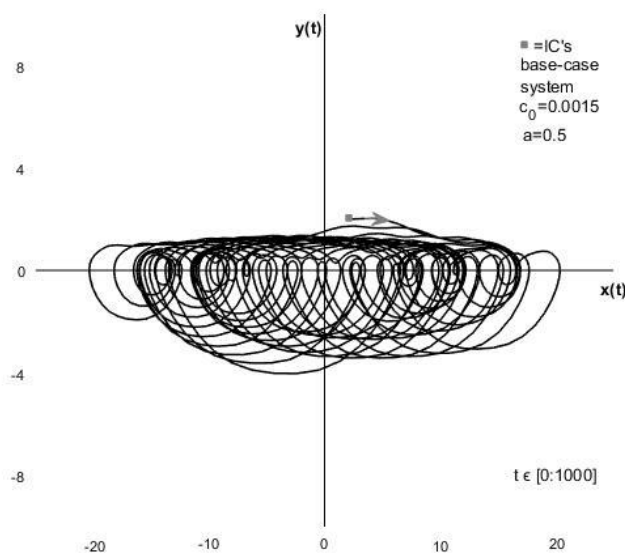


Figure D.6: Phase plane diagram for the base-case system with  $a=0,5$  and  $c_0=0,0015$ .

D.1.2.2  $c_0=0,005$

Figures D.7 and D.8 show the base-case system with the linear damping coefficient,  $c_0=0,005$ , and the nonlinear damping coefficient,  $a=0,5$ . Figure D.7 shows the position curve to the left and the velocity curve to the right, while figure D.8 shows the phase plane diagram.

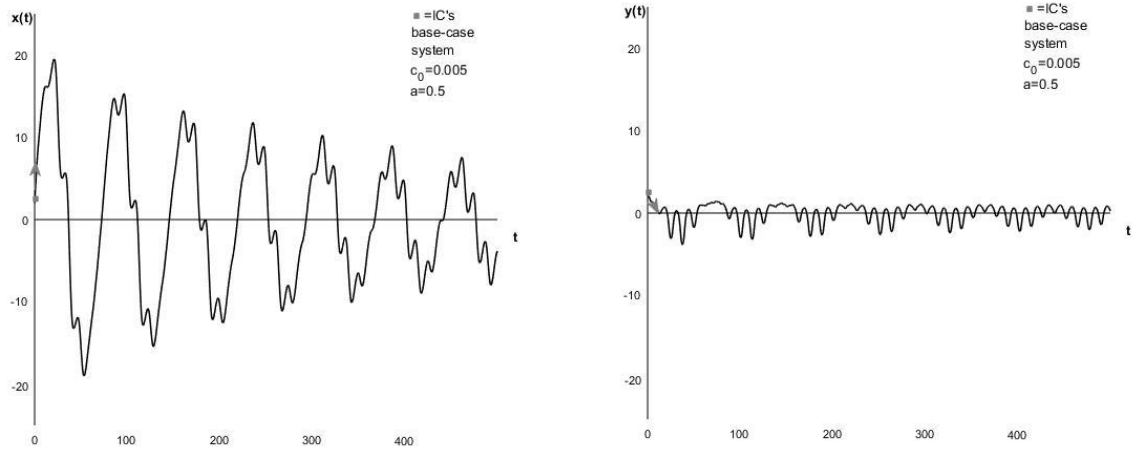


Figure D.7: Position curve(left) and velocity curve(right) for the base-case system with  $a=0,5$  and  $c_0=0,005$ .

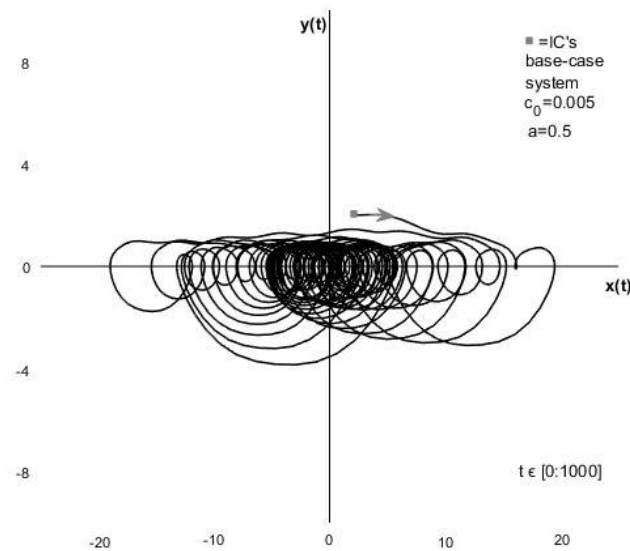


Figure D.8: Phase plane diagram for the base-case system with  $a=0,5$  and  $c_0=0,005$ .

### D.1.3 $a=1,0$

In this part, the nonlinear damping coefficient is increased to  $a=1,0$ .

#### D.1.3.1 $c_0=0,0015$

Figures D.9 and D.19 show the base-case system with the linear damping coefficient,  $c_0=0,0015$ , and the nonlinear damping coefficient,  $a=1,0$ . Figure D.9 shows the position curve to the left and the velocity curve to the right, while figure D.10 shows the phase plane diagram.

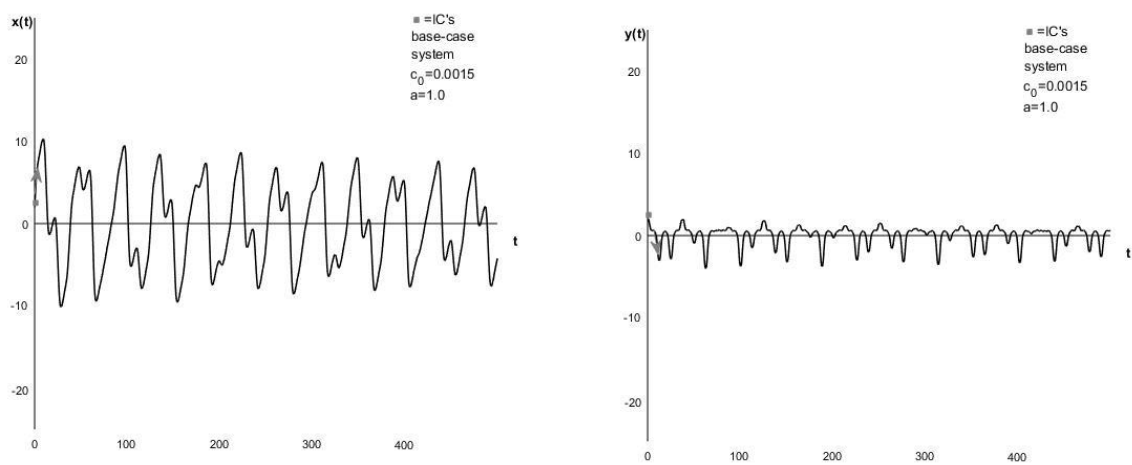


Figure D.9: Position curve(left) and velocity curve(right) for the base-case system with  $a=1,0$  and  $c_0=0,0015$ .

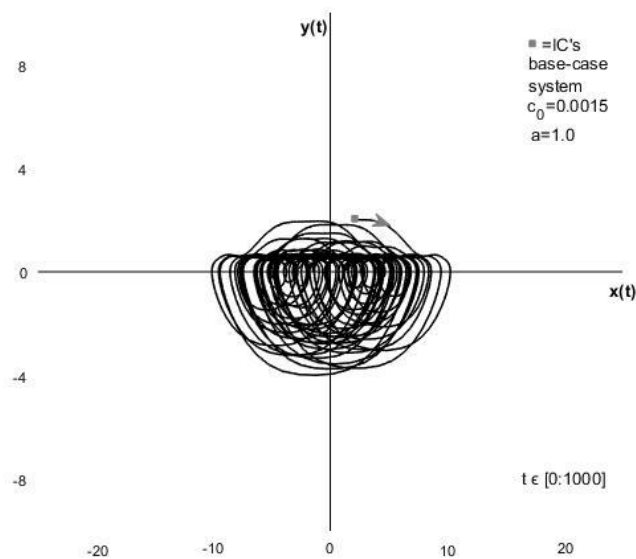


Figure D.10: Phase plane diagram for the base-case system with  $a=1,0$  and  $c_0=0,0015$ .

D.1.3.2  $c_0=0,005$

Figures D.11 and D.12 show the base-case system with the linear damping coefficient,  $c_0=0,005$ , and the nonlinear damping coefficient,  $a=1,0$ . Figure D.11 shows the position curve to the left and the velocity curve to the right, while figure D.12 shows the phase plane diagram.

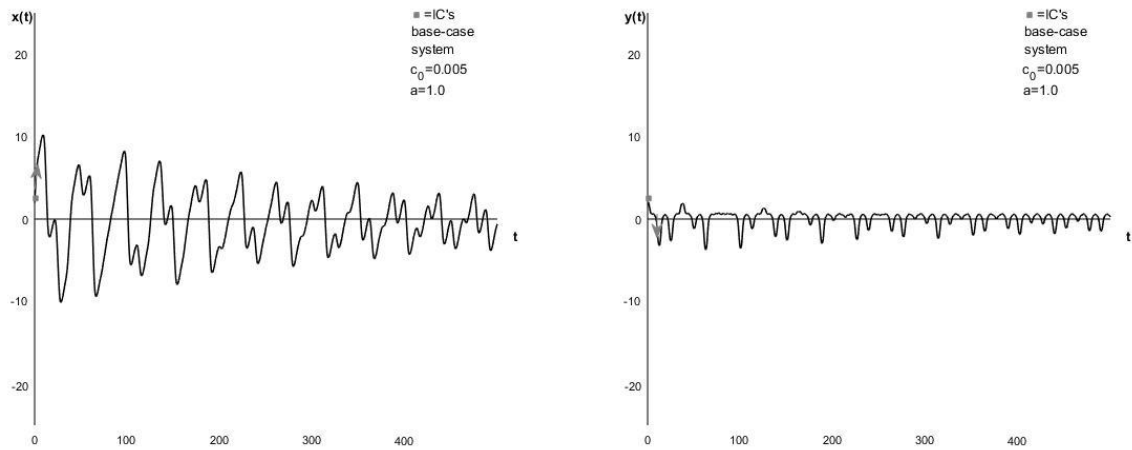


Figure D.11: Position curve(left) and velocity curve(right) for the base-case system with  $a=1,0$  and  $c_0=0,005$ .

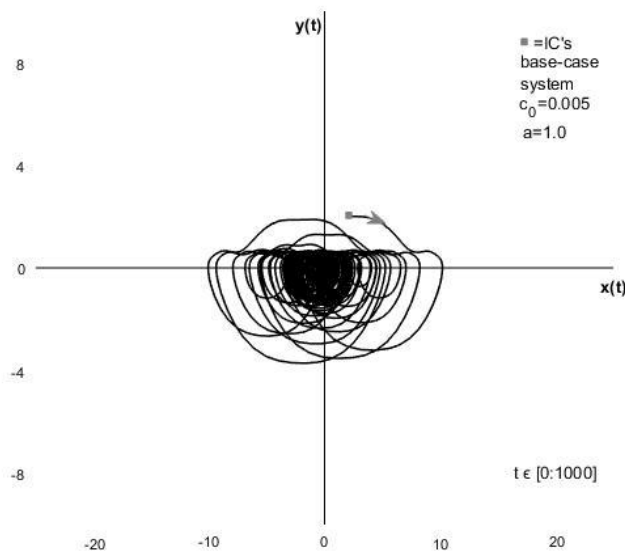


Figure D.12: Phase plane diagram for the base-case system with  $a=1,0$  and  $c_0=0,005$ .

## D.1.4 $a=1,19$

### D.1.4.1 $c_0=0,0015$

Figures D.13 and D.14 show the base-case system with the linear damping coefficient,  $c_0=0,0015$ , and the nonlinear damping coefficient,  $a=1,19$ . Figure D.13 shows the position curve to the left and the velocity curve to the right, while figure D.14 shows the phase plane diagram.

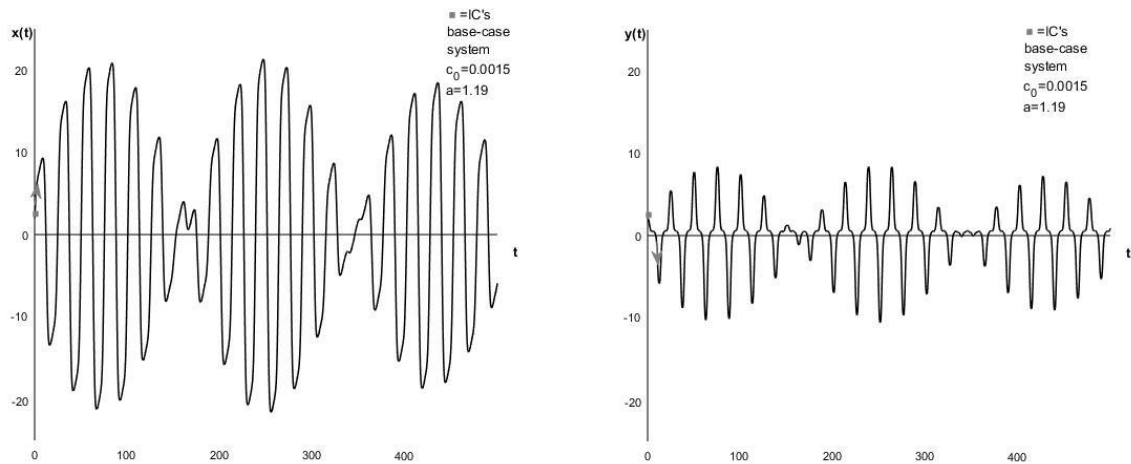


Figure D.13: Position curve(left) and velocity curve(right) for the base-case system with  $a=1,19$  and  $c_0=0,0015$ .

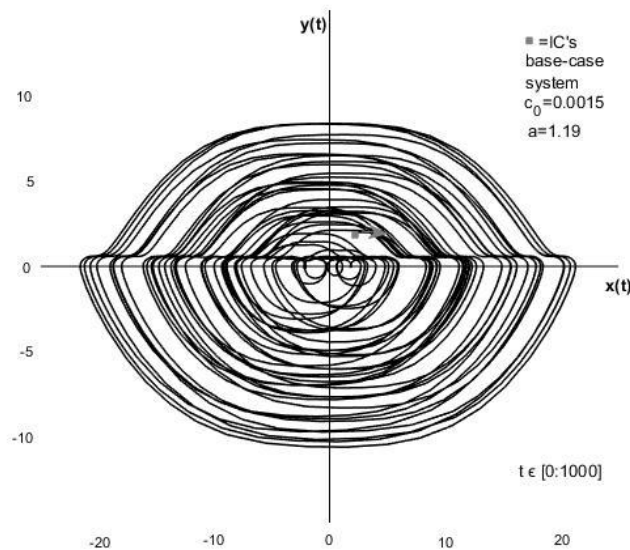


Figure D.14: Phase plane diagram for the base-case system with  $a=1,19$  and  $c_0=0,0015$ .

D.1.4.2  $c_0=0,005$

Figures D.15 and D.16 show the base-case system with the linear damping coefficient,  $c_0=0,005$ , and the nonlinear damping coefficient,  $a=1,19$ . Figure D.15 shows the position curve to the left and the velocity curve to the right, while figure D.16 shows the phase plane diagram.

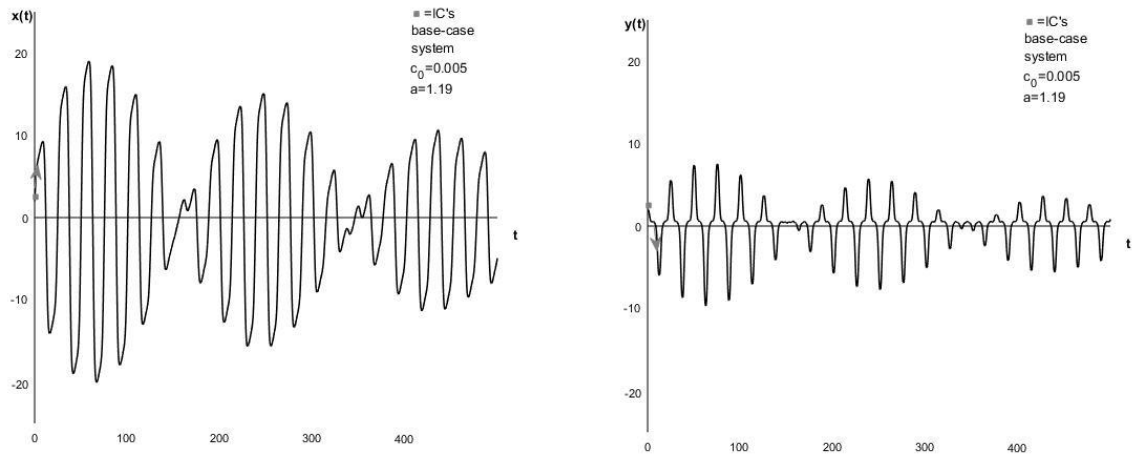


Figure D.15: Position curve(left) and velocity curve(right) for the base-case system with  $a=1,19$  and  $c_0=0,005$ .

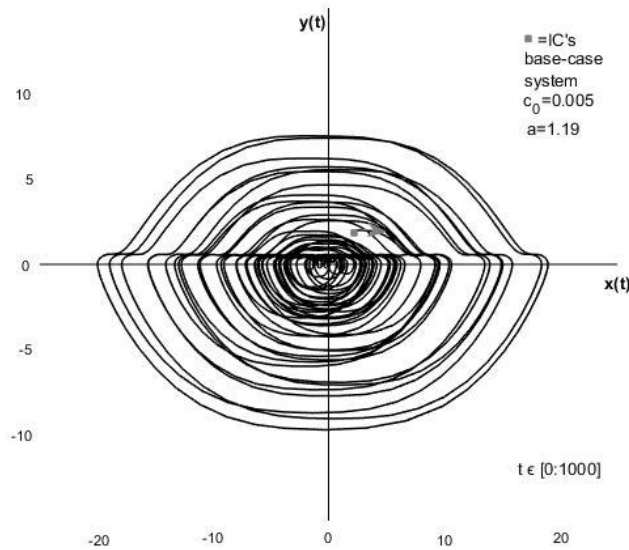


Figure D.16: Phase plane diagram for the base-case system with  $a=1,19$  and  $c_0=0,005$ .

## D.1.5 $a=1,2$

### D.1.5.1 $c_0=0,0015$

Figures D.17 and D.18 show the base-case system with the linear damping coefficient,  $c_0=0,0015$ , and the nonlinear damping coefficient,  $a=1,2$ . Figure D.17 shows the position curve to the left and the velocity curve to the right, while figure D.18 shows the phase plane diagram.

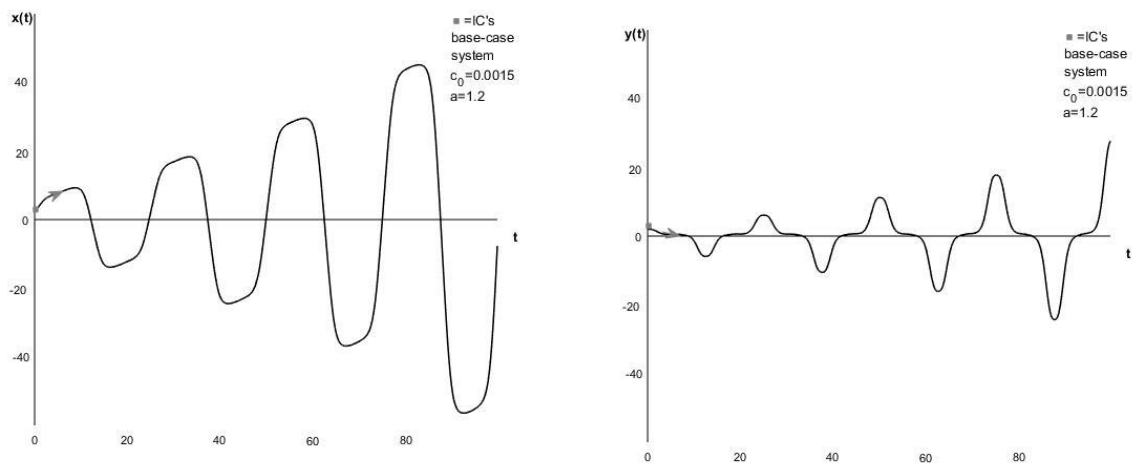


Figure D.17: Position curve(left) and velocity curve(right) for the base-case system with  $a=1,2$  and  $c_0=0,0015$ .

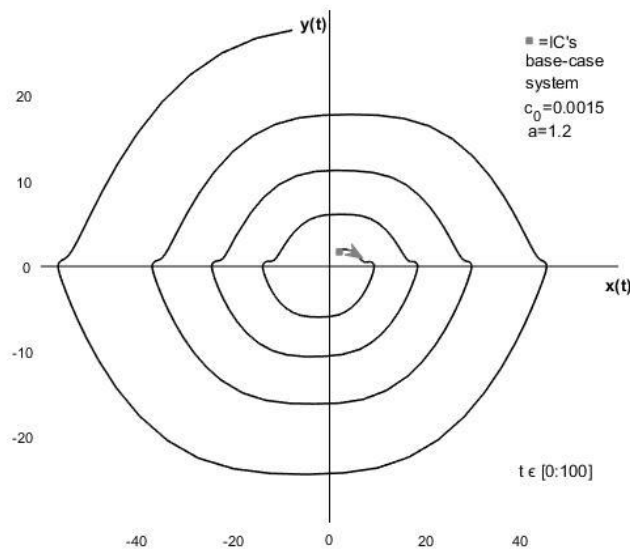


Figure D.18: Phase plane diagram for the base-case system with  $a=1,2$  and  $c_0=0,0015$ .

D.1.4.2  $c_0=0,005$

Figures D.19 and D.20 show the base-case system with the linear damping coefficient,  $c_0=0,005$ , and the nonlinear damping coefficient,  $a=1,2$ . Figure D.19 shows the position curve to the left and the velocity curve to the right, while figure D.20 shows the phase plane diagram.

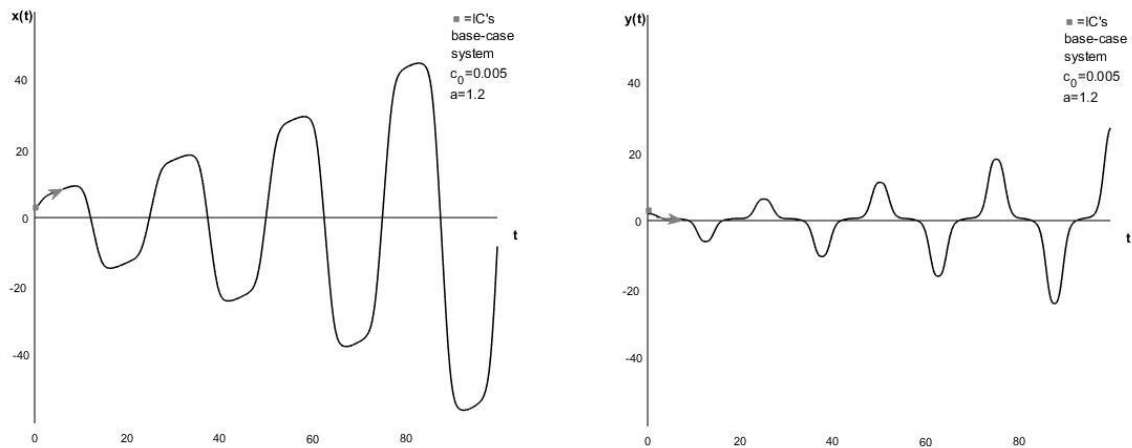


Figure D.19: Position curve(left) and velocity curve(right) for the base-case system with  $a=1,2$  and  $c_0=0,005$ .

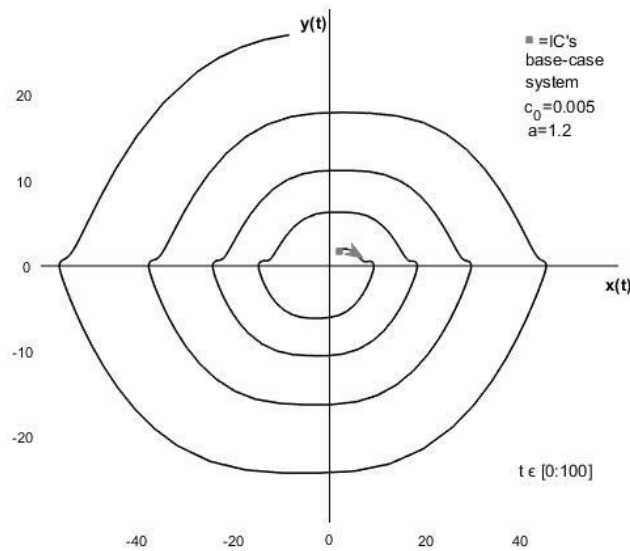


Figure D.20: Phase plane diagram for the base-case system with  $a=1,2$  and  $c_0=0,005$ .



## D.2 $\beta = \frac{1}{3}$

When the mass parameter,  $m=0,222$ , the system has a loading frequency,  $\omega$ , one third of the natural frequency,  $\omega_0$ , i.e.  $\beta = \frac{1}{3}$ .

### D.2.1 $a=0$

When  $a=0$ , the system is only subjected to linear, constant damping,  $c_0$ . Figure D.21 shows the position and velocity curve for the system with  $c_0=0,0015$ . Figure D.22 shows the system with  $c_0=0,0015$  in the phase plane. Figures D.23 and D.24 show the position and velocity curve and phase plane diagram respectively for the system with  $c_0=0,005$ .

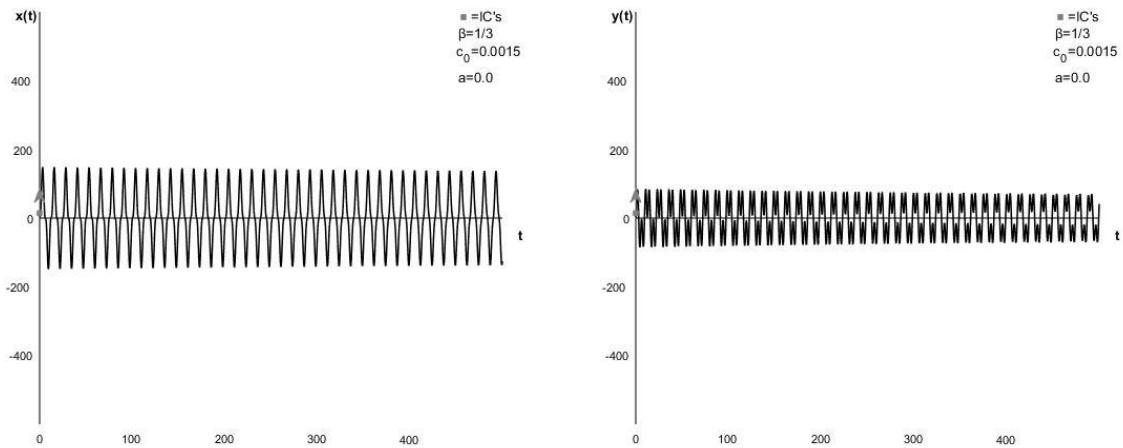


Figure D.21: Position curve(left) and velocity curve(right) for the base-case system with  $m=0,222$ , making  $\beta=1/3$ , with  $c_0=0,0015$  and  $a=0$ .

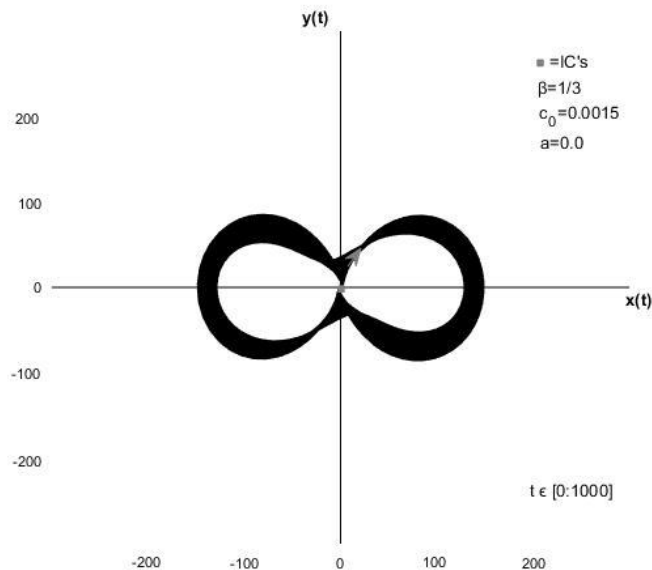


Figure D.22: Phase plane diagram for the base-case system with  $m=0,222$ , making  $\beta=1/3$ , with  $c_0=0,0015$  and  $a=0$ .

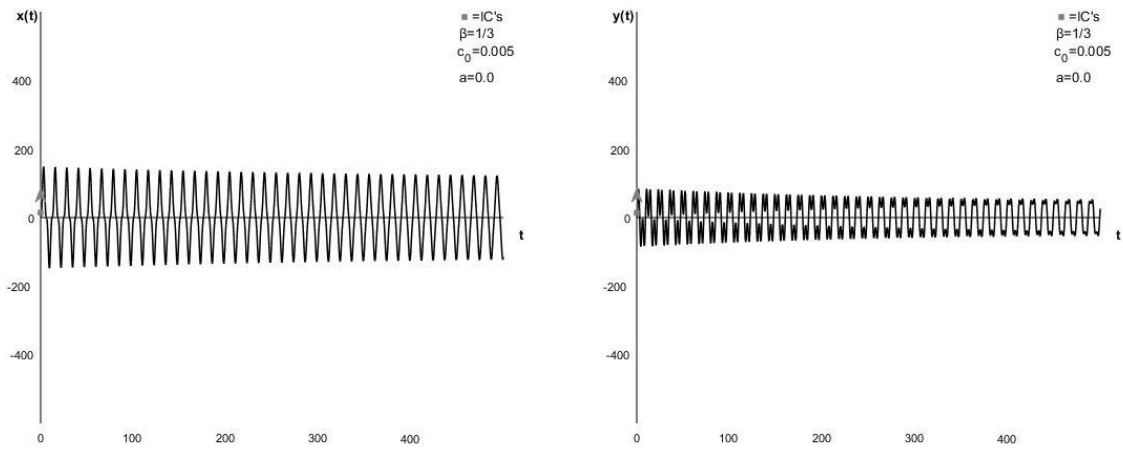


Figure D.23: Position curve(left) and velocity curve(right) for the base-case system with  $m=0,222$ , making  $\beta=1/3$ , with  $c_0=0,005$  and  $a=0$ .

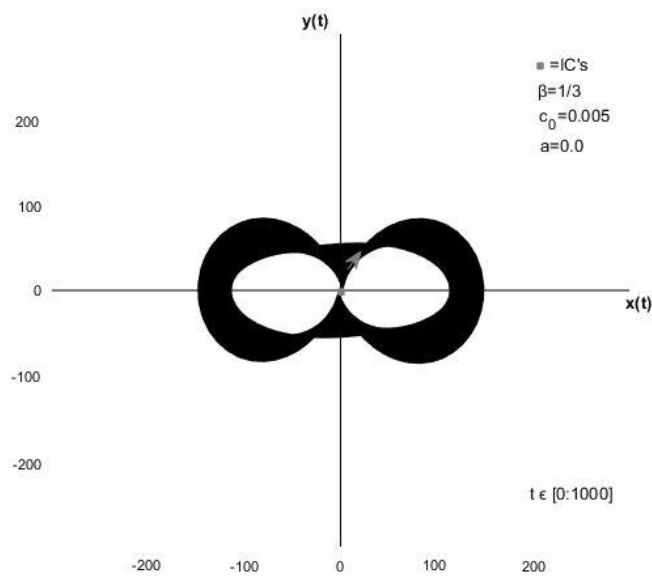


Figure D.24: Phase plane diagram for the base-case system with  $m=0,222$ , making  $\beta=1/3$ , with  $c_0=0,005$  and  $a=0$ .

### D.2.2 $a=1,0$

Figures D.25 and D.26 show the position curve, velocity curve and phase plane diagram respectively for the system with  $a=1,0$  and  $c_0=0,0015$ . Figures D.27 and D.28 show the same for the system with  $a=1,0$  and  $c_0=0,0015$ .

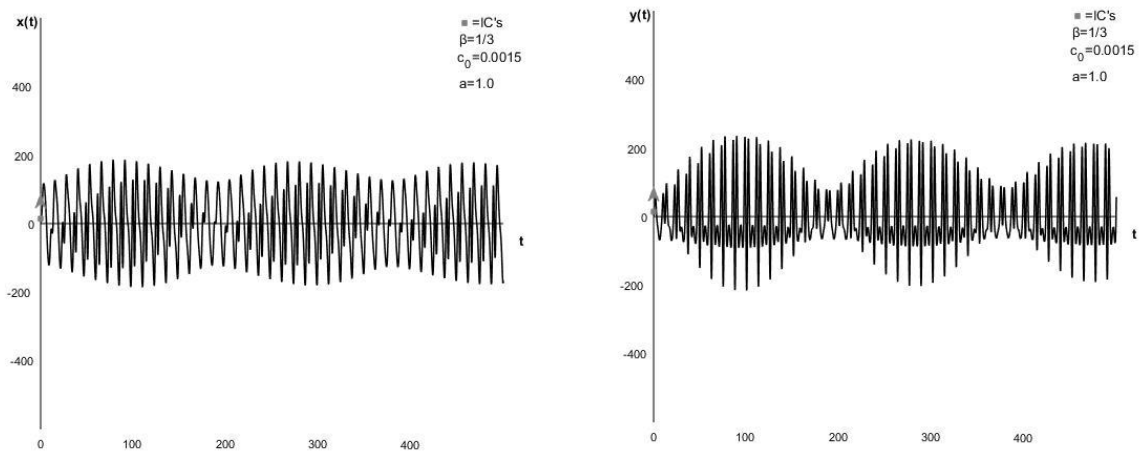


Figure D.25: Position curve(left) and velocity curve(right) for the base-case system with  $m=0,222$ , making  $\beta=1/3$ , with  $c_0=0,0015$  and  $a=1,0$ .

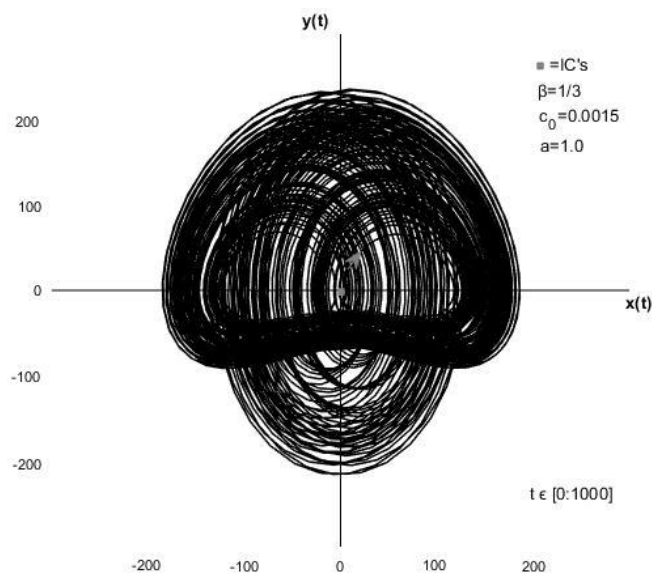


Figure D.26: Phase plane diagram for the base-case system with  $m=0,222$ , making  $\beta=1/3$ , with  $c_0=0,0015$  and  $a=1,0$ .

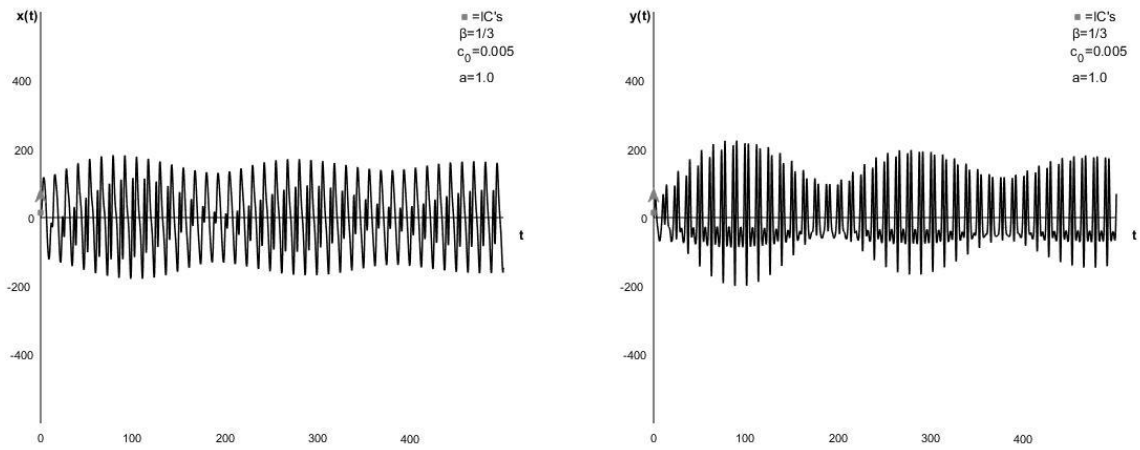


Figure D.27: Position curve(left) and velocity curve(right) for the base-case system with  $m=0,222$ , making  $\beta=1/3$ , with  $c_0=0,005$  and  $a=1,0$ .

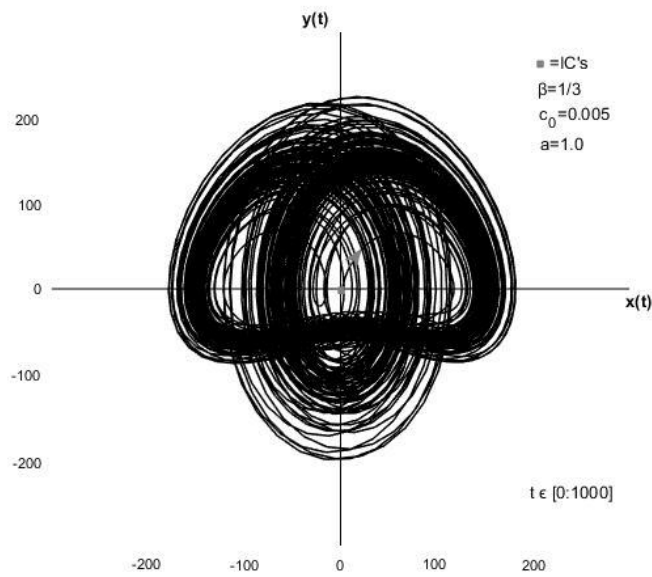


Figure D.28: Phase plane diagram for the base-case system with  $m=0,222$ , making  $\beta=1/3$ , with  $c_0=0,005$  and  $a=1,0$ .

### D.2.3 $a=2,0$

Figures D.29 and D.30 show the position curve, velocity curve and phase plane diagram respectively for the system with  $a=2,0$  and  $c_0=0,005$ . Figures D.31 and D.32 show the same for the system with  $a=2,0$  and  $c_0=0,005$ .

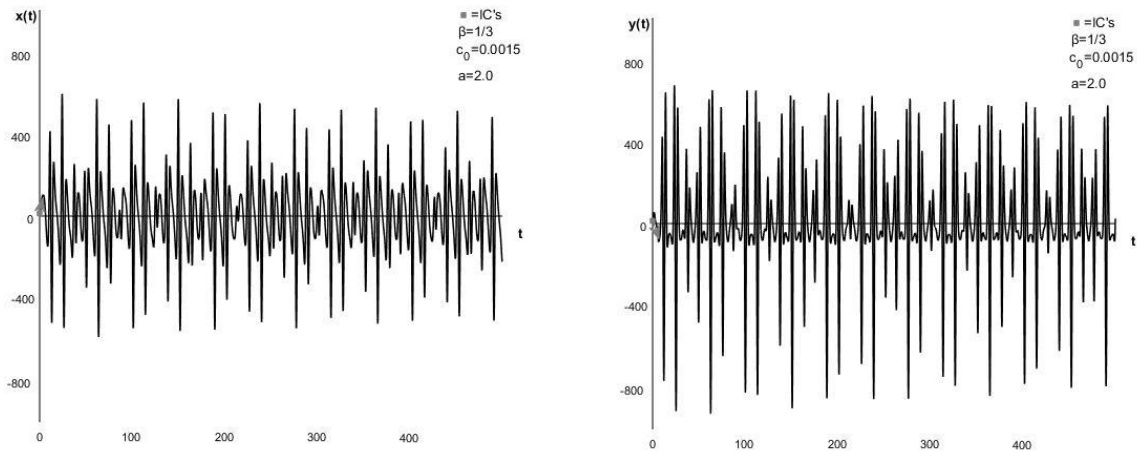


Figure D.29: Position curve(left) and velocity curve(right) for the base-case system with  $m=0,222$ , making  $\beta=1/3$ , with  $c_0=0,0015$  and  $a=2$ .

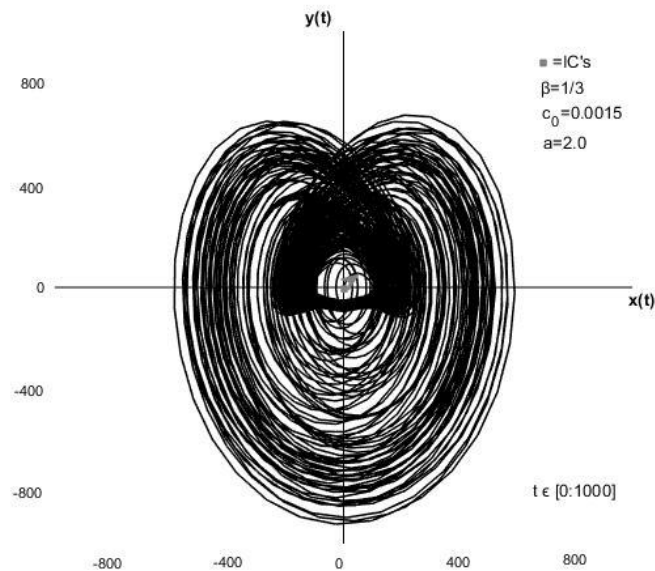


Figure D.30: Phase plane diagram for the base-case system with  $m=0,222$ , making  $\beta=1/3$ , with  $c_0=0,0015$  and  $a=2,0$ .

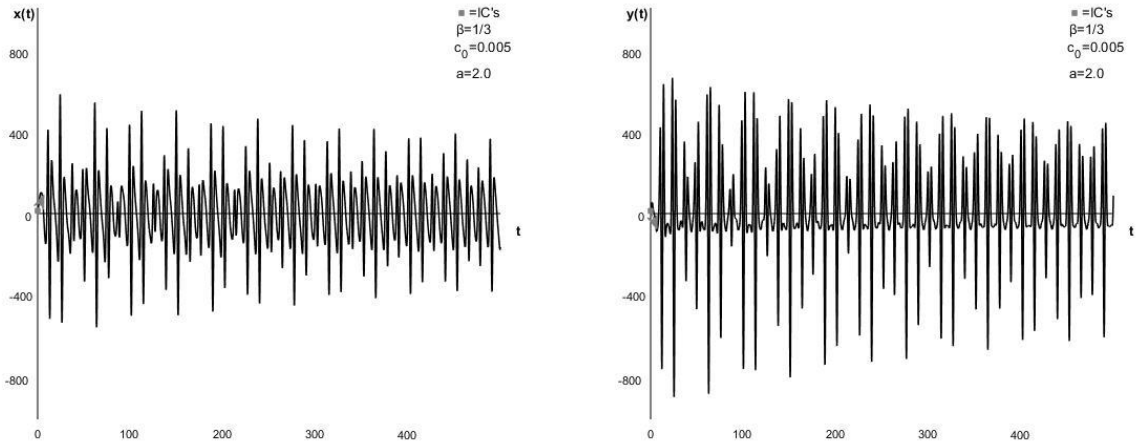


Figure D.31: Position curve(left) and velocity curve(right) for the base-case system with  $m=0,222$ , making  $\beta=1/3$ , with  $c_0=0,005$  and  $a=2,0$ .

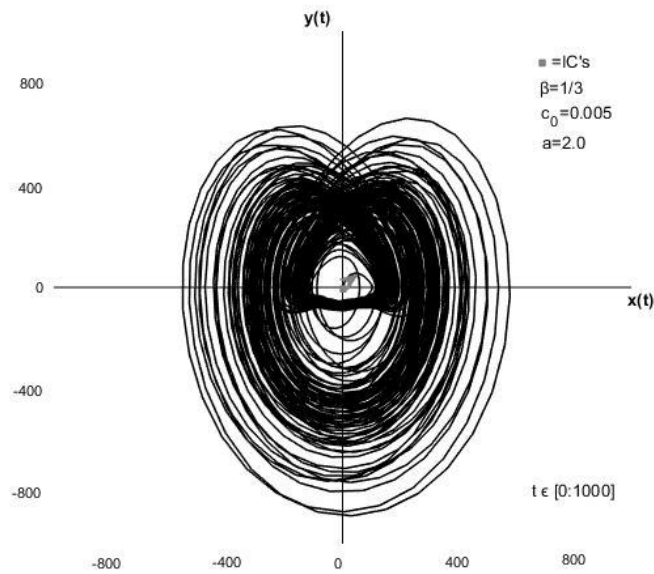


Figure D.32: Phase plane diagram for the base-case system with  $m=0,222$ , making  $\beta=1/3$ , with  $c_0=0,005$  and  $a=2,0$ .

### D.2.4 $a=3,45$

Figures D.33 and D.34 show the position curve, velocity curve and phase plane diagram respectively for the system with  $a=3,45$  and  $c_0=0,005$ . Figures D.35 and D.36 show the same for the system with  $a=3,45$  and  $c_0=0,005$ .

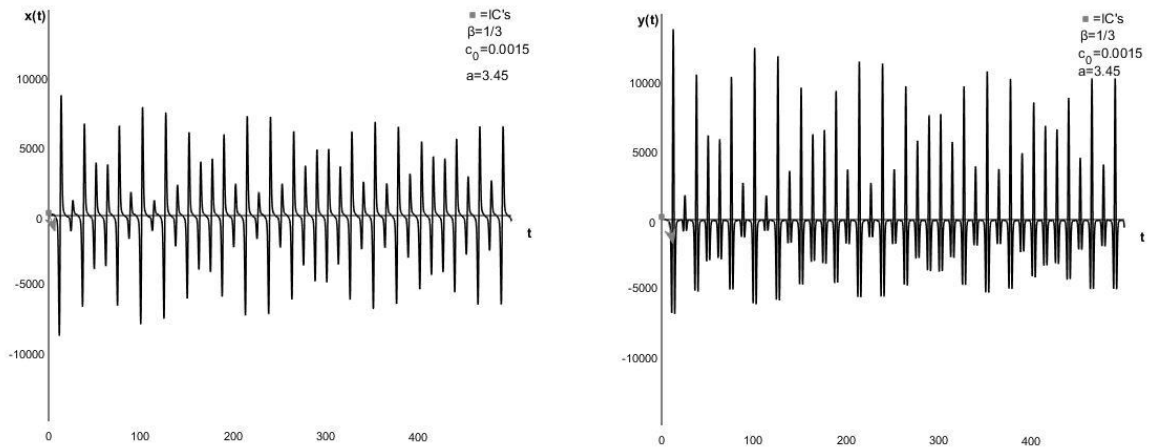


Figure D.33: Position curve(left) and velocity curve(right) for the base-case system with  $m=0,222$ , making  $\beta=1/3$ , with  $c_0=0,0015$  and  $a=3,45$ .

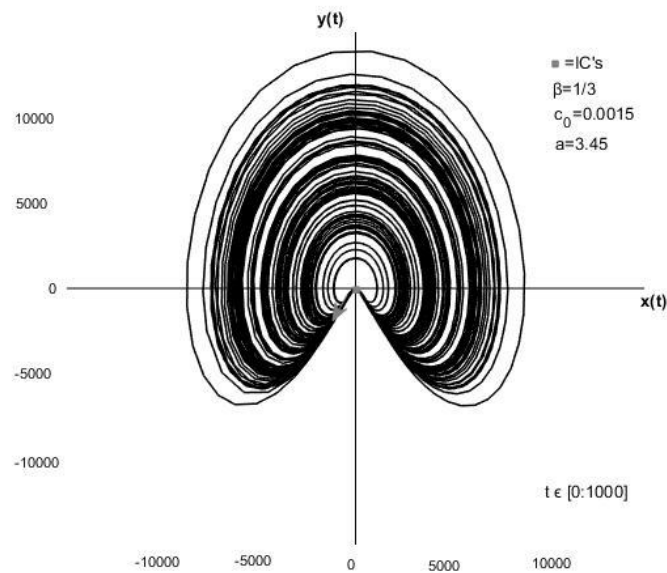


Figure D.34: Phase plane diagram for the base-case system with  $m=0,222$ , making  $\beta=1/3$ , with  $c_0=0,0015$  and  $a=3,45$ .

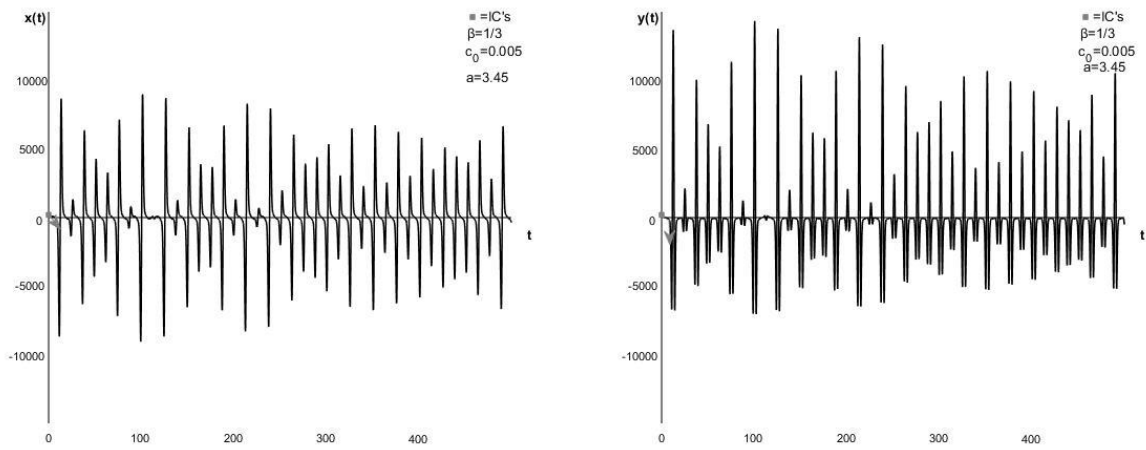


Figure D.35: Position curve(left) and velocity curve(right) for the base-case system with  $m=0,222$ , making  $\beta=1/3$ , with  $c_0=0,005$  and  $a=3,45$ .

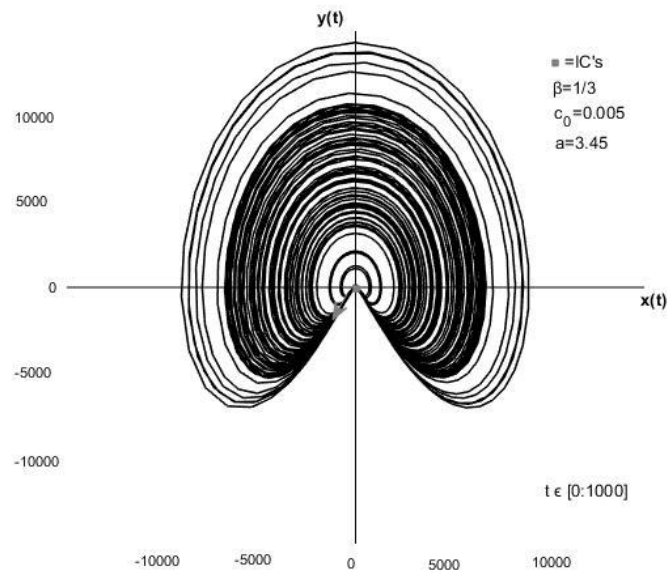


Figure D.36: Phase plane diagram for the base-case system with  $m=0,222$ , making  $\beta=1/3$ , with  $c_0=0,005$  and  $a=3,45$ .



D.2.5  $a=3,46$

Figures D.37 and D.38 show the position curve, velocity curve and phase plane diagram respectively for the system with  $a=3,46$  and  $c_0=0,005$ . Figures D.39 and D.40 show the same for the system with  $a=3,46$  and  $c_0=0,005$ .

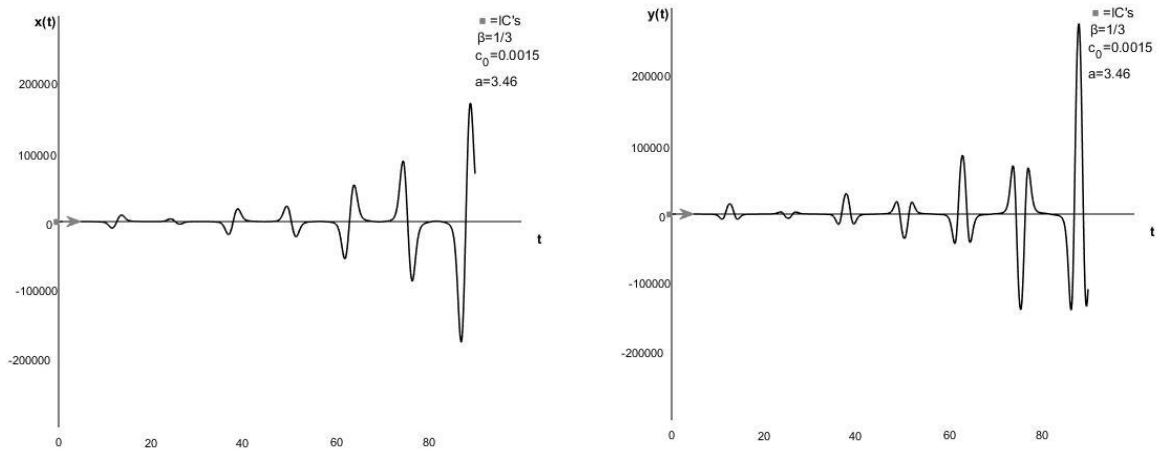


Figure D.37: Position curve(left) and velocity curve(right) for the base-case system with  $m=0,222$ , making  $\beta=1/3$ , with  $c_0=0,0015$  and  $a=3,46$ .

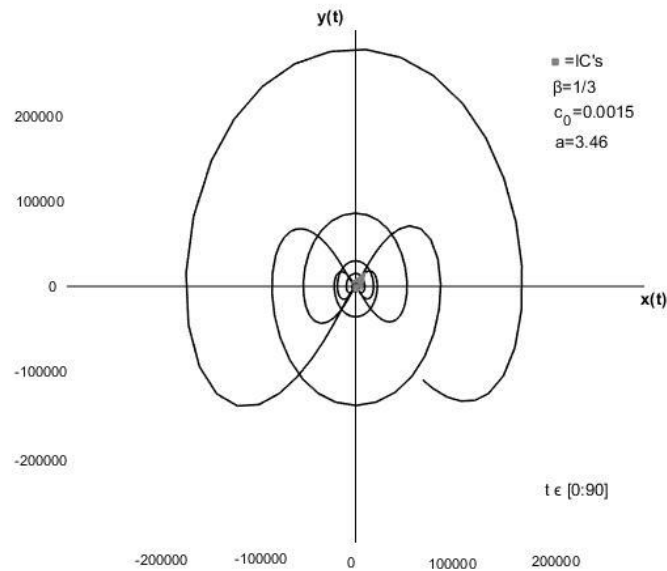


Figure D.38: Phase plane diagram for the base-case system with  $m=0,222$ , making  $\beta=1/3$ , with  $c_0=0,0015$  and  $a=3,46$ .

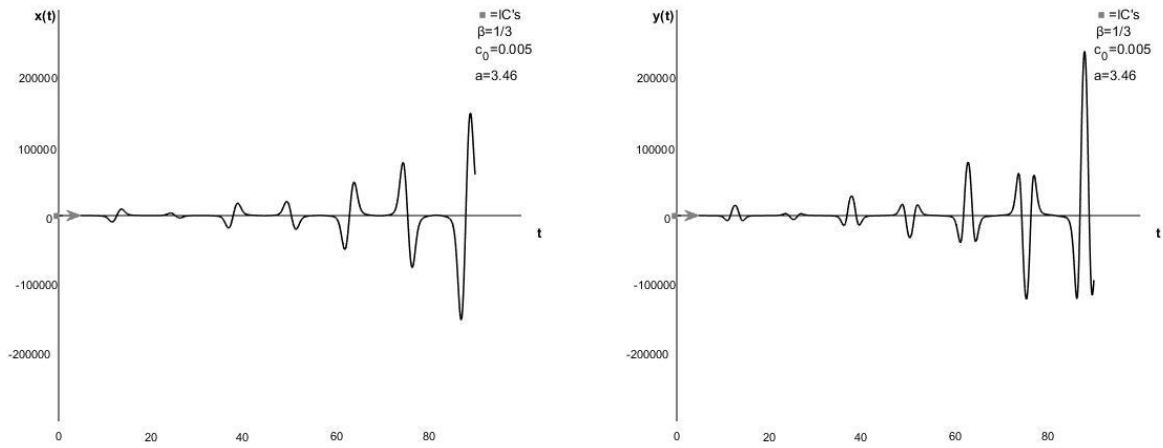


Figure D.39: Position curve(left) and velocity curve(right) for the base-case system with  $m=0,222$ , making  $\beta=1/3$ , with  $c_0=0,005$  and  $a=3,46$ .

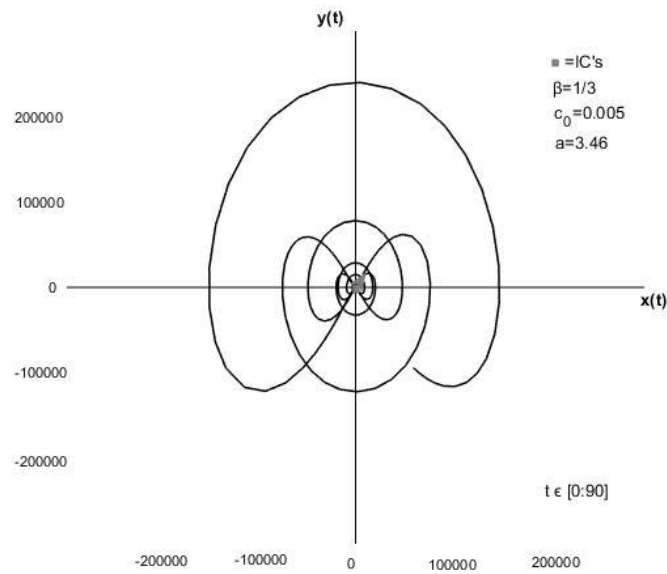


Figure D.40: Phase plane diagram for the base-case system with  $m=0,222$ , making  $\beta=1/3$ , with  $c_0=0,005$  and  $a=3,46$ .

### D.3 $\beta = \frac{1}{2}$

When the mass parameter,  $m=0,5$ , the system has a frequency,  $\omega$ , half of the natural frequency,  $\omega_0$ , i.e.  $\beta = \frac{1}{2}$ .

#### D.3.1 $a=0$

When  $a=0$ , the system is only subjected to linear, constant damping,  $c_0$ . Figure D.41 shows the position and velocity curve for the system with  $c_0=0,0015$ . Figure D.42 shows the system with  $c_0=0,0015$  in the phase plane. Figures D.43 and D.44 show the position and velocity curve and phase plane diagram respectively for the system with  $c_0=0,005$ .

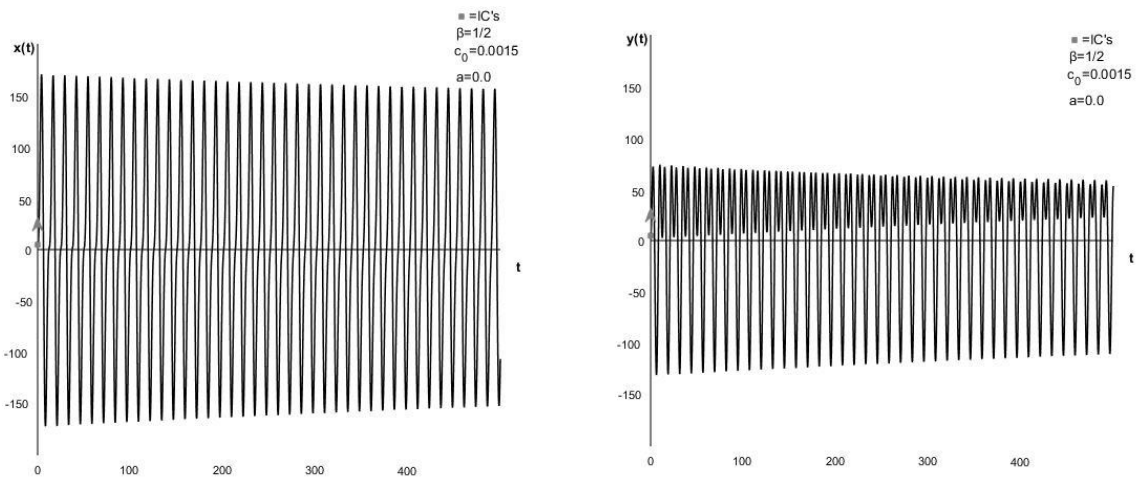


Figure D.41: Position curve(left) and velocity curve(right) for the base-case system with  $m=0,5$ , making  $\beta=1/2$ , with  $c_0=0,0015$  and  $a=0$ .

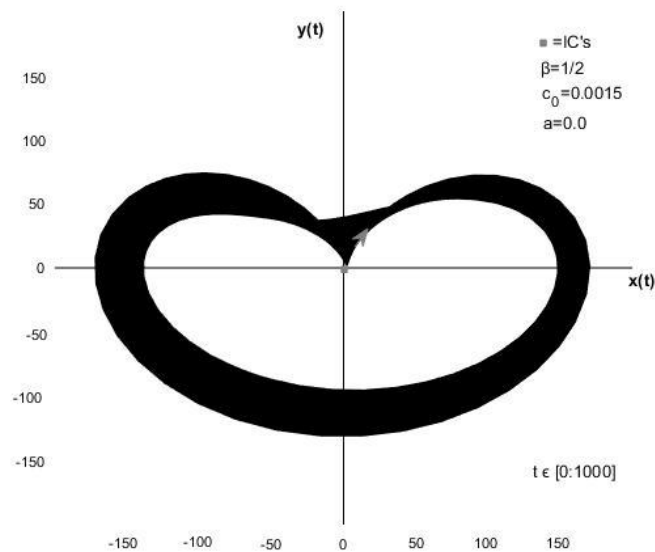


Figure D.42: Phase plane diagram for the base-case system with  $m=0,5$ , making  $\beta=1/2$ , with  $c_0=0,0015$  and  $a=0$ .

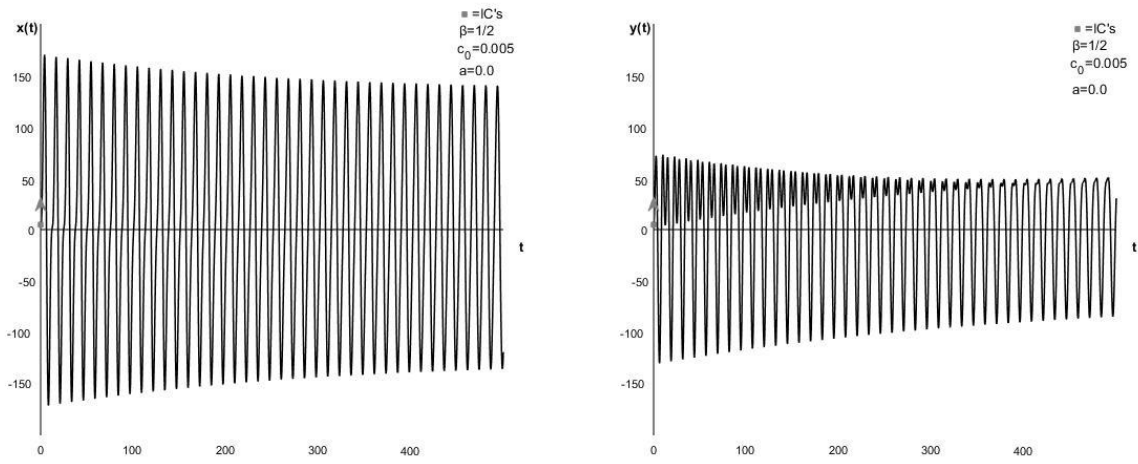


Figure D.43: Position curve(left) and velocity curve(right) for the base-case system with  $m=0,5$ , making  $\beta=1/2$ , with  $c_0=0,005$  and  $a=0$ .

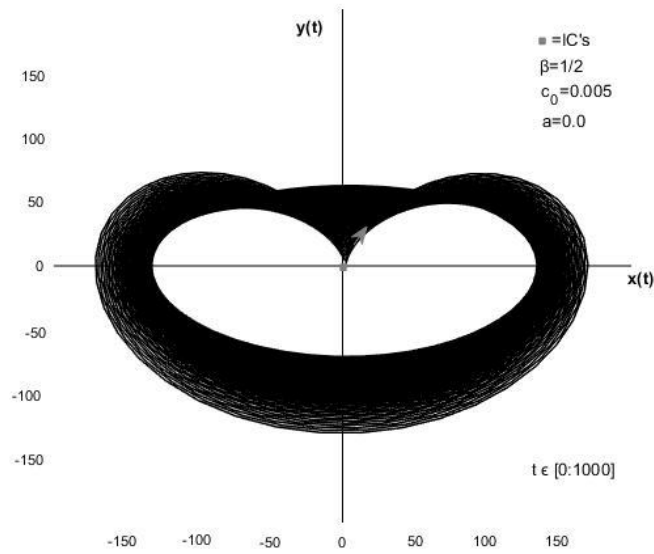


Figure D.44: Phase plane diagram for the base-case system with  $m=0,5$ , making  $\beta=1/2$ , with  $c_0=0,005$  and  $a=0$ .

### D.3.2 $a=0,5$

Figures D.45 and D.46 show the position curve, velocity curve and phase plane diagram respectively for the system with  $a=0,5$  and  $c_0=0,0015$ . Figures D.47 and D.48 show the same for the system with  $a=0,5$  and  $c_0=0,0015$ .

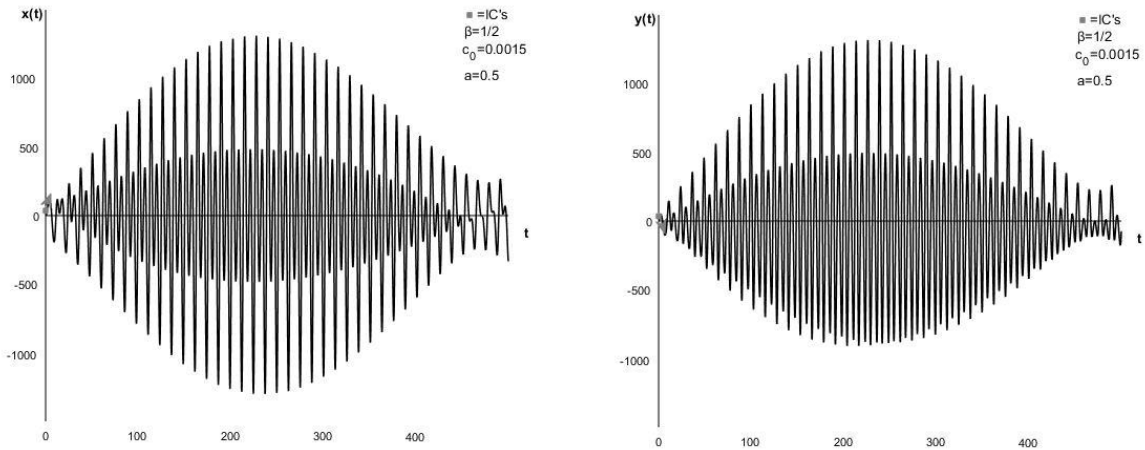


Figure D.45: Position curve(left) and velocity curve(right) for the base-case system with  $m=0,5$ , making  $\beta=1/2$ , with  $c_0=0,0015$  and  $a=0,5$ .

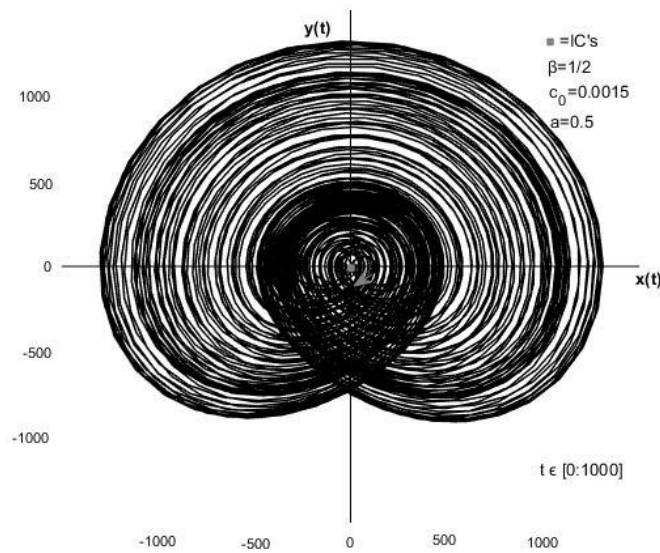


Figure D.46: Phase plane diagram for the base-case system with  $m=0,5$ , making  $\beta=1/2$ , with  $c_0=0,0015$  and  $a=0,5$ .

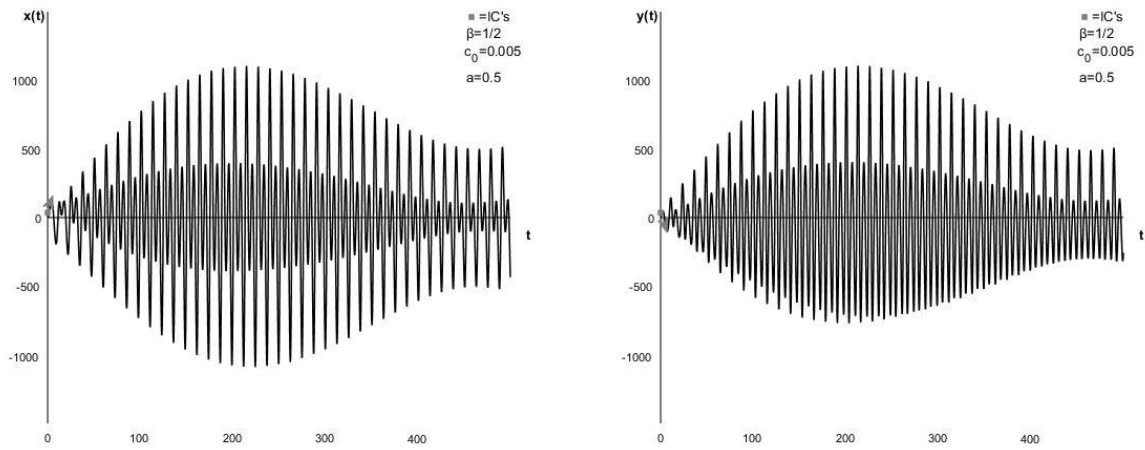


Figure D.47: Position curve(left) and velocity curve(right) for the base-case system with  $m=0,5$ , making  $\beta=1/2$ , with  $c_0=0,005$  and  $a=0,5$ .

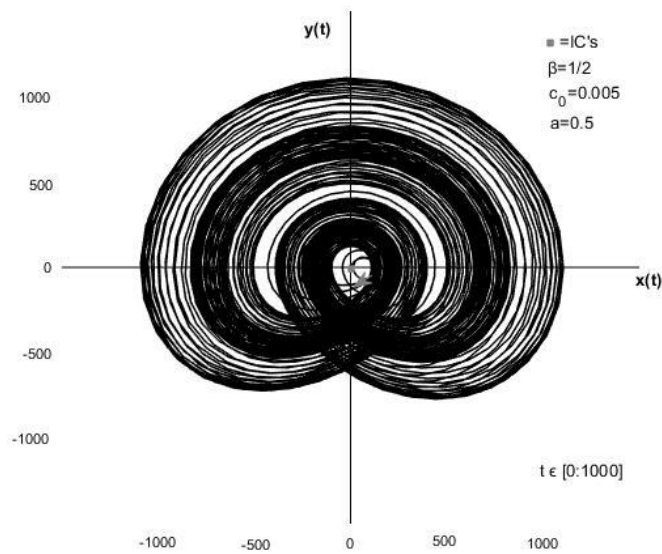


Figure D.48: Phase plane diagram for the base-case system with  $m=0,5$ , making  $\beta=1/2$ , with  $c_0=0,005$  and  $a=0,5$ .

### D.3.3 $a=1,0$

Figures D.49 and D.50 show the position curve, velocity curve and phase plane diagram respectively for the system with  $a=1,0$  and  $c_0=0,005$ . Figures D.51 and D.52 show the same for the system with  $a=1,0$  and  $c_0=0,005$ .

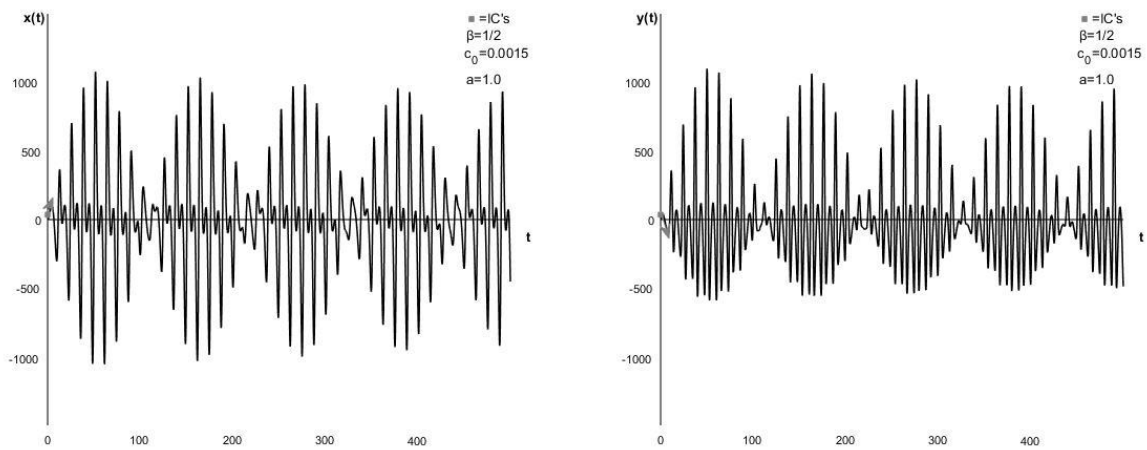


Figure D.49: Position curve(left) and velocity curve(right) for the base-case system with  $m=0,5$ , making  $\beta=1/2$ , with  $c_0=0,0015$  and  $a=1,0$ .

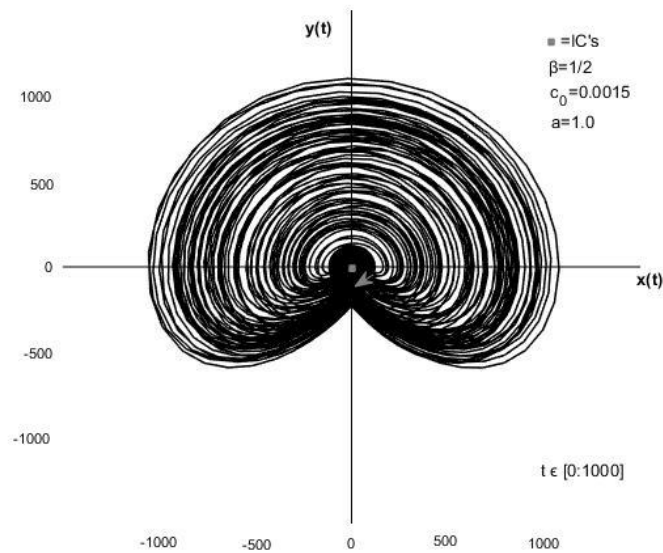


Figure D.50: Phase plane diagram for the base-case system with  $m=0,5$ , making  $\beta=1/2$ , with  $c_0=0,0015$  and  $a=1,0$ .

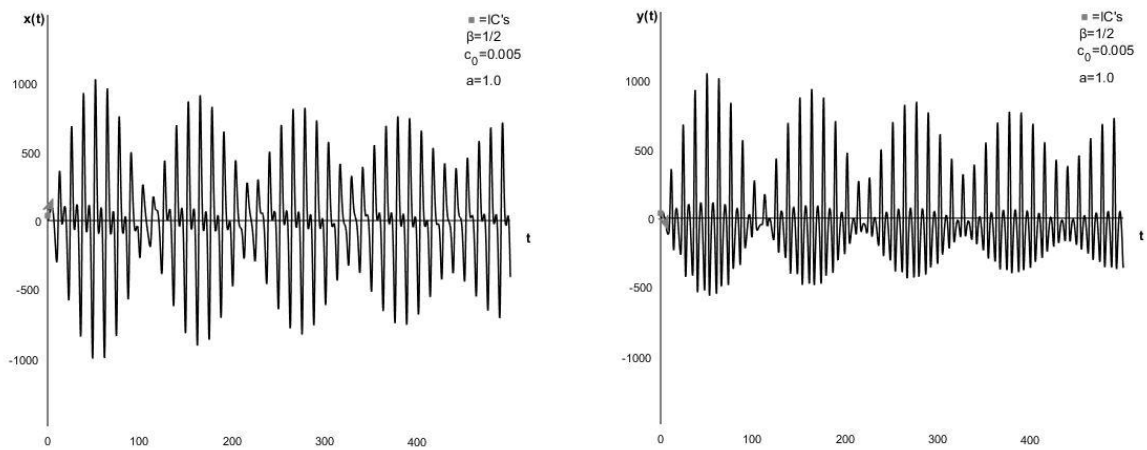


Figure D.51: Position curve(left) and velocity curve(right) for the base-case system with  $m=0,5$ , making  $\beta=1/2$ , with  $c_0=0,005$  and  $a=1,0$ .

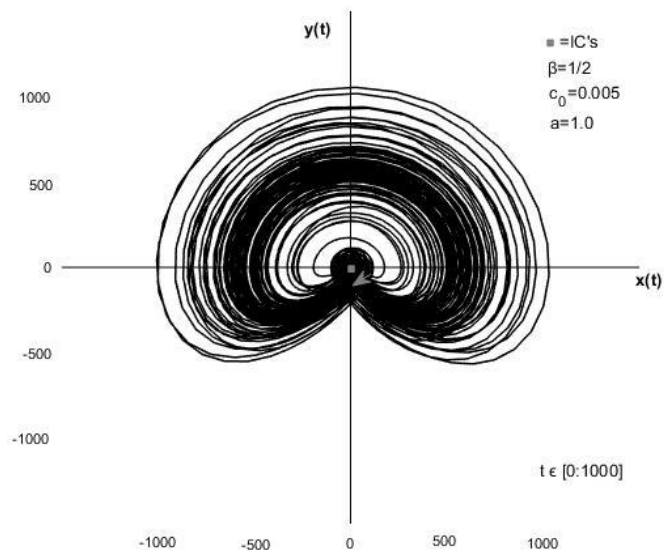


Figure D.52: Phase plane diagram for the base-case system with  $m=0,5$ , making  $\beta=1/2$ , with  $c_0=0,005$  and  $a=1,0$ .



### D.3.4 $a=1,60$

Figures D.53 and D.54 show the position curve, velocity curve and phase plane diagram respectively for the system with  $a=1,60$  and  $c_0=0,005$ . Figures D.55 and D.56 show the same for the system with  $a=1,60$  and  $c_0=0,005$ .

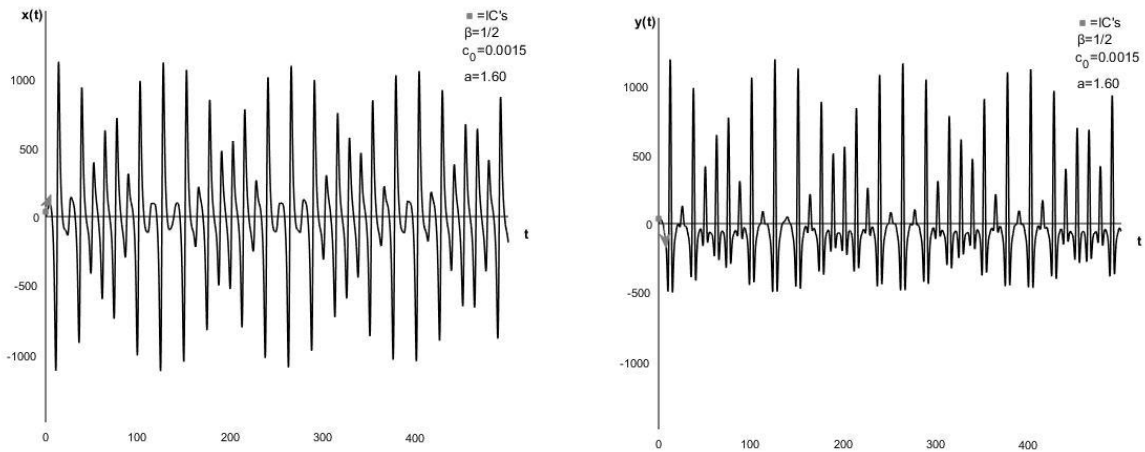


Figure D.53: Position curve(left) and velocity curve(right) for the base-case system with  $m=0,5$ , making  $\beta=1/2$ , with  $c_0=0,0015$  and  $a=1,60$ .

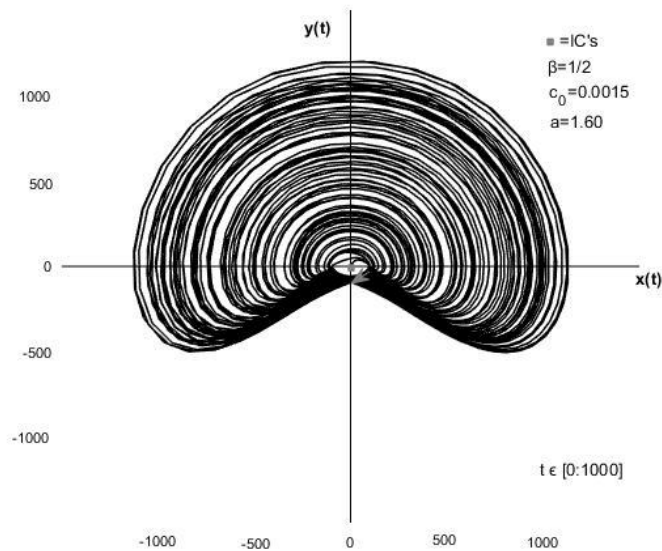


Figure D.54: Phase plane diagram for the base-case system with  $m=0,5$ , making  $\beta=1/2$ , with  $c_0=0,0015$  and  $a=1,60$ .

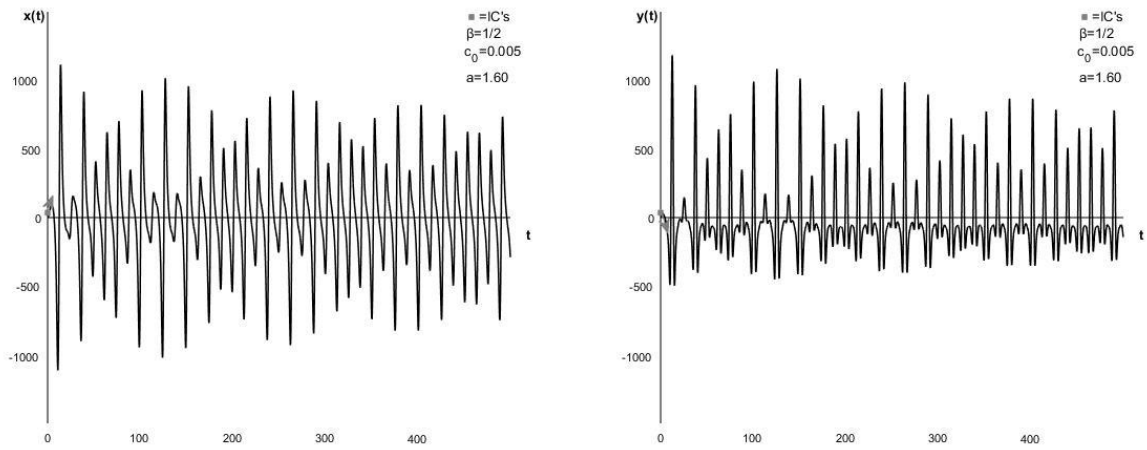


Figure D.55: Position curve(left) and velocity curve(right) for the base-case system with  $m=0,5$ , making  $\beta=1/2$ , with  $c_0=0,005$  and  $a=1,60$ .

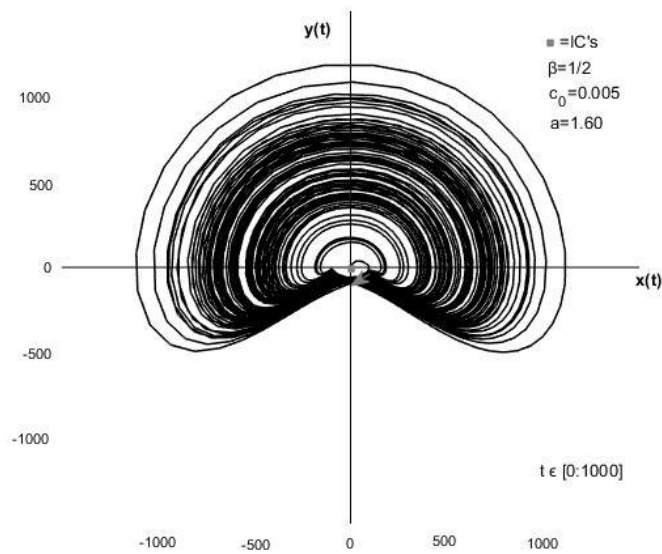


Figure D.56: Phase plane diagram for the base-case system with  $m=0,5$ , making  $\beta=1/2$ , with  $c_0=0,005$  and  $a=1,60$ .

D.3.5  $a=1,61$

Figures D.57 and D.58 show the position curve, velocity curve and phase plane diagram respectively for the system with  $a=1,61$  and  $c_0=0,005$ . Figures D.59 and D.60 show the same for the system with  $a=1,61$  and  $c_0=0,005$ .

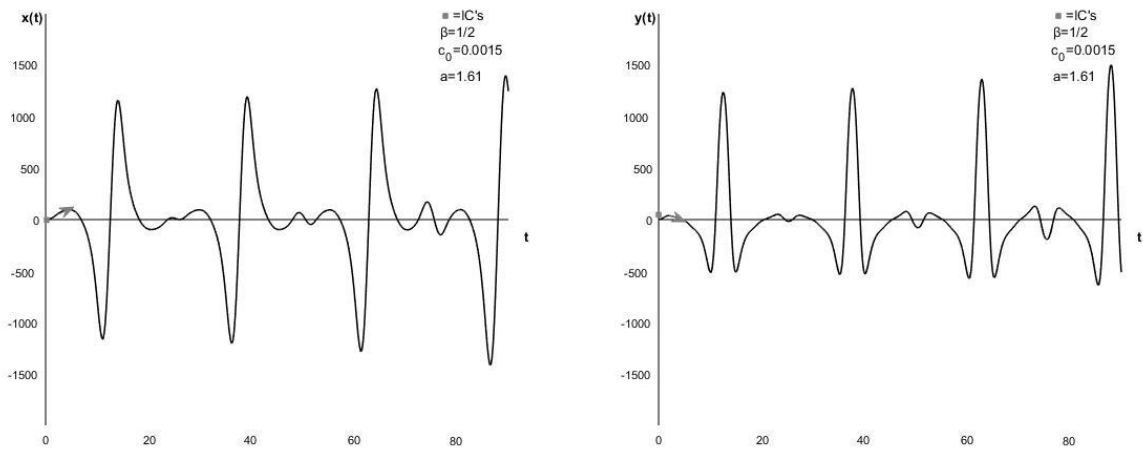


Figure D.57: Position curve(left) and velocity curve(right) for the base-case system with  $m=0,5$ , making  $\beta=1/2$ , with  $c_0=0,0015$  and  $a=1,61$ .

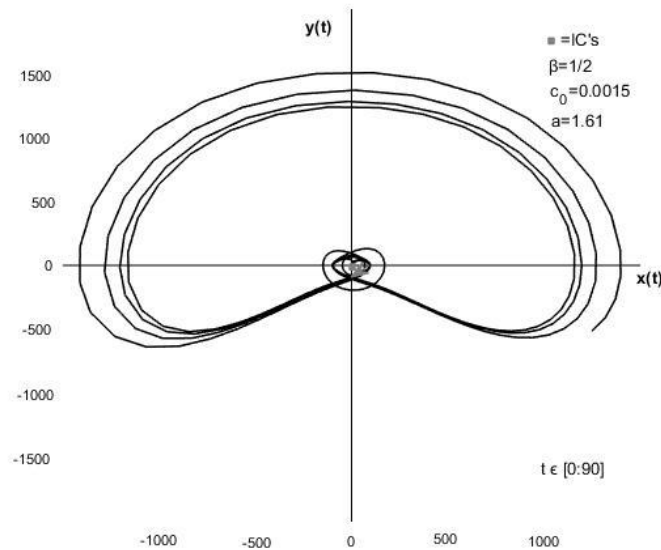


Figure D.58: Phase plane diagram for the base-case system with  $m=0,5$ , making  $\beta=1/2$ , with  $c_0=0,0015$  and  $a=1,61$ .

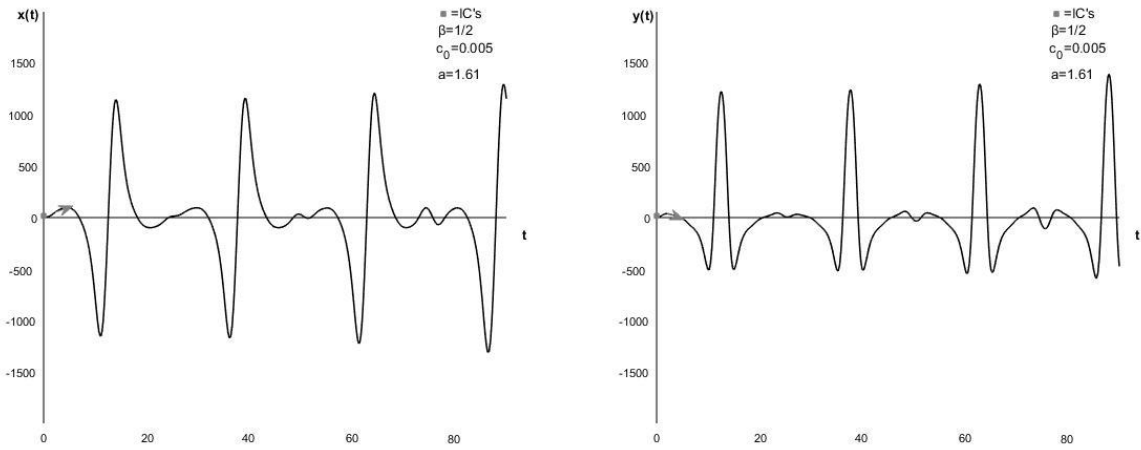


Figure D.59: Position curve(left) and velocity curve(right) for the base-case system with  $m=0,5$ , making  $\beta=1/2$ , with  $c_0=0,005$  and  $a=1,61$ .

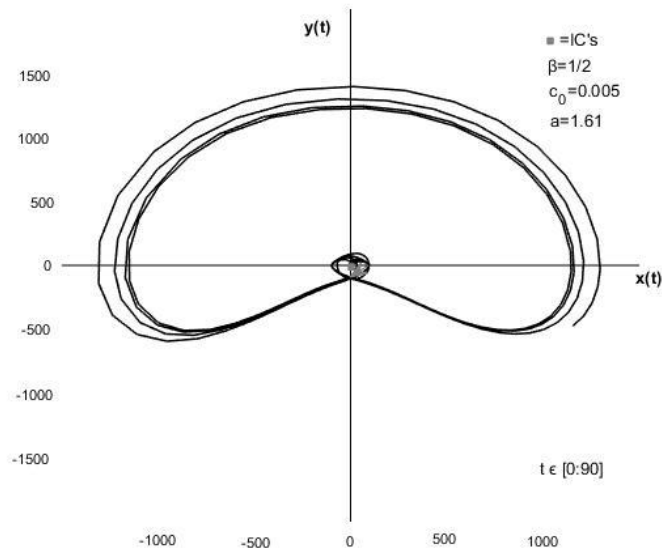


Figure D.60: Phase plane diagram for the base-case system with  $m=0,5$ , making  $\beta=1/2$ , with  $c_0=0,005$  and  $a=1,61$ .

## D.4 $\beta = 1,0$

When the mass parameter,  $m=2,0$ , the system has a frequency,  $\omega$ , equal to the natural frequency,  $\omega_0$ , i.e.  $\beta = 1,0$ .

### D.4.1 $a=0$

When  $a=0$ , the system is only subjected to linear, constant damping,  $c_0$ . Figure D.61 shows the position and velocity curve for the system with  $c_0=0,0015$ . Figure D.62 shows the system with  $c_0=0,0015$  in the phase plane. Figures D.63 and D.64 show the position and velocity curve and phase plane diagram respectively for the system with  $c_0=0,005$ .

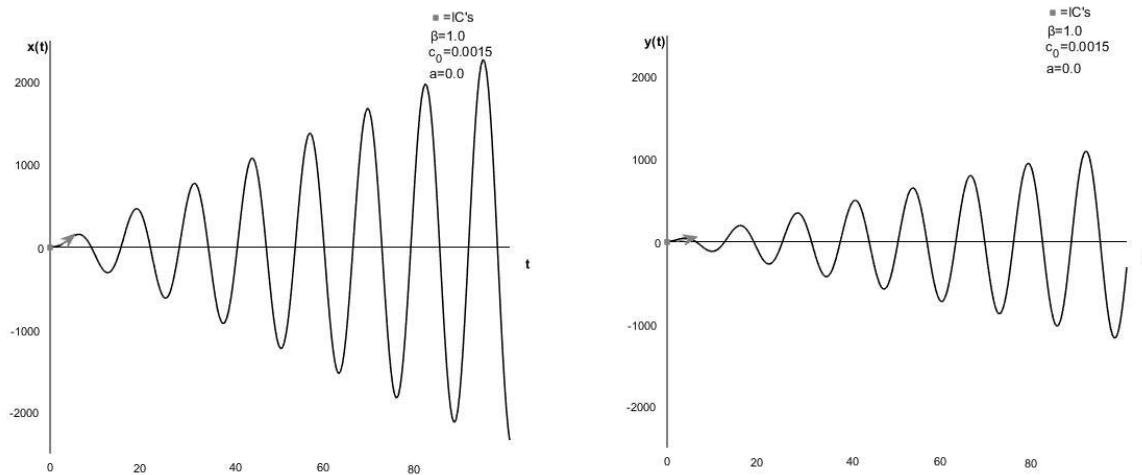


Figure D.61: Position curve(left) and velocity curve(right) for the base-case system with  $m=2,0$ , making  $\beta=1,0$ , with  $c_0=0,0015$  and  $a=0$ .

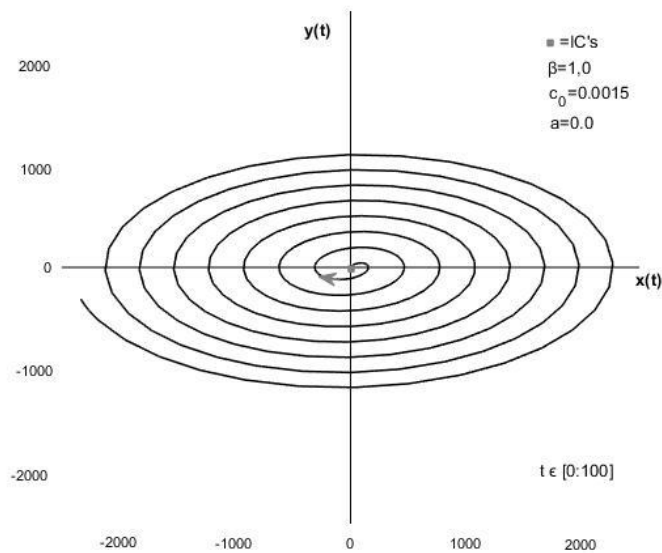


Figure D.62: Phase plane diagram for the base-case system with  $m=2,0$ , making  $\beta=1,0$ , with  $c_0=0,0015$  and  $a=0$ .

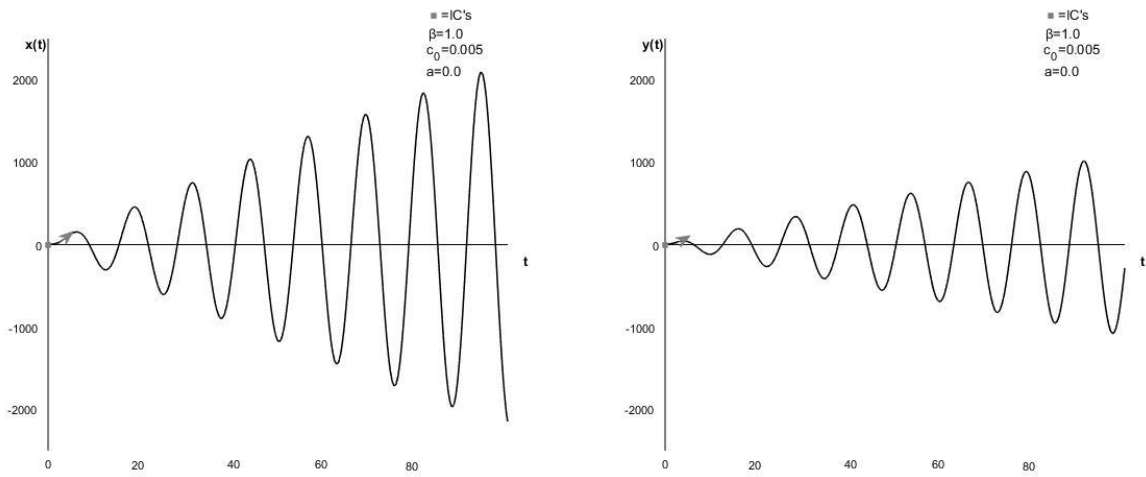


Figure D.63: Position curve(left) and velocity curve(right) for the base-case system with  $m=2,0$ , making  $\beta=1,0$ , with  $c_0=0,005$  and  $a=0$ .

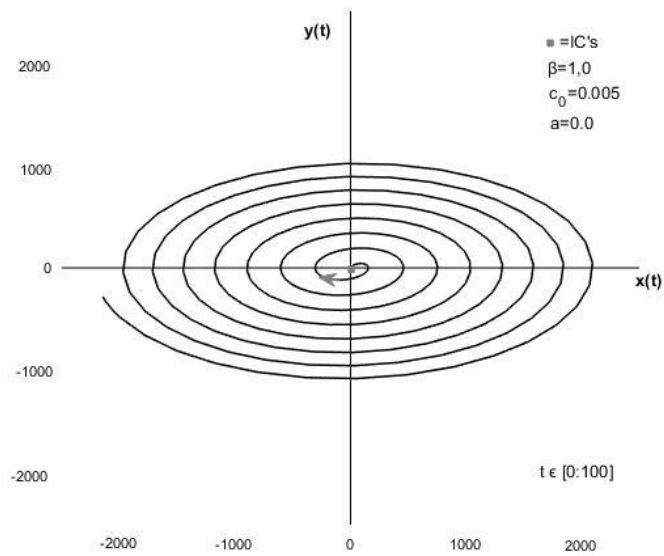


Figure D.64: Phase plane diagram for the base-case system with  $m=2,0$ , making  $\beta=1,0$ , with  $c_0=0,005$  and  $a=0$ .

### D.4.2 $a=0,5$

Figures D.65 and D.66 show the position curve, velocity curve and phase plane diagram respectively for the system with  $a=0,5$  and  $c_0=0,0015$ . Figures D.67 and D.68 show the same for the system with  $a=0,5$  and  $c_0=0,0015$ .

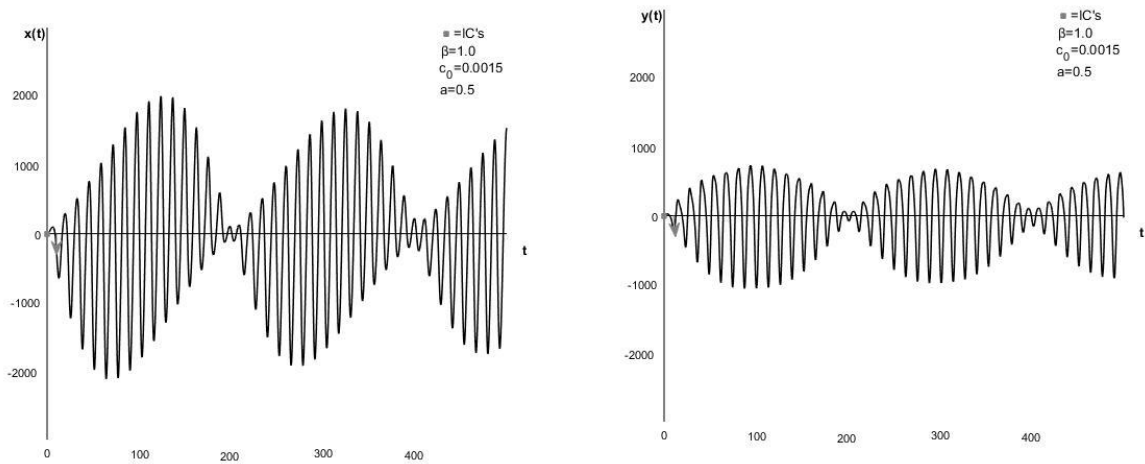


Figure D.65: Position curve(left) and velocity curve(right) for the base-case system with  $m=2,0$ , making  $\beta=1,0$ , with  $c_0=0,0015$  and  $a=0,5$ .

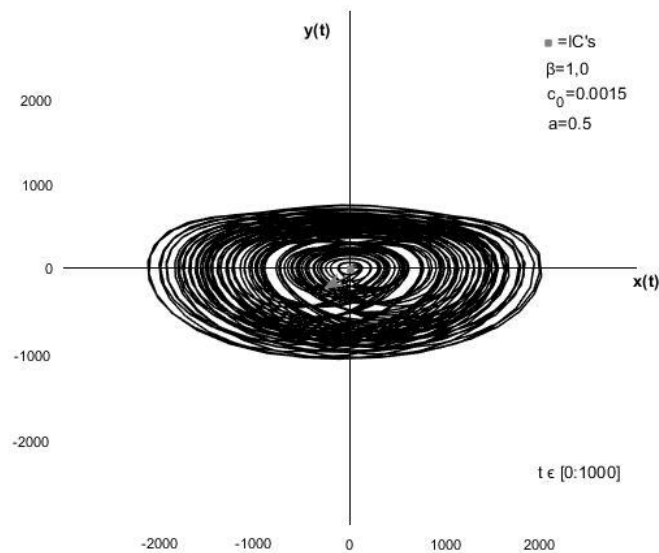


Figure D.66: Phase plane diagram for the base-case system with  $m=2,0$ , making  $\beta=1,0$ , with  $c_0=0,0015$  and  $a=0,5$ .

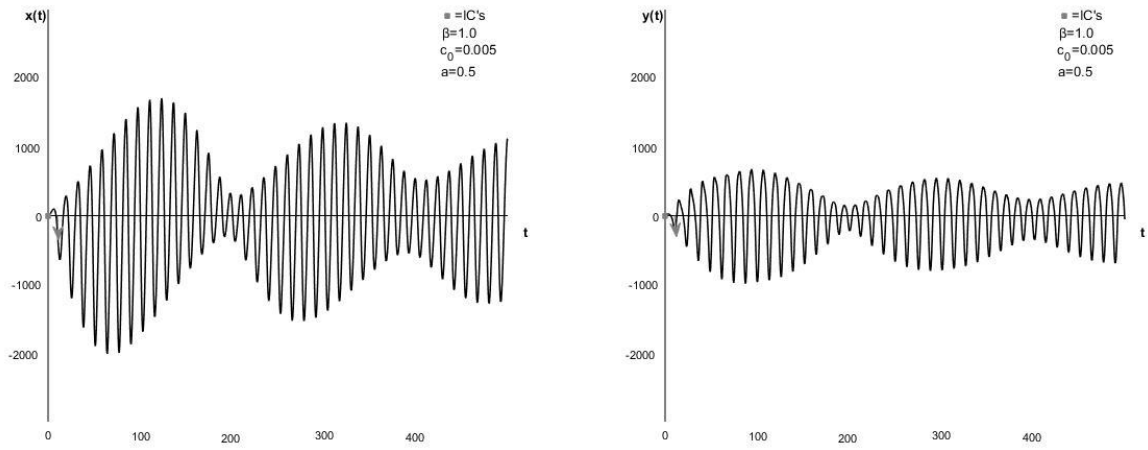


Figure D.67: Position curve(left) and velocity curve(right) for the base-case system with  $m=2,0$ , making  $\beta=1,0$ , with  $c_0=0,005$  and  $a=0,5$ .

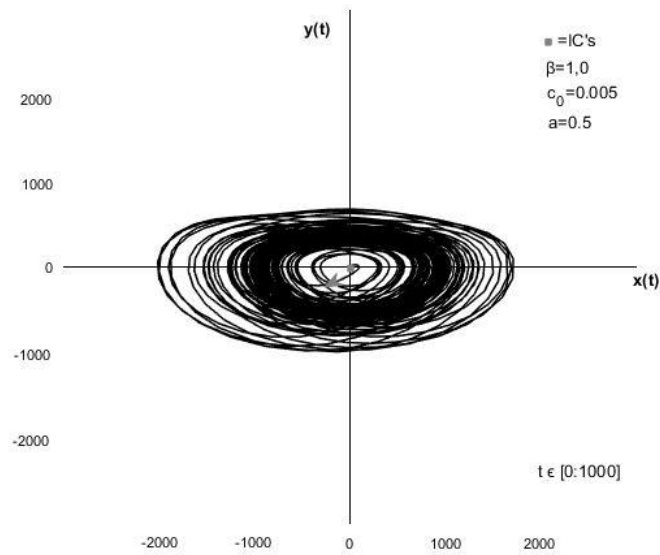


Figure D.68: Phase plane diagram for the base-case system with  $m=2,0$ , making  $\beta=1,0$ , with  $c_0=0,005$  and  $a=0,5$ .



### D.4.3 $a=1,0$

Figures D.69 and D.70 show the position curve, velocity curve and phase plane diagram respectively for the system with  $a=1,0$  and  $c_0=0,005$ . Figures D.71 and D.72 show the same for the system with  $a=1,0$  and  $c_0=0,005$ .

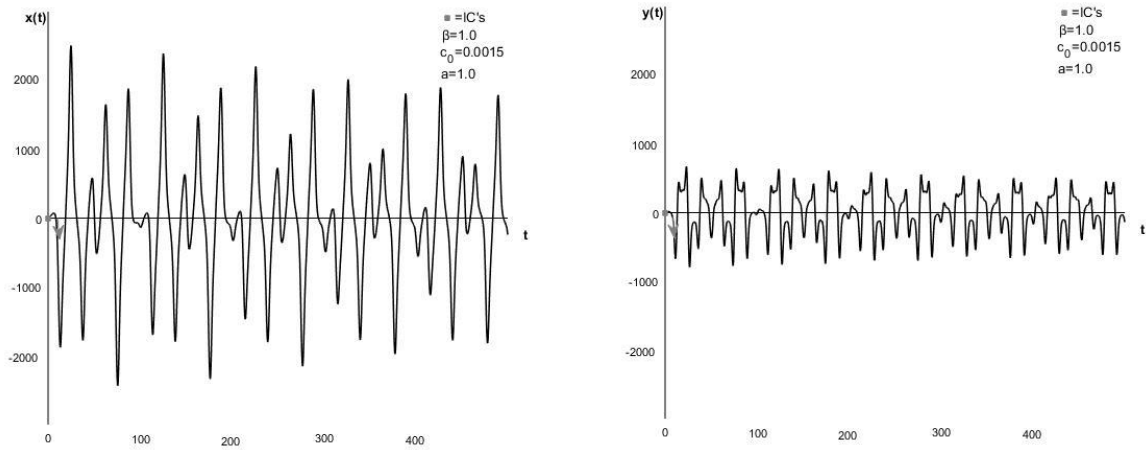


Figure D.69: Position curve(left) and velocity curve(right) for the base-case system with  $m=2,0$ , making  $\beta=1,0$ , with  $c_0=0,0015$  and  $a=1,0$ .

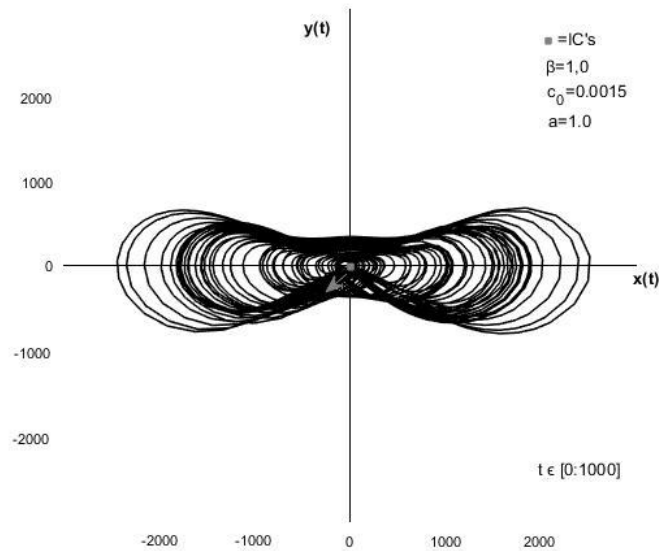


Figure D.70: Phase plane diagram for the base-case system with  $m=2,0$ , making  $\beta=1,0$ , with  $c_0=0,0015$  and  $a=1,0$ .

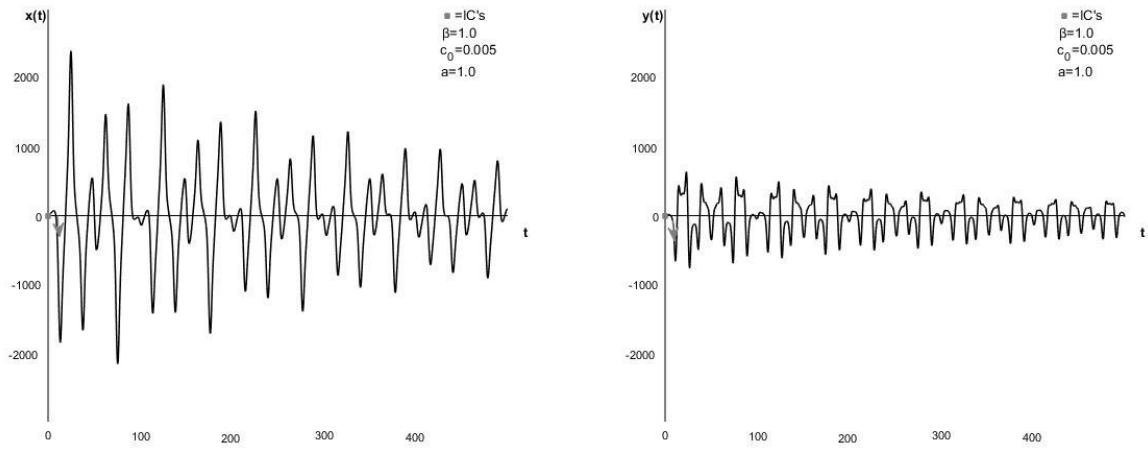


Figure D.71: Position curve(left) and velocity curve(right) for the base-case system with  $m=2,0$ , making  $\beta=1,0$ , with  $c_0=0,005$  and  $a=1,0$ .

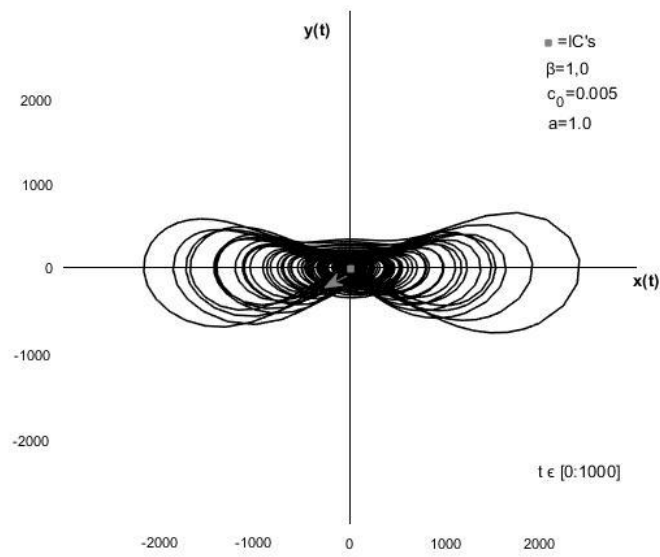


Figure D.72: Phase plane diagram for the base-case system with  $m=2,0$ , making  $\beta=1,0$ , with  $c_0=0,005$  and  $a=1,0$ .

#### D.4.4 $a=1,03$

Figures D.73 and D.74 show the position curve, velocity curve and phase plane diagram respectively for the system with  $a=1,03$  and  $c_0=0,005$ . Figures D.75 and D.76 show the same for the system with  $a=1,03$  and  $c_0=0,005$ .

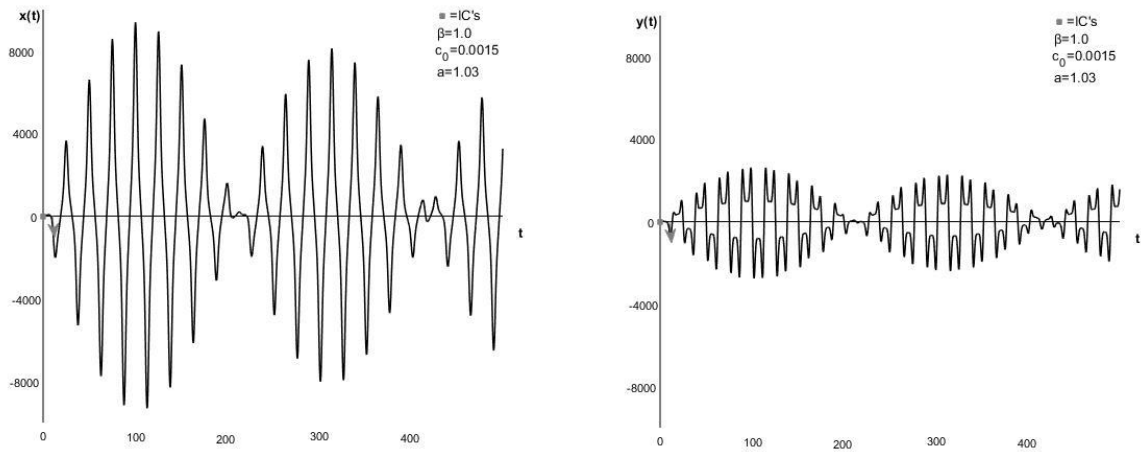


Figure D.73: Position curve(left) and velocity curve(right) for the base-case system with  $m=2,0$ , making  $\beta=1,0$ , with  $c_0=0,0015$  and  $a=1,03$ .

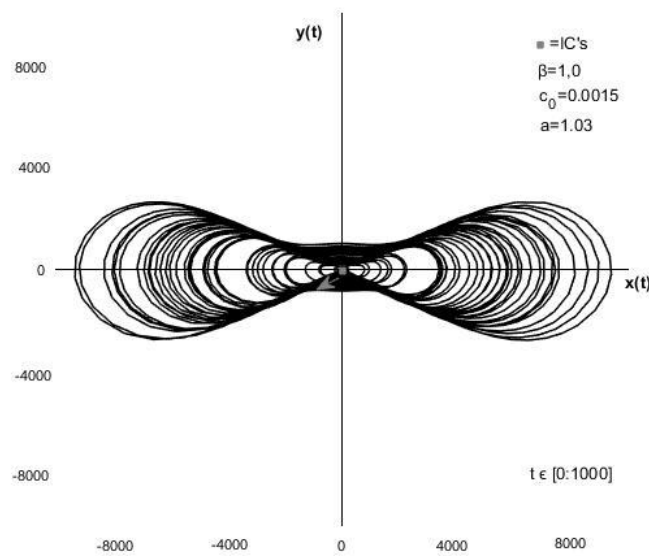


Figure D.74: Phase plane diagram for the base-case system with  $m=2,0$ , making  $\beta=1,0$ , with  $c_0=0,0015$  and  $a=1,03$ .

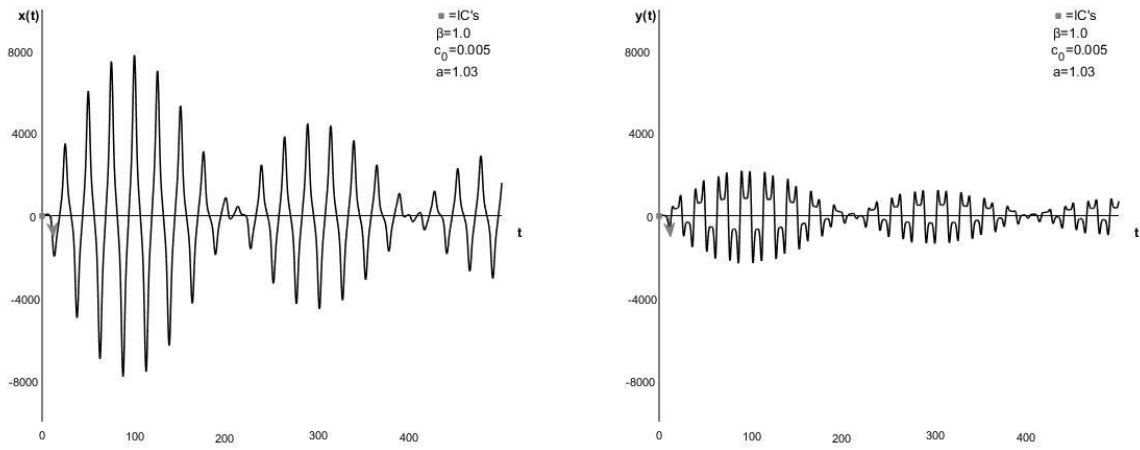


Figure D.75: Position curve(left) and velocity curve(right) for the base-case system with  $m=2,0$ , making  $\beta=1,0$ , with  $c_0=0,005$  and  $a=1,03$ .

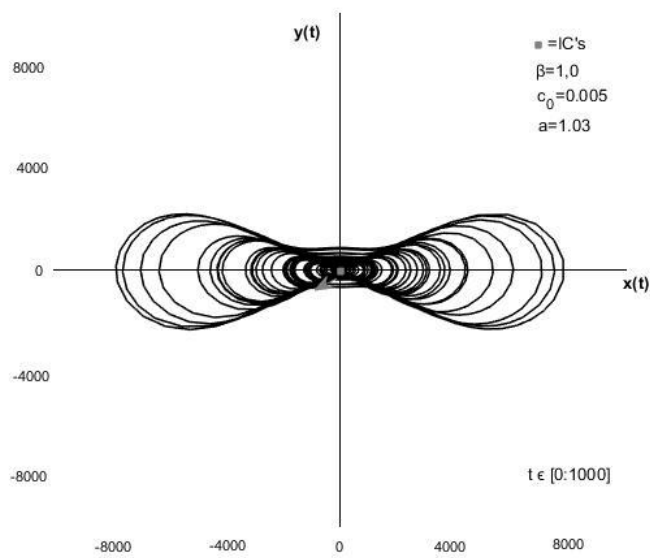


Figure D.76: Phase plane diagram for the base-case system with  $m=2,0$ , making  $\beta=1,0$ , with  $c_0=0,005$  and  $a=1,03$ .

D.4.5  $a=1,04$

Figures D.77 and D.78 show the position curve, velocity curve and phase plane diagram respectively for the system with  $a=1,04$  and  $c_0=0,005$ . Figures D.79 and D.80 show the same for the system with  $a=1,04$  and  $c_0=0,005$ .

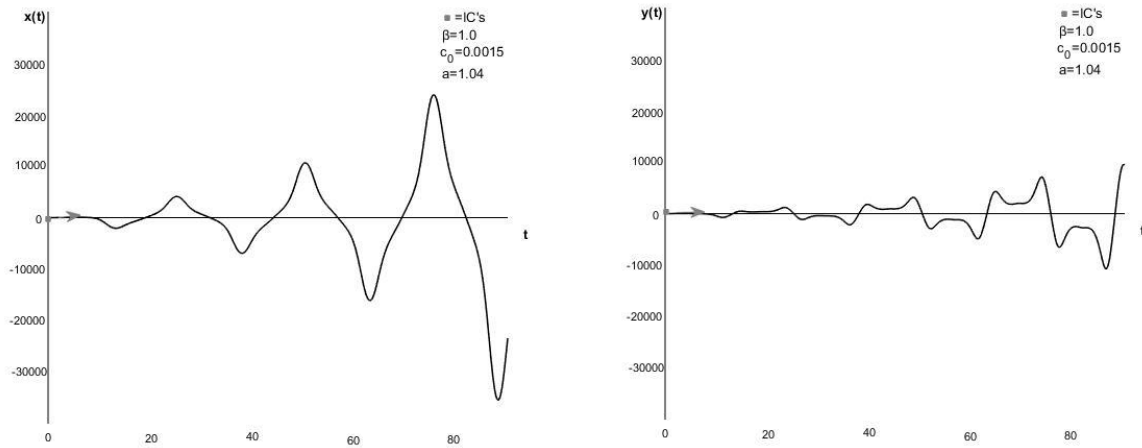


Figure D.77: Position curve(left) and velocity curve(right) for the base-case system with  $m=2,0$ , making  $\beta=1,0$ , with  $c_0=0,0015$  and  $a=1,04$ .

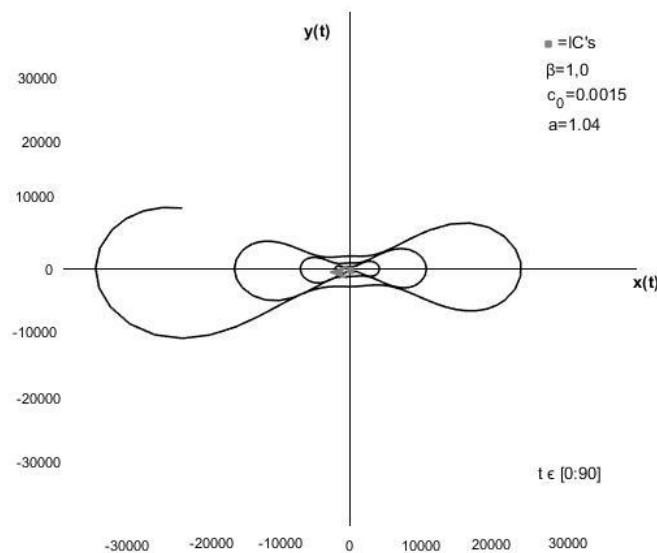


Figure D.78: Phase plane diagram for the base-case system with  $m=2,0$ , making  $\beta=1,0$ , with  $c_0=0,0015$  and  $a=1,04$ .

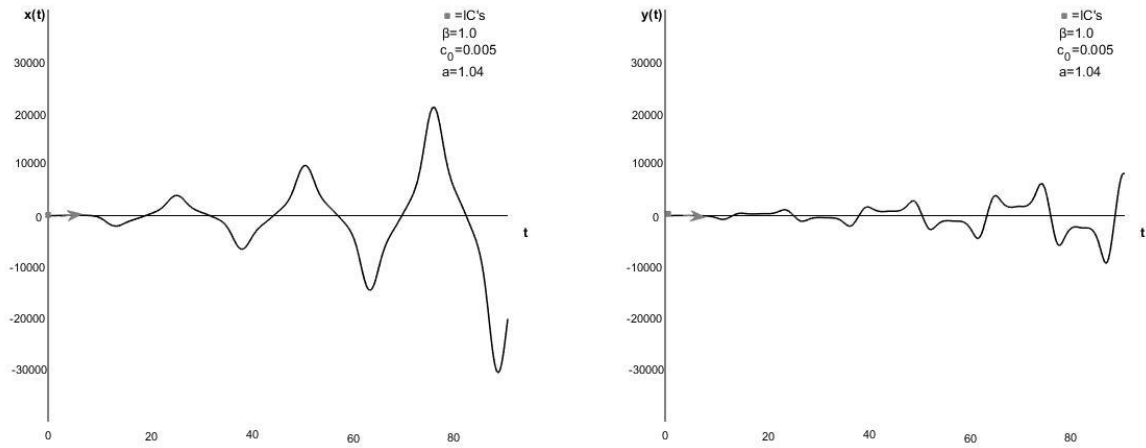


Figure D.79: Position curve(left) and velocity curve(right) for the base-case system with  $m=2,0$ , making  $\beta=1,0$ , with  $c_0=0,005$  and  $a=1,04$ .

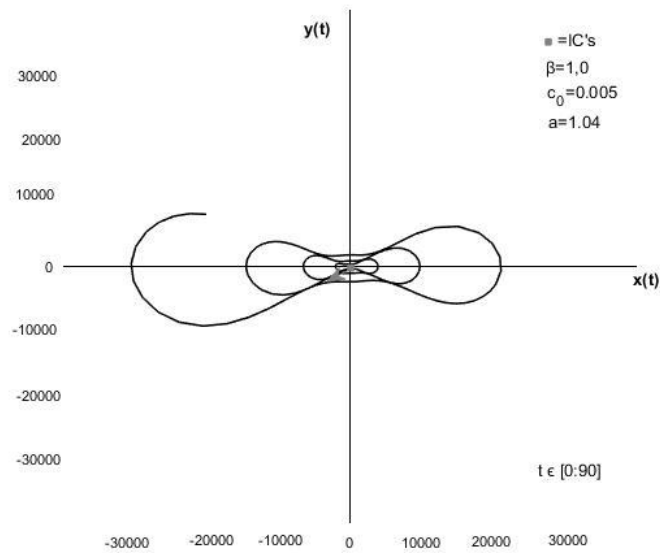


Figure D.80: Phase plane diagram for the base-case system with  $m=2,0$ , making  $\beta=1,0$ , with  $c_0=0,005$  and  $a=1,04$ .

D.5  $\beta = \frac{3}{2}$

When the mass parameter,  $m=4,5$ , the system has a frequency,  $\omega$ , is 50% bigger than the natural frequency,  $\omega_0$ , i.e.  $\beta = \frac{3}{2}$ .

D.5.1  $a=0$

When  $a=0$ , the system is only subjected to linear, constant damping,  $c_0$ . Figure D.81 shows the position and velocity curve for the system with  $c_0=0,0015$ . Figure D.82 shows the system with  $c_0=0,0015$  in the phase plane. Figures D.83 and D.84 show the position and velocity curve and phase plane diagram respectively for the system with  $c_0=0,005$ .

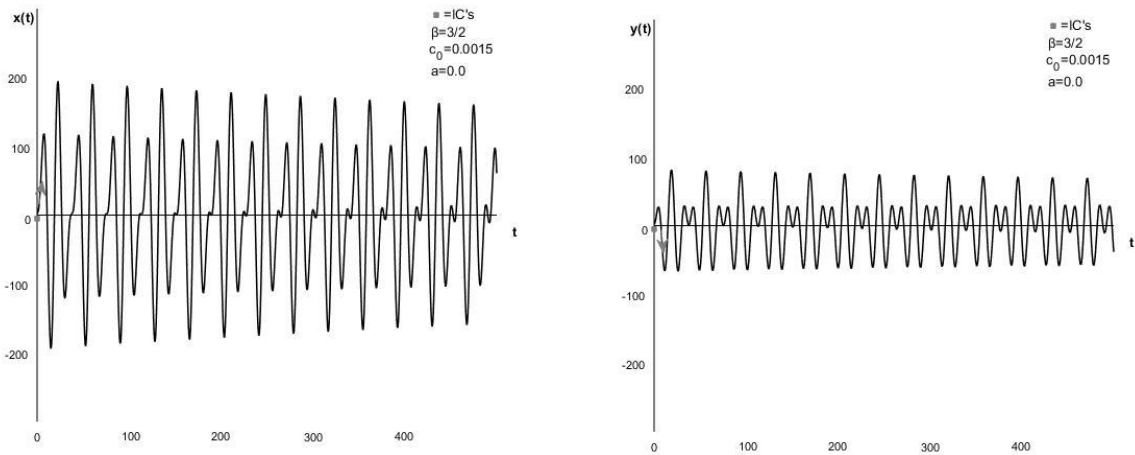


Figure D.81: Position curve(left) and velocity curve(right) for the base-case system with  $m=4,5$ , making  $\beta=3/2$ , with  $c_0=0,0015$  and  $a=0$ .

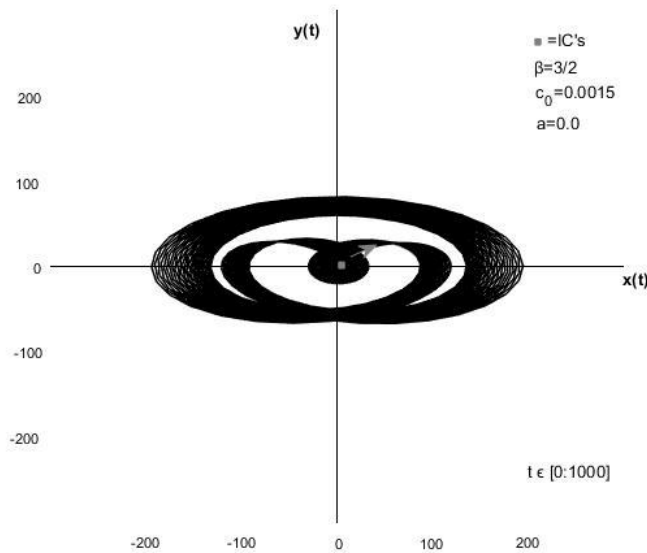


Figure D.82: Phase plane diagram for the base-case system with  $m=4,5$ , making  $\beta=3/2$ , with  $c_0=0,0015$  and  $a=0$ .

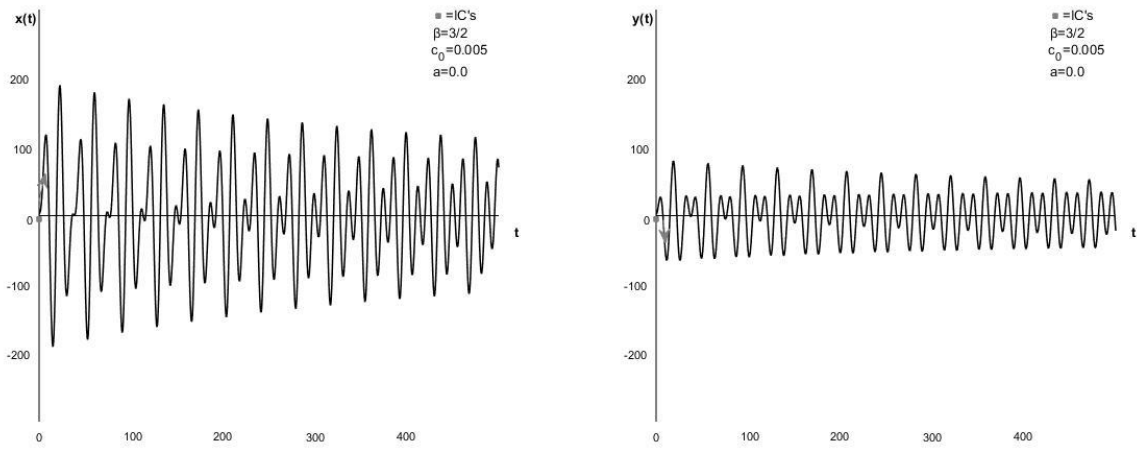


Figure D.83: Position curve(left) and velocity curve(right) for the base-case system with  $m=4,5$ , making  $\beta=3/2$ , with  $c_0=0,005$  and  $a=0$ .

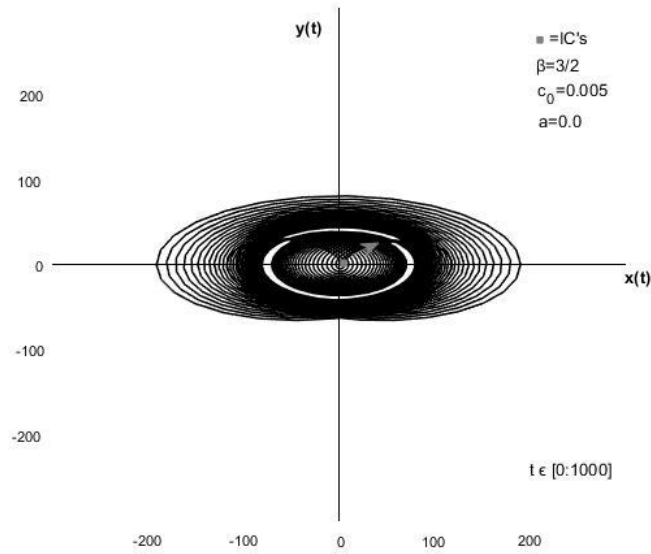


Figure D.84: Phase plane diagram for the base-case system with  $m=4,5$ , making  $\beta=3/2$ , with  $c_0=0,005$  and  $a=0$ .



### D.5.2 $a=0,1$

Figures D.85 and D.86 show the position curve, velocity curve and phase plane diagram respectively for the system with  $a=0,1$  and  $c_0=0,0015$ . Figures D.87 and D.88 show the same for the system with  $a=0,1$  and  $c_0=0,0015$ .

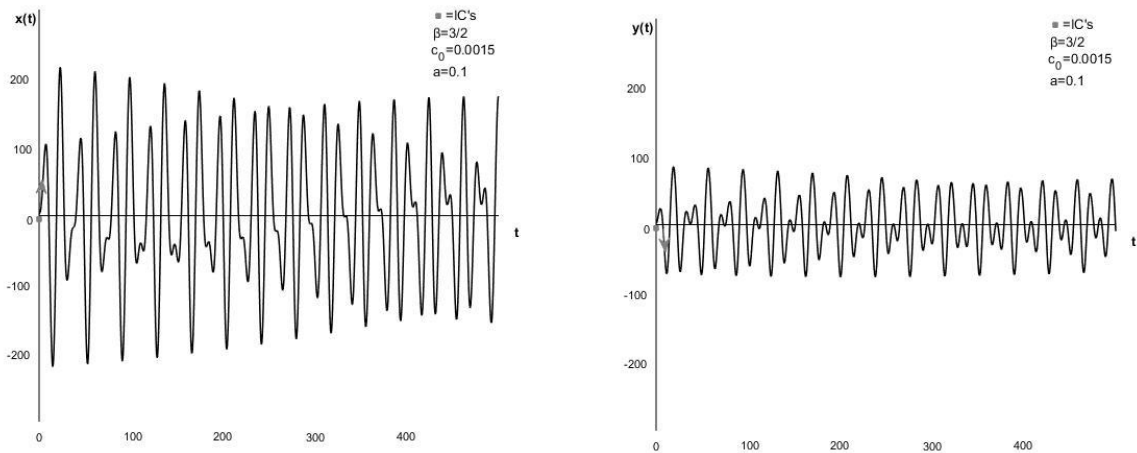


Figure D.85: Position curve(left) and velocity curve(right) for the base-case system with  $m=4,5$ , making  $\beta=3/2$ , with  $c_0=0,0015$  and  $a=0,1$ .

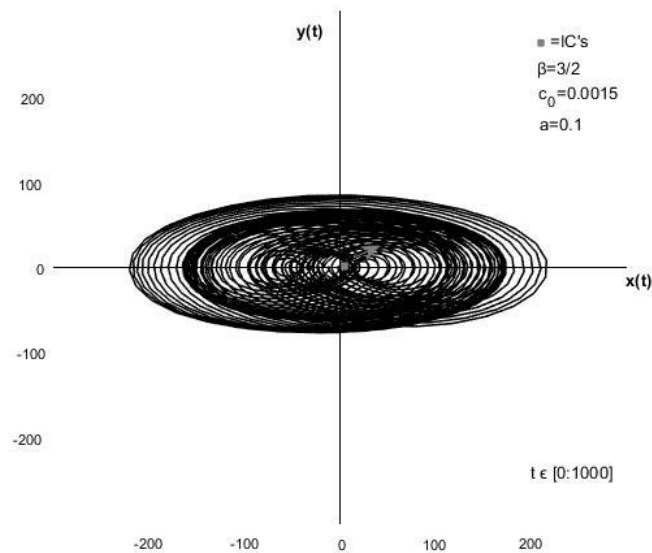


Figure D.86: Phase plane diagram for the base-case system with  $m=4,5$ , making  $\beta=3/2$ , with  $c_0=0,0015$  and  $a=0,1$ .

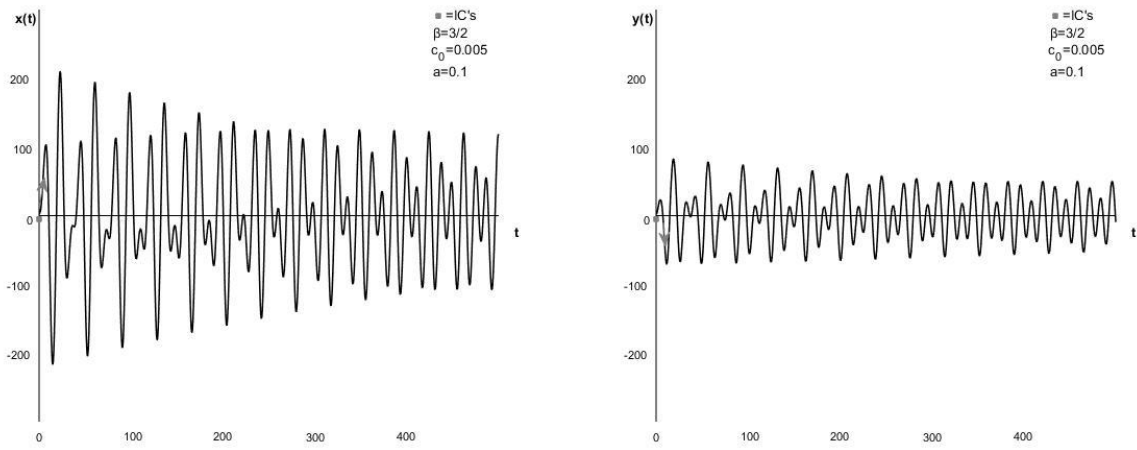


Figure D.87: Position curve(left) and velocity curve(right) for the base-case system with  $m=4,5$ , making  $\beta=3/2$ , with  $c_0=0,005$  and  $a=0,1$ .

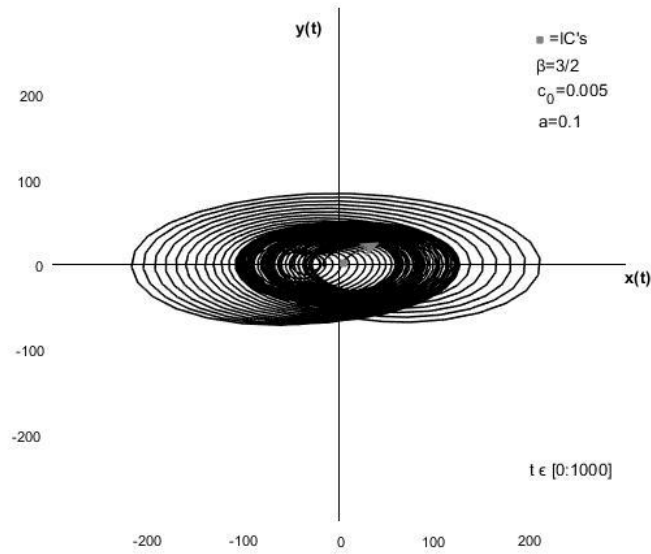


Figure D.88: Phase plane diagram for the base-case system with  $m=4,5$ , making  $\beta=3/2$ , with  $c_0=0,005$  and  $a=0,1$ .

### D.5.3 $a=0,2$

Figures D.89 and D.90 show the position curve, velocity curve and phase plane diagram respectively for the system with  $a=0,2$  and  $c_0=0,005$ . Figures D.91 and D.92 show the same for the system with  $a=0,2$  and  $c_0=0,005$ .

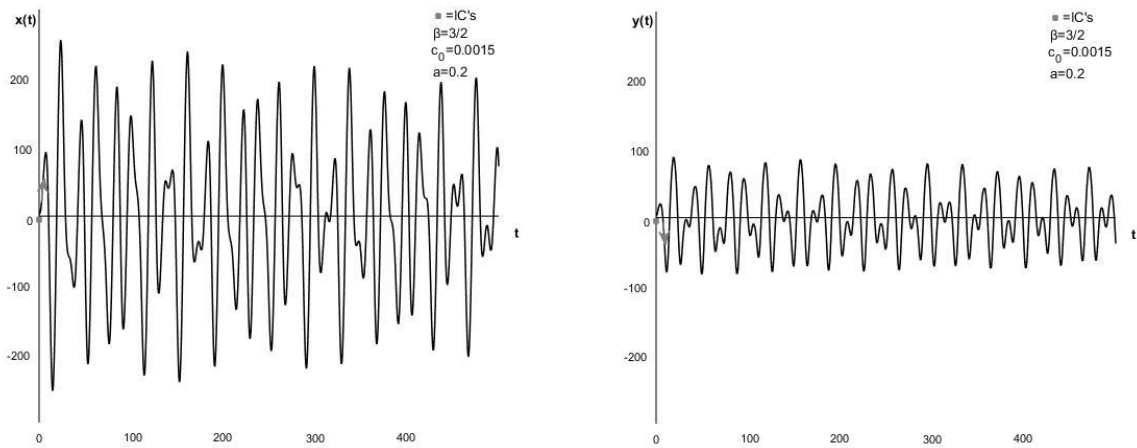


Figure D.89: Position curve(left) and velocity curve(right) for the base-case system with  $m=4,5$ , making  $\beta=3/2$ , with  $c_0=0,0015$  and  $a=0,2$ .

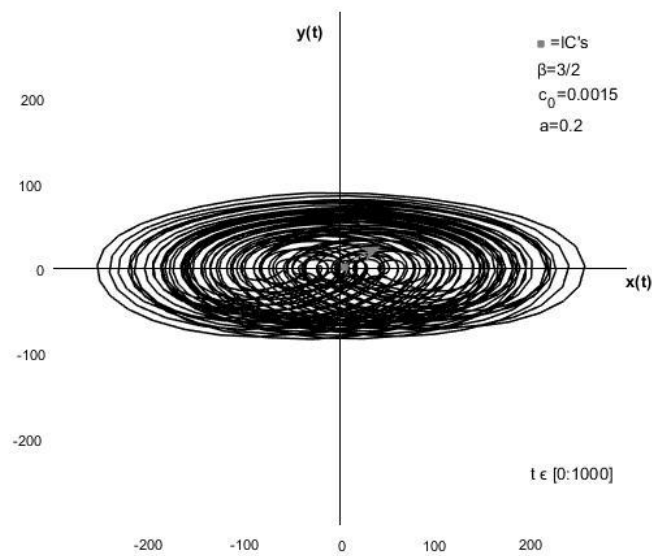


Figure D.90: Phase plane diagram for the base-case system with  $m=4,5$ , making  $\beta=3/2$ , with  $c_0=0,0015$  and  $a=0,2$ .

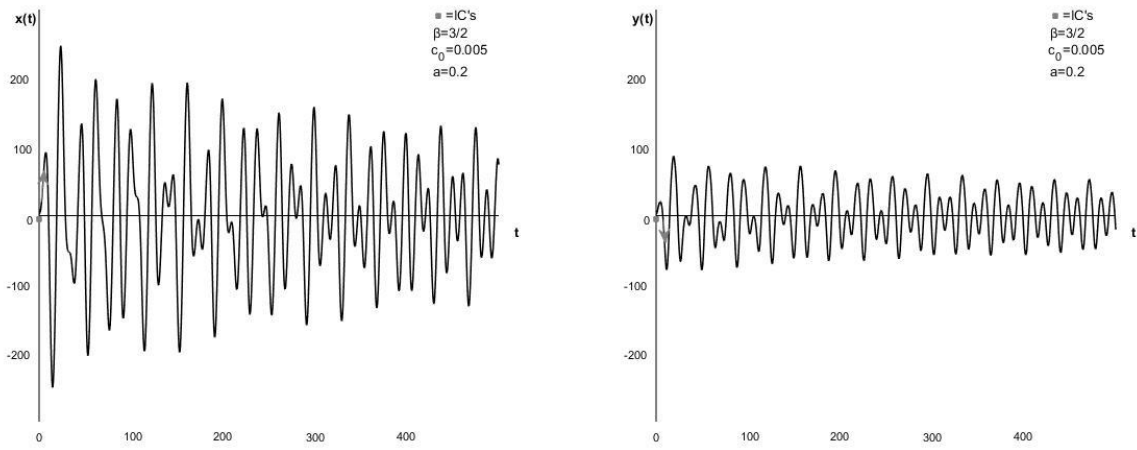


Figure D.91: Position curve(left) and velocity curve(right) for the base-case system with  $m=4,5$ , making  $\beta=3/2$ , with  $c_0=0,005$  and  $a=0,2$ .

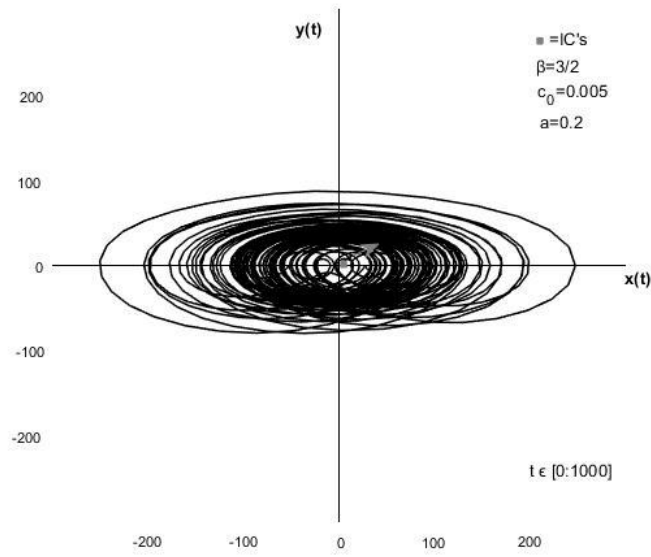


Figure D.92: Phase plane diagram for the base-case system with  $m=4,5$ , making  $\beta=3/2$ , with  $c_0=0,005$  and  $a=0,2$ .

### D.5.4 $a=0,36$

Figures D.93 and D.94 show the position curve, velocity curve and phase plane diagram respectively for the system with  $a=0,36$  and  $c_0=0,005$ . Figures D.95 and D.96 show the same for the system with  $a=0,36$  and  $c_0=0,005$ .

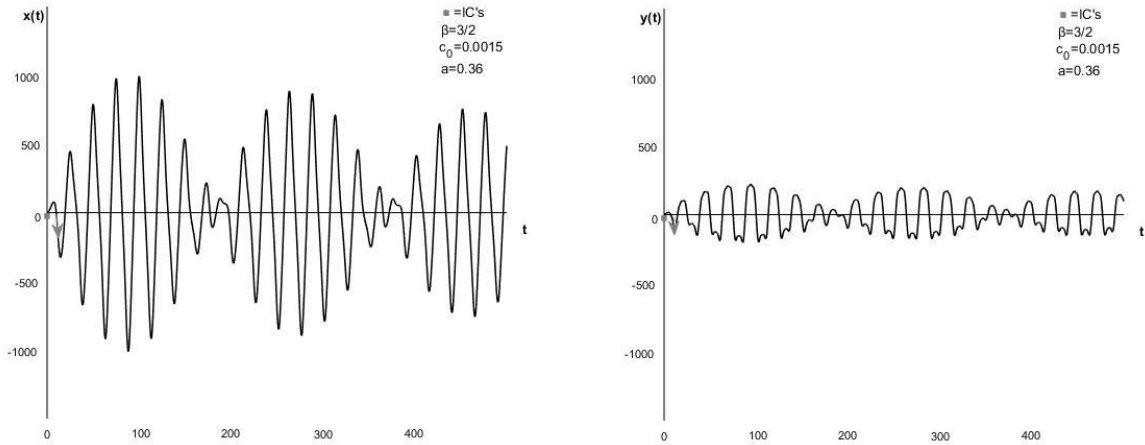


Figure D.93: Position curve(left) and velocity curve(right) for the base-case system with  $m=4,5$ , making  $\beta=3/2$ , with  $c_0=0,0015$  and  $a=0,36$ .

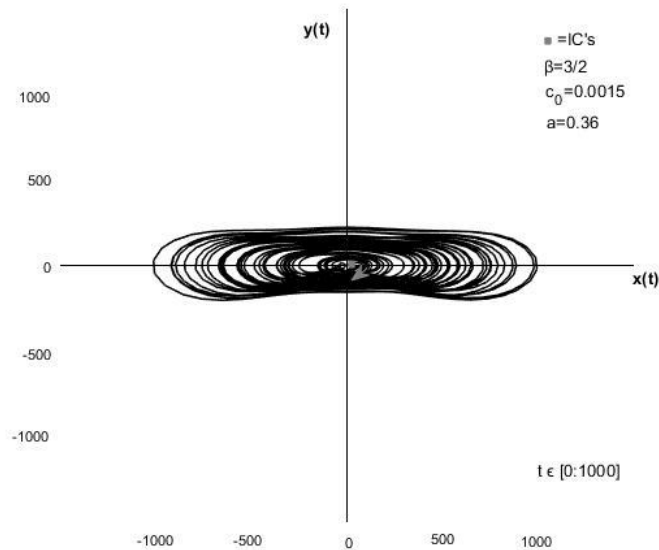


Figure D.94: Phase plane diagram for the base-case system with  $m=4,5$ , making  $\beta=3/2$ , with  $c_0=0,0015$  and  $a=0,36$ .

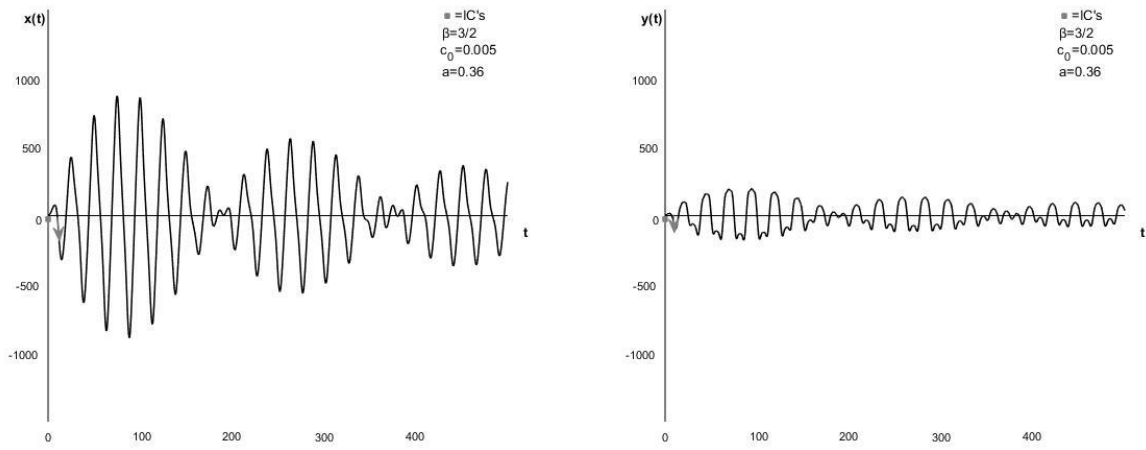


Figure D.95: Position curve(left) and velocity curve(right) for the base-case system with  $m=4,5$ , making  $\beta=3/2$ , with  $c_0=0,005$  and  $a=0,36$ .

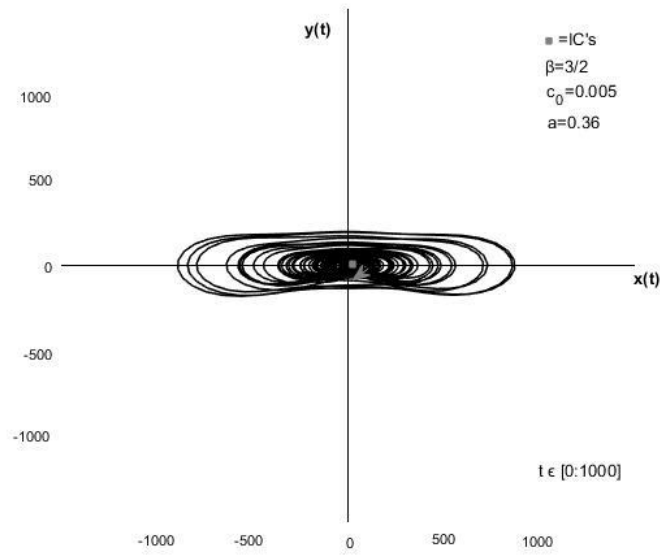


Figure D.96: Phase plane diagram for the base-case system with  $m=4,5$ , making  $\beta=3/2$ , with  $c_0=0,005$  and  $a=0,36$ .

D.5.5  $a=0,37$

Figures D.97 and D.98 show the position curve, velocity curve and phase plane diagram respectively for the system with  $a=0,37$  and  $c_0=0,005$ . Figures D.99 and D.100 show the same for the system with  $a=0,37$  and  $c_0=0,005$ .

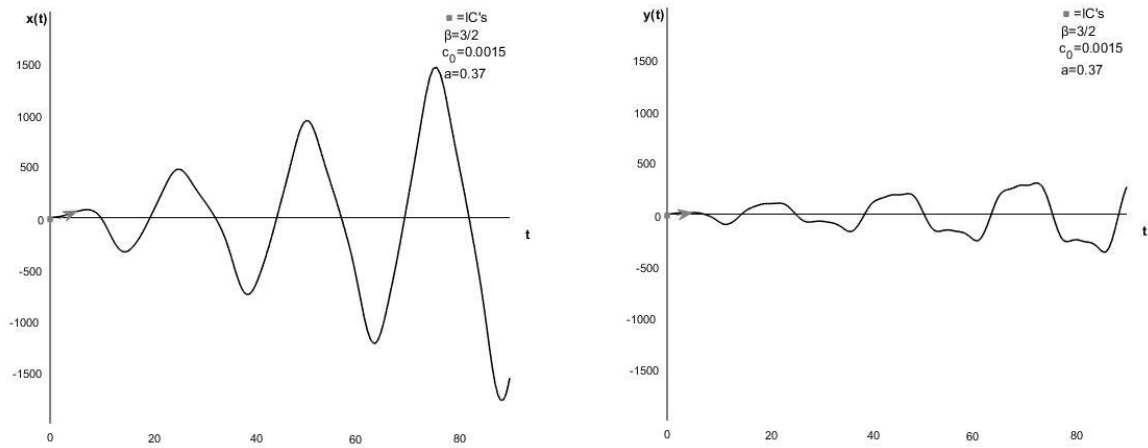


Figure D.97: Position curve(left) and velocity curve(right) for the base-case system with  $m=4,5$ , making  $\beta=3/2$ , with  $c_0=0,0015$  and  $a=0,37$ .

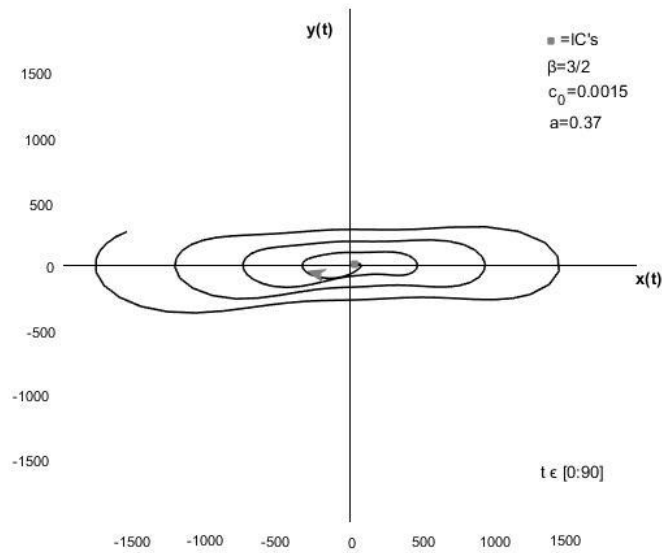


Figure D.98: Phase plane diagram for the base-case system with  $m=4,5$ , making  $\beta=3/2$ , with  $c_0=0,0015$  and  $a=0,37$ .

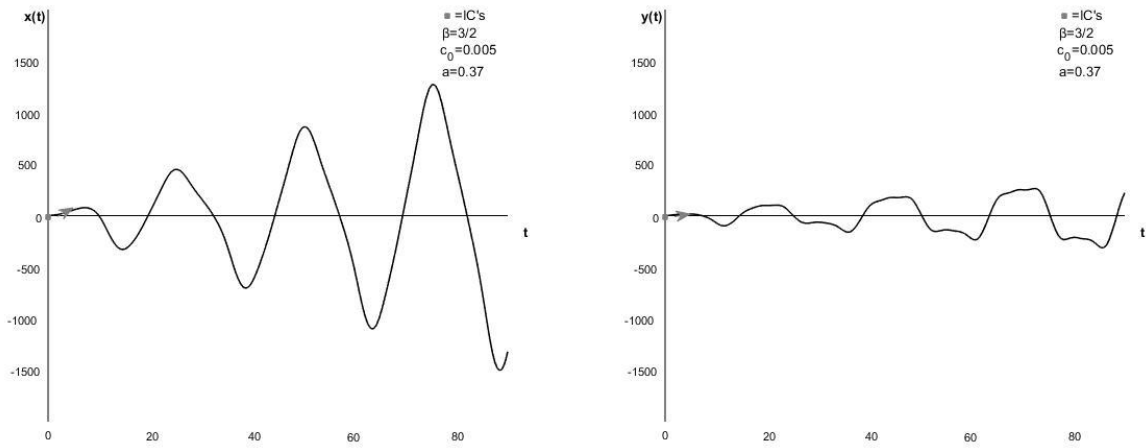


Figure D.99: Position curve(left) and velocity curve(right) for the base-case system with  $m=4,5$ , making  $\beta=3/2$ , with  $c_0=0,005$  and  $a=0,37$ .

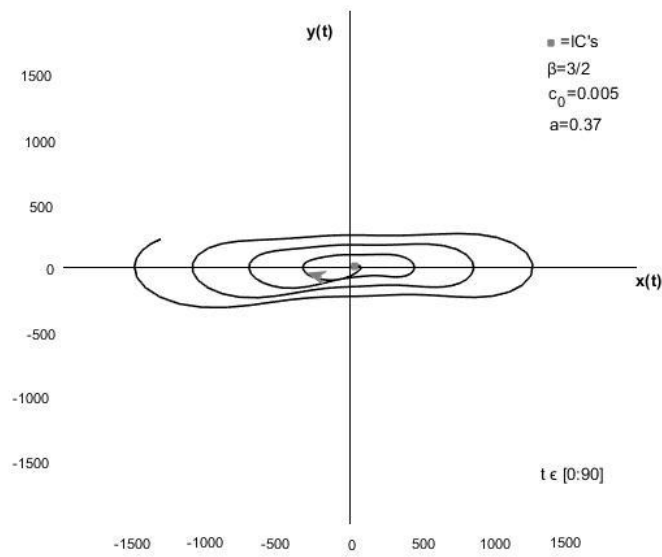


Figure D.100: Phase plane diagram for the base-case system with  $m=4,5$ , making  $\beta=3/2$ , with  $c_0=0,005$  and  $a=0,37$ .



## D.6 $\beta = 2,0$

When the mass parameter,  $m=8,0$ , the system has a frequency,  $\omega$ , is twice the natural frequency,  $\omega_0$ , i.e.  $\beta = 2,0$ . The system is presented for two values of linear, constant damping,  $c_0=0,0015$  and  $c_0=0,005$ , with an increasing nonlinear coefficient,  $a$ .

### D.6.1 $a=0$

When  $a=0$ , the system is only subjected to linear, constant damping,  $c_0$ . Figure D.101 shows the position and velocity curve for the system with  $c_0=0,0015$ . Figure D.102 shows the system with  $c_0=0,0015$  in the phase plane. Figures D.103 and D.104 show the position and velocity curve and phase plane diagram respectively for the system with  $c_0=0,005$ .

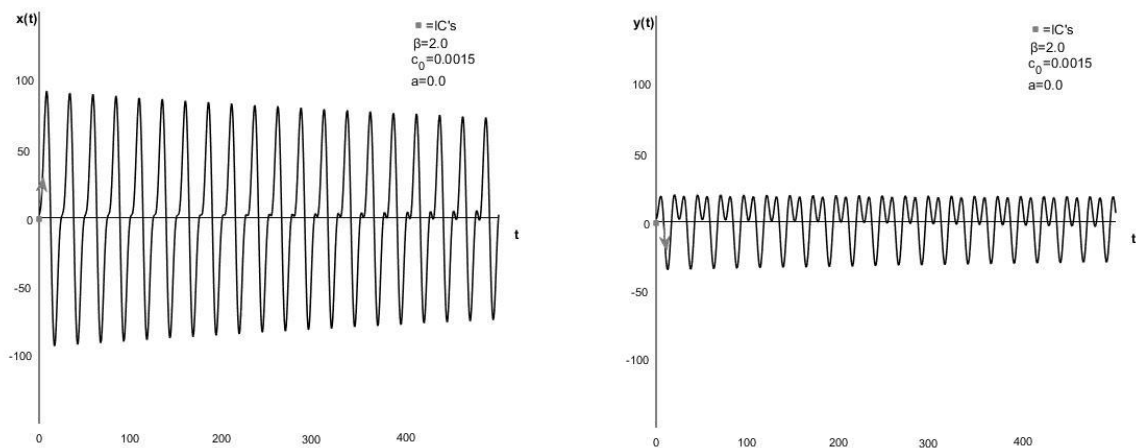


Figure D.101: Position curve(left) and velocity curve(right) for the base-case system with  $m=8,0$ , making  $\beta=2,0$ , with  $c_0=0,0015$  and  $a=0$ .

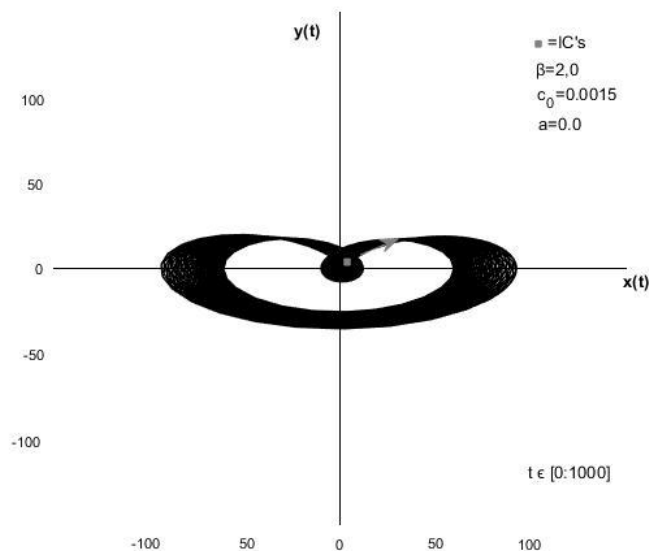


Figure D.102: Phase plane diagram for the base-case system with  $m=8,0$ , making  $\beta=2,0$ , with  $c_0=0,0015$  and  $a=0$ .

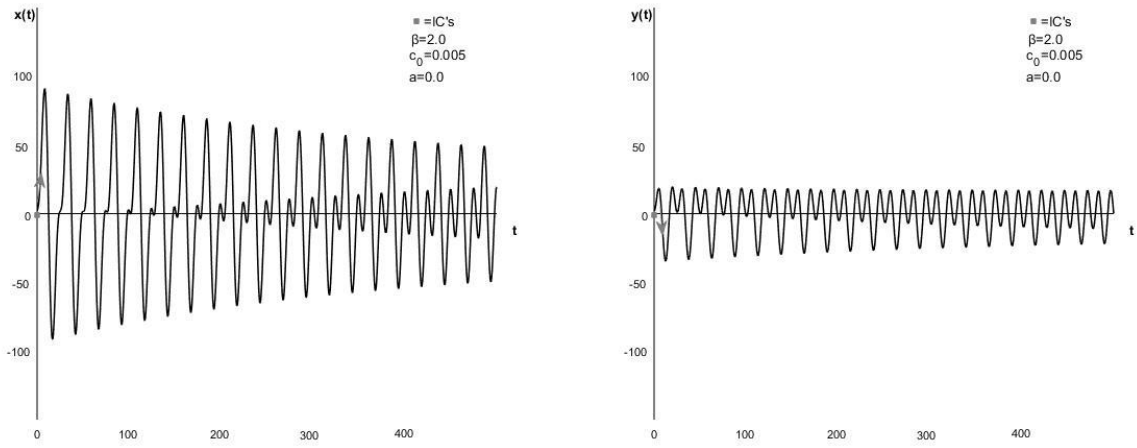


Figure D.103: Position curve(left) and velocity curve(right) for the base-case system with  $m=8,0$ , making  $\beta=2,0$ , with  $c_0=0,005$  and  $a=0$ .

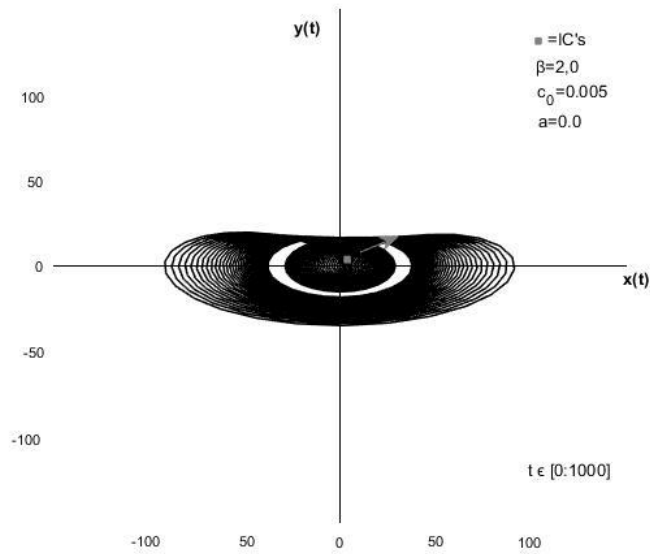


Figure D.104: Phase plane diagram for the base-case system with  $m=8,0$ , making  $\beta=2,0$ , with  $c_0=0,005$  and  $a=0$ .

## D.6.2 $a=0,01$

Figures D.105 and D.106 show the position curve, velocity curve and phase plane diagram respectively for the system with  $a=0,01$  and  $c_0=0,0015$ . Figures D.107 and D.108 show the same for the system with  $a=0,01$  and  $c_0=0,0015$ .

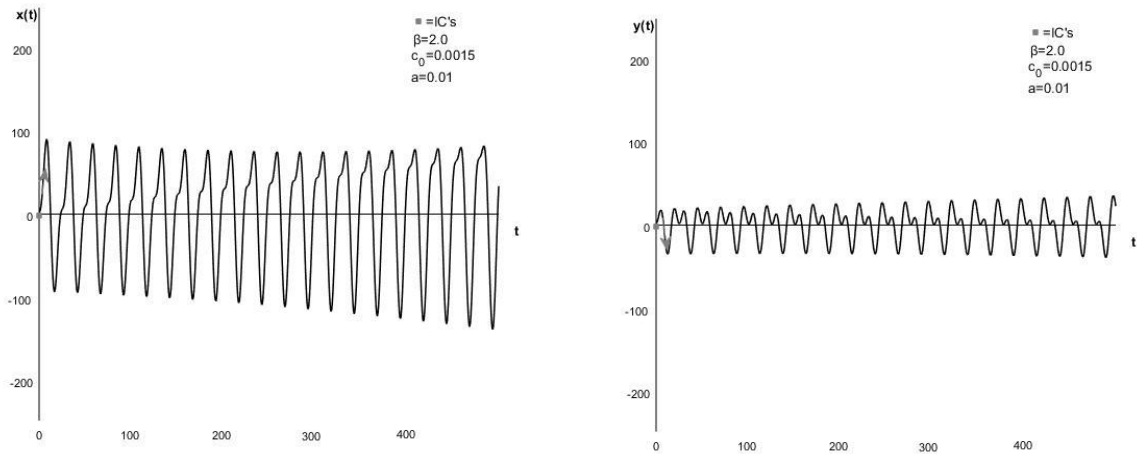


Figure D.105: Position curve(left) and velocity curve(right) for the base-case system with  $m=8,0$ , making  $\beta=2,0$ , with  $c_0=0,0015$  and  $a=0,01$ .

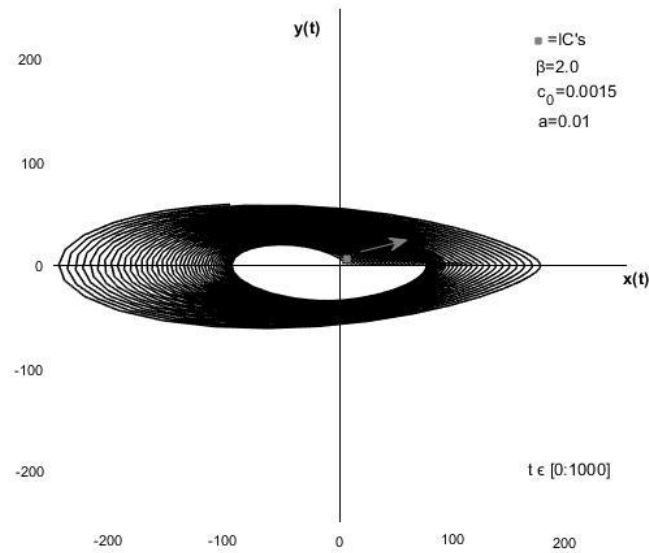


Figure D.106: Phase plane diagram for the base-case system with  $m=8,0$ , making  $\beta=2,0$ , with  $c_0=0,0015$  and  $a=0,01$ .

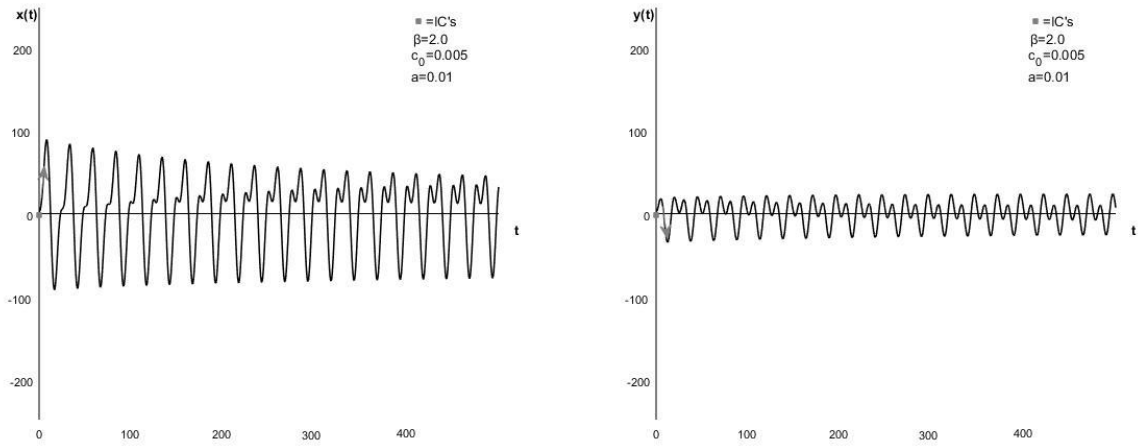


Figure D.107: Position curve(left) and velocity curve(right) for the base-case system with  $m=8,0$ , making  $\beta=2,0$ , with  $c_0=0,005$  and  $a=0,01$ .

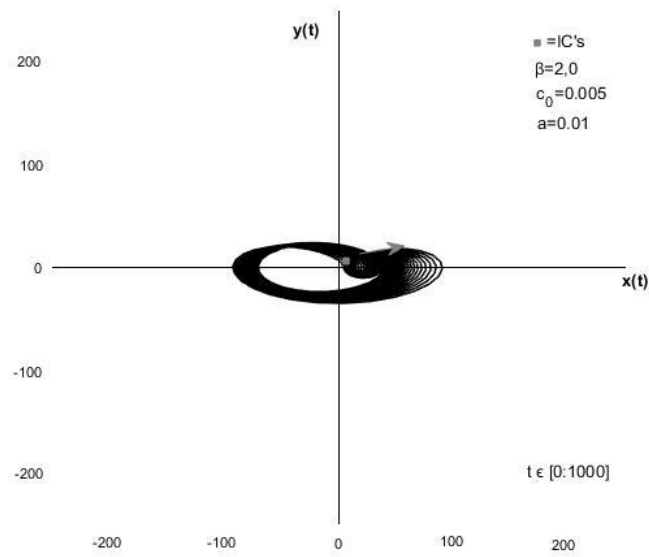


Figure D.108: Phase plane diagram for the base-case system with  $m=8,0$ , making  $\beta=2,0$ , with  $c_0=0,005$  and  $a=0,01$ .

### D.6.3 $a=0,02$

Figures D.109 and D.110 show the position curve, velocity curve and phase plane diagram respectively for the system with  $a=0,02$  and  $c_0=0,005$ . Figures D.111 and D.112 show the same for the system with  $a=0,02$  and  $c_0=0,005$ .

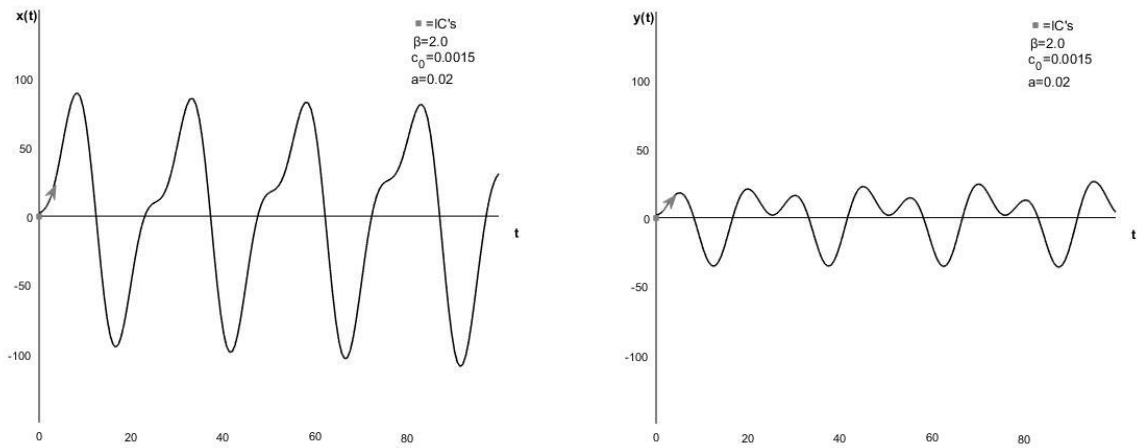


Figure D.109: Position curve(left) and velocity curve(right) for the base-case system with  $m=8,0$ , making  $\beta=2,0$ , with  $c_0=0,0015$  and  $a=0,02$ .

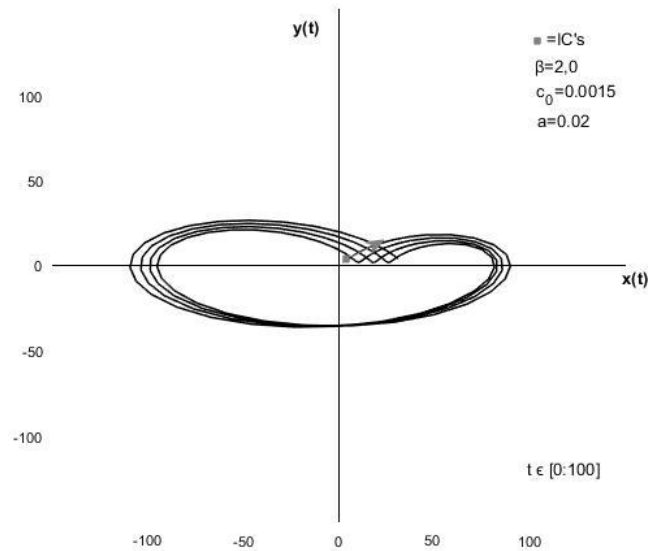


Figure D.110: Phase plane diagram for the base-case system with  $m=8,0$ , making  $\beta=2,0$ , with  $c_0=0,0015$  and  $a=0,02$ .

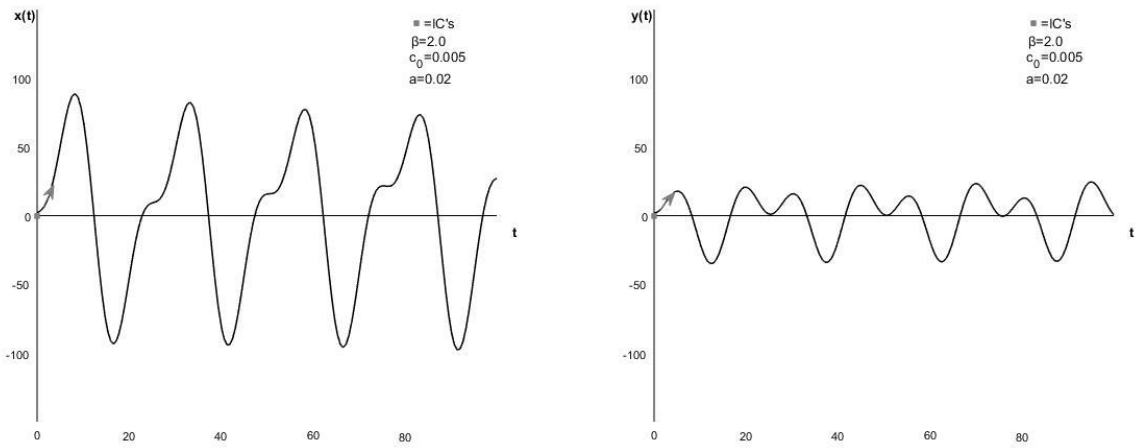


Figure D.111: Position curve(left) and velocity curve(right) for the base-case system with  $m=8,0$ , making  $\beta=2,0$ , with  $c_0=0,005$  and  $a=0,02$ .

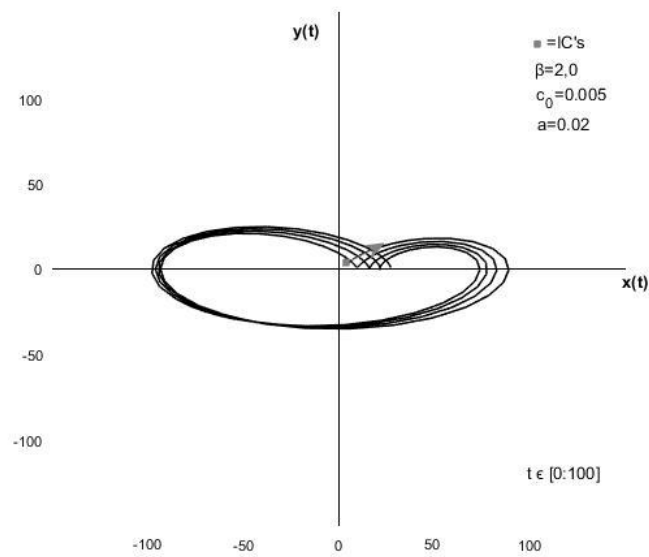


Figure D.112: Phase plane diagram for the base-case system with  $m=8,0$ , making  $\beta=2,0$ , with  $c_0=0,005$  and  $a=0,02$ .

# Appendix E

This appendix is in its entirety copied from the master thesis *“Apparent Negative Damping an Original Approach to the Oscillations of Offshore Structures”* [25] by Babbiste Reyne from 2016.

## E.1 Context

Nils Gunnar Gundersen is today a consultant in oil and gas production management. He was in the past involved in various projects and held the position of platform manager on Shell Draugen platform. The following text summarizes his testimony which was collected during an interview arranged by Ove Tobias Gudmestad on April 7, 2016.

## E.2 Interview

I was already involved with the Draugen project during its concept phase. The structure consists of a single concrete shaft of variable section located at two hundred and fifty meters deep sea. On top of it, around thirty tons of steel forming the decks and the equipment. The air gap, initially supposed to be twenty four meters, was increased of six meters during the construction after a redesign proposed by the structural engineers who explained to us that it would reduce the risk of failure due to “ringing response”; this decision might have later saved our lives. In the year 1988 when the design process had just started, the project director asked the team to set on a date to begin the production: October the sixteenth, 1993 was our answer. After a few years of exemplary management demonstrated by minimum delays and no over costs, the production started on October the nineteenth, 1993. I then took charge of the platform management that held me responsible for all that would happens on site during its life of production.

During one day of March 1995, I was working in my office when I noticed that the painting hanging in front of my desk was was not only swinging as it usually did, but punctually be lifted away from the wall before hitting it back. A hurricane was announced that day, and we could also tell by the “bangs” shrilling in the site. I then received an unexpected call from Aberdeen weather center, warning me of a very large wave coming in our direction. According to them, we had only thirty minutes to prepare. I ran to the microphone in order to quickly stop the production and to summon every present individual to the gymnasium located on the lower deck. Once everyone gathered was standing in front of the inner walls, I stood in the center of the room and told them about “Rasmus” - this is the name sailors give to the largest waves. Everyone was quiet and alert. I explained them how well the conception of the platform had been lead using a short presentation that the engineering team gave me. I finally tried to reassure everyone expressing my unconditional faith in the designers work. My short speech was concluded by this precise sentence: now we can only wait for “Rasmus” to hit us. As soon as I finished pronouncing these words, the loudest, most shivery and violent BANG I have ever heard rang out in the gymnasium. We started to feel increasingly large motions under our feet, the projector I was using for the presentation all of a sudden left its place and rolled towards a wall. Once I caught it, all and sundry sat and no one batted an eye while the room kept on pitching. I could not tell exactly how long it lasted but my guess would be more than a minute.

Once it became obvious that “Rasmus” had left, we eventually went outside. Heavy equipment that where before taped on walls had run off after their bands were cut in the shock. We had been hit by a massive wave. On the hundred and thirty four workers who where present at Draugen, some would be quite experienced as fishermen. I would allow them to fish and to hang their catches under the deck where strong winds result in an effective way of drying fish. My condition was to only use

rope and wooden elements in order not to alter the structure, and they would come up with clever solutions to strongly attach the hundreds of kilograms of seized prays. We went to the lower deck to see what happened to them. Not only this large mass of robustly roped beings had disappeared, but the wave had not even left a clue of their very existence. No significant damage however was reported, and knowing what could have happen if we had not be told of the upcoming danger, I felt at first very thankful to those who warned us. The origin of this phenomenon could not be explained and I do not know how it was detected. While the industrial Shell hardly showed a reaction, the engineering team from Norwegian Contractors saw there an excellent way to confirm the quality of their work. This occurrence lead to the installation of measuring devices on the platform which may have recorded a similar event about a year later.

Nils Gunnar Gundersen

### E.3 Complementary comments

By the description of the events, it is clear that the phenomenon that was experienced is related to exceptional wave conditions which involve high magnitudes in both velocity and period. As the investigations were advancing rose the question of the relation of directions in between the impacting flow and the oscillations. N. G. Gundersen was contacted again and asked for possible further informations about any memory he may have had of both the angle of attack of the wave, and the trajectory of the resulting oscillations.

I do not remember from which direction Rasmus was coming. The report I wrote after the event has very unfortunately been removed from the document center in the operating office in Kristiansund.

Additionally, I cannot remember the direction of the oscillations. I just remember the tremendous big “BANG” when the huge wave hit us and everybody standing along the walls immediately jumped down on to the floor. The very big oscillations must have taken around 40 to 60 seconds, but it is difficult to judge because the weather was at that time very bad and the leg moved quite a lot during this bad weather situations. The fact that there were movement in the leg was in full compliance with the design criteria.

I mentioned that I still remember the large painting I had in my office on the wall in front of me moving in all directions during bad weather situations. I always took it as a good sign that the huge vertical concrete structure behaved in accordance with all design criteria.

Nils Gunnar Gundersen

### E.4 Conclusion

Although N. G. Gundersen was understandably not able to recall the very details of the events, two hints may indicate the occurrence of a crossflow amplification of the oscillations, studied in part II.

First, the gigantic wave that is described corresponds to a great height that necessarily comes with a large period. But the vibrations that are mentioned seem to correspond to much higher frequencies that do not resemble inflow oscillations. Then, the movement of the painting at the beginning of the events is reported abnormal because it would be lifted off the wall instead of gliding along it, which implies a change of the action’s direction. Assuming the usual forces to have the same direction as the flow, the behavior of the painting may be the result of an unusual crossflow oscillation.